A Genetic Suppressor Screen identifies a novel, conserved ion channel complex as a new downstream target of RHO-1 signalling

Andrew Phillip Porter

UCL

PhD

Declaration

I, Andrew Phillip Porter, declare that the work presented in this thesis is my own. Where information has been derived from other sources, I confirm this has been indicated in the thesis.

Abstract

The small GTPase RHO-1 is an important regulator of neurotransmission. *Caenorhabditis elegans* nematodes expressing activated RHO-1 (G14V) in their cholinergic motor neurons (nRHO-1*) become hypersensitive to the acetylcholinesterase inhibitor aldicarb, demonstrating increased acetylcholine release, and acquire a highly loopy, uncoordinated locomotion.

RHO-1 inhibits diacylglycerol kinase (DGK-1), and so increases the availability of diacylglycerol (DAG), a key second messenger for release at the presynaptic membrane. Inhibiting RHO-1 in a *dgk-1* mutant causes a decrease in neurotransmitter release, demonstrating the presence of additional targets downstream of RHO-1.

During a forward genetic screen for suppressors of the loopy locomotion of nRHO-1* animals we obtained a mutant, *nz94*, which carried an additional 'fainter' phenotype, helping us identify it as an allele of *unc-80*, a large, conserved protein, important in the localization of NCA-1 and NCA-2, C. elegans homologues of the novel mammalian ion channel NALCN.

RHO-1*;*unc-80* double mutants are non-loopy, but still hypersensitive to aldicarb, indicating that the loopy locomotion and high levels of neurotransmitter release can be uncoupled. *unc-80* mutants do not suppress non-neuronal phenotypes associated with heat-shock expression of RHO-1*, such as tail swelling and sterility.

Expressing an *unc-80* transgene under a cholinergic promoter is sufficient to rescue the suppression of loopy locomotion seen in the nRHO-1*;*unc-80* double mutants, indicating that *unc-80* acts presynaptically in the same cells as nRHO-1* for the generation of this loopy locomotion.

Work from other labs shows that *unc-80* mutants suppress gain-of-function PPK-1 (PI4P5K) phenotypes, most likely through changes in the localisation of the ion channels.

Our current model involves RHO-1 binding to and activating PPK-1, increasing levels of PIP_2 and hyperactivating the NCA-1/NCA-2 channels. We suspect this ion channel complex may regulate the release of neuropeptides involved in locomotive behaviour.

Acknowledgements

I would like to thank my supervisor, Dr Stephen Nurrish, for providing me with much support and guidance during this PhD, as well as for suggesting the initial project. I would also like to thank Dr Rachel McMullan with whom I performed the genetic screen described here, and who gave a great deal of practical help throughout. My thanks also go to all the other members of the Nurrish lab who I've had the pleasure of working with throughout my PhD, and to the wider LMCB community, particularly my year group with whom I've shared the ups and downs of research and life in general.

I would especially like to thank my wife, Aliya, for her love and support, particularly during the writing of the thesis, through which we managed to make it in the end. Also to the rest of my family, with special mention to everyone who helped baby sit Benjamin so I could do some writing.

I would also like to acknowledge those at Greenwich Vineyard church whose friendship helped me through tough times, and particulary to Allan who helped proof-read.

Thanks for all the coffees, Ben, and for being a great housemate, Alex; to Darryl, Danny, Stephen, Jack and Tom for their continued friendship, and hello to Jason Isaacs.

Table of Contents

Table of Contents

List of Movies

1 - INTRODUCTION

1.1 - Neurobiology - a perspective

One of the essential properties of all living organisms is the ability to sense and respond to their environments. Multicellular organisms have the task of coordinating inputs from many different cell types and from the environment and producing a suitable, organism-wide response to changing conditions. Coordination between cells that does not require a fast output is conducted through paracrine signalling, but this is limited by the rate of diffusion and the strength of the diffused signal. More distant signalling makes use of blood or lymph for endocrine signalling, but this is still limited by the speed of transport in a liquid medium. For fast responses, multicellular organisms make use of a specialised branch of endocrine signalling - the nervous system. The individual cells of the nervous system - neurons - have adapted basic principles found in all cells - electrochemical potential, excitibility, cell-cell contacts, signalling pathways - for reception, transmission and processing of data over distance. From a mouse searching for food in a maze to a man listening his iPod, the nervous system has developed from humble beginnings to manage highly complex behaviours. The power of the nervous system arises from coupling a common unit - the neuron - into vast networks, with billions of neurons in the human brain each potentially contacting and communicating with thousands of others.

1.1.1 - C. elegans as a model organism for the study of neuroscience

In the 19th century, a debate raged between George Cuvier (1769-1832) and Geoffroy Saint-Hilaire (1772-1844), prominent scientists of the day, as to the nature of the relationship between living things (Striedter 2007). Cuvier proposed that animals be divided into four distinct groups, which shared no common ancestory; any similarities arose as a product of body parts having a similar function. Geoffroy maintained that all animals descended from a common ancestor, and that there was a common structural blueprint linking all animals together, modified between organisms on the basis of function, but constrained by a common unity of composition. One of Geoffroy's theories was that the dorsal side of vertebrates, where the central nervous system is located, is analogous to the ventral side of invertebrates, which contains the nerve cord (Hirth 2007).

While many of Geoffroy's predictions and similarities were shown to be superficial, Charles Darwin's (1809-1882) theories on the basis of common descent and evolution by natural selection provided a framework for the re-examination of these models. In our modern era of molecular analysis, we can see that homologous proteins, such as the

Notch family, control the patterning of the nervous system from the fruit fly to the mouse (Lardelli, Williams et al. 1995), and increasingly we see molecular homologies in function between the nervous systems of disparate organisms, for instance in the components of neurotransmitter release (Sudhof, Baumert et al. 1989), neuropeptide signalling (Nassel 2002) or the action of G-protein coupled receptors (GPCRs) (Fredriksson and Schioth 2005).

This perspective gives a rationale for the use of model organisms to study biology. Our brains are composed of cells not dissimilar to those found in apes or rodents, squid or sea slugs, flies or worms. These organisms offer huge practical and technical advantages in terms of scientific investigation compared with working directly in humans. Much work can be accomplished in simpler, smaller, faster-growing organisms than ourselves, and then scaled up for application to human health.

This model for conducting scientific research was used by Sydney Brenner (1927-) when he decided to work on a simple organism, one which he believed was so tractable that its entire nervous system and behaviour could be completely understood. Working in the late 1960s, Brenner wrote to Max Perutz, then head of the Medical Research Council, that 'it is now widely realized that nearly all the 'classical' problems of molecular biology have either been solved or will be solved in the next decade' (Brenner 1988) - referring to the understanding of the encoding of genetic information in DNA and the unravelling of the genetic code which was underway at the time. Instead Brenner proposed that to solve the next level of problems in biology - issues of why animals behave as they do - it would be necessary to study a single animal, 'to tame a small metazoan organism to study development directly' and for this he proposed to study a nematode worm. The fruit fly Drosophila had already been established as a model, but was deemed too complicated for the purpose (Brenner 1988). In his proposal to the MRC, Brenner wrote that 'we think we have a good candidate in the form of a small nematode worm, *Caenorhabditis briggsiae*...To start with we propose to identify every cell in the worm and trace lineages. We shall also investigate the constancy of development and study its genetic control by looking for mutants' (Brenner 1988). Interestingly, Brenner changed his mind and decided to concentrate on the related nematode *Caenorhabditis elegans*, a decision that proved of great significance decades later, as *C. briggsiae* has proven less tractable to RNA interference (Winston, Sutherlin et al. 2007), a key technique in the field of nematode biology.

Even in that initial proposal to the MRC Brenner identified some key factors which make nematode worms a favourable organism for biological manipulation. *C. elegans* is small,

a fully-grown adult is approximately 1mm in length, and passes through its lifecycle in approximately 3 days. These properties allow large numbers of animals to be grown in the laboratory. It had earlier been recognised that nematodes of this genus appeared to have an invariant cell number, and that this might make them useful for genetic study (Dougherty and Calhoun 1948).

C. elegans is a self-fertilising hermaphrodite, producing sperm and eggs separately. This aspect of the biology of the worm is highly useful to us in the laboratory, as an isogenic population can be maintained simply by picking a single individual to a fresh plate of bacteria and allowing it to self-fertilise. A single hermaphrodite may lay up to 300 eggs allowing rapid population expansion.

C. elegans does produce a low, spontaneous proportion of males, with a rather elegant developmental switch occurring in animals which carry only one copy of the sex chromosome, leading to the development of male characteristics (Hodgkin, Horvitz et al. 1979; Hodgkin 1983). Males exhibit a number of behaviours distinct from hermaphrodites, including a vulva detection pattern of movement when they encounter another worm or obstacle, and a mate-searching behaviour. Most of this behaviour is governed by an additional 205 male-specific somatic cells, including 89 neurons and 41 muscle cells. As well as assaying for male-specific behaviours, males are useful in experimentation because they allow for genetic crosses to be made allowing the generation of double mutants, backcrossing mutated animals and conducting epistasis and complementation experiments.

One of the key criticisms of Brenner's approach was that the worm appeared to be so simple that no useful mutants would be identified, although a mutant of *C. briggsae* had been identified and published much earlier (Nigon and Dougherty 1950). Brenner therefore spent the majority of his first years working with *C. elegans* screening for mutants generated by exposure to ethyl methanesulfonate (EMS), which he published in a ground-breaking paper in 1974 (Brenner 1974).

Brenner was able to identify a wide range of mutant phenotypes in the worm, relating to development and behaviour, and perform genetic mapping to place these mutants into complementation groups. These mutants are classified using a three letter code to represent the phenotype (Brenner 1974). For instance, mutants which are longer than wild-type are designated *lon* (for *lon*g), while mutants whose movement is different from wild-type are given the code *unc (unc*oordinated*)*. Similarly mutants were identified which were *eg*g-*l*aying defective (*egl)*, *let*hal (*let*) and *d*um*py* (*dpy*), amongst others. Subsequent cloning and identification of the genetic mutations responsible for these

phenotypes has identified key genes required for nervous system development or function, growth, behavioural responses, cell division and cell signalling - all essential processes common across species. This method of naming mutants has been translated into a structure for naming genes and proteins in *C. elegans* (Horvitz, Brenner et al. 1979). Gene names are three or four letters long, and written in lower case italics, for instance *unc-64* encodes the *C. elegans* homologue of the vertebrate syntaxin gene. The protein encoded by the gene is written in capitals, i.e. UNC-64 denotes the syntaxin protein.

These early screens demonstrated that *C. elegans* could be used to identify mutants defective in aspects of nervous system function, the very processes Brenner was originally interested in. For instance, UNC-5 and UNC-6 and UNC-40 are involved in axon guidance (Hedgecock, Culotti et al. 1990) and were identified in the original EMS screen (Brenner 1974) which also uncovered UNC-29, UNC-38 and UNC-63, subsequently shown to encode the nicotinic acetylcholine receptor (Lewis, Wu et al. 1980).

Much subsequent work has determined the structure of the *C. elegans* nervous system including synaptic connections (White 1986), the processes of synaptic vesicle fusion and neurotransmitter release, and the behaviours which result from a the workings of the nervous system. I will briefly review the use of C. elegans as a model organism, followed by an examination of the workings of its nervous system, and finally discuss a number of ways in which regulation of the nervous system controls a variety of complex behaviours.

1.1.2 - The small size and fast life cycle of C. *elegans* lends itself to biological analysis

An adult *C. elegans* worm is approximately 1mm in length, and 25µm in diameter (Figure 1-1), meaning that thousands of individuals can be grown on a single 55mm plate. *C. elegans* passes through four larval stages, named L1, L2, L3 and L4, before a final moulting to produce the mature adult. Under conditions of stress the animals can enter an alternative developmental stage known as dauer (Cassada and Russell 1975), which is highly resistant to dessication. At an average of 1000 animals per plate, a *C. elegans* laboratory can easily contain well over a million individuals at any one time. This is several orders of magnitude greater than for any other multicellular model system, and adds to the power of investigation in the worm.

The growth of *C. elegans* can be continued in liquid culture (Lewis 1995). Flasks containing basic nutrients allow the worms to grow in aerated liquid, and this is especially useful for cultivating even greater quantities of worms for biochemical analysis, for

instance, although the animals appear starved and their behaviour may not be equivalent to animals grown on solid plates.

The small size of *C. elegans* also lends itself to investigation using microfluidic devices (Chung, Crane et al. 2008). This rapidly growing field involves manipulating the worm using tiny quantities of liquid contained within channels created typically in PDMS. Worms tend to move in a 2-dimensional plane of liquid on the surface of an agar plate, and seem to suffer no ill effects when moving in a similar plane of liquid under microfluidic conditions. They can be manipulated and handled using liquid flow, offering the opportunity for mass handling of individual animals in an automated or semi-automated fashion. This has been applied to high-throughput genetic screening (Crane, Chung et al. 2009), and on-chip laser microsurgery (Chung and Lu 2009).

Other devices challenge the worms to move through 'artificial soil' (Lockery, Lawton et al. 2008), or to navigate mazes (Qin and Wheeler 2007). Interacting with the worm on its own scale opens up many new possibilities for experiments.

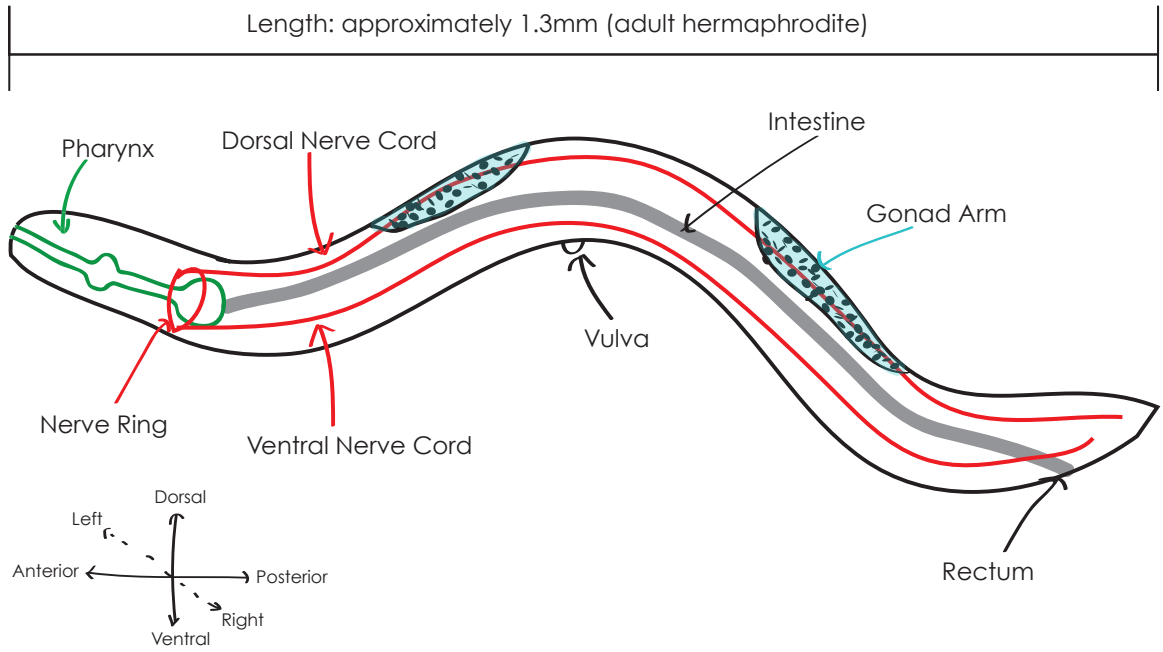

Figure 1-1 Schematic of a nematode worm

C. elegans is a self-fertilising hermaphrodite which grows to a length of approximately 1.3 mm as an adult. Food is ingested through the pharynx, a large muscular organ which grinds up bacteria, passing it through to the intestine for digestion. Dorsal and ventral nerve cords contain neurons which synapse onto the body wall muscles for the production of locomotion, while the nerve ring in the head is the site of synapses between neurons responsible for controlling behaviour.

1.1.3 - *C. elegans* is transparent, allowing detailed visual characterisation

The importance of *C. elegans* being transparent can hardly be overstated. Cells within the organism can be observed directly, including neurons. Transparency allows a number of phenotypic observations to be made with the aid of nothing more than a standard bench microscope. For instance, the pharangyl muscle contains a grinding component which breaks up bacteria for easier digestion in the intestine. This grinder pumps with a regular rhythm and is clearly visible in the head of the worm (Raizen, Lee et al. 1995); measuring the rate of grinding gives an indication of the satiety state of the organism, as well as being a useful diagnostic tool for certain mutants (Brundage, Avery et al. 1996). Similarly, the defecation cycle, in which the intestine contracts and expels waste can be clearly observed within the live worm (Avery 1997). This cycle operates on a regular timescale of around 55 seconds in a wild-type animal and is governed by known pathways, again making it an excellent diagnostic of pathways regulating rhythmic behaviours.

The transparency of the worm also allowed observation of the cell lineage to be conducted in live animals (Sulston and Horvitz 1977; Horvitz and Sulston 1980), and other features, such as the number of eggs contained within the organism can clearly be counted.

The transparency of the worm has become vital over the last 20 years since the development of green fluorescent protein and its derivatives (Chalfie, Tu et al. 1994). These proteins have transformed biology, and are ubiquitous in *C. elegans* experiments.

The list of experiments using this technology is too great to cover, but some of the aspects of cell and particularly neurobiology which have been investigated include: using tagged proteins or promoter-GFP constructs to assess the expression patterns of neurobiological proteins (McKay, Johnsen et al. 2003); tagged neuropeptides acting as reporters of secretion (Sieburth, Madison et al. 2007); tagged UNC-13 acting as a reporter of DAG levels at the presynaptic membrane (Nurrish, Ségalat et al. 1999); reconstitution of GFP across synapses to define partner cells (Feinberg, Vanhoven et al. 2008); and live reporting of the activity of neurons by using the calcium-sensitive GFP reporter cameleon (Suzuki, Kerr et al. 2003).

1.1.4 - Transformation of *C. elegans* allows the generation of genetically modified organisms

The introduction of exogenous genetic material into *C. elegans* is made possible by the way the worm processes DNA and by the presence of a syncitia of nuclei in the gonad. Direct injection of DNA into the gonad (Figure 1-1) allows, at low frequency, incorporation

of that DNA into the developing egg. In some cases this DNA is maintained as a large extrachromosomoal complex, and this can even be heritable, allowing the production of stable, transformed lines (Mello and Fire 1995).

These constructs can be integrated into the genome by the introduction of double stranded breaks by UV irradiation, after which (also at low frequency) the extrachromosomal arrays can be incorporated into the DNA of the animal. If this occurs in cells of the germline it is possible to create integrated lines (Mello, 1995).

Alternative methods for the introduction of exogenous genetic material include the use of the gene gun and, more recently, targetted introduction of DNA at specific sites in the genome using the Mos transposase (Frokjaer-Jensen, Davis et al. 2008).

1.1.5 - The genome of *C. elegans* has been fully sequenced

Ever since those original screens for mutants conducted by Sydney Brenner, the aim has been to achieve an understanding of the biology of *C. elegans* by using genetic methods. The initial approach of mutational screening combined with forward genetics and mapping is still in use today, while additional tools provide even greater advantages. The most significant of these is the complete genome sequence of *C. elegans*, obtained in 1998 (Consortium 1998). This information is accessible online, and has been used to search for orhtologues of genes in other species, as well as providing detailed information for producing gene models and rescuing constructs, and for quickly analysing sequencing data of mutant animals. This genome has been joined by sequences for four other *Caenorhabditis* species: *C. briggsae* (Gupta and Sternberg 2003), *C. remanei*, *C. brenneri* and *C. japonica*; as well as data for a number of other nematode species, all of which can be accessed online at Wormbase.org (Harris, Antoshechkin et al. 2010).

This data has been combined with the latest high-throughput sequencing machines to achieve high-resolution sequencing of individual genomes (Sarin, Prabhu et al. 2008; Shen, Sarin et al. 2008). While the original genome sequence was achieved through sequencing of thousands of large, overlapping DNA pieces, further sequence of mutant genomes can be achieved by mapping short reads back onto the original sequence and observing discrepancies.

The usefulness of the whole genome sequence is complemented by two techniques for reverse genetic analysis of *C. elegans*. Gene knockouts are currently obtained through random mutagenesis using mutagens such as UV irradiation or trimethylpsoralen (TMP) which are able to induce large deletions in the genome, and then sequencing is used to look for deletions in particular genes of interest (Jansen, Hazendonk et al. 1997; Liu,

Spoerke et al. 1999; Edgley, D'Souza et al. 2002). Large libraries containing around a million mutants can be screened for deletions in genes of interest, or individual labs can make use of the services of two gene knockout consortia at http://celeganskoconsortium.omrf.org or http://shigen.lab.nig.ac.jp/c.elegans/index.jsp rather than producing libraries of their own.

The alternative method for gene knockout is the use of RNA interference (Fire, Xu et al. 1998; Tabara, Grishok et al. 1998; Timmons, Court et al. 2001). It has been used to screen large libraries containing dsRNA against the majority of genes in the genome (Fraser, Kamath et al. 2000; Kamath, Fraser et al. 2003), and more recently to screen for mutants in the nervous system (Sieburth, Ch'ng et al. 2005).

1.2 - The nervous system of *C. elegans*

The basic unit of the nervous system is the neuron, which consists of a cell body, containing the nucleus, a long projection called an axon, and dendrites, which receive information from signalling cells (Figure 1-2). Neurons can have multiple projections for both axons and dendrites, and each dendrite can receive multiple signals, allowing a single cell to complex with potentially thousands of others. In large animals, axons can span an incredible range of distances, from less than 1mm to over a metre in length. The transmission of information along a single neuron, and communication between neurons, requires a large number of specific protein components and specialised membrane domains.

It had been shown by Luigi Galvani (1737-98) as long ago as the 18th century that there was a connection between living tissue and electricity, and early models of neuronal function saw them as wires connecting an electrical circuit. Ramón y Cajal (1852-1934) was the first to identify that, at the point of contact between cells in the nervous system, there was no direct contact, but instead there existed a gap between the cells - the synapse. This was a blow to the prevailing electrical theories of brain activity, as electrical circuits by their very nature do not contain gaps. It was left to Otto Loewi (1873-1961) to discover that neurons communicate with one another through the release of chemicals we now know as neurotransmitters. These chemicals are released from the presynaptic cell and bind to receptors on the post-synaptic cell. Synapses are defined by the presence of vesicles, which store neurotransmitter. The postsynaptic side is defined by the presence of the postsynaptic density, which includes the receptors which recognise neurotransmitter released by the presynaptic cell.

Neurons do utilise electrical signalling to transmit information along their length, and this electrical signal is converted to a chemical signal at the synapse. The transmission of a signal along the axon of a neuron requires manipulation of the electrochemical potential of the cell.

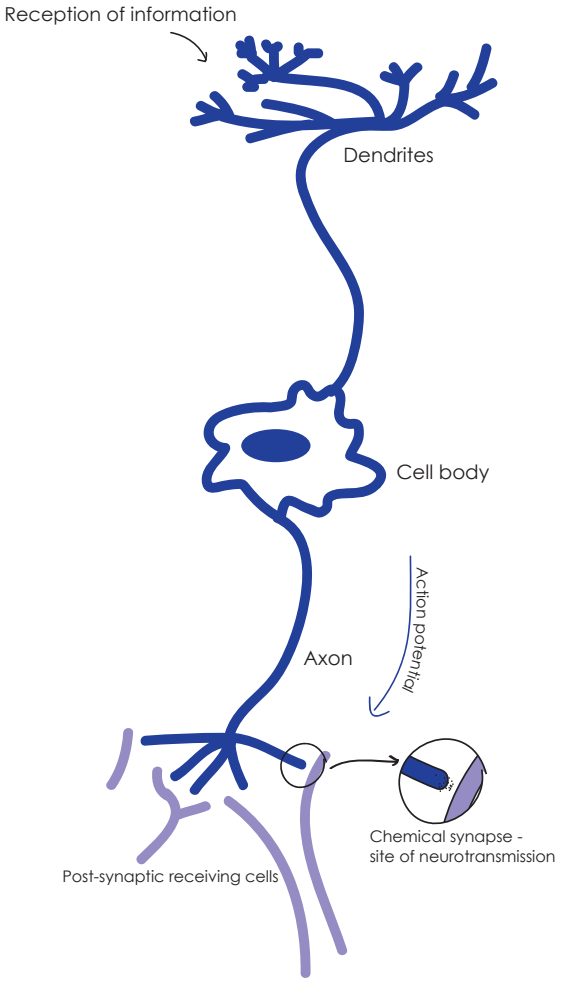

Figure 1-2 Schematic of a neuron

Neurons are cells specially adapted for the reception, processing and transmission of information. In a typical neuron, inputs are received at the dendrites, processed and transmitted along the axon to the pre-synaptic terminus, from where neurotransmitter can be released to signal to further cells.

The interior of a typical mammalian neuron is negatively charged compared with the extracellular medium, at approximately -70mV (Alberts, 2008) (although this varies significantly between cell types). The sodium potassium ATPase uses the energy from ATP hydrolysis to export three sodium ions out of the neuron while moving two potassium ions into the cell. This helps maintain the interior of the cell as negatively charged compared with the outside, and ensures a higher external concentration of sodium (Alberts, 2008).

Excitatory neurotransmitters activate receptors which can act as ion channels at postsynaptic sites. Upon reception of these neurotransmitters, these channels are opened, allowing an influx of positively charged ions, mainly sodium and calcium. This causes a local depolarisation of the membrane which triggers the opening of voltage-gated sodium channels. A rapid influx of sodium ions occurs, further depolarising the membrane. This depolarisation of a small patch of membrane is sufficient to activate voltage-gated sodium channels in neighbouring membrane regions and a wave of depolarisation spreads along the membrane of the cell. The depolarisation is terminated by the inactivation of the voltage-gated sodium channels, preventing the influx of further sodium ions, and by the opening of voltage-gated potassium channels, which allow the rapid efflux of stored potassium, rebalancing the membrane potential (Alberts, 2008).

This process generates an action potential, an 'all-or-nothing' response with a stereotypical waveform which is independent of the amplitude and waveform of the initial depolarisation (Figure 1-3). The rate of stimulation, and hence the rate of propagation of action potentials, is a key mechanism by which information is transmitted in neural networks. For instance, fast trains of action potentials in a presynaptic cell are associated with the establishment of long term potentiation (LTP) in the postsynaptic cells, particularly in the hippocampus, a region associated with learning and memory. Following the induction of LTP, a subsequent single action potential in the presynaptic cell is more likely to induce firing in the postsynaptic cell (Bliss and Gardner-Medwin 1973). Alternatively, low frequency trains of presynaptic firing can induce long term depression (LTD), where the postsynaptic cell becomes more resistant to subsequent activation.

In *C. elegans*, there is an ongoing debate about the nature of neurotransmission. While the *C. elegans* genome encodes a large and varied population of potassium channels and voltage-gated calcium channels, no voltage gated sodium channels have so far been uncovered. It is likely that the small size of neurons in *C. elegans*, along with their high resistance, allows propagation of membrane depolarisation without the requirement for voltage-gated sodium channels, in a graded response (Goodman, Hall et al. 1998) (Figure 1-3). The waveform and amplitude of graded potentials is directly coupled to that of the stimulus received by the cell. In addition, the novel ion channels NCA-1 and NCA-2, which are related to voltage-gated sodium channels but not voltage regulated, are thought to allow a leak of sodium ion into neurons which helps bring the resting potential closer to that required for excitation (Yeh, Ng et al, 2008).

There have been reports of action potentials in some *C. elegans* neurons (Mellem, Brockie et al. 2008), although these may more accurately be described as plateau potentials, in

which neurons have two equally stable membrane potentials, (in this case at -70mV and -35mV), between which they can switch in response to depolarisation (Lockery and Goodman 2009).

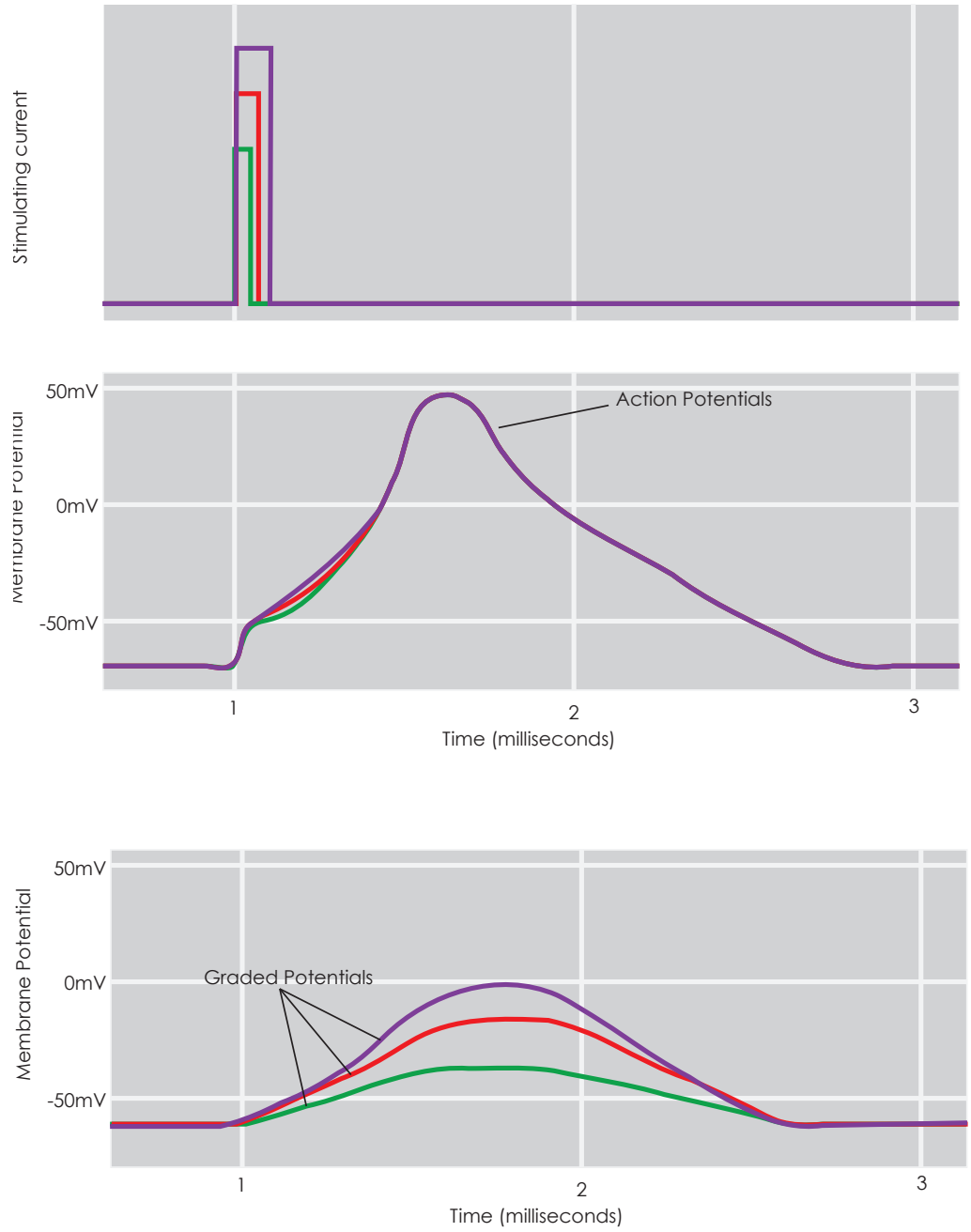

Figure 1-3 Action potentials and graded potentials

Action potentials are self-terminating, all-or-nothing potentials with a stereotyped waveform. So long as the initial depolarisation is above a pre-determined threshold, the response curve in the stimulated neuron is identical regardless of the strength of the stimulus (middle panel). This kind of response has not been observed in *C. elegans* neurons, although some have been reported to have bistable waveforms (Mellem, Brockie et al 2008). A more typical profile of the response of a C. elegans neuron is a graded response (bottom panel), where the waveform of the response is directly linked to the strength of the depolarising current. Adapted from Alberts 2008.

How these types of potential encode information is less well understood than for action potentials, but their presence in a wide variety of cell types hints at a complex 'code' of neuronal activity (Lockery and Goodman 2009).

Propagation of an action or graded potential to the synapse activates voltage-gated calcium channels and an influx of calcium ions, triggering exocytosis of synaptic vesicles and the release of neurotransmitter, which can signal to additional neurons. In this way, cells can form complex process networks of activation and inhibition, as well as rapidly communicating information over great distances. As predicted by Donald Hebb (Hebb 1949), neurons which are in proximity to each other in networks become 'wired together' by repeated stimulation, as demonstrated by phenomena such as LTP. Neurons in these networks have an intrinsic plasticity, allowing them to respond to these changes over time, which likely underpins learning and memory. One of the challenges of neuroscience is to find ways to investigate the function of neuronal networks in culture systems and in whole organisms.

1.2.1 - Reconstruction of the nervous system of *C. elegans*

C. elegans has an invariant somatic cell lineage, as demonstrated by John Sulston who showed by careful analysis of the worm using DIC microscopy that essentially every cell division occurs in the same order in every individual (Sulston, Schierenberg et al. 1983). This provides a highly useful tool for probing a wide range of biological questions. It allows a researcher to identify cells by their appearance and type, and using modern laser technology, to specifically ablate and kill specific cells during experiments (Sulston and Horvitz 1977; Sulston and White 1980; Kimble 1981). This form of development reduces the variation between individuals; in all other model organisms even genetically identical animals have differences in the number of neurons in their nervous system.

John White performed serial section electron microscopy reconstructions of the worm nervous system (White 1986). This identified 302 neurons in the adult hermaphrodite, which can be classified into 118 groups defined by their structure. The neurons in *C. elegans* generally have a simple structure, with few branches, and form approximately 5000 chemical synapses, 2000 neuromuscular junctions and 600 electrical synapses, or gap junctions in the adult hermaphrodite. Definition of synapses is by proximity, as the post-synaptic side of worm synapses generally lack the post-synaptic density seen in other organisms. While individual synapses may form differently from animal to animal, the overall structure of the nervous system is consistent.

More recent work suggests that the arrangement of the nervous system follows an optimised pattern, reducing the energetic costs of wiring the neurons together, while maintaining functionality (Chen, Hall et al. 2006).

1.2.2 - Chemical synapses in C. elegans contain two classes of vesicle

Chemical synapses define the connection between neurons, while neuromuscular junctions (NMJ) are the interface between a muscle cell and a neuron. These tend to operate in a one-to-one fashion, with each muscle cell receiving input from just one neuron. As the contraction of striated muscle is important for quick responses in organisms, the rate of action at the NMJ is required to be extremely fast. The distance between cell and muscle is between 20-30nm, meaning a diffusion time of around 100µs. The *C. elegans* neuromuscular junction is a key target of the research in this thesis. Neuromuscular junctions, like other synapses in *C. elegans,* are *en passant*, i.e. the axon runs parallel to the body wall muscles from which projections emerge to synapse onto the neuron (White 1986). Unlike NMJs in mammalian systems, which demonstrate 'all-or-nothing' action potentials, control of the C. elegans NMJ occurs through a graded response, more like that found in sensory neurons or in the mammalian central nervous system (Liu, Hollopeter et al. 2009).

Both neuromuscular junctions and chemical synapses are defined by the presence of vesicles, containing neurotransmitter ready for release and signalling to the postsynaptic cell. Two types of vesicle are observed in electron micrograph images of *C. elegans* synapses (Figure 1-4).

1.2.3 - Small synaptic vesicles

The first are small, clear vesicles of between 35–45 nm in diameter (Takamori, Holt et al. 2006), and many of these are packaged with small molecule neurotransmitters (Figure 1-4). These vesicles bear resemblance to those found in endocrine cells, although unlike in endocrine cells the vesicles are produced in the Golgi and mature as they travel to the synapse. Once in place and fully matured the vesicle can be emptied, recycled, refilled and readied for release again (Sudhof 2004). This is a highly specialised and efficient version of the endo- and exocytosis cycles seen in trafficking in many other cell types, specially adapted for neuronal signalling. It allows neuronal signalling to be sustained for long periods of time, long after an initial pool of filled vesicles produced in a more conventional fashion would have been depleted.

Vesicles were first isolated from cells using sucrose gradients to separate out structures based on their density, followed by filtering with controlled pore glass beads to separate out structures based on size. This allowed pure preparation of synaptic vesicles leading to analysis of their composition and the raising of antibodies against protein targets. It was found that many of these antibodies cross reacted with proteins from other species.

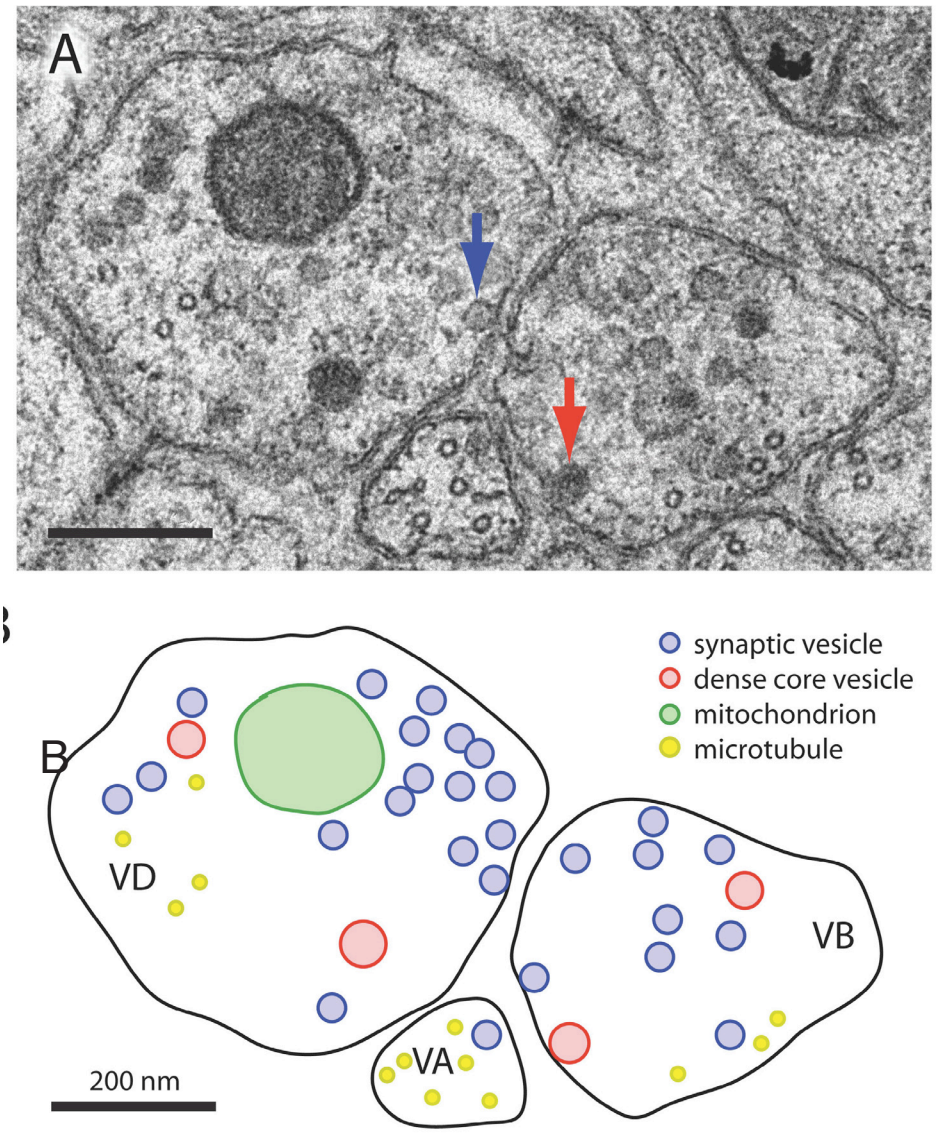

Figure 1-4 Synapses contain synaptic vesicles and dense core vesicles

Shown is a cross section through the ventral nerve cord of *C. elegans,* bisecting three neurons - VA, VB and VD. Shown below is a schematic illustrating some of the components observed in the electron micrograph - including small synaptic vesicles (blue circles) and larger, dense core vesicles (red circles). The blue arrow indicates a docked small synaptic vesicle, while the red arrow points to a docked dense core vesicle.
Taken from Hammarlund, Watanabe et al. 2008. Scale bar indicates 200 nm.

This demonstrated the conservation of structures between organisms, reinforcing the utility of genetic model organisms in neurobiology, such as that of mammalian synaptobrevin, which was found to be orthologous to the vesicle-associated membrane protein (VAMP) isolated from the electric organ of the Torpedo fish, and subsequently identified in fruit flies (Trimble, Cowan et al. 1988).

Recent mass spectrometry analysis of purified vesicles demonstrates that they contain a vast array of proteins, many present in multiple copies. Including the clathrin coat, involved in recycling, synaptic vesicles have been isolated containing over 400 distinct proteins, while a single vesicle may contain over 200 proteins in its vesicle membrane (Takamori, Holt et al. 2006). Many of these are involved in the trafficking of the vesicle, filling with neurotransmitter, or are other components of the presynaptic membrane, such as ion channels, which may be transitory 'visitors' to the synaptic vesicles themselves, incidentally incorporated into the vesicle membrane following endocytosis. The protein to lipid ratio is so high that each protein may be surrounded by only a few lipid molecules, or proteins may cluster into protein-rich domains on the vesicle membrane (Takamori, Holt et al. 2006).

1.2.4 - Dense core vesicles

The second class of vesicles observed are larger, dense-core vesicles (LDCV) range from 40–53nm, and as their name suggests appear electron-dense in EM micrographs (Figure 1-4). Unlike small synaptic vesicles, they do not cluster at defined pre-synaptic release sites, and do not recycle at the synapse. They contain larger neurotransmitter molecules, neuropeptides, synthesised in the endoplasmic reticulum, and catecholamine neurotransmitters such as dopamine and serotonin. Neuropeptides are large signalling molecules and can diffuse over long distances, ultimately binding to target receptors on neuronal and non-neuronal cells (Nassel 2002, Li 2008).

1.2.5 - Electrical synapses in C. elegans

A third class of synapse is present in the nervous system of *C. elegans*, which lacks these neurotransmitter filled vesicles. These are GAP junctions, and they comprise direct electrical linkages between cells. They allow the passage of small molecules, generally estimated at less than 1 kD in size (Flagg-Newton, Simpson et al. 1979) and 1.5nm in radius (Lo and Gilula 1979) although this varies depending on the composition of the channel and the charge on the molecules.

Molecules such as inorganic ions, cyclic AMP and inositol 1,4,5 trisphosphate (IP_3) have been shown to move through these channels (Kumar and Gilula 1996) directly coupling

the electrical potentials of linked cells. There are an estimated 600 gap junctions in the *C. elegans* nervous system (White 1986) comprising some 10% of connections in the nervous system, although their biological significance is not well understood.

GAP junctions in mammalian systems are composed of hemichannels formed of 6 subunits of connexin proteins, while innexins, a related protein family, are the structural components of GAP junctions in invertebrates (Phelan, Bacon et al. 1998; Phelan and Starich 2001). *unc-7* and *unc-9* encode innexins in *C. elegans*; they, along with *unc-1*, which encodes a stomatin which regulates GAP junction activity (Chen, Liu et al. 2007), have been implicated in the action of volatile anaesthetic compounds on the worm (Morgan, Sedensky et al. 1990), which cause a number of phenotypes including immobility. Mutations in *unc-1*, *unc-7* and *unc-9* cause uncoordinated phenotypes, indicating that GAP junctions are important for locomotion in *C. elegans* (Chen, Liu et al. 2007; Starich, Xu et al. 2009).

1.2.6 - Neurotransmitters in *C. elegans*

While direct electrical couplings between cells exist in the form of GAP junctions, the classical synapse has been the focus of most neuroscience work. Neurotransmitters released from either small synaptic vesicles or dense core vesicles bridge the physical gap between neurons, converting an electrical signal into a chemical signal. Neurotransmitters can be classified by their effects on a target cell, being either excitatory and depolarising the target, or inhibitory and hyperpolarising the target. Some, such as acetylcholine, can be excitatory or inhibitory, depending on the receptors activated. In chemical terms, we can distinguish between small molecule neurotransmitters, which includes amino acids such as glutamate, modified amino acids such as dopamine, or larger peptides which typically interact with G-protein coupled receptors, although all three neurotransmitter classes can interact with GPCRs. Each class has its own mechanisms of production; for instance neuropeptides can be regulated at the transcriptional and translational levels, while the use of amino acids for neurotransmission is linked their roles in metabolism.

1.2.6.1 - Acetylcholine

Acetylcholine is the major excitatory neurotransmitter at the human and worm neuromuscular junction, acting through the nicotinic acetylcholine receptor to stimulate muscle contraction (Rand 2007). Acetylcholine is synthesised from acetyl-CoA and choline by choline acetyltransferase, encoded by *cha-1* (Rand and Russell 1985, Figure 1-5), which generates a protein similar to that found in Drosophia and mice (Rand and Russell 1985). It is subsequently loaded into synaptic vesicles by the vesicular

acetylcholine transporter, encoded by *unc-17* (Alfonso, Grundahl et al. 1993, Figure 1-5). Once released into the synapse, acetylcholine is broken down by acetylcholine esterases which help terminate signalling. Four genes encode acetylcholine esterases in C. elegans - *ace-1*, *ace-2*, *ace-3* and *ace-4* (Combes, Fedon et al. 2000)- and a triple mutant *ace-1;ace-2;ace-3* is embryonic lethal (Johnson, Rand et al. 1988) although this mutant may actually also contain a mutation in the *ace-4* locus, making it a quadruple mutant (Combes, Fedon et al. 2000). *ace-2* is the dominant neuronal acetylcholine esterase, while *ace-1* is expressed mainly in muscle cells (Combes, Fedon et al. 2003).

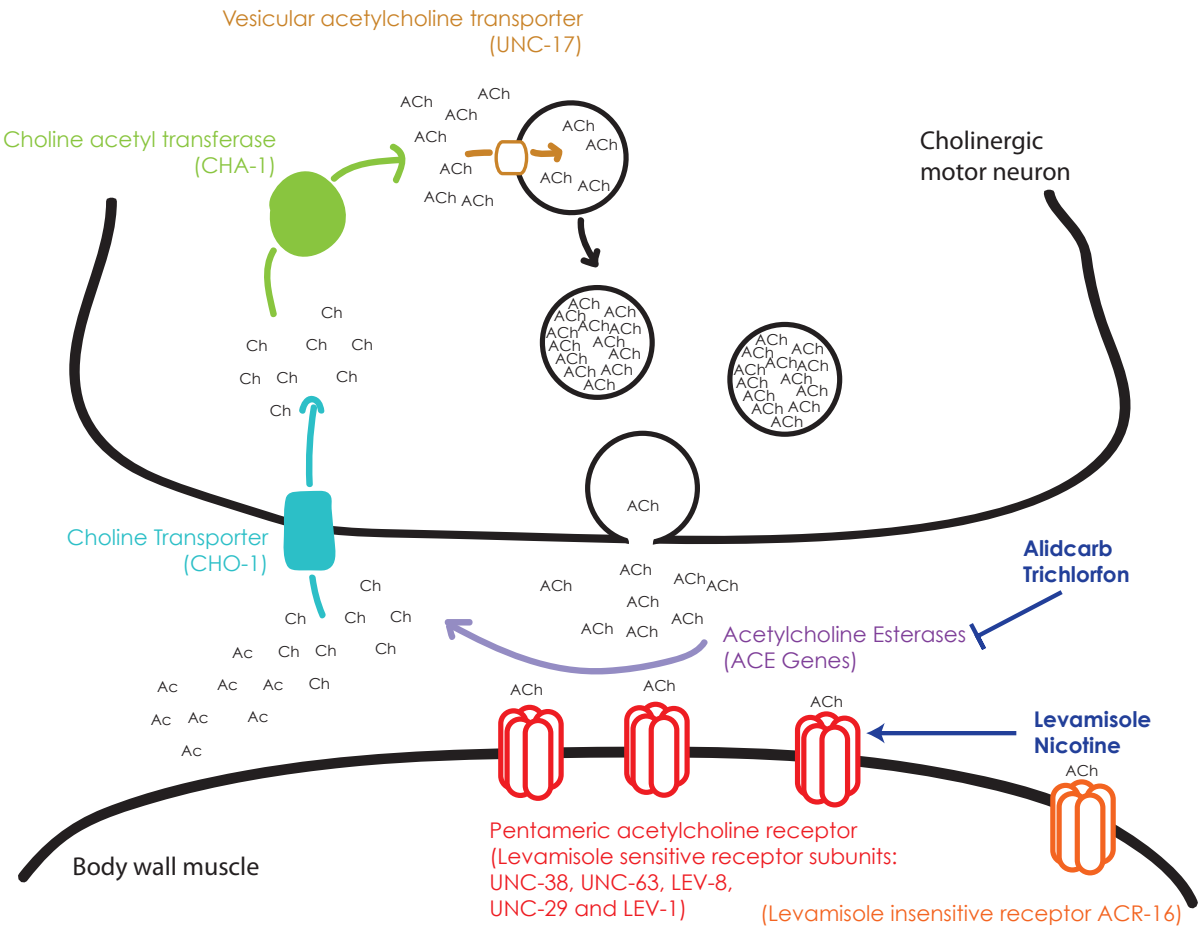

Figure 1-5 Acetylcholine signalling at the *C. elegans* NMJ

Acetycholine was the first chemical established as a neurotransmitter. It is the major excitatory neurotransmitter at the *C. elegans* NMJ, where it is released from small synaptic vesicles to stimulate receptors on the body wall muscles. In this figure, the levamisole-sensitive receptor is depicted. Acetylcholine esterases break down acetylcholine, terminating signalling, while the choline transporter, choline acetyltransferase and vesicular acetylcholine transporter combine to produce new acetylcholine molecules for loading into synaptic vesicles. Acetylcholine signaling can be peturbed by a number of a pharmacological agents, including aldicarb and trichlorfon, which inhibit acetylcholine esterases, and levamisole and nicotine which directly stimulate different populations of acetylcholine receptors. These drugs can be used to dissect pre- and post-synaptic changes in acetylcholine signalling. Adapted from Rand 2007.

While screening for neurobiological mutants, Brenner used lannate, an inhibitor of acetylcholine esterases, along with tetramisole (also known as levamisole), an acetylcholine agonist to identify mutants (Brenner 1974, Figure 1-5). Excess exposure to either chemical overstimulates acetylcholine signalling, hypercontracting the body wall muscles, and this leads to paralysis and eventually death of the animals through suppression of pumping of the pharynx. Trichlorfon has also been used as an acetylcholinesterase inhibitor, but aldicarb is the more commonly used drug to inhibit the breakdown of acetylcholine (Figure 1-5).

While having similar effects on the treated worms, levamisole and aldicarb have rather different mechanisms of action which are useful for identifying different kinds of mutants. Together, levamisole and aldicarb can be used to dissect mutants which otherwise have a similar phenotype, and provide a way of probing whether mutations act pre- or post-synaptically.

Aldicarb treatment enhances endogenous signalling, and screens have been conducted for mutants which are resistant to aldicarb (*ric*). This screening can identify mutants in which the either the reception of the acetylcholine signal has been lost, or where the production or release of acetylcholine is inhibited (Nguyen, Alfonso et al. 1995). *ric* screens use either a chronic form of acetlycholine treatment, where growth and development occur at concentrations of aldicarb which would inhibit growth in wild-type animals (Nguyen, Alfonso et al. 1995); an alternative is to use an acute assay, with high concentrations of aldicarb for short (typically 1-2 hour) exposure times (Lackner, Nurrish et al. 1999; Nurrish, Ségalat et al. 1999). The response of animals to aldicarb correlates with the level of acetylcholine release at the neuromuscular junction (Nurrish, Ségalat et al. 1999), allowing classfication of acetylcholine signalling in mutant animals.

ric screens identified general components of the release machinery, such as synaptotagmin (*snt-1*) (Nguyen, Alfonso et al. 1995) and synaptobrevin (*snb-1*) (Nonet, Saifee et al. 1998), the production of acetylcholine (*cha-1*) and its transort into vesicles (*unc-17*) (Nguyen, Alfonso et al. 1995), along with many other previously unclassified mutations, including mutations in G-protein coupled receptors (Miller, Alfonso et al. 1996). Many proteins involved in acetylcholine signalling have also been identified through screening for mutants in acetylcholine-regulated behaviours, such as egg-laying (*egl-30*) and locomotion (*unc-13*).

More recent forward genetic screens for *ric* mutants have been used to identify components of neurotransmitter release and signalling in the *C. elegans* nervous system (Sieburth, Ch'ng et al. 2005). These screens are still identifying new mutants

which suggests that these screens are not saturated, despite many repeated rounds of screening.

Treatment with levamisole has led to the identification of levamisole insensitive (*lev*) mutants; these represent mutations in the reception and processing of acetylcholine signalling. For instance, the first levamisole insensitive mutant, *lev-1*, has been shown to encode a component of the acetylcholine receptor in the body wall muscles of *C. elegans* (Fleming, Squire et al. 1997). The nicotinic acetylcholine receptors are pentameric, ligand-gated ion channels (Unwin 2005), and one of the two nicotinic acetylcholine receptors in the body wall muscles is sensitive to levamisole and a number of its constitutent parts were identified through levamisole screening (Lewis, Wu et al. 1980). The receptor is composed of five subunits - UNC-29, UNC-38 and UNC-63, along with the non-essential LEV-1 and LEV-8 subunits (Fleming, Squire et al. 1997; Richmond and Jorgensen 1999; Culetto, Baylis et al. 2004). The levamisole-insensitive receptor includes ACR-16, thought to form a homo-pentameric receptor, but other components of the structure are unknown (Touroutine, Fox et al. 2005); loss of both classes of receptor ablates acetylcholine signalling at the neuromuscular junction (Touroutine, Fox et al. 2005). A great variety of other genes encode protein associated with nicotinic acetylcholine receptors in *C. elegans* (Gottschalk, Almedom et al. 2005), which act in the trafficking and stability, or modulation of the activity of the levamisole receptor, both in the muscles and when expressed in neurons.

Acetylcholine also signals through two other classes of receptor, although their functional significance is less well understood. G-protein coupled receptors, similar to the muscarinic acetylcholine receptor found in vertebrates, are encoded by *gar-1* (Park, Lee et al. 2000), *gar-2* (Lee, Park et al. 2000, Dittman and Kaplan 2008) and *gar-3* (Park, Kim et al. 2003), all of which undergo alternative splicing, creating a great diversity of protein products. *C. elegans* also posesses a novel class of acetylcholine-gated chloride channels (Putrenko, Zakikhani et al. 2005); these do not have a mammalian homologue.

1.2.6.2 - Monoamines

Four monoamine neurotransmitters are present in *C. elegans*: serotonin and octopamine (Horvitz, Chalfie et al. 1982), dopamine (Sulston, Dew et al. 1975) and tyromine (Alkema, Hunter-Ensor et al. 2005); octopamine and tyromine are nematode-specific, while the others are found in mammalian systems.

These neurotransmitters act through a large number of receptors, identified by homology to mammalian receptors or through screens for mutants (Schafer, du Bois et al. 1996, Chase 2007).

Mutants display a wide range of phenotypes, ranging from egg-laying defects, misregulation of locomotion responses such as slowing in presence of food, changes in pumping, and modulation of learning and memory-associated behaviours, which will be explored later in the introduction.

1.2.6.3 - Glutamate

C. elegans also makes use of glutamate, which in mammalian systems carries much of the fast synaptic transmission between cells (Brockie 2006). In *C. elegans*, ten ionotropic glutamate receptors subunits have been identified (Brockie and Maricq 2003). *C. elegans* has both N-methyl-D-aspartate (NMDA) and non-NMDA receptors, which are similar to the AMPA receptors found in mammalian systems. These allow for exitatory signalling, while a third class of glutamate receptors, which allow the influx of chloride ions and are sensitive to the drug invermectin, mediate inhibitory signalling (Yates, Portillo et al. 2003).

1.2.6.4 - GABA

GABA is the major inhibitory neurotransmitter in *C. elegans*, and is used to control relaxation of body wall muscles during locomotion. While one side of the body is stimulated to contract by the action of acetylcholine, the opposite side relaxes due to the action of GABA on GABA A receptors, which encode GABA-gated chloride channels (Schofield, Darlison et al. 1987). A second class of GABA receptor, GABA B receptors, are 7-pass transmembrane proteins, which act through trimeric G-proteins to either activate potassium channels or inhibit voltage-gated calcium channels; both lead to an inhibition of the target neuron. Loss of GABA signalling has less impact on locomotion than loss acetylcholine signalling, with the main locomotive phenotype in GABA mutants being defects in switching to backwards locomotion, as the animals exhibit a ‘shrinker’ phenotype (McIntire , Jorgensen et al, 1993).

Interestingly, during defecation, GABA also controls an excitatory transmission event (Jorgensen 2005; Brockie 2006), highly unusual for an adult organism, although an important part of GABA signalling during mammalian development (Ben-Ari 2002).

1.2.6.5 - Neuropeptides

Neuropeptides are formed from large precursor molecules, processed into smaller signalling molecules by a variety of enzymes, including EGL-3 (Kass, Jacob et al. 2001) which is expressed throughout the nervous system. The *egl-3* mutants display defects in locomotion, egg-laying and mechanosensation. After processing, the basic residues at which cleavage occurs are removed from the peptide sequences by the activity of carboxypeptidase E, encoded by *egl-21*. Loss of *egl-21* causes severe phenotypes in egg laying, locomotion, mechanosensation, and defecation (Jacob and Kaplan 2003). As assayed by mass spectrometry, both *egl-3* and *egl-21* mutants have lost the majority of processed neuropeptides (Husson, Clynen et al. 2006; Husson, Janssen et al. 2007).

Neuropeptides are packaged into large dense core vesicles (DCVs), and some elements in the release of small synaptic vesicles and dense core vesicle are the same, including a possible requirement for UNC-13 in DCV exocytosis (Richmond, Davis et al. 1999; Sieburth, Madison et al. 2007), although this is debated (Hammarlund, Watanabe et al. 2008).

There is a requirement for calcium-dependent activator protein (CAPS) for release of DCV. UNC-31, the *C. elegans* CAPS homologue, is required for the release of neuropeptides (Speese, Petrie et al. 2007; Zhou, Dong et al. 2007), and requires PKC-1 activity (Sieburth, Madison et al. 2007). *unc-31* mutants are lethargic, but display either some (Miller, Alfonso et al. 1996) or no resistance to aldicarb (Charlie, Schade et al. 2006), and has little or no role in the release of neurotransmitter from small synaptic vesicles (Speese, Petrie et al. 2007). There are situations in which the requirement for *unc-31* can be bypassed, such as by increasing the activity of PKA (Zhou, Dong et al. 2007).

pkc-1 mutants are also resistant to aldicarb, but do not demonstrate any defects in release of acetylcholine from small synaptic vesicles as measured using electrophysiology (Sieburth, Madison et al. 2007). They are, however, defective in dense core vesicle exocytosis as measured by the release of a fluorescently-tagged NLP-21::YFP fusion protein (Sieburth, Madison et al. 2007).

These results indicate that the release of neuropeptides can be used by the worm's nervous system to alter locomotion rates without directly altering the release of neurotransmitter. Neuropeptides act both by direct signalling to the receiving cell (Nassel 2009), and as neurohormones, affecting many different aspects of behaviour, including foraging, egg-

laying, locomotion, as well as modulating the effects of other neurotransmitters (Li 2008, Nassel 2009).

1.3 - Analysis of behaviours in *C. elegans*

A major advantage of studying neurobiology in a whole organism is that the effects of changes in the nervous system can be observed by looking for changes in the behaviour of the animal. The neurotransmitters listed above have a wide variety of effects on the behaviour of *C. elegans*, and a number of techniques have been developed to qualitatively and quantitatively analyse behaviour in *C. elegans*.

Of particular interest to the focus of this thesis is the locomotive behaviour of the worm. Wild-type animals have a smooth sinusoidal locomotion, travelling predominantly in a forward direction when well fed. Individual animals have stereotyped responses to touch, lack of food, or encountering noxious stimuli, for example; deviations from these can be observed, and mutants identified.

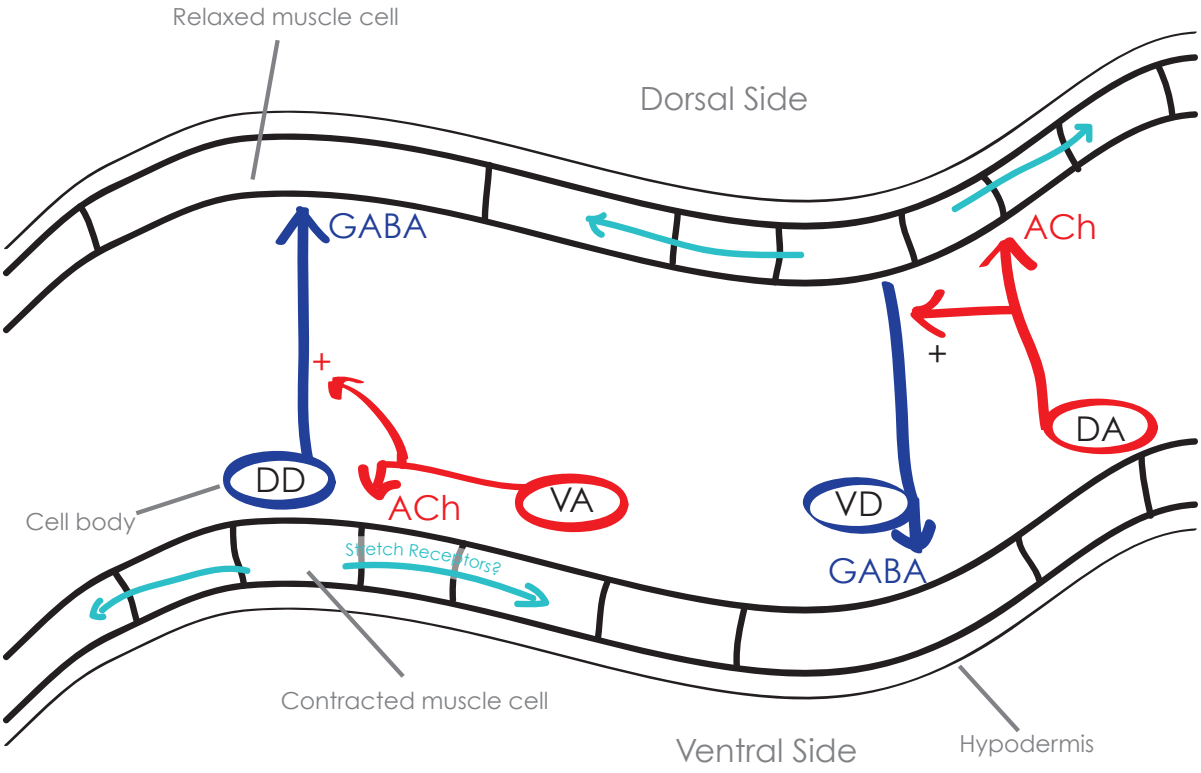

Figure 1-6 Locomotion is mediated by alternate contraction and relaxation of the body wall muscles

Locomotion in C. elegans occurs as a result of contraction of the body wall muscles on one side of the body, due to the release of acetylcholine (ACh), and the relaxation of muscles on the alternate side of the body, due to the release of GABA. The cell bodies of the motor neurons are all found in the ventral side. Some theories predict the existence of stretch receptors (light blue arrows) which coordinate contraction of the body wall muscles along the anterior/posterior axis. (Adapted from Seifert, Schmidt et al. 2006).

Measuring the number of body bends within a defined period of time, the change in the rate of locomotion between travelling on food or off food or total distance travelled in a given time provide metrics of behaviour (Hart 2005). More detailed analysis includes the use of automated tracking devices, where worms are tracked for extended periods of time and algorithms used to extract data relating to their behaviour (Feng, Cronin et al. 2004). Several packages have been developed for this purpose which either analyse individual animals in great detail (Cronin, Feng et al. 2006; Hoshi and Shingai 2006), providing data on the waveforms they produce and the amount of movement of the head relative to the body for instance, while others track multiple worms at low resolution (Ramot, Johnson et al. 2008) to obtain population-level information about the behaviour of animals in response to various stimuli. These approaches offer the possibility of standardising behavioural analysis between labs, and of revealing subtle differences and similarities between phenotypes, allowing greater degrees of classification.

1.3.1 - Locomotion is a complex, regulated behaviour

C. elegans is limited to movement in the dorsal-ventral axis. On an agar plate, the animal effectively lies on its side, with the dorsal-ventral axis perpendicular to the plane of the plate (Figure 1-1). Contractions of the 95 body wall muscles allow the production of sinusoidal waves to pass through the body of the animal, propelling the worm forwards (Seifert, Schmidt et al. 2006).

These body wall muscles are innervated by motor neurons which have their cell bodies in the ventral nerve cord, but which can synapse onto either the dorsal or ventral muscles (Figure 1-6). Three classes of motor neuron coordinate locomotion - class A and B are cholinergic neurons, releasing acetylcholine to stimulate contraction enabling backwards and forwards locomotion respectively, while class D motor neurons release GABA onto the muscles, allowing them to relax (Schuske, Beg et al. 2004). Alternating patterns of contraction and relaxation on opposite sides of the animal set up the typical sinusoidal waveform. Interestingly, animals completely lacking the neurotransmitter GABA are still capable of generating forwards and backwards locomotion; however they do exhibit more subtle locomotion defects including the ‘shrinker’ phenotype, where animals which are touched shorten, as all muscles improperly contract (Schuske, Beg et al. 2004).

Movement of the head of the animal is more complex and can occur in the left-right axis as well, enabling the head to move with a much greater degree of freedom compared to the rest of the body. This may be important for foraging behaviours, allowing the animal to chemotax to distant food sources or avoid noxious substances (Hart 2005).

Locomotion is not limited to movement in the plane of the plate. Animals are capable of climbing behaviours, evidenced by animals 'escaping' from the surface of agar plates onto the plastic sides or lids of their dishes, or climbing chunks of agar deposited on the surface. *C. elegans* also presents an interesting although poorly understood behaviour, known as nictation, where animals climb the stalks of some types of fungi, and project their heads upwards (Schuske, Beg et al. 2004). The reason for this behaviour is not known, nor is it clear that it has any physiological significance, but it is interesting to note that the environment in which we maintain *C. elegans* as a laboratory model is distinct from that which it would encounter in the wild, where the worm must navigate a three-dimensional landscape of solid and semi-solid particles and liquids.

The rate of locomotion is dependent on many factors, one of which is the presence of food. Well-fed and starved animals move at the same rate in the absence of food. When they encounter food, however, they exhibit different responses. Well-fed animals encountering food reduce their rate of locomotion, and this is known as the 'basal slowing response' (Sawin, Ranganathan et al. 2000). This is a mechanosensory response to the physical contact with bacteria and can be replicated by an encounter with small beads which have no nutritional value (Sawin, Ranganathan et al. 2000). This response requires dopamine signalling and can be mimiked by exposure to exogenous dopamine (Sawin, Ranganathan et al. 2000).

Starved animals further reduce their rate of locomotion upon encountering food, in an 'enhanced slowing response' (Sawin, Ranganathan et al. 2000). This is evidence that the animals are able to recall the history of their nutritional status, and use this to modulate their behaviour. This enhanced slowing requires serotonin signalling, as mutants which are defective in serotonin biosynthesis, such as *cat-4*, are unable to perform the enhanced slowing response (Sawin, Ranganathan et al. 2000). This demonstrates a great degree of behavioural plasticity for an organism with such a simple nervous system, and this plasticity is a key feature of other aspects of behaviour as described below.

1.3.2 - Swimming: a distinct form of locomotion, or a modified form of crawling?

C. elegans is also capable of swimming behaviour, also refered to as thrashing. In liquid, worms initiates a series of fast body bends, which occur with a frequency of between 50 and 200 per minute, depending on the age of the animal, taking on a characteristic 'C' shape, as opposed to the 'S' shape observed when crawling on a plate, leading to some to label this as a distinct form of locomotion. Swimming behaviour has been shown to be directional, allowing the worm to respond to and possibly navigate towards food sources

in a liquid environment (Pierce-Shimomura, Chen et al. 2008), a situation that the animal is highly likely to encounter in its native environment (Kiontke 2006).

It is a topic of debate whether swimming behaviour is generated by a distinct motor program, or whether swimming and crawling represent the same behaviour in different mediums (Pierce-Shimomura, Chen et al. 2008; Berri, Boyle et al. 2009). Screens for mutants incapable of swimming behaviour but capable of crawling locomotion have identified distinct a distinct set of genes - *unc-80* and *unc-79* - as more important for swimming than crawling (Pierce-Shimomura, Chen et al. 2008), although these mutants still present a crawling phenotype known as fainting (Pierce-Shimomura, Chen et al. 2008, and see discussion as the end of Chapter 5 for more information).

Other researchers have demonstrated a consistent, gradual change in locomotion when moving between media of different viscosities (Berri, Boyle et al. 2009). This research argues that if the worms are moving through or over a solid or semi-solid medium, the amplitude of body bends decreases and the frequency increases (as viewed across a single worm from head to tail). In liquid, the resistance offered by the medium is greatly decreased, and the frequency decreases while the amplitude increases, giving rise to the 'C' shape, an exagerrated form of the 'S' shape composed of a single body bend. This simpler model suggests that there is a single movement pattern in the worm, and that differences in swimming and crawling are generated by external physical properties but from a single internal pattern (Berri, Boyle et al. 2009).

This integrated model invokes the presence of stretch receptors along the length of the body of the worm which are able to sense curvature and influence the propogation of a wave along the body. It has been proposed that the long extensions of the cholinergic motor neurons act to detect flex in the animal through putatitive stretch receptors (White 1986). This input from the body of the worm itself is referred to as proprioception. While these stretch receptors have not been biologically identified, they are predicted to exist in the majority of computer models of locomotion so far developed (reviewed in Boyle, 2010). A number of mechanosensory components which have an impact on body posture and locomotion have been identified. TRP-4, part of the transient receptor potential channel superfamily, is able to respond to mechanical stresses, and the *trp-4* mutant animals have exagerated body bends with a greater amplitude than wild-type (Li et al., 2006). Rescue experiments demonstrate that is required in the single, long DVA neuron which runs the length of the worm's body, and acts as a stretch receptor (Li et al., 2006). Mutants in *unc-8*, part of DEG/ENaC channel family (which have been identified as mechanosensory components in other systems), also have a locomotive phenotype

of reduced amplitude and wavelength (Tavernarakis, Shreffler et al., 1997). Based on its expression pattern and genetic interaction with mec-6, UNC-8 is predicted to act as a stretch receptor component in *C. elegans* (Tavernarakis, Shreffler et al., 1997).

C. elegans possess a number of mechanosensory neurons which respond to external touch, important for responses when encountering food (Sawin, Ranganathan et al. 2000), as described above. A touch to the head or tail elicits a movement away from the touch. Animals can distinguish between light and harsh touch, and will also change direction in response to a tap on the plate on which they live (Chalfie and Sulston 1981) which produces reversals (Rose and Rankin 2001). This factor can cause problems in the quantification locomotive of behaviours if the plates are not handled gently, although it has also been used to address questions of habituation to touch (Rose and Rankin 2001). Habituation requires the activity of dopamine through the DOP-1 receptor; *dop-1* mutants habituate at a much higher rate than wild-type animals (Sanyal, Wintle et al. 2004).

Touch-insensitive mutants have been isolated, and the circuits for anterior and posterior touch sensitivity have been determined (Chalfie, Sulston et al. 1985) to produce a complex model for the integration of touch responses (Ernstrom and Chalfie 2002). Experiments using genetically encoded calcium sensors have shown that components MEC-4 (a sodium channel) and its associated protein MEC-2 are required within a touch sensitive neuron for the processing of mechanical sensation, but the search for the component(s) which directly senses mechanical force continues (Bounoutas and Chalfie 2007).

1.3.3 - Chemotaxis

C. elegans is able to detect a wide variety of chemical signatures, relating either to food or noxious substances, and a number of assays exist to quantify this behaviour (Ward 1973), which allowed the identification of mutants defective in chemotactic behaviour (Lewis and Hodgkin 1977) and the unravelling of the structures and genetic pathways involved. The mechanisms governing chemosensory behaviour are complex, with cycles of turning behaviour known as pirouettes (Pierce-Shimomura, Morse et al. 1999) allowing animals to change their direction and search along chemotactic gradients.

Worms respond to a variety of stimuli, including high concentrations of salt (Culotti and Russell 1978), and can chemotax to a variety of water-soluble chemicals, including nucleotides and amino acids (Ward 1973), as well as volatile organic compounds (Bargmann, Hartwieg et al. 1993). Individual neurons be assayed using microfluidic chips to expose worms to specific compounds while observing the neuronal activity using

fluorescent reporters of neuronal activity (Chronis, Zimmer et al. 2007). Worms can also adapt their responses based on their environment. 32 neurons in the head of the worm are exposed to the external environment through openings in the cuticle, while in males phasmids in the tail are also contain exposed nerve endings. Laser ablation experiments identified a number of these as responsive to specific volatile organic compounds, such as benzaldehyde (Bargmann, Hartwieg et al. 1993). Brief exposure to any of these compounds is attractive, but longer exposures of up to two hours allow the worms to adapt to the presence of the attractant (Colbert and Bargmann 1995), demonstrating the plasticity of this sensory system, and adaptation-specific mutants have been identified (Colbert and Bargmann 1995).

This response to chemosensory stimuli is modulated by the presence of food; benzaldehyde, for example, is treated as a indicator of the presence of food, making chemotaxis to this chemical worthwhile. If worms are conditioned by exposure to benzaldehyde in the absence of food, the chemical no longer acts as an attractant (Nuttley, Atkinson-Leadbeater et al. 2002). This effect is mimiked by the presence of serotonin, which acts as a signal for the presence of food, and mutants in serotonin signalling are unable to suppress adaptation to benzaldehyde in the presence of food (Nuttley, Atkinson-Leadbeater et al. 2002). This adaptation is also sensitive to the presence of high densities of *C. elegans* population, regulated through sensation of a secreted neuropeptide (Yamada, Hirotsu et al. 2010); together these variations of response indicate something of the sensitivity and processing power produced by such a small nervous system.

1.3.4 - Oxygen, light and temperature sensitivity

Soil temperature can vary by tens of degrees during the course of a day (Kiontke 2006), and temperature changes can have a large effect on growth rate (Byerly, Cassada et al. 1976) and lifespan (Lakowski and Hekimi 1996). *C. elegans* will avoid noxious temperatures outside of a range of 12^{o}C to 25^{o}C. This behaviour is dependent on a number of sensory neurons in the head of the worm; when ablated, the worm no longer tracks temperature (Mori and Ohshima 1995). When grown at temperatures between 16 and 25 degrees in the presence of food, *C. elegans* is able to migrate to its growth temperature when offered a range of temperatures as an adult (Hedgecock and Russell 1975) and track along this gradient (isothermal tracking). The presence of food is important; animals grown at a set temperature in the absence of food will not perform isothermal tracking. This behaviour is remarkably precise, allowing the animals to navigate in a range of ±0.2^{o}C outside of their growth temperature (Hedgecock and

Russell 1975). When transferred to a temperature range in the absence of food, this tracking behaviour is maintained for several hours, after which a searching behaviour is intiated to look for new sources of food (Mori 1999). This again demonstrates the plasticity of behaviour in *C. elegans* - the ability to learn and follow a pattern of behaviour is overruled once that pattern is no longer productive.

C. elegans is sensitive to the concentration of oxygen in the atmosphere, preferring a range between 5-12%, which is thought to be part of a strategy to detect anaerobic environments, such as those generated by the digestion of rotting plant matter by bacteria (de Bono and Bargmann 1998; Gray, Karow et al. 2004),. This aerotaxis behaviour can also be modulated by experience and the presence of food, thought to be integrated by the neuropeptide *npr-1* (Cheung, Cohen et al. 2005), a homologue of neuropeptide Y (de Bono and Bargmann 1998).

C. elegans also responds to light in the blue part of the spectrum; animals exposed to short wavelength light move away from the point of exposure (Ward, Liu et al. 2008). Ablation of seven ciliated neurons in the head abolished this response, which requires cyclic guanosine monophosphate (cGMP)-sensitive cyclic nucleotide–gated (CNG) channels - specifically *tax-2*, which was identified as a chemotaxis mutant (Ward, Liu et al. 2008). This phototaxis response may help animals avoid exposure to damaging levels of light, or help them navigate in the complex three-dimensional environment of the soil.

1.3.5 - Feeding is a regulated behaviour

Two other behaviours are of importance for the experiments conducted in this thesis. The uptake of food and the removal of food waste are both regulated behaviours which can be directly observed in living worms, and provide a measure of the nutritonal status of the animal, as well as providing indicators for the activity of a number of important genetic pathways. *C. elegans* feeds upon bacteria which it finds through a variety of sensing behaviours.

When it locates bacteria, they are drawn into the pharynx of the worm, where strong pharyngeal muscles and an organ known as the grinder combine to physically disrupt the integrity of the bacterial cells, making them easier to digest in the intestine (Avery and Horvitz 1987; Avery and Horvitz 1989).

Bacteria are drawn into the pharynx through the corpus, the most anterior region of the pharynx, which contracts, along with the isthmus, the central portion of the pharynx, opening the lumen and allowing bacterial entry. Bacteria which have already been

subject to grinding are expelled into the intestine by contraction of the terminal bulb. This cycle of contraction is complemented by isthmus peristalsis, where bacteria previously drawn into the pharynx are transferred to the grinder, and processed.

This feeding behaviour, which is important for the survival of the worm, also provides a useful tool for studying neuronal networks. 20 neurons innervate the pharyngeal muscles, and these neurons function separately from the rest of the *C. elegans* nervous system (Avery and Horvitz 1989; Avery 1993). Inhibition of feeding by paralysis of the pharangyel muscles provides a measure of acetylcholine release.

1.3.6 - Defecation follows a rhythmic motor pattern

Defecation in an adult hermaphrodite *C. elegans* occurs approximately once every 50 seconds when well fed (Avery 1997). The defecation motor programme (DMP) can be divided into three phases: posterior body contraction (pBoc), anterior body contraction (aBoc) and enteric muscle contraction (Emc) causing expulsion (Exp). The initial contraction of the posterior dorsal and ventral body wall muscles drives the contents of the intestine forwards (pBoc). This is followed by contraction of the anterior dorsal and ventral body wall muscles and movement of the pharynx backwards into the gut (aBoc). This pressurises the intestine, so upon contraction of the enteric muscles, which is regulated by GABA (acting in an excitatory fashion (Thomas 1990)), the anus opens and the gut contents are expelled (Exp). Other neurotransmitters, including serotonin, are involved in regulating this cycle (Segalat, Elkes et al. 1995).

The length of the cycle is determined by cyclical fluctuations in the release of calcium in the posterior intestine, and this in turn is determined by the activity of the inositol trisphophate (IP_3) receptor (Dal Santo, Logan et al. 1999), which when reduced lengthens the cycle, and when overexpressed decreases the cycle length. As such this has provided a model for studying the effects of drugs which disrupt the activity of the IP_3 cycle (Tokuoka, Saiardi et al. 2008). Cycle times are also affected by a large number of genes expressed in the intestine (Branicky and Hekimi 2006).

1.4 - The regulation of neurotransmitter release

The behaviours and analysis described above demonstrate the importance of tight control of neurotransmitter release in *C. elegans*. Locomotion is vital to the survival of worms, allowing them to avoid noxious substances and temperatures, navigate to food and to find a mate, while the strength of these responses can all be varied to account for the nutritonal status of the animal. These aspects of behaviour are dependent on the correct regulation and release of neurotransmitters such as dopamine, serotonin and

acetylcholine, and therefore the control of release must be properly managed. In the next section, I will examine the process by which neurotransmitter is released, and some of the ways in which that release can be regulated at the molecular level.

1.4.1 - The synaptic vesicle cycle

Release of neurotransmitter is stimulated by the depolarisation of the presynaptic membrane, activating voltage-gated calcium channels and allowing the entry of calcium ions. This initiates is a specialised form of exocytosis, a conserved mechanism for releasing the contents of vesicles, adapted and refined in neurons for rapid signalling. Exocytosis is confined to a distinct region of the synapse, known as the active zone, which is defined by its specific lipid and protein content. The active zone aligns with the post-synaptic density of the receiving cell such that neurotransmitter is released directly towards the post-synaptic target site, reducing diffusion time. This spatial regulation of release also helps confine neurotransmitter to the synapse, reducing off-target effects.

The machinery underpinning this release has been the subject of intense investigation for over thirty years. Early *in vitro* studies determined that fusion was an active process, requiring ATP and cytosol, and could be inhibited by the sulfydryl reagent N-ethylmalemide (NEM) (Rothman 1994). This lead to a hunt for the NEM-sensitive factor (NSF), which was identified as an ATPase (Block, Glick et al. 1988), followed by biochemical identification of three interactors of NSF, known as α/β and γ-SNAP (for soluble NSF attachment protein), the components in cytosol necessary for fusion. These SNAPs were able to interact with three previously identified neuronal proteins - syntaxin-1, VAMP2 (for vesicle associated membrane protein, also known as synaptobrevin) and SNAP-25 (for synaptosome-associated protein of 25kD) - and these proteins were named SNAREs (SNAP Receptors) (Sollner, Whiteheart et al. 1993). Using non-hydrolysable analogues of ATP to inhibit NSF and dissasembly of the protein complex, it was found that these three proteins formed a highly stable structure. They now form the basis for growing families of SNARE proteins, which have been shown to mediate membrane fusion events in all cell types.

1.4.2 - Fusion and the SNARE Proteins

SNAREs contain a domain of around 60 amino acids capable of forming helical bundles when brought together in close proximity. Four helices are required for the formation of this SNARE complex. In neurotransmission the pre-synaptic membrane-associated SNAP-25 donates two helices along with one from syntaxin, an integral membrane protein. The fourth helix is provided by synaptobrevin, which is part of the vesicle

membrane. The formation of the complex appears to occur in a stepwise fashion (Figure 1-7). Syntaxin contains an inhibitory domain which binds to its own SNARE helix and prevents formation of the SNARE complex - this is known as the closed conformation of syntaxin (Figure 1-7). Once syntaxin is in the open conformation, it is compenent to bind to SNAP-25, and this intermediate complex is able to then bind to synaptobrevin on the vesicle membrane. This forms the trans SNARE complex; once the two membranes have fused, the complex is referred to as the cis SNARE complex, with all of the components in the same membrane (for review see Palfreyman 2008).

This interaction appears to provide some level of specificity, as only specific combinations of vesicle- and presynaptic membrane-associated SNAREs are able to form SNARE complexes. For instance, vesicles containing synaptobrevin are not competent to fuse with one another or with membrane regions other than the active zone (Sudhof 2004).

Cell membranes are composed of lipid bilayers with a hydrophobic interior. Although the exact membrane conformation produced during fusion is unknown, this hydrophobic surface must interact with the charged surface of the membrane during fusion. It is thought that the formation of this highly stable SNARE complex generates the energy required to overcome the energetically unfavourable process of membrane fusion (Sudhof 2004). One early hypothesis is that SNARE proteins constitute the minimal protein machinery required for fusion of membranes, as evidenced by their ability to induce fusion between vesicles *in vitro* (Weber, Zemelman et al. 1998). Mouse knock-outs of synaptobrevin (Schoch, Deak et al. 2001) show significantly decreased regulated exocytosis (down by a factor of 100), although they retain some membrane fusion events, with spontaneous release downregulated by a factor of 10; this is most likely due to the activity of homologous proteins. Over 20 different SNARE proteins have been isolated in preparations of synaptic vesicles, although there is a potential that some of these represent contamination from other trafficking vesicles (Takamori, Holt et al. 2006).

In *C. elegans* there is an absolute requirement for SNARE proteins. *unc-64*, *snb-1, ric-4,* which encode syntaxin, synaptobrevin and SNAP-25 orthologues in *C. elegans*, are required for viability; mutations which disrupt their function cause early embryonic lethality (Nonet, Saifee et al. 1998; Saifee, Wei et al. 1998). Analysis of these dying animals demonstrated that they were still capable of some degree of movement, indicating that there are likely to be other SNARE proteins in addition to these classically recognised ones active in the worm nervous system; this movement could also be due to the effect of maternally-contributed mRNAs.

Additionally, a role has been proposed for the vesicular ATPase in membrane fusion in *C. elegans* (Liegeois, Benedetto et al. 2006). While the V-ATPase is more commonly associated with establishing a proton gradient which is required to load vesicles with neurotransmitter (Futai, Oka et al. 2000), the role in membrane fusion can be separated from this function (Liegeois, Benedetto et al. 2006), although the importance of this result has been long debated. A recent report demonstrates that the V-ATPase is able to bind directly to synaptobrevin (Di Giovanni, Boudkkazi et al. 2010) and that this interaction is mediated by calcium ions and the protein calmodulin. Injection of an interfering peptide into presynaptic cells in tissue culture was able to ihibit neurotransmitter release, demonstrating that this interaction is important for neurotransmitter release (Di Giovanni, Boudkkazi et al. 2010).

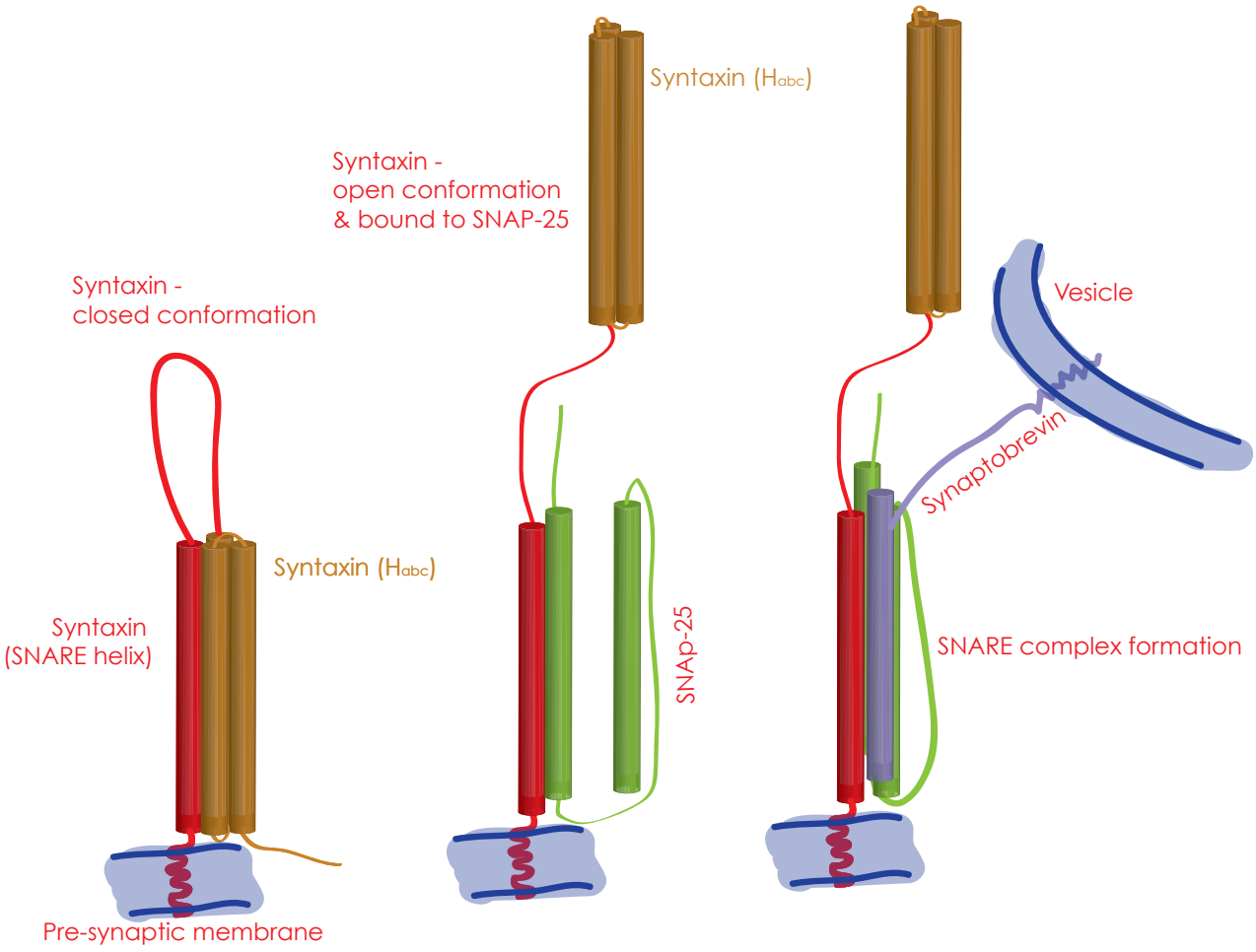

Figure 1-7 SNARE complex formation

Syntaxin is an integral membrane protein containing a SNARE helix (red) and three additional helices (Habc, brown). Syntaxin exists in two conformations - a closed conformation where the Habc helices block access to the SNARE helix - and an open conformation. In the open conformation, syntaxin is able to bind to SNAP-25 (green) and ultimately form a tight SNARE complex with SNAP-25 and synaptobrevin (purple), a SNARE protein found on vesicle membranes. Adapted from Toonen and Verhage, 2003.

1.4.3 - Docking and Priming

Before the formation of a SNARE complex can occur, vesicles must be brought into contact with the presynaptic membrane in a process referred to as docking, and prepared for release by entering a primed state by the formation of the SNARE complex. The status of individual vesicles as either docked or primed is infered through morphological, biochemical and electrophysiological criteria (see references in Palfreyman 2008), although the boundaries between these classes are becoming more blurred.

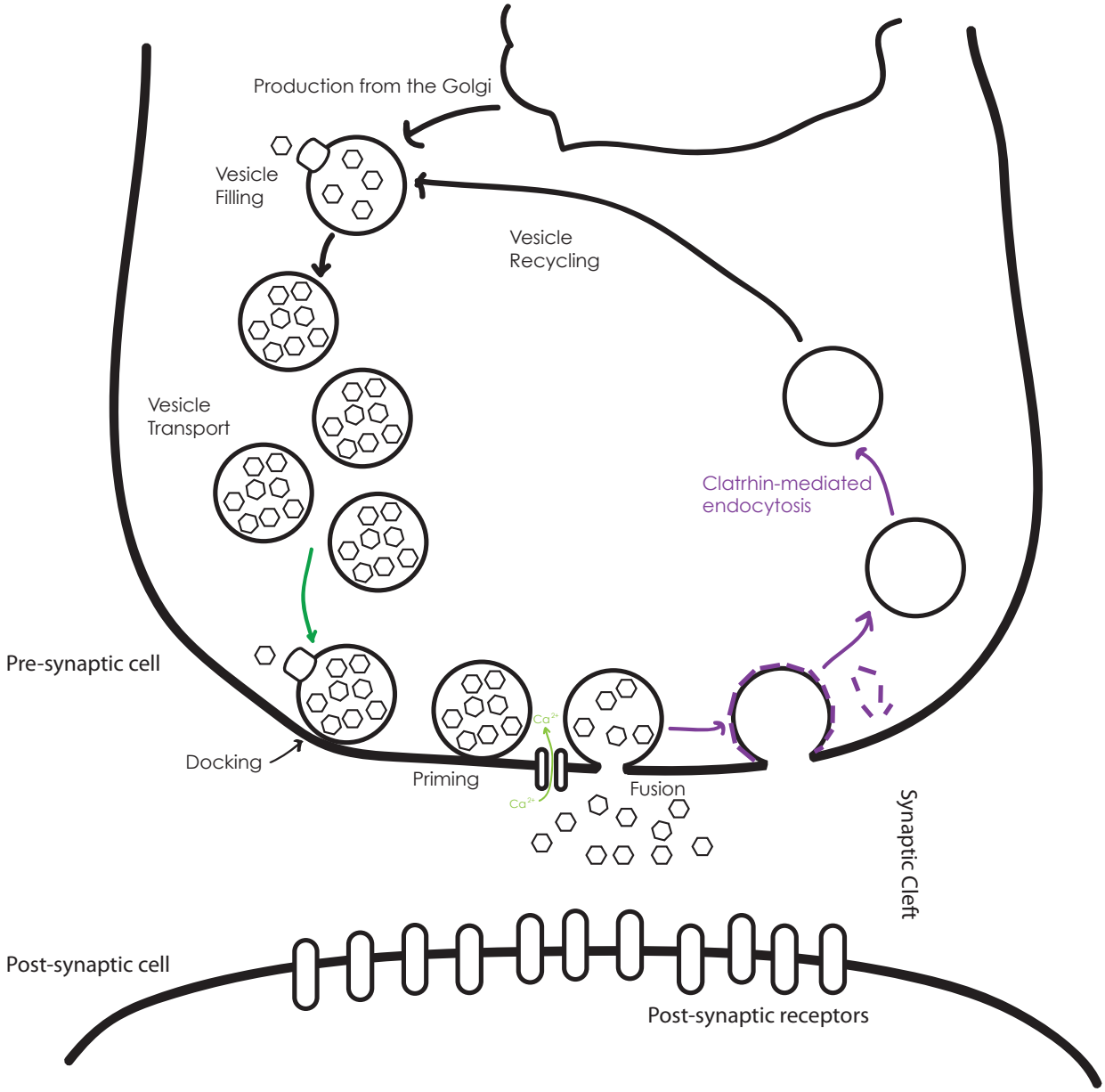

Figure 1-8 The synaptic vesicle cycle

Synaptic vesicles are produced in the Golgi and trafficked to the synapse. They are filled with neurotransmitter and stored in the synapse ready for release. They undergo a series of steps - docking, priming and fusion - mediated by a large number of synaptic proteins, allowing release of neurotransmitter into the synaptic cleft to activate receptors on the post-synaptic cell. The vesicles are recovered from the pre-synaptic membrane by a process of clathrin-mediated endocytosis, recycled back into the synapse and refilled, ready for further rounds of regulated exocytosis. Adapted from Sudhof 2004.

For instance, docking is normally considered to occur before priming (Broadie, Prokop et al. 1995), but more recent studies suggest that the primed vesicles (defined electrophysologically) may correspond to the class of vesicles considered to be docked in EM micrographs, based on their location and distance from the membrane (Hammarlund, Watanabe et al. 2008). Recent studies utilising high pressure freezing have identified reductions in docked vescile number in *unc-13* and *unc-64* mutant animals.

UNC-13 is a cytoplasmic syntaxin binding protein (Betz, Ashery et al. 1998) originally identified in early screens for *C. elegans* mutants, where *unc-13* reduction-of-function mutants were observed to be paralysed and almost completely incapable of movement (Brenner 1974). Complete loss of function of UNC-13 is lethal.

unc-13 mutants are highly resistant to aldicarb, but sensitive to levamisole, the classic phenotype of a presynaptic mutant with reduced neurotransmitter release. *unc-13* is required for synaptic vesicle release in *C. elegans* (Richmond, Davis et al. 1999). Roles for UNC-13 in both docking and priming have been suggested, and the separation of these roles is controversial, but UNC-13 appears to promote neurotransmitter release, at least in part, by binding to and altering the conformation of syntaxin, and by recognising specific membrane domains.

UNC-13 proteins contain C1 and C2 domains, originally identified as domains of protein kinase C (Nishizuka 1988). C1 domains bind to diacylglycerol (DAG), a lipid second messenger found in the presynaptic membrane (Ono, Fujii et al. 1989). Regulation of the composition of the presynaptic membrane is important for the recruitment of UNC-13 (Lackner, Nurrish et al. 1999; Nurrish, Ségalat et al. 1999). DAG defines distinct docking sites for UNC-13, which in turn is responsible for binding syntaxin and promoting SNARE complex formation. UNC-13 also contains a C2 domain; some C2 domains are sensitive to phospholipids and able to bind Ca^{2+} ions, while others may act as protein-protein interaction domains (Cho and Stahelin 2006). The C2 domain of both UNC-13 and munc13 are required for UNC-13 and munc13 to bind to syntaxin (Madison, Nurrish et al. 2005; Stevens, Wu et al. 2005).

UNC-13 binds to the N-terminus of syntaxin, and may promote the open form of syntaxin (Brose, Rosenmund et al. 2000; Madison, Nurrish et al. 2005). UNC-13 is proposed to flip syntaxin from its closed to open state, promoting the incorporation of syntaxin into the SNARE complex (Richmond, Weimer et al. 2001). Expression of a constiutively open form of syntaxin in an *unc-13* mutant is able to bypass the need for UNC-13 in priming of synaptic vesicles (Richmond, Weimer et al. 2001), although some have argued that the

loss of tomosyn is also required to completely bypass the need for UNC-13 (McEwen, Madison et al. 2006).

Tomosyn is another protein which interacts with the core release machinery during priming, and acts in an inhibitory fashion with respect to neurotransmitter release with a negative effect on priming. Tomosyn contains a SNARE domain homologous to that of synaptobrevin, and forms an inhibitory complex with syntaxin (Fujita, Shirataki et al. 1998; Yokoyama, Shirataki et al. 1999; Hatsuzawa, Lang et al. 2003). The single *C. elegans* homologue, TOM-1, is an inhibitor of both synaptic vesicle release and dense core vesicle release (Gracheva, Burdina et al. 2006; Gracheva, Burdina et al. 2007; Gracheva, Burdina et al. 2007).

Another protein thought to play a role in docking is rab3 (*rab-3*) a small GTPase associated with synaptic vesicles, mutants of which exhibit subtle defects in neurotransmission and locomotion (Nonet, Staunton et al. 1997; Mahoney, Liu et al. 2006). Rabs are commonly found on vesicles in non-neuronal cells and act to provide specificity during trafficking. They require a receptor on the target membrane, and one candidate in *C. elegans* is Rim (*unc-10*) an interactor of *rab-3,* mutants of which have an aldicarb defect (Nonet, Staunton et al. 1997). *unc-10* mutants also display a reduction in the number of docked vesicles at synapses (Weimer, Gracheva et al. 2006) and further work has demonstrated that UNC-10 and RAB-3 directly interact to recruit synaptic vesicles to the correct location in the presynaptic membrane in preparation for release (Gracheva, Hadwiger et al. 2008).

Munc18 (*unc-18*) a syntaxin-interacting protein, is also believed to play a role in docking - 80% of neurotransmission is abolished in the *unc-18* mutant, and the number of docked vesicles is dramatically reduced (Weimer, Richmond et al. 2003). The mammalian homologue - Munc-18 - is important for synaptic function, Munc-18 mice exhibit severe synaptic defects, with a complete loss in synaptic activity and the death of neurons, while the initial wiring of the nervous system is unaffected, suggesting an adult role for Munc-18 (Verhage, Maia et al. 2000). While Munc-18 and UNC-18 both bind to the SNARE protein syntaxin *in vitro* (Toonen and Verhage 2003), analysis of C. elegans *unc-18* mutant animals has revealed no difference in the localisation of UNC-64 (syntaxin) and the open form of syntaxin does not rescue mutants in *unc-18* (Weimer, Richmond et al. 2003). The precise role of munc-18 remains under investigation.

1.4.4 - Calcium sensing and release - a role for synaptotagmin

Primed vesicles represent an intermediate in exocytosis which is calcium-ion sensitive. Neurotransmitter release is temporally controlled by the influx of calcium ions via voltage-

gated calcium channels. Following the influx of calcium, neurotransmitter release can occur on the order of 100µs (Heidelberger, Heinemann et al. 1994), the fastest rate of exocytosis yet measured, because the exocytosis machinery is effectively frozen half-way through the process. One of the proteins thought to regulate this release is synaptotagmin, an integral membrane protein of the synaptic vesicle which can bind calcium. Encoded by *snt-1* in the worm, mutants are uncoordinated and have impaired synaptic transmission (Nonet, Grundahl et al. 1993). Synaptotagmin is thought to be a key sensor of calcium-regulated release (Fernandez-Chacon, Konigstorfer et al. 2001), although its precise mechanism of action is still under investigation (Koh and Bellen 2003), and it may in have other roles in the synaptic vesicle cycle which complicate this picture (Jorgensen, Hartwieg et al. 1995).

This regulation by calcium release is imperfect however, as neurons are capable of spontaneous release, which can be measured electrophysiologically and is observed as spontaneous mini-post-synaptic currents. Therefore every neuron is said to have a certain release probability, which is considerably enhanced by the influx of calcium ions. Neurons are considered to be 'reliably unreliable' in their release frequency (Goda and Sudhof 1997) and this characteristic provides an opportunity for regulation and either enhancement or depression of release.

1.4.5 - Models of release dynamics

The standard model of vesicle fusion is complete fusion of the vesicle with the presynaptic membrane, with in which the curvature of the vesicle is completely lost. A fresh vesicle is then reformed away from the active zone and membrane removed to prevent growth of the presynaptic membrane. This process utilises the clathrin-mediated endocytosis pathway (Heuser and Reese 1973; De Camilli and Takei 1996), and involves the reformation of vesicles through the action of dynamin, which scissions the budding vesicle from the presynaptic membrane (Sweitzer and Hinshaw, 1998). This endocytosis event is accompanied by refilling of the vesicle with neurotransmitter ready for additional rounds of release (Sudhof 2004).

1.4.6 - Vesicle endocytosis - a role for membrane lipid regulation

A number of key players in vesicle recycling have been identified, and play clear roles in behavioural responses in *C. elegans*. One of these is synaptotagmin, which binds to AP-2, the clathrin adaptor protein, suggesting a role in endocytosis (Fukuda, Moreira et al. 1995; Haucke and De Camilli 1999). EM imaging of *C. elegans* reveals that vesicles

are depleted in a *snt-1* mutant (Jorgensen, Hartwieg et al. 1995), although this evidence for a role in endocytosis does not rule out a role in calcium-mediated exocytosis.

Synaptojanin and endophilin, encoded in worms by *unc-57* and *unc-26* respectively, also play roles in vesicle recycling. Endophilin is a BAR-domain containing protein, and may aid the reformation of vesicles by causing bending of the membrane, but it also associates with synaptojanin via an SH3 domain, and may be responsible for its correct localisation in the presynaptic membrane (Schuske, Richmond et al. 2003). These two roles - in membrane bending and scaffolding - have been separated in a recent set of experiments in *C. elegans* (Bai, Hu et al. 2010). These demonstrate that mutations in the BAR domain of endophilin disrupt endocytosis, while mutation of the scaffolding regions do not (Bai, Hu et al. 2010), suggesting that the dominant role for endophilin is inducing membrane curvature. Interestingly, endophilin appears to cycle between the plasma membrane and synaptic vesicles, leading to a model where exchange of endophilin may help couple exocytosis and endocytosis (Bai, Hu et al. 2010).

Synaptojanin encodes a polyphosphoinositide phosphatase which is responsible for the removal of PIP_2 from the presynaptic membrane, and synaptojanin mutant mice have defects in the uncoating of synaptic vesicles (Cremona, Di Paolo et al. 1999), as do *unc-57* and *unc-26* mutants in *C. elegans* (Schuske, Richmond et al. 2003). Evidence from *C. elegans* mutants also points to a role in vesicle recycling for these proteins; *unc-26* and *unc-57* mutants are uncoordinated, and have a reduction in synaptic vesicles as observed by EM. The double mutant is no more severely affected than the single mutants (Schuske, Richmond et al. 2003) suggesting that they act in the same pathway for recycling.

The small GTPase dynamin is responsible for the fission step of endocytosis, where clathrin-coated pits separate from the plasma membrane allowing the reformation of vesicles (Sweitzer and Hinshaw 1998); in *C. elegans*, temperature-sensitive *dyn-1* mutants are highly uncoordinated at the non-permissive temperature (Clark, Shurland et al. 1997). The activity of dynamin is closely regulated. Mutations in two proteins known to interact with dynamin cause defects in synaptic transmission and more specifically a reduction in the number of synaptic vesicles, EHS-1 (Eps15) and UNC-57 (endophilin) (Salcini et al., 2001; Schuske et al., 2003), although the recent report on the nature of the endophilin scaffolding role reduces the significance of this interaction (Bai, Hu et al. 2010).

1.4.7 - Exocytosis of dense core vesicles

Neuropeptides are packaged into large dense core vesicles (DCVs), and some elements in the exocytosis of small synaptic vesicles and dense core vesicle are the same, particularly a requirement for SNARE proteins in membrane fusion (Hammarlund, Watanabe et al. 2008). The requirement for other proteins important in synaptic vesicle docking and priming, such as UNC-13 is more controversial, with some papers demonstrating a requirement for UNC-13 in DCV exocytosis (Richmond, Davis et al. 1999; Sieburth, Madison et al. 2007), while others detect no role for UNC-13 in DCV exocytosis (Hammarlund, Watanabe et al. 2008).

The protein CAPS - calcium-dependent activator protein (UNC-31 in *C. elegans*) - is structurally related to UNC-13, containing an UNC-13 homology domain, a PH domain, PI binding domain and a C2 phosphoinositide and calcium-binding motif. In *C. elegans unc-31* mutants are defective in DCV release (Speese, Petrie et al. 2007; Zhou, Dong et al. 2007) and there is an almost complete absence of docked DCVs (Hammarlund, Watanabe et al. 2008). This suggest that UNC-31 may play a complementary role with respect to dense core vesicle exocytosis to UNC-13 in small synaptic vesicle exocytosis. *unc-31* mutants are lethargic, but display either some (Miller, Alfonso et al. 1996) or no resistance to aldicarb (Charlie, Schade et al. 2006), suggesting that UNC-31 plays little or no role in the release of neurotransmitter from small synaptic vesicles (Speese, Petrie et al. 2007). There are situations in which the requirement for *unc-31* can be bypassed, such as by increasing the activity of PKA (Zhou, Dong et al. 2007) although the mechanism of action in this case is unknown.

Treatment with phorbol esters, an analogue of the membrane-bound second messenger diacylglycerol (DAG), increases the size of the readily releasable pool of both DCVs and synaptic vesicles in tissue culture preparations (Malenka, Madison et al. 1986), consistent with a role for proteins which bind to DAG. UNC-13 and PKC-1 both contain C1 domains which are able to bind DAG and phorbol esters, and in mammalian systems both MUNC-13 and PKC are required for synaptic vesicle and DCV exocytosis. In *C. elegans* however, PKC-1 appears to play a more dedicated role in DCV release, as *pkc-1* mutants do not display a reduction in synaptic vesicle exocytosis (Sieburth, Madison et al. 2007), although they do demonstrate a reduction in DCV release. Evidence from mammalian systems suggests that PKC may act to regulate DCV release through phosphorylation of SNAP-25, part of the SNARE complex (Nagy, Matti et al. 2002) or through phosphorylation of munc-18 (Barclay, Craig et al. 2003).

Unlike synaptic vesicles which continually recycle at the synapse, undergoing rounds of refilling and release, the dense core vesicle pool is restocked directly by vesicles budding from the Golgi, although a single DCV may undergo several repeated exocytosis events - each of which sees the release of only a portion of its contents (Perrais, Kleppe et al. 2004).

1.5 - The genetic pathways regulating neurotransmitter release in *C. elegans*

The synaptic vesicle cycle is a specially adapted form of exocytosis allowing regulated release of neurotransmitter. The amount of neurotransmitter released at any one time from any particular neuron can be modulated by a large number of factors, and it is these which help an organism like *C. elegans* which has only 302 neurons to produce and modulate the a wide range of behaviours described earlier. A large number of experiments have defined an extensive genetic pathway, ranging from reception of neurotransmitter at the post-synaptic membrane through to the release of acetylcholine onto the body wall muscles to initiate locomotive responses, and this pathway can be modulated to allow for changes in regulated release over time.

1.5.1 - G-protein coupled receptors are targets for neuromodulators in *C. elegans*

There are two main classes of receptor that are sensitive to neurotransmitters. The first class is ionotropic receptors, such as the nicotinic acetylcholine receptor which tend to be associated with rapid signalling. They can also induce long-lasting effects on the behaviour of neurons as well, a good example being the calcium-permeable NMDA receptor, which is associated with formation of LTP (Collingridge 2003).

The other major class of neurotransmitter receptor are the seven-transmembrane helix family of G-protein coupled receptors (GPCRs). These receptors are associated with more subtle modulation of the activity of neurons, acting over longer time periods than the fast action of ligand-gated ion channels (Nassel 2009). Neuromodulators such as serotonin and dopamine, and larger molecules such as neuropeptides, interact with these receptors, which tend to have a higher affinity for their neurotransmitter substrate than ionotropic receptors, allowing them to function at lower concentration of signalling molecules and at longer distances from the site of neurotransmitter release (Nassel 2009).

GPCRs in turn interact with heterotrimeric G-proteins, and it is these second messengers which transduce the signals through the cell. G-proteins consist of alpha, beta and

gamma subunits, and are regulated through the exchange of GDP for GTP on the alpha subunit. In their inactive state, the alpha subunit associates with GDP, which allows binding to the beta/gamma subunit and to the GPCR. Upon activation of the GPCR by ligand binding, the receptor acts as a guanine nucleotide exchange factor (GEF), and acts to substitute the GDP bound to the alpha subunit for GTP. This activates the alpha subunit, causing dissociation from the beta/gamma subunit, and binding to downstream effectors can occur.

In *C. elegans* there are 21 Gα subunits, 2 Gβ subunits and 2 Gγ subunits, expressed in many neurons and muscle cells, with 14 of the Gα subunits expressed specifically in chemosensory neurons in the head of the animal (Jansen, Thijssen et al. 1999). The Gβ and Gγ subunits bear strong homology to their mammalian counterparts, and have roles in development and locomotion, and in regulating the activity of Gα subunits, as well as some instances of direct modulation of ionotropic receptors. The main focus of interest however is on the Gα subunits themselves. The roles of a number of Gα subunits in the regulation of neuronal activity have been defined through experiments in *C. elegans*, demonstrating how they allow neurons to become responsive to neuromodulatory signals, effecting long-lasting changes in the release potential of the cell.

1.5.2 - G-alpha subunits regulate behaviour in *C. elegans*

There are worm homologues of all the mammalian classes of Gα proteins. The mammalian Gα subunits are divided into four classes: Gαs, Gαi/o, Gαq and Gα12. All four classes are represented in *C. elegans* (Jansen, Thijssen et al. 1999), and all have been demonstrated to have an impact on behaviour.

1.5.2.1 - GOA-1

The Gαo homologue GOA-1 was the first G-protein subunit demonstrated to have an effect on behaviour (Mendel, Korswagen et al. 1995; Segalat, Elkes et al. 1995). GOA-1 encodes the only clear *C. elegans* homologue of the Gαi/o family, and is 80% identical to the mammalian Gαo (Lochrie, Mendel et al. 1991), although it also bears a similar amount of identiy to Gαi. It was demonstrated that *C. elegans* mutants lacking GOA-1 activity were viable and hyperactive, with exaggerated body bends, increased rates of locomotion and increased egg-laying, accompanied by reductions in pharyngeal pumping. This led to the hypothesis that GOA-1 natively acts to regulate these behaviours.

goa-1 mutants are resistant to the effects of serotonin (Segalat, Elkes et al. 1995), a neuromodulator which causes animals to reduce their rate of locomotion, increase

pharyngeal pumping and increase egg-laying, and are hypersensitive to the effects of aldicarb (Nurrish, Ségalat et al. 1999) demonstrating an increase in acetylcholine release. Loss of GOA-1 in the cholinergic neurons, by expression of pertussis toxin (which specifically inhibits GOA-1) caused the same decreases in acetylcholine release (Nurrish, Ségalat et al. 1999), while expressing constitutively active GOA-1 in cholinergic neurons decreased acetylcholine release and rates of locomotion (Nurrish, Ségalat et al. 1999).

GOA-1 acts to reduce the amount of diacylglycerol at sites of neurotransmitter release in the presynaptic membrane (Nurrish, Ségalat et al. 1999, Figure 1-9). As described in the section detailing the synaptic vesicle cycle, DAG is an important second messenger involved in neurotransmitter release. It is through regulation of DAG levels, and through changes in the binding of UNC-13 and PKC-1 that GOA-1 is able to affect neurotransmitter release. Mutation of *goa-1* causes an increase in recruitment of UNC-13 and PKC-1 to release sites in a DAG-dependent manner (Nurrish, Ségalat et al. 1999), whereas the endogenous activity of GOA-1 is to reduce UNC-13 recruitment. However, the exact mechanism of the modulation of DAG levels by GOA-1 remains to be established.

1.5.2.2 - EGL-30

The Gαq homologue EGL-30 is also able to regulate a diverse set of phenotypes in *C. elegans*. Complete loss of function is thought to be lethal (Brundage, Avery et al. 1996), while less severe mutations reduce locomotion, pharyngeal pumping, egg-laying (Brundage, Avery et al. 1996), and are resistant to the effects of aldicarb (Miller, Alfonso et al. 1996; Miller, Emerson et al. 1999).

Expressing activated EGL-30 in the cholinergic neurons increases locomotion rates and acetylcholine release, the opposite effect of increasing GOA-1 activity (Brundage, Avery et al. 1996; Lackner, Nurrish et al. 1999).

The mechanism of EGL-30 action was initially inferred from comparisons with the mammalian homologue Gαq. Gαq activates phospholipase C, an enzyme which converts phosphatidylinositol-(4,5)-bisphosphate (PIP_2) into DAG and inositol trisphosphate (IP_3). EGL-30 has been shown to activate the *C. elegans* PLC homologue EGL-8 in transfected cells (Brundage, Avery et al. 1996), and mutations in *egl-8* mimic those of EGL-30. *egl-8* mutants are lethargic, have reduced egg-laying and are resistant to the effects of aldicarb (Lackner, Nurrish et al. 1999), and are able to suppress some (but not all) of the aldicarb sensitivity of animals expressing *egl-30* gain-of-function alleles from a heat-shock transgene (Lackner, Nurrish et al. 1999), demonstrating that *egl-8*

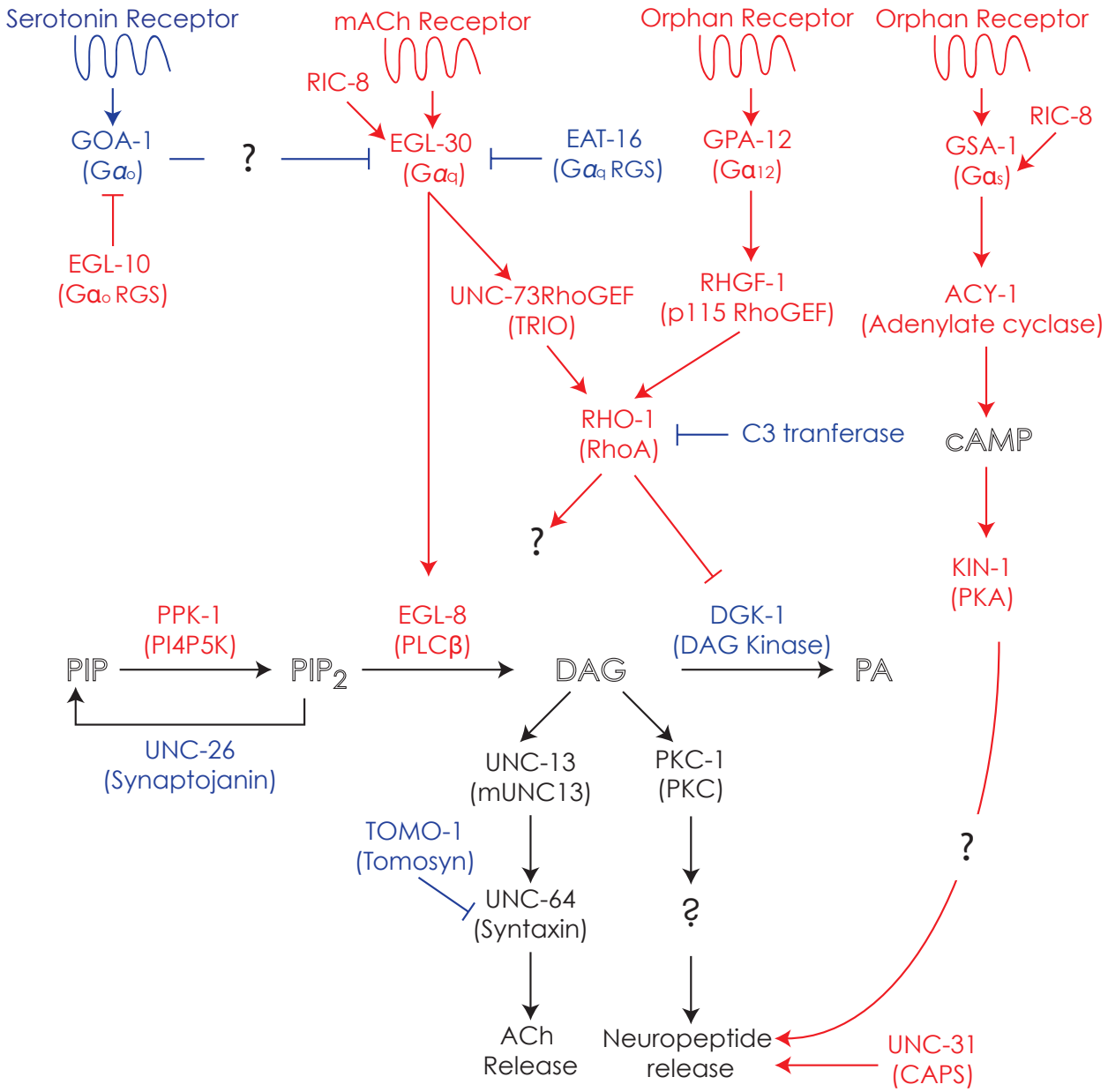

Figure 1-9 Multiple G-proteins regulate neurotransmitter release

A network of G-proteins act to increase or decrease neurotransmitter release in the C. elegans nervous system. Proteins depicted in blue act to reduce release, while those depicted in red increase neurotransmitter release. Signalling from three G-protein alpha subunits - GOA-1, EGL-30 and GPA-12 - converges on RHO-1, a membrane-bound small GTPase, which inhibits the activity of DGK-1, increasing levels of the membrane-bound second messenger in the presynaptic membrane. DAG regulates the release of both small molecule neurotransmitters and neuropeptide.

The production of DAG is also regulated by EGL-30 increasing the activity of EGL-8, the phospholipase C homologue which produces DAG from PIP_2. Evidence discussed in the text indicates that additional pathways act downstream of RHO-1 to regulate neurotransmitter release. Adapted from Perez-Mansilla and Nurrish 2009.

works downstream of *egl-30*. Mutations in *egl-8* and *egl-30* are rescued for acetylcholine release by exposure to the DAG analogue PMA, a phorbol ester (Malenka, Madison et al. 1986), suggesting that these proteins lie upstream of the pathway regulated by DAG and UNC-13. Expression of EGL-8 in motor neurons fully rescues both locomotion and the response to aldicarb, suggesting that for locomotory behaviour and acetylcholine release EGL-8 is only required in these cells. However, while *egl-30* null mutants are lethal, *egl-8* mutants are merely lethargic, suggesting additional roles for *egl-30*. Similarly, *egl-8* mutations only partially suppress the increased neurotransmitter release phenotype of *egl-30* (gain-of-function) mutants, indicating that there are additional pathways regulated by EGL-30 (Lackner, Nurrish et al. 1999).

While the classical Gαq pathway stimulates the production of DAG, leading to an increase in neurotransmitter release, EGL-30 also inhibits a pathway which leads to the removal of DAG from the membrane. As will be discussed below, screens for suppression of activated EGL-30 (Williams, Lutz et al. 2007) and subsequent research demonstrated that EGL-30 inhibits a diacylglycerol kinase, DGK-1, whose action converts DAG to phosphatidic acid.

The EGL-30 pathway is activated by arecoline, a pharamacological agent which activates the G-protein coupled muscarinic acetylcholine receptor (Lackner, Nurrish et al. 1999), although this activation may be indirect (Dittman and Kaplan 2008).

1.5.2.3 - EGL-30 and GOA-1 antagonistically regulate neuronal activity

These two G-proteins, EGL-30 and GOA-1, function antagonistically in the neuron to regulate the overall activity and amount of release of neurotransmitter, and the majority of this regulation is DAG-dependent, putting the membrane bound second messenger as a key player in the regulation of neurotransmitter release. The *goa-1;egl-30* double mutant is lethargic, and animals overexpressing gain-of-function GOA-1 are suppressed by mutations in *egl-30*, indicating that *egl-30* acts either downstream of or in parallel to *goa-1* (Hajdu-Cronin, Chen et al. 1999; Miller, Emerson et al. 1999).

GOA-1 and EGL-30 also antagonistically regulate expression of TPH-1, a key enzyme involved in serotonin biosynthesis (Tanis, Moresco et al. 2008) suggesting that this antagonistic pairing is utilised in multiple situations.

1.5.2.4 - Regulation linking GOA-1 and EGL-30

GOA-1 and EGL-30 are both regulated by RGS (regulator of G-proteins) proteins (Watson, Linder et al. 1996). RGS proteins negatively regulate the activity of heterotrimeric G proteins by functioning as GTPase activating proteins (GAPs) catalysing the intrinsic hydrolysis of Gα-GTP to Gα-GDP.

GOA-1 is negatively regulated by EGL-10 (Koelle and Horvitz 1996), and *egl-10* mutations decrease locomotion and acetylcholine release due to an increase in GOA-1 activity, while EGL-30 is negatively regulated by EAT-16 (Hajdu-Cronin, Chen et al. 1999), and *eat-16* mutants have increased rates of locomotion due to an increase in EGL-30 activity (see Figure 1-9).

The activity of these two RGS proteins is dependent upon the protein GPB-2, a Gβ5 homologue of heterotrimeric G-proteins (van der Linden, Simmer, et al, 2001). Both EGL-10 and EAT-16 contain a G-gamma like (GGL) domain, and this domain interacts with GPB-2 (van der Linden, Simmer, et al, 2001). A null mutation of *gpb-2* increases locomotion, while point mutants of *gpb-2* can either increase or decrease acetylcholine release, presumably by differentially activating either EGL-10 or EAT-16, and hence inhibiting either GOA-1 or EGL-30 (Chase, Patikoglou et al, 2001; van der Linden, Simmer et al, 2001). This protein therefore marks a point of cross-talk between these two antagonistic signalling pathways.

1.5.2.5 - GSA-1 regulates behaviour in *C. elegans*

Gαs heterotrimeric G-protein subunits commonly activate adenyl cyclase, producing the second messenger cyclic AMP (cAMP). In *C. elegans*, activation of GSA-1, the homologue of Gαs, causes hyperactive locomotion, and this effect is completely blocked by loss of ACY-1, the *C. elegans* adenyl cyclase (Schade, Reynolds et al. 2005), while mutations in *gsa-1* cause lethargy which is rescued by expression in the motor neurons (Reynolds, Schade et al. 2005). By homology to Drosophila, activation of this pathway is thought to lead to recruitment of UNC-13 in a DAG-independent fashion (Aravamudan and Broadie 2003; Speese, Trotta et al. 2003).

Activation of ACY-1 causes hyperactive locomotion which is blocked by mutations in *egl-30*, while paralysis in an *acy-1* mutant is partially rescued by activation of EGL-30 or by phorbol esters (Reynolds, Schade et al. 2005) indicating a link between these pathways, although how these pathways integrate to control locomotion is unclear. As measured by the chronic aldicarb assay there is little change in aldicarb release in *acy-1* mutants, despite their almost complete paralysis (Reynolds, Schade et al. 2005). However, the

gsa-1 (gf) mutants are hypersensitive to aldicarb in a chronic assay (Schade, Reynolds et al. 2005) suggesting a role in synaptic vesicle exocytosis. This appears to be mediated by *ric-8*, an orthologue of the mammalian protein synembryn, which acts as a receptor-independent GEF to stimulate signalling by the alpha subunit of G-proteins (Tall et al, 2003). RIC-8 stimulates signalling by both EGL-30 and GSA-1 (Reynolds, Schade et al. 2005), and the *ric-8* mutants are highly resistant to aldicarb; the *ric-8;gsa-1 (gf)* mutants are restored to a wild-type level of acetylcholine release (Schade, Reynolds et al. 2005)

Interestingly, the activation of PKAc, known as KIN-1 in *C. elegans,* is able to bypass the requirement for UNC-31 (CAPS) in dense core vesicle exocytosis (Zhou, Dong et al. 2007). This is consistent with the phenotype of *unc-31* mutants, which are highly lethargic on food but move much faster when starved (Speese, Petrie et al. 2007), suggesting the activation during starvation of an additional pathway independent of *unc-31* which acts to increase locomotion.

1.5.3 - DGK-1

Diacylglycerol is a key point of cross-talk between GOA-1 and EGL-30. A screen for animals which were resistant to the effects of serotonin, which normally causes animals to reduce their body bend rate and increase egg-laying, identified mutants in a diacylglycerol kinase, *dgk-1* (Nurrish, Ségalat et al. 1999). In an alternative experiment, *dgk-1* was identified as a mutation which caused animals to become hyperactive in their locomotion (Miller, Emerson et al. 1999). Also called *sag-1*, *dgk-1* mutants were also identified as suppressors of activated GOA-1 (Hajdu-Cronin, Chen et al. 1999), demonstrating that they act downstream of or in parallel to GOA-1 in the response to serotonin. As yet the relevant GOA-1 effector for control of DAG levels and locomotion is unknown.

The DGK-1 enzyme phosphorylates DAG to phosphatidic acid, removing the binding site for UNC-13 and PKC-1, involved in the release of neurotransmitter from both synaptic vesicles and DCVs. *dgk-1* mutants are not lethal, demonstrating that this function is not part of the core release machinery. They do however demonstrate hypersensitivity to aldicarb, resistance to serotonin and have a loopy locomotion (Nurrish, Ségalat et al. 1999), and are predicted to have increased levels of DAG and lowered levels of PA.

Expression of DGK-1 in the motor neurons of *dgk-1* mutant was sufficient to restore the response to aldicarb (Nurrish, Ségalat et al. 1999), demonstrating that, along with GOA-1, EGL-30 and EGL-8, DGK-1 acts in the motor neurons to alter levels of acetylcholine release.

egl-30;dgk-1 and *egl-8;dgk-1* double mutants have virtually wild-type levels of neurotransmitter release, suggesting that these lie in parallel pathways acting to either increase or decrease the levels of DAG, in turn increasing or decreasing the release of neurotransmitter (Miller, Emerson et al. 1999), and that there is a basal level of DAG production in these mutants.

1.5.4 - RHO GEFs regulate behaviour

Examination of *unc-73RhoGEF* mutants (Steven, Zhang et al. 2005) gave an indication of the mechanism linking EGL-30 to changes in DGK-1 activity. UNC-73 contains both Rac and Rho GEF domains, and mutations in the Rac GEF domain causes axon guidance defects (Steven, Kubiseski et al. 1998). However, mutations affecting only the Rho GEF domain were isolated, and caused reduction in locomotion and egg laying (Steven, Zhang et al. 2005), similar to severe mutations in EGL-30 although with only a small effect on acetylcholine release. Nonetheless this demonstrated a role for a Rho GEF and hence for Rho in neurotransmitter release. Loss of *unc-73RhoGEF* activity causes a severe decrease in locomotive activity, although it has little effect on the level of acetylcholine release. The likely target of UNC-73RhoGEF is the small GTPase RHO-1, and this suggests that presynaptic RHO-1 is able to regulate locomotion via changes in acetylcholine release and by some additional mechanism.

Loss of the Rho-specific GEF domain in UNC-73 suppresses the activity of EGL-30, the Gαq which also regulates the activity of EGL-8, the phospholipase C (Williams, Lutz et al. 2007). Loss of both EGL-8 and UNC-73 RhoGEF activity phenocopies *egl-30* mutants, suggesting that these two proteins represent the effectors of EGL-30 in the cholinergic neurons of *C. elegans* (Williams, Lutz et al. 2007), and *in vitro* studies suggest a close physical interaction between EGL-30 and UNC-73. The model predicts that UNC-73, as activated by EGL-30 is upstream of a target which is able to inhibit DGK-1 and increasing levels of DAG at the presynaptic membrane.

In mammalian studies, RhoA, the mammalian orthologue of RHO-1, is also regulated p115RhoGEF, which in turn is activated by a fourth class G-protein subunits, Gα12/13. The *C. elegans* homologue of Gα12/13 is GPA-12, and RNAi of this gene in an RNAi-sensitised strain (*rrp-3*) has been shown to affect locomotion (Yau, Yokoyama et al. 2003), although the deletion mutant has no effect on locomotion (Hiley, McMullan et al. 2006). The p115RhoGEF homologue, RHGF-1, which is activated by GPA-12, has in turn been demonstrated to activate RHO-1, increase UNC-13 levels at release sites, and hence stimulate neurotransmitter release (Hiley, McMullan et al. 2006). Using the mutant form of UNC-13 (H173K), which is unable to bind to DAG, completely blocks

the effects of activated RHGF-1 in increasing neurotransmitter release. This suggests that GPA-12 and RHGF-1 act to stimulate the DAG/UNC-13 dependent pathway. *pkc-1* mutations have no effect on the action of GPA-12 and RHGF-1, suggesting the presence of two pools of DAG, one of which acts through UNC-13 and the other through PKC-1. Interestingly, *rhgf-1* and *gpa-12* mutants have little effect on neurotransmitter release or locomotion (Hiley, McMullan et al. 2006) suggesting that under basal laboratory conditions this pathway is not active.

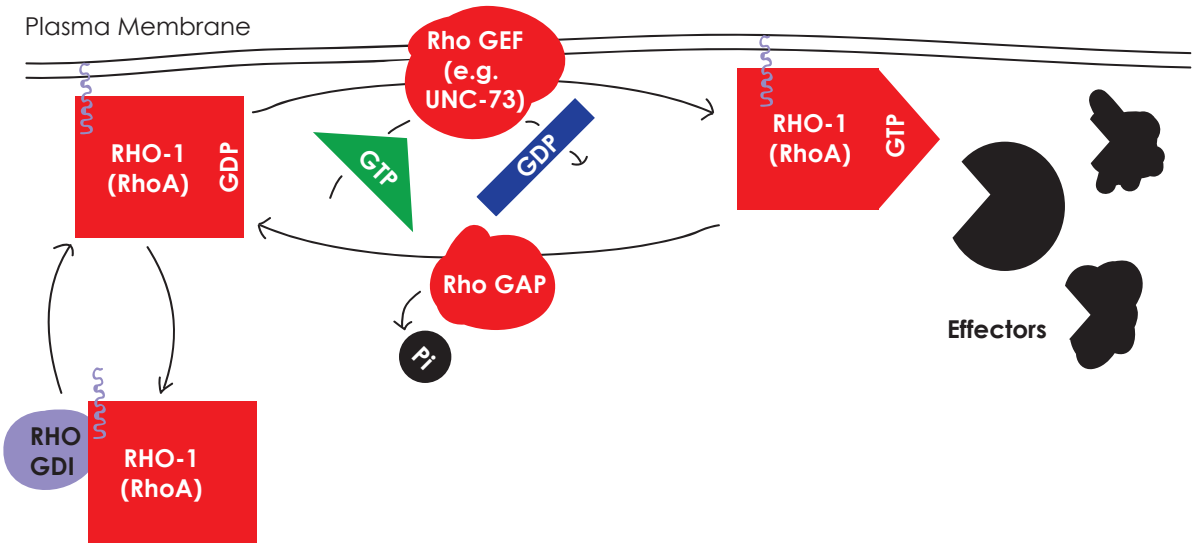

Figure 1-10 RHO-1 is a membrane-bound GTPase

RHO-1 is the C. elegans orthologue of RhoA, a small, membrane bound GTPase. It cycles between an inactive GDP-bound state and an active GTP-bound state due to the action of Rho GEFs (guanine nucleotide exchange factors) , which exchange GDP for GTP, and Rho GAPs (GTPase activating proteins), which stimulate the intrinsic GTPase activity of Rho, converting GTP back to GDP. RhoA is sequestered from the membrane by Rho GDI proteins. Adapted from Etienne-Manneville and Hall 2002.

These two RhoGEFs activate RHO-1 but with different effects. RHO-1 activated by RHGF-1 stimulates neurotransmitter release and changes in locomotion solely through the DAG/UNC-13 dependent pathway, but loss of RHGF-1 has little effect on acetylcholine release. Stimulation of RHO-1 activity by UNC-73 increases the rate of locomotion but has little effect on neurotransmitter release. This suggests that either these two proteins act redundantly, or that there are additional RhoGEFs which act in the nervous system of *C. elegans*.

1.5.5 - RHO-1

The mechanism of the link between EGL-30, UNC-73, RHGF-1 and DGK-1 lies in the activity of the small GTPase RhoA, known as RHO-1 in *C. elegans.* By homology to

mammalian systems, diacylglycerol kinases can be regulated by Rho family GTPases (van Blitterswijk and Houssa 2000). DGKθ, the closest homologue of DGK-1, is regulated by RhoA (Houssa, de Widt et al. 1999). RHO-1 is the single *C. elegans* orthologue of RhoA, and it was therefore an attractive candidate for the regulation of neurotransmitter release.

RHO-1 is a membrane-associated GTPase; it can bind guanine triphosphate (GTP) or guanine diphosphate (GDP), and is has innate enzymatic activity capable of converting bound GTP into GDP (Jaffe and Hall 2005). The exchange of one nucleotide for another induces conformational changes in the structure of RHO-1. In its GTP-bound state RHO-1 is considered to be active; switching to GDP inactivates the protein. The rate of this activity is enhanced by additional proteins known as GTPase Activating Proteins, or GAPs. The dissociation of GDP for GTP is enhanced by another set of associated proteins known as Guanine nucleotide Exchange Factors, or GEFs. Therefore the endogenous activity of RHO-1 can be further enhanced by association with these other molecules (Jaffe and Hall 2005). GAPs, despite their name, act to reduce the signalling activity of RHO-1, while GEFs, by allowing RHO-1 to enter its active state, enhance signalling through the GTPase.

RHO-1 is prenylated at its C-terminus; this allows it to interact with the cell membrane and is required for function. Another set of associated proteins, the Guanine nucleotide Dissociation Inhibitors (GDIs) extract RHO-1 from the membrane and sequester the inactive GDP-bound form (Jaffe and Hall 2005).

RhoA has been implicated in a vast range of biological processes, including development, immunity, cell shape changes and movement (Etienne-Manneville and Hall 2002, Jaffe and Hall 2005, Lundquist 2006). The first clues to the function of Rho came from observations that constitutively active Rho was able to induce the formation of stress fibres and lamellipodia in transfected fibroblasts (Ridley and Hall 1992), and much of the activity of Rho family GTPases is connected to (but not limited to) changes in cell shape and the reorganisation of cytoskeletal proteins. The roles of Rho GTPases can be broadly divided into three categories: morphology, movement and behaviour, regulating processes as diverse as wound closure, growth cone guidance and phagocytosis (Etienne-Manneville and Hall 2002).

In *C. elegans*, Rho GTPases play a number of very important roles. In the first cell division in the developing zygote, CDC-42, in complex with the polarity protein PAR-6 and the atypical protein kinase PKC-3 are required to establish polarity in the zygote (Gotta, Abraham et al. 2001). Experiments with the RHO-1 target Rho kinase (ROCK) and the

RhoGAP RGA-2 have demonstrated that a balance of RHO-1 signalling is important for morphogenesis during *C. elegans* development (Diogon, Wissler et al. 2007).

Later in development, Rho GTPases are important for elongation of the developing embryo which occurs as a result of contraction of actin rings, mediated by LET-502, which encodes the worm ortholgoue of Rho Kinase, and MEL-11, a myosin phosphatase

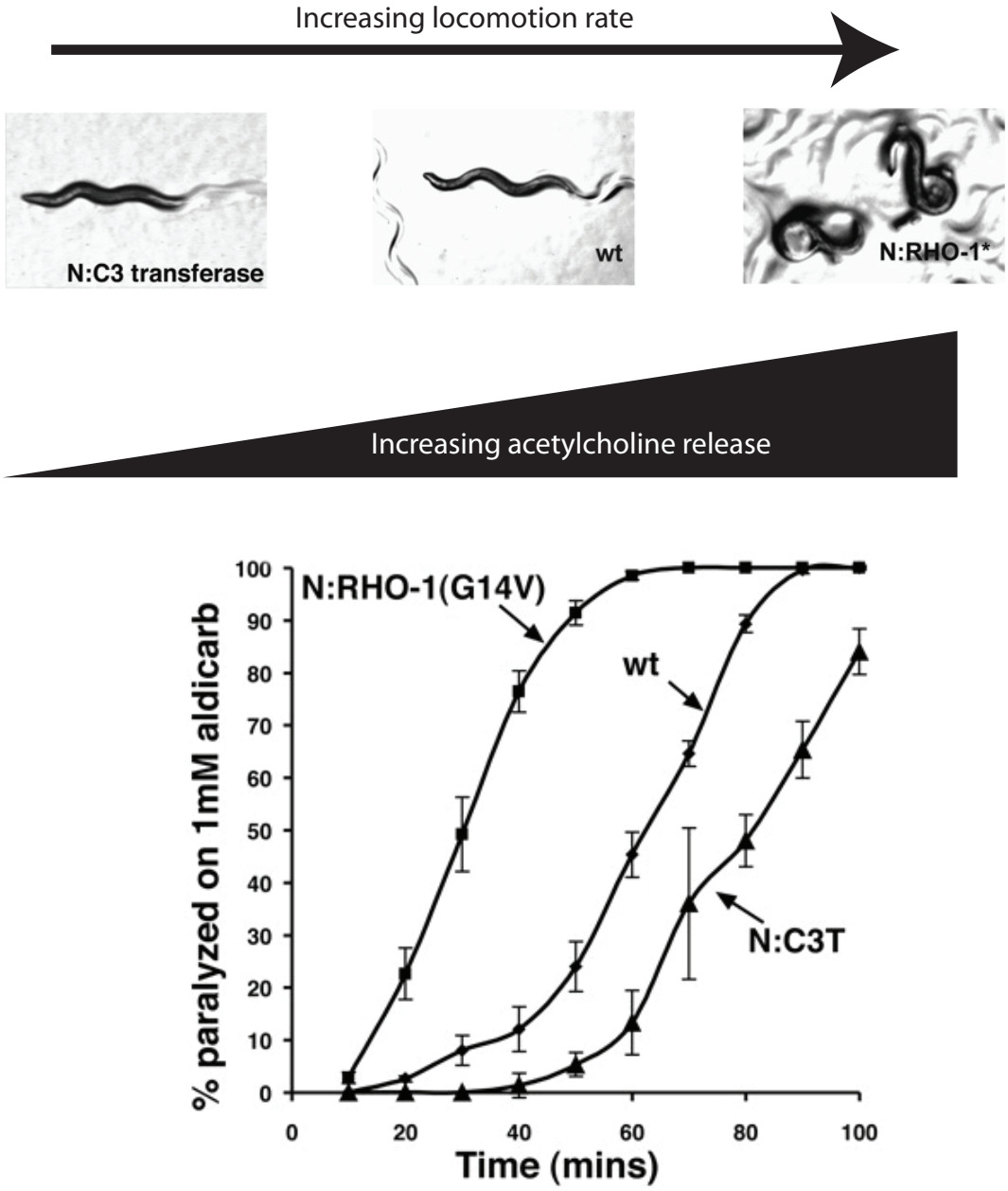

Figure 1-11 RHO-1 increases neurotransmitter release in *C. elegans*

Expression of constitutively active RHO-1, a small GTPase, under the *unc-17* promoter (N:RHO-1(G14V)) causes an increase in rate of paralysis on 1mM aldicarb, indicating that RHO-1 increases acetylcholine release. These animals also become highly loopy and uncoordinated. Alternatively, inhibiting endogenous RHO-1 with C3 transferase, a RhoA specific toxin expressed under the *unc-17* promoter (N:C3T), reduces neurotransmitter release and causes lethargic locomotion with reduced depth of body bends. From McMullan, Hiley et al. 2006

(Wissmann, Ingles et al. 1997, Wissmann, Ingles et al. 1999). RHO-1 also plays a role in the migration of hypodermal cells in C. elegans (Spencer, Orita et al. 2001), and in neuronal development; a dominant negative RHO-1 increases neurite outgrowth (Zallen, Peckol et al. 2000).

In other model systems, Rho GTPases regulate nervous system development (Govek, Newey et al. 2005) and act in synaptic transmission and there is a strong link between mutations affecting Rho GTPases and mental retardation (Govek, Newey et al. 2005). Rac and Cdc42 regulate synaptic strength in *Aplysia* (Humeau, Popoff et al. 2002, Udo, Jin et al. 2005), while inhibition of RhoB blocks stimulated release of neurotransmitter from PC12 cells (Ishida, Zhang et al. 2004). In mice, stimulation of Rho GTPase activity by cytotoxic necrotizing factor 1 (CNF1), a toxin from *Escherichia coli*, increased the ability in tasks assessing learning and memory, most likely due to alterations in synaptic connections (Diana, Valentini et al. 2007). Other roles for Rho in synaptic activity include the phosphorylation of syntaxin by the Rho effector ROCK (Sakisaka, Baba et al. 2004), loss of which impairs learning and memory in mice (Dash, Orsi et al. 2004).

A RHO-1 deletion mutant is lethal (R. McMullan, personal communication), and so the first evidence that RHO-1 plays a direct role in neurotransmitter release came with experiments on the protein UNC-73 as discussed above. Roles for Rho family GTPases in regulating behaviour had been demonstrated through mutations of the RhoGEF *vav-1*, which produces defects in pharangyl pumping, ovulation and defecation (Norman, Fazzio et al. 2005), and more recent evidence suggests that RHO-1 is the target of VAV-1 for regulating these behaviours (McMullan and Nurrish, 2011).

The Nurrish lab also become interested in RHO-1, because the mammalian homolgoue had been demonstrated to bind to DGKθ (Houssa, de Widt et al. 1999), the orthologue of DGK-1 and this binding has been demonstrated to be conserved between the *C. elegans* homologues (McMullan, Hiley et al. 2006). In mammalian cells, this interaction decreases the activity of DGK-1, preventing the removal of DAG from the membrane and hence increasing neurotransmitter release.

Expression of activated RHO-1 in motor neurons is sufficient to increase acetylcholine release, and leads to exaggerated body bends similar to those seen in a *dgk-1* mutant animal (McMullan, Hiley et al. 2006, Figure 1-11). Inhibition of endogenous RHO-1 by the expression of the RHO-1 specific inhibitor C3 transferase (Aktories and Hall 1989) from either a heatshock of motor-neuron specific promoter causes a decrease in the level of acetylcholine release (McMullan, Hiley et al. 2006), demonstrating a role for RHO-1 in the motor neurons (Figure 1-11).

While RHO-1 has been shown to have effects during development, these effects on locomotion occur post-developmentally, as demonstrated by the activation of RHO-1 from a heatshock promoter in fully developed adults. This leads to an increase in sensitivity to acetylcholine esterase aldicarb, demonstrating an increase in acetylcholine release (McMullan, Hiley et al. 2006), and an increase in the levels of DAG at existing synapses, as measured by the accumulation of fluorescently tagged UNC-13 (McMullan, Hiley et al. 2006, Figure 1-12).

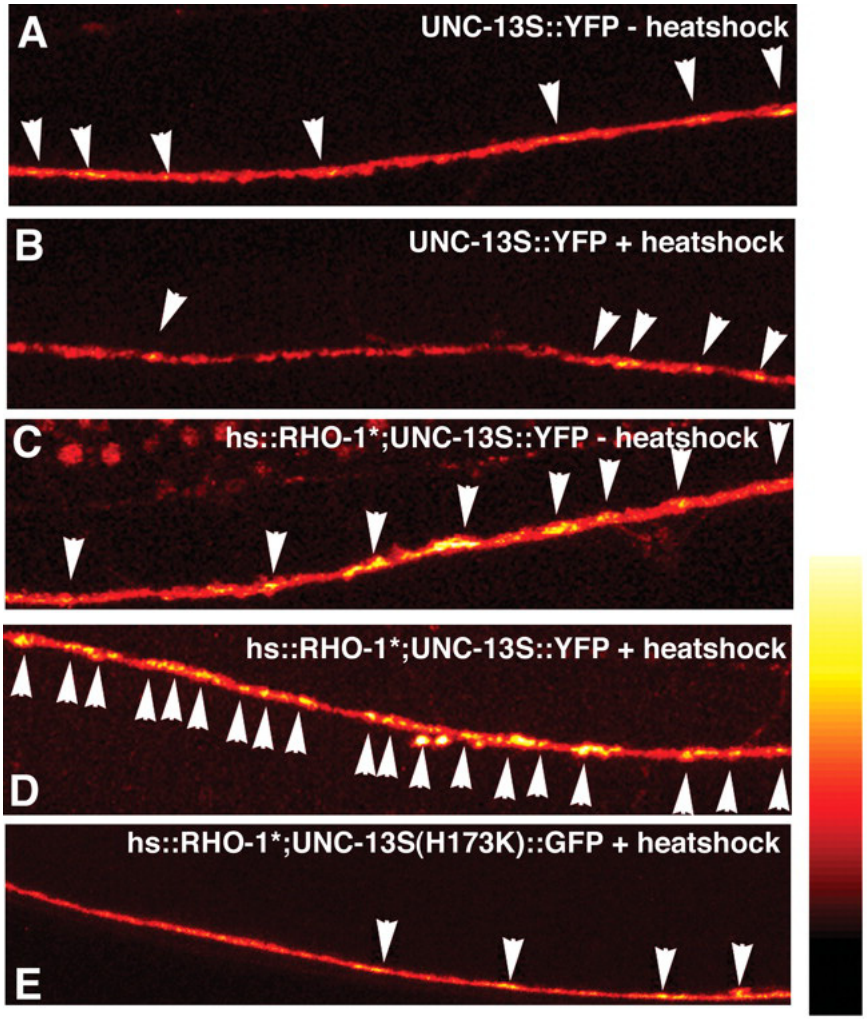

Figure 1-12 RHO-1 recruits UNC-13 to prexisting synapses

Activation of a heatshock RHO-1 transgene in adult animals causes an accumulation of YFP-tagged UNC-13 at synapses in *C. elegans*. RHO-1 inhibits DGK-1, causing an accumulation of DAG, a target for UNC-13 binding. From McMullan, Hiley et al. 2006

This recruitment of UNC-13 suggests that RHO-1 acts by inhibiting DGK-1, increasing levels of DAG, and hence increasing recruitment of UNC-13 to release sites (Figure 1-12). However, use of a mutant form of UNC-13, which contains the H173K mutation and is unable to bind to DAG (Lackner, Nurrish et al. 1999), is insufficient to completely block the effects of constitutively active RHO-1 on locomotion and sensitivity to aldicarb

(McMullan, Hiley et al. 2006), while RHO-1 still demonstrates some ability to increase neurotransmitter release in an *unc-13*(H172K);*pkc-1* double mutant (R. McMullan, personal communication).

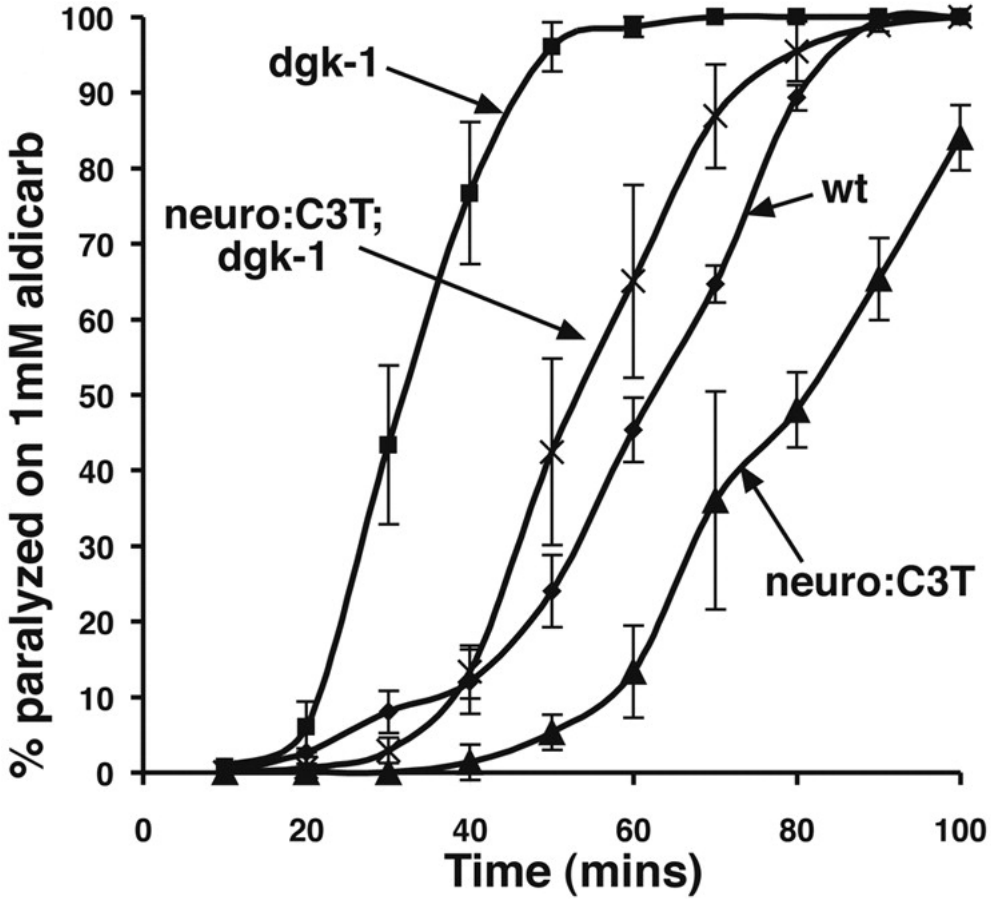

Figure 1-13 RHO-1 acts through DGK-1-dependent and DGK-1-independent pathways

Inhibition of endogenous RHO-1 activity by C3 transferase decreases neurotransmitter release as measured by rate of paralysis on 1mM aldicarb. A *dgk-1* mutant has increased levels of neurotransmitter release and is hypersensitive to aldicarb. If DGK-1 were the only target of RHO-1 in the nervous system, inhibiting RHO-1 activity by expressing C3 in a *dgk-1* mutant background should have no effect on neurotransmitter release. However, there is a reduction in neurotransmitter release in the neuro:C3T*;dgk-1* double mutant animals, suggesting that there are additional targets of RHO-1 in the *C. elegans* nervous system. It should be noted that *dgk-1* significantly suppress the effects of C3T, demonstrating that it is a major effector of RHO- in motor neurons. From McMullan, Hiley et al. 2006

A mutant form of activated RHO-1 carrying the F25N mutation demonstrates reduced binding to DGK-1 (McMullan, Hiley et al. 2006), and is unable to stimulate neurotransmitter release as effectively as RHO-1 which is wild-type at this position (McMullan, Hiley et al. 2006). This mutation was isolated by Alan Hall in early experiments with RhoA, improves the expression of RhoA in tissue culture experiments, and is generally regarded as having

little effect on the activity of the GTPase on changes in actin remodelling (McMullan and Nurrish 2007).

Further, inhibition of RHO-1 by C3 transferase in a *dgk-1* null mutant background decreases neurotransmitter release (McMullan, Hiley et al. 2006), indicating that RHO-1 has targets other than DGK-1 (Figure 1-13). If DGK-1 were the only downstream effector of RHO-1, then changes in RHO-1 activity in a dgk-1 null mutant should have no impact on acetylcholine release. However, as can be seen in Figure 1-13, inhibition of endogenous RHO-1 by C3 transferase still leads to a decrease in acetylcholine release.

Together these pieces of evidence - DAG effector mutants which do not completely block the activity of RHO-1, the F25N mutation which is able to stimulate neurotransmitter release, and the action of C3 transferase in a *dgk-1* mutant - suggest the presence of a DAG-independent, DGK-1-independent pathway by which RHO-1 is able to stimulate neurotransmitter release. However, activated RHO-1 combined with a *dgk-1* mutant background does not demonstrate any additional increase in neurotransmitter release compared with a *dgk-1* mutant alone. This is surprising because the activated RHO-1 would be expected to activate the *dgk-1* independent pathway in this genetic background. However, it is possible that the body bend rates in a *dgk-1* animal, used as a measure of the activity of the motor neurons, represent a maximum rate which cannot be increased even by activation of the *dgk-1* independent pathway.

1.6 - Aims of this thesis

The regulation of RHO-1 in its role in neurotransmitter release has been well characterised (Steven, Zhang et al. 2005; Hiley, McMullan et al. 2006; McMullan, Hiley et al. 2006; Williams, Lutz et al. 2007), although additional RhoGEFs most likely remain to be uncovered (McMullan and Nurrish 2007). It is known that RHO-1 acts to regulate DAG levels by inhibiting DGK-1, but number of experiments, including use of the RHO-1 specific inhibitor in a *dgk-1* mutant background, reveal the presence of additional RHO-1 targets, demonstrating that RHO-1 acts through both a DAG/UNC-13 dependent and independent pathway (McMullan, Hiley et al. 2006). It is the nature of this independent pathway or pathways which is under investigation here.

I have set out to characterise these through the use of a genetic screen for suppressors of activated RHO-1, as described in Chapter 3, where a number of potential targets are identified and characterised. One particularly interesting mutant was identified as an allele of the large, conserved gene *unc-80*, and characterisation of this mutant is

examined in more detail in Chapter 4, while the *unc-80* functionally related genes *unc-79, nca-1* and *nca-2*, and their effects on RHO-1 activity, are examined in Chapter 5.

Also of interest is the regulation of the core release machinery, including tomosyn (*tom-1*) and syntaxin (*unc-64*), and work in collaboration with the Fujita laboratory to examine the roles of these proteins in *C. elegans*, and characterisation of a novel phosphorylation site, is described in Chapter 6.

Finally, Chapter 7 documents my attempt to produce a new tool for the regulation of protein activity in *C. elegans*, utilising tamoxifen to regulate fusion proteins.

2 - MATERIALS AND METHODS

2.2 - Worm Maintenance

Worms were grown following conditions described in Brenner 1974. Worms are maintained on 55mm petri dishes containing 13ml worm agar, otherwise referred to as normal growth media (NGM). Plates were seeded with *E. coli* strain OP50, which is resistant to streptomycin, as food for the worms. To maintain stocks, small chunks of agar containing worms are removed from a plate using a spatula flamed in ethanol, and the chuck transferred to a fresh plate with food. Best practice is to prevent stocks becoming starved; should starvation occur worm strains are grown for a week in the presence of food before being used for any physiological assays, although starved males can be successfully used for crosses. Individual worms are picked using a flamed platinum wire.

Worms are grown at 20°C in a temperature-controlled room. To maintain strains for long periods of time without being starved, 3 or 4 L4 animals are transferred to a fresh plate with food, and the plate placed at 15°C to decrease the growth rate.

2.3 - Freezing and defrosting worm stocks

2.3.2 - Freezing

10 plates of the strain to be frozen were grown to starvation on 55mm petri dishes. The starved animals were washed in 15ml of M9 buffer and left on ice for 15 minutes. The worms settled to the bottom of the M9 buffer, and the volume was reduced by pipetting to 2ml. 2ml of molten freezing solution and agar was added and the resulting mixture divided into two 2ml aliquots and transferred to 2ml cryovial tubes (Corning). These were then placed in a polystyrene box and stored at –80°C. One vial was subsequently transferred the liquid nitrogen store.

2.3.3 - Defrosting

When defrosting animals cryovial tubes were maintained on dry ice at all times when outside the freezer or liquid nitrogen. A small amount of agar from the tube was scraped onto a fresh seeded plate using a flamed spatula before returning the cryovial. The plates were examined for live worms 1 hour after defrosting, and for up to three days subsequently. Live worms were transferred to fresh plates using a platinum wire.

In many instances defrosting caused fungal contamination, in which case the animals were bleached once sufficient stocks had been obtained (see 2.4).

Where the original cryovial was completely emptied of agar, animals were grown for re-freezing (see 2.2.1).

2.4 - Crossing worm strains

For standard crosses, 55mm petri dishes containing worm agar were seeded with 50µl of OP50, forming a small lawn (cross plate). Five larval stage 4 (L4) hermaphrodites of the first strain were transferred onto the lawn of the cross plate. Males from the second strain were picked to a fresh seeded plate and allowed to crawl free of any eggs or hermaphrodites before at least 10 males were transferred to the cross plate. In instances where mating efficiency was low, up to 50 males were transferred to the cross plate. The cross plate was placed at 15oC for between 1 and 3 days. The hermaphrodites were then singled to individual plates and the progeny examined after 3 days.

2.5 - Bleaching

2.5.2 - Removing contamination

To remove contamination, household bleach (5% solution of sodium hypochlorite) was mixed with 5M NaOH in a 1:1 ratio, and a drop (200µl) pippetted onto a fresh plate, away from the lawn of OP50 bacteria. Adult hermaphrodites were picked into the bleach:NaOH drop, and were killed and dissolved, while their eggs were unharmed. Plates were left overnight, and the lawn examined for live worms the following day; these worms were transferred to a fresh plate. Sometimes this procedure was repeated for stubborn contamination.

2.5.3 - Producing a synchronous culture

5 plates of mixed-stage worms were washed in 15ml of M9 buffer. Worms were spun at 1500rpm, pelletting them. The volume was reduced by pipetting, and the pellet was resuspended in 2ml M9, to which was added 2ml household bleach and 1ml 5M NaOH. The worms were placed on a shaker for 15 minutes, before being washed three more times in M9, before being resuspended in 2ml fresh M9. They were then pipetted to 5 fresh plates using a glass dropping pipette. The process left eggs intact which hatched into a synchronous culture.

2.6 - Microinjection

Plasmid DNA was injected into the gonad of young adult worms (best results were usually obtained by picking L4 hermaphrodities the day before injection), along with a suitable marker as described in the text, to identify the transgenic animals.

The markers used were TTX-3::GFP, which is expressed in the cell bodies and axonal processes of bilaterally symmetric head neurons AIY left and right (a gift from Oliver Hobert); UNC-122::GFP, which is expressed in the coelomocytes (a gift from Piali Sengupta) p.acr-2::GFP, which is expressed in ventral cord motor neurons VA, DA, VB, DB, DA, IL1, RMD, and PVQ (the promoter for acr-2 was a gift from Yishi Jin), and p.unc-17::GFP. The total DNA concentration in the injection mix was made up to 150ng/μl using pBluescript (Stratagene) in TE buffer. Pads for injecting the worms were made from 2% agarose on 22mm X 50mm cover slips (Chance Propper Ltd). A small drop of halothane oil (Sigma) was placed on the pad and the worm transferred to the oil. The animal was then gently stuck to the agarose pad using a platinum wire pick. If the animal failed to stick, it was transferred to a fresh drop of oil with the aim of removing excess bacteria adhering to the cuticle.

A Leica DM IRB microscope and Intracel picospritzer III injector were used to perform the injections with 0.5mm diameter injection needles (Harvard apparatus),

Once injected the worms were carefully removed from the pad by the addition of a small volume of M9 buffer that released the worm. The animal was then transferred with a platinum wire to a seeded agar plate, each injected animal to an individual plate.

The F1 generation from injected adults was screened for the transgenic marker and any positive animals singled to fresh plates. The progeny of these transgenic animals were then screened for the transgenic marker and those that contained it were considered a line of transgenic animals.

2.7 - Extraction of DNA from worms

2.7.2 - For PCR and standard sequencing

10 starved plates of worms were washed in 15ml ice-cold EN solution in a 15ml tube and spun down for 1 minute at 1000rpm at 4^{o}C, then resuspended in 2ml clean ice-cold EN solution and left to settle on ice for 10 minutes. 2.5ml cold sucrose solution (68% sucrose) was added and the tube vortexed. 3ml EN solution was then carefully layered on top of the sucrose solution. The tube was spun at 2500rpm for 10 minutes to allow all the unwanted material to pellet at the bottom. The worms banded in a thin layer and were transferred to a new tube with a glass pipette. They were washed twice with EN solution to remove any remaining sucrose. The worms were suspended in a small volume of EN solution and transferred to a 1.5ml Eppendorf tube.

500µl lysis buffer, 5µl of β-mercaptoethanol and 5µl of proteinase K (20mg/ml) were added and the tubes incubated at 65C with mixing every 15 minutes for the first 90 minutes followed by incubation overnight. The next morning a further 5µl β-mercaptoethanol and 5µl proteinase K was added and the tube incubated at 65C for a further 4 hours. DNA was then extracted using an ethanol precipitation by adding 1/10 volume 2.5M NaAc, 2ml 100% EtOH centrifuging for 30 minutes at 1300rpm. The pellet was washed with 70% EtOH and resuspended in 50µl TE buffer. The concentration was assayed using the NanoDrop spectrophotometer (Thermo Scientific).

2.7.3 - For Whole Genome Sequencing

To obtain large quantities of genomic DNA at higher purity, we made use of a modified version of the Quiagen Blood and Tissue Kit protocol. 10 plates of mixed-population worms were washed in 15ml PBS, centrifuged at 1000rpm for 1 minute, and the volume reduced to 2ml. This was repeated 3 times to remove unwanted material, such as bacteria. Following the final spin, the final 2ml was divided between between 3 1.5ml tubes (Eppendorf.) These were then placed on ice, and sonicated for bursts of 1-2 seconds, until the solution had a consistent thickness. The tubes were returned to ice, and the sonicator washed with distilled water each time. Added 20µl proteinase K (20mg/ml) and 200µl buffer AL to each tube, and tubes were incubated at 56°C with mixing every 15 minutes for the first 90 minutes followed by incubation overnight.

200µl 100% EtOH was added, the tube vortexed and the contents of each tube transfered to a DNEasy mini column (Qiagen), and the standard Qiagen washing protocols followed, before elution in 200µl of Quiagen buffer AE. The final concentration was assayed using the NanoDrop spectrophotometer (Thermo Scientific).

2.8 - Heatshock Treatment

To activate genes controlled by the heatshock response, larval stage 4 (L4) hermaphrodites were picked the day before the assay. To induce heatshock, the animals were placed at 33°C for one hour, followed 30 minutes at 20°C, and this was repeated. Where animals were then assessed for their response to pharmacological agents they were directly transferred to drug plates as described below.

2.9 - Aldicarb assays

2.9.2 - Acute Assay

Small (35mm) drug plates were filled with 5ml worm agar (see page 94) containing 1mM aldicarb (Greyhound Chromatography and Allied Chemicals Ltd) made using 100mM

aldicarb stock solution dissolved in 70% ethanol. They were seeded with 50µl OP50 and left to dry overnight with lids on. 40 larval stage 4 (L4) worms were picked onto clean seeded plates and left overnight at 20°C. The plates were blinded and the details recorded for future analysis.

The following day 25-30 adult animals were transferred to the small drug plates containing aldicarb and observed every 10 minutes for 100 minutes to record the number of worms that had paralysed.

Paralysis was defined as a worm that could not move any body wall muscles upon stimulation with a platinum wire. Worms which were paralysed were removed from the plate. A graph was drawn showing the percentage of paralysed animals against time.

To determine whether the effects of aldicarb were reversible, worms counted as paralysed were picked to plates without aldicarb and left to recover for two hours before their locomotion was observed by eye.

2.9.3 - Chronic Assay

Small (35mm) drug plates were filled with 5ml worm agar containing 0.2mM aldicarb. These were seeeded with 200µl OP50 and left to dry overnight with the lids on. The following day, 5 larval stage 4 (L4) hermaphrodites for each strain to be assayed were picked directly onto these plates, and left to grow and lay eggs for 5 days. At the end of this time the plates were examined by eye for the number of progeny and their stage of growth compared with wild-type animals grown under the same conditions.

2.10 - Levamisole assays

Small (35mm) drug plates were filled with 5ml worm agar containing 100µM levamisole (Sigma) made using a 100mM stock solution dissolved in S. Basal. They were seeded with 50µl OP50 and left to dry overnight with lids on. 40 larval stage 4 (L4) worms were picked onto clean seeded plates and left overnight at 20°C. The plates were blinded and the details recorded for future analysis.

The following day 25-30 adult animals were transferred to the small drug plates containing aldicarb and observed every 10 minutes for 100 minutes to record the number of worms that had paralysed.

Paralysis was defined as a worm that could not move any body wall muscles upon stimulation with a platinum wire. Worms counted as paralysed were removed from the drug plates. A graph was drawn showing the percentage of paralysed animals against time.

2.11 - Phorbol ester treatment

Small (35mm) drug plates were made, in which 2µg/ml phorbol-12-myristate-13-acetate (PMA) dissolved in DMSO and 1mM aldicarb were added to the worm agar. Control plates were also made which contained 1mM aldicarb and DMSO. These plates were not seeded.

Plates were left overnight to dry at 20°C. 40 larval stage 4 (L4) worms were picked onto clean seeded plates and left overnight at 20°C. The plates were blinded and the details recorded for future analysis. The following day 25-30 adult animals were transferred to either a plate containing

2µg/ml PMA alone or a DMSO control plate and left for 2 hours at 20°C to pre-treat. Animals from the PMA plate were transferred to the plate containing 2µg/ml PMA and 1mM aldicarb and the control animals were transferred to the 1mM aldicarb plate containing DMSO. The aldicarb assay was undertaken as described above.

Where the assay was designed to investigate the effects of PMA alone, the protocol above was used without the inclusion of aldicarb.

2.12 - Serotonin treatment

Small (35mm) drug plates were made, in which serotonin creatine sulphate (3.8mg/ml) (Sigma) were added to the worm agar. Control plates were also made which contained 1mM aldicarb and DMSO. These plates were not seeded.

2.13 - Dispersal Assay

Large (100mm) worm plates were filled with NGM worm agar, and OP50 bacteria was seeded around the very edge of the plate. The plates were left to dry overnight with the lids on.

The following day, mixed populations of the animals be assayed were washed from their plates with 15ml M9 and spun at 1000rpm for 1 minute to pellet the worms. Excess M9 was removed by gentle suction and the volume brought up to 15ml with fresh M9. This was repeated three times to remove OP50 from the worms.

All excess M9 was removed following the final spin, and the washed worms were transferred to the centre of the 100mm plates. A timer was started once the M9 droplet had evaporated, and the number of adult animals on and off food was recorded at intervals of 30, 60, 90 and 120 minutes.

2.14 - Defecation assays

L4 worms were picked the night before assaying. The resulting adults were transferred onto clean seeded plates and left for 5 minutes to recover. An individual animal was then observed for between 5 and 10 minutes and the time recorded every time the pBoc and Exp phase of the defecation cycle (Avery 1997) were observed using the Ethotimer software (J. Thomas, University of Washington). If an animal moved off the bacterial food in this time, the assay was terminated at that point. The average intervals between pBoc and Exp steps was calculated.

2.15 - Swimming Assays

2.15.2 -Average thrashing assay

Animals were picked the day before the experiment as larval stage 4 (L4) and left to grow overnight on fresh plates. The following day each animal to be assayed was placed into a drop of M9 buffer pipeted onto a 22mm X 50mm cover slip, using a flamed platinum wire, and left to recover for three minutes. The number of body bends was then assayed for a period of two minutes for each animal.

2.15.3 -Intial thrashing assay

Larval stage 4 animals were used for this assay. Each animal to be assayed was transferred directly into a drop of M9 buffer pipeted onto a 22mm X 50mm cover slip, and the number of body bends in the first five seconds following immersion were counted. If the animal performed 2 or more body bends it was recorded as ‘thrashing’; if it failed to perform 2 body bends it was recorded as ‘not thrashing’. 15 to 20 animals were used for each assay, and the percentage thrashing was recorded.

2.16 - Worm length assay

Worms were staged by picking larval stage 4 (L4) animals one day before the experiment. Images were taken using a Hammamatsu camera attached to a Leica dissecting scope at consistent magnification, and recorded using the MicroManager add-on to ImageJ (NIH). Worm length was determined in ImageJ by drawing a series of straight lines from the visible tip of the head to the visible tip of the tail, not including the long whip-like structure present in hermaphrodites, and then repeating this measurement, starting at the tip of the tail to the tip of the head. An average was taken of these two measurements. At least 20 animals were measured per experiment.

Width was measured at the widest point across the mid-section of the worm including the vulva, but this measurement was not used in the analysis.

2.17 - Parallel worm tracking

We made use of software developed by Daniel Ramot of the Goodman lab (Ramot, Johnson et al. 2008) to measure the speed of multiple animals and assess the effects of serotonin and PMA. Larval stage 4 animals were picked the day prior to the experiment, and small (35mm) plates were prepared with small (50µl) OP50 lawns in the centre. The plates must be very clear for optimum image processing; any plates containing dark deposits of cholesterol or clumped bacterial lawns were not used.

Animals were transferred to the plates at a point away from the OP50 lawn, and allowed to recover for 5 minutes. Videos were taken using a Hammamatsu camera attached to a Leica dissecting scope and captured using the MicroManager add-on to ImageJ (NIH).

2.18 - Bacterial protocols

2.18.2 - Transformation of chemically competent cells

A 50 µl aliquot of the chemically competent E. coli DH10β was defrosted on ice. 450µl of ice-cold 100mM $CaCl_2$ was added and the solution divided into 5 100µl aliquots. Approximately 10µl of a 20µl ligation mix (see below), or 10ng of plasmid, were added and the mixture placed on ice for 5 minutes. The bacteria were heatshocked for 2 minutes at 37°C and briefly returned to ice. 200 µl LB broth was added and the bacteria grown for 1 hour at 37°C. The bacteria were then plated onto an LB agar plate with the appropriate selection antibiotic (ampicillin at 100µg/ml, kanamycin at 25µg/ml or tetracycline at 50µg/ml) and incubated overnight at 37°C.

2.18.3 -Isolation of plasmid DNA from bacteria

Individual bacterial colonies were picked using a sterile inoculation loop and used to inoculate LB broth cultures grown at 37°C overnight with the appropriate selection antibiotic. For small scale isolation 2ml cultures were grown and the bacteria harvested by centrifugation at 1300rpm for 2 minutes. The bacteria were resuspended in 50 µl of Solution I, to which 150µl of Solution II (TENS buffer) was added, followed by 100µl of Solution III (3M sodium acetate, pH5.2). The DNA was precipitated, washed and purified using 96% EtOH and resuspended in 50 µl TE buffer with RNAse. Large-scale DNA preparations were performed using 200ml bacterial cultures and the QIAgen midi filter kit. The DNA was resuspended in TE buffer. The concentration of DNA was determined using the NanoDrop spectrophotometer (Thermo Scientific).

2.18.4 -Restriction digestion and ligation of DNA

5µg DNA was digested with 10 units of restriction enzyme (New England Biolabs or Promega) at 37°C for 2 hours unless otherwise stated. Digests were run on 1% agarose gel made with 1x TBE buffer containing 75µl ethidium bromide per 100ml of agarose gel to visualise the DNA. The DNA band was cut from the gel, cleaned using QIAquick gel extraction kit (QIAgen) and resuspended in 50µl TE buffer. Ligations were performed using T4 Quick Ligase (New England Biolabs) as per manufacturer's instructions.

5µg of purified digested vector DNA, 5µg of purified digested insert DNA, ligase buffer and 2,000 units of T4 Quick Ligase were incubated at RT for 15 minutes and then placed on ice ready for transformation.

2.19 - Polymerase Chain Reaction (PCR)

2.19.2 -Standard PCR - e.g. for sequencing unc-80 genomic regions

10pmol of each primer, 0.2mM dNTP mix, 2.5 units Taq polymerase and 1mM $MgCl_2$ were used unless otherwise stated. Sigma Taq Polymerase was used in all PCR reactions where the product was used diagnostically or for sequencing. The same PCR programme was used for all reactions with changes in the annealing temperature and extension time for different primer sets.

1) 95°C 3 minutes

1) 95°C 45 seconds

1) Annealing temperature (from 55-65°C, depending on program) 40 seconds

1) 72°C extension time

1) Back to step 2, repeat 35 times

1) 72°C 10 minutes (final extension)

1) 4°C hold

The extension time was calculated as 1 minute per 1kb of DNA being amplified rounded up to nearest 30 seconds. The annealing temperature was determined by trial and error beginning at 60°C - increasing due to non-specific amplification and decreasing due to no amplification until the correct temperature for specific amplification was found.

2.19.3 - PCR for cloning using Phusion

10pmol each primer, 0.2mM dNTP mix, 1x Phusion HE buffer, containing 1mM $MgCl_2$ (Buffer GC was used on some more difficult genomic templates), 1 unit Phusion Hot Start DNA polymerase and 1mM $MgCl_2$ were used unless otherwise stated. Phusion

polymerase (New England Biolabs) was used for all cloning as it has a significantly lower error rate than standard Taq polymerase. The same PCR programme was used for all reactions with changes in the annealing temperature and extension time for different primer sets.

1) 98°C 30 seconds
2) 98°C 10 seconds
3) Annealing temperature (from 55-65°C, depending on program) 30 seconds
4) 72°C extension time (30 seconds per kb)
5) Back to step 2, repeat 30-35 times
6) 72°C 10 minutes (final extension)
7) 4°C hold

2.19.4 -Site-directed mutagensis using Quikchange

Site-directed mutations were introduced into plasmids using the Quikchange II protocol from Agilent Technologies. 10pmol each primer, 0.2mM dNTP mix, 1x reaction buffer, containing 1mM $MgCl_2$, 2.5 units Pfu Ultra High Fidelity DNA polymerase were used in a PCR reaction along with 50 ng of the plasmid template to be mutated.

1) 95°C 30 seconds
2) 95°C 10 seconds
3) 55°C 1 minute
4) 68°C extension time (1 minute per kb of plasmid)
5) Back to step 2, repeat 18 times
7) 4°C hold

Following the PCR reaction, 10 units of DpnI restriction enzyme were added to the reaction mix, mixed thoroughly, and incubated at 37°C for 1 hour to digest the template DNA. 1 µl of the digestion mix was used to transform XL1 Blue supercompentent cells using a heat pulse: 45 seconds at 42°C and then place the reactions on ice for 2 minutes. Cells were grown in 0.5 ml of L Broth for one hour at 37°C, and the entire mix was spread onto a plate containing an appropriate selection marker.

2.20 - Sequencing of DNA

2.20.2 -Short read sequencing

200ng of purified DNA in water was dried down. This was sent to MWG Biotech with 10ng of the desired primer for sequencing. Value read sequencing was used. The sequence, clipped by MWG for sequence purity, was blasted against the known sequence using NCBI Blast to identify any base pair changes.

2.20.3 -Whole Genome Sequencing (WGS)

Whole Genome Sequencing was performed by GeneService. We purified DNA using the method above (2.6.2), and sent DNA from four mutants for sequencing. QT317 was generated by UV/TMP mutagenesis and contains allele *nz90* which confers resistance to aldicarb, and was identified by Emma Hiley, a previous PhD student in our lab (Hiley, 2006). We also sequenced three suppressors of the loopy locomotion of nRHO-1* - QT677 (*nz99*), QT788 (*nz97*) and QT834 (*nz110*) which were generated by EMS mutagenesis (see Chapter 3).

2.21 - Analysis of Whole Genome Sequencing Data

2.21.2 - Analysis of Geneservice Data

The data obtained from Geneservice included an Excel spreadsheet containing a list of all the single nucleotide polymorphisms (SNPs) predicted from analysis of the short reads by the program MAQ (Mapping and Assembly with Quality) (Li, Ruan et al, 2008). This did not contain biologically relevant information, i.e. whether the mutations affected protein-coding regions and were non-silent mutations.

To filter mutations which are likely to be background mutations in some or all of the strains, the first step was to assign a unique code to each mutation. This was done using Excel, with the formula

```
=C2&"_"&D2&"_"&F2
```

where C2 is the chromosome name, D2 is the position of the mutation, and F2 is the mutant base. We made the assumption that if all three factors are identical between two or more strains then the mutation can be counted as a background mutation. Anything common between QT317 and any other mutant is almost certainly a background mutation, as this strain was created several years before the others, does not contain the nRHO-1* transgene and was not EMS mutagenised, unlike QT677, QT788 and QT834. Anything common between the other mutants is also likely to be a background mutation, but there is a small possibility that it could represent a real, common base change that may have a suppressive effect.

To compare these codes between different mutants requires a further Excel formula:

```
=MATCH(G2,QT317_Mutations,0)
```

where G2 is the unique code generated for a particular mutation, QT317_Mutations is an array containing all the unique codes for strain QT317, and 0 specifies that only exact matches be returned as positive hits. This formula can be added to each row for each mutation in each mutant, to produce columns listing whether a mutation is present in any

of the other mutants being screened. The formula will return #N/A if no match is found; otherwise it will return a number referring to the row on which a match has been found.

This result can be used to filter for only those mutations which have no match in any of the other strains sequenced.

Once filtered, the position of the point mutations (Chromosome number and base on the chromosome) can be run through the UCSC Genome Browser (http://genome.ucsc.ed) and this will only return an output if the position corresponds to part of an annotated region - i.e. an exon, intron or 5'/3' UTR of a gene. This can be used to filter the list of mutations to only those which affect protein-coding regions, for example.

The output for each gene from the UCSC Genome browser also contains a list of intron/exon boundaries relative to the start codon of the gene. Deducting the genomic position of the start codon from the mutated base position and comparing it to this list allows us to identify whether a mutation affects an exon or an intron, and to filter only for exonic mutations.

For each mutation affecting an exon, we downloaded the cDNA sequence and used custom Excel formulas to extract the relevant codon. We then substituted the mutated base into the appropriate position in the codon (1,2 or 3), translated this mutated codon, and compared it to the wild-type codon to determine whether the mutation caused a silent or non-silent change in the protein sequence.

This analysis was performed for data from QT834, and a number of problems prevented it being rolled out to the other mutants. Firstly, the extraction of data from the UCSC Genome Browser was often incomplete (we believe this is because the browser does not have access to the most up-to-date genome annotations for the *C. elegans* genome) and therefore we miss a number of potential mutations at the start of the analysis. Secondly, due to a bug in the formulas used the predictions were often inaccurate when compared with the data on Wormbase, especially for genes transcribed from the minus strand of DNA. Finally, we uncovered a systematic error in the Geneservice data which meant that the position of the mutated base was shifted by one base compared with the wild-type genome. Thus a different program was used for analysis.

2.21.3 -Analysis using MAQGene

From GeneService we obtained both the raw data (36bp, 55bp and 76bp paired-end reads) and the results of running that data through MAQ. We had doubts about the reliability of this bioinformatic data, and re-analysed the raw data ourselves.

With the help of Janos Kriston-Vizi of the Kettler lab at the MRC LMCB, we installed MAQGene, developed in the Hobert lab (Bigelow, Doitsidou et al. 2009). MAQGene allows a user to run the program MAQ without accessing the Linux command line. Within MAQGene, the MAQ-specific commands are entered into a user-friendly webpage-format, MAQGene generates all MAQ-specific files, and produces a list of SNPs, similar to that obtained from Geneservice.

Additionally, MAQGene then interrogates these SNPs using its own specific parameters, and then maps those that pass these thresholds onto an annotated database of the worm genome. This database can be updated to hold the most up-to-date release of the *C. elegans* genome.

We ran MAQGene using the default settings detailed from the Hobert lab in their publications using their latest paramater for filtering hits - fraction of wild-type reads - at 0.86 (Bigelow, Doitsidou et al. 2009; Sarin, Bertrand et al. 2010).

The setting " Maximum sum of error qualities" is used to assess the likelihood that a particular mismatch is due to sequencing error. Each sequenced base is given a quality score based, and the authors of MAQGene recommend a setting of 100 for 36bp reads. However, our data set incudes 36, 55 and 76bp reads; longer reads could be allowed to accumulate more errors than shorter ones and still be valid. However, we are unable to specific settings for individual read lengths, and therefore left this setting at 100. This means that some longer reads have been discounted. We have yet to determine a way to run the data sets individually and then successfully recompile them for analysis.

2.21.4 -Filtering MAQGene output for background mutations

The final output from MAQGene is a list of SNPs and small deletions referred to as indels, detailing both their position in the genome, any genes which are affected by the predicted changes, and the nature of those changes – for instance, introducing premature STOP codons, or creating read-through mutations. We filtered for mutations using the same Excel formulas developed to filter the Genservice data (section 2.19.1).

2.21.5 -Matching mutations to gene names

The output from MaqGene references each mutation to the gene it hits/nearest exon etc, and outputs the orf details – i.e. the designation refers to the particular position on the cosmid on which that gene is found.

To make the data set more user-friendly, we wanted to translate these into the more common Sanger Gene names, and to add links out to WormBase.

To do this we input the list of open reading frames into the UCSC Genome Browser. MAQGene outputs a column called 'parent features' which contains the names of all the ORFs which are affected by a specific mutation. Excel's 'Text-to-Columns' feature was used to separate these into individual columns, and the data from the first column as be entered into the UCSC Genome Browser, in the 'Identifiers' box of the OrfToGene table, with the species set to Nematode and the C. elegans database chosen.

[For some reason, not all of the identifiers are matched in the Table Browser, so for Q317 Run I we get an error message like this:

Note: 35 of the 871 given identifiers (e.g. C04B4.1.1) have no match in table orfToGene, field name. Try the "describe table schema" button for more information about the table and field.

I think this is because the Table Browser doesn't have access to the most recent annotations of the genome; the majority are found however. Missing names can be found manually by searching Wormbase which has the most up-to-date genome annotations.]

The output from UCSC Genome Browser is sorted alphabetically, so to match them to their gene of origin we can use another Excel formula:

```
=VLOOKUP(V2,QT317_ID,2,FALSE)
```

where V2 refers to the particular mutation which we wish to match to a gene name, QT317_ID is the range containing the gene names; the number 2 tells the formula to look in the second column after finding a match in the first, and FALSE tells Excel to only look up exact matches.

To generate a hyperlink to the Wormbase reference for the gene of interest, the following two formulas were used. In the first cell (X2) we entered:

```
="http://www.wormbase.org/db/gene/
gene?name="&V2&";class=Gene"
```

where V2 contains the specific ORF details, and the surrounding details create the correct format for a link to Wormbase. Then in the adjacent cell, Y2, we entered: SJN466v

```
=Hyperlink(X2,U2)
```

where X2 is the link generated above and U2 is the Sanger gene name determined earlier. This creates an efficient way to link between the sequencing data and the gene details.

2.21.5.2 - Finding regions of high mutational frequency

During outcrossing, the region around the causative mutation is likely to contain a higher frequency of mutations than the rest of the genome due to unlinked mutations being lost during recombination. To search for regions with high levels of mutation we filtered the sequencing data for mutations which occur in 100% of the reads, contain only the classical G/C to A/T mutation which results from EMS, and had a quality score above 20. We then produced a histogram of this data to identify regions of high mutational frequency.

2.22 - Making UNC-80 rescuing constructs

The most complete cDNA of *unc-80* is on plasmid yk1260h6, which we obtained as a gift from Yuji Kohara. However, sequencing of this plasmid revealed that the 3' end of the cDNA is not consistent with the published sequence of *unc-80* cDNA.

We therefore decided to produce an *unc-80* minigene, constructed partly from the wild-type 5' end of the cDNA and partly from genomic DNA.

Primers UNC-80.63 and UNC-80.64 were used to clone the whole yk1260h6 by PCR. UNC-80.63 introduces a KpnI site 5' of the start condon and a NotI site just 3' of the start codon (which can be used to introduce protein tags such as GFP), while UNC-80.64 introduces a SacI site 3' of the STOP codon. The product was digested with KpnI and SacI and subcloned into a Bluescript vector cut with SacI and KpnI (plasmid SJN455).

The KpnI/SacI fragment was digested from SJN455 and subcloned into plasmid psc#205, which contains the *acr-2* promoter, cut with KpnI and SacI, and named SJN463. The *unc-80* cDNA contains an internal BlpI site, before which the sequence is wild-type.

The genomic sequence of *unc-80* from this BlpI site to the STOP codon was amplified from a *cyk-2* genomic DNA template as a substitute for the mutated cDNA sequence. Primers UNC-80.53 and UNC-80.64 were used, which cover the internal BlpI site, and introduce a SacI site 3' of the STOP codon.

SJN463 was digested with BlpI and SacI to excise the mutated cDNA sequence, while the genomic DNA PCR product was digested with BlpI and SacI, and ligated into the cut SJN463 vector. This new plasmid is *acr-2*-driven UNC-80 minigene, and was named SJN467. The unc-80 minigene in this plasmid was sequenced and found to be wild-type.

SJN467 was digested with NotI (which cleaves just after the start codon) and with SpeI and ligated into vector QT#220 cut with NotI and SpeI, which excises *p.unc-17*-driven RHO-1 from this vector. This ligated product, named SJN469, *unc-80* expression from the same vector as the nRHO-1* transgene used in this thesis.

The KpnI-SacI fragment of SJN467, containing the unc-80 minigene, was inserted into QT#42 cut with KpnI-SacI to produce a heat-shock driven unc-80 minigene, expressed from the same vector backbone as the heat-shock driven RHO-1* used in this thesis. This new plasmid was named SJN470.

The KpnI-SacI fragment of SJN467, containing the *unc-80* minigene, was inserted into QT#237 cut with KpnI-SacI to produce a synaptobrevin-driven *unc-80* minigene, and this new plasmid was named SJN471.

Plasmids SJN467, SJN469, SJN470 and SJN471 were modified to produce GFP fusion proteins by digesting the plasmid backbones with NotI and inserting the NotI fragment of KP#295, which contains the Fire GFP sequence with introns. These plasmids where named SJN483, SJN477, SJN479 and SJN481 respectively.

Plasmids SJN467, SJN469, SJN470 and SJN471 were modified to produce mCherry fusion proteins by digesting the plasmid backbones with NotI and inserting the NotI fragment of SJN445, which contains the mcherry cDNA sequence.. These plasmids where named SJN483, SJN478, SJN480 and SJN482 respectively.

2.23 - Making a constitutively active PKC-3 construct

We obtained three *pkc-3* cDNAs as gifts from Yuji Kohara - YK1447b7, YK284f7, YK526h11 – and grew these according to standard methods. These plasmids were miniprepped as detailed above, and used as a template for a PCR reaction to amplify the full-length cDNA of PKC-3. Primers PKC-3.1 and PKC-3.2 were used to amplify the coding region, and introduced unique NcoI and SacI sites at the 5' and 3' ends of the cDNA for further subcloning. PKC-3.1 also introduces a unique NotI site at the 5' end, just after the start codon, which can be used for the introduction of protein tags such as GFP.

PCR from YK526h11 produced a band of the predicted size (1800bp) for full-length *pkc-3* cDNA. When this was digested with NheI as a diagnostic test for *pkc-3* this digestion produced two bands of approximately 1200bp and 700bp, as predicted.

The *pkc-3* cDNA fragment was subcloned into plasmid pSC#205, which contains the *acr-2* promoter, which drives expression in the cholinergic neurons of C. elegans and some interneurons (Jospin, Qi et al, 2009). Diagnostic digests with NotI and SacI suggested that this cloning had been successfully accomplished, and the plasmid, APP001 was sent for sequencing, using primers PKC-3.3, PKC-3.4, PKC-3.5 and PKC-3.6.

To generate a constiutively active PKC-3 protein we used site-directed mutagenesis, following the QuikChange protocol, to modify APP001. Primers PKC-3.7 and PKC-3.8 were used to change an alanine at position 116 in the protein to glutamate, with a base change in the cDNA from GCT to GAG. These primers also introduce a silent mutation which produces a unique SacII site, which is diagnostic for successful site-directed mutagenesis. Digests of the plasmid indicated that this mutation had been successfully introduced. This plasmid was named APP002.

However, when the sequencing reactions returned, we noticed that the YK526h11 cDNA from whcih we had obtained cDNA of PKC-3 was not wild-type at the 5' end. We sequenced the other cDNA clones we had obtained, and established that YK447b7(b) had a wild-type coding sequence over these regions. We were able to make use of the the novel SacII restriction site which we introduced as a marker for the QuikChange reaction to allow swapping of 5' end of our mutant cDNA for the wildtype version found in the YK447b7(b). We therefore used PCR to amplify the relevant section of YK447b7(b) using primers PKC-3.7 and PKC-3.2, digested this product and the APP002 plasmid using SacII and SacI, and ligated these products to make a fresh constitutively active PKC-3 plasmid. This construct was named APP003.

2.24 - Making constitutively active and dominant negative CDC-42 constructs

Oligos CDC-42.1 and CDC-42.2 were used to PCR the CDC-42 cDNA from plasmid yk1443h08 (a gift from Yuji Kohara) which contains full-length CDC-42 cDNA. The PCR product was digested with NheI and SacI and subcloned into vector pPD49_73 (containing the heat-shock promter) which had also been cut with NheI and SacI. This was sequenced and shown to contain no mutations, and the plasmid was named SJN379. The PCR product was also subcloned into vector pSC#205 (containing the *acr-2* promoter) which had been cut with NheI and SacI. This was also sequenced with primers CDC-42.1 and CDC-42.2 and shown to contain no mutations, and the new plasmid was named SJN381.

To produce a constiutively active version of CDC-42, we performed site-directed mutagenesis using the Quickchange protocol and primers CDC-42.3 and CDC-42.4 primers, which introduce the mutation G12V, and also create a silent SfcI site as a marker of successful site-directed mutagenesis. These primers were used to modify plamsids SJN379 and SJN381 to produce constitutively-active CDC-42 driven by the *acr-2* promoter (APP004) and from the heatshock promoter (APP006). These plasmids

were sequenced with primers CDC-42.1 and CDC-42.2 and found to contain the G12V mutation and the SfcI site.

To produce a dominant negative version of CDC-42, we performed site-directed mutagenesis using the Quickchange protocol and primers CDC-42.5 and CDC-42.6, which introduce the mutation T17N and also create a silent AccI site as a marker of successful site-directed mutagenesis. These primers were used to modify plasmid SJN379 to produce dominant negative CDC-42 driven by the heatshock promoter (APP005). This plasmid was sequenced with primers CDC-42.1 and CDC-42.2 and found to contain the T17N mutation and the AccI site, as well as an additional silent mutation in the coding sequence.

2.25 - Solutions and buffers

2.25.5.2 - Worm NGM agar

20.8g/litre agar
2.34g/litre Bacto-peptone
50mM NaCl
Autoclave then add:
0.25M potassium phosphate
1mM $MgSO_4$
1mM $CaCl_2$
5µg/ml cholesterol
200µg/ml streptomycin
10µg/ml nystatin

2.25.5.3 - M9 buffer

0.02M KH_2PO_4
0.04M Na_2HPO_4
0.09M NaCl
0.01M $MgSO_4$

2.25.2 -Worm freezing agar

0.1M NaCl
0.05M KH_2PO_4
300g/litre glycerol
0.05M NaOH
Autoclave then add:
3mM $MgSO_4$
4g/litre Bacto-agar

T.E. Buffer

10mM Tris/Cl

1mM EDTA

2.25.3 -EN solution

10mM EDTA

100mM NaCl

Worm lysis buffer

130mM Tris pH8.5

1% SDS

50mM EDTA

0.1M NaCl

2.25.4 -S. basal

0.1M NaCl

0.05M potassium phosphate (pH6)

5mg/litre cholesterol

2.25.5 -Single worm PCR lysis buffer:

10mM Tris pH8.0

50mM KCl

2.5mM $MgCl_2$

0.45% Igepal

0.45% Tween 20

0.01% gelatin

(Stored at 4^{o}C)

2.25.6 - TBE (Tris-Borate EDTA) buffer

0.089M Tris Base

0.089M Boric acid

2mM EDTA

2.25.7 -Transformation buffer 1 (TFB1)

30mM KOAc

100mM RbCl

10mM $CaCl_2$

50mM $MnCl_2$

2.25.8 -Transformation buffer 2 (TFB2)

10mM MOPS

75mM $CaCl_2$

10mM RbCl

15% v/v glycerol

2.25.9 -L broth

1% Bacto-tryptone
0.5% Bacto-yeast extract
10mM NaCl
(Stored at 4°C)

2.25.10 - LB agar

1% Bacto-tryptone
0.5% Bacto-yeast extract
10mM NaCl
1.5% Bacto-agar
(Stored at 4°C)

2.25.11 - TENS buffer

1mM Tris/Cl pH7.5
1mM EDTA pH8
0.1N NaOH
0.5% SDS

Table 2.1 List of strains used or referenced in this thesis

Strain	Geneotype	Made By	Notes and Comments
CB1068	unc-79(e1068)III.	CGC	Unc-fainter. Stops. Stiff anterior.
CB1069	unc-80(e1069)V.	CGC	Unc-stiff anterior.
CB4856	C. elegans wild type, CB subclone of HA-8 (Tc1 pattern IX).	CGC (20/3/01)	Isolated from a pineapple field in Hawaii in 1972 by L. Hollen.Wild type. Low copy Tc1; pattern IX.
N2	wildtype (08/04/2009)	CGC	C. elegans wild type, DR subclone of CB original (Tc1 pattern I).
NM979	unc-64(js115)/bli-5(e518) III.	CGC	Heterozygotes are WT and segregate WT, Bli and L1 arrestedparalyzed animals (js115 homozygotes). Well balanced.
QT47	nzIs1 *4 I	nuz	nzIs1 [QT#42(h.s. rho-1 (G14V)); ttx-3::gfp]
QT309	nzIs29 *2		
QT622	nzEx304 [rjm050;KP307]	Rachel	Expresses G14V, F25N RHO-1 from the heatshock promoter. line 11.3
QT623	nzEx305 [rjm050;KP307]	Rachel	Expresses G14V, F25N RHO-1 from the heatshock promoter. line 11.6
QT631	nzIs1;nzIs29	Rachel	line 7.1.3
QT670	nzIs1;nzIs29;nz92	Rachel	Isolated as non-loopy suppressor of nzIs29 and nzIs1 following EMS mutagenesis of QT631
QT671	nzIs1;nzIs29;nz93	Rachel	Isolated as non-loopy suppressor of nzIs29 and nzIs1 following EMS mutagenesis of QT631
QT672	nzIs1;nzIs29;nz94	Rachel	Isolated as non-loopy suppressor of nzIs29 and nzIs1 following EMS mutagenesis of QT631
QT673	nzIs1;nzIs29;nz95	Rachel	Isolated as non-loopy suppressor of nzIs29 and nzIs1 following EMS mutagenesis of QT631
QT674	nzIs1;nzIs29;nz96	Rachel	Isolated as non-loopy suppressor of nzIs29 and nzIs1 following EMS mutagenesis of QT631
QT675	nzIs1;nzIs29;nz97	Rachel	Isolated as non-loopy suppressor of nzIs29 and nzIs1 following EMS mutagenesis of QT631
QT676	nzIs1;nzIs29;nz98	Rachel	Isolated as non-loopy suppressor of nzIs29 and nzIs1 following EMS mutagenesis of QT631
QT677	nzIs1;nzIs29;nz99	Rachel	Isolated as non-loopy suppressor of nzIs29 and nzIs1 following EMS mutagenesis of QT631
QT678	nzIs1;nzIs29;nz100	Rachel	Isolated as non-loopy suppressor of nzIs29 and nzIs1 following EMS mutagenesis of QT631
QT679	nzIs1;nzIs29;nz101	Rachel	Isolated as non-loopy suppressor of nzIs29 and nzIs1 following EMS mutagenesis of QT631
QT680	nzIs1;nzIs29;nz102	Rachel	Isolated as non-loopy suppressor of nzIs29 and nzIs1 following EMS mutagenesis of QT631
QT683	nzIs1;nzIs29;nz104	Andrew	Isolated as non-loopy suppressor of nzIs29 and nzIs1 following EMS mutagenesis of QT631
QT684	nzIs1;nzIs29;nz105	Andrew	Isolated as non-loopy suppressor of nzIs29 and nzIs1 following EMS mutagenesis of QT631
QT685	nzIs1;nzIs29;nz106	Andrew	Isolated as non-loopy suppressor of nzIs29 and nzIs1 following EMS mutagenesis of QT631
QT686	nzIs1;nzIs29;nz107	Andrew	Isolated as non-loopy suppressor of nzIs29 and nzIs1 following EMS mutagenesis of QT631
QT687	nzIs1;nzIs29;nz108	Andrew	Isolated as non-loopy suppressor of nzIs29 and nzIs1 following EMS mutagenesis of QT631
QT688	nzIs1;nzIs29;nz109	Andrew	Isolated as non-loopy suppressor of nzIs29 and nzIs1 following EMS mutagenesis of QT631
QT700	nzIs1;nzIs29;nz110	Andrew	Isolated as non-loopy suppressor of nzIs29 and nzIs1 following EMS mutagenesis of QT631
QT701	nzIs1;nzIs29;nz111	Andrew	Isolated as non-loopy suppressor of nzIs29 and nzIs1 following EMS mutagenesis of QT631

QT738	nzIs1;nz94	Rachel	QT094 and QT672
QT739	nzIs1;nz98	Rachel	QT094 and QT676
QT748	nz94;nzIs29	Rachel	nz94 rho-1 suppressor backcrossed 1 time. nzIs1 has been lost. QT733 crossed with QT672
QT749	nz97;nzIs29	Rachel	nz97 rho-1 suppressor backcrossed 1 time. nzIs1 has been lost. QT733 crossed with QT675
QT750	nz98;nzIs29	Rachel	nz98 rho-1 suppressor backcrossed 1 time. nzIs1 has been lost
QT759	z94;nzIs29*2	Rachel	QT748 backcross
QT760	nz97;nzIs29*2	Rachel	QT749 backcross
QT761	nz98;nzIs29*2	Rachel	QT750 backcross
QT775	nz98;nzIs29	Rachel	rho-1 suppressor nz98 backcrosses three times through nzIs29
QT782	z94;nzIs29	Rachel	rho-1 suppressor nz94 backcrossed three times through nzIs29
QT788	nz97;nzIs29	Rachel	rho-1 suppressor nz97 backcrosses three time through nzIs29
QT804	nz110; nzis29 1*	Andrew	This strain is him. nz110 1x backcross. QT700 crossed with QT733.
QT812	nz108; nzis29 1*		nz108 1x backcross. QT687 crossed with QT733
QT813	nz108; nzis29 1*		This strain is nz108 1x backcross. Produces males. QT687 crossed with QT733.
QT816	nz110;nzis29 2*	Andrew	This strain is 2x backcrossed nz110. QT804 crossed with QT733
QT821	nz107; nzis29 1*	Andrew	1x backcrossed. QT686 crossed with QT733. Non-loopy.
QT822	nz107; nzis29 1*	Andrew	1x backcrossed. Produces males. QT686 crossed with QT733. Non-loopy.
QT823	nz105; nzi29 1*	Andrew	1x backcrossed. QT684 crossed with QT733
QT824	nca-2(gk5); nzis29	Andrew	non-loopy; nca-2 mutation appears to suppress nRho-1*. VC9 crossed with QT733
QT825	nca-1(gk9); nzis29	Andrew	non-loopy; nca-1 mutation appears to suppress nRho-1*. QT816 crossed with QT733. 3x backcrossed
QT826	unc-64(js115);nzEx454[SJN367;cc:gfp]	Andrew	Same as QT930; use strain QT930 instead for consistency. NM979 injection. CC::GFP marker
QT827	unc-64(js115);nzEx454[SJN368;ttx-3:gfp]	Andrew	One of several successfully rescued animals from the nm979 injections with this construct. This came from injection gamma-1.
QT828	unc-64(js115);nzEx454[SJN368;ttx-3:gfp]	Andrew	One of several successfully rescued animals from the nm979 injections with this construct. This came from injection 53.1.1.
QT829	nz94; nzIs33	Rachel	Suppressor of p.unc-17::rho-1* loopy locomotion
QT830	nz94	Rachel	Suppressor of p.unc-17::rho-1* loopy locomotion
QT831	nz94; him-5	Rachel	Suppressor of p.unc-17::rho-1* loopy locomotion
QT832	nz98	Rachel	Suppressor of p.unc-17::rho-1* loopy locomotion
QT834	nz110; nzis29	Andrew	non-loopy
QT834	nz110; nzis29	Andrew	Non-loopy. 3x backcrossed
QT835	nz108; nzis29 2*	Andrew	2x backcrossed. QT813 crossed with QT309. Non-loopy
QT838	unc-64(js115);nzEx454[SJN368;ttx-3:gfp]	Andrew	One of several successfully rescued animals from the nm979 injections with this construct. This came from injection 7.6.
QT838	unc-64(js115);nzEx454[SJN368;ttx-3:gfp]	Andrew	One of several successfully rescued animals from the nm979 injections with this construct. This came from injection 7.6.

QT839	unc-64(js115);nzEx454[SJN368;ttx-3:gfp]	Andrew	One of several successfully rescued animals from the nm979 injections with this construct. This came from injection 7.13.
QT840	unc-79(e1068); nzis29	Andrew	Non-loopy, unc-79 appears to suppress nRho-1*. CB1069 and QT733
QT841	unc-80(e1069);nzis29	Andrew	Non-loopy. CB1069 crossed with QT733
QT842	nca-2(vc9);nzis29	Andrew	VC9 crossed with QT733
QT854	nzEx401 [rjm039;QT238]	Rachel	n:F25N G14V RHO-1
QT869	nzIs29;nz92*1 [labelled 689]	Rachel	NB this tube is mislabelled as QT689
QT902	nz101;nzIs29*2	Rachel	nz101 was backcrossed through nzIs29 twice and non-loopy animals were isolated
QT930	unc-64(js115);nzEx465 [SJN367;cc:gfp]	Andrew	Non-blister, which suggests construct rescues unc-64 lethality. From injection h.1.d.
QT931	unc-64(js115);nzEx466 [SJN368;ttx-3:gfp]	Andrew	Animals are non-blister, suggesting that the construct rescues the unc-64 lethality.
QT931	unc-64(js115);nzEx466 [SJN368;ttx-3:gfp]	Andrew	Animals are non-blister, suggesting that the construct rescues the unc-64 lethality.
QT931	unc-64(js115);nzEx466 [SJN368;ttx-3:gfp]	Andrew	Animals are non-blister, suggesting that the construct rescues the unc-64 lethality.
QT947	nzEx474[SJN447;KP#307] (18.3)	Andrew	This is the mouse modified estrogen receptor bound to C3 toxin. This strain is designed to only have activated C3 in the presence of tamoxifen. N2 Injection
QT948	nzEx475[SJN447;KP#307] (8.2.9)	Andrew	This is the mouse modified estrogen receptor bound to C3 toxin. This strain is designed to only have activated C3 in the presence of tamoxifen. N2 injection
QT949	nzEx476[SJN447;KP#307] (12.1)	Andrew	This is the mouse modified estrogen receptor bound to C3 toxin. This strain is designed to only have activated C3 in the presence of tamoxifen. N2 injection
QT950	nzEx477[SJn368;ttx-3]; tom-1 (ok285) (2.6.5)	Andrew	Looking for changes in the locomotion/acetylcholine release of tom-1 mutants in the presence of the phosphomimetic form of syntaxin. No changes yet detected; animals are NOT paralysed - unlike unc-64 animals rescued with this plasmid (i.e does not appear to be dominant.) Injection into tom-1 (ok285)
QT951	nzEx478[SJn368;ttx-3]; tom-1 (ok285) (1.69)	Andrew	Looking for changes in the locomotion/acetylcholine release of tom-1 mutants in the presence of the phosphomimetic form of syntaxin. No changes yet detected; animals are NOT paralysed - unlike unc-64 animals rescued with this plasmid (i.e does not appear to be dominant.)
QT952	nzEx479[SJN368;ttx-3]	Andrew	Looking for effect of syntaxin phosphomimetic form in a wild-type background.
QT953	nzEx480[APP4;QT#238]	Andrew	p.acr-2::cdc-42* (G12V) injected into wild-type animals.
QT954	nzEx481[App6;QT#238]	Andrew	hs-cdc-42*(G12V) injected into N2 animals.
QT955	nzEx[SJN376;QT#238]	Andrew	hs-cdc-42 (WT) injected into N2 animals.
QT958	unc-77(e625)IV, nz112	CGC	This strain supposed to be loopy - however, was seen to have more of a 'fainter' phenotype after thawing (like unc-80). Crossing with him-5 produced loopy animals in the F1 generation, which suggests the presence of a suppressor (which we are calling nz112, isolated presumably by accident in the lab).

QT1081	zEx534[SJN477;ttx-3];nzIs29;unc-80(e1069)	Andrew	Strain expresses GFP-tagged UNC-80 from a minigene construct under control of the unc-17 promoter. Rescues the loopy locomotion of nzIs29 animals that had been suppressed by loss-of-function of unc-80. Injection into QT841
QT1082	nzEx535[SJN477;ttx-3];nzIs29;unc-80(e1069)	Andrew	Strain expresses GFP-tagged UNC-80 from a minigene construct under control of the unc-17 promoter. Rescues the loopy locomotion of nzIs29 animals that had been suppressed by loss-of-function of unc-80. Injection into QT841
QT1083	nzEx536[SJN478;ttx-3;KP#307];nzIs29;unc-80(e1069)	Andrew	Strain expresses mCherry-tagged UNC-80 from a minigene construct under control of the unc-17 promoter. Rescues the loopy locomotion of nzIs29 animals that had been suppressed by loss-of-function of unc-80. Injection into QT841
QT1084	nzEx537[SJN478;ttx-3;KP#307];nzIs29;unc-80(e1069)	Andrew	Strain expresses mCherry-tagged UNC-80 from a minigene construct under control of the unc-17 promoter. Rescues the loopy locomotion of nzIs29 animals that had been suppressed by loss-of-function of unc-80. Injection into QT841
QT1085	nzEx538[SJN481;ttx-3];nzIs29;unc-80(e1069)	Andrew	Strain expresses GFP-tagged UNC-80 from a minigene construct under control of the snb-1 promoter. Rescues the loopy locomotion of nzIs29 animals that had been suppressed by loss-of-function of unc-80. Injection into QT841
QT1086	nzEx539[SJN481;ttx-3];nzIs29;unc-80(e1069)	Andrew	Strain expresses GFP-tagged UNC-80 from a minigene construct under control of the snb-1 promoter. Rescues the loopy locomotion of nzIs29 animals that had been suppressed by loss-of-function of unc-80. Injection into QT841
QT1087	nzEx540[SJN481;ttx-3];nzIs29;unc-80(e1069)	Andrew	Strain expresses GFP-tagged UNC-80 from a minigene construct under control of the snb-1 promoter. Rescues the loopy locomotion of nzIs29 animals that had been suppressed by loss-of-function of unc-80. Injection into QT841
QT1088	nzEx540[SJN482;ttx-3;KP#307];nzIs29;unc-80(e1069)	Andrew	Strain expresses mCherry-tagged UNC-80 from a minigene construct under control of the snb-1 promoter. Rescues the loopy locomotion of nzIs29 animals that had been suppressed by loss-of-function of unc-80. Injection into QT841
QT1089	nzEx542[SJN482;ttx-3;KP#307];nzIs29;unc-80(e1069)	Andrew	Strain expresses mCherry-tagged UNC-80 from a minigene construct under control of the snb-1 promoter. Rescues the loopy locomotion of nzIs29 animals that had been suppressed by loss-of-function of unc-80. Injection into QT841
QT1090	nzEx543[SJN482;ttx-3;KP#307];nzIs29;unc-80(e1069)	Andrew	Strain expresses mCherry-tagged UNC-80 from a minigene construct under control of the snb-1 promoter. Rescues the loopy locomotion of nzIs29 animals that had been suppressed by loss-of-function of unc-80. Injection into QT841
QT1091	nzEx536[SJN478;ttx-3;KP#307];unc-80(e1069)	Andrew	Strain expresses mCherry-tagged UNC-80 from a minigene construct under control of the unc-17 promoter. Rescues the loopy locomotion of nzIs29 animals that had been suppressed by loss-of-function of unc-80. Injection into QT841
QT1092	nzEx542[SJN482;ttx-3;KP#307];unc-80(e1069)	Andrew	Strain expresses mCherry-tagged UNC-80 from a minigene construct under control of the snb-1 promoter. Rescues the loopy locomotion of nzIs29 animals that had been suppressed by loss-of-function of unc-80. Injection into QT841

VC12	nca-1(gk9) IV	CGC	C11D2.6. Superficially wild type. This strain was provided by the C. elegans Reverse Genetics Core Facility at UBC, which is part of the International C. elegans Gene Knockout Consortium, which should be acknowledged in any publications resulting from its use. URLs: URL: aceserver.biotech.ubc.ca/cgi-bin/stable/strain.pl?class=Strain;name=VC12, URL: www.celeganskoconsortium.omrf.org/
VC9	a-2(gk5) III.	CGC	C27F2.2. Superficially wild type. This strain was provided by the C. elegans Reverse Genetics Core Facility at UBC, which is part of the International C. elegans Gene Knockout Consortium, which should be acknowledged in any publications resulting from its use. URLs: URL: aceserver.biotech.ubc.ca/cgi-bin/stable/strain.pl?class=Strain;name=VC9, URL: www.celeganskoconsortium.omrf.org/
ZM2389	unc-80(e1272);hpEx630 (pJH983; 984; 916 (punc-80;UNC-80::RFP); odr-1::GFP)	Mei Zhen	unc-80(e1272);hpEx630 (pJH983; 984; 916 (punc-80;UNC-80::RFP) with odr-1::GFP)
ZM2390	unc-80(e1272);hpIs98[odr-1::GFP; punc80;UNC-80::RFP]	Mei Zhen	Integrated version of unc-80(e1272);hpEx630 (pJH983; 984; 916 (punc-80;UNC-80::RFP) with odr-1::GFP)

Table 2.2 List of plasmids used or referenced in this thesis

Plasmid Name	Made By	Lab Book Reference	Plasmid Details	Notes and Comments	Selection Marker
APP001	Andrew	Andrew 2:42	p.acr-2::PKC-3 (contains mutations, not WT)	Cloned pkc-3 sequence from the YK526h11b cDNA with PKC-3.1 (NcoI consensus at ATG) and PKC-3.2 (SacI after stop codon.) Digested and ligated into pacr-2 (with same restriction sites.) Sequenced maxipreps 1#10 and 5#11. Contains non-silent mutations in the region 5' to the site which is to be mutated by QuikChange.	amp
APP002	Andrew	Andrew 2:57	p.acr-2::PKC-3* (contains mutations)	Performed QuikChange on APP003 (midi preps 1#10 and 5#11) using PKC-3.7 an d PKC-3.8 primers. This introduced a SacII site along with changing an alanine at position 116 to glutamate to make activated PKC-3. However, this plasmid also contains mutations in the 5' region (carried over from APP001). Do not use this plasmid - use APP003 instead.	amp
APP003	Andrew	Andrew 2:93	p.acr-2::PKC-3*	To repair the mutations in the 5' region of APP002, I did a PCR on plasmid YK1447b7 (which was sequenced as WT PKC-3 cDNA) using PKC-3.1 and PKC-3.8. This fragment has a NcoI site at the 5' and SacII site at the 3' end, and can be exchanged for the equivalent region of APP002 to repair the mutations.	amp
APP004	Andrew	Andrew 2:116	p.acr-2::cdc-42* (G12V)	Performed QuikChange of SJN381 using cdc-42.3 and cdc-42.4 primers. This introduced the G12V activating mutation, and a SfcI site (silent base changes). Sequenced maxipreps n*1 and n*3. n*1 has the correct introduced base changes (and also a silent mutation in the coding sequence).	amp
APP005	Andrew	Andrew 2:116	p.acr-2::cdc-42 DN (T17N)	Performed QuikChange of SJN381 using cdc-42.5 and cdc-42.6 primers. This introduced the T17N dominant negative mutation, and an SfcI site (silent base change). DN3 has the correct introduced base changes (and also a silent mutation in the coding sequence).	amp
APP006	Andrew		hs-cdc-42	The coding region of cdc-42 digested from SJN381 and placed under control of the heatshock promoter	AMP
APP007	Andrew		hs-nca-1	An attempt to make a rescuing version of nca-1. PCR from the longest available cDNA; but subsequent sequencing detected numerous rearrangements and mutations; this construct should not be used.	AMP
KP#305	nuz	hypers6.52	p.acr-2::ptx	oligos ptx5' and ptx3'b were used to PCR up ptx from p519 0012 and this was digested with BspHI and cloned into pSC#205 cut with NcoI and RV. The Nco and BspHI sites are destroyed. The idea is that the PCR creates flush ends with can be cloned into the RV site. NB this will generate an RI site and a run of 5 G's immediately 3' of the STOP codon.	
KP#307	nuz	hypers6.56	p.acr-2::gfp	pPD95_75 was cut with RI and filled in, it was then cut with KpnI. The resulting KpnI-RI(fillin) frament was ligated into pSC#205 cut with KpnI and RV.	amp
KP#315	Mark	ML3-42	p acr-2::egl-30(gf).	insert can be cut out w/ Nhe/Kpn.	Amp

KP#505	nuz	hypers8.5	pBS unc-64 full length rescuing construct	This contains 5kb of the unc-64 promoter, the 6.5kb coding region (with all 3 splice variants), and 450bp of 3'UTR past the B splice form (including the polyA site as determined by my recovery of cDNAs). The PstI-NheI fragment of KP#501, and the NheI-XhoI fragment of KP#502 were subcloned into pBS Not BamHI cut with PstI-XhoI.	
QT#238	nuz	nuz10.123	p.unc-17::gfp	The BamHI-SpeI fragment of KP#307 containing the Fire GFP sequence was inserted into QT#220 cut with BamHI-SpeI.	amp
rjm039	Rachel	book8	punc-17: rho-1 G14V F25N	This corrects sjn327. The 160bp SphI/BspEI fragment of sjn327 and the 175bp BamHI/SphI fragment of QT220 were inserted into QT220 cut with BamHI/BspEI. This should remove the mutations at position7 and in the Cterminus but should keep the G14V and F25N mutations. Correct plasmids were checked using BamHI and the HpaI unique site added with the mutation	amp
SJN367	nuz	nuz11.132	unc-64 T252A genomic	This generates a syntaxin mutant based on Yasu Fujita's work. The mutation also creates a BglI site. The mutation also creates a BglI site. Oligo pairs unc-64.4/unc-64.53 and unc-64.54/unc-64.52 were used on KP#505 in a PCR reaction. The products were cut with NheI/BglI and BglI/NsiI respectively and subcloned into KP#505 cut with NheI and NsiI in a 3 way ligation.	amp
SJN368	nuz	nuz11.132	unc-64 T252E genomic	This generates a syntaxin mutant based on Yasu Fujita's work. The mutation also creates a BtgI site. Oligo pairs unc-64.4/unc-64.55 and unc-64.56/unc-64.52 were used on KP#505 in a PCR reaction. The products were cut with NheI/BtgI and BtgI/NsiI respectively and subcloned into KP#505 cut with NheI and NsiI in a 3 way ligation.	amp
SJN381	nuz	nuz11.137	p.acr-2 cdc-42	for expression in the cholinergic motorneuons. Oligos cdc-42.1 and cdc-42.2 were used to PCR up the cdc-42 cdna from yk1443h08. The PCR product was digested with NheI and SacI and subcloned into pSC#205 cut with NheI and SacI.	amp
SJN447	nuz	12.127	p.acr-2::TMX C3T	This is tamoxifen sensitive oestrogen receptor fused N terminal to C3 transferase.	amp
SJN466	nuz	12.151	h.s. unc-80 minigene	This is unc-80 cdna (from yk1260h6 which lacks one predicted exon) up until the BlpI site after which it is genomic unc-80. The ATG is preceeded by a KpnI site and there is a NotI site immediately 3' to the ATG. There is a SacI site about 50bp 3' of the STOP codon. Oligos unc-80.53/64 were used on cyk-2 genomic DNA. The PCR product was digested with BlpI and SacI and subcloned into SJN462 cut with BlpI and SacI.	amp

SJN467	nuz	12.151	p.acr-2 unc-80 minigene	This is unc-80 cdna (from yk1260h6 which lacks one predicted exon) up until the BlpI site after which it is genomic unc-80. The ATG is preceeded by a KpnI site and there is a NotI site immediately 3' to the ATG. There is a SacI site about 50bp 3' of the STOP codon. Oligos unc-80.53/64 were used on cyk-2 genomic DNA. The PCR product was digested with BlpI and SacI and subcloned into SJN463 cut with BlpI and SacI.	amp
SJN469	nuz	13.5	p.unc-17::unc-80 minigene	The NotI-SpeI fragment of SJN467 was inserted into QT#220 cut with NotI-SpeI	amp
SJN470	nuz	13.5	p.hs::unc-80 minigene	The KpnI-SacI fragment of SJN467 was inserted into QT#42 cut with KpnI-SacI	amp
SJN471	nuz	13.5	p.snb-1::unc-80 minigene	The KpnI-SacI fragment of SJN467 was inserted into QT#237 cut with KpnI-SacI	amp
SJN477	nuz	13.21	p.unc-17::GFP::unc-80 minigene	The NotI fragment of KP#295, containingthe Fire GFP with introns, was inserted into SJN469 cut with NotI. Miniprep 12 was maxiprepped	amp
SJN478	nuz	13.21	p.unc-17::mcherry::unc-80 minigene	The NotI fragment of SJN#445, containing mcherry, was inserted into SJN469 cut with NotI. Miniprep 15 was maxiprepped	amp
SJN479	nuz	13.21	hs::GFP::unc-80 minigene	The NotI fragment of KP#295, containingthe Fire GFP with introns, was inserted into SJN470 cut with NotI.	amp
SJN480	nuz	13.21	hs::mcherry::unc-80 minigene	The NotI fragment of SJN#445, containing mcherry, was inserted into SJN470 cut with NotI.	amp
SJN481	nuz	13.21	p.snb-1::GFP::unc-80 minigene	The NotI fragment of KP#295, containingthe Fire GFP with introns, was inserted into SJN471 cut with NotI.	amp
SJN482	nuz	13.21	p.snb-1::mcherry::unc-80 minigene	The NotI fragment of SJN#445, containing mcherry, was inserted into SJN471cut with NotI.	amp
SJN483	nuz	13.21	p.acr-2::GFP::unc-80 minigene	The NotI fragment of KP#295, containingthe Fire GFP with introns, was inserted into SJN467 cut with NotI. Miniprep 84 was maxiprepped	amp
SJN484	nuz	13.21	p.acr-2::mcherry::unc-80 minigene	The NotI fragment of SJN#445, containing mcherry, was inserted into SJN467 cut with NotI. Miniprep 87 was maxiprepped	amp
SJN492	nuz	13.26	hs::MUNC80 full	this expresses mammalian MUNC80 from the heatshock promoter. The NheI-Spe fragment from SJN492 was inserted into SJN493 cut with NheI-SpeI.	amp
SJN493	nuz	13.28	p.unc-17::ptx	This expresses pertussis toxin from the unc-17 promoter. This will selectively inhibit goa-1 (G alpha o) in cholinergic neurons. The NheI-Spe fragment from SJN492 was inserted into SJN493 cut with NheI-SpeI.	
SJN495	nuz	13.3	p.unc-17::MUNC80	This expresses the mammalian munc80 cdna in cholinergic cells from the unc-17 promoter. The NheI-Spe fragment from SJN492 was inserted into SJN493 cut with NheI-SpeI.	
ttx-3gfp			TTX-3 gfp in ppD95.75 from Oliver Hobert	NB there are 2 XhoI sites in this construct.	amp

Table 2.3 List of primers used or referenced in this thesis

gatatccgcatattgagagctttag	unc-80.1	This is to pcr unc-80 in 3 fragments from genomic DNA in order to rescue unc-80 It primes on the top strand See Jospin et. al.
gcagtgttttatcctgaggctc	unc-80.2	This is to pcr unc-80 in 3 fragments from genomic DNA in order to rescue unc-80 It primes on the bottom strand See Jospin et. al. THIS IS THE TOP STRAND!!! WILL NOT WORK WITH UNC-80.1
agcatgtgaagtggtctgttg	unc-80.3	This is to pcr unc-80 in 3 fragments from genomic DNA in order to rescue unc-80 It primes on the top strand See Jospin et. al.
cgtggttcaaaagatgcaatcg	unc-80.4	This is to pcr unc-80 in 3 fragments from genomic DNA in order to rescue unc-80 It primes on the bottom strand See Jospin et. al. THIS IS THE TOP STRAND!!! WILL NOT WORK WITH UNC-80.3
ccgggtgctcaatcccaaaag	unc-80.5	This is to pcr unc-80 in 3 fragments from genomic DNA in order to rescue unc-80 It primes on the top strand See Jospin et. al.
cagaatgcagtcctaatatgccga	unc-80.6	This is to pcr unc-80 in 3 fragments from genomic DNA in order to rescue unc-80 It primes on the bottom strand See Jospin et. al. THIS IS THE TOP STRAND!!! WILL NOT WORK WITH UNC-80.5
cattgactagaagaatcttcatcgtg	unc-80.7	This is to sequence unc-80. Primes on top strand 5' of exon 1
catgtggatacgttgtagcattag	unc-80.8	This is to sequence unc-80 it primes on the bottom strand 3' of exon 5
gcgttgaacaattatagtgtgcggc	unc-80.9	This is to sequence unc-80 it primes on the top strand 5' of exon 6
gaggaaatgcagtacaaataac	unc-80.10	This is to sequence unc-80 it primes on the bottom strand 3' of exon 6
ggctcatttacagtcgttaggccacta	unc-80.11	This is to sequence unc-80 it primes on the top strand 5' of exon 7
gtagaggtcgaaaaatgcgacattgcttcg	unc-80.12	This is to sequence unc-80 it primes on the bottom strand 3' of exon 13
cctattttgcaaggtttctttcagcatg	unc-80.13	This is to sequence unc-80 it primes on the top strand 5' of exon 14
caattcatcgcattcgatctcgtgggtgc	unc-80.14	This is to sequence unc-80 it primes on the bottom strand 3' of exon 18
gcaccgatactatgcaccgatatgacac	unc-80.15	This is to sequence unc-80 it primes on the top strand 5' of exon 19
cagcaagcttaatacgacattttgtcg	unc-80.16	this is to sequence unc-80 it primes on the top strand 5' of exon 23
cggcgtcacgcataccacatgtatccg	unc-80.17	This is to sequence unc-80 it primes on the bottom strand 3' of exon 23
gccagaagtagagtctagaccgtgtac	unc-80.18	This is to sequence unc-80 it primes on the bottom strand 3' of exon 27
ggcgttatcaatatgttggctattatc	unc-80.19	This is to sequence unc-80 it primes on the top strand 5' of exon 28
ccgttgcagaatggcctctgtcggtgac	unc-80.20	This is to sequence unc-80 it primes on the bottom strand it primes on the bottom strand 3' of exon 32
ctctgacaacgactttcattagaggg	unc-80.21	This is to sequence unc-80 it primes on the top strand 5' of exon 33
gtgtgatcacttaacatcaaac	unc-80.22	This is to sequence unc-80 it primes on the bottom strand 3' of the last exon
ggattaagctacatgttcagcgcc	unc-80.23	This is to sequence unc-80 it primes on the bottom strand 3' of exon 1
gagatacattttctgtgataatc	unc-80.24	This is to sequence unc-80 it primes on the top strand 5' of exon 2
gggatattgcaacctcaagtgg	unc-80.25	this is to sequence unc-80 it primes on the top strand 5' of exon 4
gctgcgccgctctcacatgaagg	unc-80.26	this is to sequence unc-80 it primes on the top strand 5' of exon 6
aatgaacatgtagattgaatatg	unc-80.27	this is to sequence unc-80 it primes on the top strand 5' of exon 7
ggcactcatgaataggtggaaatg	unc-80.28	this is to sequence unc-80 it primes on the top strand 5' of exon 9
aatccccactggcgctactac	unc-80.29	this is to sequence unc-80 it primes on the bottom strand 3' of exon 3
gggtccgcctggcatcacgtgg	unc-80.30	this is to sequence unc-80 it primes on the bottom strand 3' of exon 14
attttgacaacatgtggataatg	unc-80.31	this is to sequence unc-80 it primes on the top strand 5' of exon 15
ttacacaaaactcatgaaacag	unc-80.32	this is to sequence unc-80 it primes on the bottom strand 3' of exon 18
cacgcatacgttgaacaattggtgac	unc-80.33	this is to sequence unc-80 it primes on the bottom strand 3' of exon 19
cctgttgtccttagatgcaattg	unc-80.34	this is to sequence unc-80 it primes on the top strand 5' of exon 20
gtttcacgtaaagctgagaaacc	unc-80.35	this is to sequence unc-80 it primes on the bottom strand 3' of exon 23
gttgtggtcaagcatacaacgc	unc-80.36	this is to sequence unc-80 it primes on the bottom strand 3' of exon 25
ggcctgtggatgaatgttcagc	unc-80.37	this is to sequence unc-80 it primes on the top strand 5' of exon 26
ggactgtatttcaaggatc	unc-80.38	this is to sequence unc-80 it primes on the top strand 5' of exon 28

ggactgtatttcaaggatc	unc-80.38	this is to sequence unc-80 it primes on the top strand 5' of exon 28
cctctacttcagcagcttccc	unc-80.39	this is to sequence unc-80 it primes on the bottom strand 3' of exon 30
gacccgccgactacaaatgaagacg	unc-80.40	this is to sequence unc-80 it primes on the top strand 5' of exon 31
gtgaacgcttgttcgtcgat	unc-80.41	this is to sequence unc-80 it primes on the bottom strand 3' of exon 34
ggtcaaatgctaccaggaacttc	unc-80.42	this is to sequence unc-80 it primes on the top strand in exon 35
gacgtgctagcaatttcagatcg	unc-80.43	this is to sequence unc-80 it primes on the top strand 5' of exon 37
gcgaaagttagaagaggagaag	unc-80.44	This is to pcr up the cDNA of unc-80 it primes on the top strand in exon 6
ggatgccctcatggatgcaacg	unc-80.45	This is to pcr up the cDNA of unc-80 it primes on the top strand in exon 11
ccatacacttaaacgacaaagag	unc-80.46	This is to pcr up the cDNA of unc-80 it primes on the top strand between exons 16 and 17
gaggagcttagcctcaaggagg	unc-80.47	This is to pcr up the cDNA of unc-80 it primes on the top strand in exon 23
gggggcggccgcttagaccaattgatgttgttct gttatttg	unc-80.48	This is to amplify unc-80 cDNAs. This primes on the predicted STOP codon, which is also present in the Kohara clone, on the bottom strand. It has a NotI site 3' of the STOP codon. NB as an alternative unc-80.65 has a SacI instead of NotI
ggagaacgaaaattatctgtc	unc-80.49	To sequence the cDNA of unc-80 (based on the predicted sequence from wormbase.) Primes at around 1750 in the predicted cDNA on the bottom strand.
ctagaccttatcatttgaaag	unc-80.50	For RTPCR of unc-80, to check whether the nz94 mutation is a null (nonsense-mediated decay because of premature stop codon) or a forms a truncated mRNA. Primes on the bottom strand between two exons in the predicted cDNA (start at 7680) with about 60 bases of intron inbetween (should not prime on genomic sequence.) Forward primer for unc-80.51
aaggcaaactgccctaaggcttgc	unc-80.51	For RTPCR of unc-80, to check whether the nz94 mutation is a null (nonsense-mediated decay because of premature stop codon) or a forms a truncated mRNA. Primes on the top strand between two exons in the predicted cDNA (start at 8385) with about 50 bases of intron inbetween (should not prime on genomic sequence.) Reverse primer for unc-80.50
gcatttctactggaaactgcca	unc-80.52	To sequence the cDNA of unc-80 (based on the predicted sequence from wormbase.) Primes at around 3300 in the predicted cDNA on the top strand.
ccaattggtacattccccaatct	unc-80.53	To sequence the cDNA of unc-80 (based on the predicted sequence from wormbase.) Primes at around 5100 in the predicted cDNA on the top strand.
GGAAACTGCCAGACCGGGAACGTT	unc-80.54	Cloning central portion of unc-80 cDNA, between two XhoI sites. This primes on the top strand, and is the outside primer for the first nested pcr.
GCTGCTATCATGCACCTTAAAT	unc-80.55	Cloning central portion of unc-80 cDNA, between two XhoI sites. This primes on the top strand, and is the inside primer for the second nested pcr.
CCTGGTCCAAAGTACATTCCAA	unc-80.56	Cloning central portion of unc-80 cDNA, between two XhoI sites. This primes on the bottom strand, and is the outside primer for the first nested pcr.
CGAACATGTCGGACATCATCTT	unc-80.57	Cloning central portion of unc-80 cDNA, between two XhoI sites. This primes on the bottom strand, and is the inside primer for the second nested pcr.
CCTACATGATGAATTCACTCAT	unc-80.58	Cloning the 3' end of unc-80 cDNA. Primer primes just before the 2nd XhoI site in the unc-80 cDNA. This primer primes on the top strand, and is the inside primer for the 2nd nested pcr.
CGTTCTTTTTATCCTCAATTGA	unc-80.59	Cloning the 3' end of unc-80 cDNA. Primer primes just before the 2nd XhoI site in the unc-80 cDNA. This primer primes on the bottom strand, and is the outside primer for the 1st nested pcr.
gactgaaaatatatgagaaatgt	unc-80.60	Cloning the 3' end of unc-80 cDNA. Primer primes just after the stop codon. This primer primes on the top strand, and is the inside primer for the 2nd nested pcr. (use after PolyT Not I).

GAGCTCctGGTACCtcTTAGGCGGCCG Cgaccaattgatgttgttctgt	unc-80.61	To clone the 3' end of unc-80 cDNA. Primer primes over the stop codon (TAA) with 21 bases 5' of the stop codon. A Not I site is introduced 5' of the stop codon for adding in GFP/other tags. The primer contains a Kpn I and Sac I site for sub-cloning into pcDNA 3.1 (for mammalian expression) and into hs/unc-17 vectors. BUT the SacI site is right at the end of the oligo and may not
ggggggggtaccgtccgaaaattataaagaat gc	unc-80.62	This primes over and 5' of the UNC-80 ATG on the top strand. It has a KpnI site at the 5' end. This is used to clone the 5' and of the unc-80 cdna which does not introduce a notI site.
ggggggtaccaaagaatggcggccgcgcat gttcgatacttacagcacg	unc-80.63	This is to subclone the unc-80 cdna. The primes on the top strand over the ATG and inserts an in frame NotI site immediately 3' of the ATG. It also adds a KpnI site 5' to the ATG.
gggggggagctcaaatagaacagaaaatgac tagaaatgg	unc-80.64	The is to PCR the 3' end of the unc-80 cdna. This primes on the bottom strand approx. 60bp 3' of the STOP codon. This introduces a SacI site at the 3' end.
gggggagctcaaaattaggcggccgcgacca attgatgttgttctg	unc-80.65	This is to PCR up the 3' end of the unc-80 cDNA. This primes on the bottom strand over the STOP codon and introduces a NotI site immediately before the STOP codon, followed by the STOP codon, some cDNA sequence and then a SacI site
gagcctcaggataaaacactgc	UNC-80.66	Replaces UNC-80.2 as a the correct bottom strand primer to go with UNC-80.1 for PCR of 1st large genomic region of unc-80 (See Jospin et. al.)
cgattgcatcttttgaaccacg	UNC-80.67	Replaces UNC-80.4 as a the correct bottom strand primer to go with UNC-80.3 for PCR of 2nd large genomic region of unc-80 (See Jospin et al.)
tcggcatattaggactgcattctg	UNC-80.68	Replaces UNC-80.6 as a the correct bottom strand primer to go with UNC-80.5 for PCR of 3rd large genomic region of unc-80 (See Jospin et al.)
gggggGCTAGCggATGGTGAAGAGGA AGAGCTCCGAGGAGCAG	munc-80.1	To clone the cDNA of mouse unc-80 from pcDNA3.1 vector. Primes on the top strand, over the start codon [ATG], and introduces a unique NheI site just 5' of the start codon, for cloning into the heat shock vector. Use in conjunction with munc-80.2 to clone whole of munc-80 cDNA. CONTAINS AN ERROR - THERE IS A GAP COMPARED TO WT cDNA - use munc-80.3 instead
cccccgatatccccCTAAACGTGGGACTC ATCTAGTGCTGAG	munc-80.2	To clone the cDNA of mouse unc-80 from pcDNA3.1 vector. Primes on the bottom strand, over the stop codon [TAG], and introduces a unique EcoRV site just 3' of the start codon, for cloning into the heat shock vector. Use in conjunction with munc-80.1 to clone whole of munc-80 cDNA.
ggg ggg GCT AGC ggA TGG TGA AGA GGA AGA GCT CCG AGG GCC	munc-80.3	To clone the cDNA of mouse unc-80 from pcDNA3.1 vector. Primes on the top strand, over the start codon [ATG], and introduces a unique NheI site just 5' of the start codon, for cloning into the heat shock vector. Use in conjunction with munc-80.2 to clone whole of munc-80 cDNA. Replaces munc-80.1 which contains a gap in compared to the WT munc-80 sequence.
gggggggcggccgcGAATTTCTCGAGAAG AATTCAGAAGACCCCGGG	munc-80.4	This primes on the top strand over the unique XhoI site and has a NotI site 5' to the XhoI site. This allows PCRs of the 5' end (Nhe-Not) and 3' end (XhoI-RV) to be joined together. Then the central NotI-XhoI fragment can be subcloned in without PCR.
gggggctagcaaaattataaagaATGGTGAA GAGGAAGAGCTCCGAGGGC	munc-80.5	This is the top strand and is designed to be annealed with munc-80.6, filled in, cut with NheI and NotI, to synthesize the very 5' end of munc-80
ATGCCGCGGCCGCCGTCCTGCTCCTG GCCCTCGGAGCTCTTCCTCTTCAC	munc-80.6	This is the top strand and is designed to be annealed with munc-80.5, filled in, cut with NheI and NotI, to synthesize the very 5' end of munc-80
CCCCCCCgcggccgcAGTAAAGGAGAA GAACTTTTCACTG	munc-80.7	To PCR gfp from ppd95.75 and insert into the NotI site present in the munc-80 cDNA. Primes on the top strand, just after the ATG of gfp, and introduces a NotI site.
GGGGGGgcggccgcGTTTGTATAGTTCAT CCATGCCATGT	munc-80.8	To PCR gfp from ppd95.75 and insert into the NotI site present in the munc-80 cDNA. Primes on the bottom strand, just before the stop codon of gfp, and introduces a NotI site.
ggggGCTAGCggATGtcggaacgaaaaaa gagtctg	nca-1.1	to PCR nca-1 cDNA from Kohara clone and subclone into various vectors. Primes over the start codon on the bottom strand, and introduces an NheI site 5' of the start condon.
ggggAGATCTggCTAatcaacaagggaattc cacca	nca-1.2	To PCR up cDNA of nca-1 from Kohara clone and subclone into various vectors. Primes over the stop codon (TAG) on the top strand and introduces a BglII site just 3' of the stop codon.
gagaatggactatcattgtgttca	nca-1.3	To sequence nca-1 cDNA (primes around 700 bases in, on the bottom strand).

gttgaatgtatcatcaagattct	nca-1.4	To sequence nca-1 cDNA (primes around 1400 bases in, on the bottom strand).
ccaatgccaaaagttcgaggaag	nca-1.5	To sequence nca-1 cDNA (primes around 2100 bases in, on the bottom strand).
gcaatggccactgttacaattgt	nca-1.6	To sequence nca-1 cDNA (primes around 2800 bases in, on the bottom strand).
gtgattcgagatattttatgga	nca-1.7	To sequence nca-1 cDNA (primes around 3500 bases in, on the bottom strand).
cgatcattcttcattatcactgct	nca-1.8	To sequence nca-1 cDNA (primes around 4200 bases in, on the bottom strand).
ggacatccggttattcattcatca	nca-1.9	To sequence nca-1 cDNA (primes around 5000 bases in, on the bottom strand).
ggg gGG ATC Cgg CTA atc aac aag gga att cca cca	nca-1.10	To PCR up cDNA of nca-1 from Kohara clone and subclone into pcDNA3.1. Primes over the stop codon (TAG) on the top strand and introduces a BamHI site just 3' of the stop codon.
cctgttcgttgTcgtaattctAgataacttggaaatggacgaa	nca-1.11	To introduce the e625 mutation into the nca-1 cDNA. Change is A717V (GCC --> GTC) at position 2150 in the C11D2.6c transcript. Primes on the bottom strand. Also introduces a unique XbaI site for testing the Quikchange efficacy.
ttcgtccatttccaagttatcTagaattacgAcaacgaacagg	nca-1.12	To introduce the e625 mutation into the nca-1 cDNA. Change is A717V (GCC --> GTC) at position 2150 in the C11D2.6c transcript. Primes on the top strand. Also introduces a unique XbaI site for testing the Quikchange efficacy.
cattgctgtGatcactgaaacatttgctgaaattcAagtccagttcag	nca-1.13	To introduce the hp102 mutation into nca-1 cDNA. Change is R403Q (CGA --> CAA) at position 1208 in the C11D2.6c transcript. Primes on the bottom strand. Also introduces a fourth BclI site into the cDNA for testing the Quikchange efficacy.
ctgaactggactTgaatttcagcaaatgtttcagtgatCacagcaatg	nca-1.14	To introduce the hp102 mutation into nca-1 cDNA. Change is R403Q (CGA --> CAA) at position 1208 in the C11D2.6c transcript. Primes on the top strand. Also introduces a fourth BclI site into the cDNA for testing the Quikchange efficacy.
ccccccccagctgttaaaaaatgaaCTAatcaacaagggaattccacc	nca-1.15	To PCR up cDNA of nca-1 from Kohara clone and subclone into worm expression vectors. This primes on the bottom strand over the STOP codon and adds a PvuII site 3' to the STOP codon. This produces a blunt end that can be ligated to an RV site.
ccccagctgtaaaaaatgaaCTAggcggccgcatcaacaagggaattcc	nca-1.16	To PCR up cDNA of nca-1 from Kohara clone and subclone into worm expression vectors. This primes on the bottom strand over the STOP codon and adds a NotI site immediately 5' to the STOP codon and a PvuII site 3' to the STOP codon. This produces a blunt end that can be ligated to an RV site.
gtttcaaatcataacacaagaaggatgg	nca-1.17	This is to PCR up nca-1 cdna (this is the outer nested 5' primer) and parts of the genomic nca-1 sequence. This is the top strand and primes approx. 60bp 5' of the unique KpnI site.
gtggttgaagttttgagagcaactgacg	nca-1.18	This is to PCR up nca-1 cdna (this is the inner nested 5' primer) and parts of the genomic nca-1 sequence. This is the top strand and primes 7 bp 5' of the unique KpnI site.
gatggtatgcgacaaaatagagagcc	nca-1.19	This is to PCR up nca-1 cdna (this is the inner nested 3' primer). This is the bottom strand and primes 6 bp 3' of the unique KpnI site.
gatggtatgcgacaaaatagagagcc	nca-1.20	This is to PCR up nca-1 cdna (this is the outer nested 3' primer) and parts of the genomic nca-1 sequence. This is the bottom strand and primes 90 bp 3' of the unique SacIII site.
acctccaattccttctggagc	nca-1.21	This is to sequence the nca-1 cdna. This is the bottom strand and primes over residues APEGIGG

acctccaattccttctggagc	nca-1.21	This is to sequence the nca-1 cdna. This is the bottom strand and primes over residues APEGIGG
tccttctggttcaacttctcc	nca-1.22	This is to sequence the nca-1 cdna. This is the bottom strand and primes over residues GEVEPEG
gtcactgatctgcaaatatcc	nca-1.23	This is to sequence the nca-1 cdna. This is the bottom strand and primes over residues GYLQISD
tgttaaaagagctgttcctcg	nca-1.24	This is to sequence the nca-1 cdna. This is the bottom strand and primes over residues RGTALLT
gtgtttgctaactgccattcc	nca-1.25	This is to sequence the nca-1 cdna. This is the bottom strand and primes over residues GMAVSKH
cgtcactcttgaataaattggctttcggtgc	nca-1.26	This is to replace the cdna between the KpnI and RV sites with genomic DNA, via two parts. A KpnI-Xba 5' part and a XbaI-RV 3' part. This is the top strand and primes within a non coding region approx 70bp 5' of the XbaI site. This will PCR the Xba-RV section.
caaaattcccgtagttgagaagctcggcc	nca-1.27	This is to replace the cdna between the KpnI and RV sites with genomic DNA, via two parts. A KpnI-Xba 5' part and a XbaI-RV 3' part. This is the bottom strand and primes within the cdna approx 100bp 3' of the XbaI site. This will PCR the Kpn-Xba section.
acgacgagatatccaaatgtataagtgaatttcttcaactcc	nca-1.28	This is to replace the cdna between the KpnI and RV sites with genomic DNA, via two parts. A KpnI-Xba 5' part and a XbaI-RV 3' part. This is the bottom strand and primes over the RV site within the cdna.
gcagaaatcCAGgtacagtttcaacaaatgtggggatcCagaagcagc	NALCN-1.1	To introduce the hp102-type mutation into the human NALCN cDNA. Changes R329Q (AGA --> CAG) at position 1174 in the VGCNL1-001 transcript. Primes on the bottom strand. Also introduces a unique BamHI site 3' of the mutation to check QuikChange efficacy.
gctgcttctGgatccccacatttgttgaaactgtacCTGgatttctgc	NALCN-1.2	To introduce the hp102-type mutation into the human NALCN cDNA. Changes R329Q (AGA --> CAG) at position 1174 in the VGCNL1-001 transcript. Primes on the top strand. Also introduces a unique BamHI site 3' of the mutation to check QuikChange efficacy.
cctcctgagtttgtttgttgTGgttattCtAgacaacttagaacttg	NALCN-1.3	To introduce the e625-type mutation into the human NALCN cDNA. Changes A596V (GCT --> GTG) at position 1975 in the VGCNL1-001 transcript. Primes on the bottom strand. Also introduces a unique XbaI site 3' of the mutation to check QuikChange efficacy.
caagttctaagttgtcTaGaataacCAcaacaaacaaactcaggagg	NALCN-1.4	To introduce the e625-type mutation into the human NALCN cDNA. Changes A596V (GCT --> GTG) at position 1975 in the VGCNL1-001 transcript. Primes on the top strand. Also introduces a unique XbaI site 3' of the mutation to check QuikChange efficacy.
GGGGGGtctagaGGGGGGatgCTCAAAAGAAAGCAGAGTTCCAGG	NALCN-1.5	To clone the 5' end of rat NALCN cDNA. Adds a unique XbaI site to the 5' end, which will allow cloning into the MCS of psc#205. Use in conjunction with NALCN-1.6 to clone FRAGMENT 1 of NALCN.
TGGCAGTGAACACCACCAAGCTTCC	NALCN-1.6	To clone the 3' end of FRAGMENT 1 of NALCN. 5' of this site is a XmaI site, which conmbined with the XbaI site in NALCN-1.5 allows cloning of this fragment into psc#205.
ACTTCCAGGTTCTTCGGGTAGTCC	NALCN-1.7	Clone the 5' end of FRAGMENT 2 of rat NALCN cDNA. Use with NALCN-1.8. 3' of this oligo is a unique XmaI site in the cDNA, which allows this fragment to be combined with FRAGMENT 1, and also allows cloning into psc#205.
TCTGAAGATGCCGTTACAGTCTTCC	NALCN-1.8	Clones the 3' end of FRAGMENT 2 of rat NALCN cDNA. Use with NALCN-1.7 to clone this fragment. 5' of this oligo is a unique NheI site which can be used for joining this fragment onto FRAGMENT 3, and for cloning into psc#205.
AGTTGTTCGAGAACTTTTCAGTGG	NALCN-1.9	Clones the 5' end of FRAGMENT 3 of rat NALCN cDNA. Use with NALCN-1.10 to clone the rest of this fragment. 3' of this site is a unique NheI site in the cDNA, which can be used for cloning into psc#205 and for combining with FRAGMENT 2.
gggggGAGCTCgggggCTAGATATCTAGGAGGTCATCTCC	NALCN-1.10	Clones the 3' end of rat NALCN cDNA, including the stop codon. Introduces a unique SacI site for cloning into psc#205. Also is the 3' end of FRAGMENT 3 of the cDNA. Use with NALCN-1.9 to obtain this fragment.

caaaattcccgtagttgagaagctcggcc	nca-1.27	This is to replace the cdna between the KpnI and RV sites with genomic DNA, via two parts. A KpnI-Xba 5' part and a XbaI-RV 3' part. This is the bottom strand and primes within the cdna approx 100bp 3' of the XbaI site. This will PCR the Kpn-Xba section.
acgacgagatatccaaatgtataagtgaatttcttcaactcc	nca-1.28	This is to replace the cdna between the KpnI and RV sites with genomic DNA, via two parts. A KpnI-Xba 5' part and a XbaI-RV 3' part. This is the bottom strand and primes over the RV site within the cdna.
gcagaaatcCAGgtacagtttcaacaaatgtggggatcCagaagcagc	NALCN-1.1	To introduce the hp102-type mutation into the human NALCN cDNA. Changes R329Q (AGA --> CAG) at position 1174 in the VGCNL1-001 transcript. Primes on the bottom strand. Also introduces a unique BamHI site 3' of the mutation to check QuikChange efficacy.
gctgcttctGgatccccacatttgttgaaactgtacCTGgatttctgc	NALCN-1.2	To introduce the hp102-type mutation into the human NALCN cDNA. Changes R329Q (AGA --> CAG) at position 1174 in the VGCNL1-001 transcript. Primes on the top strand. Also introduces a unique BamHI site 3' of the mutation to check QuikChange efficacy.
cctcctgagtttgtttgttgTGgttattCtAgacaacttagaacttg	NALCN-1.3	To introduce the e625-type mutation into the human NALCN cDNA. Changes A596V (GCT --> GTG) at position 1975 in the VGCNL1-001 transcript. Primes on the bottom strand. Also introduces a unique XbaI site 3' of the mutation to check QuikChange efficacy.
caagttctaagttgtcTaGaataacCAcaacaaacaaactcaggagg	NALCN-1.4	To introduce the e625-type mutation into the human NALCN cDNA. Changes A596V (GCT --> GTG) at position 1975 in the VGCNL1-001 transcript. Primes on the top strand. Also introduces a unique XbaI site 3' of the mutation to check QuikChange efficacy.
GGGGGGtctagaGGGGGGatgCTCAAAAGAAAGCAGAGTTCCAGG	NALCN-1.5	To clone the 5' end of rat NALCN cDNA. Adds a unique XbaI site to the 5' end, which will allow cloning into the MCS of psc#205. Use in conjunction with NALCN-1.6 to clone FRAGMENT 1 of NALCN.
TGGCAGTGAACACCACCAAGCTTCC	NALCN-1.6	To clone the 3' end of FRAGMENT 1 of NALCN. 5' of this site is a XmaI site, which conmbined with the XbaI site in NALCN-1.5 allows cloning of this fragment into psc#205.
ACTTCCAGGTTCTTCGGGTAGTCC	NALCN-1.7	Clone the 5' end of FRAGMENT 2 of rat NALCN cDNA. Use with NALCN-1.8. 3' of this oligo is a unique XmaI site in the cDNA, which allows this fragment to be combined with FRAGMENT 1, and also allows cloning into psc#205.
TCTGAAGATGCCGTTACAGTCTTCC	NALCN-1.8	Clones the 3' end of FRAGMENT 2 of rat NALCN cDNA. Use with NALCN-1.7 to clone this fragment. 5' of this oligo is a unique NheI site which can be used for joining this fragment onto FRAGMENT 3, and for cloning into psc#205.
AGTTGTTCGAGAACTTTTCAGTGG	NALCN-1.9	Clones the 5' end of FRAGMENT 3 of rat NALCN cDNA. Use with NALCN-1.10 to clone the rest of this fragment. 3' of this site is a unique NheI site in the cDNA, which can be used for cloning into psc#205 and for combining with FRAGMENT 2.
gggggGAGCTCgggggCTAGATATCTAGGAGGTCATCTCC	NALCN-1.10	Clones the 3' end of rat NALCN cDNA, including the stop codon. Introduces a unique SacI site for cloning into psc#205. Also is the 3' end of FRAGMENT 3 of the cDNA. Use with NALCN-1.9 to obtain this fragment.

gggggccatggcggccgcctcgtctccgacatcattagaggagg	pkc-3.1	This is to subclone the pkc-3 cDNA into various vectors. This primes on the top strand over the ATG. The start ATG is in an NcoI consensus and a NotI site is inserted in frame immediately 3' to the ATG.
gggggagctcgggggaatcagactgaatcttcccgac	pkc-3.2	This is to subclone the pkc-3 cDNA into various vectors. This primes on the bottom strand over the STOP codon. 3' of the STOP is a SacI site.
gctatgaatggaaatgggtcg	pkc-3.3	To sequence pkc-3 cDNA and other versions of this gene. Primes on the top strand, just 3' of the Nhe I site.
cacaacttttgcataagatccacg	pkc-3.4	To sequence pkc-3 cDNA and other versions of this gene. Primes on the bottom strand, in between the Nhe I and Eco RV sites.
aatgttctgattgacgctgaagg	pkc-3.5	To sequence pkc-3 cDNA and other versions of this gene. Primes on the top strand.
tggtgcaatataattgggtgttcc	pkc-3.6	To sequence pkc-3 cDNA and other versions of this gene. Primes on the bottom strand.
gacaaaactgtatatcgccgcggtgagcgacgatggaagaaaatttatc	pkc-3.7	To modify the sequence of the pkc-3 cDNA to create a constitutively active form. Primes on the top strand. Changes an alanine at position 116 to glutamate, with base change GCT to GAG. Introduces a unique sac II site into the sequence. Sequence changed from: gta tat cga aga ggt gct to: gta tat cgG CGC ggt gAG
gataaattttcttccatcgtcgctcaccgcggcgatatacagttttgtc	pkc-3.8	To modify the sequence of the pkc-3 cDNA to create a constitutively active form. Primes on the bottom strand. Changes an alanine at position 116 to glutamate, with base change GCT to GAG. Introduces a unique sac II site into the sequence.
gggggctagccatgcagacgatcaagtgcgtcg	cdc-42.1	This is to PCR and subclone the cdc-42 cdna into various expression vectors. This primes on the top strand over the ATG and introduces an NheI site.
gggggagctcctagagaatattgcacttcttc	cdc-42.2	This is to PCR and subclone the cdc-42 cdna into various expression vectors. This primes on the bottom strand over the STOP codon and introduces a SacI site.
cgtcgttggagatgTCgctgtAggtaaaacttgtctcc	cdc-42.3	This is to create cdc-42(G12V) using quikchange. Also creates an SfcI site. This primes on the top strand.
ggagacaagttttaccTacagcGAcatctccaacgacg	cdc-42.4	This is to create cdc-42(G12V) using quikchange. Also creates an SfcI site. This primes on the bottom strand.
ggagctgtcggtaaaaAttgtctActgatcagctatacc	cdc-42.5	This is to create cdc-42(T17N) using quikchange. Also creates an AccI site. This primes on the top strand.
ggtatagctgatcagTagacaaTttttaccgacagctcc	cdc-42.6	This is to create cdc-42(T17N) using quikchange. Also creates an AccI site. This primes on the bottom strand.
GGGGGGGCGGCCGCCCGAAATGAAATGGGTGCTTCAGG	tam-1.1	To clone the mouse Estrogen receptor binding domain which is responsive to tamoxifen. Introduces a NotI site 5' of the start of the coding sequence. Primes on the top strand (forward primer). No start codon, designed to be dropped into plasmids with a NotI site 3' to the start codon, and 5' to the coding sequence of the gene to be regulated by tamoxifen.
GGGGGGGGCGGCGCCGATCGTGTTGGGGAAGCCCTCTGC	tam-1.2	To clone the mouse Estrogen receptor binding domain which is responsive to tamoxifen. Primes on the bottom strand. (reverse primer) DOES NOT CONTAIN A NOT-I SITE -- DO NOT USE THIS PRIMER TO CLONE INTO A NOT-1 SITE!!
CCCCCCGGCGGCCGCGCCGATCGTGTTGGGGAAGCCCTCTGC	tam-1.3	To clone the mouse Estrogen receptor binding domain which is responsive to tamoxifen. Primes on the bottom strand. (reverse primer) Added correct NotI site, compared to Tam-1.3. USE THIS INSTEAD OF Tam-1.3!! No stop codon, designed to be dropped into plasmids with a NotI site 3' to the start codon, and 5' to the coding sequence of the gene to be regulated by tamoxifen.

3 - SUPPRESSOR SCREENING IDENTIFIES NOVEL TARGETS OF RHO-1

3.1 - Introduction

Previous work in the lab demonstrated that the small GTPase RHO-1 is able to increase neurotransmitter release in the developed *C. elegans* nervous system by increasing levels of diacylglycerol (DAG), a key second messenger (McMullan, Hiley et al. 2006). RHO-1 inhibits DGK-1, a diacylglycerol kinase, which normally acts to remove of DAG from presynaptic membrane (Nurrish, Ségalat et al. 1999). DAG is a ligand for a number of proteins involved in synaptic vesicle and dense core vesicle release, including UNC-13 and PKC-1 (Betz, Ashery et al. 1998; Lackner, Nurrish et al. 1999; Nurrish, Ségalat et al. 1999), and is a positive regulator of neurotransmitter release (Lou, Korogod et al. 2008).

Animals carrying an integrated construct containing constitutively-active RHO-1 (G14V) expressed in the cholinergic neurons using the *unc-17* promoter (Alfonso, Grundahl et al. 1993; Sieburth, Ch'ng et al. 2005; McMullan, Hiley et al. 2006) are henceforth referred to as nRHO-1*. These animals are hypersensitive to the acetylcholinesterase inhibitor aldicarb which inhibits the breakdown of acetylcholine and potentiates signalling (Nguyen, Alfonso et al. 1995). This hypersensitivity indicates increased levels of acetylcholine release (Nurrish, Segalat et al. 1999). These nRHO-1* animals also have a highly characteristic loopy locomotion (Movie 3-2) compared to wild-type animals (Figure 3-1, and see Movie 3-1 for wild-type locomotion). This loopy locomotion may be linked to the increase in acetylcholine release (McMullan, Hiley et al. 2006).

The proteins acting upstream to control the activity of RHO-1 have been well characterised, and a complex network of guanine nucleotide exchange factors (GEFs), G-proteins, G-protein coupled receptors (GPCRs) and receptor tyrosine kinases (RTKs) has been determined (see Figure 1-9) (Steven, Zhang et al. 2005; Hiley, McMullan et al. 2006; McMullan, Hiley et al. 2006; Williams, Lutz et al. 2007).

Several experiments suggest that much more remains to be discovered with respect to the pathways downstream of the RHO-1 GTPase itself. In a *dgk-1* mutant animal (in which neurotransmitter release is increased in line with an increase in DAG levels), inhibiting RHO-1 with the specific inhibitor C3 transferase (Aktories and Hall 1989) causes a reduction in neurotransmitter release (McMullan, Hiley et al. 2006). If DGK-1 were the only target of RHO-1 within the nervous system, inhibiting RHO-1 in this mutant background should have no effect on acetylcholine release. Additionally, a mutation in

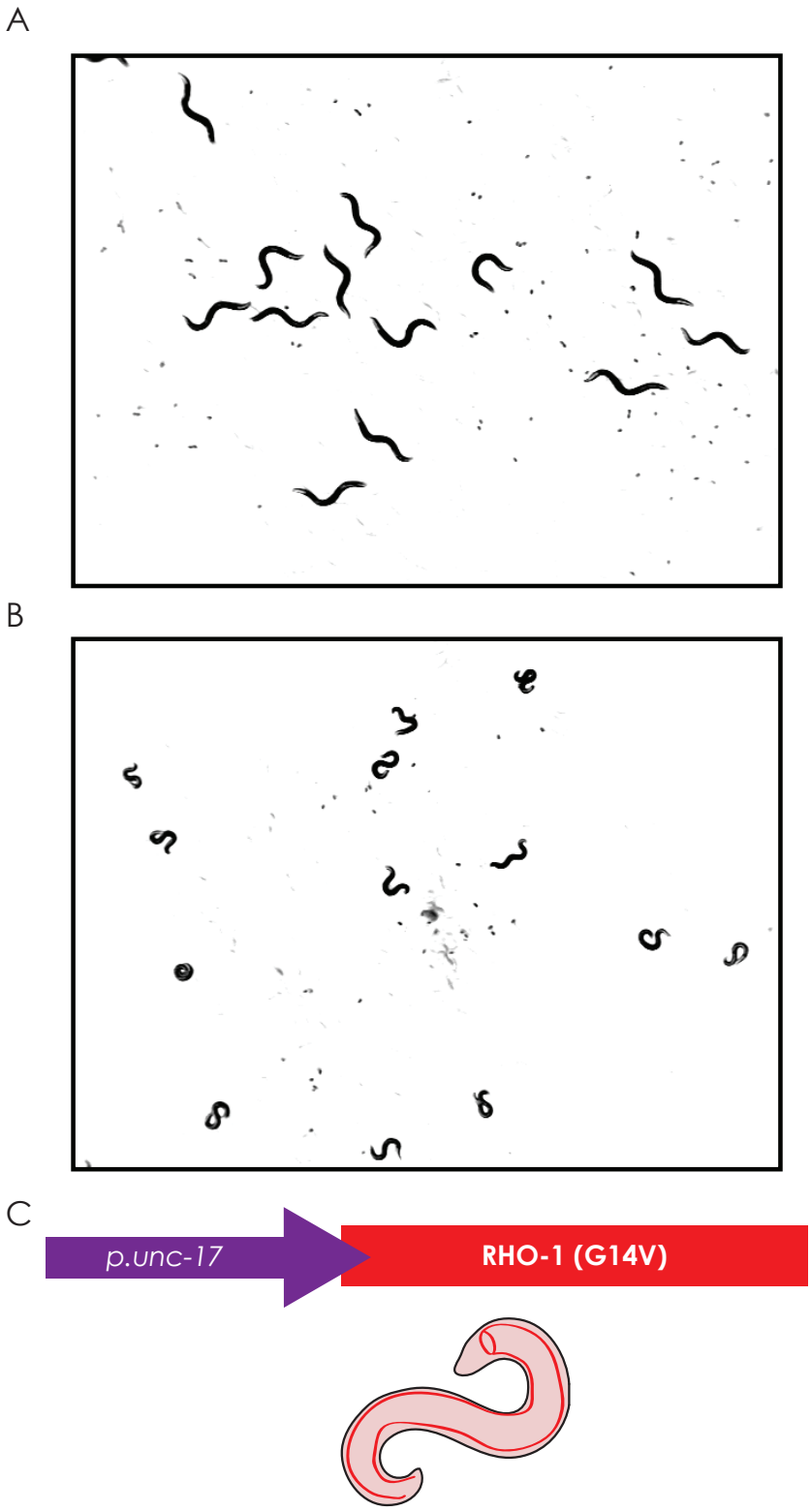

Figure 3-1 nRHO-1* animals are highly loopy compared with wild-type

A) Wild-type *C. elegans* have a smooth, sinusoidal body posture as they move across the surface of an agar plate.
B) In contrast, animals overexpressing an activated form of RHO-1, the *C. elegans* homologue of the human small GTPase RhoA, have a highly uncoordinated and loopy locomotion. These animals were staged and are imaged at the same magnification as the wild-type animals in (A), indicating that the transgene reduces the size of animals compared with wild-type.
C) The structure of the nRHO-1* transgene. Driven by the *unc-17* promoter, this transgene expresses in the cholinergic neurons (highlighted in red in the animal outline) and this expression is sufficient to drive highly loopy locomotion.

RHO-1 - F25N - specifically reduces binding to DGK-1 (McMullan, Hiley et al. 2006). This mutant form of RHO-1 is still able to drive an increase in acetylcholine release (although to a lesser degree than the non-mutant), and generate loopy behaviour. These results strongly suggests the presence of alternative targets of RHO-1 within the nervous system other than DGK-1.

Although over 40 proteins are known to be Rho effectors, they do not all share a common Rho interaction domain (Etienne-Manneville and Hall 2002), which makes it difficult to identify novel targets of Rho. In an attempt to discover some of these potential downstream targets we undertook a genetic suppressor screen using our nRHO-1* mutants. Genetic screens in *C. elegans* have proven a powerful technique for identifying neurobiological mutants (Brenner 1974; Nguyen, Alfonso et al. 1995; Miller, Alfonso et al. 1996), and suppressor screens have identified genes which interact with a variety of proteins. For instance, suppressors of activated Ras were identified as components of the MAPK pathway (Lackner, Kornfeld et al. 1994) and identification of axon guidance proteins were uncovered while screening for suppression of guidance defects caused by overexpression of UNC-5 (Colavita and Culotti 1998).

We decided to screen for suppressors of loopy locomotion, as opposed to changes in aldicarb response, for two main reasons. Firstly, there have been exhaustive screens for aldicarb resistant mutants (ric) (Nguyen, Alfonso et al. 1995; Miller, Alfonso et al. 1996), and we believed we would identify a large number of mutations which suppressed aldicarb sensitivity indirectly of RHO-1 signalling. Secondly, the loopy phenotype can be observed using a standard dissecting microscope, allowing us to screen mutants at a faster rate than a pharmacological assay; aldicarb phenotypes can be tested in a secondary screen following the initial rapid visual screen.

3.2 - Strain QT631, which carries two integrated RHO-1 transgenes, was selected for the screen

We decided to screen for suppressors of our stably integrated nRHO-1* transgene, *nzIs29*. This was integrated into transformed animals by Dr Rachel McMullan, and is carried in strain QT309, which was two-times backcrossed through wild-type to remove background mutations generated by integration. The integration maps to Chromosome II (R. McMullan, personal communication). *nzIs29* consists of the nRHO-1* plasmid QT#42, which expresses the G14V activated form of RHO-1 under a fragment of the *unc-17* promoter that has been shown not to cause any developmental defects (McMullan, Hiley et al. 2006), along with an *unc-122::gfp* marker, which produces fluorescence in the ceolomocytes.

To ensure that any mutations generated by EMS were real suppressors of RHO-1, and not simply the result of silencing the transgene, we crossed strain QT309 with QT47, which contains a second, stably-integrated RHO-1* transgene, *nzIs1*, which expresses the G14V form of RHO-1 from the heatshock promoter (hsRHO-1*) from vector pPD79.48, part of the Fire Lab Vector Kit. This integration maps to Chromosome I (S. Nurrish, personal communication.) Observations with this integrated transgene have previously been published (Hiley, McMullan et al. 2006; McMullan, Hiley et al. 2006). Heatshock RHO-1* activation has non-neuronal phenotypes, such as tail swelling and death (R. McMullan and S. Nurrish, in press), so we could not use the heatshock construct for our primary screen. We did however use this transgene to conduct secondary screening of mutant animals.

3.2.1 - A 'False Positive' screen Identified a false positive rate of 5%

To judge the level of confidence in our ability to distinguish genuinely suppressed animals from mutated animals behaving in a less loopy fashion, we conducted a small false positive screen. Here we took 5 plates of mixed population QT631 and subjected them to the same treatment regime as for EMS mutagenesis, with the exception of addition of the mutagen (Figure 3-2). These worms were subjected to pelleting by centrifugation, agitation in M9 solution for 4 hours at 20°C, and pippetting onto fresh NGM plates.

After one hour of recovery time, 44 L4s were picked to a fresh plate and left to grow to adulthood overnight. The following day, adult animals were picked to fresh plates (5 animals per plate, labelled A to I) and left for a total of 5 hours to lay eggs. After the 5 hours, the adults were removed and the eggs left to grow for two days, after which two plates were placed at 15°C, to mimic the effects of searching for temperature sensitive mutations.

After a total of 5 days growth, the plates were screened to look for any animals that looked non-loopy (i.e. had more wild-type locomotion than our QT631 starting strain).

From a total of 214 F1 animals, 14 F2s were picked which looked to be moving better than the starting QT631 strain. These were singled to individual plates. Examination of the F3 generation of these potentially suppressed animals demonstrated that their progeny were not suppressed. This experiment estimated a false positive rate of approximately 5%, but strongly suggested that these were due to behavioural variations and not spontaneous mutations or silencing of the transgene.

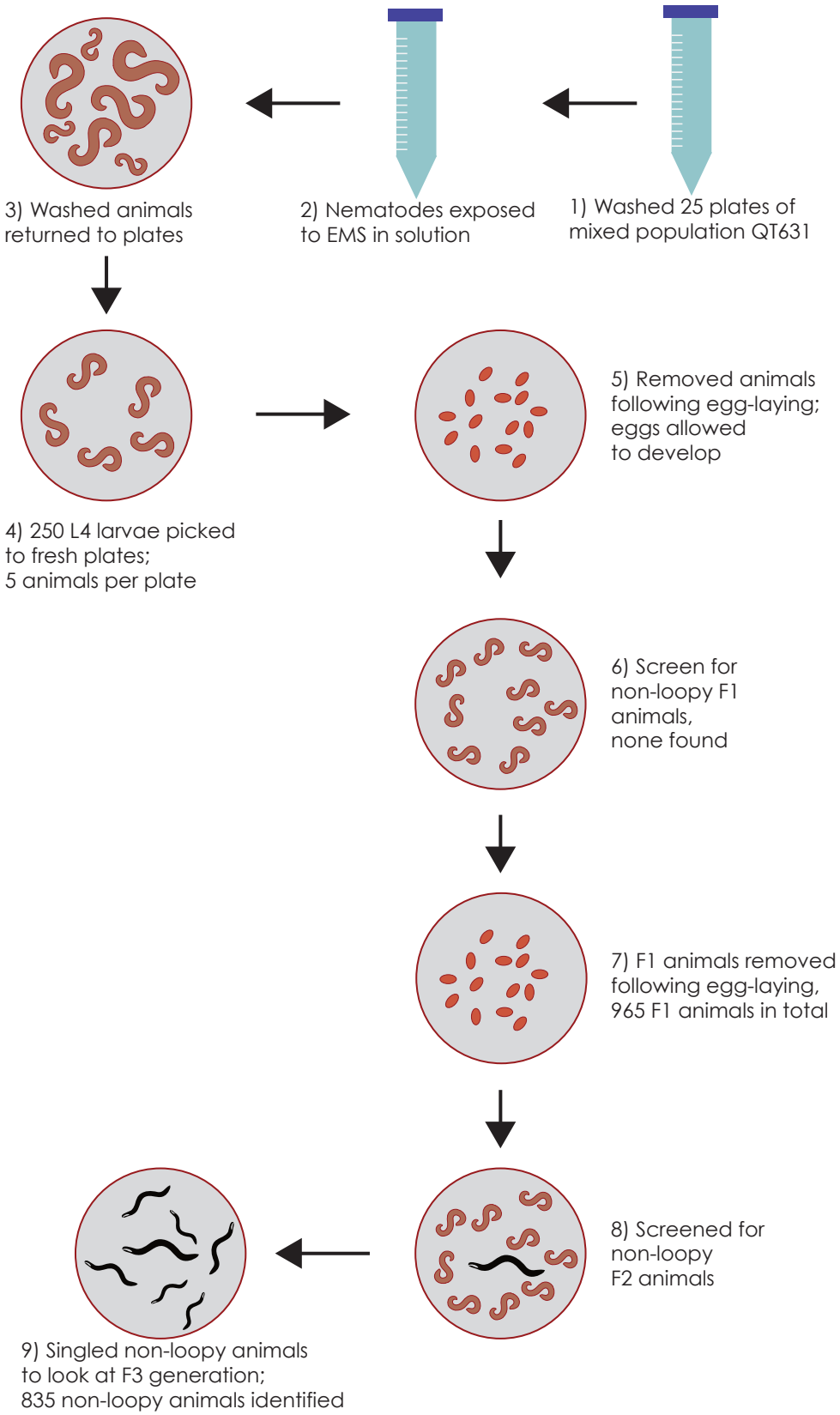

Figure 3-2 Scheme of EMS mutagenesis and screening

A mixed population of QT631 animals was exposed to 50mM EMS following washing (Steps 1-3), and 250 larval stage 4 (L4) animals were placed on fresh plates (4). These were allowed to lay eggs before being removed, and the progeny were screened for non-loopy behaviour (5 & 6). These animals were in turn singled, and their progeny screened (7 - 9).

3.3 - EMS Mutagenesis of QT631 generated 835 suspected suppressor mutants (in collaboration with Dr Rachel McMullan)

We conducted the primary screening in two parts, a small pilot screen and a larger screen, and I will consider the results from these two parts as a whole.

A total of 25 plates of mixed population QT631 animals were washed in M9 to remove excess OP50 bacteria, and then exposed to 50mM EMS for 4 hours in a solution of M9. The EMS solution was removed and disposed of, while the worms were again washed in M9, suspended in a small volume of M9, and pipetted onto a fresh plate (Figure 3-2).

Approximately 250 L4 larvae were then picked onto a total of 5 fresh plates and left to grow overnight. The L4 larvae stage contains a large number of meiotic nuclei, and it is into these which we are attempting to introduce the mutations. This way, by exposing a relatively small number of L4 animals to EMS we can screen a large number of progeny. Mutagenesis of L3 animals would increase the likelihood of 'jackpot mutations' whereby all progeny would carry the same mutation, while mutagenesis of adult animals is likely to produce chimeric mutants or non-heriditable mutations.

The following day groups of 5 adult animals were picked onto fresh plates, labelled 1 to 24 and A to AB. These animals were left to lay eggs over a period of approximately 7 hours, due to the slow egg-laying rate of this strain. The P0 adults were then removed and the eggs left to hatch (Figure 3-2).

In total, across all the plates, we captured 965 F_1 animals. As mutations could be introduced either in the developing egg or sperm of the L4 animals exposed to EMS, this allowed us to screening double the number of genomes to the number of animals exposed, i.e. we screened 1930 haploid genomes in total.

Once the F1 animals had laid eggs, the F1 adults were removed to allow the eggs to hatch. While counting and removing these F1 animals, we screened them to look for non-loopy animals. Any mutations at this stage might represent dominant mutations; however, we found no non-loopy animals in the first generation after screening, suggesting no dominant mutations were isolated.

The eggs from the F1 generation were left to grow at 15^{o}C to reduce the chances of leaky hs::RHO-1* expression (McMullan, Hiley et al. 2006; Diogon, Wissler et al. 2007). We know that RHO-1 plays significant roles in development (Govek, Newey et al. 2005), and that complete loss-of-function mutations in effectors of RHO-1 are likely to cause

lethality. We therefore grew the animals at 15°C as a potential permissive temperature, with the aim of capturing any temperature-sensitive mutations that may give partial loss-of-function at low temperature.

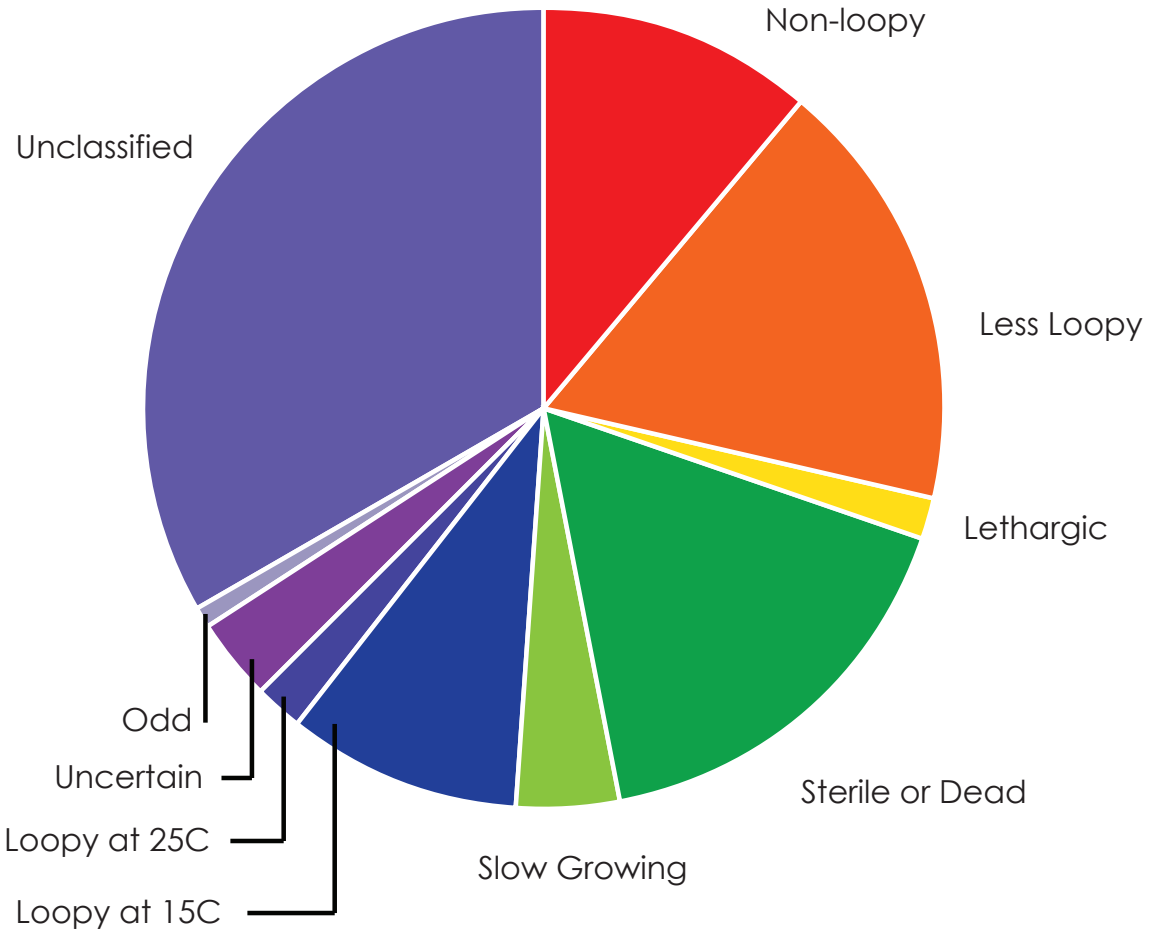

Figure 3-3 - Categories of Suppressor Mutants

After the initial screening round, we identified 835 mutants with a locomotion which was described as more like wild-type than our starting strain. Of these, the majority were either too slow growing, sterile or died before we could classify them further. Around one third of the mutants classified produced progeny which were also suppressed (i.e. non-loopy or less loopy), and could be analysed further.

3.3.1 - Further generational analysis revealed 116 strong suppressor candidates

Each plate of F2 animals was examined at least once following growth at 15°C and once after subsequent growth at 25°C before the food supply was exhausted to test for temperature sensitive mutations. During growth at 15°C we picked a total of 606 animals whose locomotion could be considered to be more like wild-type than the QT631 starting strain; many of these came from the same original plate and may contain the same suppressor mutation. When grown at 25°C we found a further 229 animals whose locomotion looked more wild-type than the starting strain.

These ‘non-loopy’ F2 were singled to their own individual plates and allowed to lay eggs. We then examined the F3 generation to see if the suppressive phenotype was maintained. Examining the progeny of a single animal gave us a clearer indication of phenotype. We assigned each plate to a category based on the overall phenotype displayed.

- Non-loopy – animals look essentially the same as wild-type
- Less loopy – animals have a higher numbers of body bends than wild-type, or assume a coiled posture, but to a lesser degree than the starting strain
- Lethargic – animals move slowly, rate of body bends reduced
- Loopy (at either 15°C or 25°C) – in the first round of screening we picked any animals that appeared to move better than the starting strain. However, when looking at a clonal population of these worms it was often clear that the mutations had not caused the animals to become non-loopy. These animals represent false positives obtained from the screen
- Sterile/dead/eggs only – plates which produced no live progeny, so were eliminated from the screen
- Unclassified - plates which produced no live progeny and on which the original mutant had died or crawled off the plate
- Slow growing – the starting strain QT631 is itself a slow growing strain, and a number of mutants appear to have acquired mutations that enhance this slow growth, making them unsuitable for further study. In hindsight, these animals should have been retained and frozen for future study, as their growth rate is incidental to the locomotion phenotype

During this round of categorisation, we also made a note of those mutants that appeared, by visual inspection, to be the most suppressed.

These results are summarised in the pie chart in Figure 3-3. A high proportion of the animals became sterile or died. 68.7% of the suppressors picked in the first round of screening were eliminated from the screen following inspection of the F3 generation, either because the animals were obviously loopy, or because the F2 animal were now homozygous for a mutation causing death, sterility or very slow growth.

This left us with 260 mutants whose locomotion was more like wild-type than the starting strain - classed as ‘Non-loopy’, ‘Less Loopy’ and ‘Lethargic’ (see Figure 3-3). Of these, 144 were in the ‘Less Loopy’ category. We decided to eliminate these from the screen, as the difference between their locomotion and that of the starting strain was insufficiently strong to enable successful backcrossing or mapping.

This left us with 116 mutants with a locomotion substantially different to the starting strain, from a starting total of 1930, of 6% of our starting total. We therefore undertook a round of secondary screening to find the best candidates to from this set of mutants.

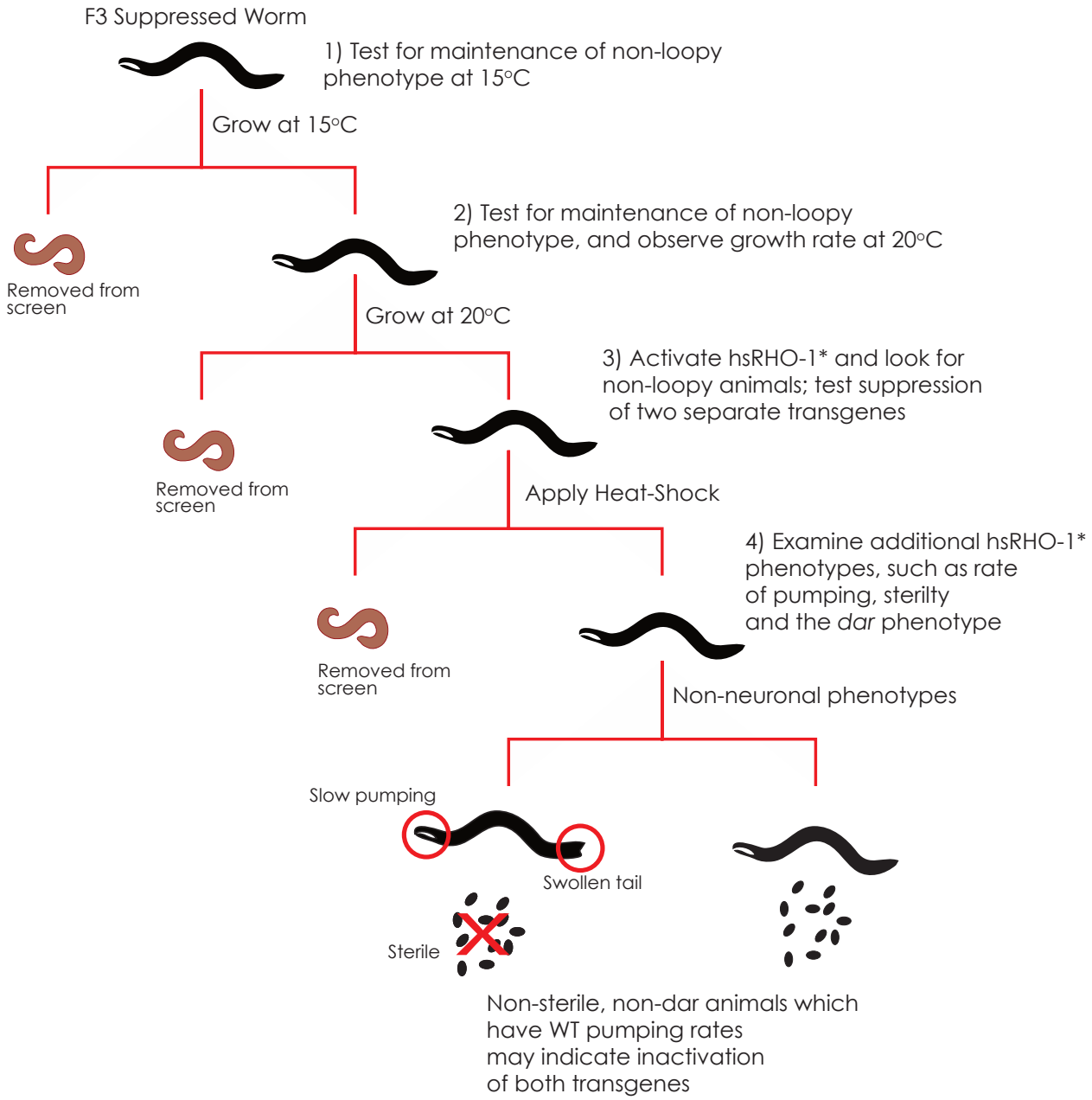

Figure 3-4 - Secondary Screening

Animals which appeared non-loopy after the initial round of screening were subjected to a number of further tests

First, we tested for maintenance of the non-loopy phenotype at both 15 and 20°C (1 & 2). Next, we looked for maintenance of the non-loopy locomotion after activation of the heatshock RHO-1* transgene (3). Finally, the animals were classified based on their additional hsRHO-1* phenotypes, such as sterility or tail swelling (4).

3.4 - Secondary Screening of Mutants (in collaboration with Dr Rachel McMullan)

3.4.1 - Screening for maintenance of the locomotion phenotype at room temperature eliminated 15 poorly suppressed mutants

From the animals that passed the first round of screening, we created an Excel spreadsheet to track all further experiments (Appendix 1). The first round of the secondary screening was to confirm the locomotion phenotypes already observed at 15°C and when grown at 20°C (Figure 3-4). To make comparisons between strains easier, we used a series of fixed categories to describe locomotion:

- Not Loopy (Suppressed)
- Less Loopy than QT631 (Partially Suppressed)
- Loopy (Not Suppressed)
- Lethargic (Partially Suppressed, locomotion different from wild-type)
- Lethargic, not loopy (Suppressed, locomotion different from wild-type)
- Lethargic, loopy (Not suppressed, slow moving)

15 mutants were relabelled as 'Loopy' following further examination. These animals appeared to have suppressed locomotion for one or two generations, with this effect reducing over time. It is not clear whether these animals represented very subtle suppressor mutations, epigenetic reduction in the activity of the transgenes, or are simply false positives, but they were discounted from the remainder of the screen.

Several mutants, as well as being non-loopy, also appeared to move slower than our wild-type animals, and were labelled as lethargic. While we were initially looking for suppressors that would return locomotion to wild-type levels, we were also interested in this lethargic phenotype, as although the rate of locomotion is reduced, the animals move with a wild-type body posture.

3.5 - Screening for maintenance of the locomotion phenotype after heatshock identified 15 potential cases of inactive nRHO-1* transgenes

One possible reason why we might see suppression of the nRHO-1 phenotype would be if we have isolated mutants in which the transgene is silenced. Transgenes are highly repetitive arrays, and so are subject to silencing by endogenous mechanisms (Mello and Fire 1995; Kelly, Xu et al. 1997). It is possible that some of our suppressors represent natural silencing of the transgene, or are mutations that enhance silencing. A number of

mutants in the RNAi pathway, such as *rde-1*, have been shown to increase the levels of silencing of transgenes (Tabara, Sarkissian et al. 1999).

The integrated nRHO-1* transgene contains an *unc-122::GFP* marker, which expresses in the coelomocytes and appears as six green dots along the body of the worm (McMullan, Hiley et al. 2006). Throughout the course of the experiments, we checked under UV light to see if this was still being expressed as an indication of the status of the transgene, and a few mutants were identified that no longer expressed this marker (e.g. mutants B.20 & D.07). These were discarded from the rest of the screen (see Appendix 1).

However, it is possible that even though this component of the transgene is being expressed, expression of RHO-1 (G14V) from the *unc-17* promoter may be down-regulated. Therefore, we tested all of our mutant animals by activating the second, hsRHO-1* transgene, which is integrated at a separate location in the genome, co-expresses *ttx-3::GFP* as a marker, and causes wild type animals to become loopy. It is less likely that both integrated transgenes are silenced, so any animals which continue to be non-loopy after activation of the heatshock gene are likely to represent genuine RHO-1 suppressors.

To test this, we grew two plates of mixed populations of each suppressor, and heatshocked one plate using our standard protocol, activating the hsRHO-1* transgene which is independently capable of generating loopy locomotion. We recorded the locomotion phenotype of these animals compared to the unheatshocked animals (Figure 3-4). 15 of the mutants tested became loopy after heatshock, suggesting that the reason for suppression in these animals is due to reduced expression of RHO-1 (G14V) from the *unc-17* promoter. For examples of the appearance of mutants following heatshock, see Figure 3-13.

This experiment also controls for an additional class of mutants which we predict would appear non-loopy. Mutations which affect expression from the *unc-17* promoter would reduce expression of nRHO-1*, making the animals appear non-loopy. However, these mutations would not affect expression from the heatshock promoter. In addition, animals with total reduction of *unc-17* (and *cha-1*, which shares the same promoter) would likely be paralysed or even dead, so we would either not see these animals in our screen, or would have discarded them due to their paralysed phenotype.

3.6 - Screening additional RHO-1 phenotypes

Although it is unlikely that a mutation would affect both transgenes, it is not impossible. While continued expression of both GFP reporters suggests that both transgenes

are operational, we also examined the functional consequences of activating heatshock RHO-1.

We took advantage of our hsRHO-1* transgene and the additional RHO-1 non-neuronal effects that occur on heatshock. These include changes in pumping and defecation rates, sterility and eventual death of the heatshocked animal, and the development of the *dar* (*d*eformed *a*nal *r*egion) phenotype (R. McMullan and S. Nurrish, in press). The *dar* and sterility phenotypes are thought to have a non-neuronal origin. We screened our suppressors to identify those which still displayed some or all of these additional RHO-1 phenotypes. These mutants likely represent:

- Mutants in which both transgenes are efficiently expressed
- True suppressors of loopy locomotion
- Neuronal-specific suppressors of RHO-1 activity

3.6.1 - 45 mutants screened suppress the sterility phenotype of heatshock RHO-1*

We picked 2 sets of 5 L4s of each suppressor strain onto two fresh plates, and heatshocked one plate using our standard protocol. Both plates were then stored at 15°C for five days, after which we compared the heatshocked plate to the control plate and examined the number of progeny. Again, we used a limited number of categories to allow easier comparison between strains. These were:

- Not Sterile, looks wild-type (Suppressed)
- Sterile, no eggs or larvae (Not suppressed)
- Eggs only, no larvae (Partially suppressed)
- Slow growth – some larvae, but growing slowly (Partially suppressed)

45 mutant strains were listed as “Not Sterile” in this test, suggesting that they are either silenced for both nRHO-1* and hsRHO-1* transgenes, or that these are general suppressors of RHO-1 function throughout the animal. As this category may contain genuine RHO-1 suppressors, we did not automatically eliminate animals which were not sterile, but used the information as part of our assessment of the best mutants to continue studying. It is also possible that locomotion and sterility defects are suppressed by independent mutations in some of these strains.

3.6.2 - 40 mutants suppress the pharyngeal pumping phenotype of hsRHO-1*

The pharyngeal muscles pump rhythmically to cause entry of bacteria into the grinder the worm. This pumping is severely reduced after heatshock RHO-1 activation, probably due

to hypercontraction of the pharangyl muscle (R. McMullan, personal communication). We assayed the rate of pumping of our mutants after heatshock. Again, we used a simple set of categories to classify the mutants based on a 2 minute inspection of the pumping rate of at least 5 animals following heatshock:

- Like wild-type (completely suppressed)
- Like QT631 with heatshock (not suppressed)
- Slower than QT631 with heatshock (not suppressed)
- Faster than QT631 with heatshock (partially suppressed)

40 mutants displayed a pumping phenotype that was faster than QT631 following heatshock – i.e. where the hsRHO-1* effect is suppressed. This did not lead to elimination from the screen, but those with unsuppressed pumping were of more interest to us, as they likely represented locomotion-specific suppressors.

3.6.3 - Protruding vulva and deformed anal region: additional heatshock RHO-1 effects

Heat-shock activated RHO-1 induces a swelling around the vulval, known as the *p*rotruding *vul*val phenotype (*pvul*), and a swelling around the tail region (*dar* phenotype) (McMullan and Nurrish, in press). While we were observing the other phenotypes, we also recorded any instances of these two phenotypes (Appendix 1). While this was not conducted in a systematic way, but it does give additional insight into the activity of the hsRHO-1 transgene in individual suppressor mutants.

3.6.4 - Growth at 20°C of suppressor mutants

We also made note of other distinguishing characteristics of the mutants. Rate of growth at 20°C was noted, as measured by the ability of a singled animal to starve a standard plate in six days. This was considered as a factor in choosing mutants to continue investigating, from the practical viewpoint that slow-growing strains are more difficult to work with.

3.6.5 - Suppressor mutants can be grouped into 3 categories

Based on all the information we had gathered from the screen, we selected 20 mutants for continuing study. The primary factor for this selection was the degree of suppression of the loopy phenotype at 20°C as our original objective was to identify suppressors of this phenotype. While cataloguing our mutants we used the designations ‘Not Loopy’ and ‘Less loopy (than QT631)’ for ease of classification, a number of animals clearly had a phenotype that was more easily distinguished from the starting strain, marked with an asterisk (Appendix 1, Column 2). In addition, we favoured those mutants which had the

least suppression of the sterility and pumping defects associated with heatshock RHO-1* activation. The 20 selected mutant animals can be arranged into three groups (Table 3-1) These classifications were performed prior to backcrossing and it is possible that additional mutations act in these strains to modify the supression of various nRHO-1* and hsRHO-1* phenotypes.

Group 1: Non-loopy at 20°C, and non-loopy and sterile after heatshock

These are the suppressors that best match our original target phenotypes. Five mutants meet these criteria - *nz94*, *nz97*, *nz98*, *nz99*, and *nz104*, although *nz94* and *nz98* are additionally categorised as lethargic. These animals fully suppress the neuronal phenotype of RHO-1 in generating loopy locomotion, but fail to suppress the sterility phenotype upon heatshock. These animals also show little suppression of the reduction in pumping of the pharyngeal muscles after heatshock.

Group 2: Non-loopy at 20°C but more loopy than wild-type after heatshock; sterile following heatshock

These animals demonstrate less effective suppression of the loopy phenotype following heatshock, suggesting that they are slightly weaker alleles compared to Group 1, that hsRHO-1* had additional effects on locomotion or because of modifying mutations in the background. Group 2 animals become sterile after heatshock, suggesting that the hsRHO-1* transgene is still active. Three suppressors make up this category, *nz100*, *nz105* and *nz110*.

Group 3: Non-loopy at 20°C, non-loopy following heatshock; non-sterile after heatshock

This group composes 10 mutants. They may represent more general RHO-1 suppressors, as the sterility effects of heatshock RHO-1 are suppressed. Not all non-neuronal phenotypes are suppressed in these mutants, however, as we still see a reduction in pumping following heatshock, and also the emergence of *dar* and *pvul* swellings in some of these mutants. The suppression of sterility of the heatshock transgene is of interest and may be pursued in future investigations. Group 3 mutants are most likely to represent loss of activity of both transgenes.

3.7 - Suppressor mutants display a range of aldicarb phenotypes

The suppressor mutants we chose for further study were all selected primarily on their ability to restore wild-type locomotion in the presence of nRHO-1*. We also know that

allele	Mutant	Movement at 20°C	Movement after heatshock	Sterility after heatshock	Pumping after heatshock
Group 1					
nz99	7.12	Not loopy	Not loopy	Sterile	Faster than QT631 w/ hs
nz97	1.03	Not loopy	Not loopy	Sterile	Like QT631 w/ hs
nz104	A.01	Not loopy	Lethargic, not loopy	Sterile	Faster than QT631 w/ hs
nz94	4.13	Lethargic, not loopy	Not loopy	Sterile	Like QT631 w/ hs
nz98	4.36	Lethargic, not loopy	Lethargic, not loopy	Sterile	Faster than QT631 w/ hs
Group 2					
nz100	13.05	Not loopy	Less loopy	Sterile	Like QT631 w/ hs
nz105	A.17	Not loopy	Less loopy	Sterile	Faster than QT631 w/ hs
nz110	A.20	Not loopy	Less loopy	Sterile	Faster than QT631 w/ hs
Group 3					
nz92	1.05	Not loopy	Not loopy	Not sterile	Faster than QT631 w/ hs
nz93	2.09	Not loopy	Not loopy	Not sterile	Like N2
nz95	15.02	Not loopy	Not loopy	Not sterile	Faster than QT631 w/ hs
nz96	2.29	Not loopy	Not loopy	Not sterile	Faster than QT631 w/ hs
nz101	13.15	Not loopy	Not loopy	Not sterile	Like QT631 w/ hs
nz102	18.06	Not loopy	Not loopy	Not sterile	Like QT631 w/ hs
nz103	8.07	Not loopy	Not loopy	Not sterile	Faster than QT631 w/ hs
nz106	D.07	Not loopy	Less loopy	Not sterile	Like QT631 w/ hs
nz107	L.09	Not loopy	Not loopy	Not sterile	Like N2
nz108	L.10	Less loopy	Not loopy	Not sterile	Like N2
nz109	L.15	Not loopy	Not loopy	Not sterile	Faster than QT631 w/ hs
nz111	D.03	Less loopy	Less loopy	Not sterile	Slower than QT631 w/ hs

Table 3-1 Mutants isolated from the screen cluster into three groups

We selected the 20 mutants displaying the most suppressed locomotion, and satisfying the criteria of observing some degree of activity of the hsRHO-1* transgene. They can be classified into three groups based on the strength of suppression of the two RHO-1* transgenes.

nRHO-1* is able to increase sensitivity to aldicarb, and therefore we wanted to see whether these suppressors of locomotion also suppressed the aldicarb phenotype. Our typical aldicarb assay lasts 100 minutes. 25-30 animals were placed on a 35mm plate containing 1mM aldicarb, in the presence of food, with each animal assayed every 10 minutes. To more rapidly assess the phenotype of all our mutants we instead looked at two time points for paralysis. We chose 50 and 80 minute time points, as these show a distinct difference between wild type and QT631. At 50 minutes around 20% of wild-type animals are paralysed (Figure 3-5, blue line) compared to over 60% of QT631 animals (Figure 3-5, red line). Looking at 80 minutes gives information about whether any of the suppressors are resistant to aldicarb compared to N2, as at this time point 70% of wild type animals are paralysed (Figure 3-5, blue line).

We observed a range of aldicarb phenotypes (Figure 3-5) across the mutants tested. The majority of mutants are as or more sensitive to aldicarb than the starting strain, suggesting that mutations in these strains only affect the locomotion phenotype of RHO-1, and do not suppress the acetylcholine release phenotype. This is evidence that these two phenotypes, which often appear together, for example in *goa-1* and *dgk-1* mutants (Lackner, Nurrish et al. 1999; Nurrish, Ségalat et al. 1999) , can be successfully separated.

Other mutants, such as *nz101* (Group 3), *nz105* (Group 1) and *nz111* (Group 3) display aldicarb profiles more similar to wild-type, suggesting that these mutant suppress both the acetylcholine release phenotype and the locomotion phenotype of nRHO-1*. Additionally, this could be evidence that these suppressors have lost activity in both transgenes.

It could be that we have introduced some mutations that are affecting aldicarb resistance in parallel to the nRHO-1* transgene effects, but we cannot distinguish between these possibilities at this stage.

3.8 - Detailed analysis of individual suppressor mutants

Following isolation of twenty strongest RHO-1 suppressor mutants from the screen, we decided to examine the behaviours of individual mutants in more detail. Our original aim

was to backcross all the mutants, analyse their responses to aldicarb and levamisole as markers of activity of the nervous system, and perform mapping experiments on the best candidates to isolate the suppressor mutations.

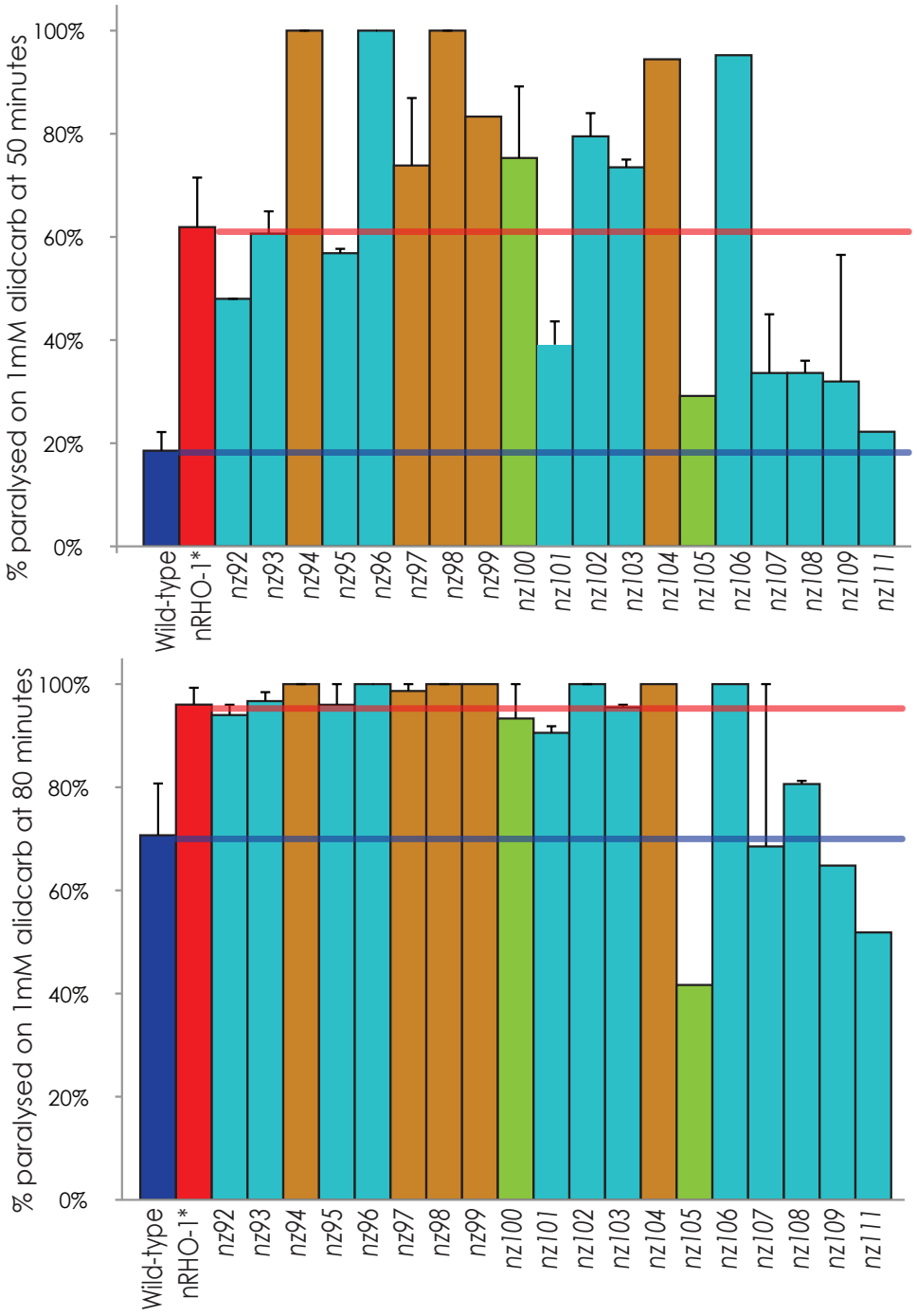

Figure 3-5 - Aldicarb phenotypes of suppressor mutants

Mutants were tested for rate of paralysis on 1mM aldicarb at 2 time points, 50 and 80 minutes. For comparrision, the red line indicates % of nRHO-1* animals paralysed, while the dark blue line indicates % wild-type animals paralysed at each time point. Mutant *nz110* was not included in this experiment (see Figure 3-9 for aldicarb curves of this mutant). Error bars indicate S.E.M. of at least two trials.

Orange bars - Group 1 Mutants, green bars - Group 2 Mutants, light blue bars - Group 3 Mutants (see Table 3-1).

During the course of this process we became particularly interested in the suppressor mutant *nz94*. Initially classified as lethargic, this mutant actually has a rare 'fainting' phenotype, which allowed us to identify it as an allele of the novel gene *unc-80*. Following this discovery, the focus of experimention was concentrated on analysis of this mutant, as detailed in Chapters 4 and 5. Therefore a number of the mutants from this screen remain to be characterised in detail, but those which have been analysed are described here.

3.8.1 - Aldicarb profile of *nz105*

The suppressor mutant *nz105* completely suppresses the locomotion phenotype of nRHO-1* and partially suppresses the loopy locomotion induced by hsRHO-1*, and was placed in Group 2 (Table 3-1). The one-times backcrossed strain, QT823 (*nz105* 1*) is shown here (Figure 3-6, see also Movie 3-3). Tracks left in the OP50 lawn indicate wild-type movement and body bends.

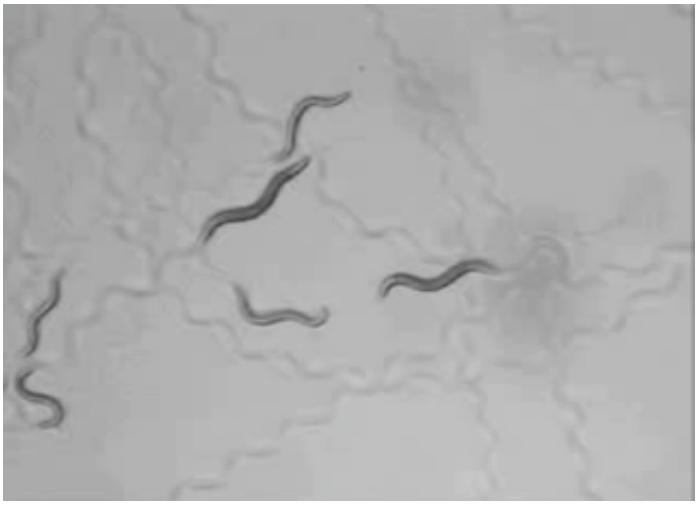

Figure 3-6 - *nz105* suppresses the loopy locomotion phenotype of nRHO-1*

nRHO-1* animals are highly loopy, but animals carrying the nz105 mutation suppress this phenotype. QT823 (nRHO-1*;nz105 1*) animals, shown here, are one-times backcrossed, and have a wild-type body posture and leave tracks similar to those of wild-type animals.

However, despite completely suppressing the locomotion phenotype of nRHO-1*, this mutation only partially suppresses the aldicarb phenotype associated with the nRHO-1* transgene (Figure 3-7). Both the strains assayed, the orginal mutant isolated from the screen and the one-times backcrossed mutant, appear hypersensitive to aldicarb compared with wild-type. Their aldicarb curves are only partially shifted to the right

compared with nRHO-1* animals alone, demonstrating that they still have high levels of neurotransmitter release.

This indicates that the nRHO-1* transgene remains active in these animals, and is able to drive high levels of acetylcholine release independently of generating loopy locomotion, although it is possible that upon further backcrossing the sensivity to aldicarb will change.

3.8.2 - Aldicarb profile of *nz110*

As already mentioned, it is possible that the suppressor mutation in *nz110* is the same as that seen in *nz105*, as they were obtained from the same plate of P_0 animals. The three times backcrossed strain appears wild-type in its locomotion (Figure 3-8, see also

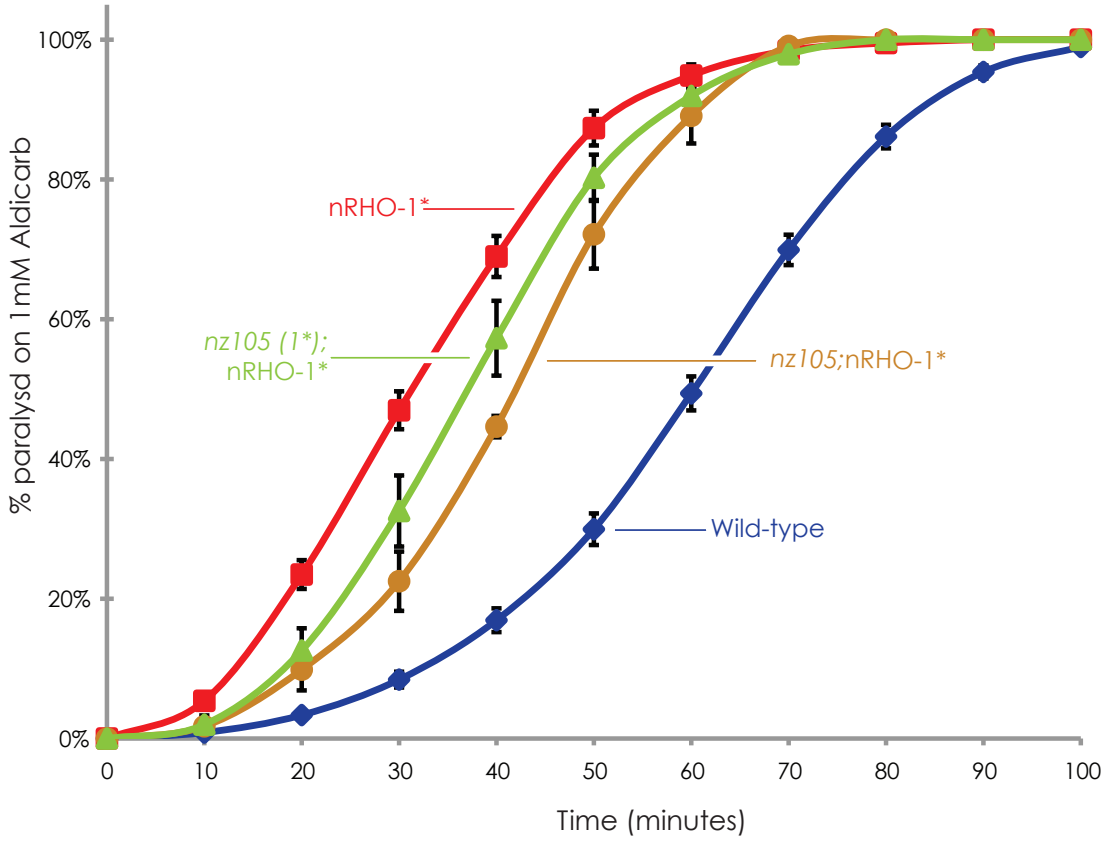

Figure 3-7 - Aldicarb profile of mutants carrying the *nz105* suppressor

Animals were exposed to 1mM aldicarb and the number of paralysed animals assayed every 10 minutes. Both lines assayed, QT684 (*nz105*, orange line, n=4) and QT823 (*nz105 1**, green line, n=6) only partially suppress the aldicarb hypersensitivity of nRHO-1*. Error bars indicate SEM.

Movie 3-4).

The aldicarb curve for the one-times backcrossed *nz110* strain appears intermediate between wild-type and QT631, as it did for *nz105*, suggesting some degree of suppression of the neurotransmitter release phenotype of nRHO-1* (Figure 3-9). A second round

of backcrossing, following the suppression of the loopy phenotype, moves the aldicarb curve to the right, while a third round of backcrossing shifts the curve to the left. These changes could indicate the presence of some modifying loci causing slight variations in the sensitivity to aldicarb in the genetic background of this mutant and potentially (by extension) in animals carrying the *nz105* suppressor.

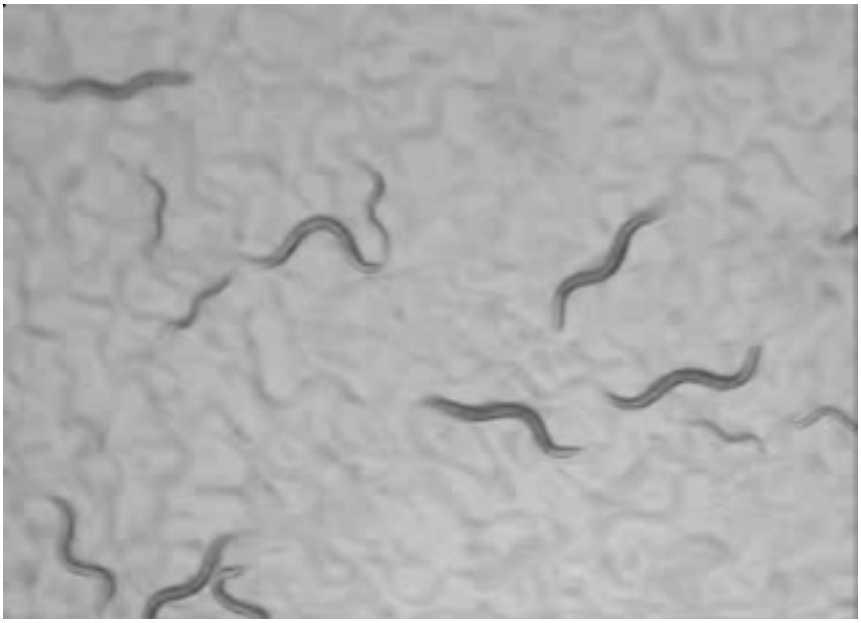

Figure 3-8 - *nz110* suppresses the loopy locomotion phenotype of nRHO-1*

Animals carrying the nz110 mutation suppress the loopy locomotion generated by the nRHO-1* transgnee. QT834 (nRHO-1*;nz110 3*) animals, shown here, are three-times backcrossed, have a wild-type body posture and leave tracks similar to those of wild-type animals.

3.9 - Aldicarb profile of *nz107* and *nz108*

nz107 and *nz108* were obtained from the same original plate, and so may contain the same suppressor mutation. Both belong to Group 3 of the mutants obtained from the screen; they strongly suppress the loopy locomotion phenotype of both transgenes, and are also capable of some suppression of the sterility and pumping phenotypes. This might indicate a reduction in the action of the transgenes, but both mutants exhibit tail swelling following heatshock, demonstrating some action of hsRHO-1*.

In the initial round of aldicarb analysis, the aldicarb profile of both *nz107* and *nz108* looked intermediate between that of wild-type and the starting strain (Figure 3-5), so *nz107* may be a more general RHO-1 suppressor.

In the more detailed neurotransmitter release analysis using the standard aldicarb assay, we see that both unbackcrossed and one-times backcrossed mutants carrying *nz107*

have an aldicarb phenotype intermediate between that of wild-type and the starting strain (Figure 3-10). This, along with the presence of the cc::gfp marker of the nRHO-1* transgene, suggests that the transgene is still functional, and that *nz107* is able to partially suppress the increase in neurotransmitter release caused by nRHO-1*.

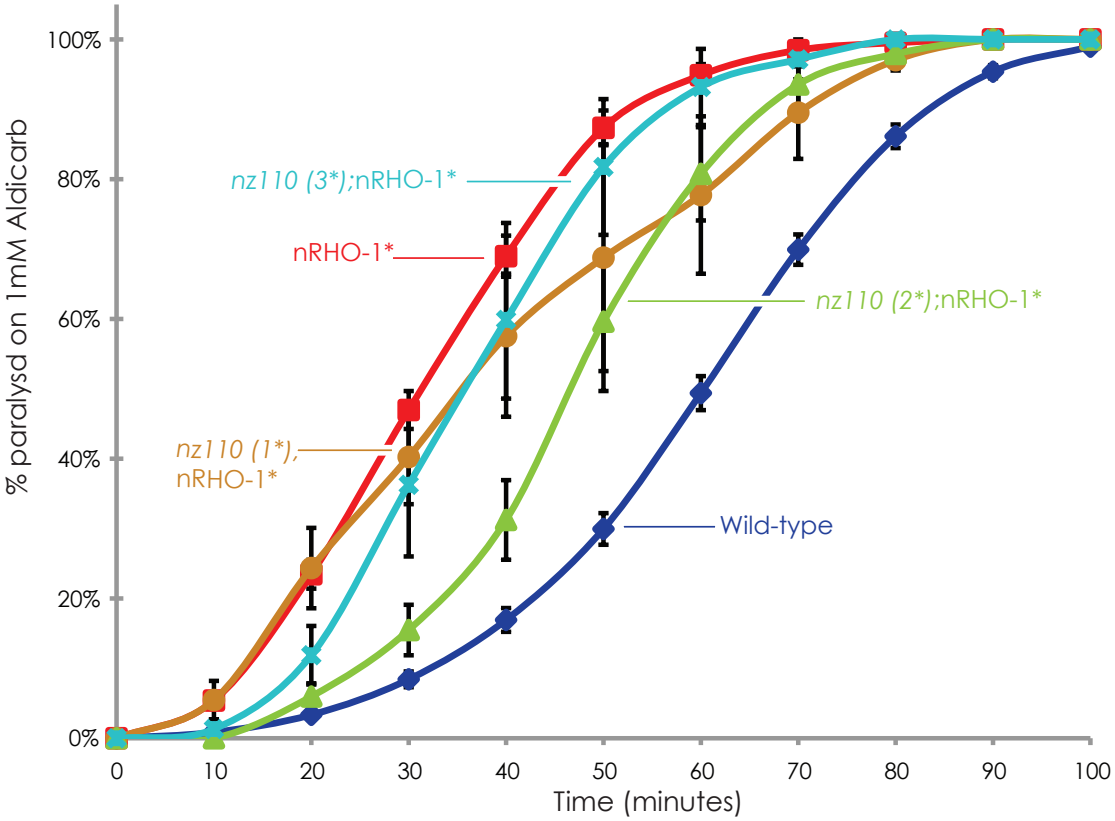

Figure 3-9 Aldicarb profile of mutants carrying the nz110 suppressor

Animals were exposed to 1mM aldicarb and the number of paralysed animals assayed every 10 minutes. All the lines assayed, QT804 (nz110 1*, orange line, n=3), QT816 (nz110 2*, green line, n=5) and QT834 (nz110 3*, light blue line, n=4) are hypersensitive to aldicarb compared with wild-type, and only slightly suppress the aldicarb sensitivity of nRHO-1*. Error bars indicate SEM.

Suppressor *nz108* demonstrates an aldicarb profile highly similar to that of the starting strain (Figure 3-11). This indicates that while this mutant can suppress the locomotion phenotype of the nRHO-1* trasgene it has little effect on the release of acetylcholine.

3.9.1 - Additional RHO-1 suppressor mutant aldicarb profiles

A number of other suppressors have been assessed using the more detailed 100 minute aldicarb assay. Although this data is for a single repeat of unbackcrossed animals, the

sensitivity to aldicarb seems to follow the same trend as the initial assessment for each mutant (Figure 3-5).

nz92 and *nz95* are hypersensitive to aldicarb and show no suppression compared to nRHO-1* animals, while *nz97* and *nz99* mutants are partially suppressed (Figure 3-12) *nz101* appears almost wild-type in its response to aldicarb (Figure 3-12).

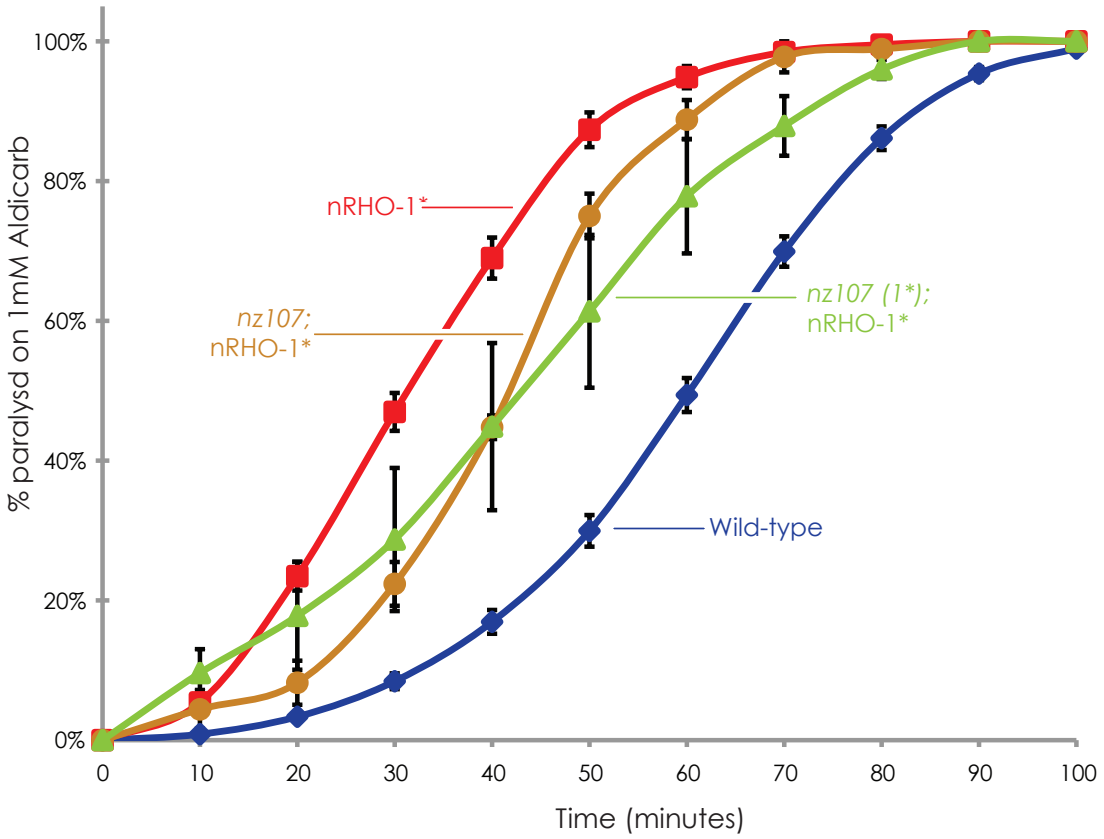

Figure 3-10 Aldicarb profile of mutants carrying the nz107 suppressor

Animals were exposed to 1mM aldicarb and the number of paralysed animals assayed every 10 minutes. Both the lines assayed, QT686 (nz107, orange line, n=3), QT821 (nz107* 1*, green line, n=6) exhibit an aldicarb phenotype intermediate between wild-type and nRHO-1* animals. Error bars indicate SEM.

While all these experiments require additional repeats, and a number of mutants remain to be assayed in detail, the data so far suggests that the majority of mutations show a far stronger suppression of the nRHO-1* locomotion phenotype than the aldicarb phenotype.

3.9.1.1 - Chronic aldicarb assay of mutants

To further assess the aldicarb phenotype of these mutants, a chronic aldicarb assay was performed (Miller, Alfonso et al. 1996)(Miller, Emerson et al. 1999). Here, instead of acutely treating the worms on plates containing 1mM aldicarb for a period of 100 minutes and observing the time of paralysis, 5 L4 worms were placed onto plates containing 0.2mM aldicarb or ethanol control and left to grow for 6 days. Wild type animals are able

to grow on this concentration of aldicarb, although more slowly than in the absence of the drug, while nRHO-1* animals have severely inhibited growth (Table 3-2).

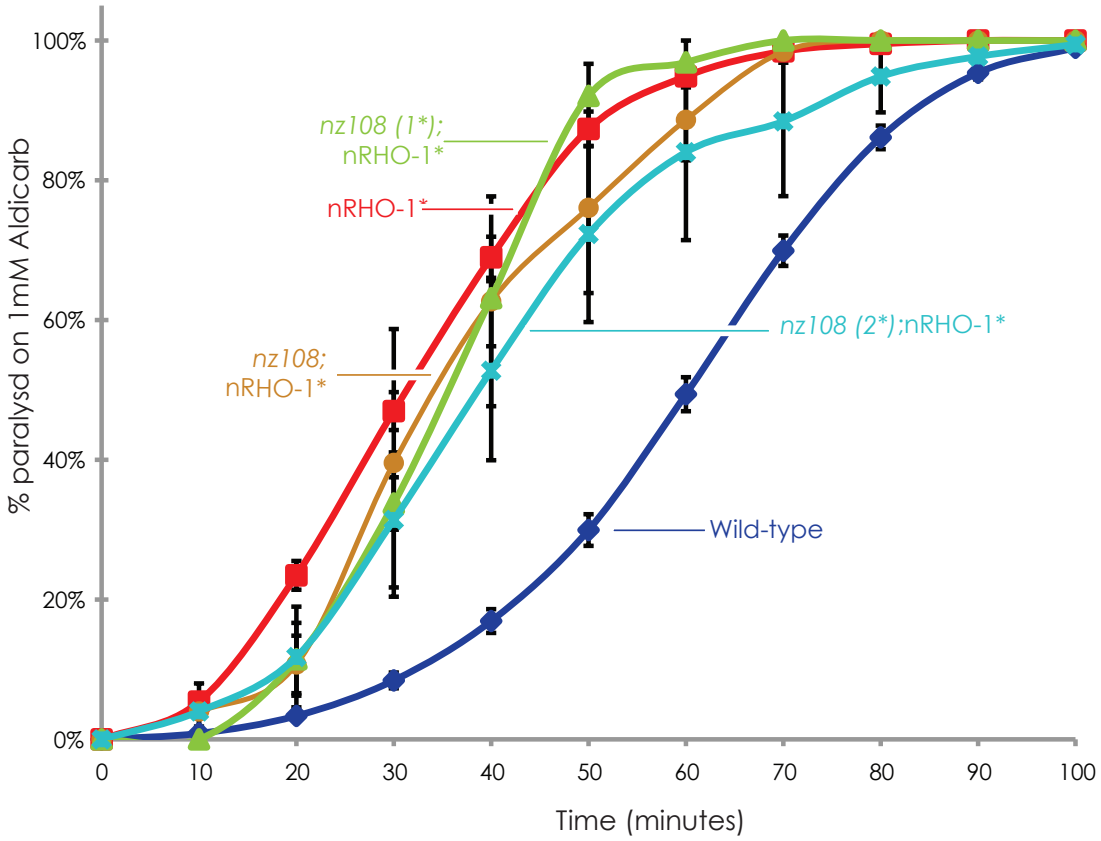

Figure 3-11 Aldicarb profile of mutants carrying the nz108 suppressor

Animals were exposed to 1mM aldicarb and the number of paralysed animals assayed every 10 minutes. All the lines assayed, QT687 (nz108, orange line, n=3), QT812 (nz108* 1*, green line, n=2) QT835 (nz108 2*, light blue line, n=5) exhibit an aldicarb phenotype very similar to that of the starting strain. Error bars indicate SEM.

When tested using this chronic assay, the suppressor mutants all tend to look more like the nRHO-1* starting strain, growing poorly in the presence of 0.2mM aldicarb (although even in the absence of aldicarb some mutants grew poorly). This demonstrates that while they are suppressed for the loopy locomotion generated by the nRHO-1* transgene, they are still releasing more acetylcholine than wild-type animals.

nz105 alone of those mutants tested is able to grow in the presence of 0.2mM aldicarb, looking more like wild-type worms, which is consistent with the initial aldicarb tests for *nz105* which showed some suppression of the aldicarb sensitivity of the starting strain (Figure 3-7).

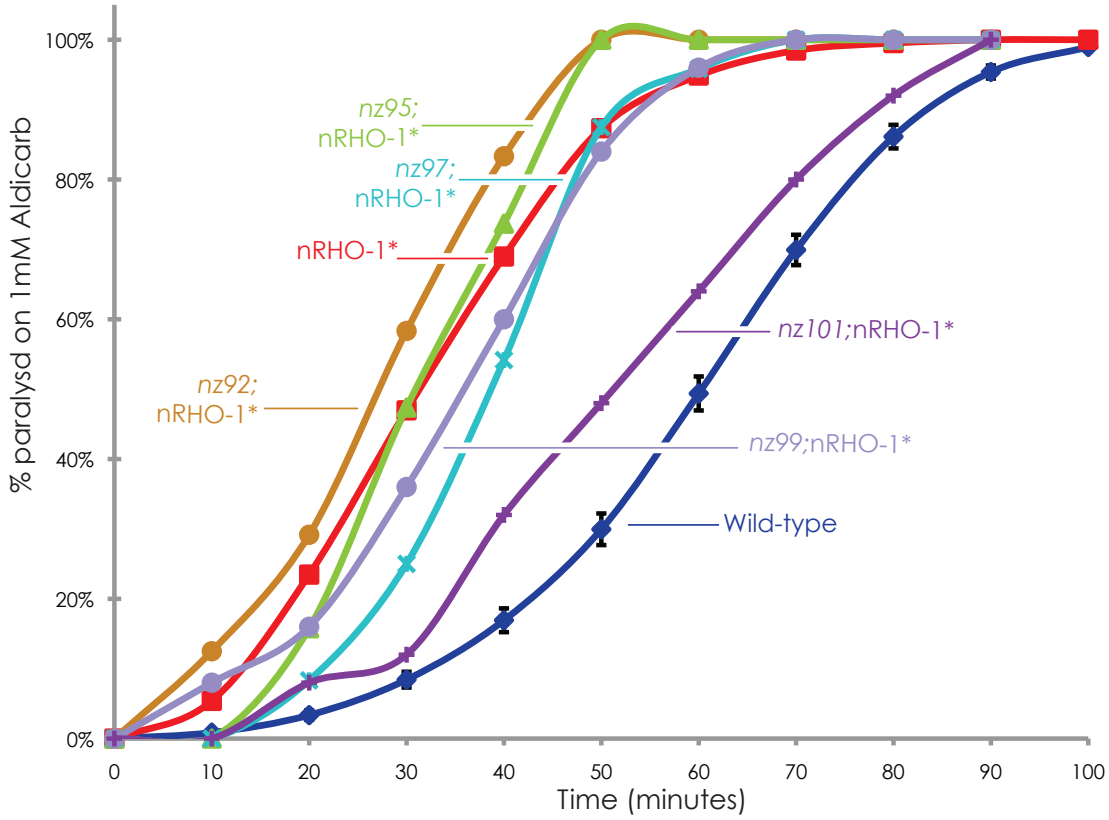

Figure 3-12 Aldicarb profiles of additional unbackcrossed mutants

Animals were exposed to 1mM aldicarb and the number of paralysed animals assayed every 10 minutes. All lines except for nRHO-1* and WT are for a single trial. Error bars indicate SEM.

3.9.2 - *nz106* suppresses the dar phenotype induced by hsRHO-1*

RHO-1 Activation of the heatshock RHO-1* transgene causes an additional phenotype to develop in the tail of the worm. This is the deformed anal region (*dar*) phenotype, commonly associated with infection by bacteria (Hodgkin, Kuwabara et al. 2000). Wild-type worms become dar in the presence of pathogen, first identified in strains contaminated with the nematode-specific pathogen *M. nematophilum,* while hsRHO-1* animals become dar even in the absence of pathogen.

We were interested to see whether any of our suppressors had an altered tail swelling response, so we examined a number of the unbackcrossed mutants, which still carry the heatshock transgene, following heatshock (Figure 3-13). As previously noted during the screening procedure, most of these animals develop tail swellings. However, suppressor *nz106* appears capable of suppressing this phenotype. As the regulation of the tail swelling involves additional, important cellular pathways downstream of RHO-1, such as

MAP Kinase signalling (Partridge, Gravato-Nobre et al. 2010 and R. McMullan, personal communication), this suppressor may be interesting for further study.

3.9.3 - Levamisole Assays of Suppressor Mutants

Strain	0mM Aldicarb	0.2mM Aldicarb
N2	*Large mixed population, food gone*	*Mixed population, food left, slow movement*
nRHO-1*	*Mixed population, food gone*	*Very few animals, food left, very slow movement*
QT688 (*nz109*)	*Small mixed population, food left*	*Most animals dead, very few worms, food left*
QT804 (*nz110 1)**	*Mixed population, food left*	*Very few worms, food left*
QT812 (*nz108 1)**	*Mixed population, food left*	*Few worms, food left*
QT822 (*nz107 1)**	*Small population, food left*	*Very few worms, food left*
QT823 (*nz105 1)**	*Large population, food gone*	*Mixed population, looks like N2, food gone*

Table 3-2 Chronic Aldicarb Assay of Mutants

5 L4 animals were grown in the presence of 0.2mM aldicarb for 6 days, and the plates were assayed for growth. Observatons are the result of two separate trials.

3.9.3.1 - Four suppressor mutants are wild-type in their response to levamisole

It is possible that a mutation that blocks increased acetylcholine release by nRHO-1* also makes muscles hypersensitive to acetylcholine, and this would result in animals which remained hypersensitive to aldicarb. To test for this we have so far tested eight of our suppressors by exposure to the drug levamisole, which directly stimulates the cholinergic receptors on the body wall muscles and is capable of causing paralysis (Nguyen, Alfonso et al. 1995). The nRHO-1* transgene itself does not affect the sensitivity of the body wall muscles to levamisole (McMullan, Hiley et al. 2006).

Four of the eight mutants tested - *nz92*, *nz97*, *nz105* 1*, *nz107* 1* - had a wild-type response to levamisole, indicating no obvious changes in the response of their body wall muscles to neurotransmitter (Figure 3-14).

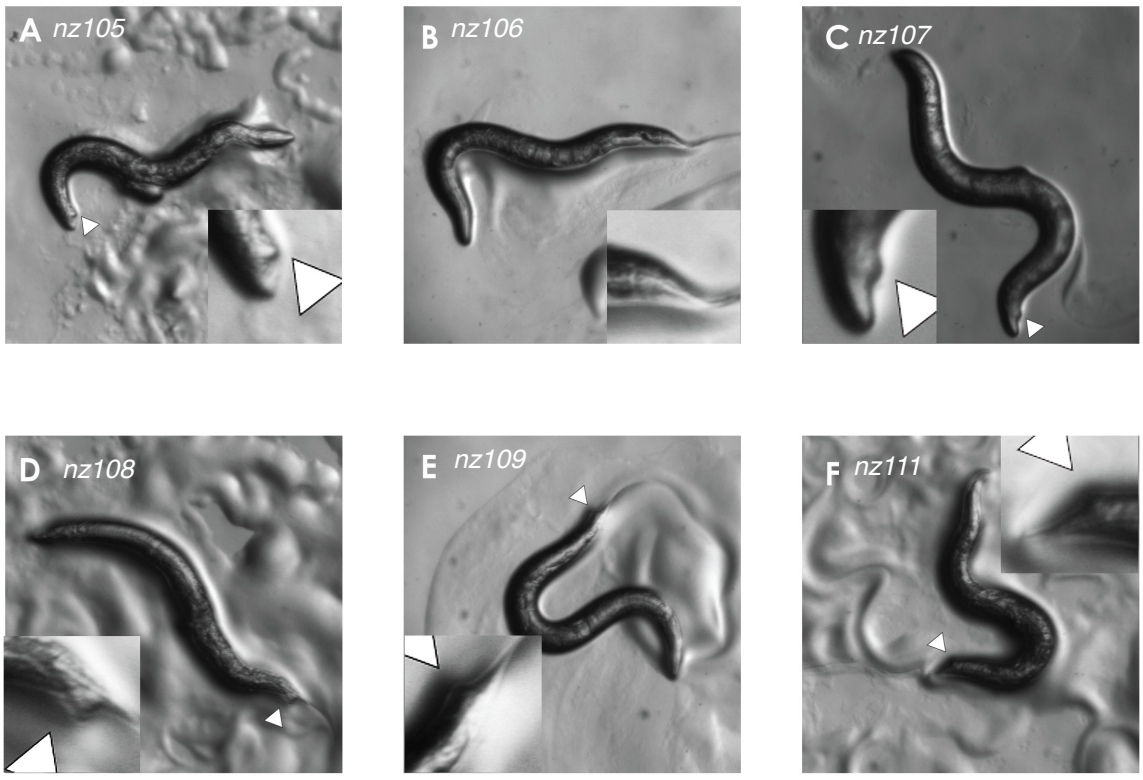

Figure 3-13 Heatshock of suppressor mutants causes tail swelling

One-day old adult animals were subjected to our standard heatshock protocol, and left to recover at 20°C. Of the animals tested, only one, the unbackcrossed QT685 carrying suppressor nz106 (b, above) fails to generate a deformed anal region (dar) phenotype.

nz97, *nz105* 1* and *nz107* 1* display aldicarb phenotypes intermediate between nRHO-1* and wild-type animals, suggesting some level of suppression of the neurotransmitter release phenotype of the nRHO-1* transgene. This suppression is unlikely to be occurring post-synaptically, as they have a wild-type response to levamisole; instead it is likely that these animals are neuronal suppressors of neurotransmitter release.

nz92 displays no suppression of the aldicarb phenotype of nRHO-1*, and is also wild-type for levamisole, suggesting that this mutant affects only the locomotion phenotype and has no effect on neurotransmitter release.

3.9.3.2 - Four suppressor mutants have an abnormal response to levamisole

Of the remaining mutants tested in levamisole assays, three - *nz101*, *nz108* 1*, *nz110* 3* - are resistant to levamisole. *nz101* had a wild-type response to aldicarb (Figure 3-12) which, combined with a resistance to levamisole, suggests that neurotransmitter release remains high in this mutant, but that the aldicarb effect is masked by a post-synaptic reduction in sensitivity to neurotransmitter. This suggests that the supression of the effects of the nRHO-1* trangene may occur post-synaptically.

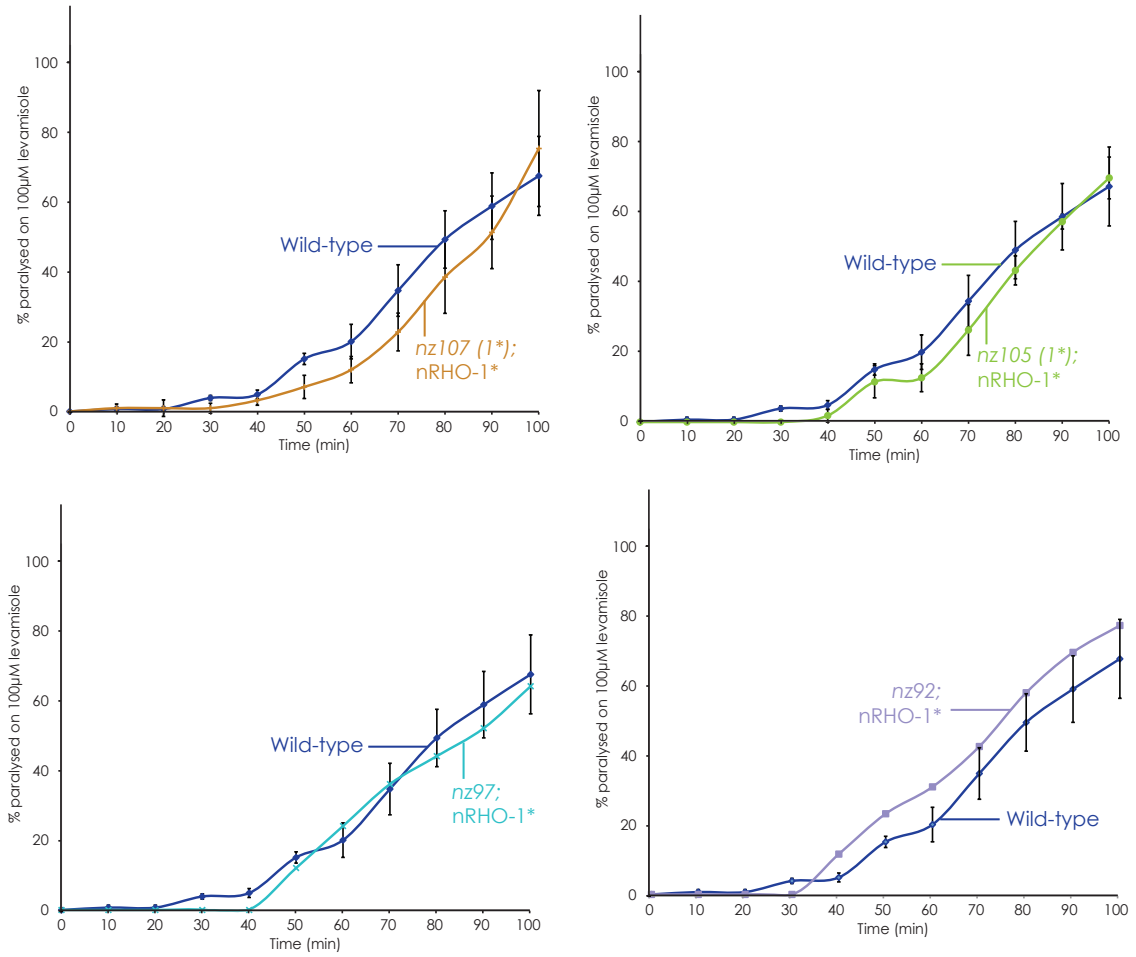

Figure 3-14 Suppressors with a wild-type response to levamisole

Animals were exposed to 100µM levamisole and assayed for paralysis over the course of 100 minutes. Error bars indicate SEM for *nz107* 1* (n=3) and *nz105* 1* (n=3); *nz92* and *nz97* data is the result of a single trial.

nz108 1* and *nz110* 3* are both hypersensitive to aldicarb (Figure 3-11) and (Figure 3-9). They are also resistant to levamisole, and together this data suggests that they have an even higher level of acetylcholine release than that suggested by the aldicarb assay alone. These mutants also represent potential post-synaptic mutations, although

homeostatic mechanisms may occur in the muscle in response to acetylcholine release, as seen in Drosophila (Davis 2006).

The final mutant tested, *nz95*, is hypersensitive to levamisole compared to wild-type animals (Figure 3-12). This suggests that the muscles are hypersensitive to acetylcholine. This mutant also appeared hypersensitive to aldicarb (Figure 3-12); hypersensitivity to both aldicarb and levamisole suggests that this mutant may have a more wild-type level of neurotransmitter release than that indicated by either experiment independently.

3.10 - Identifying the molecular nature of the nRHO-1* suppressor mutants is complicated by poor mating efficiency

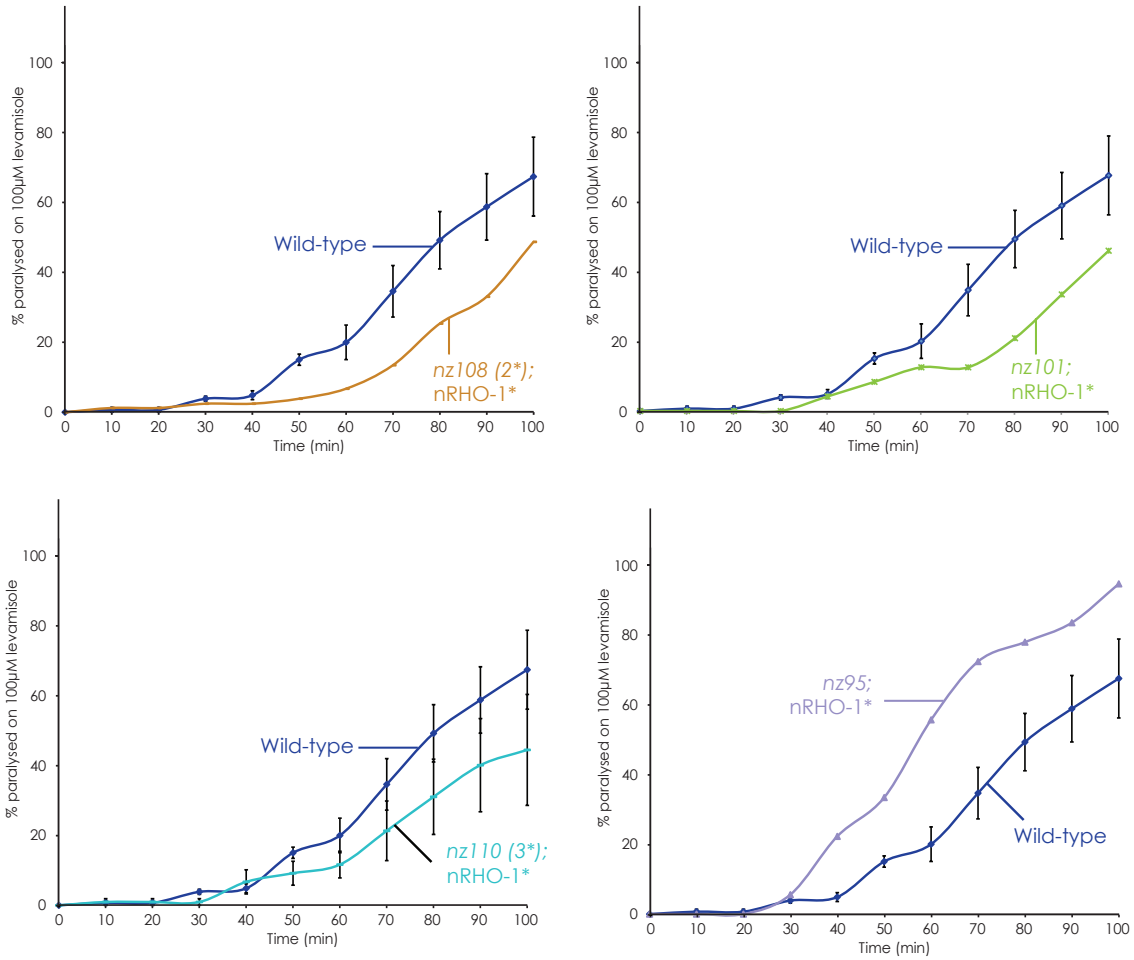

Figure 3-15 Suppressors with a non-wild-type response to levamisole

Animals were exposed to 100µM levamisole and assayed for paralysis over the course of 100 minutes. Error bars indicate standard error of the mean for *nz108* 2* (n=3) and *nz110* 3* (n=3); *nz95* and *nz101* data is the result of a single trial.

To identify the molecular nature of the suppressor mutations introduced by EMS, it is necessary to know which gene is mutated. The earliest methods for this mapping in *C. elegans* involved identifying complementation groups, and crossing with visual markers, such as dumpy or roller mutants, whose relative position on each chromosome was well known (Hodgkin 1999).

One commonly used technique for positional mapping of mutants uses strains which contain a number physiological markers. However, this approach is limited by the availability of easily distinguished markers. A later technique is to analyse the distribution of single nucleotide polymorphisms (SNPs), at positions known to be different between the Bristol strain of *C. elegans* (N2) and the Hawaiian strain (CB4856) (Wicks, Yeh et al. 2001). These can be analysed by PCR and sequencing (a laborious process) or in some cases (where the SNP changes a restriction enzyme site), by PCR and enzyme digest.

This protocol has been refined to take advantage of a 96 well plate system, and 48 SNPs that are all susceptible to the restriction enzyme DraI (Davis, Hammarlund et al. 2005). The idea is to cross a mutant with a Hawaiian animal, pick mutants and wild type animals from the cross, and then perform PCR using a prepared primer set for each SNP, digest on the plate and then run the whole plate out on an agarose gel to look for the changes in digestion.

This procedure has been published as providing a fast and effective means of identifying both the mutant chromosome, and for finer mapping of the interval that contains the mutation.

However, all of our mutations are suppressor mutations, and (with the exception of *nz94*, which will be discussed later) none of these mutations has yet been shown to have a strong phenotype in the absence of the nRHO-1* transgene. This necessitated the production of a Hawaiian strain of *C. elegans* carrying the *nzIs29* transgene (see Strains.)

However, strains carrying the nRHO-1* transgene have proven very difficult to cross, especially for crosses involving suppressor mutants carrying additional background mutations. While we had some success generating backcrossed lines for analysis using aldicarb and levamisole, difficulties backcrossing our suppressor strains reduced our access to conventional (Brenner 1974) and snip/SNP mapping techniques (Wicks, Yeh et al. 2001). We therefore made use of a technique which is quickly becoming a new standard for mapping mutants – whole genome sequencing (Sarin, Prabhu et al. 2008).

3.11 - Whole Genome Sequencing allows identification of mutations in backcrossed and unbackcrossed strains

The principle of the technique is to generate millions of short reads (usually between 36 and 76 base pairs), randomly distributed across the mutant genome. Computer algorithms are then able to align these short reads against the wild-type genome. The program then identifies bases that are different between the wild type and mutant genomes, and these sites can then be further investigated (Figure 3-16).

In previous cases, this sequencing has been performed after several rounds of standard mapping – either using the Snip/SNP mapping or by mapping to an arm of a chromosome – which then allowed the researchers to focus on the data for those fractions of the genome. We reasoned, however, that the number of protein-altering mutations in reported in these papers was low enough that, across a mutant genome, we might expect approximately 200 mutations affecting coding sequences. Of these we might be able to distinguish good candidates for further investigation, or be able to attempt rescuing experiments using pools of cosmids and fosmids to narrow down the search.

We therefore decided to proceed with the whole genome sequencing without having mapped to the mutations to a specific chromosome. Should the sequencing prove inconclusive, we could return to the traditional mapping approaches and use them to filter our (already acquired) sequencing data.

3.11.1 -Choosing strains to send for Whole Genome Sequencing

nz97 – A Group 1 suppressor (Table 3-1), *nz97* is 'Not loopy' at room temperature, so suppresses the nRHO-1* effects on behaviour, and is 'Not Loopy' following heat shock, suppressing the neuronal effects of hsRHO-1*. It does become sterile after heatshock, and does not suppress changes in pumping, showing that this mutation is specifically able to suppress the locomotive phenotype of RHO-1* (Table 3-1). This mutant has high levels of neurotransmitter release, (Figure 3-10), suggesting it does not suppress this phenotype associated with nRHO-1*. We sent strain QT788, which contains the *nz97* suppressor, and is three times backcrossed, with the aim of reducing background mutations.

nz99 – Also a Group 1 suppressor, *nz99* similarly suppresses the locomotive phenotype of nRHO-1*, but not other neuronal phenotypes (pumping and hypersensitivity to aldicarb (Figure 3-12)) or non-neuronal behaviours (sterility) (Table 3-1). The strain we selected for sequencing - QT677 - is completely unbackcrossed. With this strain, we wanted to

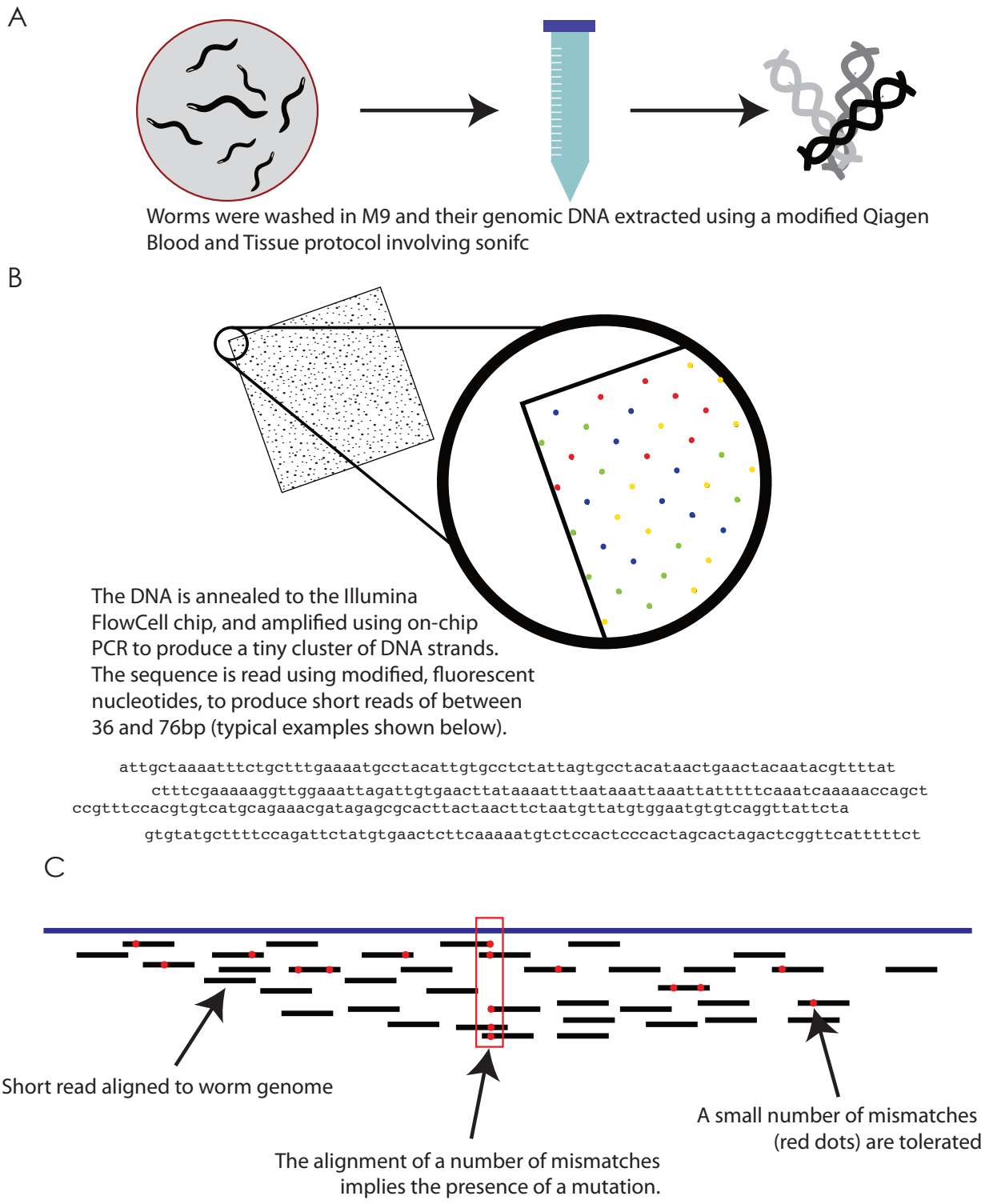

Figure 3-16 Whole Genome Sequencing

DNA was extracted from mutant animals (A) and sent to GeneService for sequencing (B). The result is millions of short reads which can be aligned against the known worm genome to predict mutations (C).

test the full capacity of the Whole Genome Sequencing approach, to see whether we could identify a mutation in an unbackcrossed, unmapped strain.

nz110 – This suppressor is in Group 2, and fully suppresses the locomotion phenotype of nRHO-1* at room temperature (Table 3-1). It does however become relatively loopy after heatshock, so is possibly a weaker suppressor than the other mutants. It displays high levels of neurotransmitter release, suggesting it does not suppress all the neuronal phenotypes of nRHO-1* (Figure 3-9). We sent strain QT834, which was three times backcrossed.

nz90 – We also included in our sequencing run a mutant from an entirely different source. Emma Hiley, a previous PhD student in the lab, identified *nz90* as an mutation which causes resistance to aldicarb (Hiley 2006). While investigating strain VC430, which contained a mutation in the Rho GEF RHGF-1, she found a second mutation that caused resistance to aldicarb. This mutation was mapped using Snip/SNP mapping to a 500kb region on Chromosome V, and the resistance to aldicarb was rescued by injecting cosmid T025B5. Genes TO2b5.1 and TO2b5.2 were injected individually and overexpression of either gene was sufficient to rescue the aldicarb phenotype.

Subsequent sequencing of the coding regions of these genes detected no mutations. Some sequencing has also been performed to look at the non-coding regions of these genes without detecting any mutations. This mutant, which had been mapped to an 3Mb interval, but for which the molecular nature of the lesion is unknown, provided a good test of the whole genome resequencing.

This mutant was generated by TMP/UV entirely separately from the EMS mutagenised nRHO-1* animals. However, this strain had been backcrossed through wild-type animals from our lab. We therefore felt confident in classifying any mutations common to this strain and our nRHO-1* mutant strains as background mutations or sequencing errors.

3.11.2 -Preparing genomic DNA for sequencing

We prepared the DNA using the Qiagen Blood and Tissue kit, and a modified protocol involving sonication (see Methods). We obtained genomic DNA and quantified it using the NanoDrop spectrophotometer (Table 3-3).

3.11.3 -Running the samples

The samples were dispatched to GeneService, who ran them on multiple lanes of the Illumina sequencing system. These produced reads of 36, 55 or 76 base pairs (see Table 3-4). All of these sequences are ‘paired end data’. During fragmentation of the

genome, DNA fragments of approximately 500 base pairs are produced. The paired end sequencing procedure reads the sequences at both ends of these fragments, and associates the data into a single file. Essentially, this provides additional spatial information, such that in the starting genome those two short reads were no more than 500 base pairs apart. This additional data can be used to constrain the search algorithms during mapping.

3.12 - Analysing the Whole Genome Sequencing Data

The runs described above generated a large amount of sequencing data for each of the mutants. Geneservice inputted this data in the program MAQ (Mapping and Assembly with Quality (http://maq.sourceforge.net/)). This program takes the millions of reads produced by the sequencing reactions and attempts to find a good match within a known sequence, in our case, the *C. elegans* genome.

These reads are then used to define a consensus, using the quality scores associated with each mapped base. The coverage of the consensus data is essentially random, but may be influenced at any given point by the ease with which a particular sequence can be amplified by PCR.

Mutant Sequenced	**QT317**	**QT677**	**QT788**	**QT834**
Suppressor Allele	*nz90*	*nz99*	*nz97*	*nz110*
DNA Concentration	509 ng/ul	205 ng/ul	815 ng/ul	225 ng/ul
Dilution (Final Concentration)	2x (250ng/ul)	1x	4x (200ng/ul)	1x

Table 3-3 - DNA extraction from suppressor mutants

Details of DNA extracted from the four mutants sent for sequencing

3.12.1 -Analysis of data obtained by Geneservice indicated a premature STOP codon in *cbp-1* within mutant QT834

Geneservice provided a list of predicted SNPs in the four mutant animals sent for sequencing. To reduce the number of SNPs which may be relevant to the analysis we filtered the SNPs by comparing across all files for any mutations occurring at exactly the

same genomic location, and introducing the same mutation, in more than one strain (see Methods). These can be considered to be background mutations, possibly present in our original starting strain, or introduced during backcrossing. This reduced the number of SNPs which are likely to represent the suppressor mutation in the strains by between 50 and 80% (Table 3-5).

Mutant Sequenced	**QT317**	**QT677**	**QT788**	**QT834**
Suppressor Allele	*nz90*	*nz99*	*nz97*	*nz110*
36bp Data	2 runs (271mb and 258mb)	2 runs (271mb and 295mb)	2 runs (200mb and 196mb)	2 runs (252mb and 278mb)
55bp Data	1 (unknown)			
76bp Data	1 run (565mb)	1 run (545mb)	2 runs (344mb and 341mb)	1 run (563mb)
Estimated Coverage	18.2 times	24.7 times	17.8 times	17.9 times

Table 3-4 - Details of sequencing reactions

The raw data from the Illumina Flow Cells was processed by Geneservice using their in-house algorithms to determine the quality of the sequencing data. Where spots on the flow cell dimmed too quickly or were too close together these were excluded from the analysis. This data was used to run the program MAQ (see text) and from this a prediction of the coverage of the genome was obtained for each mutant.

Of these remaining mutations, we initially focussed on those that introduced changes into protein coding regions of the genome. However, no annotation of the SNPs was provided by Geneservice. To attempt to overlay the details of the remaining SNPs with biologically-relevant information, we ran the details of each SNP through the UCSC Genome Browser (http://genome.ucsc.ed), and used this to identify which SNPs fell within the regions of genes. For each of these genes identified as a 'hit', we used data from WormBase (http://www.wormbase.org) to identify those SNPs which overlay an exon, and subsequently those which cause a protein coding change (see Methods for more details of this procedure).

This analysis was most thoroughly performed for the SNPs obtained from QT834 with the aim of testing the process and then applying it to the other mutants if successful.

The most severe mutation predicted by this analysis was the introduction of a premature STOP codon into the gene *cbp-1*, the *C. elegans* homologue of CREB Binding Protein.

To test the efficiency of this analysis, we sequenced the region of *cbp-1* into which this mutation had been introduced. However, the sequencing reactions demonstrated that *nz110* was wild-type for *cbp-1* in the sequenced region. Repeat bioinformatic analysis of this region indicated that the initial assignment of this mutation was incorrect.

Mutant Sequenced	**QT317**	**QT677**	**QT788**	**QT834**
Suppressor Allele	*nz90*	*nz99*	*nz97*	*nz110*
Number times backcrossed	10 (through WT)	*0*	*3, through starting strain*	*3, through starting strain*
SNPs in Geneservice File	2520	2960	3346	2675
Unique SNPs in Geneservice File	375	895	1457	862
SNPs from MAQGene analysis	2369	2809	2464	3083
Unique SNPs from MAQGene analysis	843	1278	1608	1500
Protein coding changes in MAQGene Analysis	16	42	115	44

Table 3-5 - Details of Mutations identified in sequenced DNA

The total number of mutations in each mutant is relatively consistent (from 2369 to 3346, depending on analysis) regardless of the number of times these animals have been backcrossed. After filtering for SNPs which occur in at least two strains, the number of mutations decreases drastically, with between 35 to 85% of the original SNPs being eliminated from the analysis. Using MAQGene, which ascribes biologically relevant context to the SNPs, the number of protein coding changes per mutant ranges from 16 to 115, within the range we estimated at the start of the process.

3.13 - Analysis of WGS data using MAQGene

Following this unsuccessful attempt to analyse the processed data obtained from Geneservice, we decided perform our own analysis on the raw data. As well as the processed data obtained from running MAQ, Geneservice provided us with the raw data from the flowcells.

To perform this analysis we made use of a program, MAQGene, developed in the Hobert lab (Sarin, Prabhu et al. 2008; Bigelow, Doitsidou et al. 2009;Sarin, Bertrand et al. 2010). MAQGene allows a user to run the program MAQ without accessing the Linux command line. Within MAQGene, the MAQ-specific commands are entered into a user-friendly webpage-format, MAQGene generates all MAQ-specific files, and produces a list of SNPs, similar to that obtained from Geneservice.

Additionally, MAQGene then interrogates these SNPs using its own specific parameters, and then maps those that pass these thresholds onto an annotated database of the worm genome. This database can be updated to hold the most up-to-date release of the *C. elegans* genome.

The final output from MAQGene is a list of SNPs and small deletions referred to as indels, detailing both their position in the genome, any genes which are affected by the predicted changes, and the nature of those changes – for instance, introducing premature STOP codons, or creating read-through mutations.

These files can be filtered to remove any mutations occurring at the same residue and giving rise to the same base change in at least two of the four mutants sequenced, as these are likely to represent background mutations or consistent sequencing errors. This procedure reduced the total number of mutations from a range of 3083 - 2369 to a range of 1608 - 843.

The mutations can then be sorted according to their molecular nature, for instance to list just those affecting protein coding regions. This reduces the number of mutations in each strain to between 16 and 115 which affect protein coding sequences.

3.13.1 -Distribution of mutations along chromosomes following backcrossing reveals potential locations of suppressor mutants in QT788

As backcrossing occurs, mutations close to the suppressor are likely to be maintained in the genome, while those further away and therefore unlinked are more likely to be lost. This is the essence of all mapping, whether those linked mutations produce visible

phenotypes such as dumpy or roller mutants, or whether they represent SNPs which have to be analysd through PCR and restriction digests. A recent idea in whole genome sequencing is to look for patches of the genome which have a particularly dense collection of mutations following backcrossing, as these linked mutations may indicate the locus of the suppressor mutation (Zuryn, Le Gras et al. 2010). A similar idea has recently been tested using crosses with the Hawiaan strain of *C. elegans* to identify regions linked to the candidate mutation (Doitsidou, Poole et al. 2010).

We filtered the MAQGene predictions for the cannoical G/C - A/T mutations introduced by EMS (Drake and Baltz 1976), and plotted the frequency of mutation every million bases along each chromosome for the three suppressor mutants.

QT677 provides a good control for this process, as this mutant is entirely unbackcrossed, and therefore no selection has been applied which could create linkage between the background SNPs and the causative suppressor mutation. When the G/C - A/T mutations are analysed, there are clusters of mutations present on each chromosome, as would be expected through a random introduction of mutations by EMS (Figure 3-17, A). After filtering these mutations for quality (see Methods for details) the distribution appears to cluster on Chromosome III (Figure 3-17, B). This cluster does not represent any artificial selection causing association to the causative mutation, but may instead indicate a susceptibility to mutation in this region, or result from selection pressure occuring at the population level during screening.

For QT788 the initial analysis did not reveal a single concentration of SNPs (Figure 3-18, A). However, after filtering for quality, a single peak of SNPs can be seen to clearly cluster on Chromosome II (Figure 3-18, B). Although far from definitive, this provides a good target for investigation of the potential suppressor mutation.

In QT834, neither the unfiltered nor the filtered data provide a good target for further investigation (Figure 3-19). In fact, the total number of SNPs which pass the quality filter is very low compared to the other two mutants. There is a slightly denser concentration of SNPs on Chromosome IV, as indicated by the red arrow, but it is not possible at this stage to determine whether this is significant.

3.13.2 -QT834 (*nz110*) contains a mutation in *unc-31* (CAPS)

Without strong positional information from mutant QT834, we took a candidate approach to analysing our data. From the filtered output from MAQGene, we obtained a list of 44 missense mutations predicted to be present in the QT834 (*nz110*) genome (Appendix 2). The remainder of the predicted mutations are either silent, intronic or in intergenic

regions, so we focused first on those predicted to be capable of altering protein-coding regions. Interestingly, we found no predicted premature STOP codons in the data produced from MAQGene. Although premature STOP codons are not the only type of mutation capable of disrupting gene function, they are an important class of mutation and, in previous studies, mutants regularly contain 5-10 premature STOP codons per genome (Sarin, Prabhu et al. 2008; Bigelow, Doitsidou et al. 2009; Sarin, Bertrand et al. 2010).

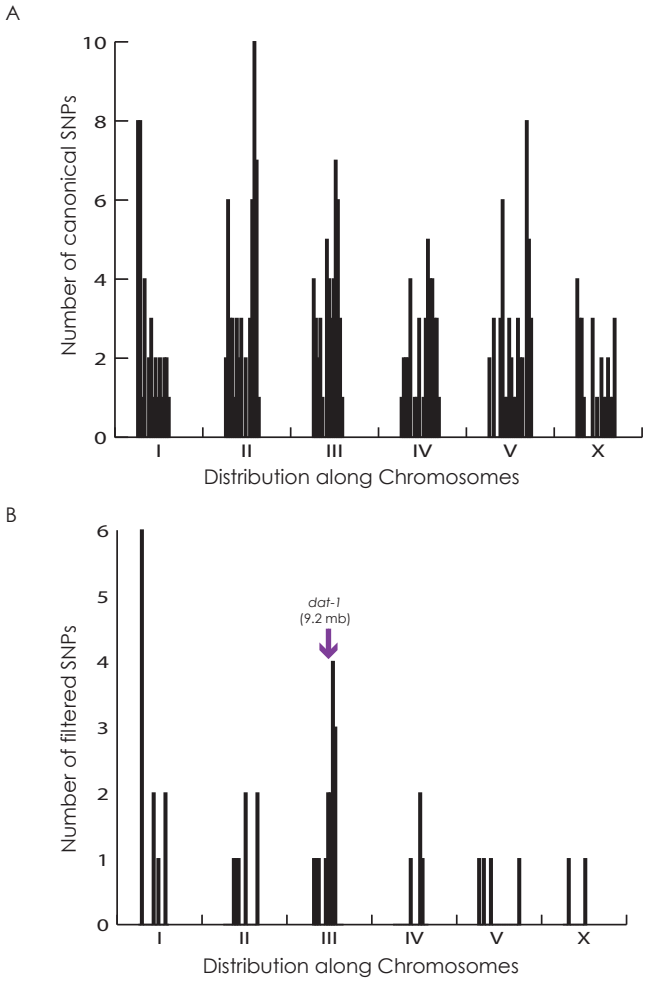

Figure 3-17 Distribution of SNPS in QT677 (*nz99*)

QT677 is a completely unbackcrossed mutant, and therefore its distribution of SNPs should represent the natural introduction of mutations into the genome by EMS. In the unfiltered data (A), there are peaks of C/G to A/T SNPs (coding and non-coding) on each chromosome. As can be seen from the filtered data (B), there is a higher concentration of SNPs on Chromosome III. This cannot be attributed to the causative mutation being present on this chromosome as no selection has occurred to drive this accumulation; rather it is the stochastic nature of mutations to be unevenly distributed at this level of analysis However, this region on chromosome III corresponds to the location of a strong candidate mutation in *dat-1* (purple arrow), suggesting that there may be some bias, even without backcrossing.

Without the detection of a specific class of strong mutant, we next examined the list of mutations for genes known to be involved in synapse function. One candidate suppressor mutation is in the gene *unc-31*, which encodes the *C. elegans* homologue of CAPS, a protein involved in the release of dense core vesicles (Speese, Petrie et al. 2007).

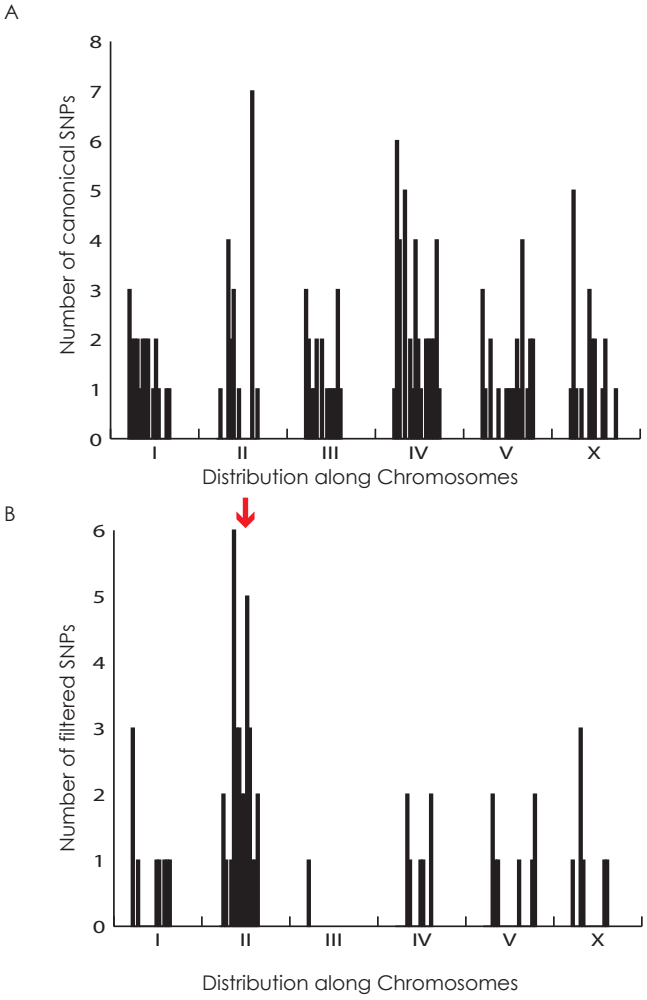

Figure 3-18 Distribution of SNPS in QT788 (*nz97*)

The unfiltered distribution of all C/G to A/T SNPs (coding and non-coding) in QT788 does not indicate a strong selection for any particular chromosome, as there are spikes in frequency along each chromosome (A).

After filtering for quality (B), a strong peak of SNP concentration emerges on Chromosome II (red arrow), suggesting that these SNPs may be linked to a causative and selected mutation in this region.

These contain neuropeptides, as well as some small molecule neurotransmitters such as serotonin and dopamine, and are far larger than the small synaptic vesicles which release acetylcholine. We were interested in this potential mutation because neuropeptides act as neuromodulators through activation of seven-pass transmembrane receptors, and we

thought that this kind of signal might well be involved in the modulation of the extent of body bends in *C. elegans*.

The predicted *unc-31* mutation causes a GCA->GTA[Ala->Val] change in the protein. We sequenced this region of *unc-31* from the QT834 (*nz110*) mutant, and confirmed the predicted change using Sanger sequencing (Figure 3-20). This mutation falls in the Munc-13 homology domain. Dr Muna Elmi is currently attempting to rescue the *unc-31* mutation using *unc-31* wild-type sequences from a fosmid covering that region.

3.13.3 -QT677 (*nz99*) contains a premature STOP codon in *dat-1*, a dopamine reuptake transporter

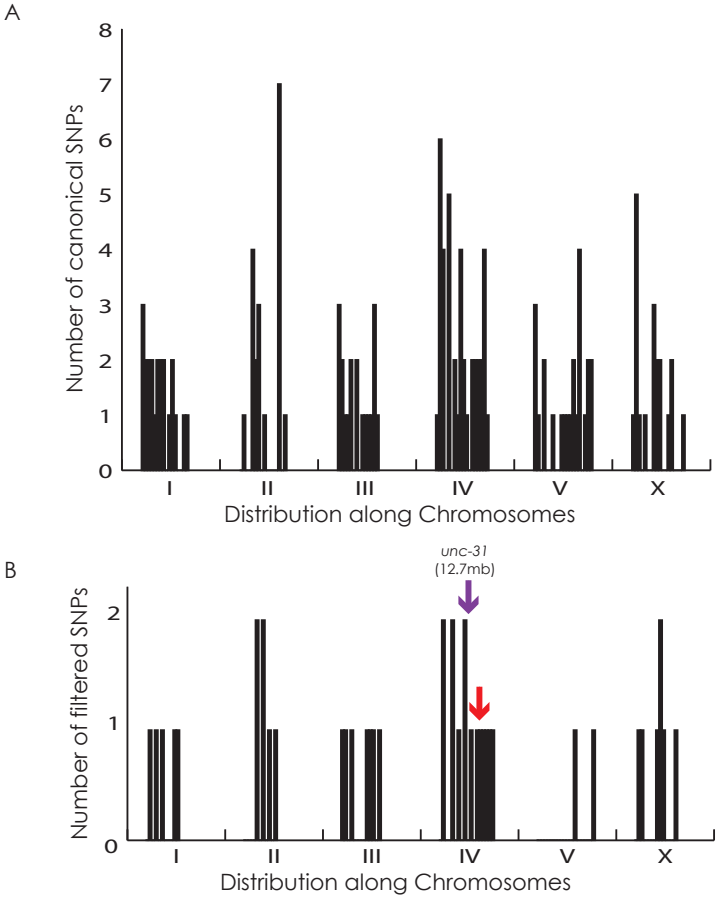

Figure 3-19 Distribution of SNPS in QT834 (*nz110*)

The unfiltered distribution of C/G to A/T SNPs (coding and non-coding) in QT834 does not indicate a strong selection for any particular chromosome, as there are spikes in frequency along each chromosome (A). After filtering for quality, the majority of the SNPs on each chromosome are lost (B). Chromosome IV maintains the highest density of SNPs, indicated by the red arrow.

In the absence of positional information for the suppressor mutation in QT677, we took a candidate approach to the mutations obtained from analysis using MAQGene. We

produced a list containing 42 protein-coding alterations, including 39 single nucleotide polymorphisms and 3 small insertions/deletions causing frameshifts. Looking first for strong alleles, we found a single predicted premature STOP codon, in *dat-1*, the dopamine reuptake transporter, which works to remove dopamine from the synapse after release (Jayanthi, Apparsundaram et al. 1998).

We sequenced the region of *dat-1* predicted to contain the STOP codon using sanger sequencing, which confirmed the presence of the mutation (Figure 3-21). This is our top candidate for the suppressor mutation, because it occurs in a protein important for synaptic signalling and particularly the control of locomotion.

3.13.4 -Analysis of QT788 indicates that the suppressor mutation may localise to one of two regions on Chromosome II

With the analysis of the distribution of SNPs in QT788 we saw a clear concentration on Chromosome II (Figure 3-18). This suggests that the mutation localises to this chromosome. Our analysis from MAQGene predicts a total of 115 protein coding changes in this mutant, of which 29 localise to Chromosome II.

We examined the distribution of canonical G/C - A/T mutations on this chromosome in more detail (Figure 3-22) and saw that these mutations cluster into two peaks on the chromosome. Within those peaks there are only 8 mutations which are able to cause protein coding changes. While this analysis cannot say that one of those mutations is the suppressor mutation, these provide good candidates for further investigation.

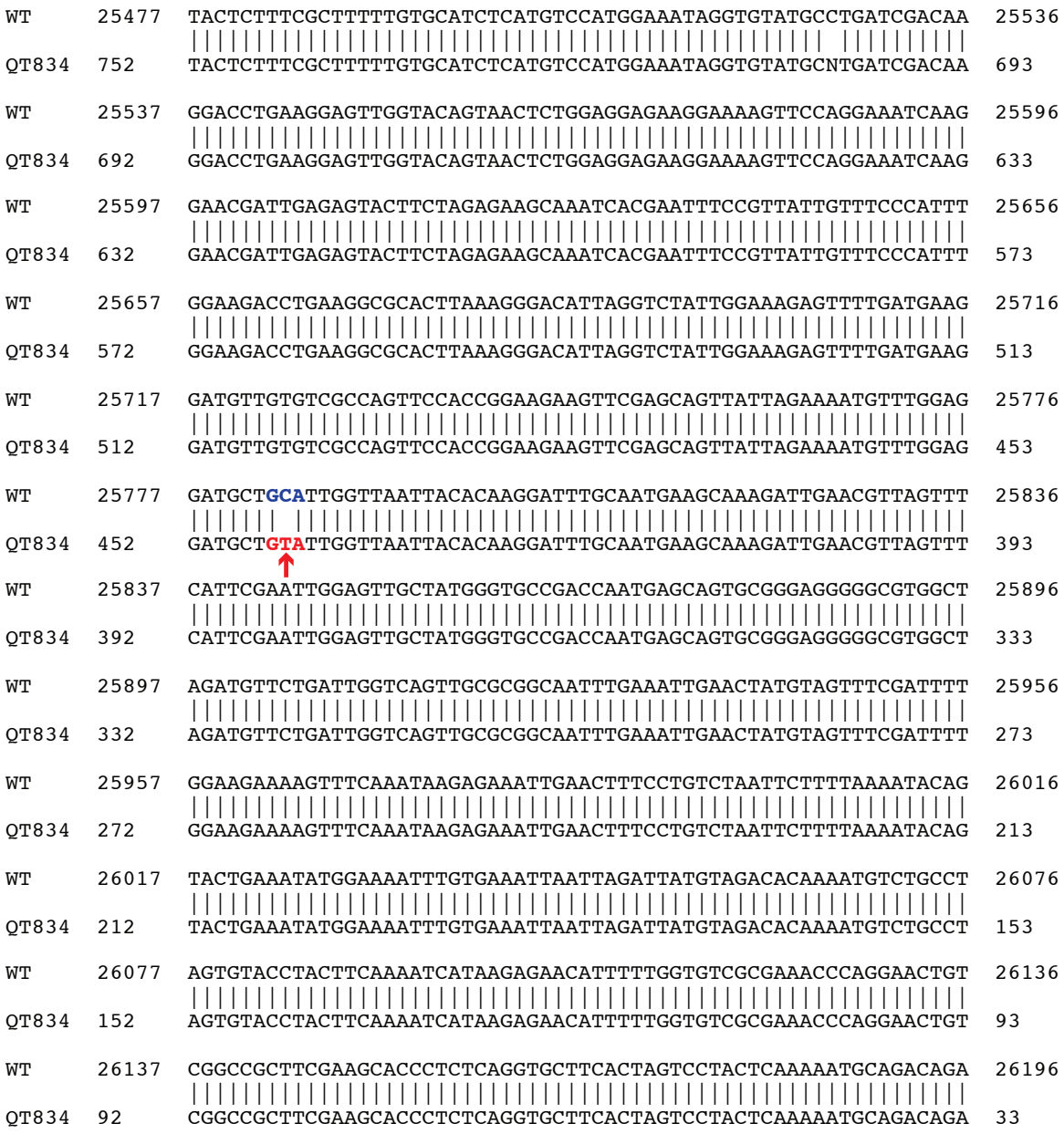

Figure 3-20 Mutant QT834 (*nz110*) contains a mutated version of *unc-31*

Sanger sequencing of genomic DNA from QT834 confirmed a mutation in the *unc-31* gene giving rise to a mutated codon (red lettering) compared to the wild-type sequence (blue lettering). The single nucleotide change is indicated by the red arrow.

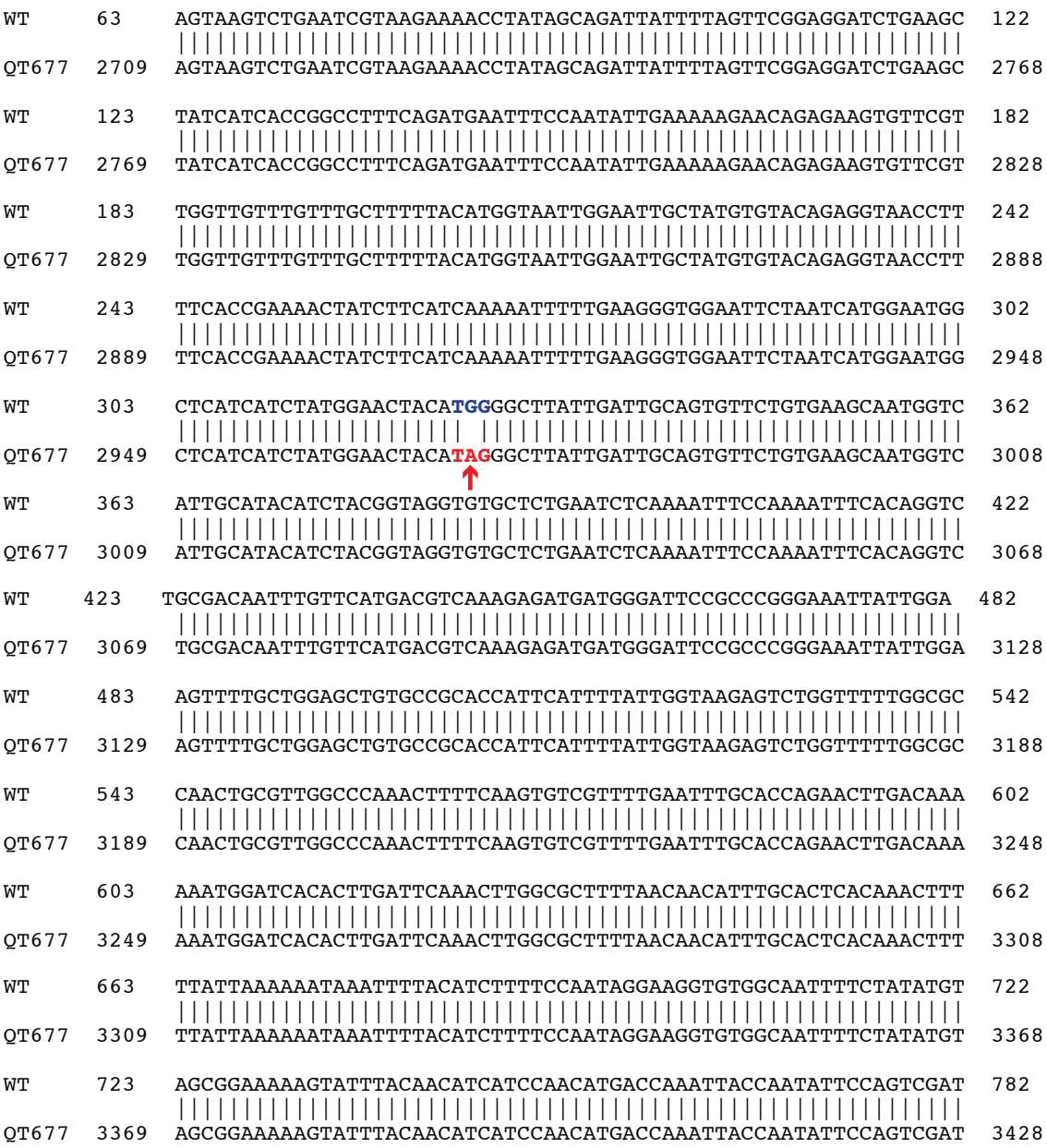

Figure 3-21 Mutant QT677 (*nz99*) contains a premature stop codon in dat-1

Sanger sequencing of genomic DNA from QT677 confirmed a mutation is introduced into the dat-1 gene in QT677. The mutation introduces a premature STOP codon (red lettering) with the single nucleotide change indicated by the red arrow.

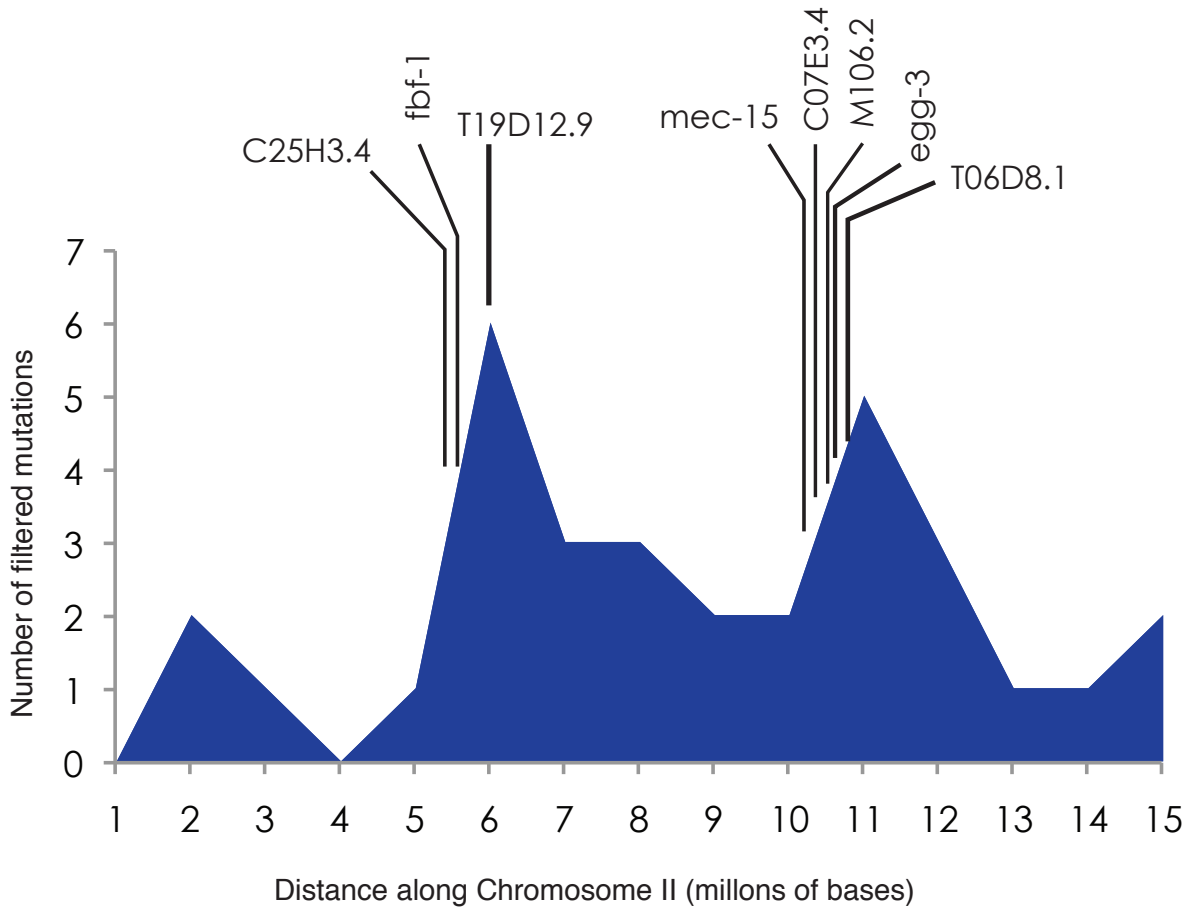

Figure 3-22 Detailed analysis of chromosome II mutations from QT788 (*nz97*)

Analysis of the distribution of mutations in QT788 highlighted a concentration of mutations on Chromosome II. Here that distribution is shown in more detail. There are two peaks of mutation frequency around 6 and 11mb along the chromosome. These have been overlayed with details of those mutations capable of causing protein-coding changes. This analysis suggests that one of these 8 mutations may be responsible for suppressing the loopy phenotype of nRHO-1*.

3.14 - Discussion

3.14.1 -Screening

The overall aim of the screen was to identify novel downstream targets of RHO-1 which regulates neurotransmitter release in *C. elegans*. We chose the loopy locomotion phenotype of our nRHO-1* animals as a marker, as it is distinct from wild-type locomotion and can be observed without special equipment (i.e. does not require high power microscopy or UV light) or use of drugs, e.g. aldicarb. We considered screening for animals which suppressed the the alidcarb hypersensitivity of nRHO-1*, but decided against this primarily to avoid repeating the *ric* (resistant to aldicarb) screens performed by other labs (Miller, Alfonso et al. 1996). (A summer student tried a pilot screen using aldicarb resistance, but obtained a high number of false positive results).

Screening on locomotion produced a very large number of candidates (835 mutants from 2000 haploid genomes screened), but many of these suppressor mutants either died, were sterile, or did not appear to be suppressed on further examination.

At a concentration of 50mM, EMS is predicted to mutate G/C bases to A/T bases (the most common EMS-induced mutation) at a rate of $7x10^{-6}$ per G/C base, and to introduce loss-of-function or reduction-of-function mutations into the average-sized gene at a rate of $1x10^{-4}$ to $5x10^{-4}$ per mutagenised gamete (Anderson 1995). This rate was estimated by Sydney Brenner based on his original screen for mutant phenotypes, (Brenner 1974), and has been reinforced by a large number of other screens (for review see (Jorgensen and Mango 2002)). Together these studies estimate that to identify a mutation in any given average-sized gene (of around 10kb), it would be necessary to screen approximately 2000 animals.

Subsequent investigation using whole genome sequencing, analysing unbackcrossed mutants, has given us the most direct examination of the effects of EMS mutagenesis in *C. elegans* (Sarin, Bertrand et al. 2010). These experiments estimate a slightly higher mutational frequency of $1x10^{-5}$ per G/C base, and a broader specificity for mutations, with 66% of detected mutations creating G/C to A/T transitions, although it is not clear whether non G/C to A/T mutations were introduced by EMS or whether they represent spontaneous mutations; other studies report a relationship closer to the standard G/C to A/T bias of EMS (Flibotte, Edgley et al. 2010). These studies also identified a significant bias for mutations to be introduced into gene rich regions on the arms of the *C. elegans* chromosomes (Sarin, Bertrand et al. 2010). This more detailed examination predicts a loss-of-function mutation rate similar to that of Brenner's original paper (Sarin, Bertrand

et al. 2010). These studies also reveal the presence large number of spontaneous mutations in any given laboratory strain, and while many of these are removed by backcrossing, the process of crossing itself introduces fresh mutations (Sarin, Bertrand et al. 2010).

Based on this data, our screen, of 1930 haploid genomes, is potentially large enough to hit every average-sized gene in the genome once. Our primary round of screening identified 116 suppressor mutants, which strongly suggests, given the small size of the screen, that there are a large number of RHO-1 suppressor mutations.

One of our identified mutants, *nz94*, has a fainter phenotype which allowed us to identify it as an allele of *unc-80* (see Chapter 4), a gene with 10,000 coding bases, approximately five times larger than the 'average-sized' gene. We identified another mutant with this fainting phenotype, *nz98* (which may have derived from the same original mutated animal) but did not obtain any other 'fainter' mutants. As another large gene, unc-79, also gives rise to a fainting phenotype, this suggests that our screen is far from saturated, and that further screening will identify additional alleles and additional suppressor genes. To conduct an even larger scale screen, we could adapt the dispersal assay, (which will be discussed in Section 4.4) to remove the subjective element from our screening. Briefly, animals would be placed in the centre of a large NGM plate, without food, and allowed to migrate to food at the edges of the plate. nRHO-1* worms are severly impaired in this behaviour, and no nRHO-1* animals reach the food within 2 hours (Figure 4-7); we could therefore select suppressors from those animals which are able to reach food at this time point.

Nonetheless, our primary round of screening identified 116 suppressor mutants. While this justified our decision to screen based on locomotion, it also raised questions of whether the control of locomotion is too complex a phenotype to allow isolations of suppressors which specifically interact with our nRHO-1* transgene, as opposed to having some gross reduction in locomotion activity. We addressed these concerns in a number of ways, discussed in the following sections.

3.14.2 -Suppressor screening identifies animals which move in a wild-type fashion

One advantage of the design of a suppressor screen is that we were trying to identify animals that look and move in a more wild-type manner than our starting strain. There are indeed many potential mutations to reduce the rate of locomotion which could act independently of RHO-1 regulation – for instance, mutations in SNARE complex genes,

such as syntaxin (*unc-64*) will block neurotransmitter release and should suppress locomotion phenotypes. However, these animals are either highly lethargic or the mutations are lethal (Saifee, Wei et al. 1998). Lethargic movement is as distinct from wild-type locomotion as loopy behaviour is, so by focussing on animals which move with wild-type locomotion we should avoid mutations in the core release machinery, for instance. This is not a perfect solution, as weak hypomorphs of *unc-64* , for example, may be sufficient to reduce neurotransmitter release without lethality or excessive lethargy.

We identfied and retained two lethargic mutants - *nz94* and *nz98* - and the nature of these mutations and their relationship to RHO-1 will be explored in Chapter 4. The remaining mutants isolated in the screen had essentially wild-type locomotion, and the quality of this locomotion tended to improve where we were able to backcross the mutants.

3.14.3 -Levamisole analysis demonstrates we have isolated a number of mutants with wild-type post-synaptic responses

If high levels of acetylcholine release are responsible for loopy locomotion, we predict another class of indirect suppressors are mutations which alter the body wall muscle sensitivity to acetylcholine. We use levamisole, which directly stimulates the acetylcholine receptors on the body wall muscles, to test the muscle activity. From the mutants examined so far, four of eight displayed wild-type responses to levamisole (Figure 3-14), while one was hypersensitive to levamisole (Figure 3-15), suggesting that a post-synaptic change in the response to acetylcholine is unlikely to be responsible for suppression in these strains, although these results are from a mixture of partially backcrossed and unbackcrossed animals, and so firm conclusions cannot yet be drawn.

Three other strains demonstrate resistance to levamisole (Figure 3-15), but these animals continue to display hypersensitivity to aldicarb, suggesting that both pre- and post-synaptic signalling is being disrupted in these mutants. This analysis demonstrates that a simple model of post-synaptic suppression, whereby the muscles are less sensitive to acetylcholine, is unlikely, but further experiments are needed to confirm this.

3.14.4 -Screening for locomotion produces mutants with a range of aldicarb phenotypes

As previously mentioned, we were concerned that a screen for suppression of the aldicarb response to nRHO-1* would mainly identify genes where mutations cause resistance to aldicarb, either indirectly or through processes already characterised.

We have subsequently assayed the aldicarb sensitivity of a number of our mutants, and have seen a wide range of phenotypes, from those which appear to completely suppress the aldicarb phenotype of nRHO-1* mutants, those intermediate between nRHO-1* and WT, or completely unsuppressed, and even some more sensitive to aldicarb than the starting strain in both the acute assays (Figures 3-5, 3-9, 3-10, 3-11 and 3-12). This indicates that the high levels of acetylcholine release do not correlate directly with loopy locomotion. We do not as yet have evidence for a class of loopy, aldicarb-resistant animals. The lack of this class suggests that while high levels of release do not generate loopy behaviour, loopy behaviour may either require high levels of release for sufficiently exagerated body bends to occur, or may in fact induce high levels of release through some feedback mechanism involving the putatitive motor neurons stretch receptors.

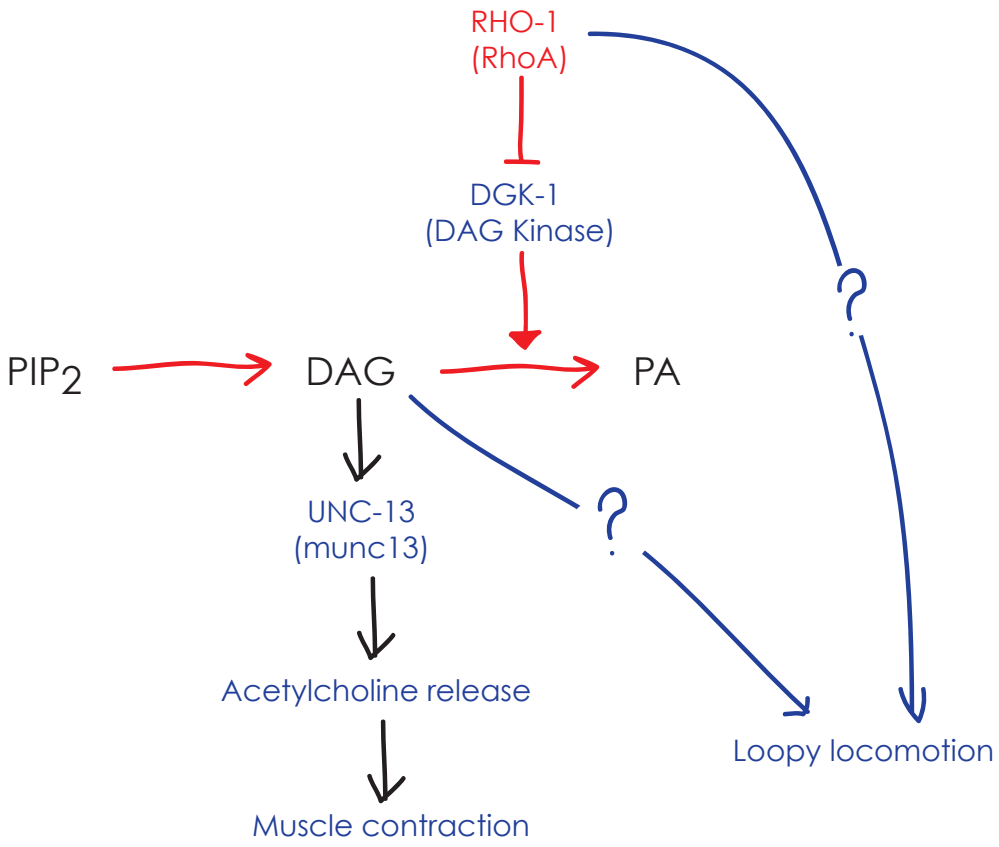

Figure 3-23 RHO-1 independently regulates acetylcholine release and loopy locomotion

We identified a large number of mutants which, despite being non-loopy, have high levels of acetylcholine release. This suggests that RHO-1 independently regulates these two phenotypes. However, we have yet to identify a loopy animal which is resistant to aldicarb, suggesting that these two aspects remain linked.

While there is an overlap between the group of mutants which are non-loopy and are suppressed for the aldicarb hypersensitivity of nRHO-1*, screening on aldicarb sensitivity alone would have been likely to miss the range of other mutations capable of suppressing loopy locomotion, confirming our choice of loopy locomotion as a phenotype to study in our primary screen.

3.14.5 -Secondary Screening

The presence of a heatshock transgene in our starting strain allowed us to ensure that the mutations we had isolated suppressed the activity of RHO-1 from two separate transgene. Transgenes, even those which are integrated into the genome, are prone to silencing because of their highly repetitive nature. The nRHO-1* transgene contains a GFP marker, and silencing of the entire transgene would lead to loss of GFP expression; we therefore verified using a UV dissecting microscope that our suppressor mutants displayed GFP expression.

However, it is possible that a reduction in the activity of the transgene might leave GFP expression relatively unaffected while reducing the activity of RHO-1 to a level below that required for loopy locomotion. Activating the second transgene and increasing RHO-1* levels in the nervous system as well as all other tissues by means of heatshock provided a good secondary test for true suppressor mutants.

3.14.5.1 - hsRHO-1* induces a number of phenotypes in many of the suppressor mutants

It is possible that both transgenes could be silenced (although this situation would require reduction in RHO-1 activity but retention of GFP expression in both instances), in which case the animals will always look non-loopy, even after the induction of heatshock.

However, heatshock-activated RHO-1* generates a number of additional phenotypes, including sterility (McMullan and Nurrish, 2011). This phenotype persists in over half of the mutants which we maintained from the screen (Groups 1 and 2, Table 3-1), suggesting that the heatshock transgene is functional and they are truly suppressing the loopy locomotion generated by RHO-1*.

A substantial proportion of the mutants we maintained, those in Group 3, are non-loopy and non-sterile (although this non-sterility designation still includes animals which have a low brood size, and grow more slowly than the starting strain.) This group of suppressors is the most likely to represent loss of activity in both transgenes, or potentially loss of activity of the heatshock response itself, such as mutations in *hsf-1*.

Group 3 may also contain more general suppressors of RHO-1, able to suppress both loopy locomotion (which as a neuronal origin) and sterility (which may not have). While not the phenotype we originally set out to detect, this suppression of the sterility induced by heatshock activation of RHO-1* is an interesting observation and these mutants may provide a source for further examining this phenotype of RHO-1.

As described in Section 3-6, a number of mutants which suppress the locomotion phenotype fail to suppress the reported hsRHO-1* effects on slowing pharangyl pumping and lengthening the defection cycle (McMullan and Nurrish, 2011). However, there is a range of suppression of these phenotypes and mutants classed as Group 2 and Group 3 (Table 3-1) may prove an interesting source for separating out pathways which act downstream of RHO-1* in different tissues. We also examined the *dar* phenotype following heatshock and found that the majority of the mutants tested display this phenotype (Figure 3-13, and Appendix 1), suggesting tail swelling acts through a different pathway to loopy locomotion behaviour. *nz106* suppresses the *dar* phenotype (Figure 3-13) and therefore is worth further investigation as it may represent a more general RHO-1* suppressor, while *nz107*, *nz108*, *nz109* and *nz111* suppress all heatshock RHO-1* phenotypes except tail swelling (Table 3-1 and Figure 3-13), and therefore might form the basis for an enhancer screen.

While we see a range of phenotypes across our identified suppressor mutants, from suppression of almost all RHO-1* phenotypes except tail swelling to animals which suppress only loopy locomotion, we cannot rule out that some of this diversity arises from second site mutations not directly connected to the suppression of loopy locomotion. Further backcrossing, identification of the causal mutations and rescue experiments will be required to confirm these intial observations.

3.14.6 -Backcrossing mutants was complicated by poor mating efficiency

Of the mutants selected, a number originate from the same plate, meaning they could be carrying the same mutation. Plate 1 gave rise to *nz92* and *nz97*, plate 4 to *nz94* and *nz98*, plate A to *nz104*, *nz105* and *nz110*, plate D to *nz106* and *nz111* and plate L to *nz107*, *nz108* and *nz109* (Table 3-1). If we assume that all mutants from the same plate represent the same mutation (which is a conservative estimate) we are left with 11 separate mutations. Even where animals have been obtained from the same plate we see some differences in our assays; most likely this represents behavioural variation, or additional background mutations.

The genome of lab strains, particularly following mutagenesis and even after backcrossing, is considerably more 'dirty' than previously imagined, calling into question whether we can really talk about the effects of single mutations, or whether we have to consider the entire genetic background of a mutant (Sarin, Bertrand et al. 2010). Based on whole genome sequencing, backcrossing has been shown to be effective at reducing the mutational load (Flibotte, Edgley et al. 2010; Sarin, Bertrand et al. 2010), although it also creates the opportunity for the introduction of fresh mutations, presumably introduced during meiosis or by spontaneous mutagenesis during DNA replication.

Given the need to reduce the background load of mutations, we undertook to backcross our mutant strains. To enable us to follow the first cross more easily, we used a strain which produces a high incidence of males (*him-5*) carrying only the nRHO-1* transgene and lacking the hsRHO-1* transgene (QT733), and crossed them with our suppressor animals. These are marked with *unc-122::gfp* which expresses GFP in the coelomocytes,. In the F1 generation, the animals should be loopy (because the suppressor is now heterozygous, and none of the suppressors demonstrated an obvious dominant phenotype because we saw no suppression in the first generation of the screening process (Figure 3-2), and the *nzIs1* transgene will be retained on only one chromosome. The *nzIs29* transgene remains homozygous during the cross.

We let these F1 animals self-fertilise, and looked for non-loopy animals in the F2 generation, where the suppressor is now homozygous, and is able to suppress the loopy locomotion of the *nzIs29* transgene. To ensure that these animals had definitely undergone one round of backcrossing, we looked for F2 animals that had lost the *ttx-3::gfp* marker of the hsRHO-1* transgene but retained the *unc-122::gfp* marker of the nRHO-1*. In some instances we found backcrossed animals that had acquired the *him-5* mutation. We used males from these lines to cross into strain QT309, which carries the nRHO-1* transgene without the *him-5* mutation.

On reflection, this loss of the hsRHO-1 transgene was unfortunate. Even after the initial screening the heatshock RHO-1* would have been a useful tool to have retained in these strains. It would have been better to either cross only with starting strain (QT631) and follow suppression by heatshock, and then reintroduce nRHO-1* as necessary.

Animals carrying nRHO-1* tend to grow more slowly than wild-type animals and mate less efficiently, and this effect is compounded when the strains also carry hsRHO-1*. This made the process of backcrossing more difficult than expected. While we did manage to backcross a number of the mutants (e.g. *nz110* in QT834 is 3 times backcrossed) the

success varied from strain to strain and limited which mutants we were able to analyse in more detail.

One step which might improve the efficiency of analysis of these mutants would be to cross them all with wild-type males and look for additional phenotypes in the absence of the nRHO-1* transgene. These animals could be crossed again with nRHO-1* to ensure that the additional mutation is linked to the suppressive effect, and then backcrossing could be conducted in the absence of the transgene. Another approach would be to cross our strains with a non-integrated nRHO-1* transgene, follow the suppressor mutation in animals carrying the extrachromosomal array, and examine animals which have lost the array for any additional phenotypes. As already mentioned, *nz94* and *nz98* displayed an additional phenotype allowing faster identification of the suppressive allele (Chapter 4).

3.14.7 - Putting suppressor mutations into complementation groups

This difficulty in crossing strains carrying the nRHO-1* transgene has so far prevented us from establishing complementation groups to establish whether different mutants represent alleles of the same gene, by looking for crosses which continue to suppress the loopy phenotype (although there are rare examples of non-allelic non-complementation in the nervous system which could complicate this process (Yook, Proux et al., 2001)

Having yet to perform this analysis we do not know how many different genes we have isolated in our screen. This is why the classification and grouping based on locomotion, sterility and aldicarb assays are important to try to distinguish between our mutants, although different alleles of the same gene may cause different phenotypes. In addition, where mutants derive from the same original plate we consider that these may contain the same mutation, until otherwise shown. Due to these technical difficulties, we chose to use the technique of whole genome sequencing (WGS) as a way of identifying suppressor mutants.

3.14.7.1 - Choosing mutants for whole genome sequencing

When we sent three mutants for whole genome sequencing, we used several methods in the hope of finding distinct suppressor mutants. We chose mutants which came from different original plates, so that they must have been mutations introduced into different animals, itself reducing the probability that they are in the same gene or, at the very least, by the laws of probability, that they are the same mutation.

Next, we chose mutants which had some distinct levels of behaviour in our tests. *nz97* and *nz99* were both Group 1 mutants, whereas *nz110* is in Group 2 (not entirely suppressing the locomotion phenotype of hsRHO-1*).

However, it is still possible that these suppressors could all represent mutations in the same gene. During the analysis of the whole genome sequencing data, we were careful to only count as background those mutations which are identical both in position and in the nature of the predicted mutation (i.e. Chromosome I, base 204567 A-T) in at least two strains. Although not impossible, it is highly unlikely that we have isolated exactly the same mutation from two independent strains. Therefore, even if the mutations are allelic, we should still have the capacity to detect them from our analysis.

3.14.7.2 - Whole Genome Sequencing without positional information

We were able to take advantage of this relatively new technique in our attempt to identify the nature of three of our suppressor mutants. As detailed above, these were chosen without detailed knowledge of their genetic position or the nature of the mutations. Should data from whole genome sequencing prove inconclusive, additional rounds of conventional mapping (Snip/SNP mapping and complementation analysis) could be used subsequently to filter the data. In this way, we felt we were able to test the current limits of the technology, to ask the question: is it possible to identify the nature of a suppressor mutation simply by looking at high-resolution data representing the entire genome?

Papers published using this technique (Sarin, Prabhu et al. 2008; Shen, Sarin et al. 2008) suggest that although the total number of mutations introduced into a genome by EMS mutagenesis is very high, the number of mutations which change a protein-coding sequence represent a small proportion of that total. The number that introduce premature stop codons, a common source of strong mutations, is even lower. We reasoned that it might be possible to produce a list of potential mutants, numbering around 50 to 100, and then inject pools of fosmids or cosmids covering those regions to look for rescue. Therefore we might be able to determine the suppressor mutant phenotypes without any conventional mapping. Mutations occuring in non-coding DNA or in miRNAs can also be identified from WGS, but might require more positional information to identify causal mutations.

We included one mutant which was entirely unbackcrossed. A recent paper investigated the effectiveness of backcrossing mutants, and found that while the first few rounds of backcrossing are able to remove a percentage of extraneous mutations, subsequent

crosses are less successful, because they allow the introduction of new mutations (Sarin, Bertrand et al. 2010). The source of these mutations is not entirely clear, and may be due to a low level of mutagenesis from the environment, or from inefficient DNA repair mechanisms involved in chromosome segregation and meiosis. Nonetheless, backcrossing does reduce the mutational load of an individual genome, but we wanted to test a completely unbackcrossed mutant We would always have the option of performing those backcrosses, identifying a degree of positional information, and returning to the whole genome data for that region. We see this workflow as being very fluid, even to the extent that, should a mutation fall in a region of low coverage, it would be possible to send further samples of the original genomic DNA, and having these sequenced. The data from the sequencing is in the form of short reads which are additive; more data can be obtained at any time.

3.14.7.3 - Geneservice bioinformatics analysis was unreliable

Our initial work centred around the analysis of the data sent to us by Geneservice. This included the raw output from the sequencing machines, the same data but formatted and filtered by quality into FASTQ files (the short read format as mentioned above), and a final run of this data through the program MAQ. This final level of analysis was limited in its usefulness as we did not have the details of parameters used, and although it identified numerous mutations across the genome, we had no biological information on the potential changes to protein coding genes which we were hoping to use to filter the data.

We used custom equations in Excel in an attempt to map the mutations back onto the genome and assign biologically relevant details to our data. This was conducted in most detail for mutant QT834, but attempts to confirm one predicted mutation in *cbp-1* suggested that the GeneService bioinformatics analysis was unreliable.

3.14.7.4 - MAQGene provides a user-friendly platform for whole genome sequence analysis

As detailed in the results, we set up the program MAQGene, developed by the Hobert lab for analysis of whole genome sequencing data (Bigelow, Doitsidou et al. 2009). This program uses the Apache server to link the short read files, the MAQ program itself, and a MYSQL database containing the annotations of the *C. elegans* genome. It allows a user to run MAQ from webpage-style interface, to easily re-run using different parameters, and to extract biologically useful information.

There are errors in the prediction software, however; a predicted coding change in QT788, AAT->AAA (asparagnine to lysine in the gene mpz-1) actually occurs in an intron of MPZ-1. This highlights the need to use the most up-to-date genome data from WormBase, as well as the need to manually confirm and sequence potential candidates.

3.14.7.5 - Comparision between data generated in this thesis and published whole genome sequencing mutants

The most complete analysis published of whole genome sequencing data obtained from mutants exposed to EMS is found in data from the Hobert lab (Sarin, Bertrand et al. 2010), where 14 mutants are analysed. These range from unbackcrossed strains to strains which have been backcrossed 10 times. They found that backcrossing reduces the mutational load, but that even backcrossed mutants have a high number of protein coding changes in their genome, ranging from 24 to 96 per genome.

We compared our data with this published data set (Table 3-6). The total number of mutations, including background and EMS-induced mutations, is on average twice as high in our strains as in those publised by the Hobert lab ($p<0.001$). The number of mutations which can be attributed to EMS mutagenesis is also twice that seen in the published data (1307.25 compared with 610.9, $p<0.05$). While significantly higher than the average, our data do fit within the range of mutations seen in the Hobert data, however, where mutants contain from 324 to 3746 mutations per strain.

We consider three potential reasons why our mutational load is higher on average than those of the strains in the Hobert lab. Firstly, different lab strains of wild-type animals may contain different numbers of mutations due to genetic drift, estimated at around 40 unique mutations introduced spontaneously over 200 generations (Denver, Dolan et al. 2009). We may be observing a laboratory-specific difference in rates of mutation in our data. This could account for some of the increase in mutation rate across all four strains.

Secondly, our mutagenesis procedure may dffer subtly from that used in the Hobert lab, such that the animals are exposed to a higher concentration of EMS (although we also see a higher than average mutation rate in QT317 which was generated independently of the others by exposure to UV/TMP). This would account for an increased number of mutations that are non-background. i.e. specific to each strain. Mutations introduced by or linked to the integration of the nzIs29 transgene should be eliminated as background mutations and not increase the number of EMS induced mutations as they would likely occur in more than one strain.

Thirdly, as the number of mutants sequenced increases, the number of mutations which can be classified as background also increases. Were we to sequence additional mutants isolated from the screen we would be likely to see a reduction in the predicted mutagen-induced mutations.

Despite the increase in the total number of coding changes induced by EMS in our strains compared with the Hobert lab data, the average number of protein coding changes induced by EMS is consistent with the published data (54 compared with 62, $p>0.05$). This could be due to a filtering effect of the probability of hitting a protein-coding region which means that more than a two-fold increase in total mutations is required to significantly increase the number of protein-coding changes, or it could indicate that our nRHO-1* animals are less tolerant of protein-coding changes than the genetic backgrounds used in the Hobert lab.

3.14.7.6 - WGS identified only a single premature STOP codon in four separate mutants

We anticipated identifying causative mutations through WGS without backcrossing or mapping because the predicted number of protein-coding mutations in a single animal is low enough to be able to manually sort through and identify candidate mutations, and the number of severe mutations (including premature STOP codons) is even lower (Sarin, Bertrand et al. 2010).

However, in our mutants, we found only a single premature STOP codon in all three nRHO-1* mutants sequenced, and none in strain QT317 (generated by UV/TMP). We wondered whether this could be an indication of the intolerance of nRHO-1* mutants for severe mutations. However, in the data for mutants from the Hobert lab (Sarin, Bertrand et al. 2010), 8 out of 14 mutants have either zero or one premature STOP codon generated by EMS, so our data is consistent with this range.

3.14.7.7 - MAQ, the underlying program for MAQGene, cannot successfully combine reads of varying lengths

One issue we faced when running this data ourselves was that the Geneservice data included reads of varying lengths (36, 55 and 76bps). This raises a problem when attempting to use the program MAQ for analysis. MAQ, and hence MAQGene, which uses MAQ as part of its programming, uses a number of variables for assessing whether a read is a good match for the genome. These include the number of mismatches in the first 28 bases (usually set to 2), and the total number of mismatches across the length

of the read. However, assuming a constant level of mis-reading within the sequencing machinery, the number of bases which misalign to the genome because of sequencing errors will be higher in a 76bp fragment than a 36bp fragment. However, MAQ does not take into account the read length; the number of mismatches is fixed at the start of the run.

What this means in practice is that if the number of mismatches is set to a low threshold, then 76bp reads will be unnecessarily discounted, while the 36bp reads will have an appropriate level of thresholding. However, if the threshold is set higher, to allow more 76bp reads to be incorporated successfully, error-ridden 36bp reads will now be allowed through.

Without fundamentally changing the code within MAQ, it is not possible to fully optimise this approach for different length reads. In previous studies, the read length for each mutant tends to be constant, and there is some debate as to whether long read lengths significantly improve the ability to find SNPs. Given that cyclical workflow discussed earlier, it would certainly be helpful if these parameters in MAQ were made more flexible. Longer reads give a much higher degree of certainty in positioning, and are especially useful for predicting deletions. In the future, we may wish to add additional sequence to our mutants, and at that stage 152bp reads may be viable. Ideally we would like to be able to combine all of our data into one run and have these variables adjust to the specific inputs.

In the absence of such a system, we have tended to rely on setting low thresholds, and only counting long reads with few errors. It is interesting to note that the *unc-31* mutation predicted in QT834(*nz110*) is not seen if the thresholds are set higher, suggesting that erroneous 36bp data is now being allowed to affect the number of mutant/wild-type reads at that position.

With respect to the data obtained from Geneservice, this too includes a mutation in *unc-31*, however it is 1 base pair different from that predicted by MAQGene. We believe there is a systematic error in the Geneservice data which means that the SNP predictions are misaligned by 1bp. This could be because they used a different version of the *C. elegans* genome, or because of some error introduced during the analysis. Taking this error into account, the Geneservice data appears to include the *unc-31* mutation we see from our own analysis. However, being unannotated, it was not spotted earlier.

3.14.8 -Screening and analysis provide a platform for future work on targets of RHO-1

During the course of this screen we have identified 20 mutants which suppress the loopy locomotion of the nRHO-1* transgene. While later chapters contain detailed analysis of one of these mutants, we have obtained a large amount of data around the remaining

	Allele	Total number of mutations	EMS Induced	EMS-induced proten coding changes
QT317	nz90	2369	843	16
QT677	nz99	2809	1278	42
QT788	nz97	2464	1608	115
QT834	nz110	3083	1500	44
Average		2681.25	1307.25	54.25
Sarin et al 2010		1022.4	610.9	62.4

Table 3-6 - Comparrison of WGS data to published data

We compared the data generated by sequencing our four mutant strains to the data published in Sarin et al, 2010, which lists the number of mutations identified in 14 EMS mutagenised strains. We see that our total number of mutations is significantly higher than those in the published data ($p<0.001$). The mutations attributable to EMS mutagenesis (as opposed to background mutations) is also higher on average than those in the Sarin data set ($p<0.05$). The number of protein coding changes induced by EMS is within the range seen in the published data ($p>0.05$). Significance was assessed using a 2-tailed T-test.

animals, which will hopefully be of use in future experiments. That data is collated here, along with candidate mutations where these have been identified.

3.14.8.1 - QT834 (*nz110*) contains a mutation in *unc-31* (CAPS)

QT834 contains the suppressor mutation *nz110*, and has been backcrossed three times. These animals are highly suppressed for the loopy locomotion of nRHO-1*, and were identified as a top candidate by visual inspection (Appendix 1). We can be confident that these are true suppressors of nRHO-1*, rather than being due to malfunction of the transgene, because these animals become sterile upon activation of hsRHO-1*, but still remain less loopy than unsuppressed hsRHO-1* animals (Table 3-1).

These animals have high levels of neurotransmitter release, as measured by the aldicarb assay, and this level of neurotransmitter release has increased during backcrossing (Figure 3-9). This suggests that in the unbackcrossed strain there is an additional mutation which partly suppresses aldicarb hypersensitivity, and may be of interest in its own right

if deemed suitable for future examination. These animals are partially suppressed for their response to levamisole, which suggests that their post-synaptic response to acetylcholine is reduced (Figure 3-15). Combined with their hypersensitivity to aldicarb this suggests that the level of neurotransmitter release in these animals is actually greater than in the starting strain, as the levamisole phenotype would normally mask the aldicarb hypersensitivity. This also suggests that a simple model of reduction in neurotransmitter release sensitivity is insufficient to explain the suppression of locomotion.

Further investigation using MAQGene failed to identify any strong suppressors (e.g. premature STOP codons, altered splice sites) (Appendix 2), while analysis of the distribution of SNPs did not give any clear indication of the potential location of the suppressor mutant. We became interested in a mutation in *unc-31* as a potential candidate, however; and sequenced this mutation to demonstrate it was present in QT834. *UNC-31* is required for the release of dense core vesicles and the neuropeptides they contain (Speese, Petrie et al. 2007), and it is possible that these neuropeptides may perform some modulatory function with respect to locomotion, and one that we detect the action of through our levamisole assay.

A double nRHO-1*;*unc-31*(e928), the cannonical mutation of *unc-31* also has non-loopy locomotion (R. McMullan, personal communication), indicating that loss of *unc-31* activity is able to suppress loopy locomotion. Interestingly, an *unc-31* null mutation is able to suppress some of the increased locomotion phenotype of *egl-30* (gain-of-function) mutants (Charlie, Schade et al, 2006), although the animals still have a tendancy to coil (Charlie, Schade et al, 2006). *egl-30* is a known activator of RHO-1 signalling in the nervous system. In addition, the *unc-31;egl-30* (gf) mutant still has high levels of acetylcholine release (Charlie, Schade et al, 2006), consistent with the results observed with the *nz110* mutant.

The predicted *unc-31* mutation in *nz110* generates only a small change in the coding sequence, replacing an alanine residue with valine (Figure 3-21). However, this residue is at a conserved point when compared to CAPS homologues from other species, and is part of the MUNC-13 homology domain. We expect this to be a weak hypomorph of *unc-31*, because the behaviour of the animals is distinct from previous mutations in this gene. The mutant behaviour associated with *unc-31* loss-of-function is for the animals to be paralysed while in the presence of food, but capable of wild-type locomotion in its absence. Our animals, meanwhile, have a locomotion phenotype indistinguishable from wild-type. This suggests however that we may have isolated a mutation which specifically blocks only a part of *unc-31* function (Charlie, Schade et al, 2006).

Our working model is that *unc-31* is the supressor of nRHO-1* in this strain. Further to this work will be attempts to rescue the QT834 mutant with an wild-type copy of *unc-31*, either isolated as genomic DNA from by a fosmid or from a cDNA driven by a cell-specific promoter. In preliminary rescue experiments with an *unc-31* containing fosmid, 1 in 3 lines were rescued for loopy locomotion. We intend to generate an *unc-31* cDNA which we can place under cell-specific promoters to determine the site of action of *unc-31* with respect to RHO-1.

The mutation we have isolated in *unc-31* appears relatively mild, and we will therefore introduce this mutation in the *unc-31* cDNA, and test whether this mutant form of *unc-31* is able to rescue more severe mutations of *unc-31.*

Should this hypothesis prove incorrect, it will be necessary to perform some positional mapping to reduce the potential number of protein coding suppressor mutants from its current level of 44, so that rescue experiments can be performed on the remaining candidates.

3.14.8.2 - QT677 (nz99) contains a mutation in the dopamine reuptake transporter *dat-1*

QT677 contains the *nz99* suppressor. *nz99* is placed in Group 1 as one of the strongest neuronal suppressors. QT677 worms become sterile on activation of the hsRHO-1* transgene, demonstrating that the transgene is indeed active in this strain, and remains non-loopy. This also shows specificity for suppressing neuronal activity of nRHO-1*.

These animals also appear hypersensitive to aldicarb, in both the two time point and standard aldicarb assay. This suggests that increased acetylcholine release does not necessarily give rise to loopy locomotion. Understanding the additional requirements for loopy locomotion will be an important goal for future research.

With this mutant we tested the full capacity of whole genome sequencing to establish the nature of an unbackcrossed mutation without standard positional information. In an unbiased assessment of the mutations as provided by MAQGene, we detected 1278 mutations, of which 42 caused changes in protein coding genes. If fosmids covering each of these mutations were injected in pools of 5, it would only require a maximum of 8 sets of injections to begin to look for rescue in this strain.

However, we were also able to identify one strong suppressor candidate, a mutation in *dat-1*, the dopamine transporter. While suppressor mutations do not have to severely

alter protein function, STOP codons are a common source of strong mutations. This, coupled with the known roles for dopamine in locomotion, make this a good candidate.

DAT-1 is a plasma membrane associated transporter, and part of the same family as the GABA transporter SNF-11 and the serotonin reuptake transporter MOD-5. It is expressed in 8 dopaminergic neurons in adult hermaphrodites (Flames and Hobert 2009). Dopamine acts a neurohormone, regulating global behavioural states, and is

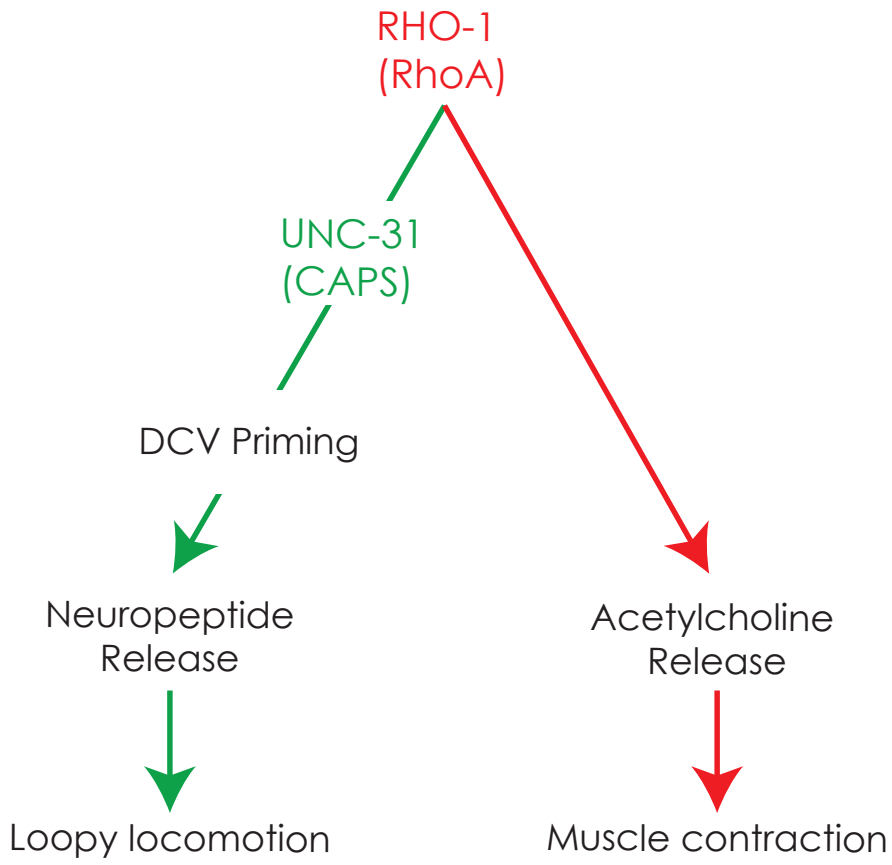

Figure 3-24 Mutations in *unc-31* suppress the loopy phenotype of nRHO-1*

We identified an *unc-31* mutation in strain QT834, and subsequent evidence confirms that loss of *unc-31* activity reduces the loopy locomotion of nRHO-1*, but retain high levels of acetylcholine release. As *unc-31* (CAPS) is responsbile for priming dense core vesicles, we suggest that neuropeptide signalling may be invovled in the generation of loopy locomotion.

important for behaviours such as slowing on food sources (Sawin, Ranganathan et al. 2000; Chase, Pepper et al. 2004) and the frequency of turning behaviour (Hills, Brockie et al. 2004). Transfer of dopamine via DAT-1 requires the movement of two sodium ions and one chloride ion, and it has been suggested that in addition to the ionic movement

associated with transport, DAT-1 can act as a depolarising ion channel in its own right (Carvelli, McDonald et al. 2004).

Loss of *dat-1* reduces the reuptake of dopamine, increasing dopamine signalling which has the effect of slowing animals down and preventing vigorous motor activity (McDonald, Hardie et al. 2007). This may indirectly reduce the loopy locomotion of nRHO-1* animals (Figure 3-25). Interestingly, dat-1 mutants have defects in swimming behaviour, a phenotype we also observe in other suppressors of nRHO-1* loopy behaviour (see Chapters 4 and 5) . Alternatively, *dat-1* mayb be acting as a ion channel, depolarising the presynaptic membrane and increasing neuronal activity (Carvelli, McDonald et al. 2004). If this action were regulated by RHO-1*, then increasing RHO-1 activity might lead to further increases in neuronal activity, generating loopy behaviour.

Direct sequencing confirmed the presence of the mutation in *dat-1*, a critical step before rescue experiments are to be conducted (Figure 3-21). We will now construct double mutants between nRHO-1* and cannonical *dat-1* mutants, and attempt to rescue the dat-1 mutation in QT677 by injection of fosmid DNA covering the *dat-1* locus, as well as by injection of *p.dat-1::*DAT-1::GFP (a gift of the Blakely lab).

Additionally, artificially increasing dopamine levels in these mutants may reduce loopy locomotion. Preliminary experiments to treat nRHO-1* animals with dopamine suggest that this may be the case (S. Nurrish, personal communication.) An alternative experiment would be to use cocaine treatment to inhibit the activity of the DAT-1 transporter in nRHO-1* background to see whether this decreases loopy locomotion.

3.14.8.3 - QT788 has a number of mutations which cluster on Chromosome II

QT788 contains suppressor *nz97*, which fully suppresses loopy locomotion while having no suppressive effect on sterility or pharyngeal pumping. It is hypersensitive to aldicarb (Figure 3-5) in our initial analysis, but slightly suppresses the aldicarb sensitivity of nRHO-1* (Figure 3-10). It is completely wild-type in its response to levamisole (Figure 3-12).

We had some difficulty running the QT788 data using MAQGene. For QT788 we obtained two runs of 76bp data, along with two runs of 36bp data. When we loaded this into the computer using our standard parameters, the analysis failed to complete. Only by omitting one set of 76bp data could we obtain a completed analysis. The analysis in this thesis omits the QT788_76bp_B dataset; if in future the source of this malfunction can be identified then a more complete analysis can be performed.

Analysis of the distribution of SNPs was most successful for this mutant, as it identified a strong linkage to Chromosome II), and particularly to two regions on this chromosome. While evidence that the suppressor mutation is on Chromosome II requires additional study, the current evidence suggests that one of only 8 mutations which affect protein coding regions may be the suppressor mutation. As these mutations are relatively close together on the chromosome, between two and four sets of fosmid injections could be performed to look for rescue of the loopy phenotype as a fast way to determine whether any of these are good candidate mutations. Alternatively, we could perform RNAi of nRHO-1* mutants, taking advantage of the SID-1 strains developed by the Chalfie lab which enhance RNAi effects in the nervous system (Calixto et al., 2010).

The genes mutated in the high-frequency peaks on Chromosome II are:

- C2H3.4 - filamentous baseplate protein Ligatin
- *fbf-1* - FEM-3 mRNA binding protein
- T19D12.9 - Permease of Na/PO4 transporter
- *mec-15* - Fbox - ubiquitin ligase adaptor
- C07E3.4 - Protein tyrosine phosphatase
- M106.2 - Novel nematode protein
- *egg-3* - alternative splicing factor / protein tyrosine phosphatase
- T06D8.1 - mucin-like cell surface protein

Of most immediate interest are the two protein phosphatases *egg-3* and C07E.4, as these could conceivably be part of regulated signalling pathways downstream of RHO-1. *mec-15* mutants have a neuronal phenotype and are insensitive to gentle touch; *mec-15* is required for specification of these neurons (Bounoutas, Zheng et al. 2009). It is conceivable that loopy locomotion could arrise from improper activation of mechanosensory pathways leading to repeated writhdrawl actions, and loss of mechanosensation might suppress this. Ultimately rescue experiments will be required to identify the causative suppressor mutation.

3.15 - Conclusions

3.15.1 -Additional screening of mutants is a powerful way of refining a screen

Only by screening for suppression of additional phenotypes generated by our hsRHO-1* transgene could we systematically hone our list of candidate suppressors. This approach of using a second transgene under a separate promoter is recommended for future screens where appropriate, as it also reduces the probability of suppressors being purely due to reduced function of the original transgene.

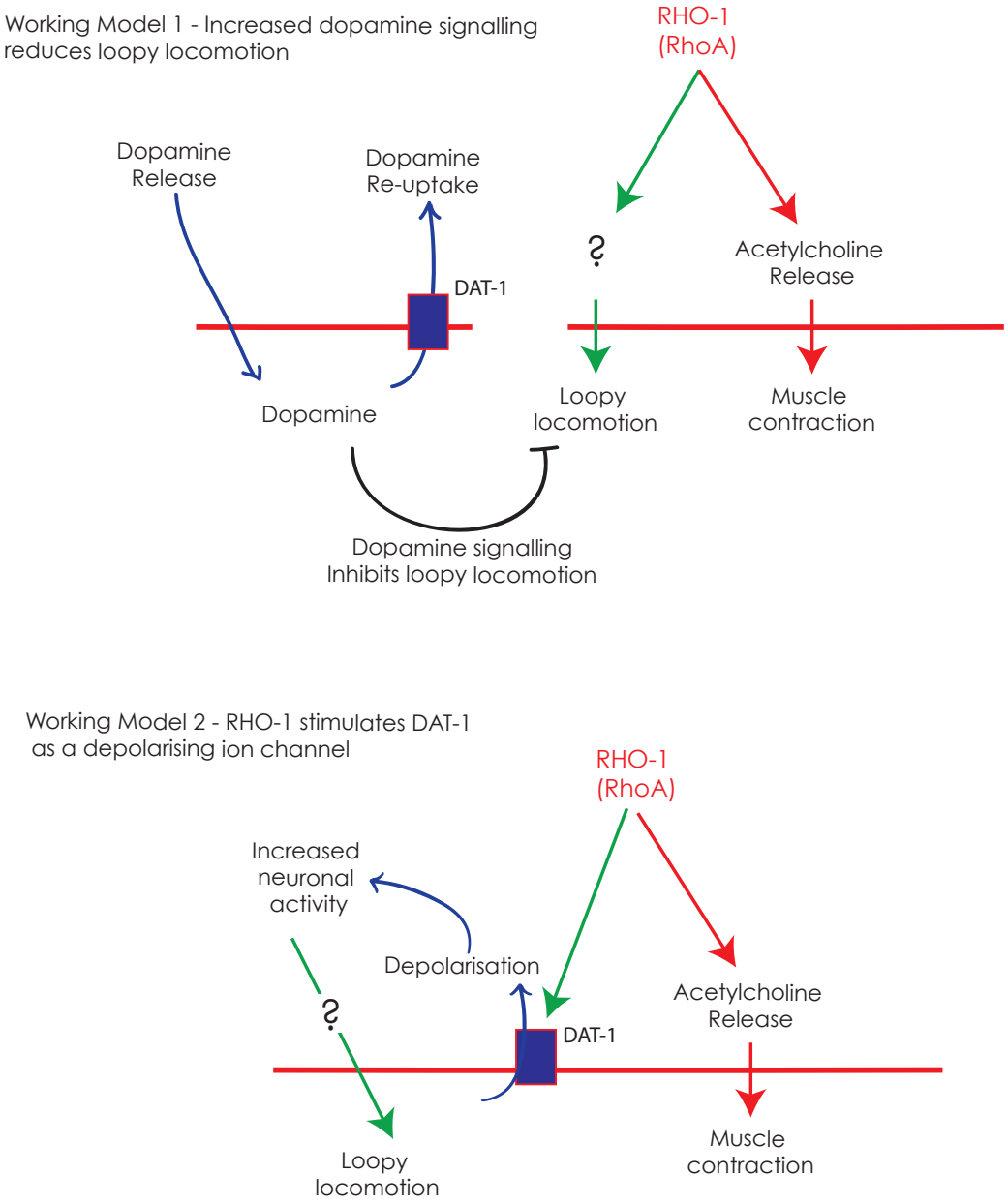

Figure 3-25 A *dat-1* mutation appears to suppress the loopy phenotype of nRHO-1*

We identified a premature STOP codon in *dat-1*, the gene encoding the dopamine reuptake transporter. This suggests that high levels of dopamine signalling may be responsible for reducing loopy locomotion (Model 1). The mutant, QT677, is hypersensitive to acetylcholine, suggesting that excess dopamine signalling does not reduce the effects of nRHO-1* on acetylcholine release. Alternatively, RHO-1 may stimulate DAT-1 to act as a depolarising ion channel (Model 2), and this may lead to increased loopy behaviour.

3.15.2 -Aldicarb phenotype of suppressor mutants is not linked to their locomotive suppression

As previously discussed, while we chose to screen with reference to locomotion, once we had obtained our mutants we wanted to see whether these locomotion-suppressed mutants were also suppressed in their aldicarb phenotype.

As we looked across the range of our 20 mutants, we saw some which were completely suppressed for aldicarb phenotype, and others which showed no change in aldicarb response.

This is interesting because our original hypothesis about the locomotion phenotype was that it was caused by the excess release of acetylcholine onto the body wall muscles, causing hypercontraction and the appearance of a loopy or coiled posture.

We favour a model where increased acetylcholine release is necessary, but not sufficient, for loopy locomotion . Consistent with this we have never observed a class of mutant with loopy locomotion which are wild-type in their response to aldicarb. The *unc-31* mutation suggests that at least one of the additional requirements is the release of neuropeptides.

3.15.3 -Whole Genome Sequencing provides a powerful tool for mutant analysis

Using whole genome sequencing we have obtained a large amount of data on the nature of mutations in our suppressor mutants. However, simply by looking at the raw data, and even with analysis of the distribution of SNPs following backcrossing, it is not possible to definitively identify the nature of the suppressor mutants. Additional experiments are required, although these (injection of rescuing constructs) can be performed after only a few weeks of sequencing and analysis, rather than at the end of up to a year or more of conventional mapping.

Sequencing multiple mutants from a screen is an invaluable way of reducing the list of mutations by eliminating those which are common between animals. Some of these will have been introduced through mutation in the lab, others occur as the result of sequencing errors from the system. Those which occur as systematic errors, or sites which are commonly prone to mutation, could be stored in a shared database and systematically eliminated from, or at least highlighted in, any future analysis. In all cases, mutations unrelated to the suppressor will be identified. Although we are not interested in these mutations ourselves, it would be advantageous to the *C. elegans* research community to create a database to which details of these mutations could be uploaded and searched by other groups. Ideally, this could be linked to the gene descriptions already present on Wormbase, but such a facility is not yet available.

Backcrossing, while not essential for detecting mutations, does provide valuable linkage information for reducing the list of causative mutations. While the mutation in *dat-1* in QT677 may indeed prove to be the suppressor, it is fortuitous that the mutation introduced a STOP codon into this gene. To successfully use this technique without further positional

information will require better prediction of the role of changes in miRNA, as well as the ability to predict in silico the effects of changes in promoter sequences and 3' and 5' UTRs of genes.

4 - UNC-80 ACTS DOWNSTREAM OF RHO-1 IN THE C. ELEGANS NERVOUS SYSTEM

4.1 - Introduction

Our screen for suppressors of the loopy locomotion induced by overexpressing constitutively active RHO-1 (G14V) in the cholinergic motor neurons (nRHO-1*) identified over 800 mutants with more wild-type locomotion than our starting strain, which we classified as 'less loopy' or 'not loopy'. These mutants were examined for the maintenance of suppression over a number of generations, their ability to suppress a second, integrated heat-shock activated transgene (hsRHO-1*) and their level of suppression of non-neuronal RHO-1 phenotypes. From this additional analysis we refined our original list of mutants to 20 strong suppressors, as detailed in Chapter 3.

Included in this group of twenty suppressors were two mutants, derived from the same plate, which suppressed the loopy locomotion of the starting strain, producing animals without the exaggerated body bends associated with nRHO-1*, but which were also lethargic in their locomotion when compared to wild-type. Our original aim for the screen was to identify mutants which moved with wild-type locomotion in an attempt to avoid isolating mutants in pathways which only indirectly suppressed the nRHO-1* transgene. The suppression of the body bend phenotype in these two strains - *nz94* and *nz98* - was strong enough for us to include them in our list of 20 strong suppressors, despite their lethargic locomotion. The initial characterisation of these mutants was conducted in collaboration with Dr Rachel McMullan.

4.2 - *nz94* and *nz98* suppress phenotypes associated with neuronal activation of RHO-1

Both of these mutants show strong suppression of the loopy phenotype from both the neuronal and heatshock transgenes of the starting strain. These mutations do not suppress the non-neuronal phenotypes seen on activation of heat-shock RHO-1 (G14V). Activation of hsRHO-1* causes the animals to become sterile, to develop the tail swelling phenotype associated with hsRHO-1* activation, and animals which have been heatshocked die within 2 days of treatment, which is consistent with our observations of the QT631 starting strain.

hsRHO-1* activation also causes a reduction in the rate of pharyngeal pumping, as seen in the starting strain. Pumping of the pharynx is neuronally regulated, indicating that there is some specificity of suppression of RHO-1* phenotypes with respect to locomotion.

These results with two separate transgenes suggest that these mutations are specifically suppressing the activity of RHO-1 in the nervous system.

Observing these effects of hsRHO-1* in these mutants also provides evidence that suppression of loopy locomotion is not due to a defect in RHO-1* expression, as we would expect any such defect to result in a reduction in all RHO-1* phenotypes.

4.2.1 - *nz94* mutants have a fainting locomotion

On closer inspection of the locomotion of these suppressed animals we observed that while the animals remained motionless for extended periods of time compared to wild-type, they were still capable of wild-type body bends. When left undisturbed, *nz94* animals appear to be highly lethargic or even paralysed. However, tapping the plate or touching individual animals with a platinum wire induces a strong response, with the animals briefly moving with wild-type body bends, but stopping abruptly where wild-type animals continue moving.

While backcrossing these mutants we were able to remove the background hsRHO-1* transgene in the mutant strain. We subsequently obtained a line (which we named QT830) which had spontaneously lost the expression of *unc-122*::GFP, the marker for the nRHO-1* transgene. We believe this line represents the suppressor mutation in the absence of both the hsRHO-1* and nRHO-1* transgenes; however, we have not formally assayed the loss of the nRHO-1* transgene.

We took this opportunity to assess the locomotion of the animals in the absence of the neuronally-acting transgene, and observed that the animals did indeed move with this unusual fainting phenotype. The video time series in Figure 4-1 demonstrates that when the animals are stimulated by a nose tap they move with wild-type body bends, but stop moving prematurely compared to wild-type animals (see Movie 4-1 for wild-type response to nose tap, and Movie 4-2 for *nz94* response).

This was reminiscent of a phenotype originally identified by Leon Avery, and subsequently referred to as ‘fainting’, which is described on Wormbase as:

“Alternating periods of stopping and moving; Motion is interrupted by periods of inactivity lasting several seconds.”

So far, this unusual and subtle phenotype has been seen to result from mutations in only four genes – loss of function mutations of the large, unclassified yet conserved genes *unc-79* or *unc-80*, or the double mutant of novel ion channels *nca-1;nca-2* (Humphrey,

Hamming et al. 2007). (The actual period of inactivity of these mutants, if left undisturbed, can last much longer than several seconds as seen from the video time series).

We were therefore interested in whether our suppressors represented mutations in any of these genes, or whether we had identified a novel fainter mutation.

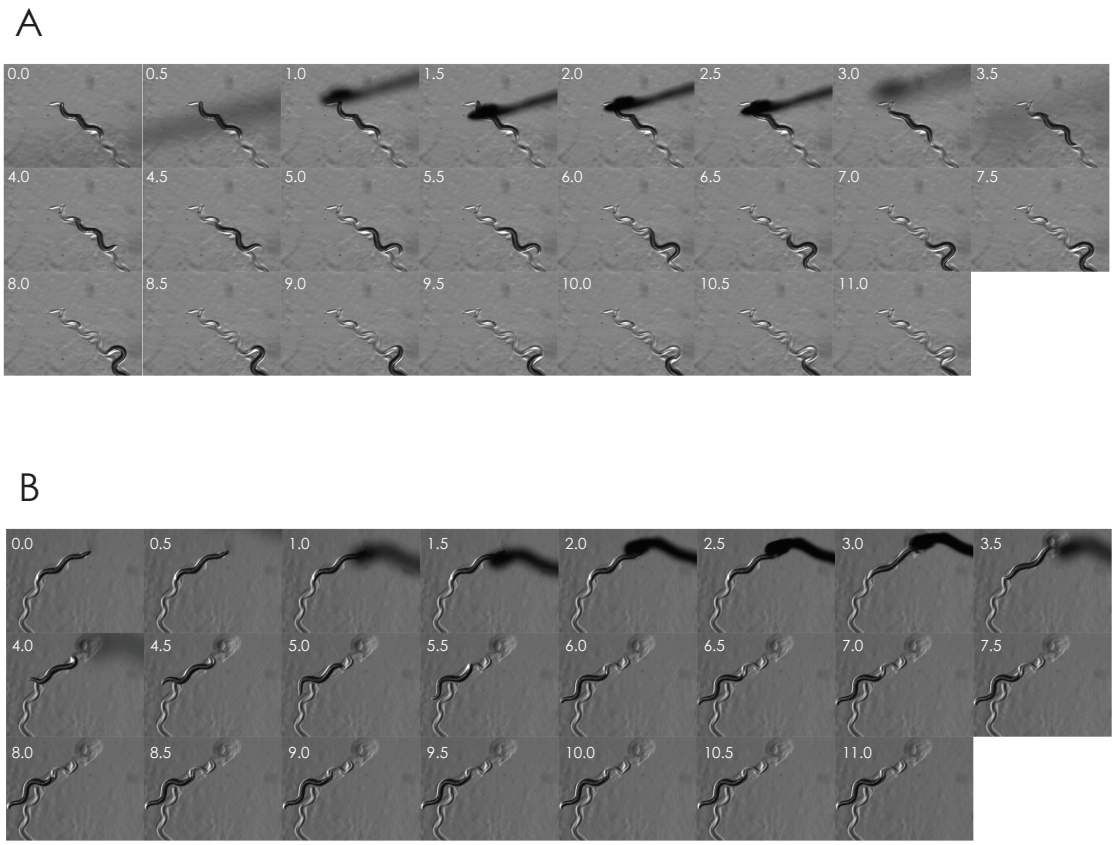

Figure 4-1 *nz94* has a fainting locomotion

Touching the nose of a wild-type worm with a platinum wire induces backwards locomotion with a number of body bends (A). Mutant *nz94* failed to respond normally to a nose touch (B). Its initial response appeared wild-type, from time 4.0 to 6.0 it produces two body bends, moving backwards. However, the animal then pauses for the remainder of the video. This is reminiscent of the 'fainting' locomotion common to *unc-80*, *unc-79* and *nca-1;nca-2* mutants. See also Movies 4-1 and 4-2.

4.2.2 - Suppressor mutant *nz94* fails to complement mutations in the large, conserved gene *unc-80*

We made use of the QT830 strain that lacked the nRHO-1* transgene but retained the fainting locomotion to perform complementation analysis of the mutation. We thought it highly unlikely that we had isolated a double mutant of *nca-1* and *nca-2* from our screen, and instead concentrated on comparing the *nz94* mutation to the two single mutations known to cause fainting locomotion.

We crossed *nz94* with the *unc-79* mutant CB1068, which has fainting behaviour and contains the reference mutation *e1068* (although the molecular nature of this mutation

remains to be determined). All animals in the F1 generation were wild-type, suggesting that mutations are able to complement mutations, and that these represent alleles of different genes.

We also crossed *nz94* with the *unc-80* mutant CB1069; this mutation introduces a splice site mutation into and causes fainting locomotion. We found that *nz94* failed to complement this mutation in *unc-80*, with the F1 generation displaying the fainting phenotype (data not shown), suggesting that *nz94* represented a mutation in this *unc-80*.

4.2.3 - *nz94* contains a premature STOP codon in the *unc-80* locus

Complementation analysis strongly suggested that *nz94* represents a mutation in *unc-80*. Although uncommon, there are examples of nonallelic non-complementation, where two mutations in separate proteins generate the same phenotype while both mutations are heterozygous as when either mutation is homozygous. Usually this involves proteins which act together in the same complex or the same pathway, for instance proteins which regulate the synaptic vesicle cycle (Yook, Proulx et al. 2001). To determine whether *nz94* truly is an *unc-80* mutation, we set out to sequence the coding region of this gene.

We designed a set of primers to cover the exons of *unc-80* (see Primer list). We generated fragments of genomic DNA from strain QT830, which carries the *nz94* mutation. We initially performed PCR and sequencing using genomic DNA purified from this strain. A number of the sequencing reactions failed to work successfully, so we complemented this source of DNA by using the technique of single worm PCR to generate fragments for sequencing (see Methods).

The positions of these reactions relative to the gene structure of are shown in Figure 4-2.

When the sequencing data returned bases which failed to match the wild-type genomic sequence we re-sequenced these areas, where possible using primers to perform PCR on the opposite strand of DNA from that originally sequenced to control for sequencing errors. In all cases except one (highlighted with an arrow, Figure 4-2) these subsequent sequencing reactions returned wild-type sequence, suggesting that the original mismatches were due to sequencing errors.

PCR reactions covering Exon 28 of the F25C8.3b isoform of *unc-80* returned a sequence differing from wild-type, where a wild-type guanine nucleotide had been substituted for a mutant adenosine. When this mutation was plotted onto the wild-type cDNA it generated

a premature stop codon in this exon, where a tryptophan residue (TGG) is replaced with a STOP codon (TGA). This exon is present in all predicted splice forms of *unc-80*.

All subsequent sequencing reactions covering this region returned a result different from wild-type, and were all in agreement with each other. We therefore identified a mutation introducing a premature stop codon into Exon 28 of *unc-80*. The base-pair sequence from one of these sequencing reactions is shown in Figure 4-3.

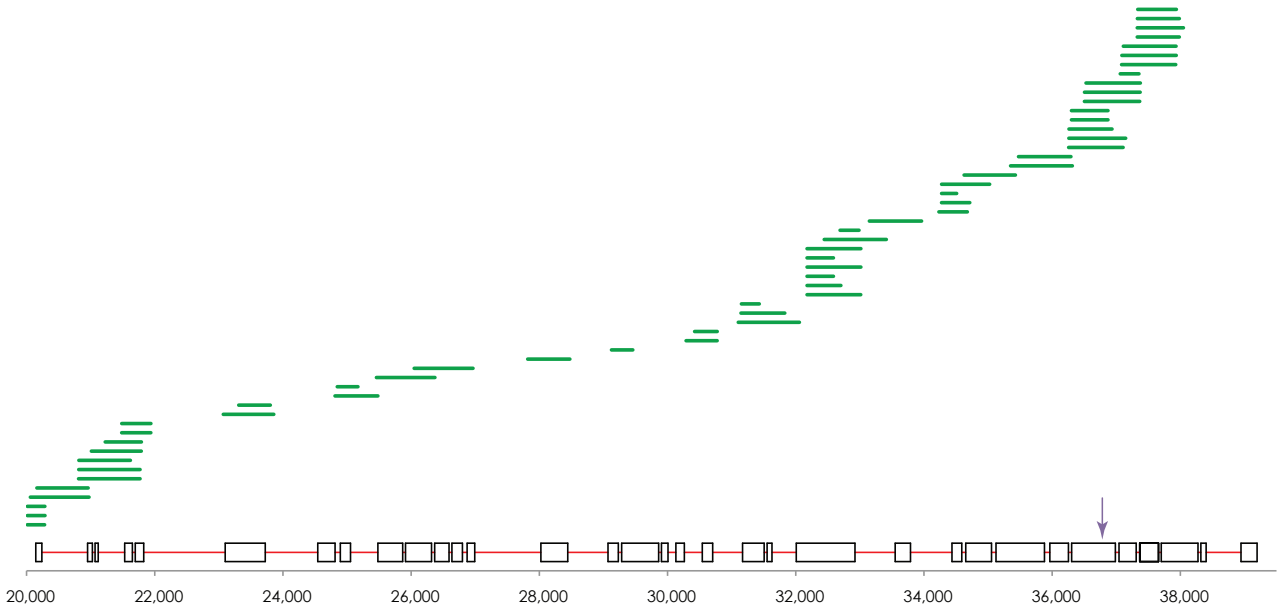

Figure 4-2 *nz94* contains a premature STOP codon in *unc-80*

We designed primers to sequence the coding region of the *unc-80* gene. The regions sequenced are represented by the green lines. Wherever we found disagreement between our sequence data and the published sequence we repeated the sequencing. Only at one region, indicated by the arrow, did we find a consistent difference between our mutant and the published *unc-80* sequence, confirmed by four PCR reactions.
Exons are represented by open boxes, introns as thin red lines.

We suggest that this premature stop codon results in either a truncated form of *unc-80* or, through nonsense-mediated decay of the coding mRNA (Hodgkin, Papp et al. 1989; Conti and Izaurralde 2005), in a complete loss-of-function of this protein, and that it is the mutation in this gene which is responsible for the fainting phenotype we observe. Although UNC-80 is a large protein of between 3166 and 3263 amino acids, and this mutation is in the 3' end of the cDNA sequence, other previously identified loss-of-function mutations cluster in this region. This suggests that *unc-80* is susceptible to mutations affecting this part of its coding sequence (Figure 4-4).

Our evidence so far indicates that the mutation is recessive, which would suggest it does not produce a dominantly-interfering truncated protein.

The *nz98* mutant, which also demonstrates fainting locomotion, was obtained from the same original plate as the mutant described here. We believe it most likely contains the same mutation identified in the line, but we have yet to sequence this region in to confirm this.

```
W.T.    36262   AGTCAGTACTTAATTTCTGATAATTGTTCCTCTTTTTTTAAGGAAAGAAAAAAGATCCAC   36321
                ||||||||||||||||||||||||||||||||||||||||||||||||||||||||||||
nz94    1       AGTCAGTACTTAATTTCTGATAATTGTTCCTCTTTTTTTAAGGAAAGAAAAAAGATCCAC   60

W.T.    36322   TGCGGTTGCATGGGAAGCTGCTGAAGTAGAGGAACAACAAAAGGAAACGTATCGACGGCC   36381
                ||||||||||||||||||||||||||||||||||||||||||||||||||||||||||||
nz94    61      TGCGGTTGCATGGGAAGCTGCTGAAGTAGAGGAACAACAAAAGGAAACGTATCGACGGCC   120

W.T.    36382   ACGTGATACTCTTCTTCAATTGATAGCAGCTTATATAGAAATGGCGTCGGTCCGTCTGAA   36441
                ||||||||||||||||||||||||||||||||||||||||||||||||||||||||||||
nz94    121     ACGTGATACTCTTCTTCAATTGATAGCAGCTTATATAGAAATGGCGTCGGTCCGTCTGAA   180

W.T.    36442   AGAACTTACCAAACTAGGTGCAAACCTAGAACACGCCAAGATTCCTGACGTGCTTGACCA   36501
                ||||||||||||||||||||||||||||||||||||||||||||||||||||||||||||
nz94    181     AGAACTTACCAAACTAGGTGCAAACCTAGAACACGCCAAGATTCCTGACGTGCTTGACCA   240

W.T.    36502   CAAATGCTATGTGAAACTTGGAGAAGTTGCATTGGCCTTGTTGAAAGTTGCTCCCTATGA   36561
                ||||||||||||||||||||||||||||||||||||||||||||||||||||||||||||
nz94    241     CAAATGCTATGTGAAACTTGGAGAAGTTGCATTGGCCTTGTTGAAAGTTGCTCCCTATGA   300

W.T.    36562   TTTATCAACTACAACGTGTCACGGTCTTCAGAAATATTTCCAGATAATACTACCAGTTAC   36621
                ||||||||||||||||||||||||||||||||||||||||||||||||||||||||||||
nz94    301     TTTATCAACTACAACGTGTCACGGTCTTCAGAAATATTTCCAGATAATACTACCAGTTAC   360

W.T.    36622   TGATTGGAGTATAGAGTCTAACAGGAGTGCTCTCAATATTATTCTACGACGATTAGACAA   36681
                ||||||||||||||||||||||||||||||||||||||||||||||||||||||||||||
nz94    361     TGATTGGAGTATAGAGTCTAACAGGAGTGCTCTCAATATTATTCTACGACGATTAGACAA   420

W.T.    36682   AACACTATCCAAGATTGCCAAACGTCAAAGTTTTCGAAAAAGAGCTATTTGGATAGCACT   36741
                ||||||||||||||||||||||||||||||||||||||||||||||||||||||||||||
nz94    421     AACACTATCCAAGATTGCCAAACGTCAAAGTTTTCGAAAAAGAGCTATTTGGATAGCACT   480

W.T.    36742   TTCATCGTGGATTAATGGCATTTGTGATACTCTAAATGCATTTCCGTACATCGCACATCT   36801
                |||||||||  ||||||||||||||||||||||||||||||||||||||||||||||||||
nz94    481     TTCATCGTGAATTAATGGCATTTGTGATACTCTAAATGCATTTCCGTACATCGCACATCT   540
                         ↑
W.T.    36802   TCATCCACTTCGAACAATAACACAGCTATGCTTGAGAATGATGGTTGGAGATCCATGTGT   36861
                ||||||||||||||||||||||||||||||||||||||||||||||||||||||||||||
nz94    541     TCATCCACTTCGAACAATAACACAGCTATGCTTGAGAATGATGGTTGGAGATCCATGTGT   600

W.T.    36862   TGAAGATAGCGCAGCTTCCACCGCACTTCATCCAACAACTGTTTTACATCCAACTCCACC   36921
                ||||||||||||||||||||||||||||||||||||||||||||||||||||||||||||
nz94    601     TGAAGATAGCGCAGCTTCCACCGCACTTCATCCAACAACTGTTTTACATCCAACTCCACC   660

W.T.    36922   GCCTCAAACTTTT   36934
                |||||||||||||
nz94    661     GCCTCAAACTTTT   673
```

Figure 4-3 *nz94* contains a premature STOP codon in *unc-80*

We sequenced the *unc-80* gene in *nz94* and detected a consistent mutation generating a premature STOP codon. As seen here the alignment to the wild-type *unc-80* genomic sequence (upper sequence) is perfect except for one base (indicated by a red arrow) where the *nz94* mutant introduces a change from a guanine to an adenosine base.

4.2.4 - The UNC-80 protein is conserved from nematodes to mammals

The large gene, stretching over ten kilobase in cDNA alone, is predicted to produce a protein with molecular weight over 300kD. This very large protein has close homologues in other nematode species, such as *C. briggsae*, with which it shares 87% homology, and orthologues have been identified across the animal kingdom with poorer degrees of conservation (24% homology to the mouse homologue).

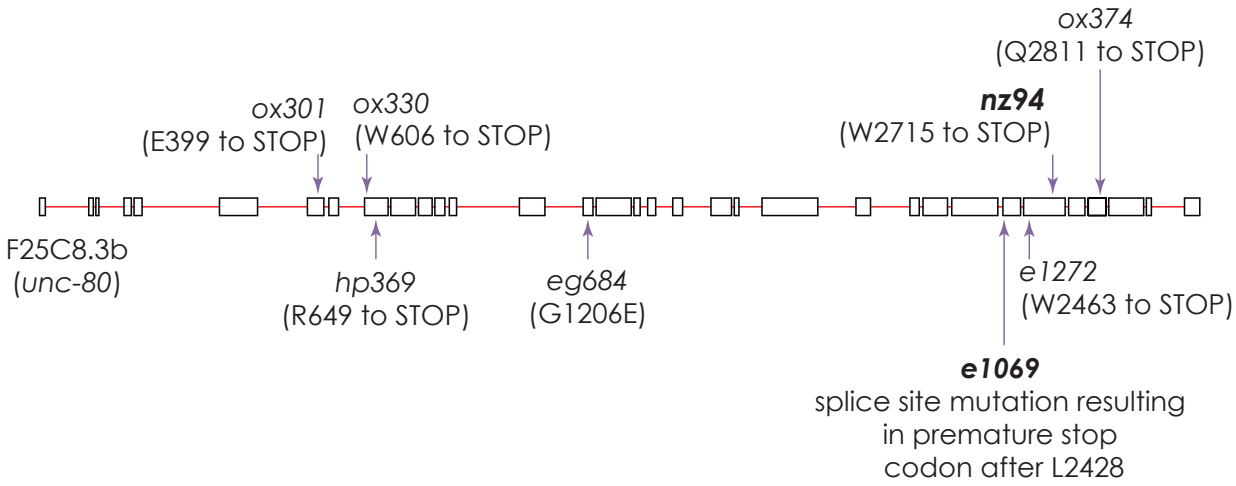

Figure 4-4 Known alleles of *unc-80*

The published *unc-80* alleles are shown here mapped onto the same gene model. They appear to cluster in two main regions, at the 5' and 3' end of the gene, which could indicate a particular susceptibility to mutation in those regions.

Interestingly, there are no domains of known function so far identified in the UNC-80 protein, apart from a predicted Armadillo repeat of relatively low homology (Pierce-Shimomura, Chen et al. 2008).

While the overall homology between species is relatively low, some regions of the protein are very highly conserved. Sequence analysis of the mouse homologue of UNC-80 predicts the existence of four potential transmembrane helices, marked in yellow in Figure 4-5. These four regions are relatively well conserved between highly disparate species (highlights in blue and purple), suggesting that they have some functional significance. Whether they are indeed transmembrane helices remains to be determined. Associated with these predicted helices are further regions of high conservation, marked in green across the various species listed.

This pattern of disparate patches of homology interspersed with regions showing no conservation is reminiscent of large proteins commonly classified as scaffolds. These often contain multiple protein-protein interaction domains, which are conserved between species, and large, flexible linker domains, which tend to be poorly conserved.

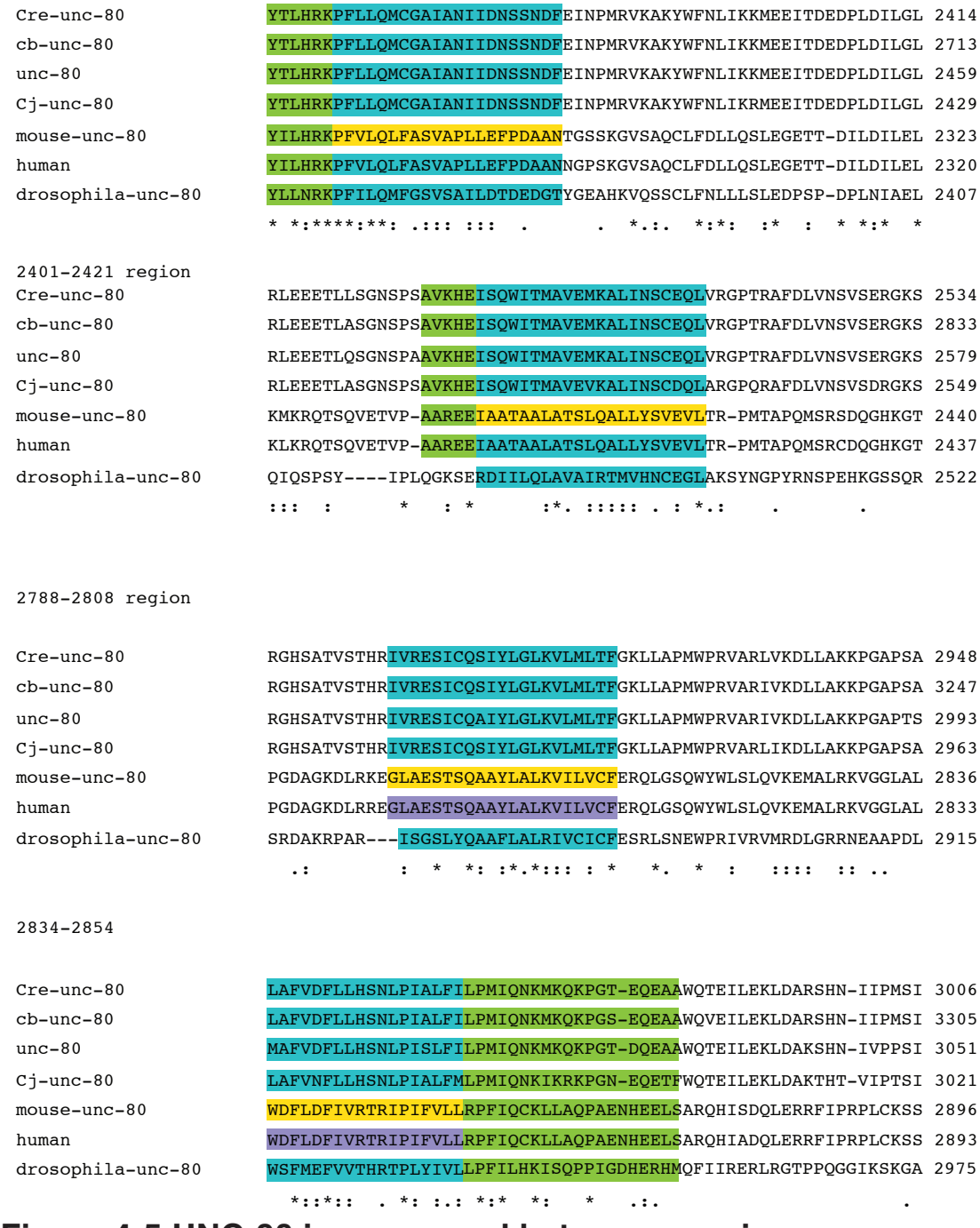

Figure 4-5 UNC-80 is conserved between species

While the UNC-80 protein in C. elegans contains no domains of known function, it does share homology to a number of other proteins in other species. The mouse homologue (listed here as mouse-*unc-80*) has been annotated to contain four potential transmembrane domains (highlighted in yellow). These sequences are relatively well conserved between other species, as are a number of adjacent sequences labelled in green.

4.3 - unc-80 (e1069) mutants are able to suppress the loopy locomotion of nRHO-1 mutants*

While complementation and sequencing confirmed that mutant *nz94* carries a mutation in the gene, there are likely to be many other genomic variations in this strain since it was

generated by EMS mutagenesis. We therefore tested whether other *unc-80* mutations are able to suppress of the loopy locomotion of nRHO-1* animals. We crossed males of strain QT733, carrying the nRHO-1* transgene, with strain CB1069 which carries a splice-site mutation in *unc-80* and has a fainting phenotype.

While being fainter in their locomotion, the body posture assumed by these *unc-80* mutants (Figure 4-6, C, and see Movie 4-5) looks identical to wild-type animals (Figure 4-6, A, and see Movie 4-3) in distinct contrast to the loopy body posture of nRHO-1* animals (Figure 4-6, B, and see Movie 4-4).

We examined the F2 generation following the cross for animals which were expressing (the marker for the nRHO-1* transgene) but which did not appear to have loopy locomotion. We picked these animals to fresh plates and allowed them to self-fertilise. The offspring of these animals are also non-loopy, and have a fainting phenotype. The animals obtained from this cross were labelled as strain QT841, and all the animals were positive for the nRHO-1* GFP marker. They are homozygous for the nRHO-1* transgene, and are consistently non-loopy.

This demonstrates that this allele of *unc-80* can also suppress the loopy phenotype of nRHO-1* (Figure 4-6, D and see Movie 4-7). All further experiments with respect to *unc-80* were performed using this strain and the *e1069* allele, as it likely contains fewer background mutations to our allele, and has been used in a number of prior publications.

4.4 - *unc-80*;nRHO-1* double mutants move efficiently towards food

unc-80 mutants have also been identified, using a dispersal assay, as suppressing a hypomorphic (synaptojanin) allele (Jospin, Watanabe et al. 2007). We therefore also used a dispersal assay to quantitatively measure the extent to which the *unc-80* mutation suppresses the loopy locomotion phenotype of nRHO-1* mutants.

When placed in the centre of a 10 cm plate without food, wild-type animals efficiently move towards food seeded at the edge of the plate, with 83±1% of animals on the food at 60 minutes (Figure 4-7, B, Table 4-1). In contrast, no nRHO-1* mutants are able to reach the food during the 60 minutes of the experiment, possibly due to an increased rate of reversals or a failure of chemotaxis (Table 4-1). The *unc-80*;nRHO-1* double mutants are able to suppress this inability to reach food during the dispersal assay as significantly more of these animals are on food at 60 minutes (76±6%, $p<0.001$, Table 4-1). Of the *unc-80* single mutants, despite their fainting locomotion, 63±4% of animals are on food at

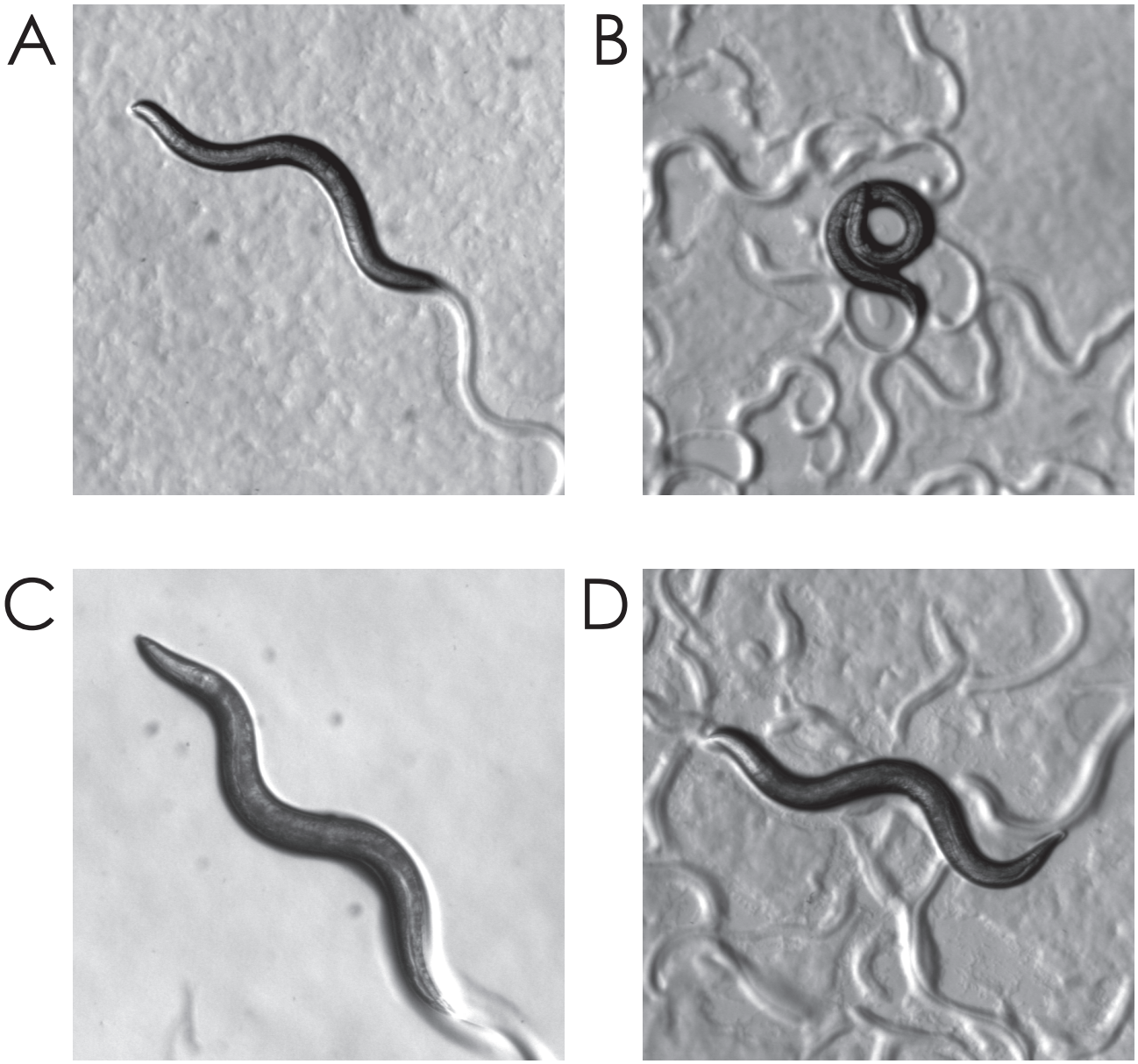

Figure 4-6 *unc-80* mutations suppress the loopy locomotion of nRHO-1*

nRHO-1* mutants are highly loopy (B) compared to wild-type animals (A). A double mutant, *unc-80*;nRHO-1* (D), regains the smooth sinusoidal locomotion of a wild-type animal. The *unc-80* single mutant, while having a fainter phenotype, is also non-loopy (C).

60 minutes, demonstrating that, although fainter, they are capable of efficient chemotaxis in this assay.

Interestingly, the double mutant, *unc-80*;nRHO-1* animals move more efficiently than the single mutant, with 76±6% of animals on food at 60 minutes, suggesting that there is some synergism between these two mutations, although this difference is not significant (Table 4-1).

4.5 - Rescue of the *unc-80* mutation

Since we have seen suppression of the loopy phenotype of nRHO-1* mutant animals by two alleles of *unc-80*, *nz94* which introduces a premature STOP codon, and *e1069*, a splice-site mutation, this represents strong evidence that it is loss of function of the gene itself which suppresses the loopy locomotion phenotype. To confirm this we wanted to rescue the mutation and restore loopy locomotion in these double mutations using a wild-type copy of the *unc-80* gene. We also wanted to determine the site of action of with respect to the suppression of the nRHO-1* loopy phenotype.

To this end we generated an *unc-80* minigene. The most complete *unc-80* cDNA available, yk1260h6, shows good homology to the genomic sequence of at its 5' end, but is aberrantly spliced at the 3' end. We therefore used the 5' sequence of the cDNA fused to the 3' genomic sequence, which we obtained by PCR from wild-type DNA. We also introduced a unique NotI restriction site into the 5' end of the cDNA to allow the insertion a GFP or mCherry fluorescent tag (see 2.22 for more details.)

The *unc-80* tagged and untagged minigenes were placed under the control of four different promoters to allow us to assess the site of action of with respect to suppression of nRHO-1* (Figure 4-8). These were the heatshock promoter from vector pPD79.48, which drives expression in most cells in the organism, although with a neuronal bias (Stringham, Dixon et al. 1992); the synaptobrevin (*snb-1*) promoter, which expresses in all neurons (Nonet, Saifee et al. 1998), and the *acr-2* and *unc-17* promoters, both of which express in neurons that produce acetylcholine, although with a few subtle differences of expression: the *acr-2* promoter expresses in some interneurons (Jospin, Qi et al. 2009) and the *unc-17* promoter drives some intestinal expression (Duerr, Han et al. 2008).

4.5.1 - Pan-neuronal expression of *unc-80* from the *snb-1* promoter rescues the suppression of loopy locomotion in an *unc-80*;nRHO-1* double mutant

The expression pattern described for *unc-80* indicates expression in neurons and vulval muscles (Jospin, Watanabe et al. 2007; Yeh, Ng et al. 2008); we therefore thought it likely that a neuronally expressed construct would rescue the suppression.

We generated transgenic animals by injecting *unc-80*;nRHO-1* double mutants (QT841) with SJN471 (p.*snb-1*::*unc-80*), at a concentration of 5ng/µl, along with a *ttx-3*::GFP co-injection marker. We obtained 2 independent lines in which all animals carrying the *ttx-3*::GFP marker are loopy, demonstrating that pan-neuronal expression of the *unc-*

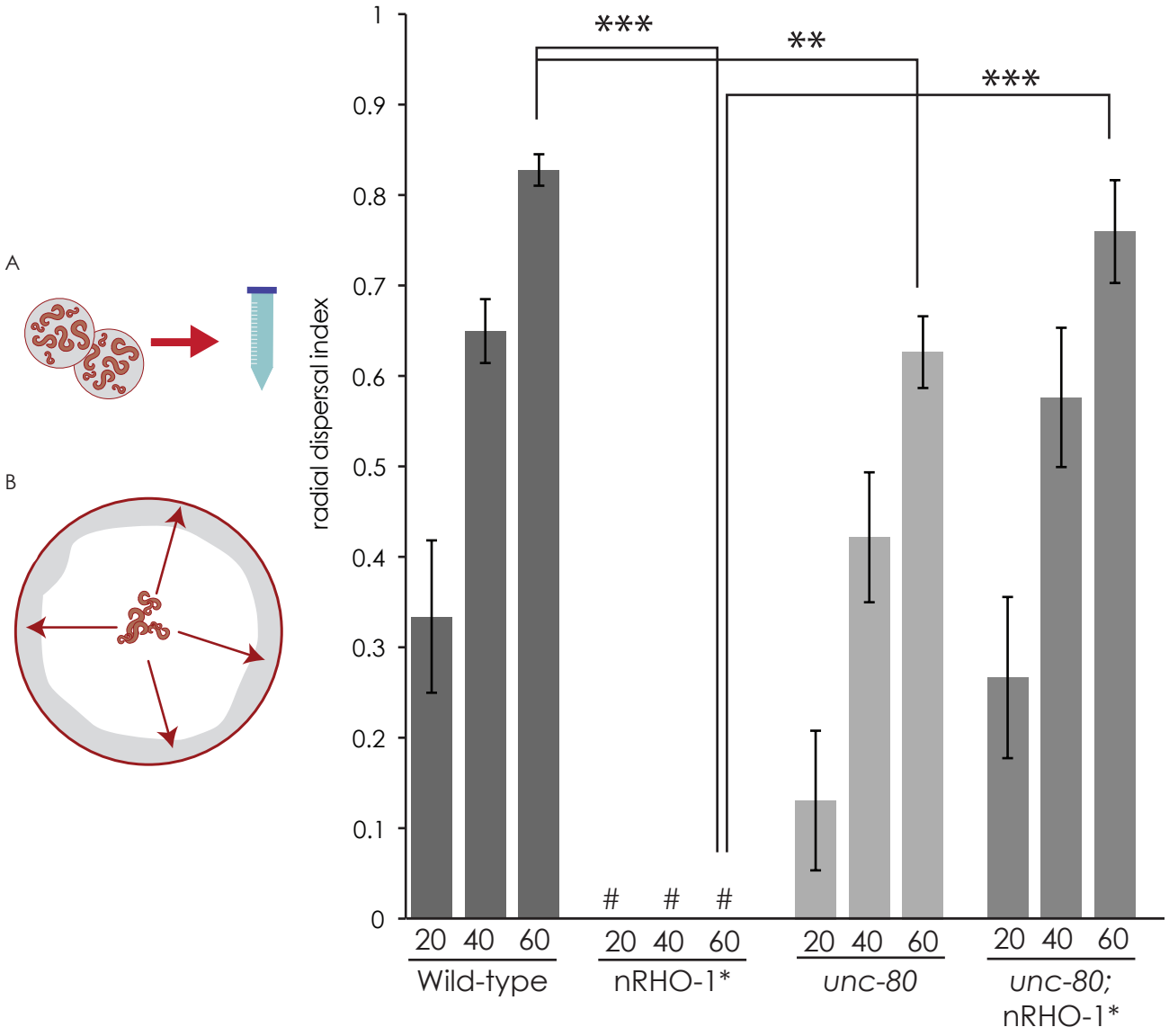

Figure 4-7 *unc-80* mutations rescue the inability of nRHO-1* to chemotax efficiently

The highly loopy phenotype of nRHO-1* mutants severely impairs their locomotion ability. Mixed populations of animals are collected in M9 (A), and placed in the centre of a large 10cm plate ringed with food (B). Animals migrate over time to the food at the edge of the plate, and the radial dispersal index indicates the proportion of animals on food, with 1 being all on food and 0 being none on food.

Wild-type animals efficiently move to the food, while nRHO-1* mutants are incapable of reaching the food during the 60 minute assay. *unc-80*;nRHO-1* double mutants are able to move efficiently to the food, demonstrating that the *unc-80* mutation suppresses the inefficient chemotaxis of nRHO-1* animals ($p<0.001$).

unc-80 single mutants, being fainter, reach food at a slower rate than wild-type animals. The *unc-80*;nRHO-1* double mutants reach food faster than *unc-80* mutants alone, suggesting some co-suppression, although this is not statistically signficant.

*** = $p<0.001$, ** = $p<0.01$. Statistics calculated using a 2-tailed T-test. # = none of the animals reached food during the recorded interval. n=8 for all strains.

80 minigene from the *snb-1* promoter construct is able to rescue the suppression of nRHO-1*.

We injected *unc-80*;nRHO-1* animals with SJN481 (p.*snb-1*::GFP::*unc-80*) along with the *ttx-3*::GFP marker at a concentration of 6ng/µl, and obtained 2 independent lines. All animals carrying the co-injection marker are loopy. A representative animal is shown in Figure 4-9 (and see Movie 4-7).

unc-80;nRHO-1* animals were also injected with SJN482 (p.*snb-1*::mCherry::*unc-80*) along with an *unc-17*::GFP marker,at a concentration of 12ng/µl. We obtained 3 independent lines, all of which produce loopy locomotion in animals carrying the co-injection marker.

Animals carrying the SJN481 and SJN482 plasmids were frozen for future reference (see Strains list). QT1086, carrying p.*snb-1*::GFP::*unc-80*, was selected for further analysis, and is referred to through the remainder of this chapter as *unc-80*;nRHO-1*;*p. snb-1*::GFP::*unc-80.* Unfortunately animals carrying the untagged SJN471 plasmid were not frozen down; these animals could be generated again by re-injecting the plasmid into QT841.

These constructs were not integrated into the genome of the rescued animals, but instead carried as extrachromosomal arrays. Animals not carrying the construct remain as non-loopy, fainter animals as an internal control for the effects of transformation.

4.5.2 - Cholinergic expression of *unc-80* under the *unc-17* promoter rescues nRHO-1* loopy locomotion in an *unc-80*;nRHO-1* double mutant animal

The nRHO-1* transgene is expressed only in cholinergic neurons, under the control of the *unc-17* promoter. *unc-17*, which encodes the worm synaptic vesicle acetylcholine transporter (VAChT), is required in cholinergic neurons for the loading of acetylcholine (Alfonso, Grundahl et al. 1993) and expresses in cholinergic neurons (Duerr, Han et al. 2008).

We generated transgenic animals by injecting *unc-80*;nRHO-1* double mutants (QT841) with SJN469, p.*unc-17*::*unc-80*, at a concentration of 5ng/µl, along with a *ttx-3*::GFP co-injection marker. We obtained 3 independent lines in which all animals carrying the *ttx-3*::GFP marker were loopy.

We also injected *unc-80*;nRHO-1* animals with either SJN477 (p.*unc-17*::GFP::UNC-80) at a concentration of 15ng/µl, or SJN478 (p.*unc-17*::mCherry::UNC-80) at a concentration

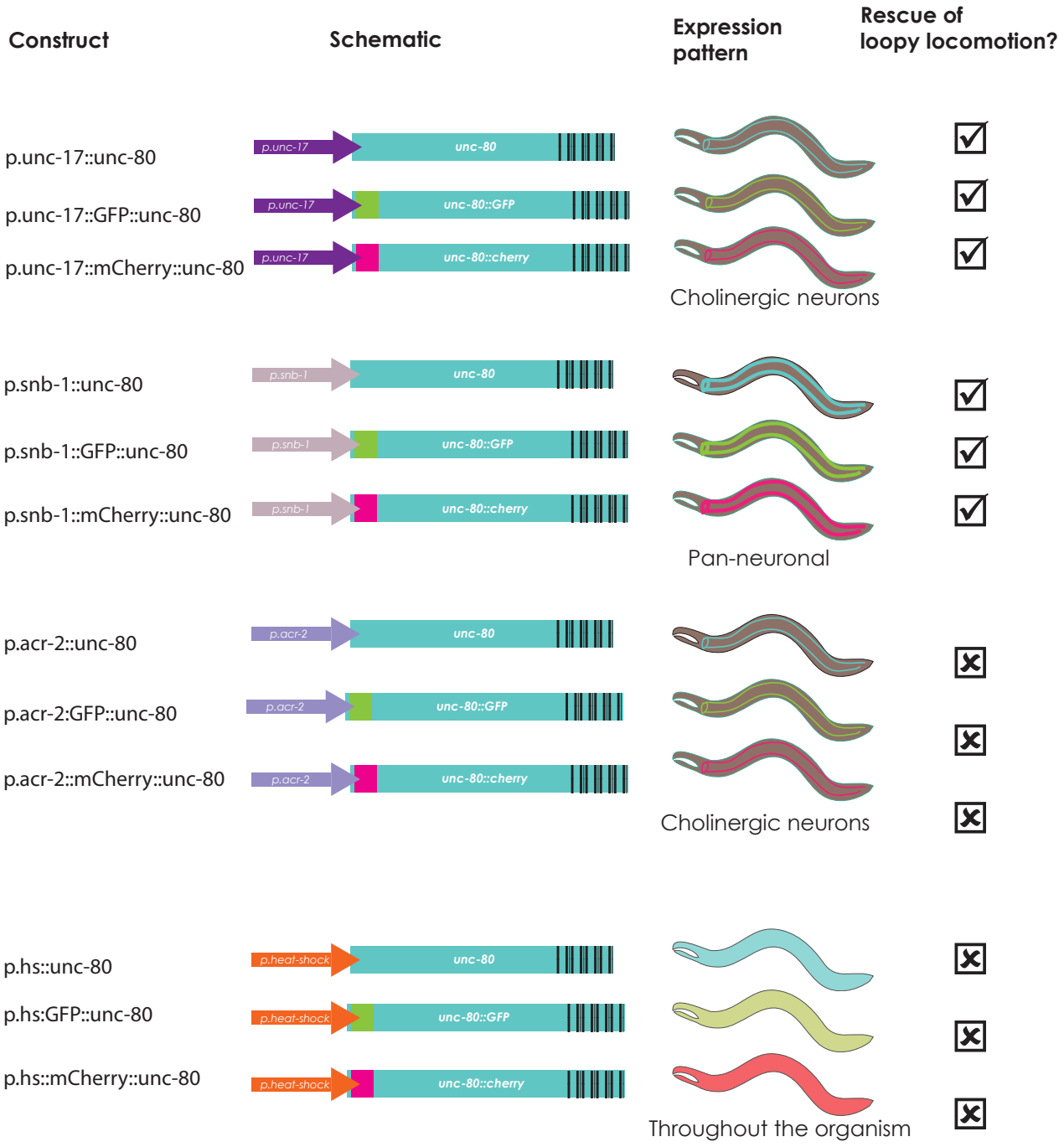

Figure 4-8 UNC-80 rescuing constructs

We generated a range of UNC-80 constructs using part 5' cDNA (solid blue section) and part genomic 3' DNA (striped section), along with versions tagged with either GFP (green) or mCherry (pink). These were placed under the control of four promoters: *unc-17*, *acr-2*, *snb-1* and heatshock. We observed rescue with UNC-80 constructs driven from the *unc-17* and *snb-1* promoters, partial rescue with the *acr-2* promoter, and have yet to observe rescue from the heatshock promoter.

of 5.5 ng/µl, along with the *ttx-3*::GFP or an *unc-17*::GFP marker respectively. We obtained 2 independent lines for each set of injections. All animals carrying the co-injection marker are loopy. A representative animal expressing p.*unc-17*::GFP::UNC-80 is shown in Figure 4-9 (and see Movie 4-8).

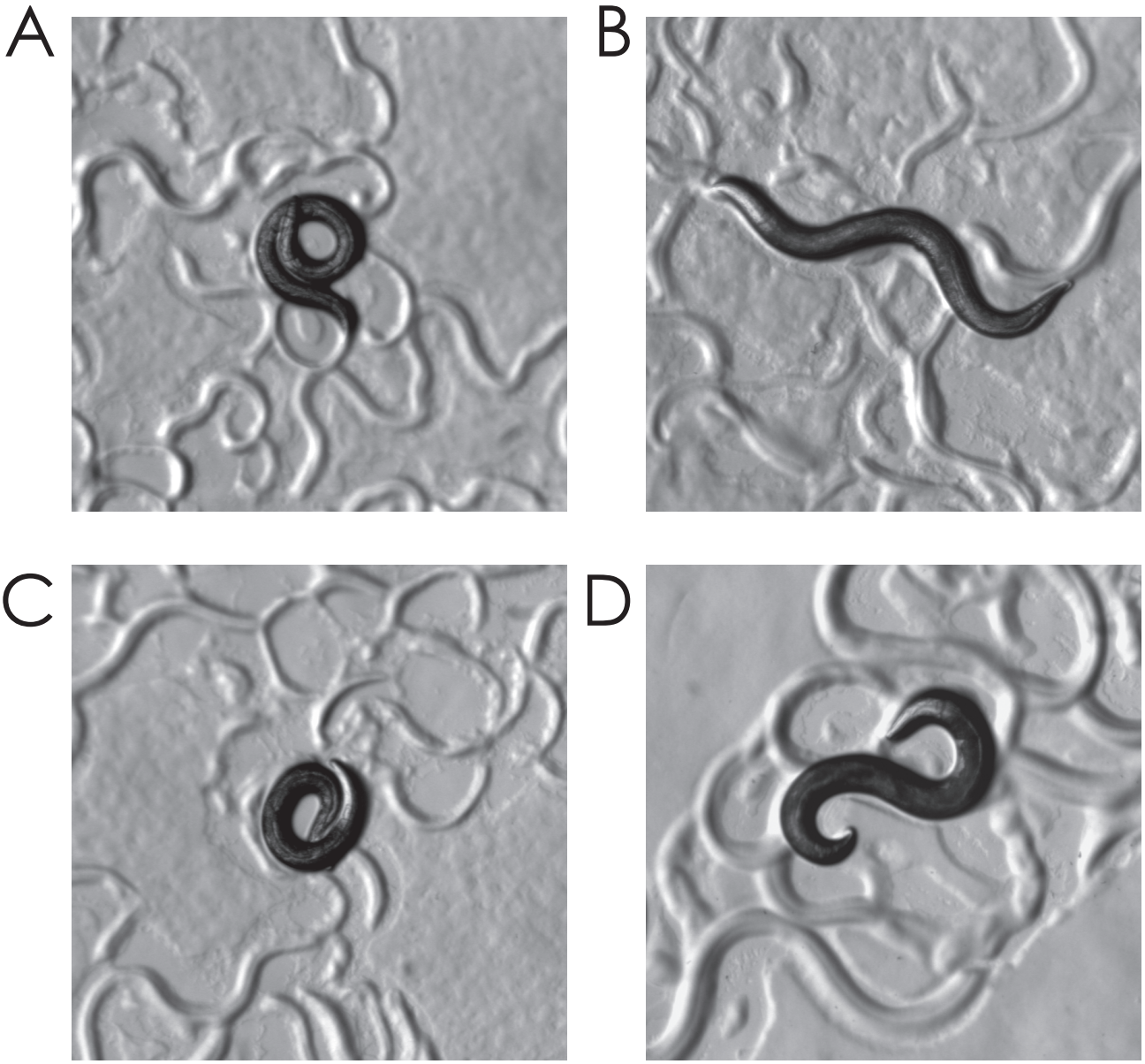

Figure 4-9 Rescue of the *unc-80* suppression phenotype by neuronal expression of UNC-80

nRHO-1* mutant animals are highly loopy (A), and the *unc-80*;nRHO-1* double mutant restores wild-type body posture (B). GFP-tagged UNC-80, expressed either pan-neuronally from the synaptobrevin promoter (C) or in the cholinergic motor neurons from the *unc-17* promoter (D) is sufficient to restore loopy locomotion in *unc-80*;nRHO-1* animals.

Animals carrying the SJN477 and SJN478 plasmids were frozen for future reference (see Strains list). Unfortunately animals carrying the untagged SJN469 construct lost the expression of their extrachromosomal arrays before they could be frozen down; these

animals could be generated again if necessary by reinjecting the plasmid into strain QT841.

These results demonstrate that UNC-80, expressed using the *unc-17* promoter, is able to restore the loopy locomotion phenotype in *unc-80*;nRHO-1* double mutants, and that UNC-80 and RHO-1* act within the cholinergic motorneurons to generate loopy phenotype.

4.5.3 - GFP-tagged UNC-80 protein is visible in neurons in rescued *unc-80*;nRHO-1* double mutant animals

Using the high-power fluorescent microscope (Zeiss widefield, Axioplan 2) we examined the animals carrying the rescuing constructs for expression of the tagged *unc-80* transgenes. Animals expressing UNC-80 from the synaptobrevin promoter do not show detectable levels of GFP or mCherry, although they are rescued for the locomotion phenotype. This suggests that very low levels of expression of UNC-80 are able to rescue the loopy locomotion phenotype.

The line QT1082, which expresses GFP-tagged UNC-80 under the *unc-17* promoter do show GFP expression in neurons (Figure 4-10).

No mCherry expression has been detected in lines carrying the mCherry-tagged constructs. The p.*unc-17*::GFP::UNC-80 construct was injected at a concentration three times higher than that in the other rescuing injections. This suggests that the level of expression of UNC-80 protein is too low to produce a detectable fluorescent signal in the remainder of the rescued lines. This may also be due to differences in the efficiency of transformation between these independently-generated lines. Future work to integrate these transgenes directly into the genome may increase GFP expression, or the rescuing plasmids could be reinjected at higher concentration.

As the loopy locomotion of these animals is rescued, we surmise that only a low level of UNC-80 expression is required to rescue this phenotype. This strain, QT1082, is used in further analysis in this chapter, and is referred to as *unc-80*;nRHO-1*;p.*unc-17*::GFP::UNC-80.

4.5.4 - Limited rescue of loopy locomotion in *unc-80*;nRHO-1* mutants has been obtained with UNC-80 expressed under the *acr-2* promoter

We injected *unc-80*;nRHO-1* animals with SJN467, p.*acr-2*::UNC-80, at a concentration of 5ng/µl, along with a ttx-3::GFP co-injection marker. We obtained 4 independent lines,

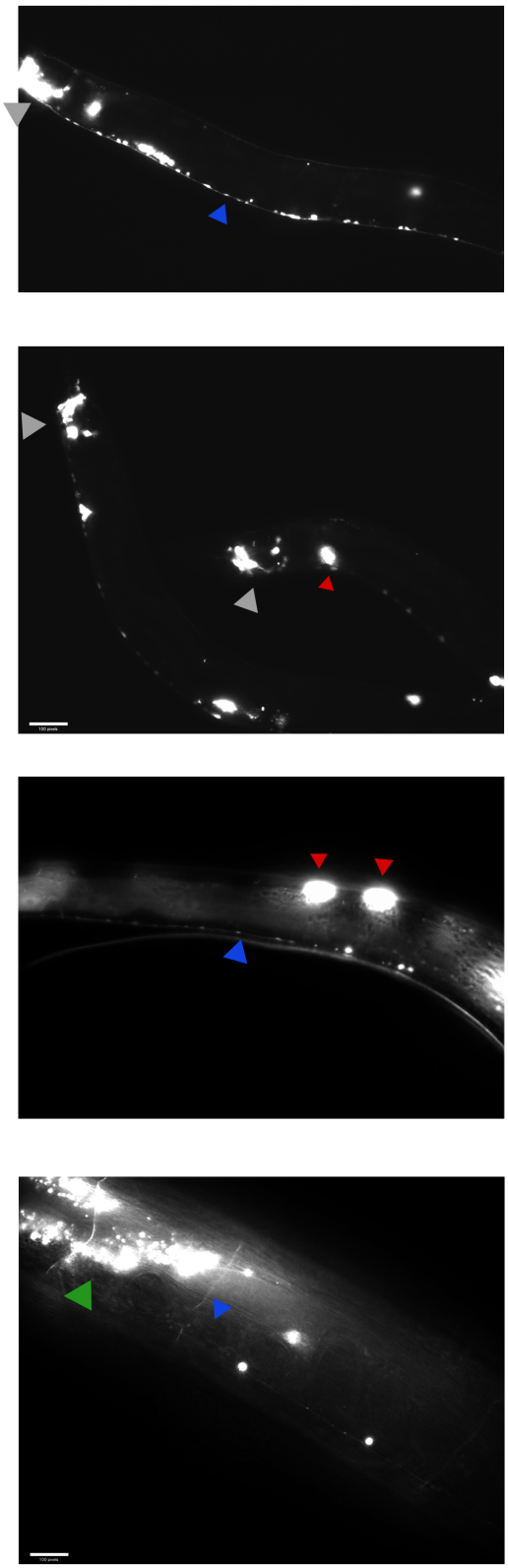

Figure 4-10 One rescued line expresses neuronal GFP

We have assayed all our rescued lines for expression of GFP- and mCherry-tagged UNC-80. While we see rescue of the loopy phenotype in all our rescued lines, we see expression of the GFP-tagged protein in only one line, QT1082, shown here. We see expression in the nerve ring (grey arrows) and in the nerve cord and commisures (blue arrows). We also observe some non-specific GFP expression (green arrow.) These animals also express the nRHO-1* co-transfection marker *unc-122*::GFP (red arrows).

only one of which produced any loopy animals, and not all animals carrying the co-injection marker were loopy.

The *acr-2* promoter drives expression in the ventral cord motor neurons VA, DA, VB, DB, DA, IL1, RMD, and PVQ (Jospin, Qi et al. 2009), and its expression overlaps considerably with that of the *unc-17* promoter, and yet so far we have been unable to rescue the loopy phenotype using this promoter. This may be due to subtle differences either in the level or specificity of expression between these promoters. Further injections, at a higher concentration, may yield lines which fully rescue the loopy phenotype. A similar difference was observed between *p.unc-17* and *p.acr-2* in the rescue of *pkc-1* mutants (D. Sieburth, personal communication.)

4.5.5 - UNC-80 expressed from a heatshock promoter does not rescue the loopy locomotion of *unc-80*;nRHO-1* mutant animals

Next, we wanted to test whether the timing of expression of UNC-80 protein was important for its function with respect to the loopy phenotype of nRHO-1*. To conduct this experiment, we created a number of transgenic lines carrying the rescuing construct under the control of the heatshock promoter.

unc-80;nRHO-1* animals were injected with the SJN470 (p.hs::UNC-80) construct at a concentration of 5ng/µl, along with a co-injection marker. One independent line was obtained. When grown at 20°C, none of these lines displayed loopy locomotion. We used our standard heat-shock protocol (staged adults, placed at 33°C for thirty minutes, followed by a rest at 20°C for one hour, and then repeated) to activate the heatshock response. However, none of the animals carrying the co-injection marker became loopy, and all retained the fainter phenotype, as did our rescued lines.

We next injected animals with SJN479 (p.hs::GFP::UNC-80) at a concentration of 10ng/µl, double the previous concentration, along with a p.*acr-2*::mCherry co-injection marker. We obtained 3 independent lines, and performed our heatshock protocol on all three. No animals carrying the co-injection marker became significantly loopy following heat-shock.

We next tried a range of more severe heatshock protocols to attempt to induce rescue.

- 1 hour at 33°C, recovery for 30 minutes at 20°C, repeated once
- 1 hour at 33°C, recovery for 30 minutes at 15°C, repeated once
- 1 hour at 37°C, recovery for 30 minutes at 15°C, repeated once
- Growth for 2 hours at 33°C

None of these protocols was able to induce loopy locomotion.

4.5.6 - GFP-tagged UNC-80 is visible in one line following heatshock

One possible explanation for the lack of rescue would be if the heatshock protocol is unable to induce expression of UNC-80 in these lines. We looked for expression of the GFP-tagged form of UNC-80 following these protocols, and some GFP expression is seen in neuronal cells. Only one line (2.6) has so far demonstrated expression of this construct (Figure 4-11). The expression appears to be mainly neuronal, despite the activation of the heatshock response throughout the organism.

While we have been able to establish that UNC-80 is required neuronally for rescue of the loopy phenotype, we cannot determine whether UNC-80 is required for correct development of the nervous system, has a function in adult neurons, or a combination of these possibilities.

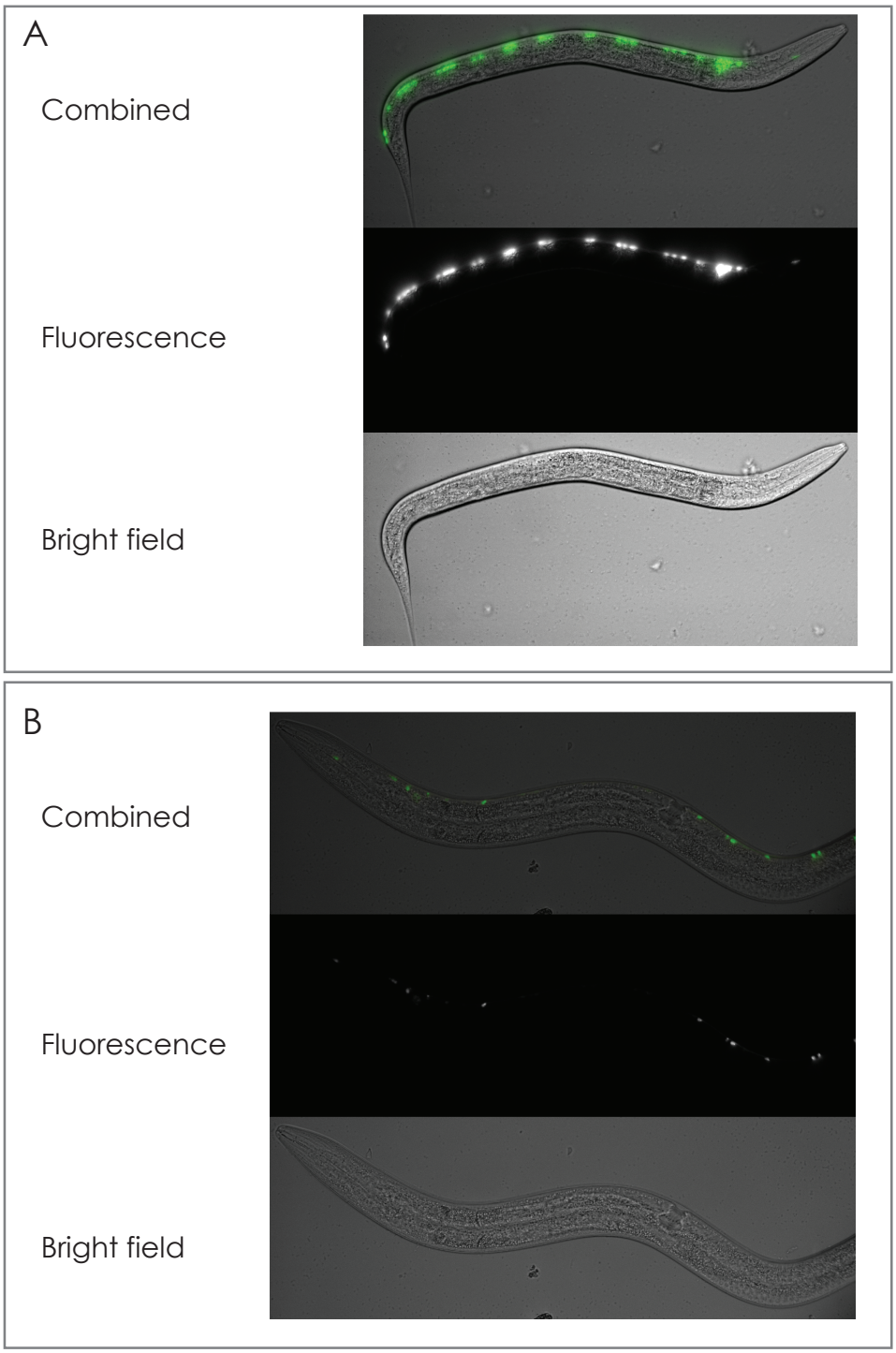

Figure 4-11 heatshock-driven GFP-tagged UNC-80 protein expresses in the nervous system

We have assayed all our lines carrying heatshock-driven GFP- and mCherry-tagged UNC-80. Only one line, Injection Line 2.6, demonstrated any expression of the tagged protein. As shown here, this line expresses GFP-tagged UNC-80 in the ventral nerve cord of larval animals (A) and adults (B) following heatshock. No expression has been observed in non-neuronal tissues.

Locus 1 \ Locus 2	Wild-type	unc-80	nRHO-1*	with p.snb-1::GFP::UNC-80	with p.snb-1::mCherry::UNC-80	with p.unc-17::GFP::UNC-80
Wild-type	0.83 ± 0.02	0.63 ± 0.04, p<0.01	0 ± 0.0	-	-	-
unc-80	0.63 ± 0.04, p<0.01	-	0.76 ±0.06, p<0.01	-	-	-
unc-80;nRHO-1*	0.76 ±0.06, ns	0.76 ±0.06, ns	0.76 ±0.06, p<0.01	0 ± 0, p<0.01	0.19 ± 0.26, p<0.01	0.01 ± 0.0, p<0.01

Table 4-1 Dispersal assay statistics

Summary of dispersal assay data Animals were constructed from a combination of locus 1 and locus 2. Numbers given indicate the radial dispersal index (at the 60 minute time point) +/- S.E.M. The statistical significance was calculated using a 2-tailed T-test.

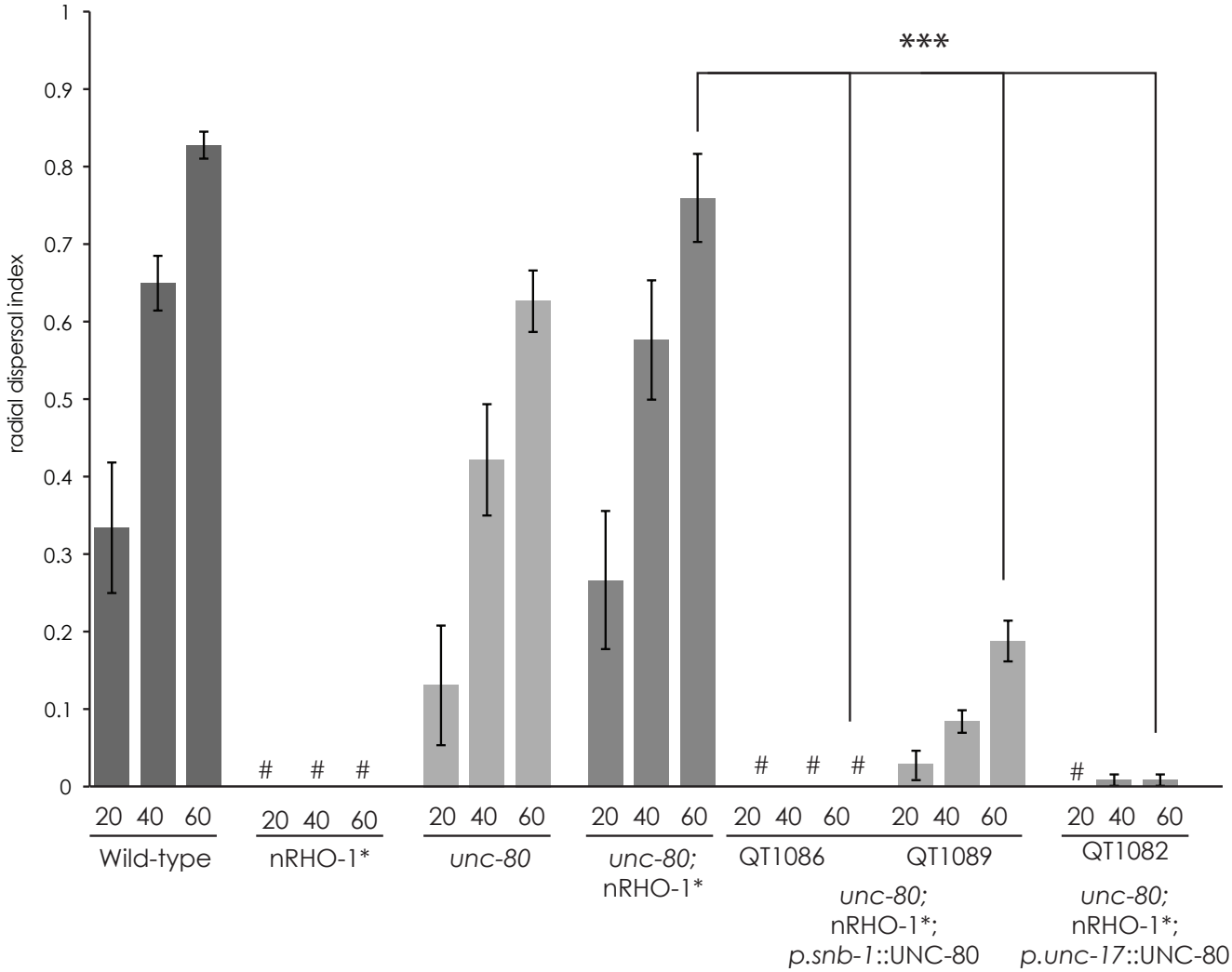

Figure 4-12 Dispersal assay of UNC-80 rescuing constructs (with Dr Rachel McMullan)

We tested two lines of animals rescued with *unc-80* under the synaptobrevin promoter and tagged with either GFP (QT1086) or mCherry (QT1089). Animals rescued with the GFP-tagged *unc-80* construct were unable to reach food for the duration of the experiment (marked with #), while animals rescued with the mCherry-tagged construct are slightly less loopy, with 18% reaching food after 1 hour.

Animals rescued with *unc-80* tagged with GFP and expressed from the *unc-17* promoter (QT1082) are completely rescued for loopy locomotion, with just 1% of animals on food at 1 hour.

*** = p<0.001, ** = p<0.01. Statistics calculated using a 2-tailed T-test. # = none of the animals reached food during the recorded interval. n=8 for all strains except QT1089 (n=6).

4.6 - Quantifying the level of rescue of the loopy phenotype of *unc-80*;nRHO-1* mutants from UNC-80 transgenes, in collaboration with Dr Rachel McMullan

While we can see by visual inspection that the *unc-80*;nRHO-1* animals expressing UNC-80 protein in the nervous system appear to be completely rescued for the loopy locomotion induced by the nRHO-1* transgene, we wanted to test their locomotion using the dispersal assay introduced earlier.

4.6.1 - Pan-neuronal expression of wild-type UNC-80 rescues the locomotion phenotype of *unc-80*;nRHO-1* mutants

In the dispersal assay, the *unc-80*;nRHO-1* double mutant is able to efficiently reach food after 1 hour (76±6% on food), while nRHO-1* animals are unable to reach food (0% on food after 1 hour).

We tested two independent lines of *unc-80*;nRHO-1* double mutants which have been rescued with UNC-80 expressed pan-neuronally from the synaptobrevin promoter. One of these lines, *unc-80*;nRHO-1*;*p.snb-1*::GFP::UNC-80, completely rescued the locomotion phenotype of the nRHO-1* transgene, with no animals reaching the food after 1 hour (Figure 4-12, Table 4-1). The second independent line tested, *unc-80*;nRHO-1*;p.snb-1::mCherry::UNC-80, demonstrated slightly weaker rescue of the suppression, with 18±2% on food after 1 hours; this is still significantly fewer animals reaching the food than seen in the non-rescued animals (Figure 4-12, Table 4-1). Differences in these two strains may be due to differences in the level of expression from the two transgenes.

4.6.2 - Cholingergic expression of wild-type UNC-80 rescues the locomotion phenotype of *unc-80*;nRHO-1* mutants

Double mutant *unc-80*;nRHO-1* animals, rescued with UNC-80 expressed from the *unc-17* promoter, which drives expression in the cholinergic neurons, are rescued for the suppression of the nRHO-1* loopy phenotype, and only 1% of animals reach the food after 1 hour of the dispersal assay (Figure 4-12).

This demonstrates that expression of UNC-80 in the same cells as RHO-1* is sufficient to completely rescue the suppression of the nRHO-1* phenotype observed in the *unc-80* mutant background.

4.6.3 - UNC-80 rescuing transgenes do not induce loopy behaviour in *unc-80* single mutants

To test whether the UNC-80 transgenes alone are responsible for the loopy behaviour seen in these animals, we crossed *unc-80*;nRHO-1* rescued animals with mutant animals to remove the nRHO-1* transgene from the genetic background while retaining the *unc-80* mutation.

unc-80 mutants expressing wild-type UNC-80 from either the synaptobrevin pan-neuronal promoter or the cholinergic promoter are non-loopy, demonstrating that the transgenes themselves are not responsible for the loopy locomotion seen in the *unc-80*;nRHO-1* rescued animals, and do not have a dominant effect on locomotion.

4.6.4 - UNC-80 rescuing constructs do not rescue fainting behaviour in *unc-80* mutant animals

Interestingly, the mutant animals expressing exogenous UNC-80 protein from both the *unc-17* and *snb-1* promoters appear to retain the fainting phenotype of the mutant animals (see Movies 4-17 and 4-18), although the *p.unc-17* transgene appears to restore more wild-type locomotion than the *p.snb-1* transgene. This suggests that the loopy behaviour and the fainting phenotype vary in their requirement for UNC-80 protein, and that either higher level of UNC-80 expression are required to rescue fainting, or that overexpression of UNC-80 causes fainting locomotion.

4.6.5 - UNC-80 rescuing constructs do not induce loopy locomotion in wild-type animals

We crossed the *unc-80*;*p.unc-17*::UNC-80 and *unc-80*;*p.snb-1*::UNC-80 animals with wild-type animals, and looked for lines in which the animals not carrying the transformation marker lacked a fainting phenotype. We obtained lines in which these extrachromosomal arrays are present in wild-type animals. These animals are non-loopy, indicating that the arrays themselves are do not drive loopy locomotion in a wild-type background. By eye, these transformed animals appear to have a subtle reduction in locomotion compared with untransformed animals, which would indicate that overexpression of UNC-80 is able to induce fainting locomotion on a solid surface. This suggests that mild overexpression is able to induce a dominant negative effect.

4.7 - *unc-80* mutants display defects in swimming behaviour

We have had difficulty finding an assay to successfully quantify fainting behaviour on a solid surface. If we examine body bends per minute, a common measure of locomotion rates, or use the dispersal assay (Figure 4-7) we see a reduction in the average locomotion rate of *unc-80* mutants, but this does not give a true picture of fainting locomotion, which allows wild-type movement interspersed with long pauses. We attempted to write a custom algorithm to measure pausing behaviour from videos analysed using the Parallel Worm Tracker (Ramot, Johnson et al. 2008), but experienced difficulties in this approach due to the sensitivity of *unc-80* animals to touch stimulation - analysing populations of individuals inducing movement in non-moving animals complicates the analysis of fainting.

We therefore looked at an additional phenotype displayed by mutants to attempt to quantify the behavioural effects of these rescuing transgenes. *unc-80* animals are noted to have a defect in swimming behaviour (Pierce-Shimomura, Chen et al. 2008). *unc-80* mutants are reported to thrash at a much slower rate than wild-type animals, which vigorously thrash when immersed in liquid. We decided to use this phenotype as a quantitative marker of the level of fainting in our mutant animals.

4.7.1 - *unc-80* mutants thrash less than wild-type when immersed in M9

It has long been known that *C. elegans* can survive long-term immersion in liquid. Wild-type animals thrash vigourously in liquid, and this behaviour has been shown to be directed, with animals capable of chemotaxing towards food in a liquid environment.

After immersion in a drop of M9 and being left to acclimatise for 3 minutes, wild-type animals thrash at a rate of 98±7 thrashes per minute (Figure 4-13, and Movie 4-9). In contrast, *unc-80* mutant animals thrash signifcantly less, at 39±10 times per minute in M9 (Figure 4-13 and Movie 4-10) ($p<0.001$).

We had previously described the *unc-80*;nRHO-1* double mutant as having a fainting locomotion. In the dispersal assay, these animals are able to successfully reach food after 1 hour, demonstrating that although fainter they are capable of sufficient locomotion for chemotaxis. In liquid, these animals thrash significantly less than wild-type, at a rate of 48±16 times per minute ($p<0.001$, Figure 4-13 and Movie 4-11). While not a statistically significant difference, this is a greater degree of thrashing than seen in *unc-80* single mutants.

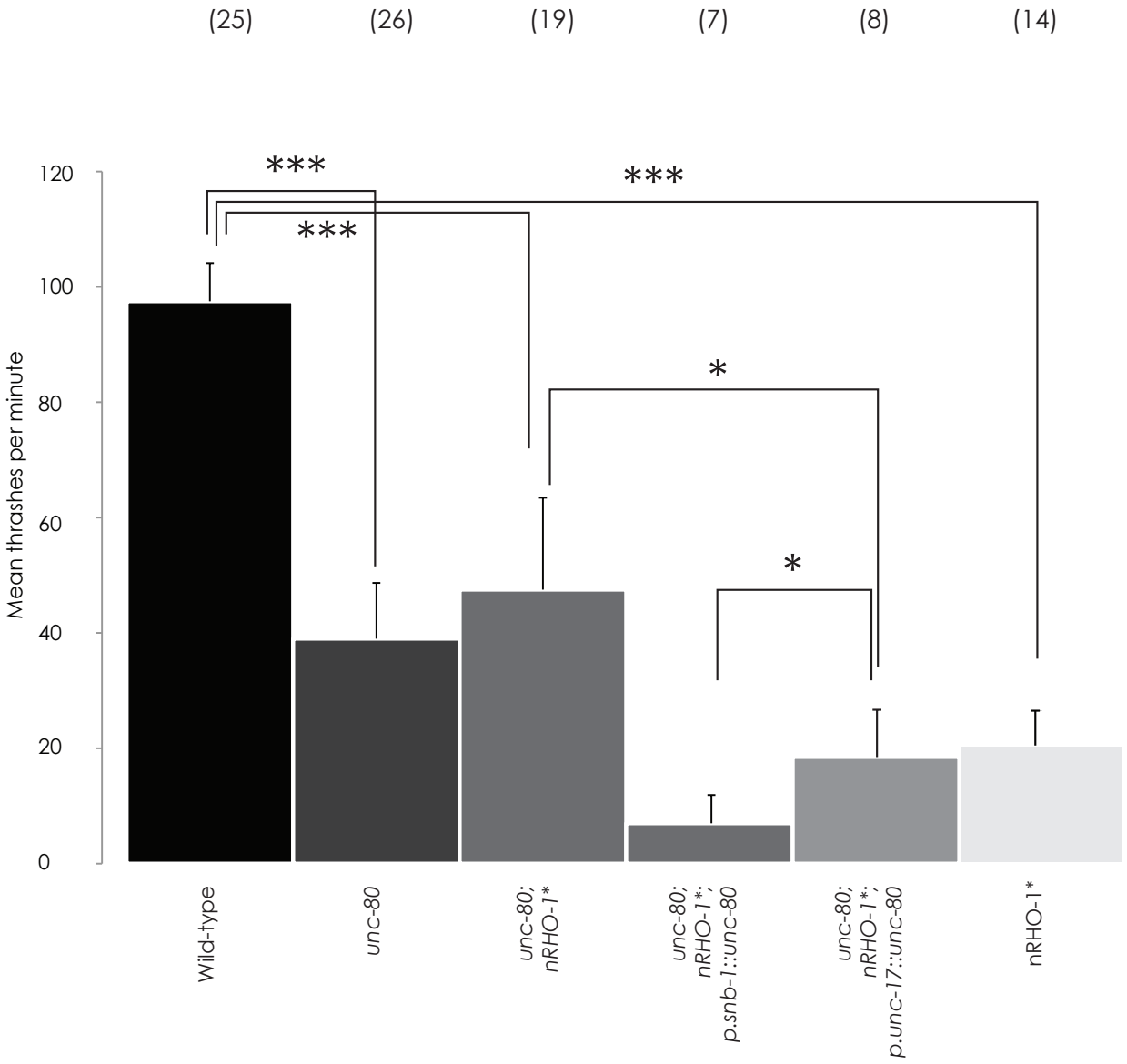

Figure 4-13 Mean thrashing assays of *unc-80* mutants

The *unc-80* mutants fail to thrash at the same rate as wild-type animals in M9. After being left for three minutes recovery, the number of thrashes in 2 minutes is counted, and an average taken for each worm. Wild-type animals thrash at 98 thrashes per minute, while *unc-80* animals thrash significantly less at 39 thrashes per minute. This indicates fainting behaviour in these animals. *unc-80*;nRHO-1* mutants also fail to thrash efficiently, at 48 thrashes per minute, demonstrating that these animals are also fainter.
nRHO-1* animal thrash significantly less than wild-type, but this appears to be due to their loopy locomotion (18 thrashes per minute).
Animals rescued with the UNC-80 transgenes are not rescued for swimming efficieny, although it is not clear whether this is due to their loopy locomotion phenotype or the retention of the fainting phenotype, as they now swim significantly less than *unc-80*;nRHO-1* double mutants. Animals expressing UNC-80 under the *unc-17* promoter swim more efficiently than those expressing UNC-80 from the synaptobrevin promoter (19 and 7 thrashes per minute respectively).
Error bars represent standard errors of the mean. Numbers in brackets indicate number of animals assayed.

4.7.2 - UNC-80 expressed from the *unc-17* cholinergic promoter does not rescue swimming behaviour in an *unc-80*;nRHO-1* double mutant

Animals expressing wild-type UNC-80 in the cholinergic neurons under the *unc-17* promoter in an *unc-80*;nRHO-1* mutant thrash at a rate of 18±7 thrashes per minute in M9 after 3 minutes recovery time (Figure 4-13 and Movie 4-12). This indicates an increase in the severity of the swimming phenotype compared to the double mutants.

These animals are highly loopy, and it may be that this uncoordination prevents successful thrashing. This hypothesis is supported by the behaviour of nRHO-1* mutants, which thrash at a rate of 18±10 thrashes per minute (Figure 4-13 and Movie 4-13), significantly less that wild-type.

4.7.3 - UNC-80 expressed pan-neuronally suppresses thrashing behaviour in an *unc-80*;nRHO-1* double mutant

unc-80;nRHO-1* mutants expressing UNC-80 wild-type protein from a synaptobrevin promoter thrash at a rate of just 7±5 thrashes per minute (Figure 4-13 and Movie 4-14). As with the *unc-17*-driven expression of UNC-80, this not only fails to rescue the fainting behaviour, it actually appears to increase the swimming defect, most due to an increase in loopy behaviour.

4.7.4 - Measuring mean thrashes per minute cannot distinguish between uncoordinated, loopy behaviour and fainting behaviour in liquid

These rescued strains do not demonstrate rescue of the *unc-80* fainting phenotype. However, the rescue of suppression of loopy behaviour induced by the nRHO-1* transgene means that these animals are highly uncoordinated, and this loopy behaviour also reduces thrashing in liquid, for reasons likely to be unrelated to the function of UNC-80.

The role of *unc-80* was further assayed in a second swimming assay. It has been reported that on immersion in liquid, *unc-80* mutants become rigid and fail to thrash. In our mean thrashes assay, we allowed time for recovery and *unc-80* mutants do then thrash, but at a slower rate than wild-type. We therefore decided to assay the initial response of animals to immersion in liquid in an attempt to find a stronger phenotype to distinguish *unc-80* mutants from wild-type animals.

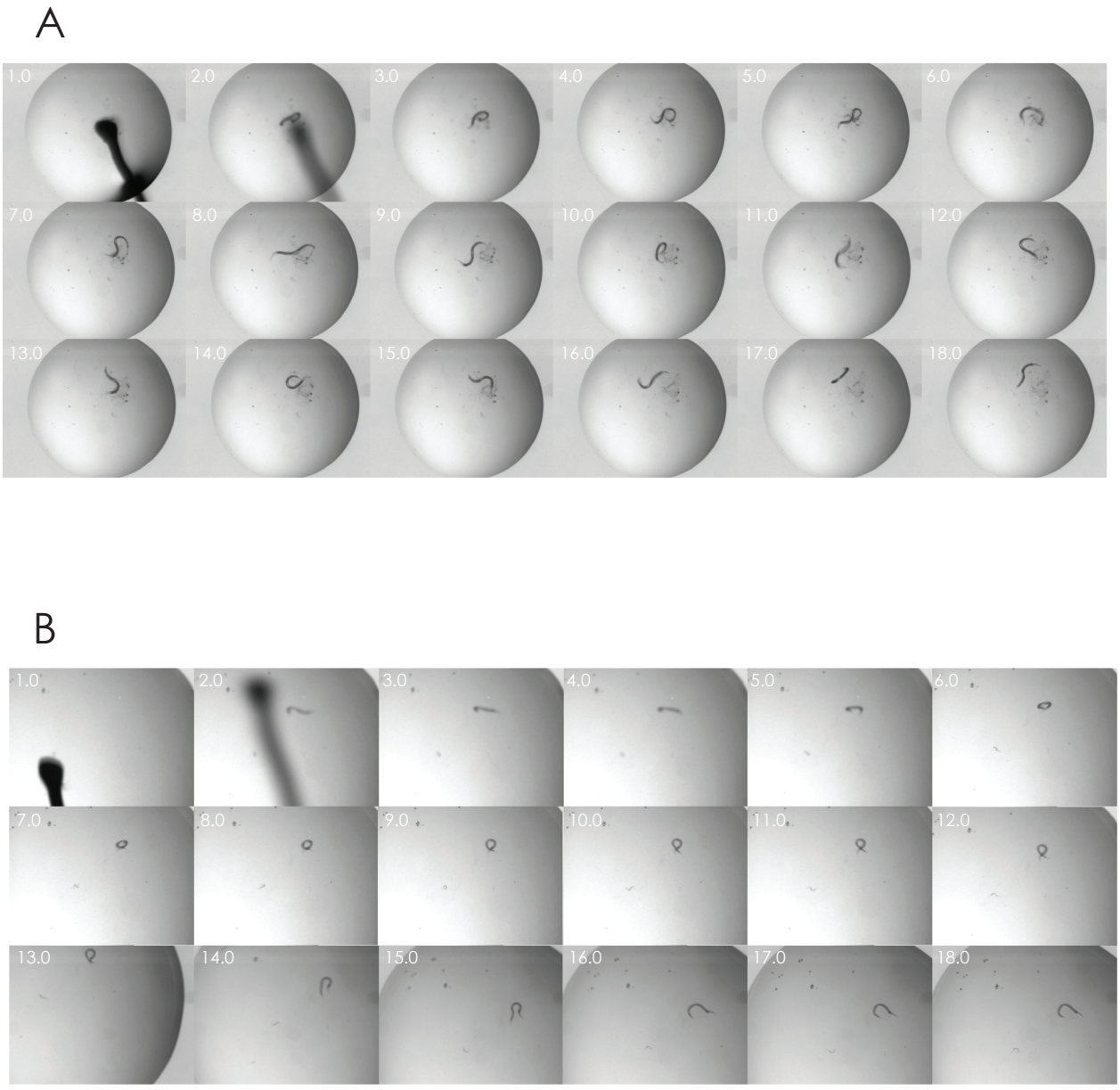

Figure 4-14 *unc-80* mutants fail to thrash on immersion in M9

unc-80 mutants (B) fail to thrash after immersion in M9. Unlike wild-type animals (A), which undergo body bends immediately on immersion in M9, *unc-80* animals retain a curled posture for most of the video.
(Numbers indicate time in seconds).

4.7.4.1 - *unc-80* mutants fail to thrash on immersion in M9

When immersed in M9, wild-type animals begin thrashing almost immediately. As can be seen in Figure 4-14, the animal undergoes several distinct body movements over the course of the first few seconds following immersion, and these continue for the duration of the video clip from which the still images were taken (Movie 4-15). In contrast, the *unc-80* mutant (Figure 4-14,B) remains immobile, with a slightly bent posture, for 10-12 seconds after immersion, uncurling slightly towards the end of the clip (Movie 4-16).

This immobility provides a good measure of the fainting phenotype, as seen in Figure 4-15. 82±13% of wild-type animals demonstrate 2 thrashes within 5 seconds of initial immersion, compared to just 21±12% of *unc-80* mutant animals. This is a statistically significant decrease in thrashing behaviour ($p<0.001$).

We can now assay whether the UNC-80 transgenes are able to rescue this behaviour in an *unc-80* background.

4.7.5 - UNC-80 expressed from the *unc-17* promoter partially rescues the fainting phenotype of *unc-80* mutants

unc-80 mutants expressing wild-type UNC-80 protein in their cholinergic neurons from the *unc-17* promoter thrash 36±15% of the time on immersion in M9 (Figure 4-15). This is less than 50% of the wild-type level, but does demonstrate a slight increase in thrashing compared to the *unc-80* mutant alone, indicating partial rescue of this swimming defect, and suggesting that UNC-80 is required in the cholinergic neurons for wild-type thrashing behaviour.

4.7.5.1 - UNC-80 expressed from the synaptobrevin promoter does not rescue thrashing behaviour in an mutant

As UNC-80 expressed just in the cholinergic neurons was unable to completely rescue the thrashing behaviour of mutants, we tested whether there is a requirement for UNC-80 in additional neurons for wild-type swimming behaviour. However, animals expressing wild-type UNC-80 protein pan-neuronally from the *snb-1* promoter thrash just 10±12% of the time on immersion in M9, a decrease when compared to *unc-80* mutants alone (Figure 4-15), although more repeats are required to assess the significance of this result.

4.7.6 - Overexpression of UNC-80 suppresses thrashing behaviour in wild-type animals

We hypothesised that the UNC-80 transgenes might be having a dominant negative effect on thrashing behaviour and decided to test their effect in a wild-type background.

When tested in the thrashing assay, UNC-80 expressed from either the *unc-17* promoter or the synaptobrevin promoter suppressed thrashing in a wild-type animal (Figure 4-15). 44±21% of wild-type animals expressing UNC-80 in their cholinergic neurons were able to thrash on immersion in M9, compared with 82±13% of wild-type animals. The reduction in thrashing behaviour was more severe with UNC-80 expressed pan-neuronally, where just 12% of the transformed animals were able to thrash on initial immersion (Figure 4-15), although this is the result of only a single experiment and so needs further investigation.

These results indicate that lack of UNC-80 function, in an *unc-80* mutant, or excess expression of UNC-80 from an exogenous transgene are both able to interfere with normal thrashing and locomotion.

4.8 - Drug assays of *unc-80* mutants

While mutations in the conserved gene *unc-80* are able to suppress the loopy locomotion phenotype induced by nRHO-1*, we were also interested in whether these mutations had a suppressive effect on the excess neurotransmitter release phenotype of nRHO-1* mutants. We use a pharmacological assay where the rate of paralysis in response to aldicarb, an acetylcholine esterase inhibitor, is a function of the amount of acetylcholine released from the neurons and the sensitivity of the muscles to that neurotransmitter (Nurrish, Ségalat et al. 1999).

As previously mentioned, nRHO-1* mutant animals are hypersensitive to aldicarb, indicating high levels of neurotransmitter release (McMullan, Hiley et al. 2006). We wanted to test whether mutants were able to suppress this aldicarb hypersensitivity phenotype as well as the loopy locomotion of nRHO-1*.

4.8.1 - *unc-80* mutants display a slight hypersensitivity to aldicarb

We first assayed whether the *unc-80* single mutants displayed a phenotype when exposed to aldicarb. *unc-80* single mutant animals demonstrate a slight hypersensitivity to aldicarb, paralysing faster than wild-type on 1mM aldicarb (Figure 4-16). After 50 minutes, 41±6% of mutant animals are paralysed, compared with 30±2% of wild-type animals. Although

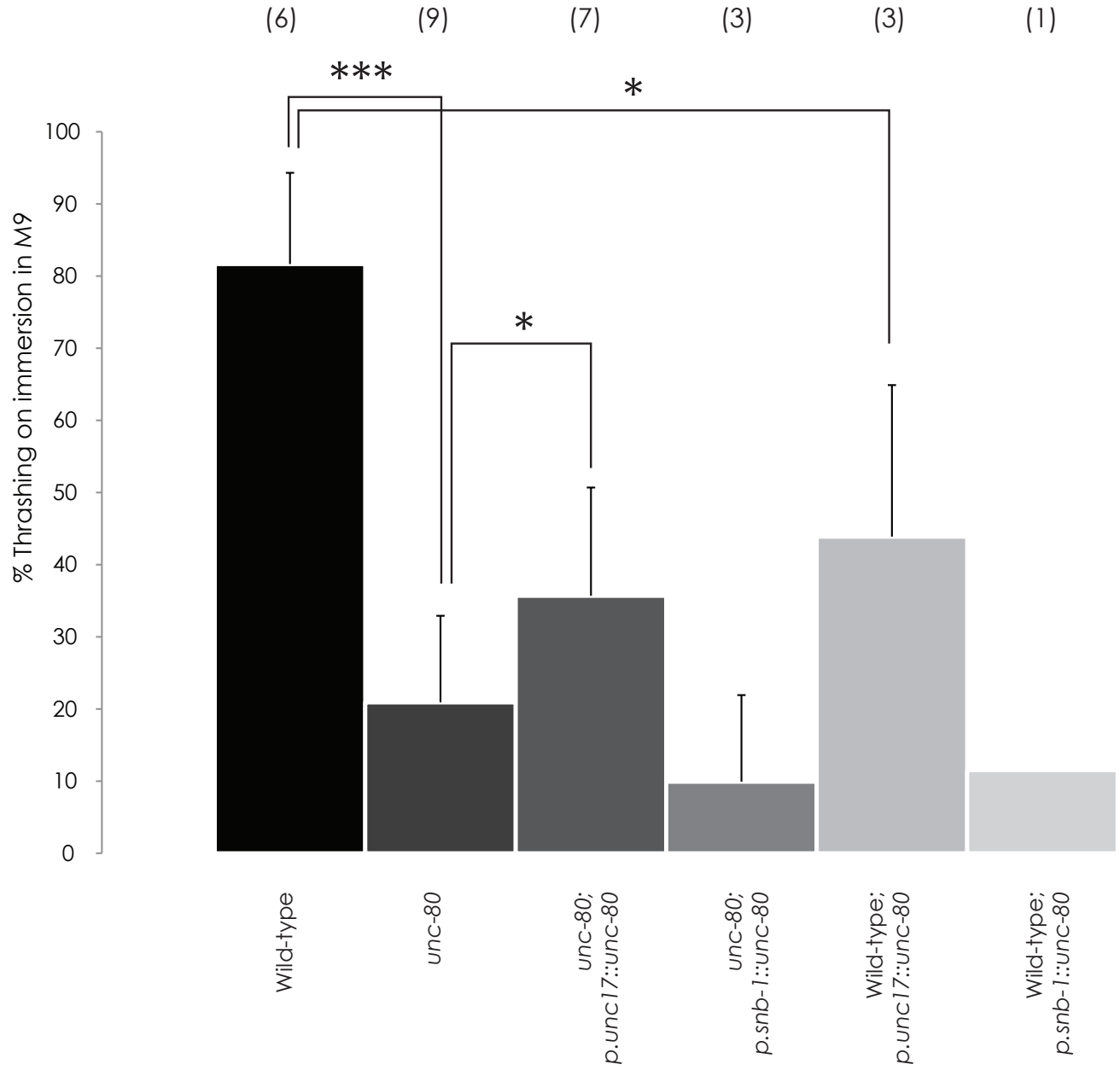

Figure 4-15 *unc-80* mutants initial thrashing assays

When wild-type animals are immersed in M9, they thrash vigorously. *unc-80* animals fail to thrash on immersion significantly more often than wild-type.
unc-80 animals rescued with UNC-80 expressed from either the *unc-17* promoter or the synaptobrevin promoter do not recover thrashing to wild-type levels, although these results do not reach significance.
Wild-type animals expressing UNC-80 either from the *unc-17* promoter or the synaptobrevin promoter thrash less efficiently than wild-type animals.
Error bars indicate standard errors of the mean. Numbers in brackets represent experimental repeats.

this is not a statistically significant change (p>0.05) (Table 4-2.), it implies that there is a trend towards increased acetylcholine signalling at the neuromuscular junction in *unc-80* mutant animals.

4.8.2 - Mutations in *unc-80* do not suppress the aldicarb hypersensitivity of nRHO-1* mutants

As previously demonstrated, nRHO-1* mutants are hypersensitive to aldicarb (McMullan, Hiley et al. 2006, and see also Figure 1-13). *unc-80*;nRHO-1* double mutant animals display a strong hypersensitivity to aldicarb compared to *unc-80* single mutant animals (Figure 4-16). At 50 minutes on 1mM aldicarb, 80±6% of the double mutant animals are paralysed, compared to 41±6% of the *unc-80* single mutant animals, a highly significant increase in paralysis (p<0.001) (Table 4-2). This demonstrates that the nRHO-1* transgene is able to potentiate the release of neurotransmitter even in an *unc-80* mutant background (Figure 4-16).

Percentage of animals paralysed at 50 minutes on 1mM aldicarb

Locus 1 \ Locus 2	**Wild-type**	***unc-80***	**nRHO-1***	**with p.*unc-17*::GFP::UNC-80**	**with p.*snb-1*::GFP::UNC-80**
Wild-type	30 ± 2.3, n=52	41 ± 6.0, n=18, p=0.08	87 ± 2.5, n=37, p<0.0001	-	34, n=1
unc-80	41 ± 6.0, n=18, p=0.08	-	79 ± 6.1, n=10, p<0.0001	70 ± 7.5, n=2	45, n=1
nRHO-1*	87 ± 2.5, n=37, p<0.0001	79 ± 6.1, n=10, p<0.0001	-	-	-
unc-80*;nRHO-1	79 ± 6.1, n=10, p<0.0001	*unc-80*;nRHO-1* compared with *unc-80* p<0.0001	*unc-80*;nRHO-1* compared with nRHO-1* p=0.025	96 ± 1.7, n=5, p=0.02	72 ± 13, n=4, p=0.62

Table 4-2 Statistical analysis of alidicarb data at 50 minute time point

Aldicarb data relating to *unc-80* and nRHO-1* is summarised here with statistics derived from the 50 minute time-point data. Statistics conducted using a 2-tailed unpaired T-Test. Data relating to PMA treatment is given within the body of the text.

The double mutant animals paralyse slightly slower than the nRHO-1* single mutants, of which 87±5% of animals are paralysed after 50 minutes exposure to 1mM aldicarb, demonstrating some slight suppression of the neurotransmitter release phenotype of nRHO-1*, although this result is not statistically significant (p>0.05) (Table 4-2).

This data suggests that there is separation between the loopy behaviour (which can be completely suppressed by mutations in *unc-80*) and the release of acetylcholine (which is not strongly suppressed by *unc-80* mutations). This is similar to the situation seen in many of the other suppressors isolated from the screen which have non-loopy locomotion with high levels of neurotransmitter release (see Chapter 3, particularly Figure 3-5).

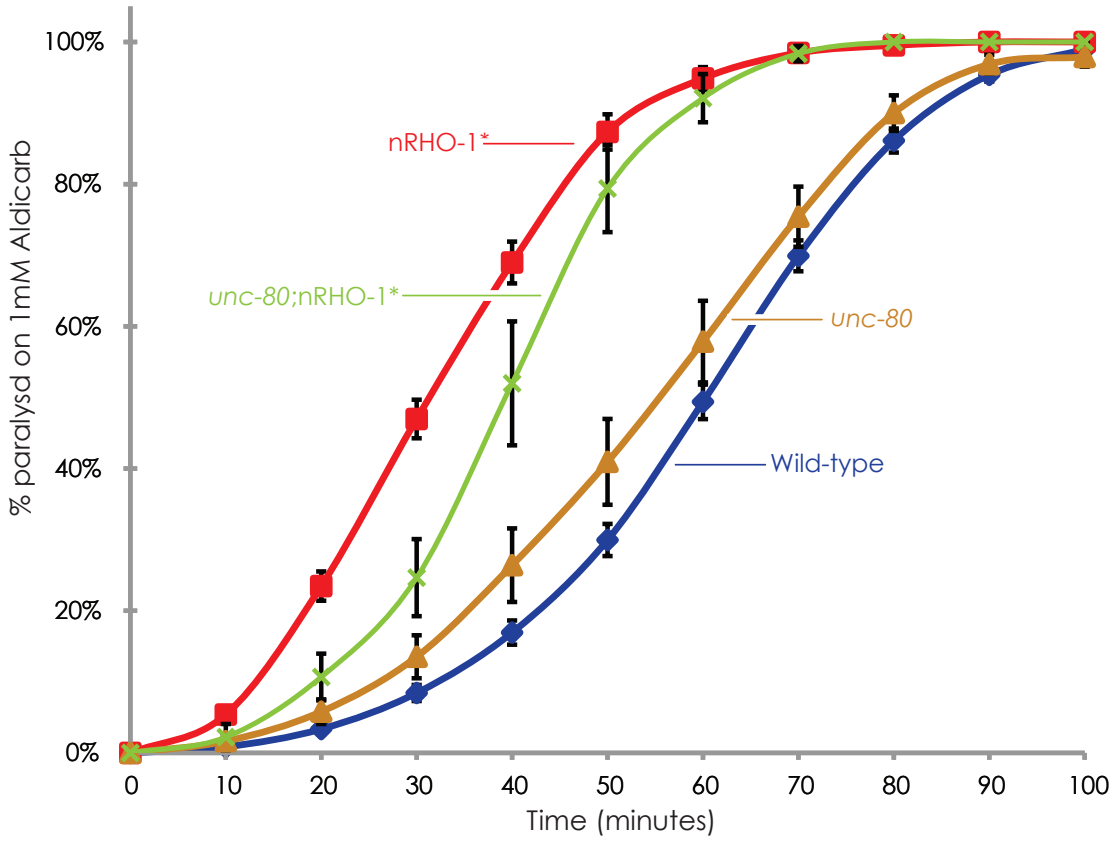

Figure 4-16 *unc-80* mutations only slightly suppress the aldicarb phenotype of nRHO-1* animals

Between 25 and 30 animals are placed on plates containing 1mM aldicarb, and assayed for paralysis with a nose touch every 10 minutes. Animals are counted as paralysed if they fail to complete the propogation of one wave of body bends following touch.
We observe a slight increase in the sensitivity of *unc-80* single mutants to aldicarb (orange line, n=18) compared to wild-type (blue line, n=52). nRHO-1* animals are hypersensitive to aldicarb (red line, n=37), and this hypersensitivity is only slightly decreased in an *unc-80*;nRHO-1* double mutant (green line, n=10).

4.8.2.1 - UNC-80 expressed pan-neuronally rescues the decrease in aldicarb hypersensitivity of *unc-80*;nRHO-1* mutant animals

We tested whether our rescuing transgenes, which restore loopy locomotion, were able to restore the slight decrease in aldicarb sensitivity observed in *unc-80*;nRHO-1* double mutants when compared to nRHO-1* animals alone. When expressed from the pan-neuronal p.*snb-1* promoter, the aldicarb curve shifts to the left of that seen in *unc-80*;nRHO-1* mutant animals (Figure 4-17). At 50 minutes, 96±2% of the *unc-80*;nRHO-1*;*p.snb-1*::GFP::UNC-80 animals are paralysed compared with 80±6% of the *unc-80*;nRHO-1*, which is a stastically significant increase in paralysis ($p<0.05$) (Table 4-2).

This suggests that *unc-80* is required neuronally to enhance the potentiation of acetylcholine release by nRHO-1*.

4.8.2.2 - Cholinergic expression of *unc-80* is not able to rescue the decrease in aldicarb senitivity seen in an *unc-80*;nRHO-1* mutant

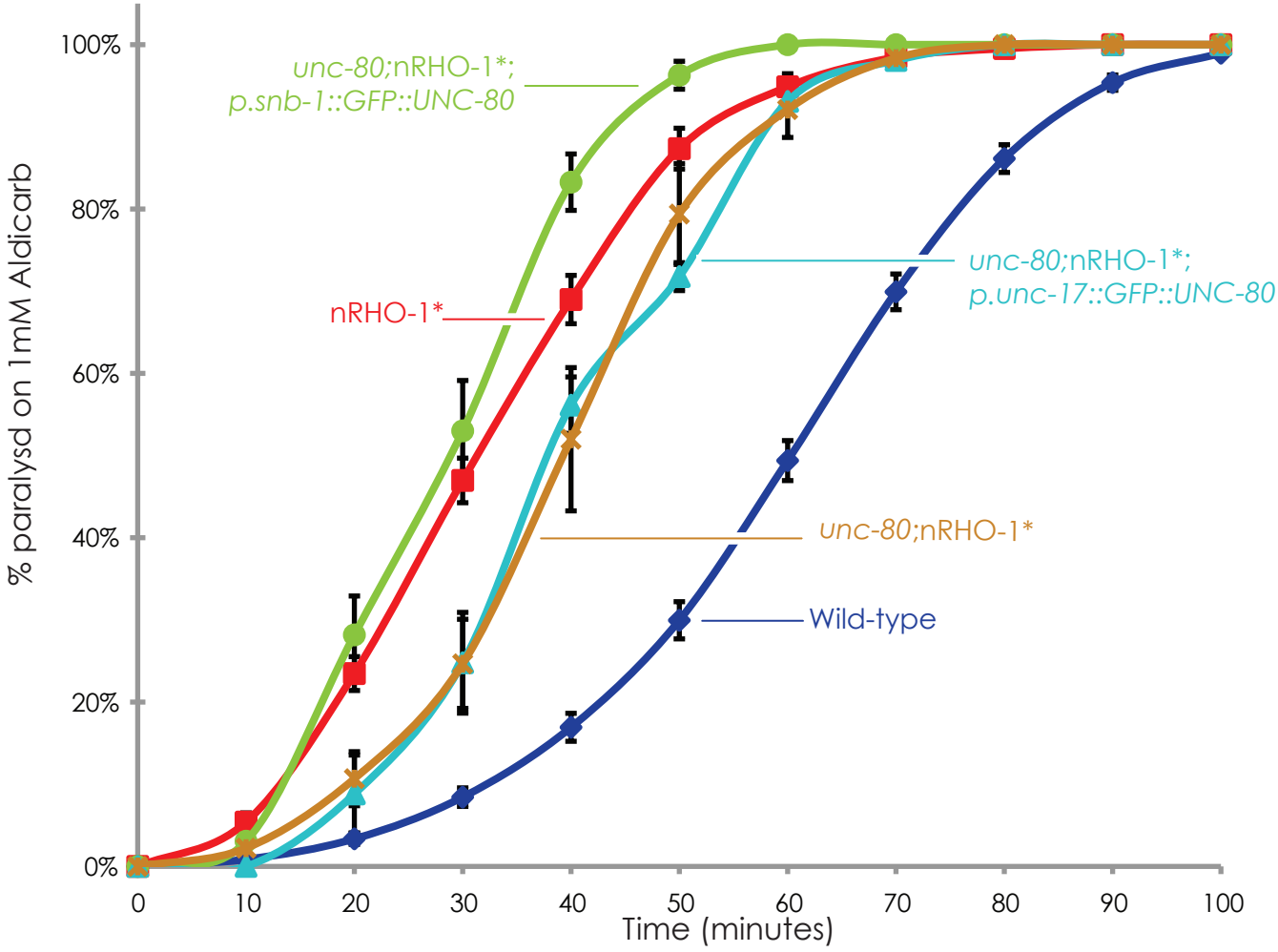

Figure 4-17 The *p.snb-1*::GFP::UNC-80 transgene increases aldicarb sensitivity in an *unc-80*;nRHO-1* mutant animal

unc-80;nRHO-1* mutant animals (orange line, n=10) demonstrate a slight decrease in acetylcholine release compared with nRHO-1* animals (red line, n=37). Expressing UNC-80 from the *snb-1* promoter increases acetylcholine release in these mutant animals (green line, n=5), while expression from the *unc-17* promoter (blue line, n=4) has no effect on neurotransmitter release.

UNC-80 expressed from the *unc-17* promoter, which also drives expression of the nRHO-1* transgene, has no effect on the aldicarb sensitivity of *unc-80*;nRHO-1* double mutant animals (Figure 4-17). 72±5% of *unc-80*;nRHO-1*;*p.snb-1*::GFP::UNC-80 animals are paralysed at 50 minutes compared with 80±6% of *unc-80*;nRHO-1* ($p>0.05$) (Table 4-2).

Along with the result for the pan-neuronal expression of UNC-80, this suggests that UNC-80 is required neuronally, in cells other than those expressing UNC-17, for a portion of the acetylcholine release enhanced by expressing nRHO-1*. These results could also be due to differences in the levels of expression between the two transgenes; assaying additional transformed lines may help resolve this.

4.8.2.3 - Cholinergic expression of UNC-80 in an *unc-80* mutant animal causes hypersensitivity to aldicarb

Another explanation for the results observed in *unc-80*;nRHO-1 animals rescued with exogenous UNC-80 protein is that the transgene itself, expressed from the synaptobrevin promoter, is increasing acetylcholine release independently of the nRHO-1* transgene, and the two together have an additive effect. We tested this by assaying the aldicarb sensitivity of *unc-80* single mutant animals expressing exogenous UNC-80 from either the *snb-1* or the *unc-17* promoter.

In a single trial, we saw no change in aldicarb response in animals carrying the p.*snb-1*::GFP::UNC-80 trasgene (Figure 4-18), although this experiment needs to be repeated before firm conclusions can be drawn. From two trials with *unc-80* single mutants carrying the p.*unc-17*::GFP::UNC-80 construct we saw an increase in sensitivity to aldicarb, although more repeats are required to confirm this result and assess its significance (Table 4-2).

Should these results hold, they suggest that overexpression of UNC-80 can cause hypersensitivity to aldicarb under some conditions, in this instance when expressed in the cholinergic neurons from the *snb-1* promoter, or from the *unc-17* promoter in combination with the nRHO-1* transgene.

The *snb-1* promoter expresses in cholinergic neurons and in all other neurons; the difference between results with these transgenes may be due to the effects of UNC-80 in those additional cells, or due to differences in levels of expression between the two transgenes. Assaying additional transformed lines may allow us to distinguish between these possibilities.

4.8.3 - *unc-80* mutants response to levamisole

An increase in the sensitivity of animals to aldicarb could be due to an increase in the release of acetylcholine from the motor neurons, or result from an increase in the sensitivity of the muscles to acetylcholine (see Chapter 3 (McMullan, Hiley et al. 2006).

Animals carrying a mutation in *unc-80* paralyse faster than wild-type animals on the drug levamisole. Levamisole directly stimulates the post-synaptic acetylcholine receptors on the body wall muscles, and induces paralysis at a rate proportional to the sensitivity of those receptors. The *unc-80* response curve is shifted to the left of the wild-type curve, which suggests that the *unc-80* mutation is having an effect on the body wall muscles (Figure 4-14). This effect is not stastically significant, 19±7% of *unc-80* mutant animals are paralysed at 50 minutes, compared with 9±1% of wild-type animals (Table 4-3). However, it is possible that the unc-80 hypersensitivity to aldicarb is due, in part at least, to a change in muscle sensitivity.

4.8.4 - *unc-80*;nRHO-1* double mutants are resistant to levamisole

We tested the *unc-80*;nRHO-1* double mutants for their response to the agonist levamisole. The response curve is shifted to the right compared with wild-type, nRHO-1* and *unc-80* mutant animals, suggesting that some interaction between the nRHO-1*

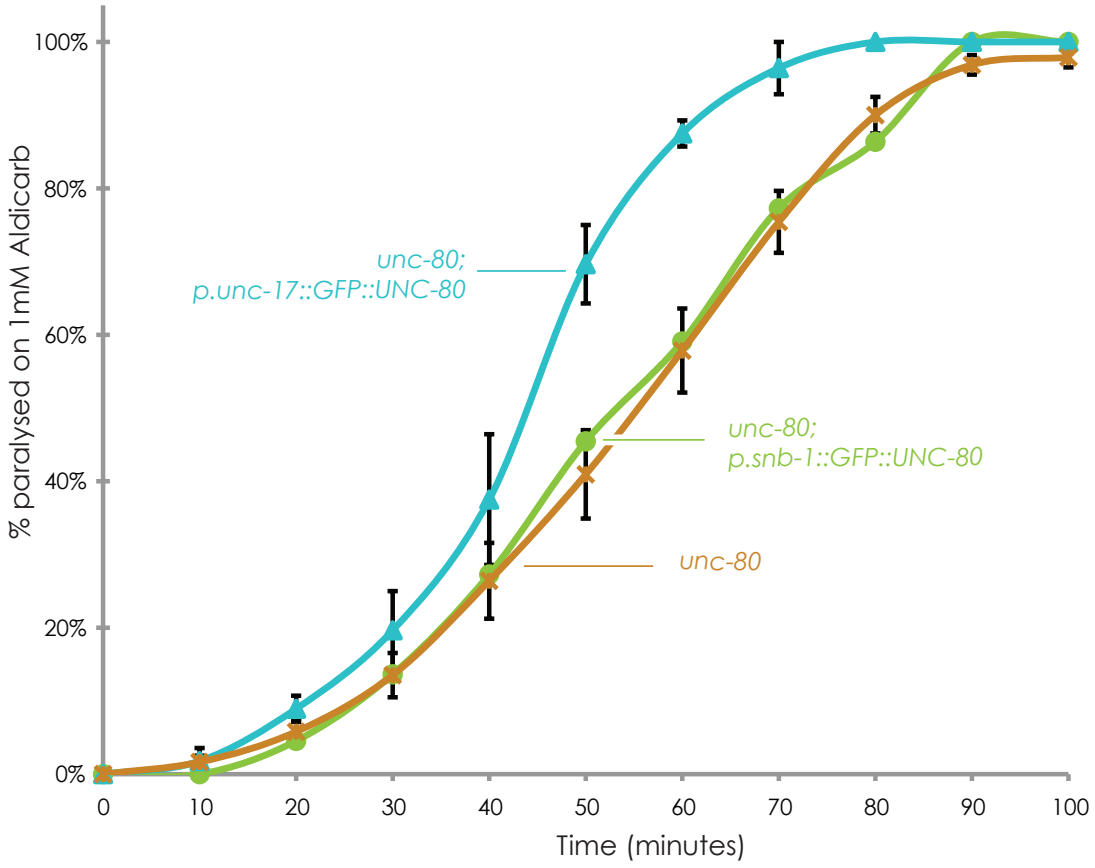

Figure 4-18 The p.*unc-17*::GFP::UNC-80 transgene increases aldicarb sensitivity in an *unc-80* mutant

Expression UNC-80 from the *unc-17* promoter in an *unc-80* mutant background increases sensitivity to aldicarb (blue line, n=2) compared with *unc-80* mutant animals alone (orange line, n=18) while expression of UNC-80 from the *snb-1* promoter has no effect on aldicarb sensitivity (green line, n=1).

transgene and the *unc-80* mutation is causing a decrease in the sensitivity of the body wall muscles to levamisole.

At 50 minutes, 7±1% of these animals were paralysed on 100µM levamisole, compared to 19±7% of *unc-80* single mutant animals ($p<0.05$) and 27±7% of nRHO-1* single mutants (which approaches significance, $p=0.06$), indicating that these double mutants are resistant to the effects of levamisole (Table 4-3). This reduction in sensitivity to levamisole, suggests that in these mutants the aldicarb assay underestimates the levels of acetylcholine release as the muscles are less sensitive to acetylcholine (Figure 4-16). In turn, this suggests a possible homeostatic compensation mechanism, where the muscle sensitivity to neurotransmitter is reduced in an attempt to balance the effects of excess neurotransmitter release.

4.8.5 - Expressing UNC-80 in the nervous system rescues the levamisole resistance of *unc-80*;nRHO-1* animals

We tested whether the expression of the UNC-80 transgenes was able to rescue the levamisole resistance of the *unc-80*;nRHO-1* double mutant animals.

Percentage of animals paralysed at 50 minutes on 100µM levamisole

Locus 1 \ Locus 2	**Wild-type**	***unc-80***	**nRHO-1***	**with p.*unc-17*::GFP::UNC-80**	**with p.*snb-1*::GFP::UNC-80**
Wild-type	9 ± 1.2, n=14	19 ± 6.7, n=9, p=0.11	27 ± 6.6, n=8, p<0.03	–	–
unc-80	19 ± 6.7, n=9, p=0.11	–	7 ± 1.7, n=5, p=0.02	52 ± 6.2, n=2	27 ± 0.5, n=2
nRHO-1*	27 ± 6.6, n=8, p<0.03	7 ± 1.7, n=5, p=0.06	–	–	–
unc-80*;nRHO-1	7 ± 1.7, n=5, p=0.4	*unc-80*;nRHO-1* compared with *unc-80* p=0.06	*unc-80*;nRHO-1* compared with nRHO-1* p=0.02	74, n=1	75, n=1

Table 4-3 Statistical analysis of levamisole data at 50 minute time point

All levamisole data in this chapter is summarised here with statistics derived from the 50 minute time-point data. Statistics conducted using a 2-tailed unpaired T-Test.

unc-80;nRHO-1* animals expressing UNC-80 from the synaptobrevin promoter are hypersensitive to levamisole, with 75% of the animals paralysed at 50 minutes compared with 7±1% of the *unc-80*;nRHO-1* mutant animals (Figure 4-20). Similarly, animals expressing UNC-80 from the *unc-17* promoter are also hypersensitive to levamisole, with 74% of animals paralysed at 80 minutes (Figure 4-15). Although these figures are the results of only a single trial, they suggest that presynaptic expression of UNC-80 can induce changes in the sensitivity of the body wall muscles to acetylcholine.

4.8.6 - Expressing UNC-80 in the nervous system of *unc-80* mutants causes hypersensitivity to levamisole

To test whether the ability of the UNC-80 transgenes to increase sensitivity to levamisole is dependent on the presence of the nRHO-1* transgene, we assayed the levamisole sensitivity of animals carrying UNC-80 transgenes in an *unc-80* mutant background. Animals expressing UNC-80 protein from the synaptobrevin promoter have essentially the same levamisole response as *unc-80* mutants (with 27±1% paralysed at 50 minutes compared to 19±7% of *unc-80* mutants, Figure 4-21), suggesting that alone this transgene does not affect signalling.

UNC-80 expressed from the *unc-17* promoter causes a hypersensitivity to levamisole in *unc-80* mutant animals (Figure 4-21), with 52±6% of animals paralysed at 50 minutes, (Table 4-3). This could reflect a difference between rescue in all motor neurons and

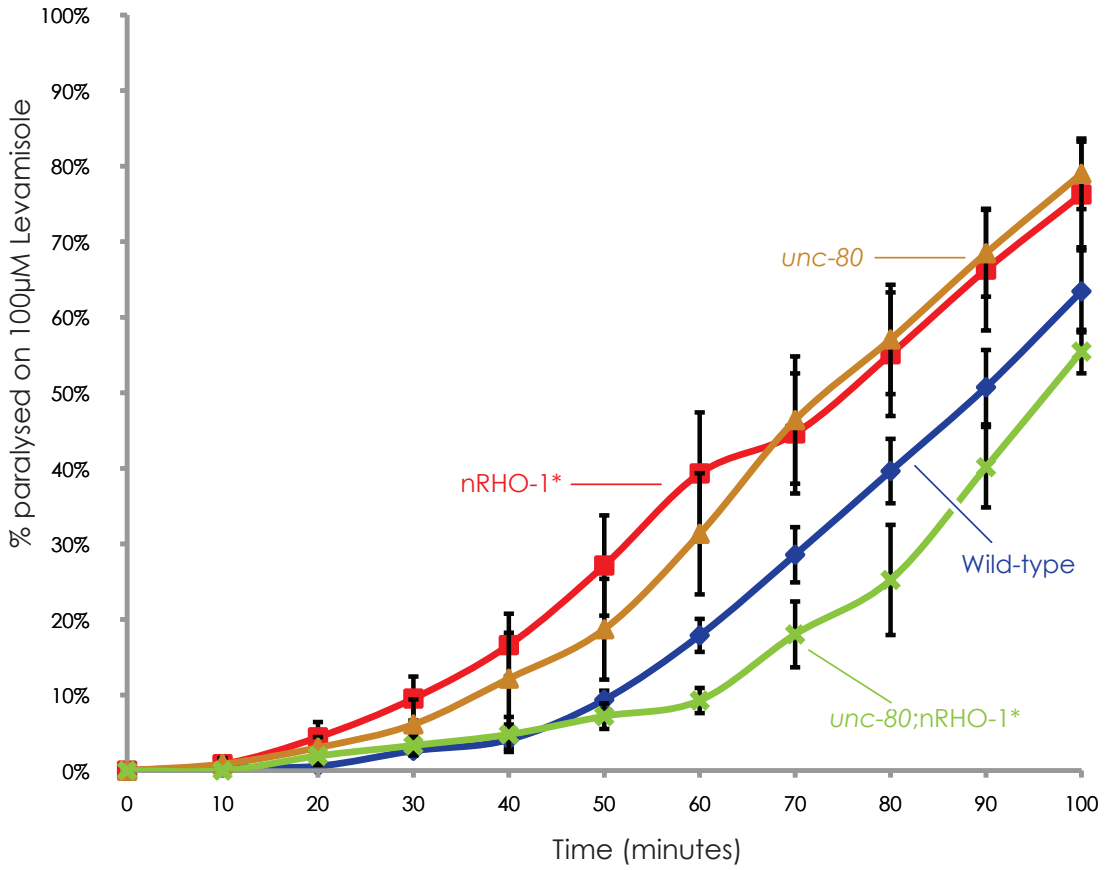

Figure 4-19 *unc-80*;nRHO-1* double mutants are resistant to levamisole

Between 25 and 30 animals are placed on plates containing 100µM levamisole, which directly stimulates contraction of the body wall muscles, and assayed for paralysis with a nose touch every 10 minutes. Animals are counted as paralysed if they fail to complete the propogation of one wave of body bends following touch.
We observe an increase in the sensitivity of *unc-80* single mutants to levamisole (orange line, n=9) compared to wild-type (blue line, n=14). nRHO-1* animals are also hypersensitive to levamisole in these assays (red line, n=8). The double mutant *unc-80*;nRHO-1* is resistant to the effects of levamisole (green line, n=5).

rescue only in the cholinergic motor neurons, suggesting a potential role for GABA release.

These preliminary results, based on two repeats for each transgene, must be repeated at least two more times before drawing any strong conclusions about effects on levamisole response. Taken together however, these results suggest that overexpression of some GFP::UNC-80 transgenes increases sensitivity to levamisole, and that addition of the nRHO-1* transgene enhances this effect.

We have seen that loss of *unc-80* allows for a reduction in levamisole sensitivity in nRHO-1* animals. These overexpression experiments demonstrate the opposite phenotype. This suggest a possible role for UNC-80 in neurons increasing muscle sensitivity to acetylcholine. Whether this change in sensitivity plays a role in the observed loopy behaviour remains to be determined (see discussion at the end of Chapter 5).

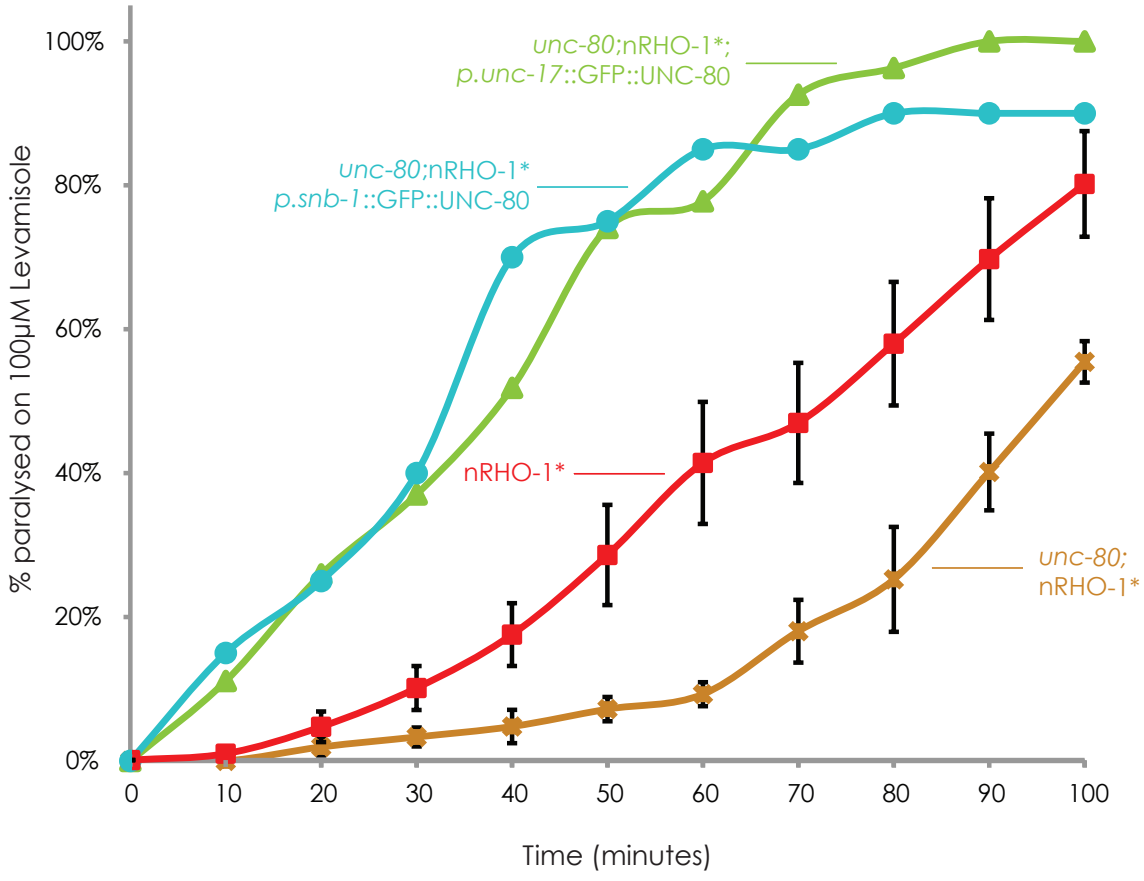

Figure 4-20 Rescue of the *unc-80* suppression phenotype by neuronal expression of UNC-80

The double mutant *unc-80*;nRHO-1* is resistant to the effects of levamisole (orange line, n=5). We tested the lines expressing GFP::UNC-80 under the control of either the *unc-17* promoter (green line, n=1) or the synaptobrevin promoter (blue line, n=1). These results are based on a single repeat, but do suggest that the GFP::UNC-80 constructs can increase sensitivity to levamisole in an *unc-80*;nRHO-1* double mutant.

4.9 - *unc-80* mutants are able to respond to phorbol esters

One theory to explain the suppression of loopy behaviour of the nRHO-1* transgene by mutants would be if these mutants were generally able to suppress the activity of the nervous system. This would be consistent with their published role, alongside the *nca-1* and *nca-2* ion channels, in propagating neuronal activity in certain neurons in *C. elegans* (Yeh, Ng et al. 2008). Ye et al suggest that NCA-1 and NCA-2, acting as sodium leak channels, could bring the neuronal membrane potential closer to its excitation threshold, allowing for passive propogation of nerve impulses to the synapse.

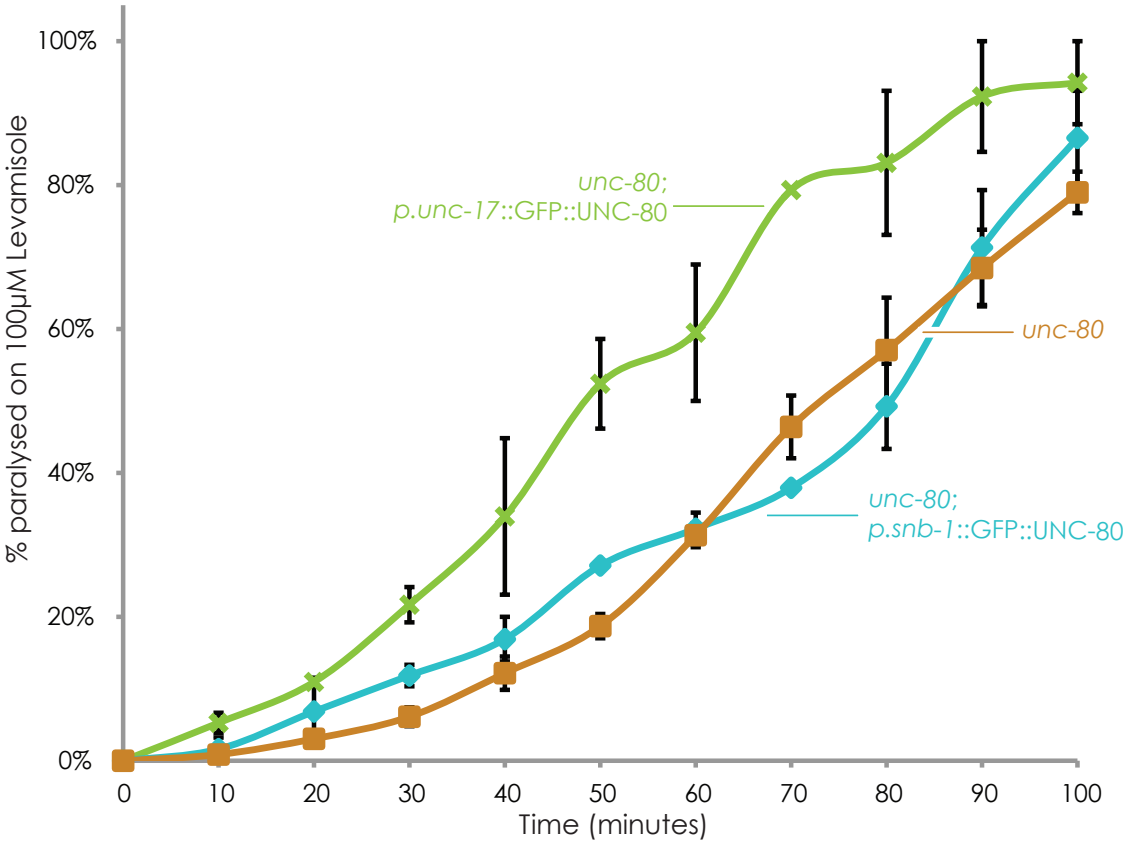

Figure 4-21 The UNC-80 rescuing transgenes increase levamisole sensitivity in an *unc-80* mutant

The *unc-80* mutants display a slight hypersensitivity to levamisole compared to wild-type animals (Figure 4-19). Addition of GFP::UNC-80, under the control of the synaptobrevin promoter, does not alter this response (blue line, n=2). Expressing GFP::UNC-80 from the *unc-17* promoter in an *unc-80*;nRHO-1* mutant causes an increase in the sensitivity to levamisole (green line, n=2)

This model provides a simple explanation for the fainting phenotype – when the activity of the nervous system reaches some given threshold, the animal is able to move normally despite the absence of the NCA-1 and NCA-2 channels; below that threshold the animal remains motionless. It is possible that this threshold is higher in a fainter, meaning they remain motionless for a greater period of time than wild-type animals, although strong stimulation, such as a nose touch, is sufficient to induce movement.

One way to test whether *unc-80* mutants are globally reducing the activity of the nervous system is to see their effect on pharmacological agents which stimulate neuronal activity. One compound with which we can achieve this stimulation is the phorbal ester PMA, which is an analogue of diacylglycerol (DAG). DAG is a key second messenger in the nervous system and is removed from the presynatpic membrane by diacylglycerol kinase (DGK-1) (Nurrish, Segalat et al. 1999) which in turn is inhibited by RHO-1 (McMullan, Hiley et al. 2006), and acts to stimulate release of neurotransmitter (Lou, Korogod et al. 2008)

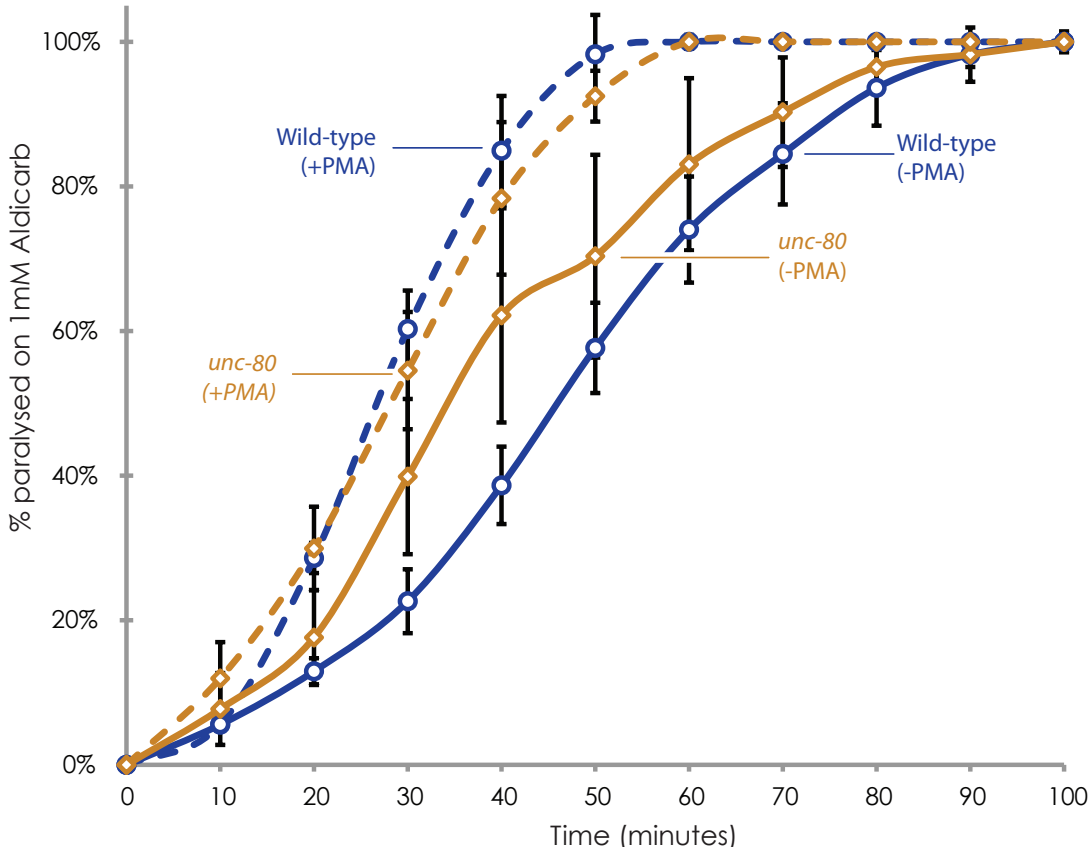

Figure 4-22 *unc-80* mutants can respond to PMA by increasing sensitivity to aldicarb

Animals are pre-incubated with either PMA or a DMSO control for 2 hours. Between 25 and 30 animals are placed on plates containing 1mM aldicarb and either PMA or DMSO and assayed for paralysis with a nose touch every 10 minutes. Animals are counted as paralysed if they fail to complete the propogation of one wave of body bends following touch. These experiments are conducted off food.
Wild-type animals on PMA (dotted blue line, n=12) paralyse faster than wild-type animals on the DMSO control plates (solid blue line, n=12). We see a similar increase in the response of *unc-80* mutants exposed to PMA (dotted orange line, n=5), which paralyse faster than the *unc-80* animals on the DMSO control plates (solid orange line, n=5).

By stimulating mutant animals with PMA we can test two things. First, if the overall activity of the nervous system is lowered by *unc-80* mutations, this should result in a

resistance to the effects of PMA. Secondly, as PMA is an analogue of DAG which acts downstream of nRHO-1 to promote release of neurotransmitter we can start to define the position the mutation with respect to other parts of the neurotransmitter release pathway.

The assay is a modified form of the aldicarb assay: animals are placed on plates containing either PMA or DMSO control, with food, for two hours preincubation. Worms are then picked to plates containing aldicarb and either PMA or DMSO, and assayed for paralysis.

When exposed to a combination of PMA and aldicarb, wild-type animals paralyse faster compared with control animals, (100±1% of animals paralysed at 50 minutes, compared to 49±8% of animals on control plates) (Figure 4-22). We observe a similar increase in the rate of paralysis in *unc-80* mutants exposed to PMA, with 100±0% of animals paralysed at 50 minutes exposure to PMA and aldicarb, compared with 61±25% of animals paralysed on the DMSO control plates (Figure 4-13).

This indicates an increase in the activity of the nervous system in *unc-80* animals as a result of PMA stimulation (Figure 4-22) in line with that seen for wild-type. This suggests that there is no gross reduction in nervous system activity, and that *unc-80* acts in a pathway upstream of or in parallel to PMA, and hence to diacylglycerol.

4.10 - Mutations in *unc-80* suppress the small body size of nRHO-1* animals

We noticed that the animals carrying the nRHO-1* transgene looked smaller than wild-type animals. Animals were staged by picking L4 animals, and then images were taken using the Micromanager add-on to the ImageJ software. Animals were measured from the tip of the head to the tip of the tail (with each animal being measured twice and the average taken).

nRHO-1* animals are significantly smaller than wild-type animals by about 20% (Figure 4-23). The reason for this size difference is unclear.

The double mutant *unc-80*;nRHO-1* animals, as well as having a more wild-type locomotion, also have a partially restored body size – with their head to tail measurements being intermediate between wild-type and nRHO-1* (Figure 4-23, and see Figures 4-6 and 4-9 for representative images taken at the same magnification.)

We have yet to test whether this phenotype is rescued by addition of the transgenes, although by eye the rescued animals appear smaller than animals not carrying the *unc-80* transgenes.

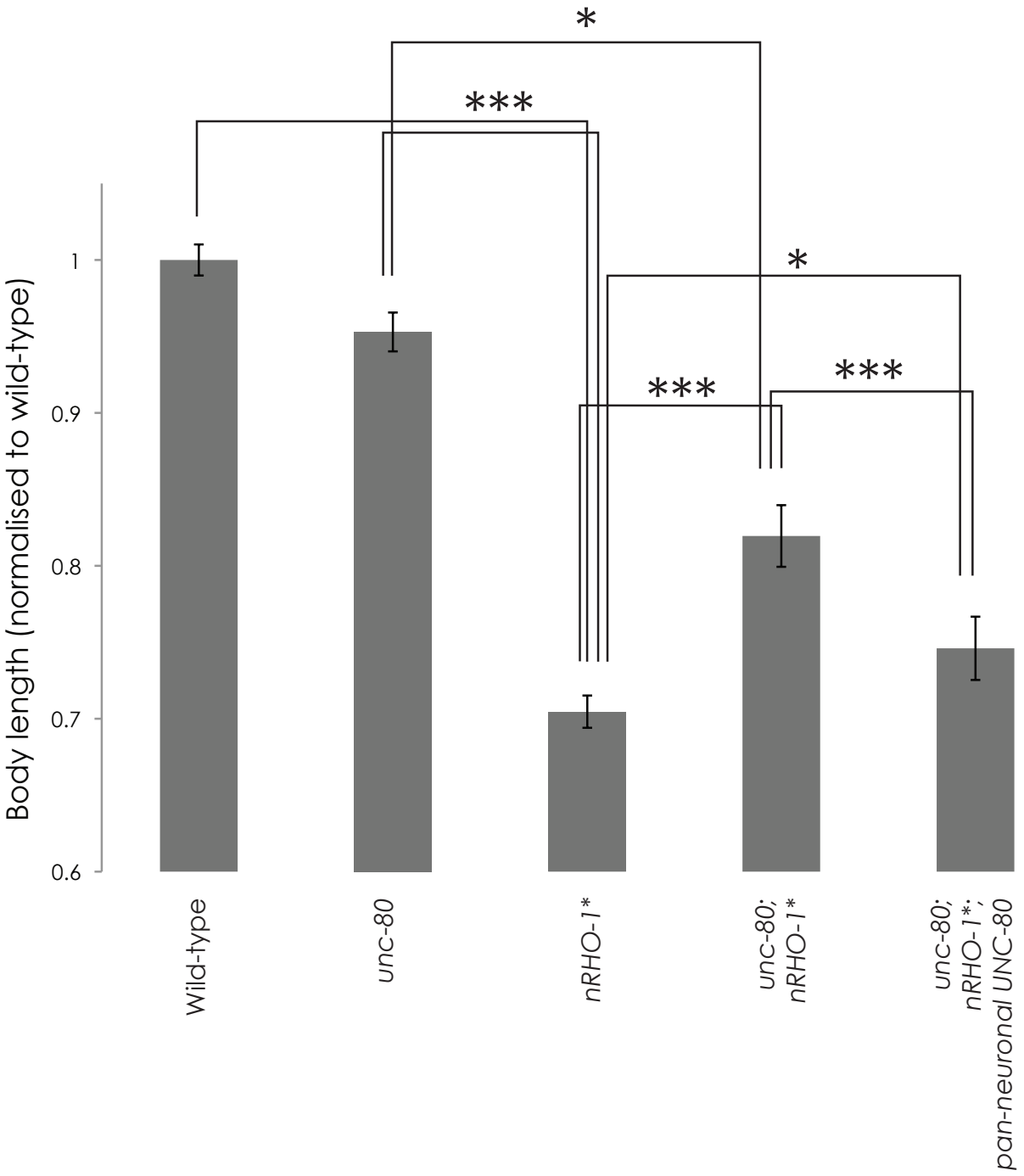

Figure 4-23 *unc-80* mutations suppress the small body size of nRHO-1* mutants

The length of animals was assayed from images captured using Micromanager and ImageJ. Two recordings were taken for each animal. nRHO-1* mutants are significantly smaller than wild-type animals or *unc-80* mutants, and this difference is partially suppressed in the *unc-80*;nRHO-1* double mutants. A pan-neuronal UNC-80 transgene under the control of the *snb-1* promoter partially rescues the suppression of small body size in a *unc-80*;nRHO-1* double mutant animal. Error bars indicate standard errors of the mean. Numbers in brackets indicate number of animals observed. (Significance assessed using a 2-tailed T-test. * = $p<0.05$, *** = $p<0.001$)

4.11 - Defecation assays

unc-80 mutants exhibit fainting locomotion on a solid surface, and have reduced thrashes in liquid, although they are capable of both swimming and crawling during short bursts of activity. The propogation of movement is a rhythmic behaviour, and we speculated that they might show defects in other regulated behaviours, such as defecation.

We tested the animals for any potential defects in defecation, which is a tightly controlled cycle lasting about 50 seconds in a well-fed adult animal (Avery 1997). About 50 genes are known to play a role either in the length of the defecation cycle or in controlling its frequency, and around 20 of these act in the intestine itself (Branicky and Hekimi 2006).

The Defecation Motor Program (DMP) consists of three stages which occur over the course of approximately 5 seconds: a posterior body contraction (pBoc), an anterior body contraction (aBoc), and expulsion of the gut contents (Exp). The expulsion step is the only one that requires neuronal function. It is regulated by GABA acting in an excitatory fashion (Beg and Jorgensen 2003). These steps reoccur with approximately 45 second of pause in between.

4.11.1 -unc-80 mutants have a mildly disrupted defecation cycle.

In the assays conducted here, in wild-type animals the pBoc occurs every 59±5 seconds, while the Exp step occurs every 62±13 seconds, slightly longer intervals than the recorded average (Figure 4-24).

unc-80 mutants display a slight increase in the length and variability of their defecation cycle, with pBoc occurring every 65±13 seconds, and Exp every 71±21 seconds (Figure 4-24). This suggests that UNC-80 has a small role in the defecation motor program, particularly in the step involving the release of GABA. A future experiment would be to test our animals rescued with UNC-80 expressed pan-neuronally to see if they recover from this defect.

4.11.2 -nRHO-1* mutants display a defect in defecation

nRHO-1* mutant animals were also assayed for their defecation cycle. We observed that they displayed fewer Exp steps than wild-type animals, resulting in an increase in the average interval between these steps from 62±13 seconds in wild-type to 104±30 seconds in nRHO-1* mutants (Figure 4-24). This is a previously unreported phenotype for these animals. Their pBoc cycles also become highly variable, occurring on average every 49 seconds, but with a standard error of the mean of 36 seconds.

*4.11.3 -unc-80;*nRHO-1* mutants have increased defecation cycle length compared to *unc-80* mutant animals

There is a significant increase in the length of defecation cycles to 96±11 seconds for the pBoc and 103±13 seconds for the Exp steps (Figure 4-24). The Exp phenotype is very similar to that of the nRHO-1* single mutants, suggesting that the mutation has no effect on this nRHO-1* phenotype.

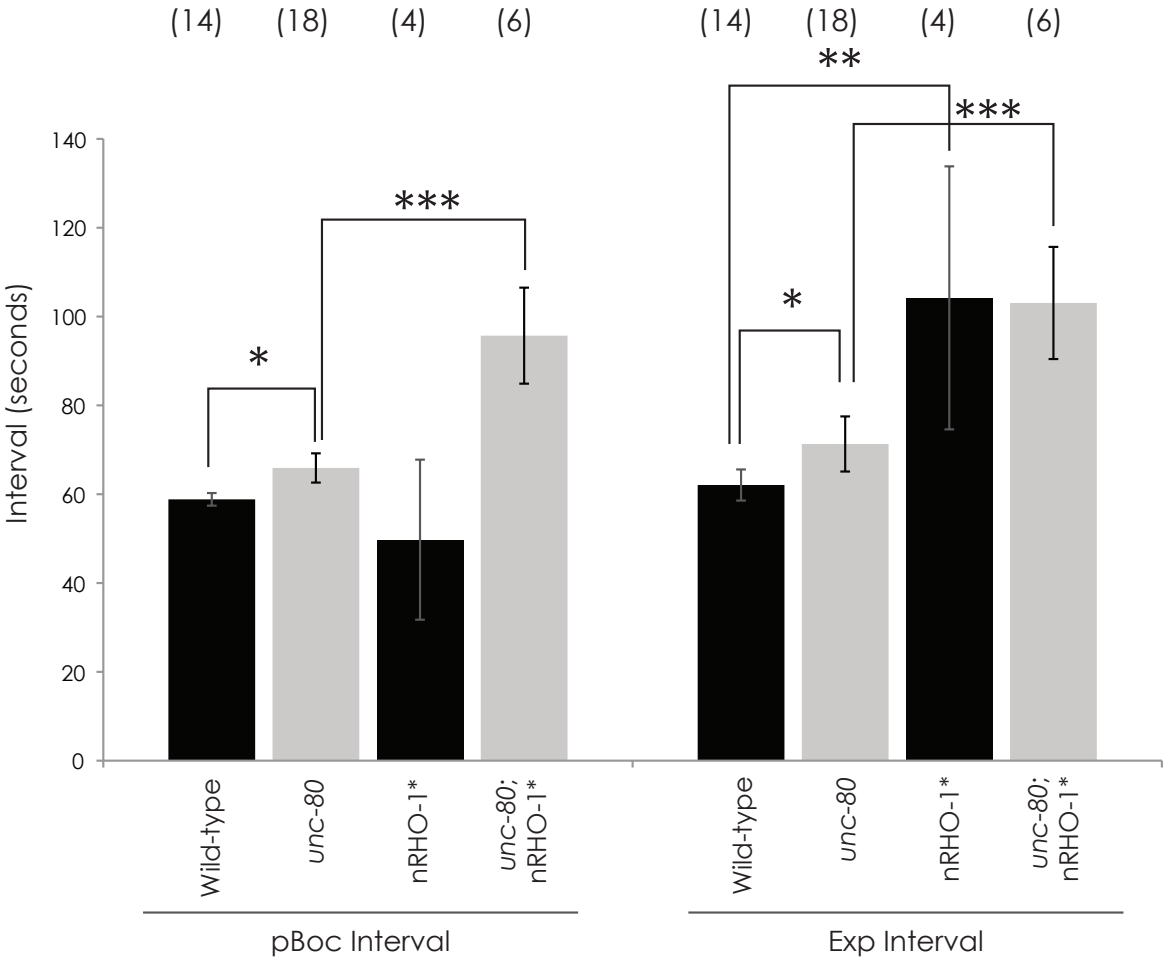

Figure 4-24 Defecation assay of *unc-80* and nRHO-1* mutants

Animals were observed for periods of 5 minutes, during which each pBoc and Exp was recorded using the program EthoTimer. Average intervals for each step were obtained for each mutant, with the overall average being plotted here.
unc-80 animals display a lengthening of their defecation cycle compared to wild-type animals. nRHO-1* mutants display a defect in the frequency of Exp steps compared to wild-type.
Error bars indicate standard errors of the mean. Numbers in brackets indicate number of animals observed. (Significance assessed using a 2-tailed T-test. * = $p<0.05$ ** = $p<0.01$ *** = $p<0.001$)

4.12 - The F25N mutation in RHO-1 bypasses the suppressive effects of loss of UNC-80 with respect to loopy locomotion

Through the screen we were aiming to identify proteins which acted downstream of RHO-1* in neurotransmitter release. We knew from the experiment with *dgk-1* mutants expressing C3 transferase (McMullan, Hiley et al. 2006) that there must be additional targets of RHO-1, as inhibition of RHO-1 still reduces the level of neurotransmitter release in this mutant background (McMullan, Hiley et al. 2006).

As demonstrated earlier in this chapter *unc-80* mutations have very little effect on the neurotransmitter release phenotype of nRHO-1*, but completely suppress the loopy locomotion phenotype. We considered that *unc-80* acted in parallel with *dgk-1* with respect to acetylcholine release. Therefore, to block the ability of nRHO-1* to increase acetylcholine release we sought to block both the *unc-80* and *dgk-1* pathways.

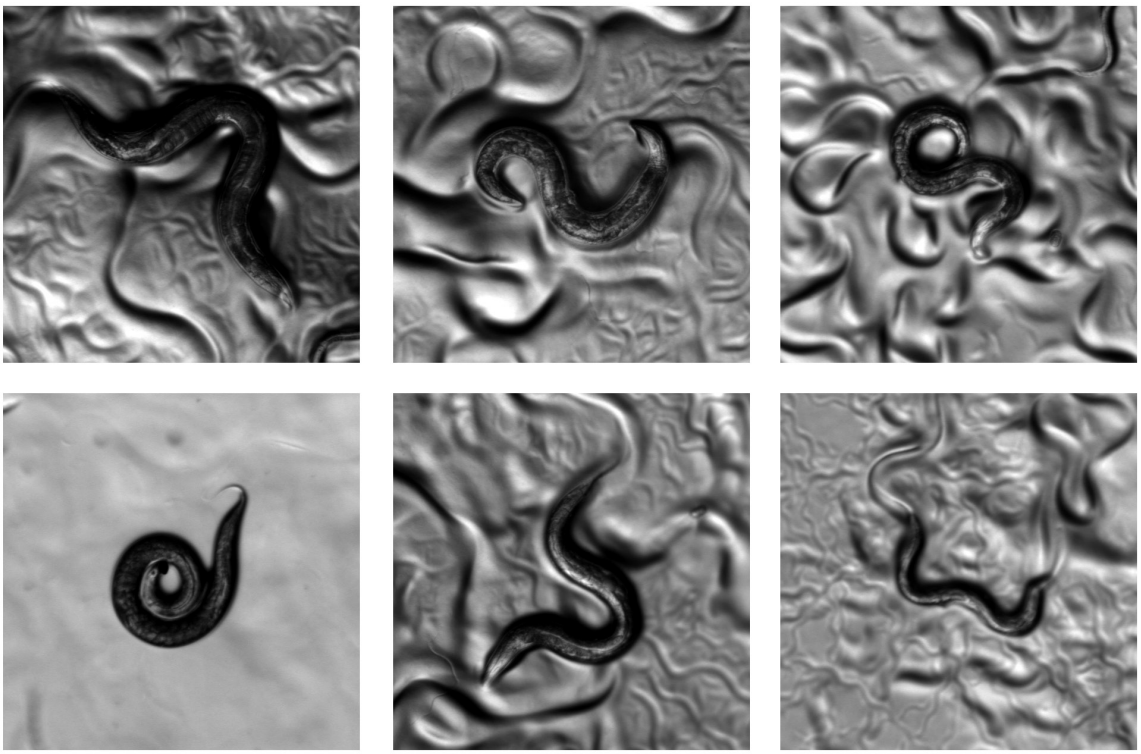

Figure 4-25 *unc-80*;nRHO-1(F25N)* double mutants are loopy

unc-80 animals were injected with plasmid RJM39 at a concentration of 1ng/µl. One transformed line, Line 6, produced loopy animals. This line was very unstable, and lost expression of the co-injection marker after three or four generations. These images were taken of F2 generation animals carrying the *unc-17*::GFP co-injection marker.

To test this, we made use of an additional RHO-1 mutant which carries the mutation F25N along with G14V. This mutation was isolated by Alan Hall, and is common in many

constructs containing the human homologue, RhoA, where it is used to increase the stability of transgenic RhoA protein when expressed in bacteria.

Another effect of this mutation, however, is to significantly reduce the interaction between RHO-1 and DGK-1 (McMullan, Hiley et al. 2006). It has been speculated that the wide-spread use of this point mutation might have led to additional RHO-1/RhoA pathways being overlooked (McMullan and Nurrish 2007).

The RHO-1(G14V F25N) construct, under either the heatshock or *unc-17* promoter, is able to increase levels of neurotransmitter release, although to a lower level than the RHO-1(G14V) construct (McMullan, Hiley et al. 2006). Constructs carrying the F25N point mutation still cause the animals to become highly uncoordinated and loopy, demonstrating that the *dgk-1*-independent pathway is able to drive behavioural changes in a similar way to the *dgk-1*-dependent pathway.

As the *dgk-1*-dependent pathway is important for increasing levels of neurotransmitter release, and the pathway incorporating is necessary for loopy locomotion, we wanted to examine the phenotype of an *unc-80*;nRHO-1(F25N)* mutant, to see whether both the locomotion and the neurotransmitter release pathways activated by RHO-1 would be suppressed.

4.12.1 -Neuronal expression of RHO-1(G14V F25N) in an *unc-80* mutant causes loopy locomotion

We injected plasmid RJM39, carrying RHO-1(G14V F25N) under control of the *unc-17* promoter, directly into *unc-80* mutants, along with *unc-17*::GFP as a co-injection marker. RJM39, as with all RHO-1 constructs we have used, can cause pathfinding defects and even death in animals misexpressing the construct.

RJM39 constructs tend to create rather unstable extrachromosomal arrays (R. McMullan, personal communication.) We have not been able to maintain stable lines expressing this construct.

However, we were able to sustain one or two generations of animals carrying the nRHO-1(F25N)* construct. These animals clearly became loopy in comparison to untransformed animals (Figure 4-25).

4.12.2 -The loopy phenotype of *unc-80*;nRHO-1(F25N)* animals is not associated with pathfinding defects

We had coinjected an *unc-17*::gfp construct which allowed us to check for pathfinding defects, which are a possible cause of uncoordinated locomotion. In the animals which demonstrated a loopy phenotype, we could not see any gross changes in the morphology of the nervous system which might explain the changes.

4.12.3 -Heatshock expression of RHO-1(G14V F25N) in an *unc-80* mutant causes loopy locomotion

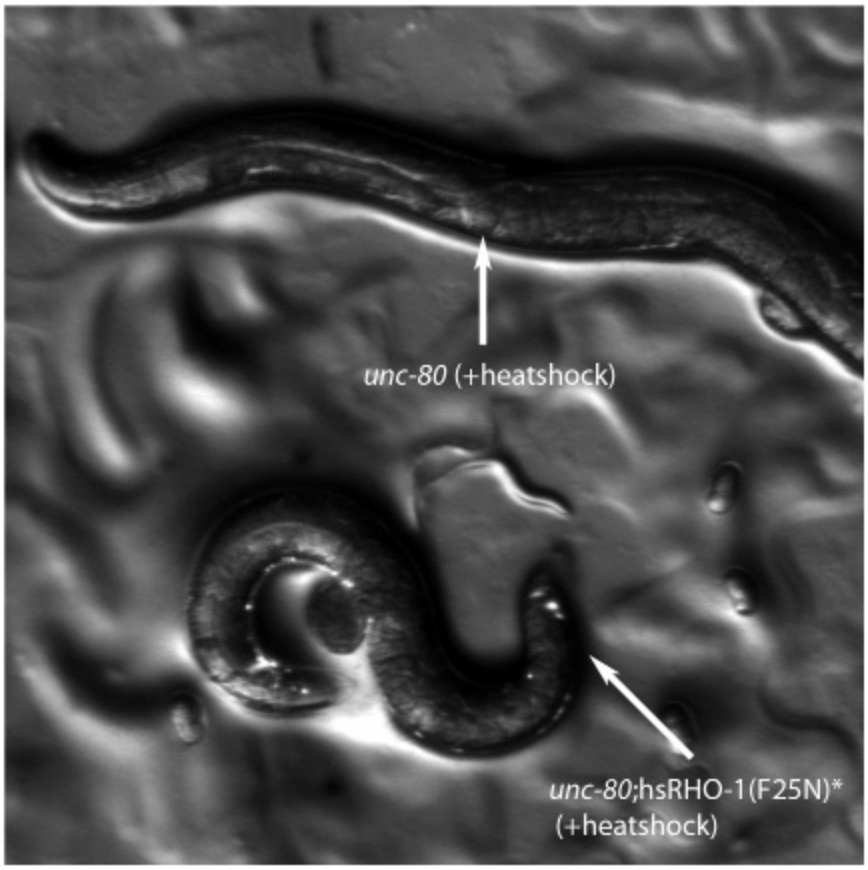

Figure 4-26 *unc-80*;hsRHO-1(F25N)* double mutants are loopy

unc-80 animals carrying the hsRHO-1(F25N)* transgene become loopy following heatshock, unlike *unc-80* mutant animals, which are unaffected by heatshock, or *unc-80*;hsRHO-1* mutant animals. This image was taken with the UV light switched on, showing the *unc-17*::GFP marker. *unc-80* animals not carrying the marker do not become loopy following heatshock.

We crossed *unc-80* mutants with a previously generated RHO-1(G14V F25N) heatshock-inducible line (hsRHO-1(F25N)*). This construct is not integrated, so by looking for animals which lack the coinjection marker we can control for the effects of heatshock on the *unc-80* mutant background.

The double mutant *unc-80*;hsRHO-1(F25N)* is non-loopy and appears fainter prior to heatshock. Following heatshock, the animals carrying the RHO-1 array become highly loopy within a period of four hours (Figure 4-26). Animals not carrying the RHO-1 construct remain non-loopy (Figure 4-26). This is in marked contrast to unc-80 animals upon heatshock activation of RHO-1*, which do not become loopy.

We grew the worms are at 15°C, to reduce unwanted activity of the heatshock transgene. When adult animals which are non-loopy are subjected to heatshock, they develop loopy locomotion, demonstrating that this effect occurs in developed animals.

4.12.4 -unc-80 mutants do not suppress the additional phenotypes of hsRHO-1(F25N)*

When *unc-80*;hsRHO-1(F25N)* animals are subjected to heatshock, we see that after 4 days of growth there are no progeny from the heatshocked animals. The sterile adults develop the *dar* phenotype associated with hsRHO-1* expression.

This demonstrates that UNC-80 is not required for the non-neuronal functions of RHO-1 which manifest even with the F25N mutation.

4.12.5 -unc-80 mutations do not suppress the increase in aldicarb sensitivity caused by activation of the hsRHO-1(F25N)* transgene

Wild-type animals carrying the hsRHO-1(F25N)* transgene become hypersensitive to aldicarb following heatshock (Figure 4-27, Table 4-3). *unc-80* mutants carrying this transgene also become hypersensitive to aldicarb following heatshock (Figure 4-27, Table 4-3)

Activation of the hsRHO-1(F25N)* transgene in an unc-80 mutant background induces slightly less hypersensitivity to aldicarb than in a wild-type background, in a situation which appears analagous to that seen in Figure 4-16, where *unc-80* mutants partially suppress the aldicarb sensitivity induced by the nRHO-1* transgene, although this difference is not stastically significant ($p>0.05$)..

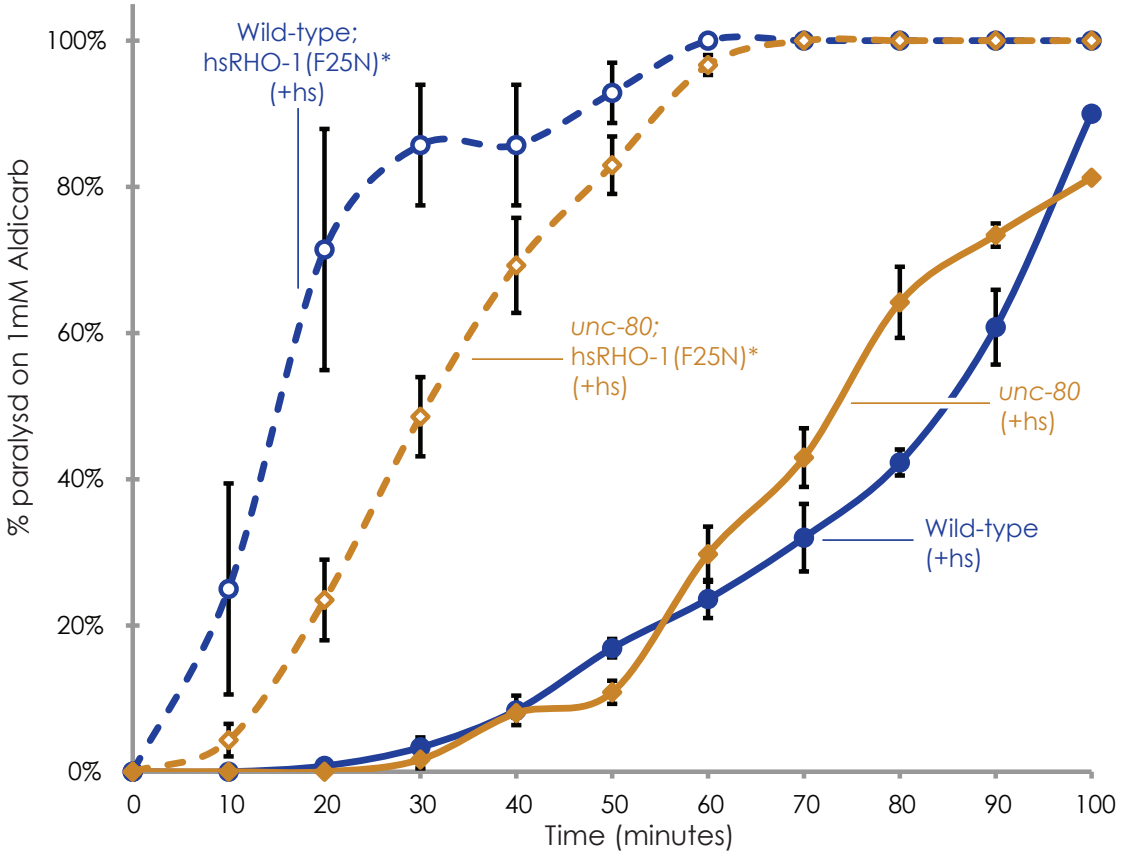

Figure 4-27 hsRHO-1(F25N)* increases sensitivity to aldicarb

unc-80 animals carrying the hsRHO-1(F25N)* transgene become hypersensitive to aldicarb following heatshock (orange dotted line, n=6) compared to *unc-80* animals without the transgene (solid orange line, n=5). Wild-type animals expressing the hsRHO-1(F25N)* transgene also become hypersensitive to aldicarb following heatshock (dotted blue line, n=3) compared with animals not carrying the transgene (n=5).

Percentage of animals paralysed at 50 minutes on 1mM aldicarb

	Locus 2	
Locus 1	***without hsRHO(F25N)* transgene***	***with hsRHO(F25N)* transgene***
Wild-type (+heatshock)	17 ± 1.3, n=6	93 ± 4.1, n=3, p<0.0001
***unc-80* (+heatshock)**	11 ± 1.6, n=5	83 ± 3.9, n=6, p<0.0001

Table 4-3 Statistical analysis of aldicarb data at 50 minute time point

Analysis of effect of activation of the hsRHO(F25N)* transgene summarised here with statistics derived from the 50 minute time-point data. Statistics conducted using a 2-tailed unpaired T-Test.

4.12.6 -Heatshock expression of RHO-1(G14V F25N) in an *unc-80*;nRHO-1* mutant causes loopy locomotion

When RHO-1 is wildtype at residue 25 (nRHO-1*), its ability to generate loopy locomotion is impaired by loss of *unc-80*. When the F25N mutation is introduced into RHO-1, this somehow bypasses the requirement for UNC-80 in developing loopy locomotion phenotype.

Here I consider three potential explanations (see Figure 5-26).

i) The F25N mutation reduces signalling to a RHO-1 effector. Loss of signalling to this effector bypasses the requirement for *unc-80* in the generation of loopy locomotion.

ii) The F25N mutation is able to signal to a new effector, one which is not a target of F255 RHO-1* and this is independently able to generate loopy locomotion in the absence of UNC-80 function.

iii) The F25N mutation reduces signalling to a RHO-1 effector, allowing additional RHO-1 signalling through the remaining pathways. This extra signalling is able to generate loopy locomotion in the absence of *unc-80*.

To partially distinguish between these hypotheses, we generated an animal carrying both the nRHO-1*construct (expressed from the *unc-17* promoter) and RHO-1*(F25N) under the heatshock promoter, in an *unc-80* background.

Prior to heatshock, these animals are non-loopy - the loss of *unc-80* suppresses the loopy phenotype of nRHO-1*, as previously observed. These animals are grown at 15^{o}C to avoid unwanted activation of the hsRHO-1*(F25N) transgene.

Upon heatshock, the animals become highly loopy and uncoordinated in the same manner as the *unc-80*;nRHO-1*(F25N) animals.

This result appears to rule out hypothesis (i). If the F25N mutation were to reduce signalling to an effector of RHO-1*, and this loss of signalling was able to bypass the requirement for in loopy locomotion, then the expression of RHO-1* in the cholinergic motor neurons should negate this effect and restore non-loopy locomotion.

We cannot yet distinguish between the remaining hypotheses (ii) and (iii), as both are consistent with the results observed here.

4.13 - Discussion

nz94 is a mutant able to suppress the loopy phenotype of nRHO-1*. This mutant was discovered to have an additional fainting locomotion, which helped us identify it as an allele of the large, conserved gene *unc-80* (Figure 4-4). We subsequently found that an additional *unc-80* mutation was also able to suppress this loopy locomotion phenotype (Figure 4-5), and successfully rescued this with transgenes expressed either pan-neuronally or in the cholinergic neurons, where the nRHO-1* transgene is expressed (Figure 4-9).

Two other classes of mutations - in the large, conserved protein *unc-79*, and in the double mutant *nca-1;nca-2* - also generate a fainting locomotion. These proteins are thought to form part of a novel neuronal complex.

The relationship between *unc-79, nca-1* and *nca-2* and the nRHO-1* transgene will be assessed in the following chapter, after which I will discuss in detail the results from both sets of experiments, as we believe that these proteins are connected by a common pathway.

5 - THE NCA-1/NCA-2/UNC-79 ION CHANNEL COMPLEX IS REQUIRED FOR THE LOOPY LOCOMOTION PHENOTYPE OF NRHO-1* ANIMALS

5.1 - Introduction

Following our discovery that mutations in *unc-80* are sufficient to suppress the loopy phenotype of nRHO-1* animals, we next explored the potential for other mutations associated with *unc-80* to interact with our nRHO-1* mutant animals.

unc-80 and *unc-79* share a common fainter phenotype (Pierce-Shimomura, Chen et al. 2008; Yeh, Ng et al. 2008), where periods of normal locomotion are interrupted by extended periods of inactivity.

Early reports that *unc-80* mutants were hypersensitive to the general anaesthetic halothane demonstrated that *unc-79* mutants were similarly hypersensitive, and that the double mutant was only slightly more sensitive than either single mutant (Sedensky and Meneely 1987; Morgan, Sedensky et al. 1988). Hypersensitivity of both mutants to halothane is suppressed by mutations in *unc-1* (Morgan, Sedensky et al. 1990), a stomatin which forms part of gap junctions - direct electrical couplings between muscles cells and cells of the nervous system. This is suggestive of proteins which act in a common pathway.

The UNC-79 and UNC-80 proteins do not share any significant homology to each other. *unc-79* (Figure 5-1, A) is a large gene, with a predicted 2092 amino acids in its largest splice form, and is conserved from nematodes to mammals, although it does not contain any domains of known function, aside from a predicted armadillo repeat domain structure (Pierce-Shimomura, Chen et al. 2008), which is also predicted for *unc-80*.

The fainting phenotype has been reported for only one other class of mutants, the double mutant *nca-1*;*nca-2*. A number of mutations have been identified for both of these proteins (Figure 5-1, B and C).

The novel ion channel NCA-1 (also called UNC-77), and its homologue, NCA-2, are the *C. elegans* homologues of the 24-transmembrane-spanning mammalian ion channel NALCN (Jospin, Watanabe et al. 2007; Yeh, Ng et al. 2008), part of the protein family which includes voltage-gated sodium and calcium channels (Yu, Yarov-Yarovoy et al. 2005; Snutch and Monteil 2007).

This ion channel and its *C. elegans* homologues are unusual in that the S4 transmembrane segments lack some of the charge residues (K and R) found at every third position in the S4s of the voltage-gated sodium, calcium and potassium channels which make up the rest of the family. In addition, its selectivity filter contains a novel EEKE motif, a mixture between the EEEE found in the voltage-gated calcium channels and the DEKA motif of voltage-gated sodium channels (Lee, Daud et al. 1999). These changes make NALCN permeable to calcium, potassium and sodium ions. It appears to be a voltage-independent channel (Lu, Su et al. 2007).

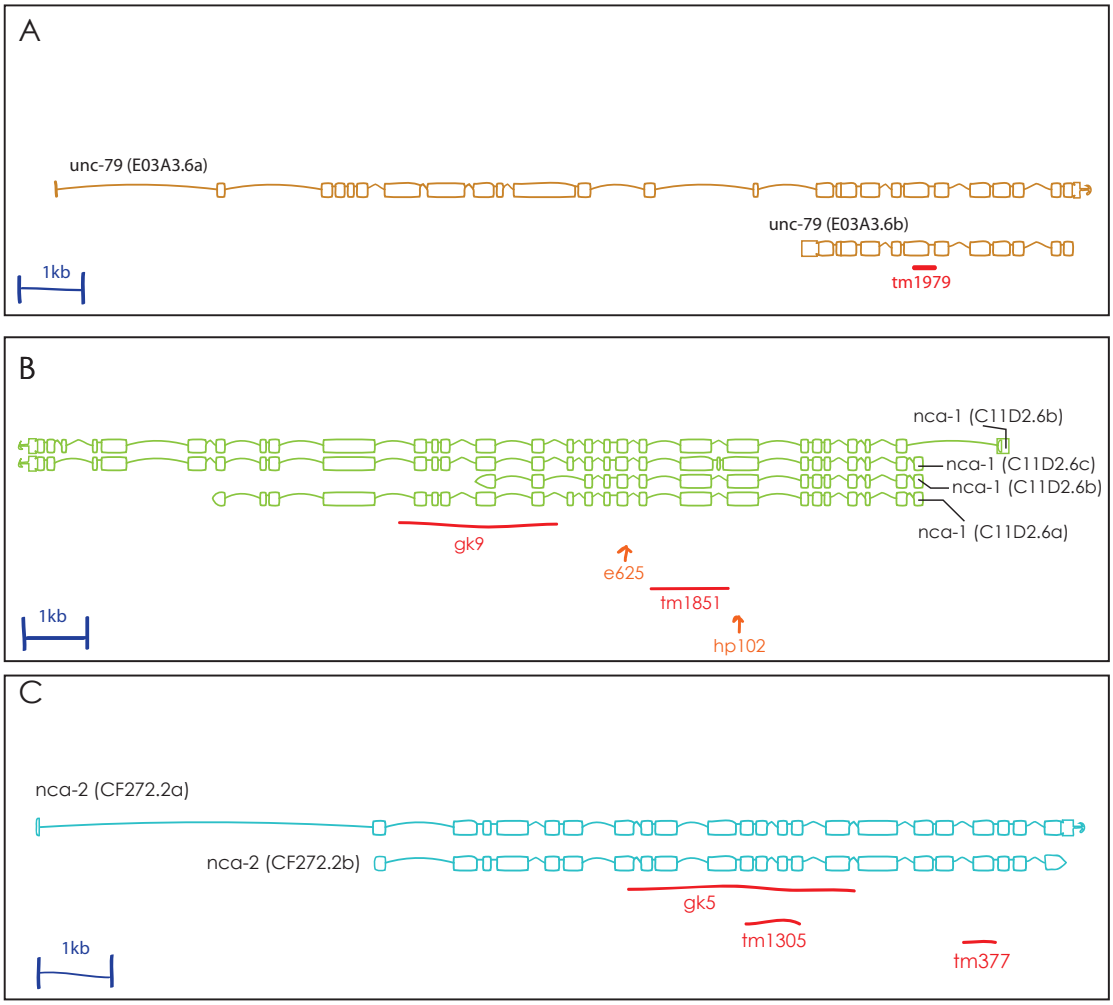

Figure 5-1 Gene models of *unc-79, nca-1* and *nca-2*

Alongside *unc-80* two other sets of mutations are known to generate fainting locomotion. These are mutations in the large conserved protein *unc-79* (A), and the double mutant of *nca-1* (B) and *nca-2* (C), which code for the *C. elegans* orthologues of the mammalian NALCN ion channel. Scale bars indicate 1kb. Deletions are highlighted in red, known point mutations in orange. The molecular nature of an additional *unc-79* mutation, e1068, has not yet been determined. (Data obtained from Wormbase).

In *C. elegans*, UNC-79, NCA-1, NCA-2 and UNC-80 staining is extrasynaptic, and does not colocalise with synaptic markers such as synaptobrevin (Yeh, Ng et al. 2008). Loss of UNC-80 or UNC-79 protein leads to a loss of NCA-1 punctate staining in the nerve

cord (Yeh, Ng et al. 2008). This suggests that UNC-79 and UNC-80 somehow regulate the localisation of NCA-1. Interestingly, loss of NCA-1 protein also leads to a diffuse rather than punctate staining for UNC-80 and UNC-79 (Yeh, Ng et al. 2008), suggesting that all these proteins are all dependent on one another for their localisation.

Loss of UNC-79, UNC-80 or the ion channel proteins themselves generates the same phenotypes – fainting behaviour and altered anaesthetic sensitivity. Having seen that loss of UNC-80 is able to suppress the loopy locomotion of nRHO-1* mutants, we therefore decided to test whether loss of UNC-79, NCA-1 or NCA-2 were also able to suppress this phenotype. For these experiments we made use of the following alleles - *unc-79* (*e1068*), *nca-1* (*gk9*) and *nca-2* (*gk5*). While the *e1068* mutation is the cannonical allele for *unc-79*, its molecular nature is undetermined. The *gk9* and *gk5* alleles are both large deletions in the *nca-1* and *nca-2* genes (Figure 5-1).

5.2 - Fainter mutant animals display a swimming defect

While fainting locomotion on a solid surface is difficult to quantify, we found that studying the behaviour of *unc-80* mutants in liquid was much easier to quantify (Chapter 4). We used two distinct assays for analysing *unc-80* mutants. In the first, the 'Mean thrashes per minute' assay, we allowed worms to recover for three minutes after immersion in M9, then counted the number of thrashes over a two minute period. *unc-80* fainter mutants thrash less than wild-type animals in this assay (Figure 4-13).

The second test involves placing an animal in a drop of M9, and recording whether it completes two body bends in the first 5 seconds following immersion. *unc-80* animals display a defect in this initial thrashing assay (Figure 4-15).

We therefore decided to test whether these results are replicated with the other mutants under investigation in this chapter.

5.2.1 - unc-79 mutants exhibit a swimming defect on initial immersion and following recovery in M9

On a solid surface, *unc-79* mutants move with a fainting locomotion (Sedensky and Meneely 1987). In line with our experiments conducted on *unc-80* mutants and previously published data on the swimming efficiency of these animals (Pierce-Shimomura, Chen et al. 2008), we assayed the response of *unc-79* mutants to immersion in M9. When initially placed in liquid, just 10±2% of *unc-79* animals thrash in the first 5 seconds of immersion, compared with 82±6% of wild-type animals (Figure 5-2, A).

When assayed over two minutes, having been allowed to recover for 3 minutes, *unc-79* animals thrash significantly less than wild-type animal (Figure 5-2, B).

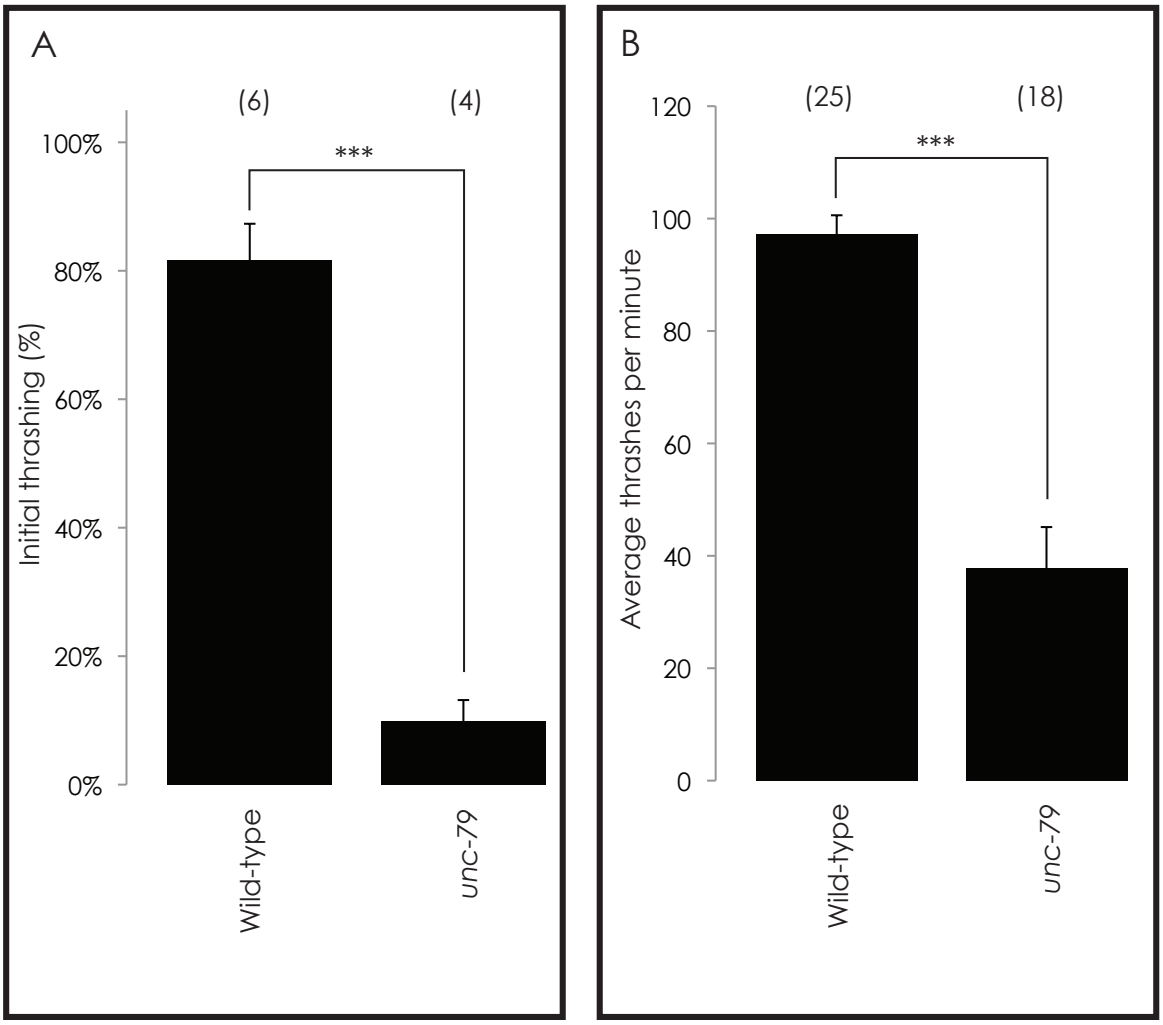

Figure 5-2 Swimming assays of *unc-79* mutants

We assayed the behaviour of *unc-79* animals in liquid using two distinct assays. A) Initial thrashing assay. Animals were placed in a drop of M9, and assayed for thrashing behaviour for 5 seconds after immersion. *unc-79* animals thrash significantly less often than wild-type animals in this assay. Each repeat consists of measuring the response of at least 15 animals. B) Mean thrashes per minute. Animals were allowed to recover for 3 minutes following immersion in M9, and then the total number of thrashes counted for two minutes. *unc-79* exhibit fewer thrashes per minute than wild-type animals.
Error bars indicate standard errors of the mean. Numbers in brackets indicate number of animals observed. (Significance assessed using a 2-tailed T-test. *** = $p<0.001$)

These assays indicate that while initally inert following immersion in M9, by three minutes *unc-79* mutants have begun to thrash, although this rate of thrashing is below that seen in wild-type animals.

5.2.2 - *nca-1* mutants are wild-type in their swimming behaviour

In the majority of assays reported so far (Jospin, Watanabe et al. 2007; Pierce-Shimomura, Chen et al. 2008; Yeh, Ng et al. 2008), *nca-1* appears to act redundantly with *nca-2* and thus *nca-1* single mutants appear to be wild-type in their behaviour. In our swimming assay, there was no significant difference in the rate of thrashing of *nca-1* mutant animals compared with wild-type animals (Figure 5-3).

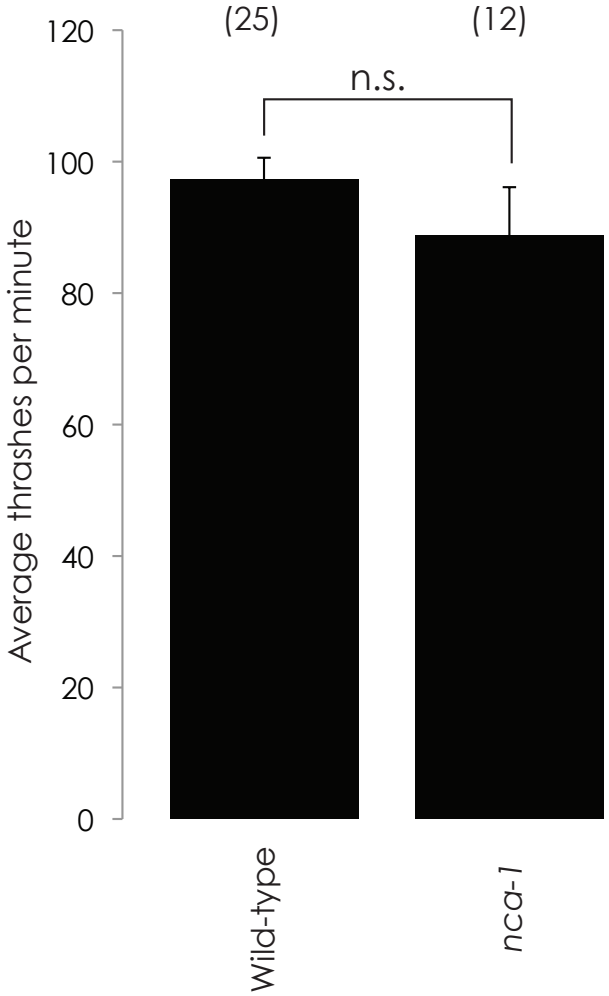

Figure 5-3 Swimming assays of *nca-1* single mutants

Animals were assayed for total thrashes after 3 minutes of recovery in M9. *nca-1* single mutant animals exhibit no significant difference in their number of thrashes compared to wild-type animals. Error bars indicate standard errors of the mean. Numbers in brackets indicate number of animals observed. (Significance assessed using a 2-tailed T-test. n.s. = not significant)

5.2.3 - *nca-1;nca-2* double mutants exhibit swimming defects

nca-1 and *nca-2* mutants are highly homologous (Figure 5-6), and the loss of both genes is required for the establishment of the fainting phenotype. We generated double

mutant animals through crossing *nca-1* (VC12) animals with *nca-2* (VC9). Each strain naturally produces a low incidence of male animals, which we used for these crosses. The resulting strain, QT961, has a fainting phenotype on solid surfaces (Movie 5-1).

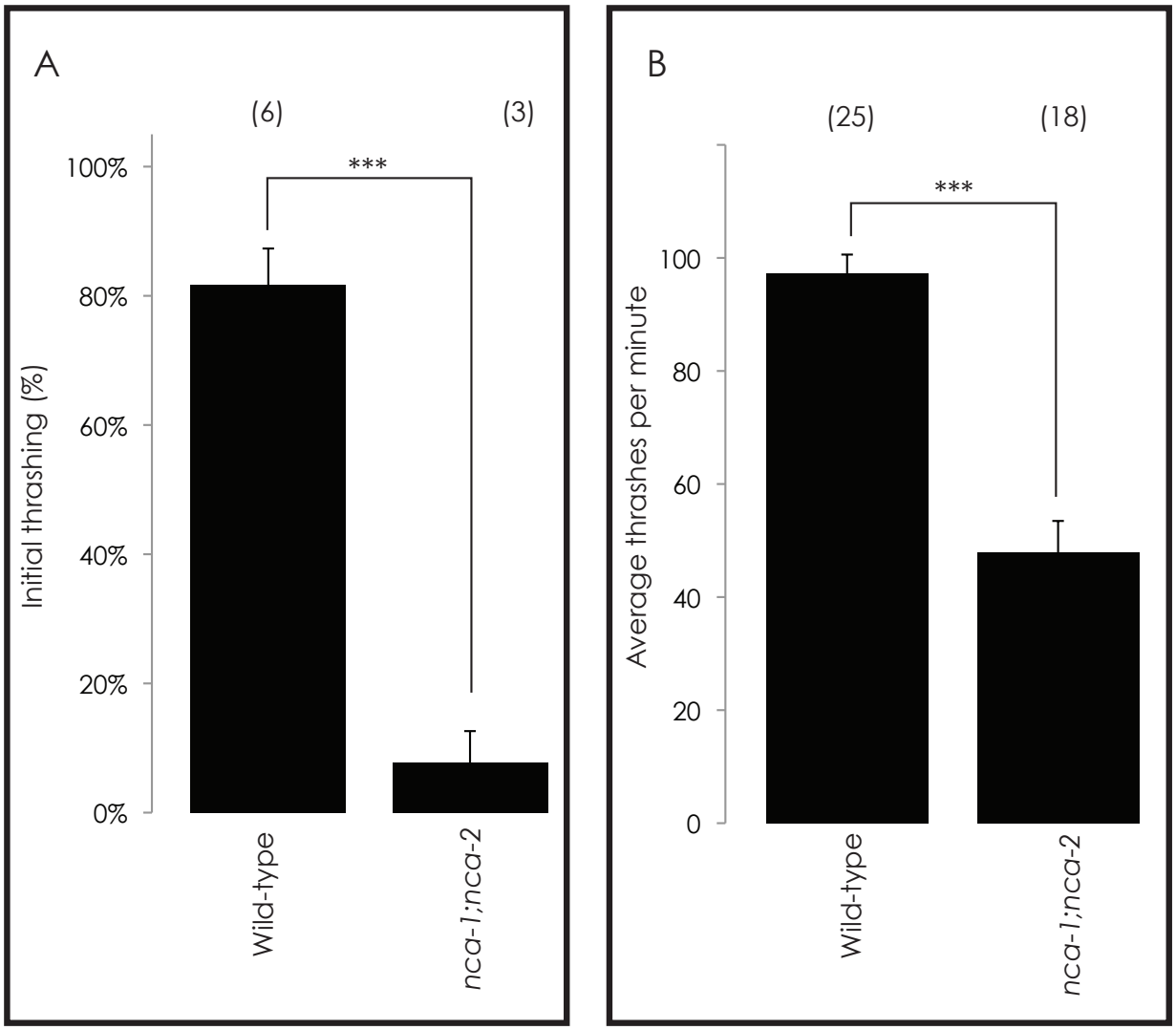

Figure 5-4 Swimming assays of *nca-1;nca-2* mutants

We assayed the behaviour of *nca-1*;*nca-2* mutants in liquid using two assays. A) Animals were placed in a drop of M9, and assayed for thrashing behaviour for 5 seconds after immersion. *nca-1*;*nca-2* double mutant animals thrash significantly less often than wild-type animals in this assay. B) Animals were assayed for total thrashes after 3 minutes of recovery in M9. *nca-1*;*nca-2* animals have significantly fewer thrashes per minute than wild-type animals.
Error bars indicate standard errors of the mean. Numbers in brackets indicate number of repeats (A) and number of animals observed (B). (Significance assessed using a 2-tailed T-test. *** = $p<0.001$)

When initially immersed in liquid, the *nca-1*;*nca-2* double mutants fail to thrash (Figure 5-4, A), while their mean thrashing rate after three minutes recovery is significantly reduced compared to wild-type animals (Figure 5-4, B).

5.3 - Loss of UNC-79 function is sufficient to suppress the loopy locomotion phenotype of nRHO-1* animals

To test whether a loss-of-function mutant of *unc-79* might be able to suppress the loopy locomotion phenotype of nRHO-1* mutants in the same way as loss-of-function mutations in *unc-80*, we constructed a double mutant between CB1068, carrying *e1068*, the canonical *unc-79* mutation, and QT733, a line carrying *nzIs29*, the integrated nRHO-1* transgene with unc-122::GFP marker. The molecular nature of the *e1068* mutation is unknown.

In the F2 generation we found non-loopy animals carrying the nRHO-1* transgene marker of unc-122::GFP (Figure 5-5, C). These animals also display the *unc-79* fainting locomotion, indicating that while the *unc-79* mutation suppresses loopy locomotion, the nRHO-1* transgene has no apparent effect on the fainting behaviour.

This demonstrates that UNC-79 is required for the propagation of the loopy locomotion phenotype associated with over-expression of gain-of-function RHO-1 expressed in the cholinergic neurons of *C. elegans*.

5.4 - Loss of NCA-1 function is sufficient to suppress the loopy phenotype of nRHO-1* animals

In the literature, *nca-1* and *nca-2* single mutants are reported to be essentially wild-type (Yeh, Ng et al. 2008). It requires the double mutant *nca-1*;*nca-2* for animals to display the fainting locomotion associated with *unc-79* and *unc-80* mutants.

NCA-1 and NCA-2 are highly homologues (58%, alignment using Clustal online tools, Figure 5-6) and the loss of one appears to be compensated for by the presence of the other with respect to locomotion and general anaesthetic sensitivity phenotypes (Humphrey, Hamming et al. 2007). There are some reports of a very subtle fainter phenotype in the single mutants, observed through detailed analysis of locomotion using computer vision processing (Pierce-Shimomura, Chen et al. 2008), but generally these mutants are considered to be wild-type.

We crossed strain VC12, which carries a deletion in *nca-1*, with strain QT733, which carries the nRHO-1* transgene. In the F2 generation we found animals which were non-loopy but carried the nRHO-1* unc-122::gfp marker, demonstrating that the single mutation in *nca-1* is sufficient to suppress the loopy phenotype of nRHO-1* (Figure 5-5, D). These animals do not throw any loopy animals, demonstrating that these are homozygous for the both the *nca-1* mutation and the nRHO-1* transgene. The double

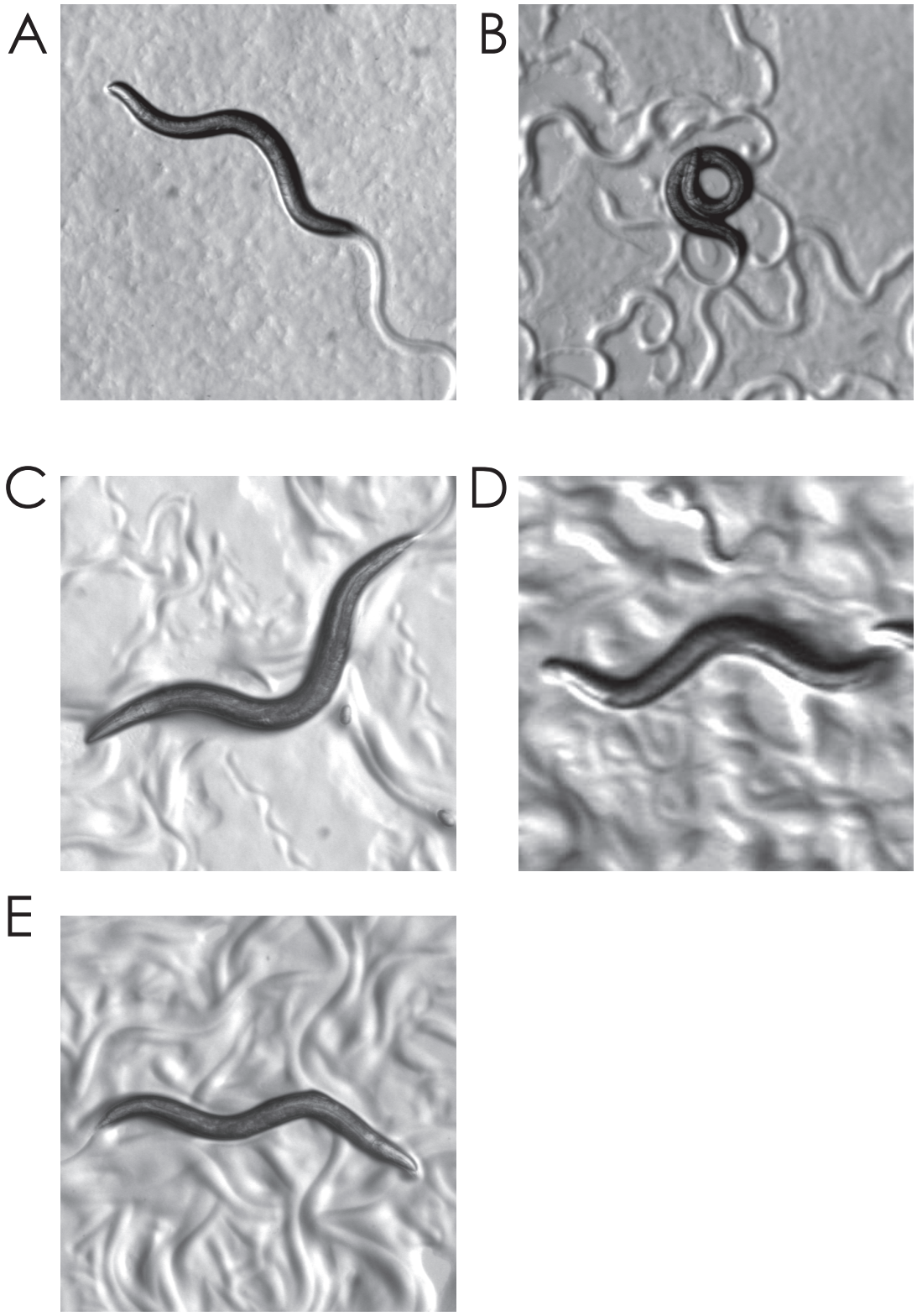

Figure 5-5 Mutations in *unc-79, nca-1* and *nca-2* suppress the loopy phenotype of the nRHO-1* transgene

nRHO-1* mutants are highly loopy (B), compared with wild-type (A). Double mutants *unc-79*;nRHO-1* (C), *nca-1*;nRHO-1* (D) and *nca-2*;nRHO-1* (E) are all non-loopy, demonstrating that loss-of-functon of *unc-79*, *nca-1* or *nca-2* is able to suppress the loopy phenotype associated with nRHO-1*.

mutant animals do not exhibit fainting locomotion on a solid surface. This is the first report of a strong phenotype associated with a loss-of-function mutation of this gene.

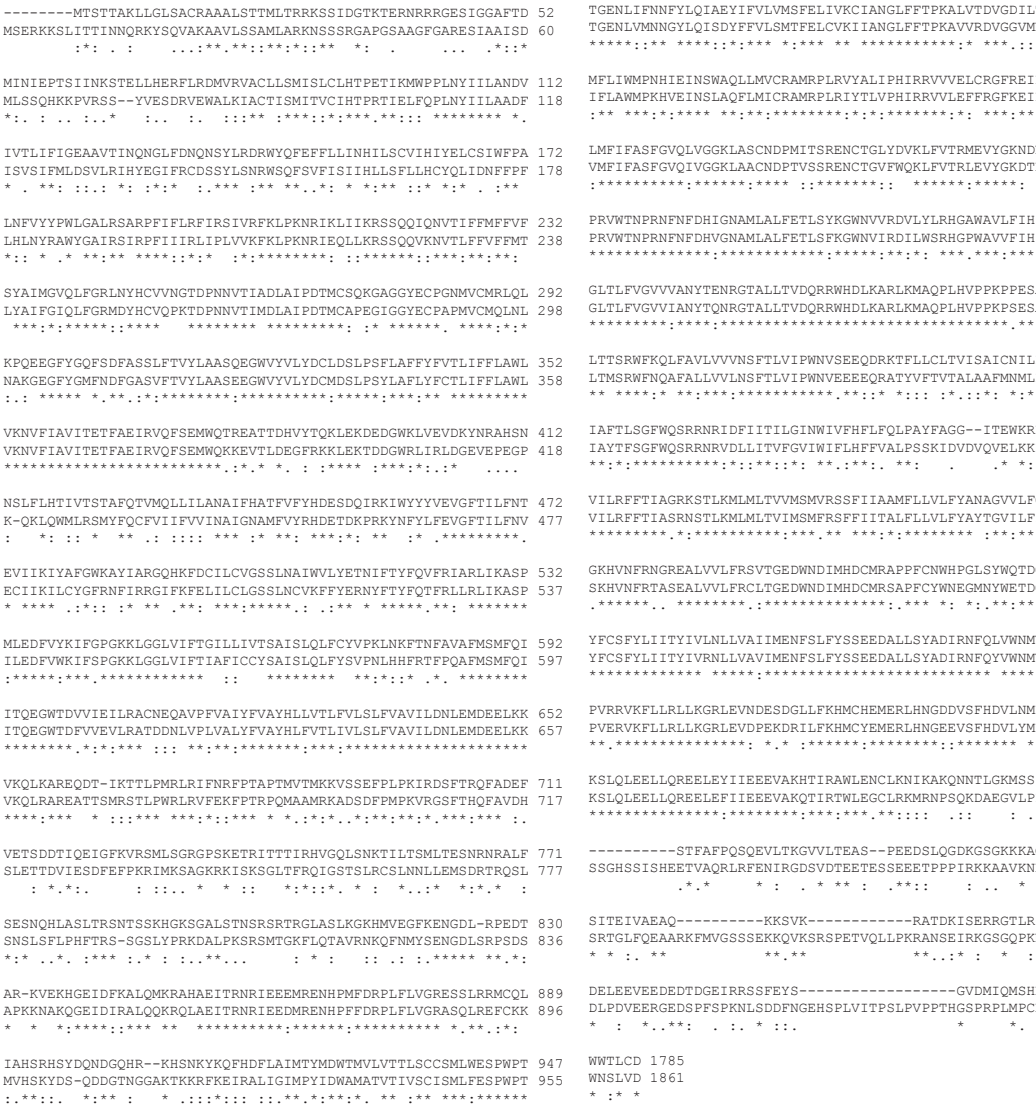

Figure 5-6 Alignment between NCA-1 and NCA-2

The worm homologues of NALCN, NCA-1 and NCA-2, are highly similar, as shown here with an alignment between the two longest predicted translations of each gene (NCA-2 top sequence, NCA-1 bottom sequence).

5.5 - Loss of NCA-2 function is sufficient to suppress the loopy phenotype of nRHO-1* animals

Following our discovery that the *nca-1* single mutant is capable of suppressing nRHO-1* loopy locomotion, we crossed *nca-2* VC9 animals with strain QT733 (nRHO-1*). In the F2 generation, as with the *nca-1* cross, we found animals which were non-loopy and carried the unc-122::gfp marker of the nRHO-1* integrated transgene, demonstrating that the single mutation in *nca-2* is also sufficient to suppress the loopy phenotype of nRHO-1* (Figure 5-5, E). These animals do not throw any loopy animals, demonstrating

that these are homozygous for the both the *nca-2* mutation and the nRHO-1* transgene. The double mutant animals do not demonstrate fainting locomotion on a solid surface. This is the first demonstration of a strong independent phenotype for the *nca-2* single mutation.

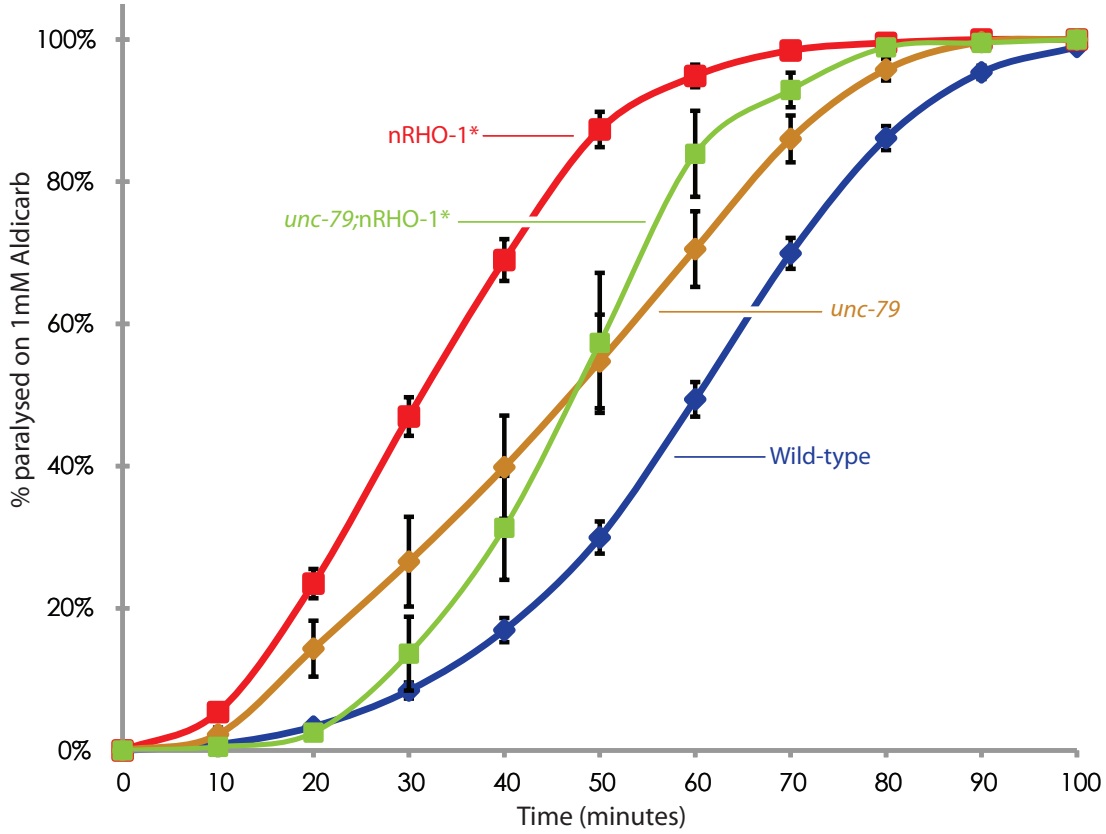

Figure 5-7 Aldicarb Assays - *unc-79* mutants

unc-79 single mutants (n=12) are hypersensitive to aldicarb compared with wild-type animals. The double mutant *unc-79*;nRHO-1* animals (n=7) paralyse faster than *unc-79* single mutants, and slower than nRHO-1* mutants. Error bars indicate the S.E.M.

This result, coupled with that in Section 5.4 suggests that *nca-1* and *nca-2* have independent roles within *C. elegans* nervous system. To our knowledge this is the first experiment to demonstrate non-redundancy of these genes, and may give some insight into why *C. elegans* has retained two highly similar copies of this protein (Figure 5-6) which is present as a single copy in Drosophila, mouse and human genomes.

We would need to perform rescue experiments for *unc-79*, *nca-1* and *nca-2* to confirm that these are genuinely the mutations which are able to suppress the loopy phenotype of nRHO-1*. However, the probability of all three mutants tested containing a second-site mutation capable of suppressing the loopy locomotion of nRHO-1* is very low, suggesting that the loss of *nca-1*, *nca-2* or *unc-79* function is likely to be the reason for restoration of normal locomotion in the presence of the nRHO-1* transgene.

5.6 - Neurotransmitter release assays of NCA complex mutants

NCA-1, NCA-2, UNC-79 and UNC-80 are considered to form part of a novel ion channel complex (Jospin, Watanabe et al. 2007; Yeh, Ng et al. 2008, Lu, Su et al. 2009), hereon referred to as the NCA complex, although its subunit composition is unknown at present. We had previously seen that mutations in *unc-80*, while sufficient to suppress the loopy locomotion of nRHO-1* animals is insufficient to suppress the hypersensitivity to aldicarb generated by nRHO-1* (Figure 4-16). We wanted to test what effect, if any, the other components of the NCA complex have on neurotransmitter release, and its regulation by nRHO-1*.

Percentage of animals paralysed at 50 minutes on 1mM aldicarb

Locus 1 \ Locus 2	**Wild-type**	***unc-79***	***nca-1***	***nca-2***	**nRHO-1***
Wild-type	30 ± 2.3, n=52	55 ± 6.6, n=12, p=0.0016	36 ± 5.0, n=9, p=0.35	77 ± 4.9, n=5, p=0.0001	87 ± 2.5, n=37, p<0.0001
unc-79	55 ± 6.6, n=12, p=0.0016	–	–	–	57 ± 9.8, n=7, p=0.8
nca-1	36 ± 5.0, n=9, p=0.35	–	–	41 ± 10.2, n=6, p=0.7	55 ± 5.0, n=7, p=0.02
nca-2	77 ± 4.9, n=5, p=0.0001	–	41 ± 10.2, n=6, p=0.01	–	53 ± 3.2, n=4, p=0.01
nRHO-1*	87 ± 2.5, n=37, p<0.0001	57 ± 9.8, n=7, p=0.02	55 ± 5.0, n=7, p=0.0002	53 ± 3.2, n=4, p=0.04	–
***nca-1* (gf)**	77 ± 4.7, n=9, p<0.0001	–	nca-1(gf) compared with nca-1 p<0.0001	–	nca-1(gf) compared with nRHO-1* p=0.06

Table 5-1 Statistical analysis of aldicarb data at 50 minute time point

All aldicarb data in this chapter is summarised here with statistics derived from the 50 minute time-point data. Statistics conducted using a 2-tailed unpaired T-Test. Data relating to PMA treatment is given within the body of the text.

5.6.1 - Aldicarb responses of *unc-79* mutants

5.6.1.1 - unc-79 mutants are hypersensitive to aldicarb

unc-79 single mutants are hypersensitive to aldicarb compared to wild-type (Figure 5-7), with 55±7% of animals paralysed at 50 minutes, compared with 30±2% of wild-type animals. This suggests that, despite their reduction in locomotion rate due to the fainting phenotype, that these animals have increased levels of neurotransmitter release. It remains a possibility that a second site mutation alters aldicarb sensitivity in these mutants, and therefore testing additional *unc-79* alleles, and performing rescue experiments would enable us to determine whether *unc-79* is the mutation responsible for this increase in aldicarb sensitivity. .

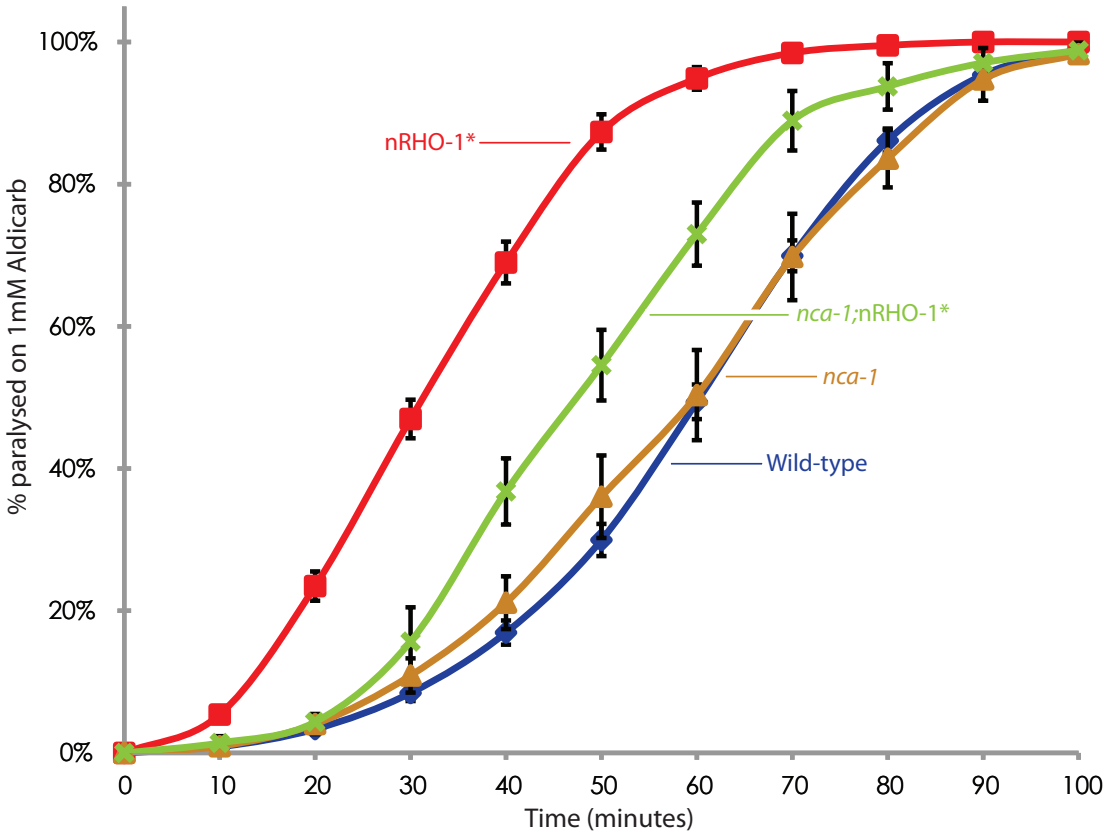

Figure 5-8 Aldicarb Assays - *nca-1* mutants

nca-1 single mutants have a wild-type response to aldicarb (n=9). The *nca-1*;nRHO-1* double mutant animals paralyse faster than *nca-1* mutant animals on 1mM aldicarb (n=7). However, their rate of paralysis is less than that of nRHO-1* animals.
Error bars indicate the standard error of the mean.

5.6.1.2 - *unc-79*;nRHO-1* double mutants are hypersensitive to aldicarb

The double mutant *unc-79*;nRHO-1* mutants paralyse faster than wild-type on 1mM aldicarb (Figure 5-7). These animals paralyse at a slightly faster rate than *unc-79* single mutants in the second half of the assay, indicating that the nRHO-1* transgene is able to increase neurotransmitter release in this mutant background. However, their rate of paralysis is less than that of the nRHO-1* single mutant. This suggests that the lack of *unc-79* limits the extent to which nRHO-1* can increase neurotransmitter release.

5.6.2 - Aldicarb responses of *nca-1* mutants

5.6.2.1 - *nca-1* single mutants are wild-type in their response to aldicarb

Animals carrying a deletion in *nca-1* (*gk9*) have a wild-type response to aldicarb (Figure 5-8), with 36±6% of animals paralysed at 50 minutes compared to 30±2% of wild-type

animals. This follows the rest of the literature which reports that the *nca-1* single mutant appears wild-type under all conditions so far tested.

5.6.2.2 - *nca-1*;nRHO-1* double mutants are hypersensitive to aldicarb

The double mutant *nca-1*;nRHO-1* animals are non-loopy, as the *nca-1* mutation alone is able to suppress the loopy phenotype of nRHO-1*. These double mutants paralyse faster than wild-type or *nca-1* single mutants (Figure 5-8) on 1mM aldicarb, a highly significant increase (Table 5-1). This indicates that the nRHO-1* transgene is still active and able to increase neurotransmitter release in this mutant, although the level of release is less than that seen in an nRHO-1* single mutant, implying that some suppression of the nRHO-1* activity occurs in an *nca-1* single mutant background.

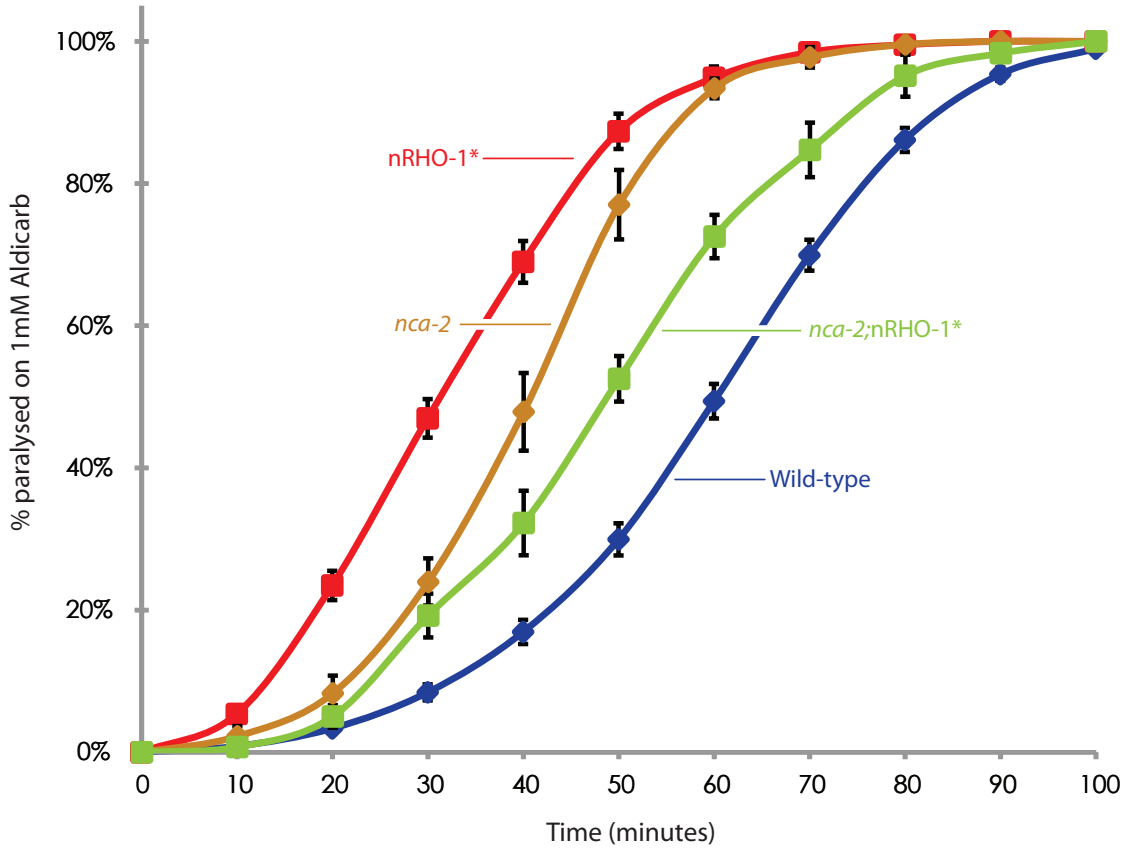

Figure 5-9 Aldicarb Assays - *nca-2* mutants

nca-1 single mutants have a wild-type response to aldicarb (n=9). The *nca-1*;nRHO-1* double mutant animals paralyse faster than *nca-1* mutant animals on 1mM aldicarb (n=7). However, their rate of paralysis is less than that of nRHO-1* animals.
Error bars indicate the standard error of the mean.

5.6.3 - Aldicarb responses of *nca-2* mutant animals

5.6.3.1 - nca-2 mutants are hypersensitive to aldicarb

Unlike *nca-1* (*gk9*) mutants, which appear wild-type for their response to acetylcholinesterase inhibitor treatment, *nca-2* (*gk5*) single mutants paralyse much faster than wild-type animals on 1mM aldicarb (Figure 5-9). 77±5% of *nca-2* single mutant animals paralyse at 50 minutes compared with 30±2% of wild-type animals (Table 5-1).

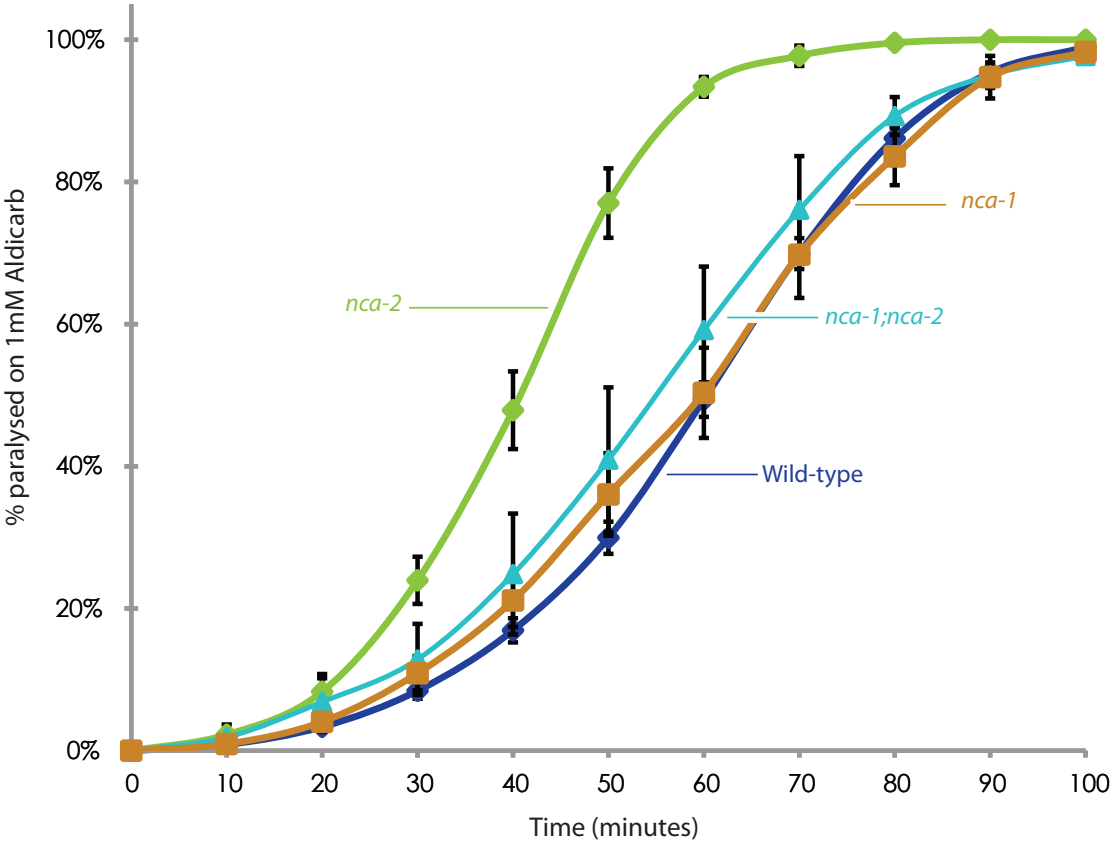

Figure 5-10 Aldicarb Assays - *nca-1;nca-2* mutants

The double mutant of *nca-1*;*nca-2* displays a fainter phenotype reminiscent of that seen in *unc-79* and *unc-80* mutants. The response of these animals to aldicarb appears wild-type (n=6). The aldicarb hypersensitivity observed in the *nca-2* single mutants is not seen in the double mutant animals.
Error bars indicate the standard error of the mean.

Along with the ability of the *nca-2* single mutant to suppress the loopy phenotype of nRHO-1* animals, this result implies that the *nca-1* and *nca-2* proteins are not entirely redundant and have distinct functions within the nervous system of the worm. However, this result is also consistent with a second site mutation increasing sensitivity to aldicarb, and testing additional *nca-2* mutants, and performing rescue experiments, would help determine whether *nca-2* is the causative mutation.

5.6.3.2 - *nca-2*;nRHO-1* mutants are hypersensitive to aldicarb

The non-loopy *nca-2*;nRHO-1* double mutants paralyse faster than wild-type animals on aldicarb but paralyse at a slower rate than *nca-2* single mutant animals (Figure 5-9). With *nca-2* mutants being hypersensitive it is not possible to determine whether the hypersensitivity of the double mutant (compared to wild-type) reflects activity of the nRHO-1* transgene, or is due to the effects of the *nca-2* mutation alone.

The rate of paralysis of the double mutant is less than that of the nRHO-1* single mutant, which suggests there is an interaction between nRHO-1* and *nca-2* with respect to neurotransmitter release such that *nca-2* suppress some of the effects of the nRHO-1* transgene, but further experiments are required to understand this relationship.

5.6.4 - *nca-1;nca-2* double mutants are wild-type for their response to aldicarb

The *nca-1*;*nca-2* double mutant exhibits a fainter phenotype similar to that seen in the *unc-79* and *unc-80* single mutants (Figure 5-10). When tested in their response to aldicarb, they appear wild-type, with 41±10% of animals paralysed at 50 minutes, compared with 30±2% of wild-type animals at the same time point.

The hypersensitivity seen in *nca-2* single mutant animals is not present in the double mutant. Potentially this hypersensitivity might reflect a change in the activity of NCA-1, compensating for the loss of NCA-2. When both NCA-1 and NCA-2 proteins are absent, the effect is lost. This result is also consistent with loss of a second-site mutation in the *nca-2* mutant which has been lost during the cross.

5.7 - Levamisole response of NCA complex mutants

The changes in aldicarb response observed in the NCA complex mutants could result either from increased acetylcholine release (a presynaptic event) or from increased sensitivity of the body wall muscles (a post-synaptic event). To distinguish between the two, we use levamisole, a cholinergic agonist, to directly stimulate the body wall muscles and subsequently assay the post-synaptic response.

5.7.1 - *unc-79* mutants are hypersensitive to levamisole

When exposed to 100µM levamisole, *unc-79* animals paralyse faster than wild-type animals (Figure 5-11). 25±9% of *unc-79* mutant animals are paralysed at 50 minutes, compared with 9±1% of wild-type animals (Table 5-2), although this result is not statistically

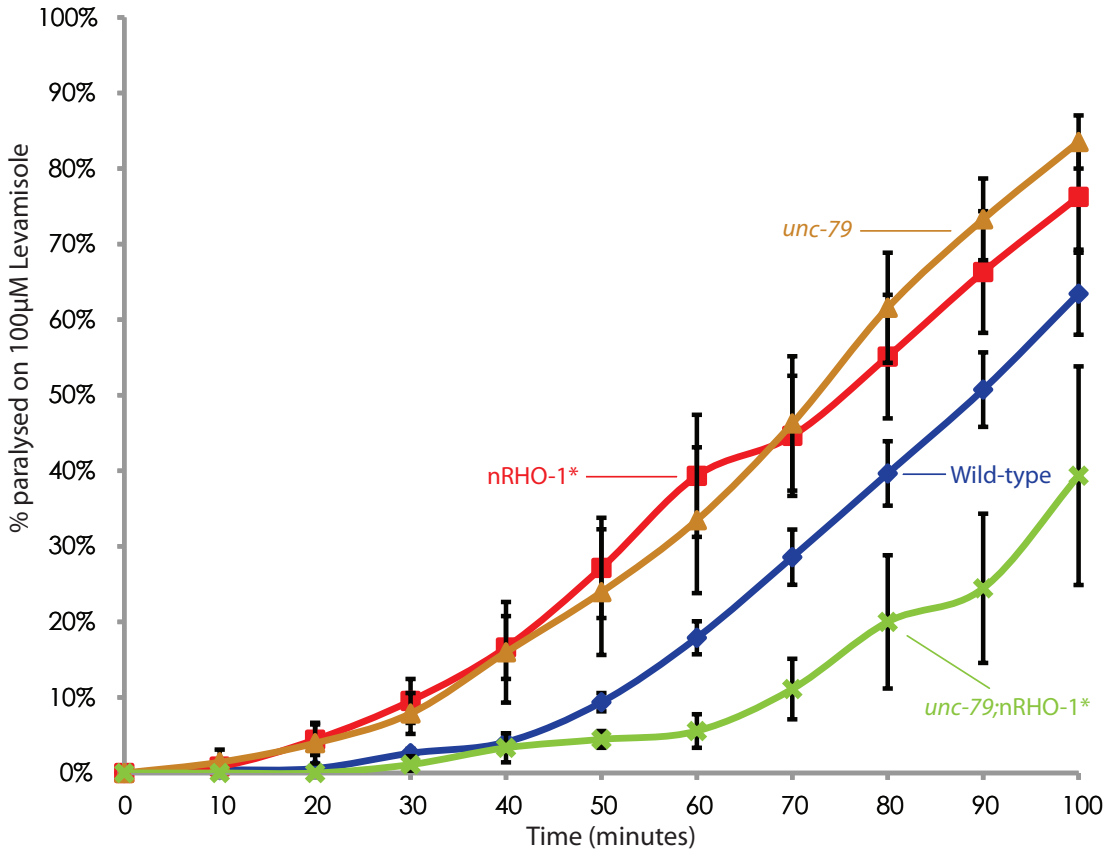

Figure 5-11 Levamisole assay - *unc-79* mutant animals

We observe an increase in the sensitivity of *unc-79* single mutants to levamisole (orange line, n=6) compared to wild-type (blue line, n=14). nRHO-1* animals also appear hypersensitive to levamisole in these assays (red line, n=8). The double mutant *unc-79*;nRHO-1* is resistant to the effects of levamisole (green line, n=3).
Error bars indicate the standard error of the mean.

significant, most likely due to the relatively large variations in the response levamisole between repeats. More repeats might achieve significance, but the trend suggests that the body wall muscles of *unc-79* animals are hypersensitive to acetylcholine.

unc-79 mutants are also hypersensitive to aldicarb, which enhances the signalling effect of endogenously-released acetylcholine. Together these two experiments suggest that the absolute level of acetylcholine release in *unc-79* animals may be closer to that of wild-type animals than suggested by the aldicarb assay; if the body wall muscles become hypersensitive to compensate for decreased signalling, this will give rise to hypersensitivity to both levamisole and acetylcholine.

5.7.2 - *unc-79*;nRHO-1* double mutants are resistant to levamisole

The non-loopy, fainter, *unc-79*;nRHO-1* mutants, which are hypersensitive to aldicarb, are resistant to levamisole, compared to the *unc-79* and nRHO-1* single mutants with

Percentage of animals paralysed at 50 minutes on 100µM levamisole

Locus 1 \ Locus 2	**Wild-type**	***unc-79***	**nRHO-1***	**nca-1**	**nca-2**
Wild-type	9 ± 1.2, n=14	25 ± 8.3, n=6, p=0.6	27 ± 6.6, n=8, p=0.03	–	–
unc-79	25 ± 8.3, n=6, p=0.6	–	4 ± 1.1, n=3, p=0.3		–
nca-1	16 ± 6.3, n=5, p=0.2				7 ± 1.7, n=5
nca-2	–	–	7 ± 1.7, n=5, p=0.02	23 ± 13.2, n=5, p=0.6	–
nca-1 (gf)	17 ± 5.3, n=4, p=0.2			*nca-1* (gf) compared with *nca-1* p=0.9	–
nRHO-1*	27 ± 6.6, n=8, p=0.03	4 ± 1.1, n=3, p=0.01	–	–	–

Table 5-2 Statistical analysis of levamisole data at 50 minute time point

All levamisole data in this chapter is summarised here with statistics derived from the 50 minute time-point data. Statistics conducted using a 2-tailed unpaired T-Test.

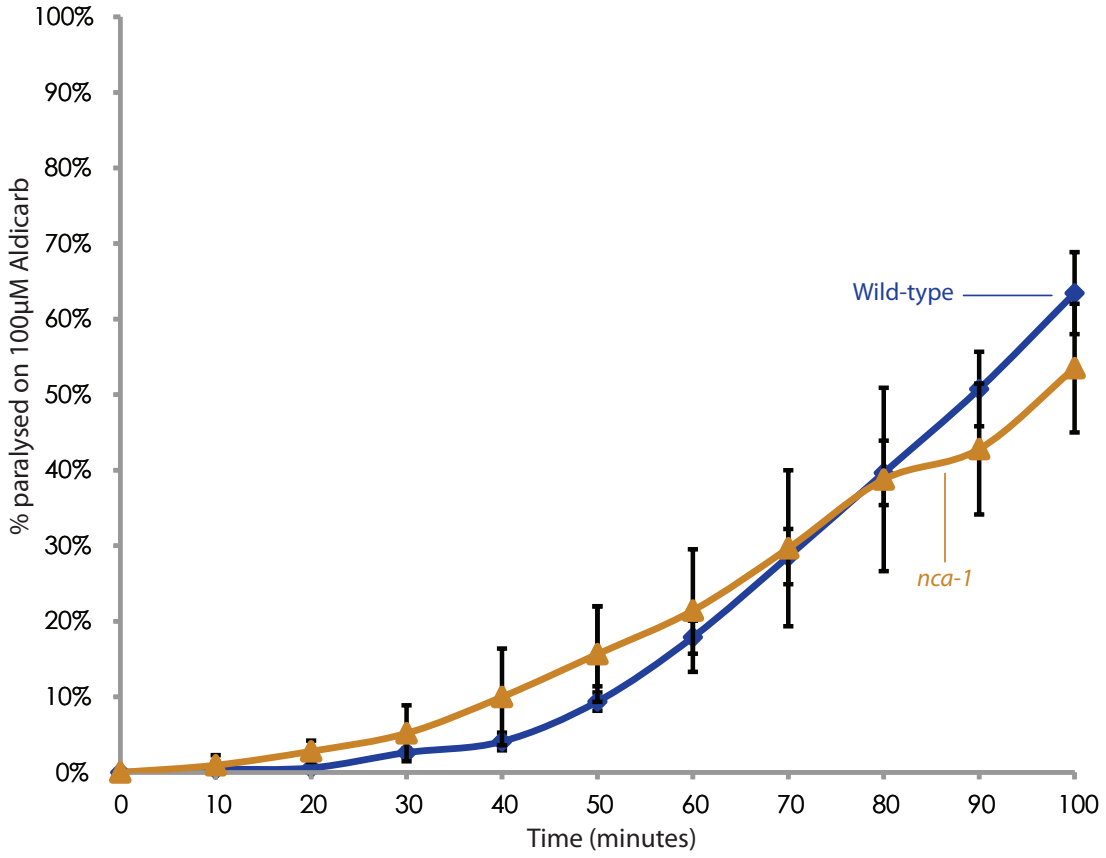

Figure 5-12 Levamisole assay - *nca-1* mutant animals

nca-1 single mutant animals, which have wild-type locomotion, display no change in levamisole response compared to wild-type animals (n=5).
Error bars indicate the standard error of the mean.

the response curve shifted to the right (Figure 5-11). At 50 minutes, just 4±1% of the double mutants are paralysed, a stastically significant decrease compared with the *unc-79* single mutant animals (Table 5-2).

Thus two mutants, *unc-79* and nRHO-1*, which alone give hypersensitivity to levamisole, when combined produce resistance to levamisole. This suggests that some combined effect of the nRHO-1* transgene in an *unc-79* mutant background is able to decrease the muscle sensitivity to acetycholine.

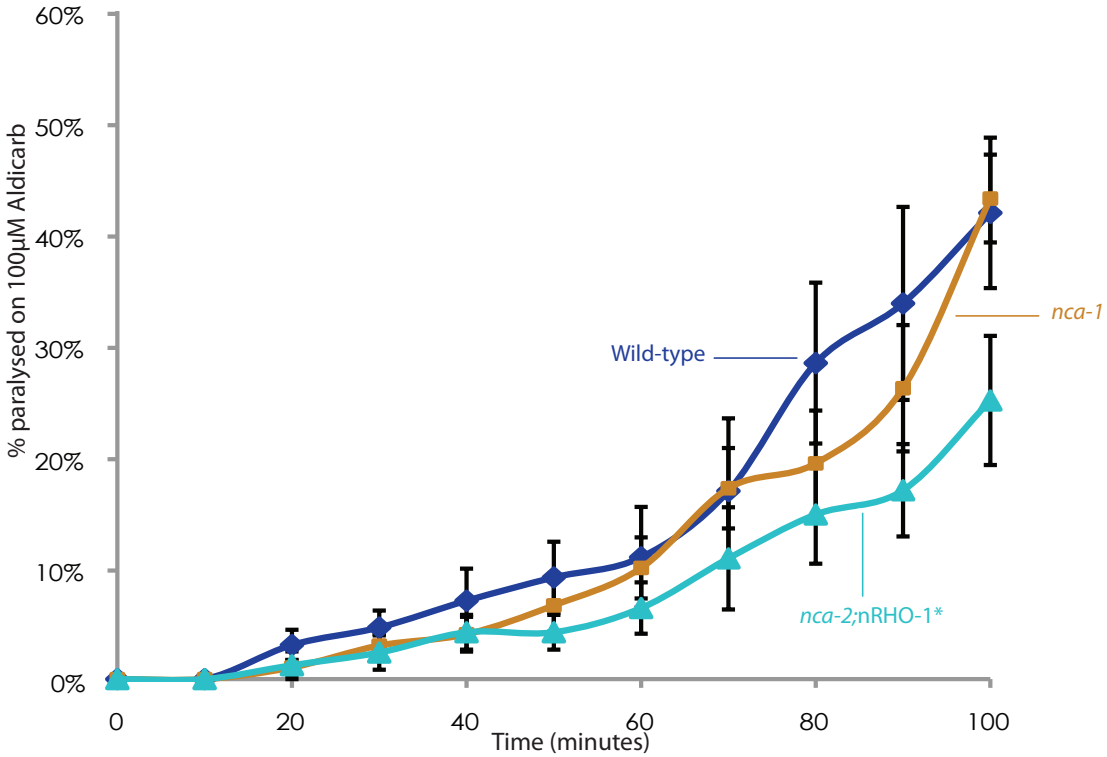

Figure 5-13 Levamisole assay - *nca-2* mutant animals

nca-2 single mutant animals which have wild-type locomotion, have a wild-type response to levamisole (n=8). nca-2;nRHO-1* double mutants are slightly resistant to levamisole when compared with wild-type animals (n=7). (n=5 for wild-type animals. These experiments were conducted with a separate batch of 100µM levamisole on which the wild-type animals paralysed slower than normal. Therefore comparrisons are made to the controls obtained only from this ste of experiments) Error bars indicate S.E.M.

5.7.3 - Levamisole responses of *nca-1* and *nca-1;nca-2* mutants

5.7.3.1 - *nca-1* mutant animals have a wild-type response to levamisole

We tested the levamisole phenotype of *nca-1* mutant animals. These animals have wild-type locomotion, and wild-type response to aldicarb (Figure 5-12), with no difference observed at 50 minutes compared with wild-type animals (Table 5-1). We also observe that these animals show no discernible levamisole phenotype. 16±6% of *nca-1* animals are paralysed at 50 minutes, compared with 9±1% of wild-type animals, which is not a statistically significant difference (Table 5-2).

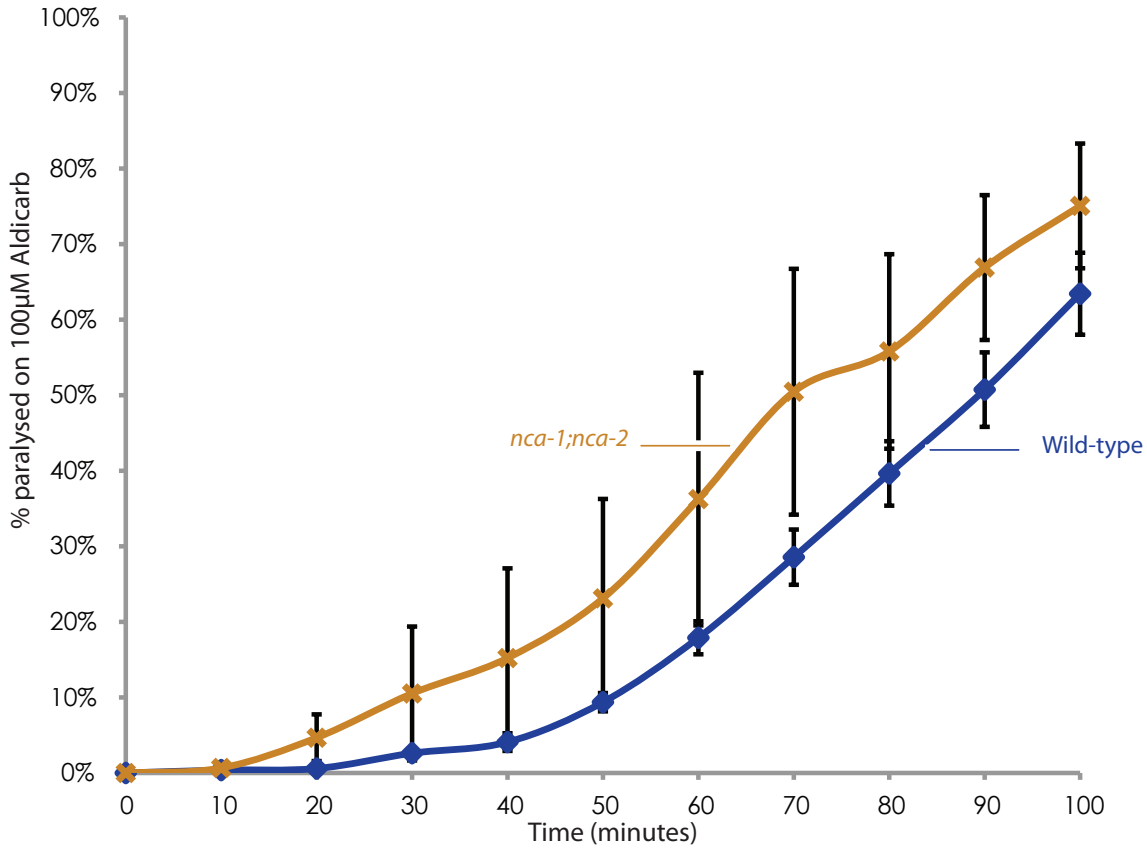

Figure 5-14 Levamisole assay - *nca-1;nca-2* mutant animals

nca-1;nca-2 double mutant animals, which have fainting locomotion, are hypersensitive to levamisole with respect to wild-type animals. Error bars indicate the standard error of the mean.

5.7.3.2 - *nca-2* mutant animals have a wild-type response to levamisole

We tested the levamisole phenotype of *nca-2 (gk5)* mutant animals. These animals have wild-type locomotion, but appear hypersensitive to aldicarb (Figure 5-12) when

compared with wild-type animals (Table 5-1). However, these animals are wild-type in their response to levamisole (Figure 5-13). 16±6% of *nca-1* animals are paralysed at 50 minutes, compared with 9±1% of wild-type animals, which is not a statistically significant difference (Table 5-2).

5.7.3.3 - nca-1;nca-2 double mutants display slight hypersensitivity to levamisole

We have already seen that *unc-79* and *unc-80* animals, which display fainting locomotion, are hypersensitive to the agonist levamisole. We tested the levamisole response of *nca-1*;*nca-2* double mutant animals, which also have a fainting locomotion, and see that these animals display a hypersensitivity to levamisole, with the response curve shifted to the left (n=5) (Figure 5-14). The difference at 50 minutes is not statisically significant, however (Table 5-2).

5.8 - Treatment with phorbol esters stimulates neurotransmitter release in NCA complex mutants

One theory to explain the suppression of loopy behaviour of the nRHO-1* transgene by loss-of-function NCA complex mutants would be if these mutants had a defect where the nervous system could not be stimulated by nRHO-1*. This also offers a simple explanation of the fainting phenotype. I would suggest that the fainter mutants could have a non-specific neuronal defect where their neurons are unable to maintain high levels of activity, causing them to pause for long intervals unless stimulated, for instance by a harsh nose touch.

One way to test whether these mutations are globally reducing the activity of the nervous system is to look in conditions where the nervous system is stimulated, such as stimulation with the DAG analogue PMA If the overall activity of the nervous system is lower in *unc-79*, *nca-1*, *nca-2* or *nca-1*;*nca-2* mutants should result in a resistance to the effects of PMA as assayed by aldicarb. Secondly, we can start to define the position the NCA complex genes in the neurotransmitter release pathway with respect to DAG signalling.

5.8.1 - unc-79 mutants respond to phorbol esters by increasing acetylcholine release

Wild-type animals respond to PMA by becoming hypersensitive to aldicarb, with the response curve shifting to the right in the presence of the drug (Figure 5-15). Without PMA, 67±7% of animals are paralysed at 50 minutes; when exposed to PMA, 99±1% of animals are paralysed at this time point (Table 5-3).

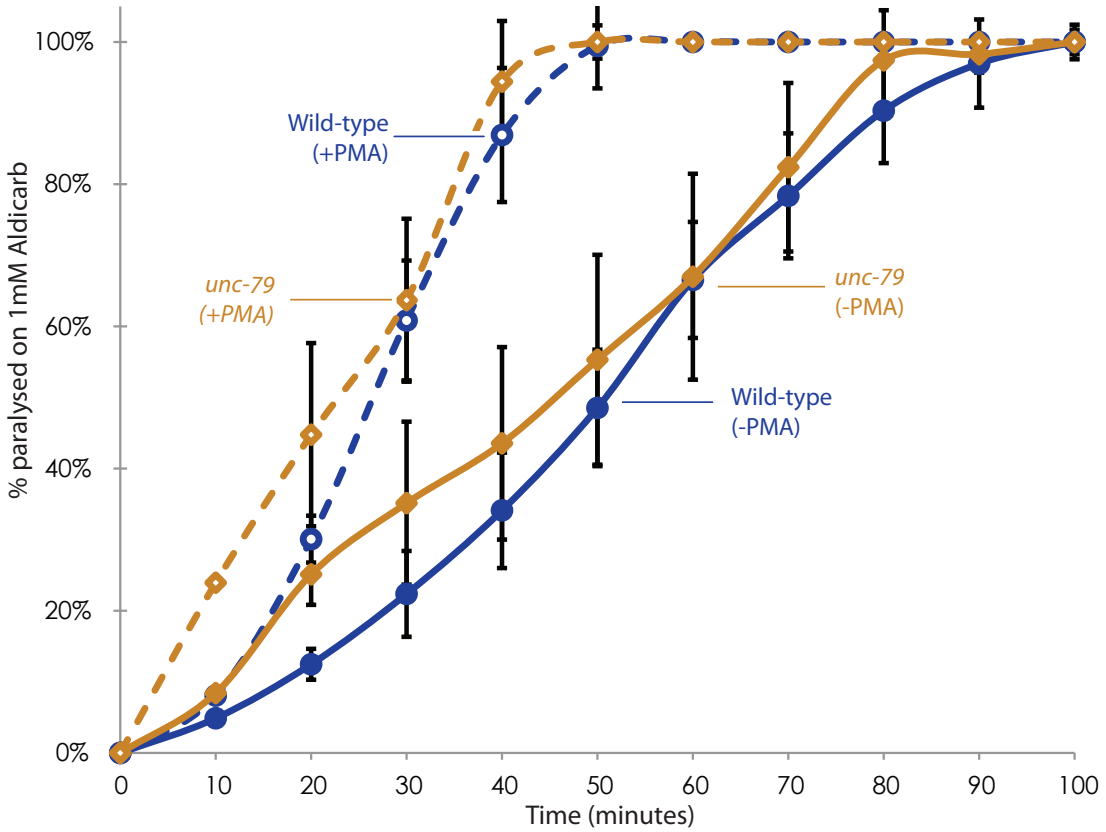

Figure 5-15 PMA assays - *unc-79* mutant animals

unc-79 mutants were assayed for paralysis on a combination of either aldicarb and PMA (a diacylglycerol analogue which stimulates neurotransmitter release) or on control aldicarb and DMSO plates. *unc-79* mutants exposed to PMA (dotted orange line, n=4) become hypersensitive to aldicarb compared to *unc-79* mutants on control plates (solid orange line, n=4). This shift of the curve to the left is also seen in wild-type animals exposed to PMA (blue lines, n=7).
Error bars indicate the standard error of the mean.

unc-79 animals display a similar response to PMA as wild-type; 98±2% of animals paralysed at 50 minutes, compared with 64±12% of animals without PMA (Table 5-3), and this change is borderline significant (p=0.07). This data indicates that UNC-79 acts upstream of or in parallel to the pathway activated by PMA.

5.8.2 - *nca-1* mutants respond to phorbol esters by increasing acetylcholine release

nca-1 mutants are able to respond to PMA and increase their sensitivity to aldicarb, as demonstrated by a shift to the left of the response curve (Figure 5-17). After two hours pretreatment with PMA or DMSO, the animals were placed on plates containing PMA or DMSO along with 1mM aldicarb. On the DMSO-treated plates, 45±4% of *nca-1* animals are paralysed at 50 minutes, whereas when treated with PMA 88±6% of animals were paralysed at the same time point, a stastisically significant change (Table 5-3). .

This indicates that, as with the *unc-79* result, NCA-1 acts either upstream of or in parallel to the pathway activated by PMA.

Percentage of animals paralysed at 50 minutes on 1mM aldicarb

	With DMSO control	***With PMA***
Wild-type	67 ± 7.1, n=9	99 ± 0.9, n=9, p=0.002
unc-79	64 ± 12.0, n=4	98 ± 1.6, n=4, p=0.07
nca-1	45 ± 4.4, n=5	88 ± 6.1, n=5, p=0.008
nca-2	62 ± 10.1, n=3	77 ± 13, n=3, p=0.5
nca-1;nca-2	17, n=1	96, n=1

Table 5-3 Statistical analysis of aldicarb and PMA data at 50 minute time point

Treatment with aldicarb and PMA is summarised here with statistics derived from the 50 minute time-point data. Statistics conducted using a 2-tailed paired T-Test.

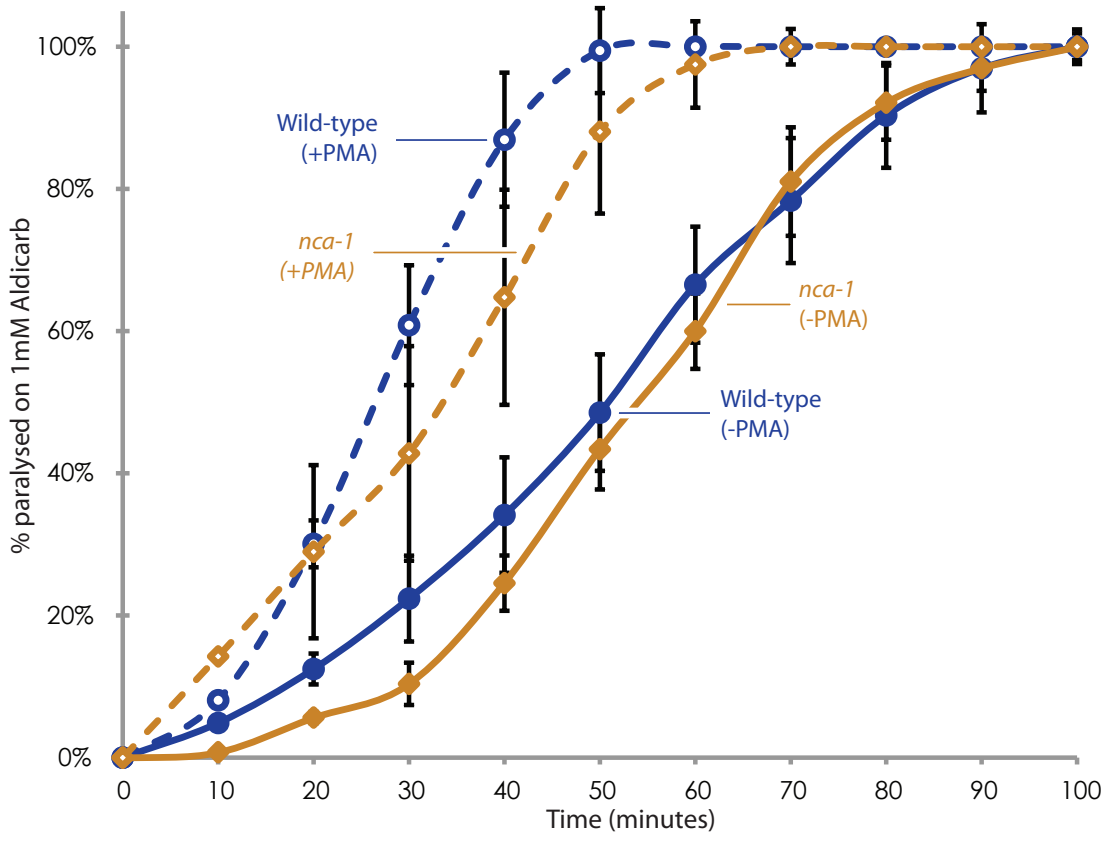

Figure 5-16 PMA assays - *nca-1* mutant animals

nca-1 mutants were assayed for paralysis on a combination of either aldicarb and PMA or on control aldicarb and DMSO plates. *nca-1* mutants exposed to PMA (dotted orange line, n=5) become hypersensitive to aldicarb compared to *nca-1* mutants on control plates (solid orange line, n=5).

5.8.3 - *nca-2* mutants partially block the increase in acetylcholine release stimuated by treatment with phorbol esters

nca-2 mutants are able to respond to PMA and increase their sensitivity to aldicarb (Figure 5-17). After two hours pretreatment with PMA or DMSO, the animals were placed on plates containing PMA or DMSO along with 1mM aldicarb. On the DMSO-treated plates, 62±10% of *nca-2* animals are paralysed at 50 minutes, whereas when treated with PMA 77±13% of animals were paralysed at the same time point (Table 5-3), although this change is not statisically significant. This suggests that the nca-2 mutation is having a suppressive effect on the action of PMA, although the response curve is still partially shifted to the left in the presence of the drug.

Given that nca-2 single mutants are hypersensitive to aldicarb, and only partially responsive to PMA (in contrast to other NCA complex mutants) it will be essential to confirm that a second site mutation is not modulating ACh release in these animals.

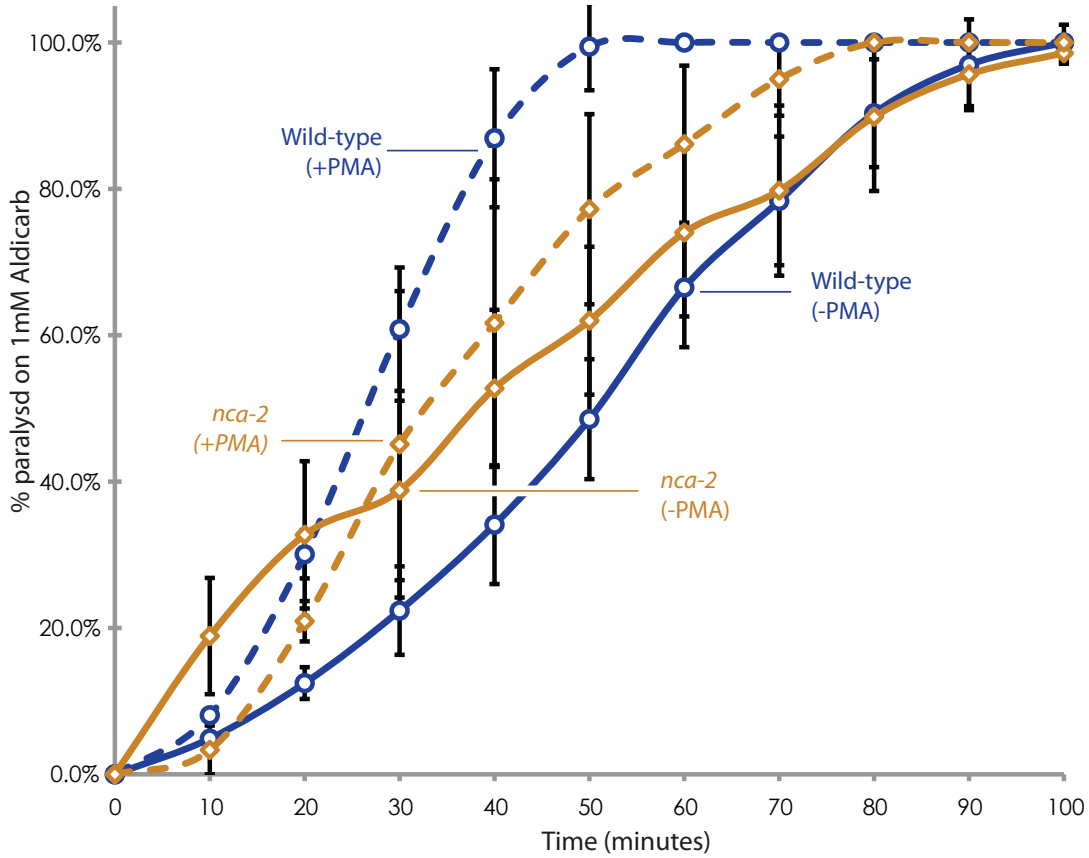

Figure 5-17 PMA assays - *nca-2* mutant animals

nca-2 mutants were assayed for paralysis on a combination of either aldicarb and PMA or on control aldicarb and DMSO plates. *nca-1* mutants exposed to PMA (dotted orange line, n=3) become hypersensitive to aldicarb compared to *nca-1* mutants on control plates (solid orange line, n=3).

Error bars indicate the standard error of the mean.

5.8.4 - *nca-1;nca-2* double mutants are sensitive to the effects of PMA

We tested the response of *nca-1*;*nca-2* fainter mutants to PMA, a DAG analogue, by assaying their response to aldicarb in the presence of either PMA or a DMSO-control.

Animals on the control plates paralyse at the same rate as wild-type animals on the control plates, demonstrating no underlying change in the response to aldicarb. When treated with PMA, *nca-1*;*nca-2* mutant animals become hypersensitive to aldicarb, paralysing at a faster rate (Figure 5-18). Without PMA, 17% of animals are paralysed at 50 minutes, whereas 92% of animals treated with PMA are paralysed at the same time point.

This result is obtained from only a single repeat, and so needs further trials for corroboration. However, the trend identified from this experiment indicates that loss of *nca-1* and *nca-2* in the same animals has no effect on the response to PMA.

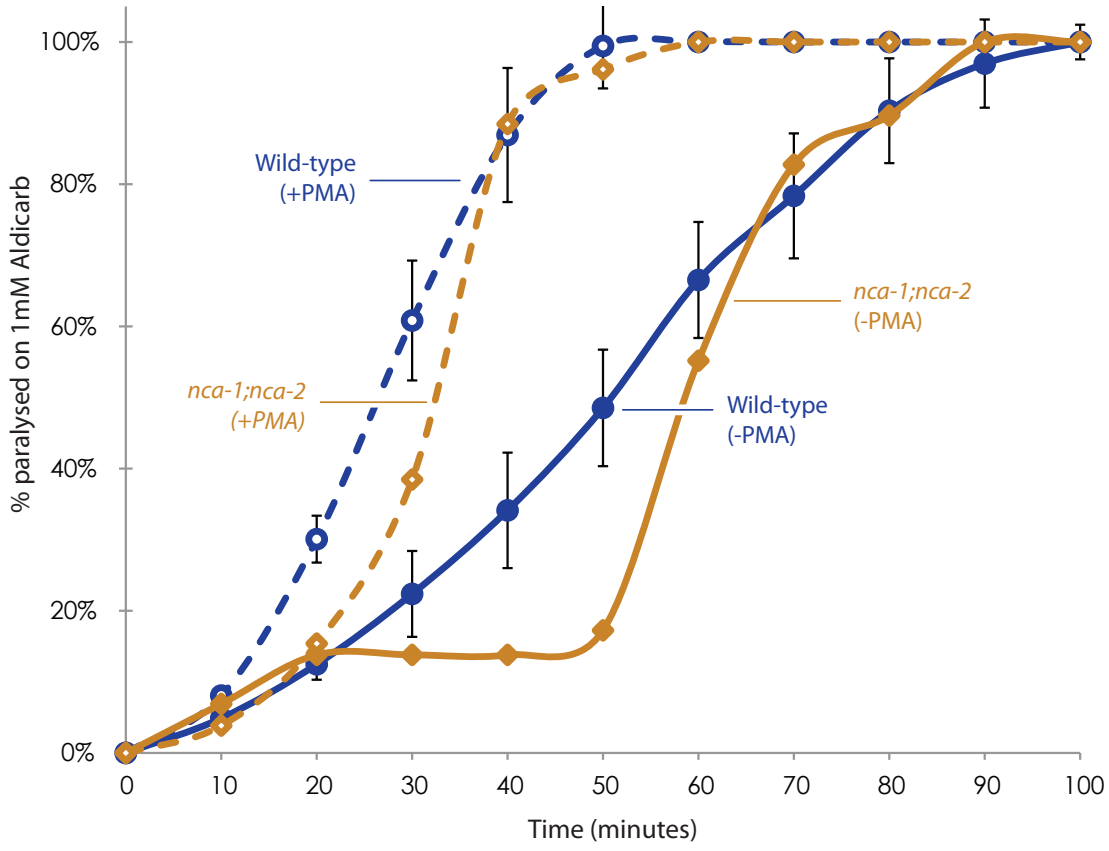

Figure 5-18 PMA assays - *nca-1;nca-2* mutant animals

nca-1;*nca-2* mutants were assayed for paralysis on a combination of either aldicarb and PMA or on control aldicarb and DMSO plates. *nca-1*;*nca-2* mutants exposed to PMA (dotted orange line, n=1) become hypersensitive to aldicarb compared to *nca-1*;*nca-2* mutants on control plates (solid orange line, n=1).
Error bars indicate the standard error of the mean.

5.9 - *nca-1*(gf) mutants phenocopy nRHO-1* mutant animals

5.9.1 - *nca-1*(gf) mutants are highly loopy

The gene originally isolated as *unc-77* (Brenner 1974) for its loopy phenotype (Figure 5-19, B) has subsequently been identified as an allele of *nca-1* (Yeh, Ng et al. 2008). This mutant carries the mutation *e625* (Figure 5-1), which introduces a mutation A717V in the sixth predicted transmembrane domain of the second repeat of the protein. This residue is conserved between species, as is a mutation in the sixth transmembrane domain of the first repeat (*hp102*, R403Q, Figure 5-1). Both of these represent dominant mutations in the protein, and the loopy locomotion phenotype can be suppressed by mutations in *unc-79* or *unc-80,* possibly due to los of NCA-1 localisation (Yeh, Ng et al. 2008).

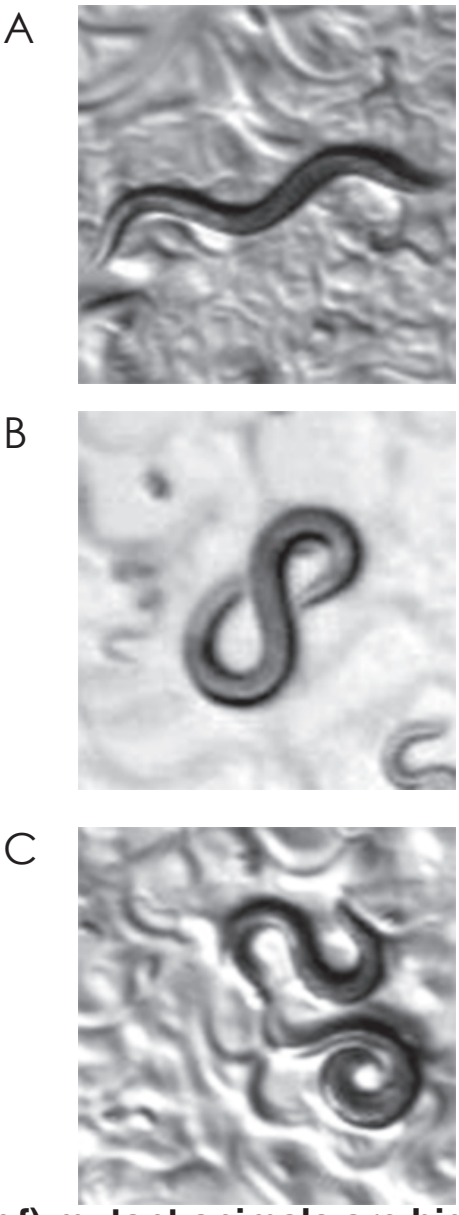

Figure 5-19 *nca-1*(gf) mutant animals are highly loopy

Animals carrying a gain-of-function mutation in the *nca-1* gene (B) become highly loopy when compared with wild-type animals (A). This loopy locomotion is reminiscent of that seen in nRHO-1* mutant animals (C).

The loopy phenotype of these animals is highly similar to that seen in the nRHO-1* mutants (Figure 5-19, B and Movie 5-2). We therefore speculated that these animals may also have high levels of neurotransmitter release.

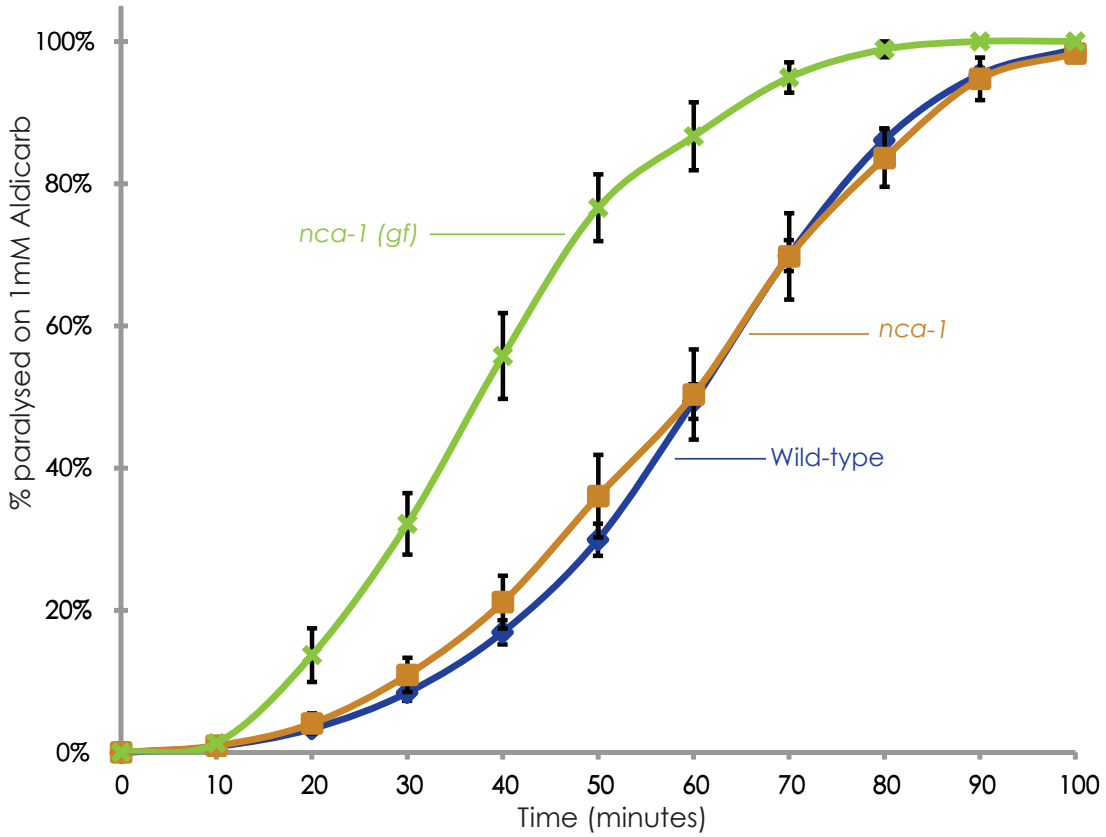

Figure 5-20 *nca-1*(gf) mutant animals are hypersensitive to aldicarb

Animals carrying a gain-of-function mutation in the *nca-1* gene are hypersensitive to the acetylcholinesterase inhibitor aldicarb, as demonstrated by a shift in their response curve to the left compared with wild-type and *nca-1* (loss-of-function) mutants (n=9).
Error bars indicate the standard error of the mean.

5.9.2 - *nca-1*(gf) mutants are hypersensitive to aldicarb

We tested the response of mutants carrying the e625 dominant mutation in *nca-1* for their response to 1mM aldicarb. Unlike animals which have a deletion in *nca-1*, which are wild-type in their response to aldicarb, *nca-1*(gf) mutants are hypersensitive to aldicarb, with 77±5% of animals paralysed at 50 minutes, compared with 30±2% of wild-type animals (Figure 5-20, Table 5-1).

5.9.3 - *nca-1* mutants are wild-type in their response to levamisole

Mutants with a deletion in *nca-1* display a wild-type response to levamisole (Figure 5-21). Animals carrying the *nca-1*(gf) mutation are also wild-type for their response to levamisole (Figure 5-20, Table 5-2). Along with their hypersensitivity to aldicarb, this

indicates that these animals have excess levels of acetylcholine release compared to wild-type and that the *nca-1*(gf) mutation acts presynaptically.

It would be useful to express *nca-1*(gf) cDNA from cell-specific promoters, such as the *unc-17* promoter, to determine the site of action of *nca-1* with respect to increasing aldicarb sensitivity.

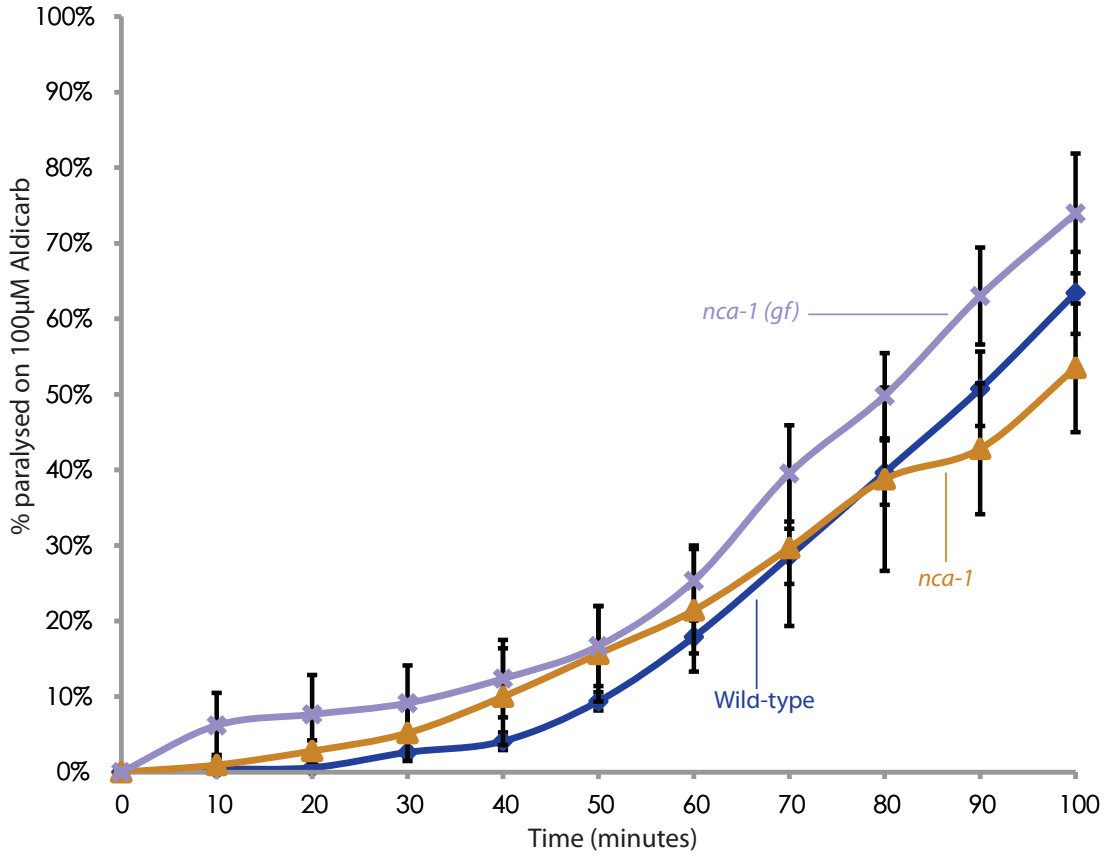

Figure 5-21 *nca-1*(gf) mutants have a wild-type response to levamisole

nca-1(gf) mutants are wild-type in their response to levamisole.
Error bars indicate the standard error of the mean.

5.9.4 - *nca-1*(gf) mutants have a defect in their swimming behaviour

The highly loopy *nca-1*(gf) animals display a defect in their ability to thrash in liquid. We previously used this assay, where animals are suspended in a drop of M9 solution, allowed to recover for three minutes, and the number of thrashes recorded for the following two minutes, to assay fainting behaviour (Chapter 4, and Figure 5-2,3 & 4), but also observed a defect in the swimming behaviour of highly loopy nRHO-1* mutant animals, resulting in fewer thrashes per minute than wild-type animals (Figure 5-22). *nca-1* mutant animals

also show a drop in their rate of thrashing in liquid compared with wild-type animals (Figure 5-22), to 31±2 thrashes per minute, compared with 97±3 for wild-type. While this drop appears similar to that seen in nRHO-1* mutant animals, *nca-1*(gf) mutant thrash rate remains significantly higher than that seen in nRHO-1* mutant animals.

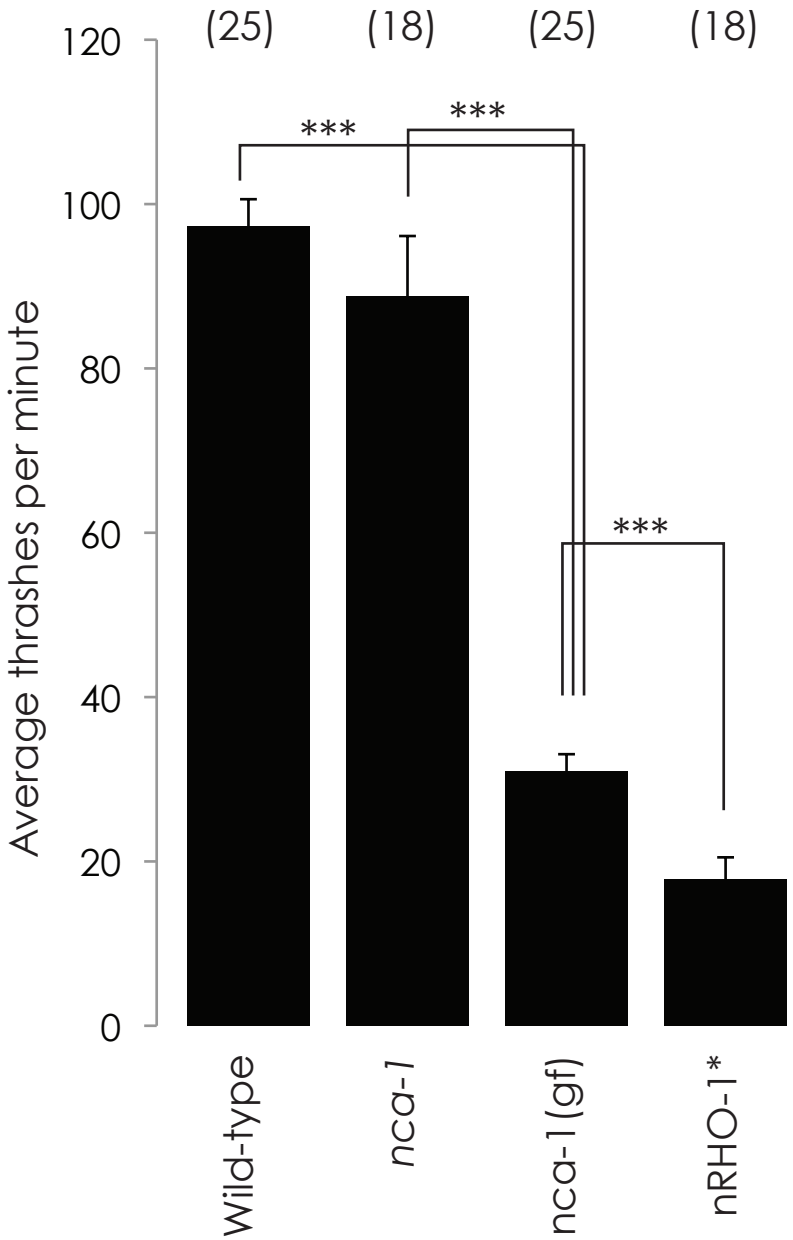

Figure 5-22 *nca-1*(gf) mutants demonstrate a defect in swimming

When placed in M9 and allowed to recover for 3 minutes, *nca-1*(gf) mutants thrash significantly less often than either *nca-1* single mutant animals or wild-type animals. Their loopy locomotion is likely to be the cause of this defect. However, their mean number of thrashes per minute is significantly different from that exhibited by the nRHO-1* mutants.

Error bars indicate standard errors of the mean. Numbers in brackets indicate number of animals observed. (Significance assessed using a 2-tailed T-test. *** = $p<0.001$)

5.9.5 - *nca-1*(gf) mutants have a defect in the Exp step of the defecation cycle

We had previously observed a defect in the Exp step associated with nRHO-1* mutant animals, and therefore we tested the gain-of-function *nca-1* mutants to see whether they displayed a similar defecation defect.

nca-1(gf) mutants are wild-type in the pBoc step of the defecation cycle (Figure 5-23), although there is an increase in the variability of this step compared with wild-type animals. The expulsion step of the defecation cycle is significantly longer than in wild-type animals (Figure 5-23). There is an even more significant increase in average expulsion interval in nRHO-1* mutant (Figure 5-23) compared with wild-type animals, but there is no significant difference between nRHO-1* animals and *nca-1*(gf) mutant animals. Together these data suggest that the defecation cycle is operating normally within these two mutant animals (as demonstrated by wild-type pBoc intervals), but that not every pBoc is followed by an Exp step. The Exp step requires the release of GABA acting as an excitatory neurotransmitter (Beg and Jorgensen 2003), and our result suggests a possible defect in GABA release in gain-of-function mutations in both NCA-1 and RHO-1.

5.10 - Strain QT958 contains a spontaneous suppressor of *nca-1*(gf)

When conducting these experiments with the gain-of-function allele of *nca-1*, we thawed out animals from strain DR1089, which had been frozen and stored at -80°C for a number of years since being obtained from the CGC. On thawing, the animals which survived the freezing process were non-loopy, and their progeny were also non-loopy. We also observed that these animals appeared to have a fainting locomotion phenotype.

The description of strain DR1089 described them as being highly uncoordinated, and did not contain any reference to this fainter phenotype. Knowing that *unc-80* and *unc-79* mutations can suppress the loopy aspect of *nca-1*(gf) mutants, we speculated that they had spontaneously acquired a suppressor mutation.

We crossed the strain carrying *nz112* with *him-5* animals, and in the F2 generation obtained animals with two distinct phenotypes. One set of animals bred true for the loopy phenotype associated with the gain-of-function *nca-1* mutation. The other set of animals, however, bred true for a fainter phenotype. We named the unknown suppressor as *nz112*.

We crossed this strain with *unc-80* and *unc-79* mutants to see whether this mutation was complementary with either of them. However, in the F1 generation following crosses

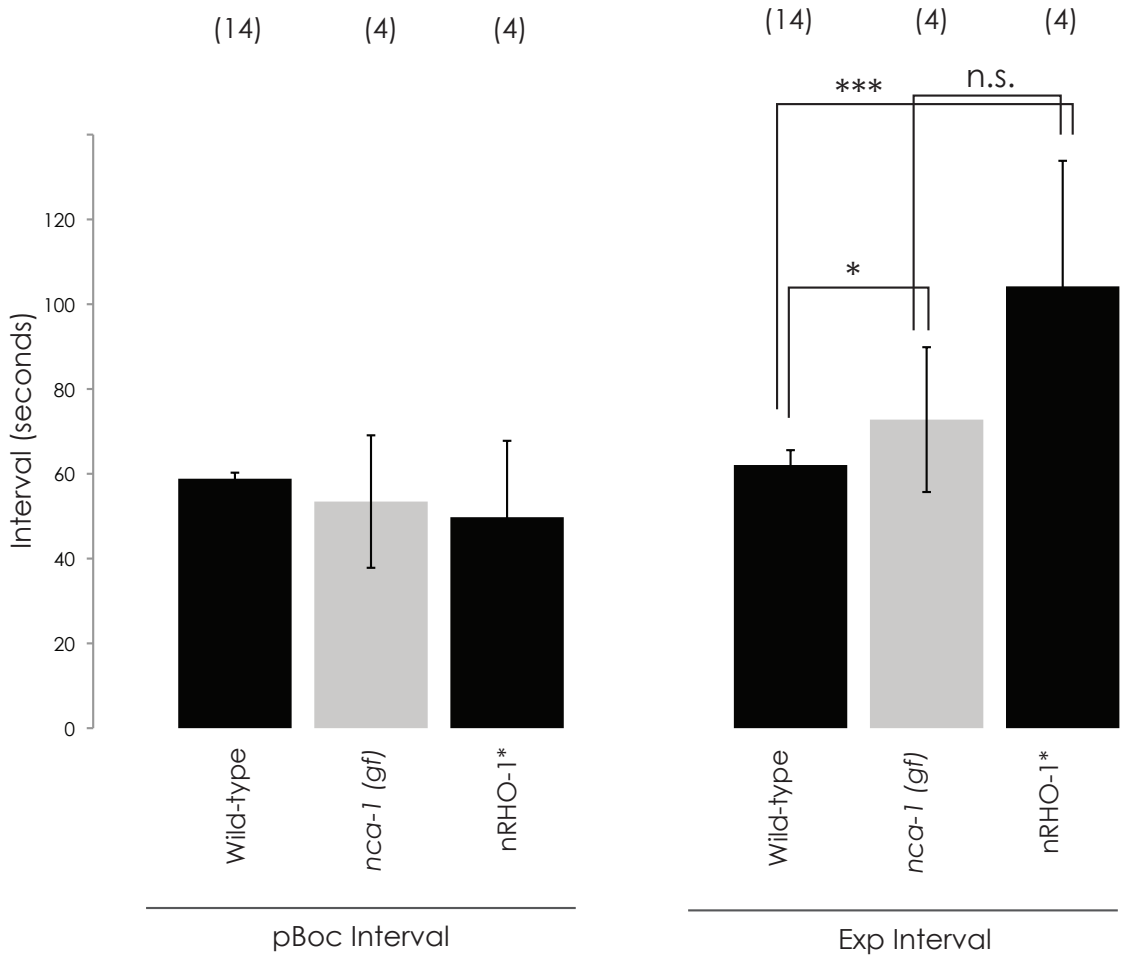

Figure 5-23 *nca-1*(gf) mutants display a defect in defecation

nca-1(gf) mutants display a significant increase in the length of the explulsion step of defecation compared with wild-type animals. They are not defective in the cycle as a whole, as demonstrated by the regular pBoc interval.
nRHO-1* animals also display an increase in the expulsion interval but no change in the pBoc interval. This suggests that in both mutants they are failng to initiate Exp following every pBoc.
Error bars indicate standard errors of the mean. Numbers in brackets indicate number of animals observed. (Significance assessed using a 2-tailed T-test. * = $p<0.05$ *** = $p<0.001$)

with both *unc-79* and *unc-80* some fainter mutants were obtained. This result suggests that this mutation is able to complement both of these genes. This experiment needs to be repeated, but this mutant remains of interest for the future. We would also like to cross these animals with nRHO-1* to see test whether *nz112* is able to suppress the loopy behaviour of those animals.

5.11 - Gadolinium treatment failed to induce fainting behaviour in *C. elegans*

It has been reported that the ion gadolinium (Gd^{3+}) is a specific inhibitor of the NALCN ion channel (Lu, Su et al. 2007) in tissue culture experiments. It has also been successfully used to block the effects of NCA-1, which causes an increase in cell death when

transfected into HEK293 cells (Yeh, Ng et al. 2008). We therefore speculated that it might act as a specific inhibitor of the NCA-1 and NCA-2 ion channels in live *C. elegans*, and potentially induce a fainting phenotype.

We added gadolinium from a 100mM stock diluted in dH_2O to our NGM plates, giving final concentrations of 10mM, 1mM, 100µM, 10µM and 0µM (control). L4 animals were picked the day before the assay, and 30 were placed on these plates, with food, and left on for either 6 hours or 24 hours. No effect on locomotion was observed in the treated animals compared to control animals.

We performed the same experiment with age-matched nRHO-1* animals, to see whether gadolinium treatment was able to suppress the loopy locomotion phenotype of these animals. After 6 hours and 24 hours of treatment, no change was observed in the locomotion of these animals compared to controls.

It is possible that highly charged gadolinium ions react with the materials of the NGM plates and becoming unavailable to treat the worms. We therefore tested the response of wild-type animals to concentrations of 10mM, 1mM, 100µM, 10µM and 0µM (control) dissolved in 1% agarose plates. However, after exposure up to 24 hours, no difference was observed with control. We also tested *nca-1* and *nca-2* single mutant animals under these conditions, speculating that with a background reduction in channel activity we may see an effect of gadolinium exposure, but no effects were seen after 24 hours of growth.

As an additional measure, we washed mixed populations of wild-type animals into gadolinium solutions at concentrations of 10mM, 1mM, 100µM and 10µM and 0µM (control). At time points of 2, 6 and 24 hours, 200µl of solution containing a mixed population of animals was transferred to NGM plates for examination. No effect on locomotion was observed compared with control-treated animals.

5.12 - Cloning NCA-1 introduces cDNA rearrangements

We wanted to produce an *nca-1* rescuing construct which would allow us to restore NCA-1 function in an an *nca-1* mutant, to test whether this was sufficient for recovery of loopy locomotion in *nca-1*;nRHO-1* mutant animals, and determine the site of action of NCA-1 with respect to fainting locomotion in the *nca-1*;*nca-2* double mutant animals. We also designed primers to allow us to introduce the two known gain-of-function mutations into our rescuing construct by site-directed mutagenesis, to analyse the effects of these mutations when expressed under cell-specific promoters.

We obtained the full-length predicted cDNA of *nca-1*, contained in plasmid YK1346e10 produced by Yuji Kohara. However, upon sequencing this plasmid, we detected a number of variations compared to the wild-type predicted cDNA. Including two gaps of 22 and 138 base pairs respectively, and several point mutations. We decided to attempt to use this cDNA sequence, despite the differences to wild-type, cloned this cDNA into the heat-shock expression vector. However, upon sequencing, this plasmid, APP7, contained a number of rearrangements of the *nca-1* sequence.

Subsequent attempts to clone the *nca-1* cDNA were also unsuccessful. We hypothesise that the cDNA contains sequences toxic to bacteria which creates a selection pressure in culture to remove or mutate these sequences. Similar problems have been reported with the NALCN cDNA sequence (D. Ren, personal communication.), and we have so far been unable to produce a stable plasmid containing the NALCN mouse cDNA sequence (the original vector was a gift from D. Ren.)

We therefore made an NCA-1 minigene which contains some introns that are not spliced in bacteria, and thus we hypothesise that this construct fails to produce the toxic element of the NCA-1 protein during replication in *E. coli*. Preliminary experiments suggest we can rescue *nca-1* mutants with this minigene (M. Elmi, personal communication).

5.13 - Discussion of Chapters 4 and 5

5.14 - A fainter mutation suppresses the loopy phenotype of nRHO-1* mutant animals

During our screen for suppressors of the loopy behaviour of animals expressing constitutively-active RHO-1 from the *unc-17* promoter (nRHO-1*), we identified two mutants, *nz94* and *nz98*, isolated from the same original plate, which were non-loopy. These animals continued to be non-loopy upon activation of a second constitutively-active RHO-1 transgene driven by the heatshock promoter (hsRHO-1*), indicating that these are genuine suppressors of the activity of RHO-1*.

We observed that these two mutants had an additional phenotype - as well as being non-loopy they appeared lethargic, and upon further investigation were reclassified as fainters, because they were capable of wild-type locomotion upon stimulation but tended to remain motionless unless disturbed.

This phenotype has so far been ascribed to only three classes of mutants - *unc-80* and *unc-79* single mutants, and the double mutant *nca-1*;*nca-2*. We found that *nz94* failed to complement a known mutation in *unc-80*, and sequenced the *unc-80* gene in *nz94*. Sequencing revealed a premature STOP codon towards the five prime end of the gene

(Figure 3-4). While we have yet to assay this position in *nz98*, we believe it is likely to contain the same mutation due to its originating from the same plate in the screen.

Mutations in *unc-80* cluster in two locations, one towards the 5' end of the gene where we found nz94, and another at the 3' end (Figure 4.4). This clustering may be revealing regions that are important for function. As a further experiment, we would like to demonstrate that *nz94* represents a true null mutation by assaying for the cDNA of *unc-80*, or by examining the protein levels by western blot.

5.15 - unc-80 and *unc-79* mutations suppress the loopy locomotion of nRHO-1*

For further assays we decided to use an allele of *unc-80*, e1069, which had been previously characterised and backcrossed, as this was likely to contain fewer background mutations. This allele is also able to suppress the loopy locomotion of nRHO-1* animals (Figure 4-6).

We also tested an allele of *unc-79*, e1068, which shares a fainter phenotype with *unc-80*, and demonstrated that loss of activity of UNC-79 is also able to suppress the loopy locomotion of nRHO-1* (Figure 5-5).

We were able to successfully demonstrate rescue of the suppression of loopy locomotion in *unc-80*;nRHO-1* double mutants by using a number of UNC-80 minigenes (Figure 4-8). Pan-neuronal expression, under the synaptobrevin promoter, was able to restore loopy locomotion (Figure 4-9), demonstrating that UNC-80 is required neuronally for RHO-1 to generate loopy locomotion. We were also able to rescue the suppression by expressing UNC-80 in the cholinergic motor neurons, using the *unc-17* promoter (Figure 4-9). This same promoter is used to drive the expression of the nRHO-1* transgene, indicating that *unc-80* is required presynaptically in the same cells as RHO-1* for the generation of loopy locomotion.

We tested the efficiency of rescue using a dispersal assay, and found that expression from both of these promoters was sufficient to restore chemotaxis in nRHO-1* mutant animals (Figure 4-12).

We have been unable to obtain rescue using heatshock expression of UNC-80, so cannot rule out a developmental role for UNC-80 in the nervous system. We have seen little expression of the GFP or mCherry tagged forms of the UNC-80 minigene following heatshock in animals carrying these constructs (Figure 4-11). It may be that these large transgenes do not express well from the heatshock promoter, and that insufficient protein is being expressed to rescue the phenotype. Additional experiments, perhaps

utilising other conditional expression systems (see Chapter 7) may allow us to answer the question of whether UNC-80 is required for the development of loopy locomotion. We may also be able to answer this question by examining heat-shock driven rescue of other components of the NCA complex, such as NCA-1, which is smaller than UNC-80 and may express at higher efficiency from the heatshock promoter.

We have also been unable to rescue the loopy locomotion phenotype by expressing *unc-80* from the *acr-2* promoter; this promoter has a largely overlapping expression pattern to *unc-17*, and so additional experiments, injecting our rescuing constructs at higher concentration, may reveal that this lack of rescue is due to inefficient expression. Alternatively, lack of rescue may result from subtle differences in the expression pattern of these two promoters which may in turn shed light on the cell-specificity of UNC-80.

A large body of literature points to a relationship between *unc-80* and *unc-79*, another large, unclassified gene (Sedensky and Meneely 1987; Morgan, Sedensky et al. 1988; Morgan, Sedensky et al. 1990; Humphrey, Hamming et al. 2007; Pierce-Shimomura, Chen et al. 2008; Yeh, Ng et al. 2008). They appear to function in the same pathway with respect to anaesthetic sensitivity, locomotion and localisation of the NCA-1 and NCA-2 ion channels.

The work in this thesis demonstrates that *unc-79* mutants are also able to suppress the loopy phenotype of nRHO-1* mutant animals (Figure 5-5). However, to be confident of this result we would like to test additional alleles of *unc-79*, and to generate UNC-79 rescuing constructs. These would also enable us to determine the site of action of *unc-79* with respect to the suppression of nRHO-1* loopy locomotion, but we have reason to believe that UNC-79 is working in the same cells as UNC-80. Rescue experiments will also be important for testing whether the *unc-79* mutation is genuinely able to increase sensitivity to aldicarb (Figure 5-7).

UNC-79 and UNC-80 are two large proteins which do not share any common domains, apart from a predicted armadillo repeat domain (Pierce-Shimomura, Chen et al. 2008), nor do they share homology to any other proteins so far classified. They are however conserved between species, indicating that they may play some important biological function (Humphrey, Hamming et al. 2007). Both are expressed in neurons in *C. elegans* (Jospin, Watanabe et al. 2007; Yeh, Ng et al. 2008) and their homologues are expressed in the nervous systems of Drosophila and mice (Humphrey, Hamming et al. 2007). Loss of function of the Drosophila homologue of *unc-79*, dunc79, causes a hesitant walking phenotype reminiscent of the fainting locomotion observed in *unc-79* mutants in *C. elegans* (Humphrey, Hamming et al. 2007). This represents quite striking conservation of

function between two distantly related species. This hesitant walking phenotype is also observed in mutants of the single Drosophila homologue of NALCN, known variously as narrow abdomen or α1U (for unusual α1 subunit). Loss-of-function of this gene also disrupts the circadian rhythms of flies, reducing their activity in anticipation of daylight (Lear, Lin et al. 2005; Zhang, Chung et al. 2010). It is tempting to see disruption of circadian rhythms as further evidence of a role for NALCN and its associated factors in the regulation of rhythmical behaviours.

Complete loss of function of the mouse homologue of UNC-79, mUNC79 (also known as Leightweight (Lwt)) is lethal, with the mice dying 24 hours after birth due to interupted respiratory rhythms (Speca, Chihara et al. 2010). Loss of NALCN in mice is also lethal with the animals dying from similarly interupted respiration (Lu, Su et al. 2007). This suggests a potential role for NALCN and munc79 in regulating respiration, which is also a rhythmical behaviour.

Early work on *unc-80* and *unc-79* mutants focused on their role in the response to general anaesthetics. *unc-80* and *unc-79* were shown to be hypersensitive to the halothane class of general anaesthetics (Sedensky and Meneely 1987; Morgan, Sedensky et al. 1988), which bucked the trend at the time of mutants affecting anaesthetic sensitivity affecting all classes equally. This was a very exciting development, because it indicated that the target of these drugs might be specific neuronal proteins, as opposed to some general lipid-membrane disrupting mechanism proposed by contemporary theories. The Drosophila homologue of *unc-79*, dunc79, has also been shown to be hypersensitive to halothane (Humphrey, Hamming et al. 2007), indicating a conservation of function between species. Lwt/+ heterozygotes are hypersensitive to the intoxicating effects of ethanol (Speca, Chihara et al. 2010), an effect also seen in *unc-79* and *unc-80* mutant animals as measured by an increase in swimming activity (Speca, Chihara et al. 2010).

Early work on *unc-79* and *unc-80* mutants isolated a number suppressors of hypersensitivity to halothane, including *unc-9* (Sedensky and Meneely 1987; Boswell, Morgan et al. 1990) and *unc-1* (Morgan, Sedensky et al. 1990; Rajaram, Sedensky et al. 1998). *unc-1* and *unc-9* mutants possess a 'kinker' mutation ('The animal moves or rests with uncharacteristic muscle spasms causing loss of smooth sinusoidal motion or body posture. Movement is often characterized by severe bending motions, more sharply angled and/or much deeper than stereotypical sinusoidal body bends of the control animals' Wormbase via Fernandes, J and Yook, K); other kinker mutations *unc-7* and *unc-24* also suppress the hypersensitivity of *unc-79* and *unc-80* to halothane. *unc-7* and *unc-9* encode stomatins, which form part of the gap junctions. Gap junctions

regulate the flow of ions in the nervous system, while *unc-1* and *unc-24* encode innexins, which associate with ion channels and lipid rafts. This places *unc-79* and *unc-80* into pathways which regulate neuronal activity and behaviour, as well as a connection to mutations which cause kinking and coiling behaviour. *unc-8* mutations also suppress the hypersensitivity of *unc-80* and *unc-79* mutants, and *unc-8* is potentially part of a mechanosensory complex involved in proprioception (Tavernarakis, Shreffler et al., 1997).

The double mutant *unc-79*;*unc-80* is only slightly more sensitive to anesthetic than either of the single mutants, and these experiments suggested that *unc-79* and *unc-80* act in the same pathway, and placed *unc-79* genetically upstream of *unc-80*. In our experiments we see that both *unc-80* and *unc-79* suppress the action of nRHO-1* in loopy locomotion placing them downstream of RHO-1 (Figures 4-6 and 5-5). It would be instructive to see whether mutations in any of *unc-1*, *unc-7*, *unc-9* or *unc-24* interact with our nRHO-1* transgene, or whether triple mutants (such as nRHO-1*;*unc-80;unc-1*) would have restored loopy locomotion due to suppression of the effects of the loss of *unc-80* function. Preliminary data from the lab suggests that *unc-1* interacts with *dgk-1*, a known target of RHO-1 signalling (S. Nurrish, personal communication.)

Other targets of general anasethetic have subsequently been identified. *goa-1* mutants are resistant to the effects of anaesthetic (van Swinderen, Metz et al., 2001), while *egl-30*(lf) mutants are hypersensitive (Hawasli, Saifee et al., 2004). These proteins also regulate the activity of RHO-1 and the levels of neurotransmitter release. Syntaxin (*unc-64*) mutants have a range of anaesthetic phenotypes depending on the specific mutations, suggesting a role for the core release machinery in anaesthetic response (van Swinderen, Saifee et al., 1999). The mechanism of general anaesthesia is still not well understood, and the identification of a genetic interaction between *rho-1* and *unc-79* and *unc-80* may provide a fresh perspective for investigating this medically important phenomena. It would also be useful to test the sensitivity of nRHO-1* animals to halothane. It is also interesting to note that screens for response to anaesthetic in worms use observations of locomotion - body bends, dispersal assays - and this may explain some of the overlap between locomotion mutants and anaesthetic response.

5.16 - *nca-1* and *nca-2* single mutants suppress the loopy locomotion of nRHO-1* animals

While the effects of *unc-79* and *unc-80* on anaesthetic sensitivity were being investigated, a further class of fainter mutants was identified. Loss of function of both *nca-1* and *nca-2* produces a fainting locomotion identical to that of *unc-80* and *unc-79*. These genes

encode the two *C. elegans* orthologues of the mammalian protein NALCN (for Sodium (Na+) Leak Channel, Non-selective). NALCN was first identified as a novel four repeat ion channel (Lee, Cribbs et al. 1999), initially classed as a leak channel (Lu, Su et al. 2007), but since shown to be regulated by neuropeptide signalling and Src family kinases (Gilon and Rorsman 2009; Lu, Su et al. 2009; Swayne, Mezghrani et al. 2009; Wang and Ren 2009). It is voltage-independent, at least in the voltage ranges tested so far (Lu, Su et al. 2007). Its putative ion selectivity filter contains a novel EEKE motif, a combination of the EEEE motif of calcium channels and DEKA found in sodium channels, which makes it permeable to calcium, sodium and potassium ions.

We tested whether mutations in the two *C. elegans* orthologues were able to suppress the loopy locomotion of nRHO-1*. Surprisingly, given that the single mutants do not display a fainting locomotion phenotype, both single mutants were able to suppress the loopy locomotion of nRHO-1* animals (Figure 5-5). This the first evidence that *nca-1* and *nca-2* are not completely redundant. It suggests that NCA-1 and NCA-2 have overlapping but distinct activities which cannot be entirely compensated for through the activity of the homologous protein.

5.17 - NALCN-MUNC-80-MUNC79 form a complex in neurons

A number of pieces of evidence suggest that the action of UNC-80 and UNC-79 is mediated, at least in part, through binding to NCA-1 or NCA-2. First, loss of *nca-1* and *nca-2* phenocopies the effects of *unc-80* and *unc-79* mutations with respect to the fainter phenotype and hypersensitivity to halothane (Sedensky and Meneely 1987; Morgan, Sedensky et al. 1988). Secondly, loss-of-function mutations in any of the genes leads to a mislocalisation of the remaining proteins in *C. elegans* suggesting that they play a role in localisation or trafficking of each other in a reciprocal fashion (Humphrey, Hamming et al. 2007; Jospin, Watanabe et al. 2007; Yeh, Ng et al. 2008). Third, by analogy to the mammalian systems, where MUNC80 has been shown to bind to NALCN in a MUNC79 dependent fashion (Lu, Su et al. 2009; Wang and Ren 2009) we anticipate that the *C. elegans* proteins will form a complex, although this has yet to be confirmed by biochemical analysis. We therefore think the major mechanism by which loss of *unc-80* suppresses the loopy phenotype of nRHO-1* mutants is through mislocalisation or misregulation of the NCA-1 and NCA-2 ion channels (Figure 5-24). For simplicity I will refer to this putative UNC-80/UNC-79/NCA-1/NCA-2 complex as the NCA complex.

nca-1, *nca-2* and *unc-80* play a role in synaptic transmission as seen from electrophysiological recordings from body wall muscles in an *nca-1*;*nca-2* mutant animal

(Jospin, Watanabe et al. 2007, Yeh, Ng et al. 2008). The frequency of spontaneous release is either wild-type (Jospin, Watanabe et al. 2007) or decreased (Yeh, Ng et al. 2008), while the amplitude of evoked release was decreased (Yeh, Ng et al. 2008). Interestingly, the recordings of miniature postsynaptic currents in some mutants exhibit near wild-type release, while others show virtually no activity (Jospin, Watanabe et al. 2007; Yeh, Ng et al. 2008). This raises the possibility that we are observing the physiological effects, or causes, of fainting locomotion; animals being assayed may be fixed in one of two states - normal locomotion, or fainting locomotion - which may correspond to the two states of wild-type release, or lack of release.

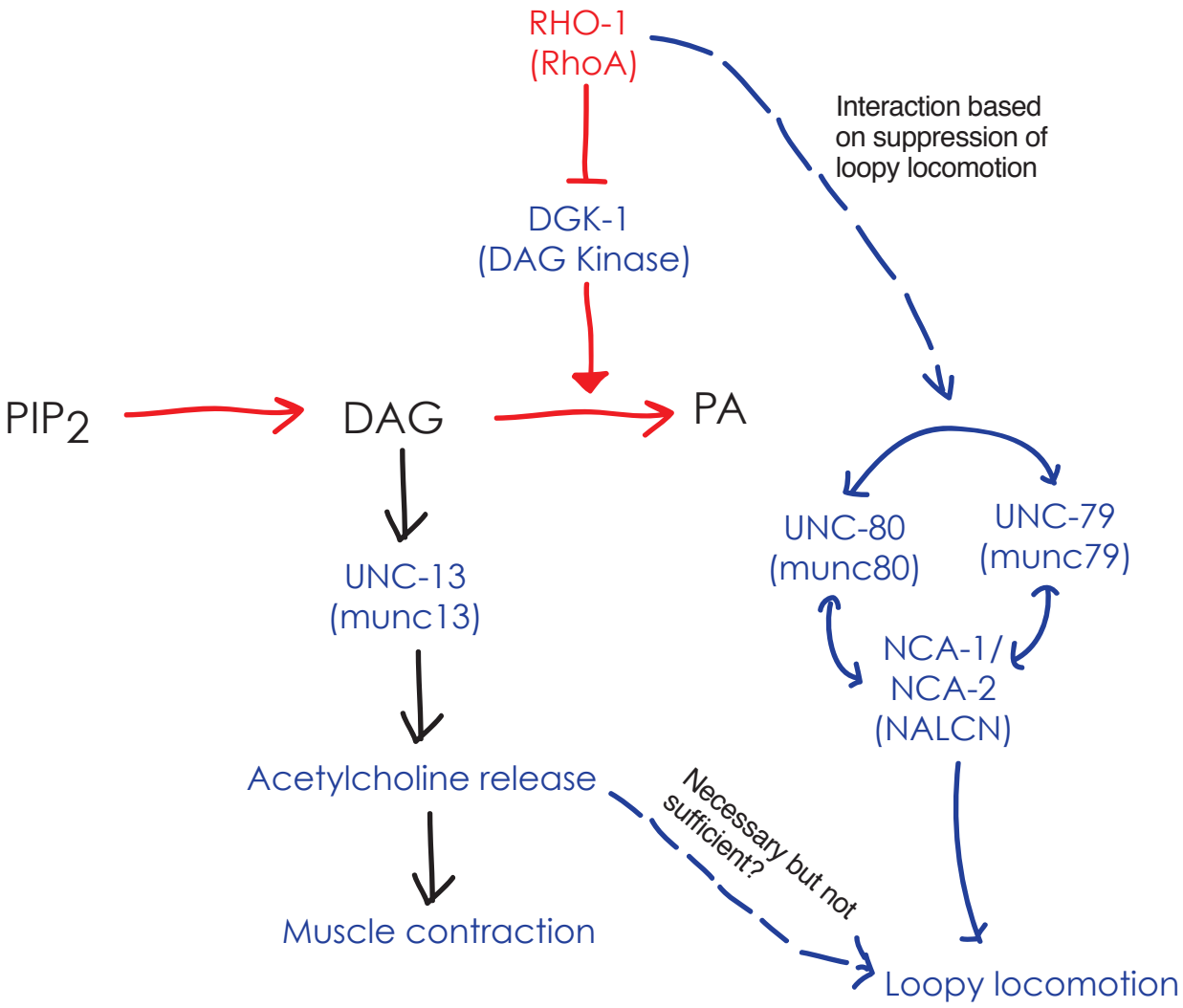

Figure 5-24 The NCA complex is downstream of RHO-1

Loss of the activity of any component of the putatitve NCA complex - the NCA-1 and NCA-2 ion channels, or the potential scaffolding proteins UNC-79 and UNC-80 - is sufficient to suppress the loopy locomotion phenotype of nRHO-1* mutant animals. The loss of any of these proteins has only a partial suppressive effect on the aldicarb release phenotype of nRHO-1* mutants which, along with experiments with the DAG analogue PMA, suggest that the NCA complex acts in parallel (or downstream) of the action of RHO-1 to increase DAG levels in the presynaptic membrane.

Recordings from HSN (neurons involved in egg-laying) using cameleon, a genetically encoded Ca^{2+} sensor, demonstrated a failure to transmit signals to the synapse from the soma in some individuals, while others were capable of normal transmission (Yeh, Ng et al. 2008). This is consistent with the proposed mammalian role for NALCN of enhancing neuronal activity (Lu, Su et al. 2007; Lu, Su et al. 2009; Swayne, Mezghrani et al. 2009). More recently, the NALCN channel has been demonstrated to be sensitive to variations in the extracellular calcium levels (Lu, Zhang et al. 2010). Reduction in extracellular calcium concentrations activate the NALCN-UNC-80 complex in a G-protein dependent manner, leading to an increase in neuronal excitibility (Lu, Zhang et al. 2010).

A number of studies have indicated the wider physiological role of NALCN (and by extension the homologues of UNC-80 and UNC-79) in human health. NALCN plays a role in the release of insulin from the Islets of Langerhans in the pancreas of mice (Swayne, Mezghrani et al. 2009; Swayne, Mezghrani et al. 2010) where it is activated by muscarinic receptors and G-protein signalling. The sensitivity of NCA complex mutants to anaesthetics (Humphrey, Hamming et al. 2007) and ethanol (Speca, Chihara et al. 2010) is significant as these are two major factors influencing human health and medical treatment. The *lightweight* mutant animals also demonstrate an increased preference for ethanol, as well as increased sensitivity. Complete loss of function of NALCN (Lu, Su et al. 2007) or the *unc-79* homologue (Speca, Chihara et al. 2010) in mice is lethal, and mice are thought to die from interrupted respitory rhythms, indicating an essential function for these genes.

Conflicting reports have emerged about a role for NALCN in schizophrenia (Souza, Rosa et al. 2010; Wang, Liu et al. 2010), while a role for the Drosophila homologue in regulating circadian rhythms (Humphrey, Hamming et al. 2007; Zhang, Chung et al. 2010) has led to some suggestions of links to manic depression.

5.17.1 -Rescue experiments hint at dominant negative effects of overexpressing UNC-80 protein in neurons

As described above, we generated a set of constructs for expressing wild-type UNC-80 protein. We obtained rescue of the loopy phenotype of *unc-80*;nRHO-1* animals using these, but it appeared as if the animals had retained a fainting locomotion. To test this, we crossed out the nRHO-1* transgene and observed by eye that *unc-80* mutant animals carrying these constructs retained a fainting locomotion. We saw the same effect in wild-type animals, suggesting that expressing UNC-80 from either the *snb-1* or the *unc-17* promoters had a dominant-negative effect on UNC-80 activity. We also saw that these

constructs failed to rescue swimming behaviour in *unc-80* mutants (Figure 4-13 & 4-15), and induced a reduction in swimming behaviour in wild-type animals (Figure 4-15).

Loss of UNC-80 protein appears to alter the localisation of NCA-1 (Jospin, Watanabe et al. 2007; Yeh, Ng et al. 2008) and we suggest UNC-80 (and potentially UNC-79) may act in a scaffolding role. Scaffolds have been observed to cause defects when both absent or overexpressed. When absent, components in a pathway are not brought together at the correct location in a cell, while ovexpressing scaffolds can lead to the titration of components away from each other, causing a dominant negative effect.

We suggest that overexpression of UNC-80 produces such a dominant negative effect due to titration of components of the NCA complex, and that this causes a similar locomotive phenotype to loss of function of the NCA complex. We may in the future be able to use this dominant negative effect as an assay - we could create constructs expressing fragments of the UNC-80 protein with the aim of disrupting normal NCA complex function, and then biochemically and bioinformatically anaylse those fragments with the aim of determining more about the structure and function of UNC-80.

The size and conservation of UNC-79 and UNC-80 suggest that they may have multiple conserved protein/protein interactions, and it would be interesting to test whether other components of our neurotransmitter release pathway, including RHO-1, EGL-30, UNC-73 and DGK-1 are able to bind to these proteins.

5.18 - NCA complex mutants response to aldicarb and levamisole

5.18.1 -The fainter mutants tend towards hypersensitivity to aldicarb

We tested the response of *nca-1*, *nca-2*, *nca-1*;*nca-2*, *unc-79* and *unc-80* mutants to the acetylcholine esterase inhibitor aldicarb, and the acetylcholine agonist levamisole. These experiments were intended to pharmacologically probe the activity of the nervous system of the mutants and the response of their body wall muscles to acetylcholine as a way to uncover the effects of the mutations on neurotransmission.

unc-79 mutants are more sensitive to aldicarb than wild-type animals (Figure 5-7), and more sensitive than *unc-80* mutants, which also display a slight hypersensitivity to aldicarb (Figure 4-16). However, *nca-1*;*nca-2* double mutants are essentially wild-type for aldicarb sensitivity (Figure 5-10).

The *nca-2* single mutant, while being wild-type in locomotion, displays a strong hypersensitivity to aldicarb (Figure 5-9). The loss-of-function mutant of its paralogue, *nca-1,* displays no aldicarb phenotype (Figure 5-10), while a gain-of-function mutation in *nca-1* leads to aldicarb hypersensitivity (Figure 5-19). This may not indicate a direct role for the NCA-1 channel in acetylcholine release; the gain-of-function allele may be a neomorphic mutation which makes the channel more permable to sodium ions, constitutively depolarising the neurons, or to calcium, initating membrane fusion , causing an increase in the release of neurotransmitter.

Whether these results reflect real differences in the activity of UNC-79, UNC-80, NCA-1 and NCA-2, or is simply a result of differences in the strength or penetration of the two mutations, or additional background mutations, is not clear. Therefore it would be useful to test additional alelles of these genes to see whether this trend continues, or is related in some way to the specific mutations tested here. There is a second deletion mutant of *nca-1*, *tm1851*, a 1213bp deletion, and two of *nca-2*, tm377 (which deletes 355bp of genomic sequence) and *tm1305*, a 794 base pair deletion which overlaps with the gk5 deletion studied here (Figure 5-1), while a number of additional *unc-79* and *unc-80* mutants are also known and could be obtained for testing (Figures 5-1 and 4.4). Testing these additional mutants might give further insight into the aldicarb effects seen in the *nca-2* mutant tested.

However, it remains a possibility that the NCA complex does play a role in acetylcholine release. The increase in aldicarb sensitivity in a *nca-2* mutant may be due to a compensatory increase in the activity of the NCA-1 channel. The differences in the aldicarb sensitivities of *unc-79* and *unc-80* mutants may be due to changes in the localisation or activity of the NCA-1 and NCA-2 ion channels, which are mislocalised in these mutant backgrounds (Yeh, Ng et al. 2008).

To confirm a role for these proteins in acetylcholine release we would like to examine the aldicarb sensitivity of rescued animals. In the experiments conducted so far with the UNC-80 rescuing transgenes, we see an increase in aldicarb sensitivity in an *unc-80* mutant expressing UNC-80 from an *unc-17* promoter, and no change when UNC-80 is expressed from the synaptobrevin promoter. These experiments need to be repeated, and additional rescued lines tested, but if the results with the *unc-17* promoter remain consistent, this increase in aldicarb sensitivity could be attributed to changes in the activity or localisation of the NCA-1 and NCA-2 ion channels.

5.18.2 -nRHO-1* is able to increase sensitivity to aldicarb in NCA complex mutants

We tested whether the increase in acetylcholine release was affected by mutations in the NCA complex genes. *unc-80* mutants only partially suppress the aldicarb hypersensitivity of nRHO-1* animals (Figure 4-22), while *unc-79*;nRHO-1* (Figure 5-15), *nca-1*;nRHO-1 (Figure 5-16) and *nca-2*;nRHO-1* (Figure 5-17) mutants have an aldicarb sensitivity intermediate between nRHO-1* and wild-type. Again, this suggests that there is a small some role for the NCA complex in neurotransmitter release, but also indicates that reduction in release is unlikely to be the main mechanism for suppressing the loopy locomotion of nRHO-1* mutants. Other mutants isolated in our screen also had little or no effect on acetylcholine release and yet had wild-type locomotion (Chapter 3, Figure 3-5).

Preliminary experiments with the UNC-80 transgenes indicate that expressing UNC-80 pan-neuronally in an *unc-80*;nRHO-1* mutant is able to rescue the suppression of acetylcholine release seen in these animals (Figure 4-17), although expression from the unc-17 promoter has no effect in these double mutant animals (Figure 4-17). This may indicate a requirement in cells other than the cholinergic neurons for UNC-80 with respect to the aldicarb sensitivty generated by nRHO-1*, unlike loopy locomotion, which can be successfully rescued with cholinergic expression of UNC-80. This experiments are preliminary, and the data from additional transformed lines will help us address whether differences in rescue are due to physiological effects of expression in different cell types, or simply due to differences in the level of expression between the two transgenes, although all transgenes are expressed at a sufficient level to rescue loopy locomotion.

5.18.3 -Fainter mutants tend towards hypersensitivity to levamisole

The response of animals to aldicarb is a product of the amount of acetylcholine released, and the sensitivity of the muscles to stimulation by acetylcholine. We therefore tested the animals for their response to levamisole, which directly stimulates the body wall muscles. We see that mutants displaying fainter locomotion (*unc-79*, *unc-80* and *nca-1*;*nca-2*) are hypersensitive to levamisole (Figures 5-14, 4-19 and 5-16). This might suggest that there is an overall reduction in acetylcholine release in these mutants, coupled with an increase in the sensitivity of the muscles as part of a homeostatic response. This is consistent with the electrophysiological data obtained from *nca-1*;*nca-2* double mutant animals, and has been observed at the Drosophila neuromuscular junction.

nca-1 single mutants are wild-type in their response to levamisole (Figure 5-16), and *nca-2* mutants remain to be tested. It would be enlightening to determine the levamisole response of *nca-2* mutants to determine whether the cause of the hypersensitivity to

aldicarb is a muscle sensitivity alteration, although we cannot rule out a second site mutation in *nca-2* and rescue experiments would be required to confirm this hypothesis.

We tested whether this change in levamisole response is rescued in a *unc-80* mutant expressing our UNC-80 rescuing constructs. As with the aldicarb phenotype, we see differences between constructs expressing pan-neuronally, which have no effect on levamisole sensitivity, and constructs expressing in the cholinergic neurons, which increase sensitivity to levamisole (Figure 4-21).

5.18.4 -unc-79;nRHO-1* and *unc-80*;nRHO-1* double mutants are resistant to levamisole

While animals displaying fainting locomotion are hypersensitive to levamisole, introducing the nRHO-1* array into these animals causes a reduction in sensivity to levamisole. While nRHO-1* and *unc-80* single mutant animals are hypersensitive to levamisole, the *unc-80*;nRHO-1* double mutant is resistant to levamisole even compared with wild-type animals (Figures 4-19) We see a similar striking change in levamisole sensitivity in an *unc-79*;nRHO-1* double mutant. *unc-79* mutants are hypersensitive to levamisole, but the *unc-79*;nRHO-1* double mutant is resistant (Figure 5-11).

We suggest that loss of the NCA complex function, as regulated by *unc-79* and *unc-80*, may allow for a greater degree of homeostasis to occur at the neuromuscular junction than in wild-type animals. Homeostasis is a mechanism for maintaining activity in biological systems at a predefined set point, such that increases in activity at one point in a system are resisted by decreases at another point (for review of this phenomena in the Drosophila nervous system, see Davis 2006). We speculate that the loss of the NCA complex may facilitate homeostatic effects in the the *C. elegans* nervous system, such that in the presence of high levels of acetylcholine release, mediated by the nRHO-1* transgene, the body wall muscles are able to reduce their response to acetylcholine more than in a wild-type background. We would like to test this hypothesis by generating an *nca-1*;*nca-2*;nRHO-1* triple mutant, entirely lacking in NCA complex activity, which we predict would have a reduced sensitivity to levamisole compared with nRHO-1*, *nca-1* or *nca-2* single mutants.

We also tested whether loss of UNC-80 function is responsible for this reduction in sensitivity to levamisole by assaying the levamisole sensitivity of *unc-80*;nRHO-1* mutant animals rescued with the UNC-80 transgenes. Although we have only conducted this experiment once, these animals appear hypersensitive to levamisole compared with the *unc-80*;nRHO-1* and the nRHO-1* mutant animal (Figure 4-20).

The *nca-1*(gf) mutant animals demonstrate a wild-type levamisole response, however, suggesting that activation of this complex alone is insufficient to affect the activity of the body wall muscles.

If loss of activity of the NCA complex somehow enhances homeostatic regulation, we would predict that loss of the complex would enhance release of neurotransmitter in mutants which have reduced levels of release. *unc-26* (synaptojanin) mutants have reduced levels of spontaneous release; this level of release is increased in combination with loss of *unc-80* or *nca-1*;*nca-2* (Jospin, Watanabe et al. 2007).

5.18.5 -NCA complex mutants respond normally to phorbol ester treatment

One concern is whether mutations in the NCA complex specifically block increased neuronal activity due to nRHO-1*, or if they are able to block any increase in neuronal activity. We tested whether NCA complex mutants are able to suppress the effects of PMA, a phorbol ester and DAG analogue. We reasoned that if these mutants were reducing the overall activity of the nervous system we would see a reduction in their aldicarb sensitivity in response to PMA. We see that with all three fainter mutants *unc-80*, *unc-79* and *nca-1*;*nca-2*, and in the single mutant *nca-1*, stimulation with PMA increases the sensitivity to aldicarb in line with the responses seen in wild-type animals. This indicates that mutations in the NCA complex genes do not prevent all increases in motor neuron activity.

It also suggests that this complex acts in a pathway either upstream of in parallel to that regulated by PMA, and endogenously by DAG. This is consistent with our results which indicate that mutations in the NCA complex have only a partial suppressive effect on the neurotransmitter release phenotype of nRHO-1*, while completely suppressing the loopy phenotype, although they may act in parallel for acetylcholine release with DGK-1 (see later).

Interestingly, in an *nca-2* mutant, PMA does not stimulate acetylcholine release to wild-type levels. We have previously seen high levels of acetylcholine release in the *nca-2* single mutant compared with both the *nca-1* single mutant and *nca-1*;*nca-2* double mutant, and this experiment with PMA also produces a result which is against the pattern seen with other NCA complex mutants. This is most likely due to a second site mutation in this strain, and either further backcrossing or the use of an additional mutant may shed light on this matter.

5.19 - UNC-80 and nRHO-1* play a role in body size

There may be additional points of interaction between the nRHO-1* activity and the NCA complex. We observe a stastically significant decrease in the size of age-matched nRHO-1* animals compared with wild-type controls, (Figure 4-23) which is partially suppressed in an *unc-80*;nRHO-1* double mutant animal (Figure 4-23). The source of this change is unknown; possible reasons may include an overall reduction in growth rate, changes in metabolic rates due to increased activity, or reductions in energy intake due to defects in chemotaxis or feeding.

We also observe that both nRHO-1* and *nca-1*(gf) mutants are highly loopy. (Figure 5-19). This suggests that overactivation of the NCA complex is sufficient to drive loopy locomotion behaviour. Interestingly, these *nca-1*(gf) mutants also become hypersensitive to aldicarb, indicating an increase in acetylcholine release (Figure 5-20).. Since loss of activity of the NCA complex only partially suppresses the excess neurotransmitter release generated by the nRHO-1* transgene, we surmise that this increase in acetylcholine release may be due to the NCA-1 channel becoming highly permeable to either sodium or calcium ions, and inducing neurotransmitter release through depolarisation of the nervous system. This effect may therefore be a neomorphic mutation.

In addition, *nca-1*(gf) mutants display a defect in the Exp step of defecation, similar to that seen in nRHO-1* mutants (Figure 5-23). This step is regulated by the release of the neurotransmitter GABA, and this observed defect suggests that this may be regulated by the NCA complex and RHO-1.

Taken together, these additional phenotypes suggest that the NCA complex and RHO-1 may combine to regulate a number of processes in *C. elegans*.

5.20 - Loopy locomotion and fainting may be part of different pathways

We observed that while the loopy phenotype of nRHO-1* is suppressed in an *unc-80* background, these double mutants retain the fainting locomotion exhibited by *unc-80* mutant animals. *unc-80* mutants have a number of locomotive defects, including a fainting locomotion on solid surfaces and a reduction in swimming behaviour in a liquid medium. If an integrated model of *C. elegans* locomotion is correct (Berri, Boyle et al. 2009), then these represent different aspects of the same phenotype .

When we reintroduce a rescuing transgene into *unc-80*;nRHO-1* mutant animals, we completely rescue the loopy behaviour (Figures 4-9 and 4-12). However, animals

expressing even a pan-neuronal UNC-80 transgene appear to retain the fainting locomotion (see Movie 4-7) on a solid surface. This suggests that there is a difference in the requirement for UNC-80 in mediating loopy locomotion and and preventing fainting. There may be a non-neuronal component to fainting behaviour not rescued by this transgene, or the level of expression from this transgene may be insufficient to rescue fainting.

We also examined the swimming phenotype of *unc-80* animals carrying these rescuing transgenes (Figures 4-13 and 4-15). This demonstrates that animals carrying the UNC-80 transgenes, under either a pan-neuronal or *unc-17* promoter, retain some of the swimming defect of *unc-80* mutants, even in the absence of the nRHO-1* transgene. Interestingly, the *p.unc-17*-driven transgene appears to restore more wild-type behaviour than the *p.snb-1*-driven transgene (see Movies 4-16 and 4-17).

One possibility is that the *p.snb-1* transgene is having some dominant negative effect on behaviour; to test this we crossed these transgenes into a wild-type background, and saw that they were able to induce some defects in swimming in wild-type animals (Figures 4-13 and 4-15). If UNC-80 is acting as a scaffold, we may be observing dominant negative effects of overexpression. Further experiments with varying levels of transgene expression, and by examining rescue in unc-79 and nca-1;nca-2 mutant animals will shed further light on this differential requirement of the NCA complex in fainting and loopy behaviour.

5.21 - The NCA complex may be regulated by PIP_2

unc-79, *unc-80* and *nca-1*;*nca-2* mutants increase the frequency of spontaneous release in hypomorphic *unc-26* mutants (Jospin, Watanabe et al. 2007). They also partially rescue the locomotion defect in animals carrying a hypomorphic allele of *unc-26* (Jospin, Watanabe et al. 2007), and increase the number of synaptic vesicles present in presynaptic terminals (Jospin, Watanabe et al. 2007). UNC-26 is a PIP_2 phosphatase, and the *unc-26* hypomorphic mutants have an increase in PIP_2 levels. This can be mimicked by overexpressing PPK-1, which encodes a PI4P5 kinase, which generates PIP_2. *unc-80* mutants are also able to suppress the locomotion defects of PPK-1 (overexpression) animals (Jospin, Watanabe et al. 2007), suggesting a link between *unc-80* and PIP_2 levels. *unc-80* mutants fail to rescue null alleles of *unc-26*, suggesting that they cannot bypass the endocytosis defect in these more severly affected mutants.

PPK-1 encodes a PI4P5 kinase, which generates PIP_2, while synaptojanin encodes a lipid phosphatase which removes PIP_2 from the presynaptic membrane. PIP_2 is an

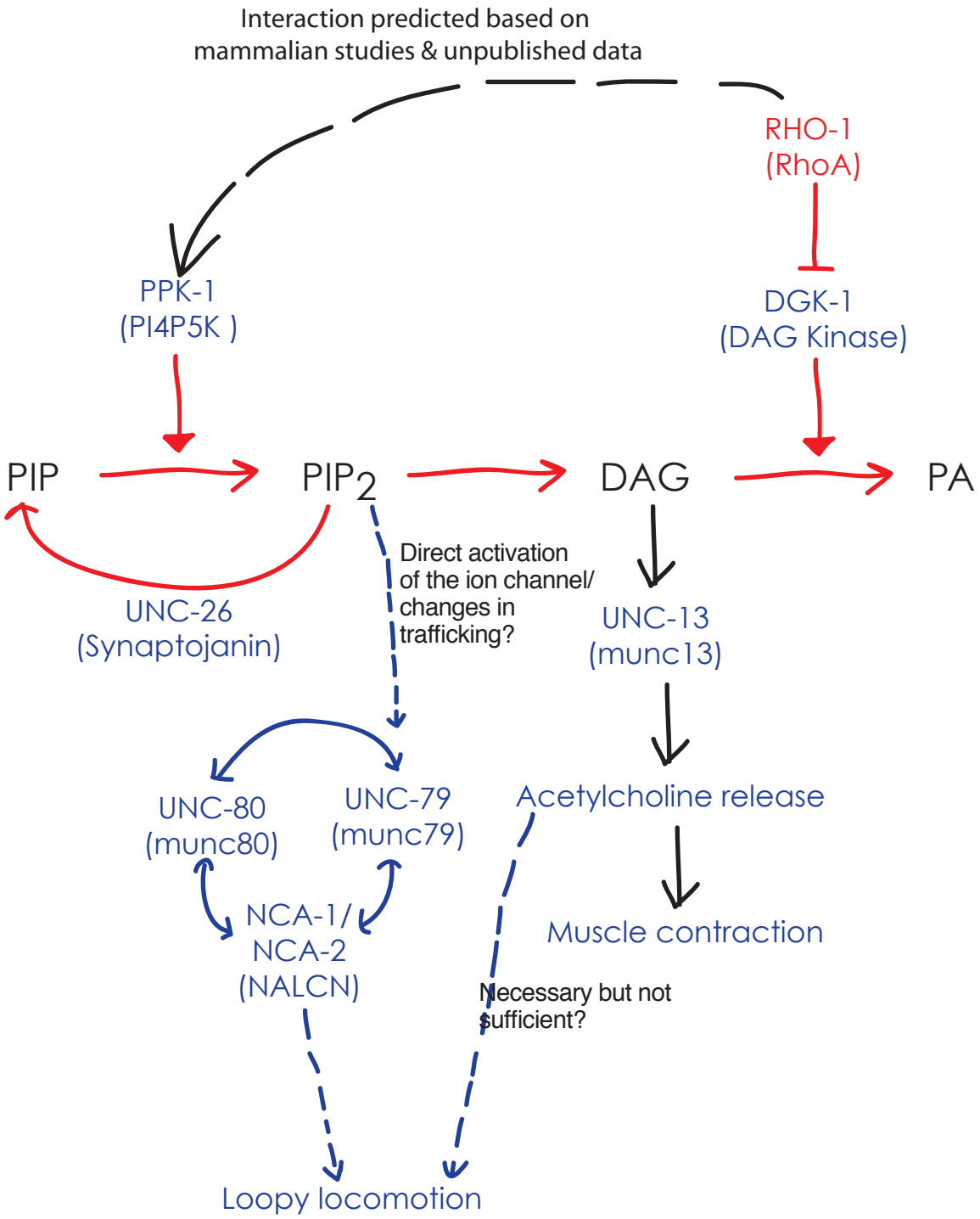

Figure 5-25 The NCA complex may be regulated by PIP_2

unc-80 mutants are able to suppress the behavioural effects of either loss of function *unc-26* or PPK-1-overexpressing animals. This suggests that the NCA complex may be regulated either directly or indirectly by PIP_2. RhoA is able to bind to an activate PI4P5K, and we suggest a model in which excess RHO-1 activity stimulates production of PIP_2, driving the activity of the NCA complex and generating loopy locomotion.

activator of ion channel activity, the lipid from which DAG and IP_3 are generated, and an important marker of membrane domains in the presynaptic membrane (Niggli 2005). It has been proposed that excess PIP_2 may misregulate the localisation or activity of the NCA-1 and NCA-2 ion channels (Jospin, Watanabe et al. 2007).

RhoA is known to enhance the activity of PI4P5K, and subsequently the production of PIP_2, through activation of Rho kinase (Oude Weernink, Schulte et al. 2000; Santarius, Lee et al. 2006) and through direct binding to PI4P5K (Ren, Bokoch et al. 1996). Unpublished data from our laboratory has demonstrated binding of RHO-1 to PPK-1 in COS cells (Dr Muna Elmi, personal communication). We propose that this activated RHO-1 stimulates activity of PPK-1, leading to an excess production of PIP_2 (Figure 5-25). We hypothesise that excess PIP_2 either directly activates the NCA complex, or causes a change in the trafficking of the complex; with either mechanism leading to the changes in neuronal activity which produce loopy locomotion.

5.22 - The F25N mutation in RHO-1* bypasses the requirement for *unc-80* in loopy behaviour

During experiments to understand the relative importance of pathways mediated by *dgk-1* and those mediated by *unc-80*, we transformed *unc-80* mutant animals with a mutant version of RHO-1 which contains the F25N mutation. When expressed from either the *unc-17* neuronal promoter, or from the heatshock promoter, expression of this version of RHO-1 generated loopy locomotion in *unc-80* mutant animals.

RHO-1 increases neuortransmitter release through inhibition of DGK-1 and via a DGK-1 independent pathway, and we therefore tested whether the NCA complex represents this DGK-1 independent pathway. We tested whether a heat-shock driven version of RHO-1(F25N)* (a mutation which blocks binding to DGK-1) was able to induce loopy locomotion in the presence of the nRHO-1* transgene. Following heatshock, the *unc-80* animals carrying both transgenes became highly loopy. This suggests that it is not the lack of binding to a specific effector, such as DGK-1, which is responsbile for the ability of this mutation to bypass the requirement for UNC-80 (Figure 5-26).

This result demonstrates that NCA complex mutants do not have a general neuronal defect which makes loopy locomotion impossible, and b) either there is a third pathway independent of both DGK-1 and the NCA complex which can generate loopy locomotion and increase acetylcholine release, or that the F25N mutation increases signalling through the exisiting pathways such that it can bypass the loss of NCA complex function.

It will be informative to perform similar experiments in an *unc-79* mutant background; following our previous work we would predict that the *unc-79,* would also fail to suppress loopy locomotion generated by the RHO-1(F25N)*, as we believe that *unc-80* and *unc-79* work through a common pathway.

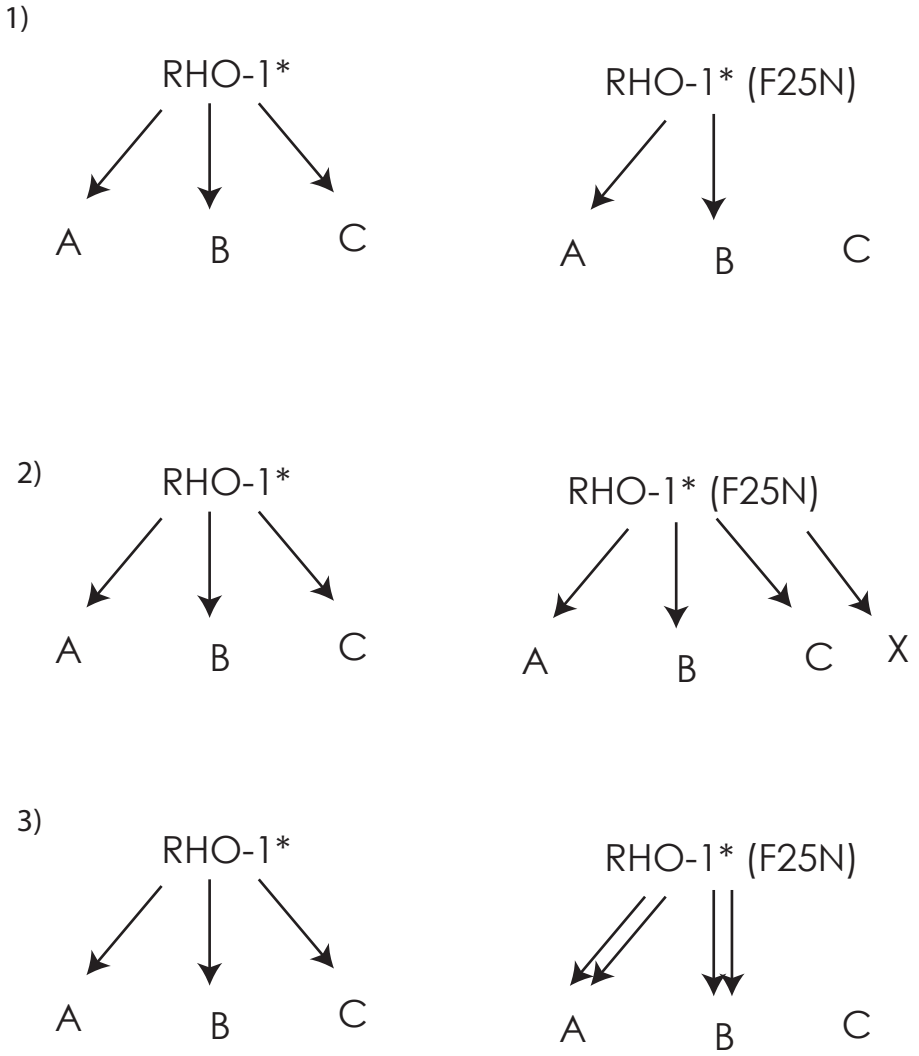

Figure 5-26 The F25N mutation bypasses the requirement for UNC-80 in loopy locomotion

RHO-1(F25N)* is able to drive loopy locomotion in a *unc-80* mutant background. We proposed three models for this action. 1) Loss of binding to an effector bypasses the requirement for UNC-80. 2) The F25N mutation induces binding to a novel effector which independently generates loopy locomotion. 3) The loss of binding to an effector allows excess signalling through existing pathways. Model 1 has been discounted as the F25N mutation bypasses the requirement for UNC-80 even in the presence of the F25 form of RHO-1. We cannot yet distinguish between the other two models.

5.23 - More quantitative methods for assaying the effects of loss-of-function of the NCA complex are required

While the fainting locomotion of *unc-79*, *unc-80* and *nca-1*;*nca-2* mutants is well described, it still remains somewhat mysterious. We can identify a number of different

phenotypes in these mutant animals which may be related. First, fainting locomotion, where animals remain at rest for long periods of time (Figure 4-1). Secondly, a reduction in locomotion as measured in the dispersal assay (Figure 4-7), which may be related to reduced rates of locomtion, or a defect in chemotaxis. Third, defects in two assays of swimming behaviour - mean thrashes after recovery, and initial thrashing (Figures 4-13, 4-14, 4-15, 5-2, 5-3 and 5-4).

We were interested in whether our rescuing constructs for UNC-80 were able to restore wild-type swimming behaviours, and found that animals rescued either in the entire nervous system or in the cholinergic neurons still displayed a swimming defect (Figures 4-13 and 4-15), suggesting that either that UNC-80 is required in cells other than neurons for the reduction of fainting behaviour, or that the absolute levels of UNC-80 expression are important. We assayed whether these constructs were able to cause swimming defects in wild-type animals, and found a reduction in swimming behaviour (Figure 4-15). This strongly suggests a dominant-negative effect of these constructs, which is consistent with a scaffolding or trafficking role for UNC-80.

We would like to expand these experiments by overexpressing UNC-79 rescuing constructs in a wild-type background to look for defects in swimming behaviour.

5.24 - Conclusions and future work

We have demonstrated that loss-of-function mutations in the genes *unc-79*, *unc-80*, *nca-1* and *nca-2* can suppress the loopy locomotion behaviour associated with nRHO-1*, while having only a small effect on the increase in neurotransmitter release generated in nRHO-1* mutant animals.

The protein products of these genes are thought to form a novel, regulated ion channel complex, which is located at perisynaptic regions in the neurons of *C. elegans*, and plays a role in the propogation of neuronal signalling in certain neurons. We also have evidence that loss of function of *unc-80* suppresses a reduction in the size of nRHO-1* animals, suggesting multiple points of interaction between these genes.

Evidence from the literature suggest that this NCA complex may act downstream of PIP_2, and we propose that regulation of PPK-1, a PI4P5K by RHO-1 may cause misregulation or mislocalisation of this complex, leading to a generation of loopy locomotion.

Our results indicate that a novel, conserved ion channel complex, involved in many biologically interesting processes, such as the response to ethanol and general anaesthetics, and responsible for similar phenotypes in distantly related organisms incuding flies and worms, is regulated by the action of RHO-1.

Evidence strongly suggests a link between the NCA complex and the overproduction of PIP_2 (Jospin, Watanabe et al. 2007), and this is part of our working hypothesis for the link between RHO-1 activity and changes in the NCA complex. Our model suggests that PPK-1 functions downstream of RHO-1 in the nervous system. To further investigate this link, we are currently conducting experiments to reduce the activity of PPK-1 in adult neurons using RNAi. Several methods allow cell-targetted RNAi in *C. elegans*, and we are expressing complimentary sequences of PPK-1 cDNA, one from a cell-specific promoter and the second from a heat-shock to generate double-stranded RNA in adult animals. Preliminary experiments suggest that reducing PPK-1 activity in nRHO-1* animals by RNAi is able to suppress the loopy locomotion phenotype of nRHO-1* (M. Elmi, personal communication.)

We would also predict that if PPK-1 is regulated by RHO-1, PIP_2 levels would increase in the nRHO-1* animals. We could test this using PIP_2 reporters to measure the levels of PIP_2 in nRHO-1* animals and following heat-shock activation of RHO-1.

The screen which identified *unc-80* as a suppressor of RHO-1* was conducted based on the loopy locomotion phenotype. While mutations in *unc-80* and the rest of the NCA complex strongly suppress loopy locomotion, they only partially suppress the aldicarb hypersensitivity of nRHO-1* mutant animals, and we have seen this with separation between locomotion and acetylcholine release in other mutants isolated from our screen (Chapter 3). This strongly suggests that our original hypothesis that high levels of acetylcholine release are responsible for loopy behaviour is oversimplistic, and that we are in fact looking for a second factor which promotes loopy behaviour. We were interested in whether there was a general reduction in neuronal activity in NCA complex mutants, but our experiments with PMA (summarised in 5.18.5) suggest that this is not the case, at least at a gross level of activity. This lack of a straightforward explanation, coupled with the successful rescue of the loopy phenotype with exogenous UNC-80 leads to the question: 'What mechanism requires the NCA-1 and NCA-2 ion channels to allow the nRHO-1* transgene to stimulate loopy locomotion?' I would like to propose a number of hypotheses which can be subjected to further investigation.

Given the isolation of mutations in *unc-31*, which has an established role in the exocytosis of dense core vesicles (see Section 3.14.8.1), there may be a role for neuropeptide release in the production of loopy locomotion. This neuropeptide release would provide a second factor to modulate the muscle response to high levels of acetylcholine release, perhaps acting in a homeostatic fashion. This explanation would go some way to explain the mechanism by which presynaptic changes affect levamisole response in the nRHO-

1*;unc-80 and nRHO-1*;unc-79 double mutant animals (5.18.3 and 5.18.4). To test this hypothesis we could attempt to assay neuropeptide release in the various mutant backgrounds using tagged neuropeptides (Sieburth, Madison et al 2007). Physiologically, the release of these peptides could also be part of a mechanism to regulate turning behaviour as a component of locomotion, for instance in the regulation of chemotaxis. The NALCN ion channel is regulated by the neuropeptide Substance P (Lu, Su et al. 2009), and it may be that a neuropeptide, whose release requires UNC-31 activity, is involved in the regulation or activity of the NCA complex in *C. elegans* (Figure 5-27).

A second hypothesis involves the relationship between the NCA complex and unc-8, a proposed mechanosensory channel. It could be that the NCA complex represents part of the proprioceptive stretch receptor complex long hypothesised to regulate body posture. Overactivation of this complex by RHO-1, possibly by increasing levels of PIP2, might directly lead to changes in locomotion; again, in a physiological situation, this could be part of the regulation of search behaviours. The NCA complex could also be a regulator of stretch response, for instance through the release of neuropeptides as described above. Loss of this stretch receptor could lead to a failure to propogate waves successfully, leading to what we observe as a fainting phenotype.

A further possibility involves the role that the NCA complex appears to play in regulating rhythmical behaviours. A recent publication suggests that an NCA-1 homologue acts as a central pattern generator (CPG) controlling breathing in a snail (Lu and Feng 2011). Again, misregulation of this CPG could lead to an increase in the rate of wave production; loss could lead to fainting behaviour.

5.24.1 - Future work

A large network of regulated G-protein signalling pathways have been shown to control acetylcholine release in *C. elegans* (Perez-Mansilla and Nurrish 2009), and EGL-30 (Gαq), GOA-1 (Gαo/i) and GPA-12 (Gα12) are known to converge on RHO-1 (Figure 5-27). We will generate double mutants between these G-proteins and the NCA complex mutants to test whether loss of activity of the NCA complex is able to suppress the hyperactive locomotion and increased neurotransmitter release phenotypes of *egl-30* (gf) and *goa-1*. Subsequently we can use mutations in other members of this signalling complex, such as EGL-8 (PLCb) and UNC-73 to epistatically place the NCA complex into our existing pathways. This would be the first example of this G-protein signalling network regulating the function of an ion channel in *C. elegans* neurons. G-proteins regulate ion channel function in mammalian neurons and, if this finding is

upheld, it would bring the *C. elegans* nervous system even closer as a model organism to the the mammalian system (Perez-Mansilla and Nurrish 2009).

Based on our work with the *nz110* suppressor which may due to a mutation in *unc-31* (see Section 3.14.8.1), we will examine the potential for a role of the NCA complex in the release of neuropeptides. We would also like to look at the localisation of the NCA complex in nRHO-1* mutant animals using our GFP- and mCherry-tagged rescuing transgenes of UNC-80. We would like to confirm that the loss of the ion channel components of the complex is the source of both fainting locomotion and the suppression of nRHO-1* loopy behaviour by assaying the effects of an NCA-1 rescuing transgene which has recently been generated in the lab.

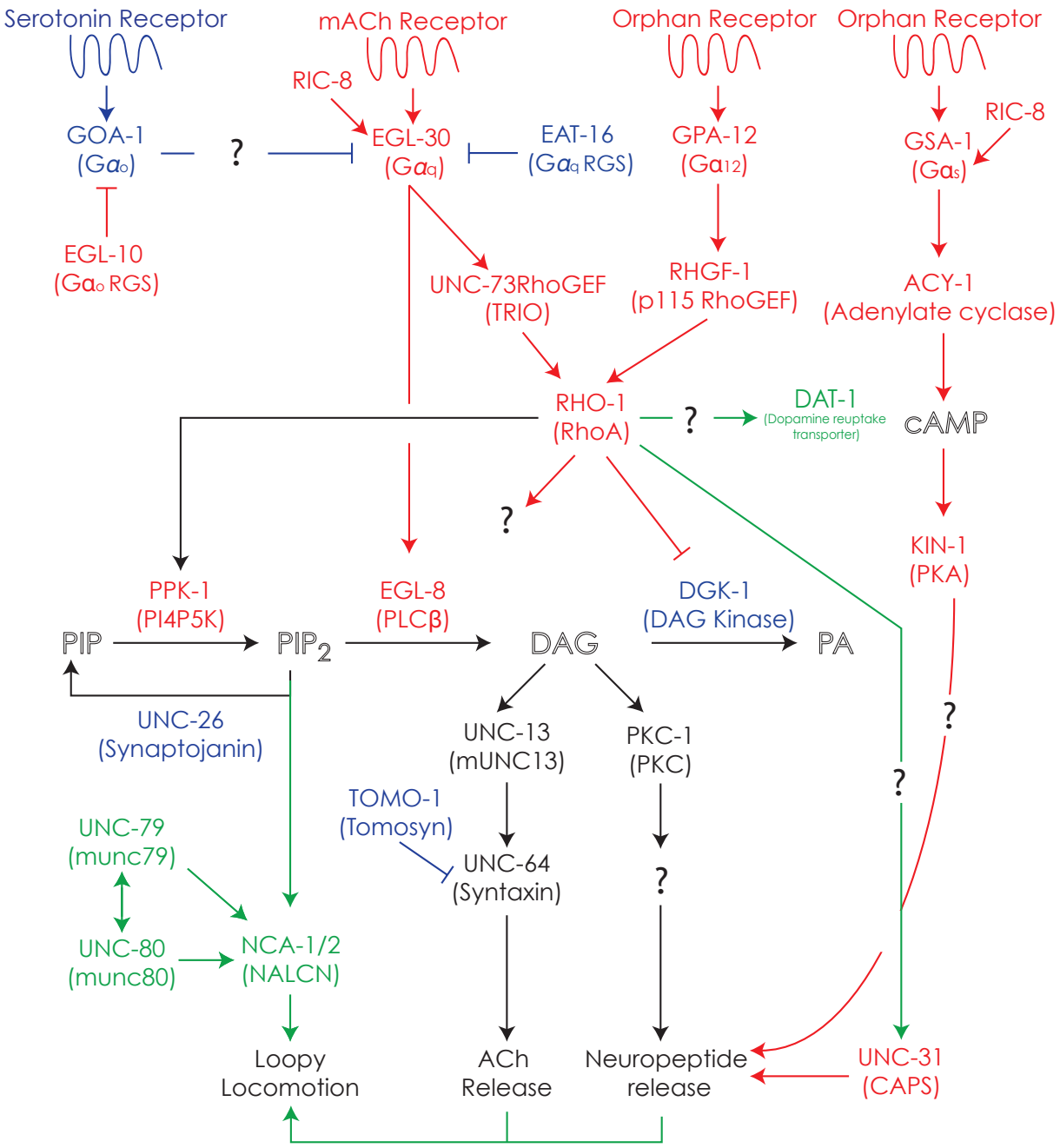

Figure 5-27 The NCA complex and neuropeptide release are required for loopy locomotion induced by nRHO-1*

Loss of any components of the NCA complex in *C. elegans* suppresses the loopy locomotion phenotype induced by nRHO-1*. Mutations in the NCA complex also suppress mutations associated with excess PIP_2 levels, putting the NCA complex downstream of PPK-1, which may be regulated by RHO-1*. Mutations in *unc-31* (CAPS) are also able to suppress loopy locomotion (Chapter 3), suggesting a role for neuropeptide release in loopy locomotion, possibly through regulation of the NCA complex, homologous to the action of substance P on the mammalian homologue NALCN. Mutations in *dat-1* also appear to suppress loopy behaviour (Chapter 3). These mutations have only a small effect on acetylcholine release, suggesting that they act in parallel pathways. However, our model suggests that high levels of acetylcholine release are necessary but not sufficient for loopy locomotion.

Green arrows and protein names relate to interactions which drive loopy behaviour.

6 - SYNTAXIN MAY BE REGULATED BY A NOVEL APKC PHOSPHORYLATION

6.1 - Introduction

The release of neurotransmitter in *C. elegans* is tightly regulated, and part of a complex network of interlinked G-proteins signalling pathways (Perez-Mansilla and Nurrish 2009), many of which converge on nRHO-1* (Chapters 3-5).

The pathways examined so far extend from the reception of neuromodulatory signals, through changes in DAG levels at the presynaptic membrane, to changes in priming of synaptic vesicles. Further regulation occurs at the level of exocytosis.

For example, fusion is mediated, at least in part, by the SNARE complex, (see section 14.2 for a detailed introduction.) Syntaxin (UNC-64), an important member of the SNARE complex, interacts with mUNC-13 (UNC-13), one of the key diacylglycerol (DAG) binding proteins whose localisation is regulated by the activity of RHO-1 in the worm nervous system.

A key regulator of syntaxin is the protein Tomosyn (*Tom-1*) (Section 1.4.3). Tomosyn binding is able to dissociate the binding of munc18 from syntaxin (Fujita, Shirataki et al. 1998), disrupting a key step in vesicle priming, and tomosyn acts as an inhibitor of invoked, calcium-dependent neurotransmitter release *in vitro* (Fujita, Shirataki et al. 1998; Baba, Sakisaka et al. 2005). In *C. elegans*, the single tomosyn homologue, *tom-1*, has been identified as an endogenous inhibitor of neurotransmission (Dybbs, Ngai et al. 2005). *tom-1* mutants have a higher evoked release as measured electrophysiologically in *C. elegans*; this appears to be as a result of increased numbers of primed vesicles rather than overall structural changes to the nervous system (Gracheva, Burdina et al. 2006). Loss of *tom-1* is able to overcome some of the defects in neurotransmission observed in an *unc-13* mutant animal (Gracheva, Burdina et al. 2006; McEwen, Madison et al. 2006). Tomosyn also plays a role in the release of neuropeptides in *C. elegans* (Gracheva, Burdina et al. 2007; Gracheva, Burdina et al. 2007).

Tomosyn is structurally related to the Drosophila protein lethal giant larvae (LGL) with which it shares a similar WD40 repeat domain (Fujita, Shirataki et al. 1998), and the yeast homologues of both proteins bind the yeast homologue of syntaxin and function in regulated exocytosis in budding yeast (Lehman, Rossi et al. 1999) (Figure 6-1).

LGL is a tumor suppressor, and competes with the polarity protein PAR-3 to form a complex with the small GTPase CDC-42, Par-6 and an atypical protein kinase C

(Yamanaka, Horikoshi et al. 2003). The Fujita lab at the MRC LMCB has maintained an interest in tomosyn, and they hypothesized that a similar complex might exist for the regulation of neurotransmitter release. Tomosyn is capable of binding to Par-6 and Syntaxin, Par-6 is capable of recruiting atypical protein kinase C, and this turn could act to regulate neurotransmitter release by phosphorylating syntaxin (Figure 6-1).

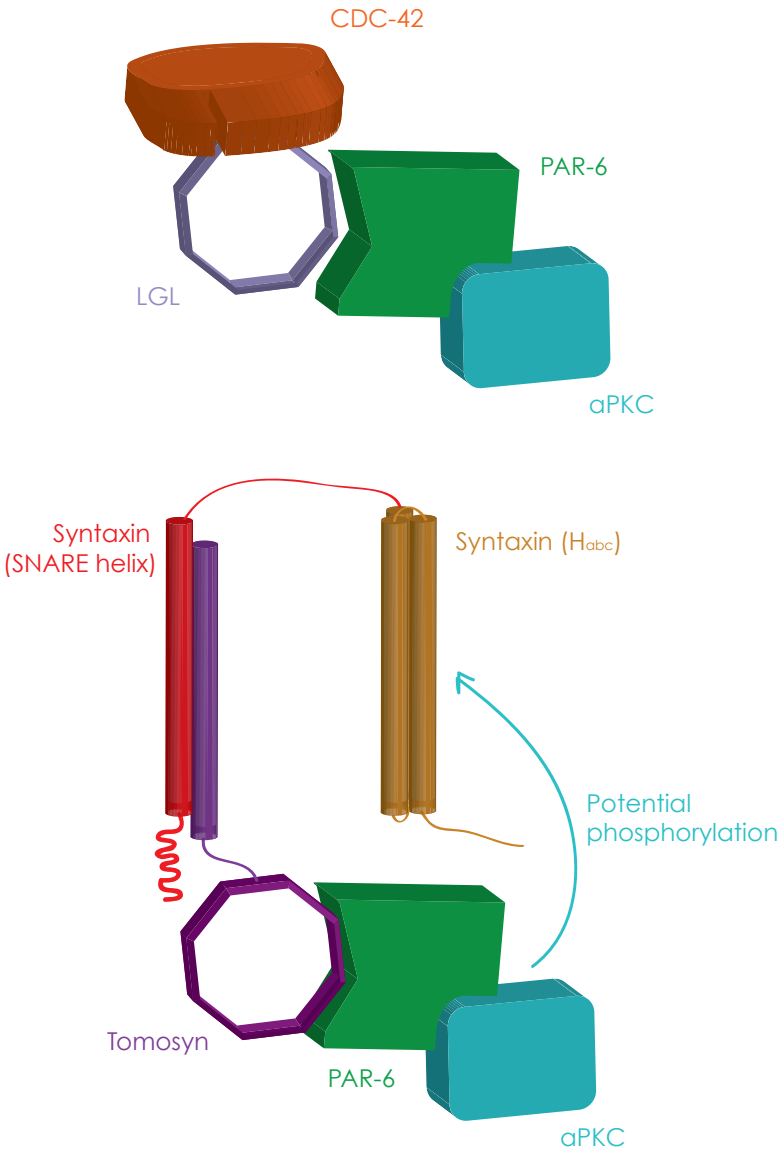

Figure 6-1 Similarities between the Par complex and the Syntaxin/tomosyn complex

Tomosyn, a syntaxin binding partner (dark purple), resembles LGL (purple), one of the constituents of the polarity complex. Both contain a WD40 domain (purple octagon), which allows interaction with PAR-6 (green). This observation led to the hypothesis that there might be a vesicle fusion complex, involving tomosyn, PAR-6 and an atypical PKC (blue) (B) which is able to regulate the function of syntaxin by phosphorylation.

The Fujita lab identified 4 potential aPKC phosphorylation sites in syntaxin, all of which are conserved in the worm homologue, UNC-64 (Figure 6–2). The potential for an

atypical protein kinase C to phosphorylate each of these in sites mammalian syntaxin was tested in vitro through site-directed mutagenesis of each site. Only one, the most 3' of the four potential threonine residues (T252), was actively phosphorylated by aPKC in vitro (Y. Fujita, personal communication.) No reports currently exist for in vivo evidence of a phosphorylation at this residue, which is conserved in syntaxin homologues involved in regulated exocytosis (Littleton, Chapman et al., 1998). The equivilent site in the Drosophila protein Syntaxin 1 (T254) was found to be mutated to isoleucine in a screen for temperature-sensitive paralysis mutants, and the T254I mutation was thought to reduce regulated exocytosis (Littleton, Chapman et al., 1998).

Syntaxin homologues implicated in constitutive exocytosis have either isoleucine or leucine at this position, and do not interact with synaptobrevin (Littleton, Chapman et al., 1998), and this site is considered as part of a neuron-specific interaction domain involved in fusion (Littleton, Chapman et al., 1998). A more recent investigation of this mutant suggests that in fact a mutation to isoleucine at this residue increases rates of both regulated and constitutive exocytosis (Lagow, Bao et al., 2007), and that T254 acts to slow the rate of exocytosis, while I254 increases opportunities for interaction within the SNARE complex, and therefore increase rate of exocytosis.

MTKDRLSALKAAQSEDEQDDDMHMDTGNAQYMEEFFEQVEEIR
GSVDIIANNVEEVKKKHSAILSNPVNDQKTKEELDELMAVIKR
AANKVRGKLKLIENAIDHDEQGAGNADLRIRK**T**QHS**T**LSRRFV
EVMTDYNKTQTDYRERCKGRIQRQLDIAGKQVGDEDLEEMIES
GNPGVFTQGIITD**T**QQAKQTLADIEARHNDIMKLESSIRELHD
MFMDMAMLVESQGEMVDRIEYNVEHAKEFVDRAVAD**T**KKAVQY
QSKARRKKIIILIVVTILIGFVSLWLIQYIPGI

T = potential aPKC sites
T = only active aPKC site

Figure 6-2 aPKC sites in UNC-64

UNC-64 is the C. elegans homologue of syntaxin, which forms part of the SNARE complex and is a positive regulator of neurotransmitter release. The amino acid sequence is shown here. Syntaxin contains four potential sites of phosphorylation by atypical protein kinase C (highlighted) but only that marked in red is an in vitro target.

Whether an as-yet undetected phosphorylation event is occuring at this threonine residue remains to be determined. The Fujita lab speculated that there may be a functional effect of this phosphorylation of syntaxin, and wanted to pursue this investigation in a

whole organism. We therefore began a collaboration to investigate the T252 residue of syntaxin as a potential in vivo aPKC site.

6.2 - Rescuing syntaxin mutants

To test the potential impact of this phosphorylation site, we decided to replace the *C. elegans* wild-type syntaxin (UNC-64) with mutated forms carrying specific mutations to the threonine phosphorylation site.

Three plasmids were generated in the lab for these experiments. Plasmid KP#505 contains the wild-type genomic coding sequence of *unc-64*, covering all three predicted splice variants (Saifee, Wei et al. 1998). This construct also contains 5kb of the *unc-64* promoter region, and 450bp of 3' UTR sequence.

This plasmid was modified by site directed mutagenesis to produce two mutant versions of syntaxin, also controlled by the endogenous promoter.

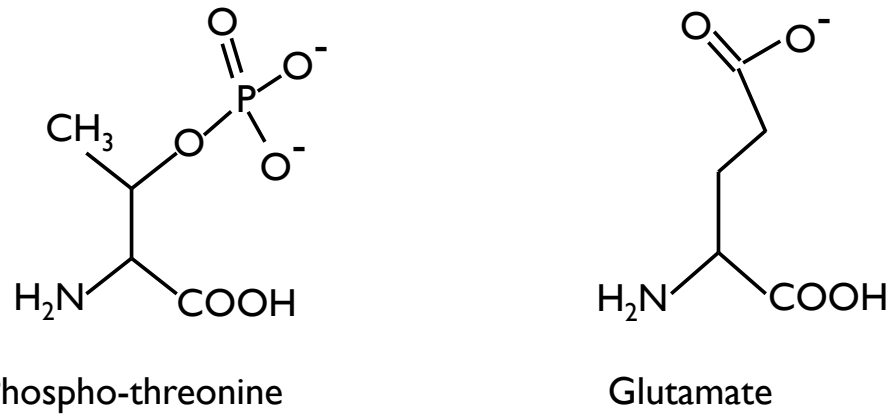

Figure 6-3 Comparision of the structure of phospho-threonine and glutamate

To mimic constitutive phosphorylation at threonine 252 in UNC-64, we substituted the threonine residue for a glutamate residue. The negatively-charged carboxyl group mimics the negative charge added to the theronine residue upon phosphorylation. To generate a mutant incapable of being phosphorylatd at this residue, we also substituted the threonine residue for an alanine residue (not shown.)

Plasmid SJN367 was generated from KP#505 and contains the mutation T252A, which modifies the threonine residue 252, which is the predicted aPKC phosphorylation site, to an alanine residue, which cannot be phosphorylated.

Plasmid SJN368 was also generated from KP#505 by site-directed mutagenesis, and modifes the predicted T252 phosphorylation site to a glutamate residue (Figure 6-3). Both glutamate and threonine are polar and hydrophilic amino acids, but glutamate carries a charge, unlike threonine, and this is intended to mimic the effects of the addition

of a phosphate group at this position in the protein, generating an artificial, constitutively-phosphorylated residue (Figure 6-3). .

Together, these plasmids allow us to test whether we can rescue loss of syntaxin function, and subsequently whether lack of ability to phosphorylate this site, or effective constitutive phosphorylation at this site has an effect in *C. elegans*.

6.2.1 - NM979 is a heterozygous balanced syntaxin deletion mutant

Complete loss of syntaxin function is lethal, either embryonically or at the L1 larval stage, or causes growth arrest at L1 (Saifee, Wei et al. 1998). To conduct these experiments, we used a heterozygous balanced deletion mutant of syntaxin, NM979 (*unc-64*(*js115)/ bli-5(e518*) III), into which we injected the rescuing plasmids along with *ttx-3::*GFP or *unc-122*::GFP as a co-injection markers

To look for rescue we look for lines where all adult animals express the GFP co-injection markers and no longer display the blister phenotype, and where the GFP-negative animals are L1 lethal.

6.2.2 - Loss of endogenous syntaxin in NM979 can be rescued by expression of wild-type syntaxin from a transfected plasmid

The plasmid carrying wild-type syntaxin under its own promoter, KP#505, had previously been injected into NM979 mutant animals (S. Nurrish, personal communication), and a total of 3 stable lines obtained, named QT415, QT416 and QT417. These also contain an *unc-122*::GFP co-injection marker, which expresses GFP in the coelomocytes along the body of the transformed worms, and plasmid KP#282, which expresses CFP-tagged VAMP, under the control of the *acr-2* promoter, as a marker for the structure of the nervous system in these animals.

These three lines produced GFP-positive animals which were successfully able to reach maturity. By eye, the locomotion of these animals appears like that of wild-type animals.

This demonstrates that plasmid KP#505, which expresses wild-type syntaxin from its endogenous promoter, can successfully rescue the loss of endogenous syntaxin function in NM979 mutant animals.

6.2.3 - The syntaxin mutant T252A is able to rescue the lethality of syntaxin-null mutant animals

The non-phosphorylatable form of syntaxin, T252A (Plasmid SJN367) was injected into the strain NM979 at a concentration of 25 ng/µl, along with an *unc-122*::gfp plasmid as a co-injection marker.

We obtained one independent line in which all the GFP-positive animals which were able to survive to adulthood, which we named QT930. By eye, these animals appear to be wildtype in their locomotion (see Movie 6-2).

6.2.4 - Phosphomimetic syntaxin (T252E) is able to rescue the lethality of syntaxin-null animals, but the rescued animals are highly lethargic

We injected the phosphomimetic form of syntaxin, T252E (Plasmid SJN368) into the NM979 animals at a concentration of 25 ng/µl, along with a *ttx-3*::gfp co-injection marker. We obtained three independent lines - QT827, QT838 and QT839 - in which all GFP-positive animals survive to adulthood. These animals appear to grow normally, but are strongly lethargic, almost to the point of paralysis (Movie 6-3).

The fact of their survival and normal growth suggests that this mutation allows at least some level of normal syntaxin function, sufficient to rescue the null mutation in this strains.

As this phenotype could result from insufficient syntaxin function caused by poor expression of this construct, rather than as a direct result of mimicking phosphorylation at T252, we reinjected at a higher concentration. This time we obtained a further two independent lines, and these animals are also strongly lethargic.

Upon nose touch, the animals respond with subtle body movements, showing some level of sensitivity and some limited movement, but these animals are essentially paralysed under normal conditions.

6.3 - Drug assays of rescued animals

All three syntaxin constructs – wild-type, T252A and T252E - are able to rescue loss of syntaxin in the NM979 mutant. The wild-type and T252A constructs appear to rescue back to wild-type behaviour, at least at the level of gross morphology, while the T252E construct produces viable animals which are paralysed, or at least highly lethargic. A possible explanation for this paralysis is that the phosphorylation site T252 is required for inhibiting neurotransmitter release. Therefore we wanted to see whether animals which contained the version of syntaxin not able to be phosphorylated at this residue might have higher levels of neurotransmitter release.

6.3.1 - Syntaxin mutants rescued with wild-type syntaxin are slightly hypersensitive to the acetylcholinesterase inhibitor aldicarb

To establish a baseline for our neurotransmitter release experiments, we tested the aldicarb response of the syntaxin mutants rescued with wild-type syntaxin. The three independent lines, QT415, QT416 and QT417 paralyse faster on 1 mM aldicarb than wild-type, with 49%, 53% and 67% of animals paralysed at 50 minutes, compared with 30% for wild-type animals (Figure 6-4).

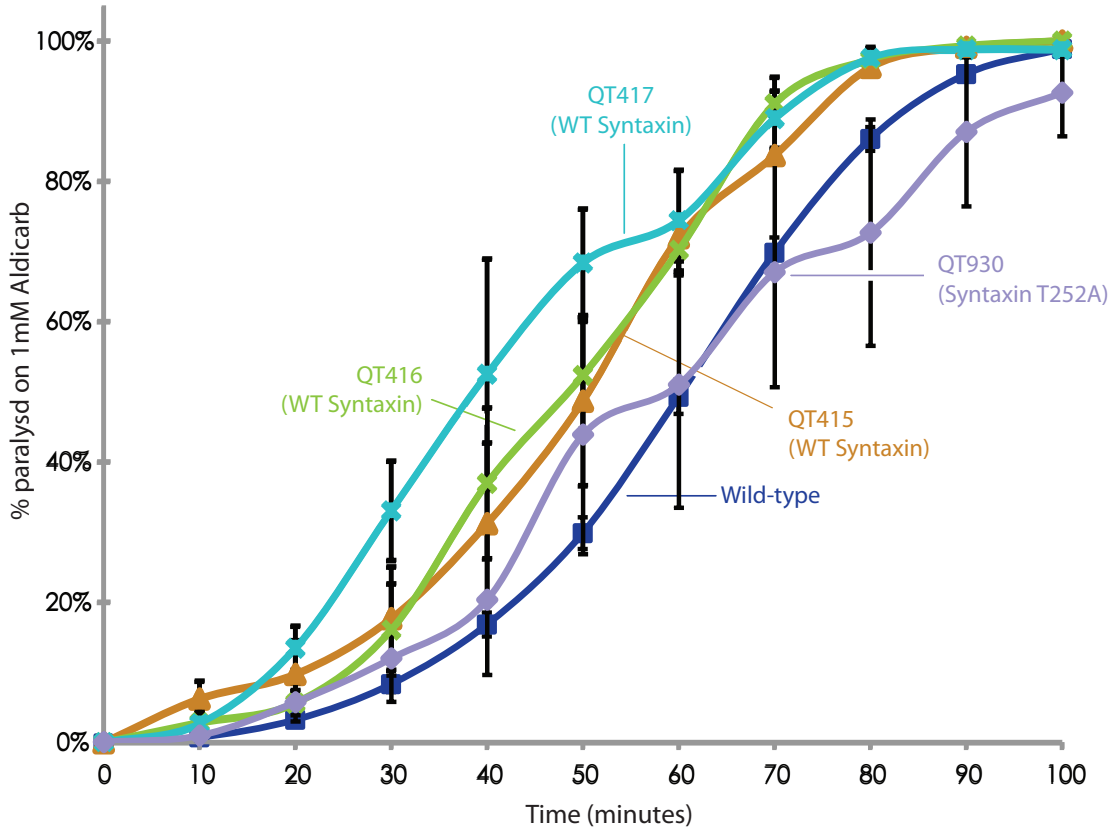

Figure 6-4 Aldicarb assays of syntaxin mutants rescued with wild-type syntaxin

The syntaxin mutant, NM979, when rescued with wild-type syntaxin expressed from the syntaxin promoter, becomes slightly hypersensitive to the acetylcholine esterase inhbitor aldicarb. Three independent lines, QT415 (orange curve, n=4), QT416 (green curve, n=5) and QT417 (light blue curve, n=6), carrying the rescuing construct, paralysed faster on 1mM aldicarb than wild-type animals (blue curve.)
Hypersensitivity to aldicarb indicates increased release of the neurotransmitter acetylcholine. This suggests that the wild-type syntaxin cDNA not only rescues the syntaxin deletion, but actually promotes neurotransmitter release compared to animals expressing endogenous levels of syntaxin.

6.3.2 - Syntaxin mutants rescued with mutant syntaxin T252A are wild-type in their response to aldicarb

While we speculated that the animals containing a form of syntaxin unable to be phosphorylated at the in vitro aPKC site might have lower levels of neurotransmitter release, these animals are wild-type in their response to aldicarb, indicating that their levels of acetylcholine release are normal (36% paralysed at 50 minutes compared to 30% for wild-type animals, Figure 6-5).

Compared with syntaxin mutant animals rescued with a wild-type syntaxin construct, these animals are slightly resistant to aldicarb (Figure 6-5), potentially indicating that this construct is less efficiently able to rescue neurotransmitter release. More investigation is required to determine whether this is a significant difference.

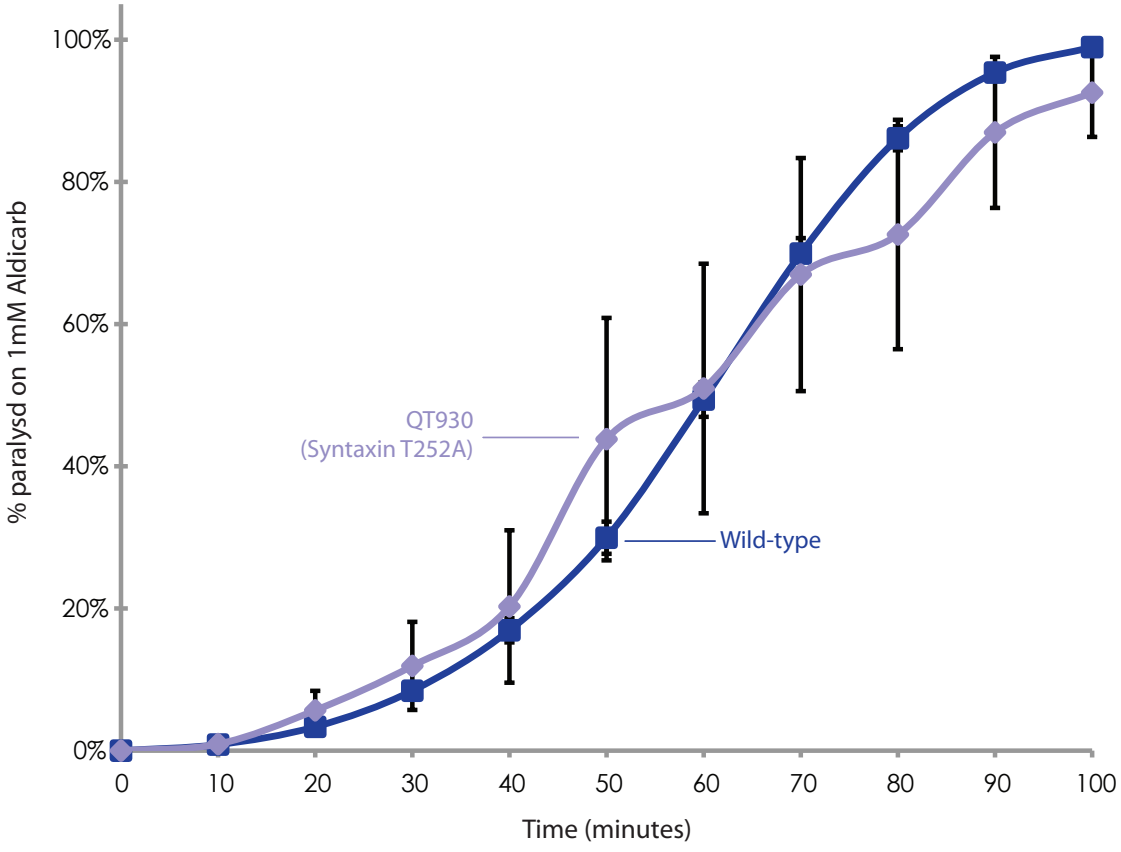

Figure 6-5 Aldicarb assay of syntaxin mutants rescued with mutant syntaxin

We obtained one independent line of syntaxin mutant animals (NM979) rescued with a plasmid containing a mutant version of syntaxin, SJN367. This plasmid contains a mutation altering an in vitro aPKC phosophorylation residue, threonine, to an alanine residue that is unable to be phosphorylated. The aldicarb profile of these mutants, QT930 (purple curve, n=4) appears the same as wild-type animals.
When exposed to 1mM aldicarb, these animals paralyse at the same rate as wild-type animals, suggesting that this mutated residue is not important in the regulation of release of acetylcholine under basal conditions.

6.3.3 - Syntaxin mutant animals rescued with phosphomimetic syntaxin T252E are resistant to aldicarb

The animals rescued with syntaxin are so lethargic that an accurate aldicarb assay is difficult to perform. If we use our standard criteria for paralysis, essentially all the animals would be counted as paralysed at the start of the experiment.

To enable the experiment to be performed, we used a different criteria for paralysis for these animals. They respond to a harsh nose touch with very small body movements, and this simple response diminishes during an alidcarb assay. Therefore we counted as paralysed those animals which failed to respond to nose touch in any way.

Using this criteria, the animals appear resistant to aldicarb, compared to wild-type animals assayed in the normal manner (where we count as paralysed any animals unable to propogate a full wave of body bends from head to tail.) The animals produced from the second set of injections are more resistant to aldicarb than those produced in the first set, but it is difficult to draw strong conclusions given the problems with performing this assay.

Interestingly during these experiments, we see that some of the animals which are counted as not paralysed towards the end of the experiment move faster and respond more strongly to nose touch than they did at the beginning of the experiment. This suggests that aldicarb is enhancing the exisiting, very low level of neurotransmitter release to allow greater responses from the body wall muscles.

6.3.4 - Automated tracking of syntaxin mutants

To further assay the effects of these two mutant versions of syntaxin on the whole animal we decided to make use of the computer vision package Parallel Worm Tracker (Ramot, Johnson et al. 2008). This program analyses videos taken of multiple worms as they move across an agar plate, and provides information on their average speeds. This can be used to produce an automated drug assay, such as looking for rate of paralysis on aldicarb, or to compare the rate of locomotion between strains.

6.3.5 - Syntaxin mutants rescued with phosphomimetic syntaxin are highly lethargic, but capable of some movement

One question we continue to return to is whether the T252E mutant form of syntaxin is causing the animals to become lethargic because it is a hypomorphic form of syntaxin due to a misfolding of the protein, or whether the change at this site mimics a regulated response causing the animals to become highly lethargic.

We measured the speed of the syntaxin mutant animals rescued with T252E on food using the Parallel Worm Tracking software, and found that they move at an average speed of 0.005 mm/sec. This is 15 times slower than wild-type animals, which move at an average speed of 0.076 mm/sec on food.

We recorded a video of these animals at a very low framerate over a 10 hour period. Interestingly, when played back at 100 times normal speed the animals appear to move like wild-type animals. This suggests that the syntaxin protein is capable of driving neurotransmitter release, but at a very low rate compared to wild-type.

6.3.6 - Syntaxin mutants rescued with phosophomimetic syntaxin move faster when exposed to PMA

If this mutant version of syntaxin is simply misfolded, it might allow a low level of neurotransmitter release, but prevent increases in release in response to normal regulators. We wanted to test whether these were still able to respond to PMA, a phorbol ester and diacylglycerol (DAG) analogue, a key second messenger in neurotransmitter release.

Again we made use of the parallel worm tracker to record the speeds of animals moving on PMA compared to their rate on food.

Wild-type animals show a fast response to PMA, with an increase in their average speed to 0.11 mm/sec after 10 minutes exposure to the drug (Figure 6-7).

The animals rescued with the T252E form of syntaxin also show a response to PMA, increasing their average speed to 0.009 mm/sec as measured by the worm tracker. Although this speed is still well below that seen in wild-type animals, the relative increase in average speed is around 80%, similar to the 70% increase in speed seen in wild-type animals for the same period of exposure (Figure 6-7). This suggests that the T252E mutation acts in pathway parallel to that activated by PMA signalling.

6.3.7 - Animals rescued with the T252A form of syntaxin respond normally by slowing in their response to serotonin

While we are unable to establish whether the phosphomimetic mutation is causing the animals to move slowly because of some function of that phosphorylation site as opposed to misfolding of the protein, another approach is to find situations in which the mutant which is unable to be phosphorylated is unable to slow down. If phosphorylation at T252 is able to cause slowing of movement, we hypothesised that the alanine mutation might

prevent this slowing from occuring. We therefore sought conditions under which the animals would naturally reduce their rate of locomotion.

One condition in which we know that *C. elegans* reduces its rate of locomotion is in the presence of food, which is signaled by increases in the levels of serotonin. Animals exposed to serotonin have fewer body bends and a slower rate of locomotion than animals on control plates (Horvitz, Chalfie et al. 1982; Segalat, Elkes et al. 1995).

We tested whether we could observe this response in wild-type animals using the parallel worm tracker. Figure 6-8 shows a histogram representing the speeds of wild-type animals on food. When animals are exposed to serotonin for 15 minutes, this distribution shifts to the left, showing that the animals are slowing in response to serotonin.

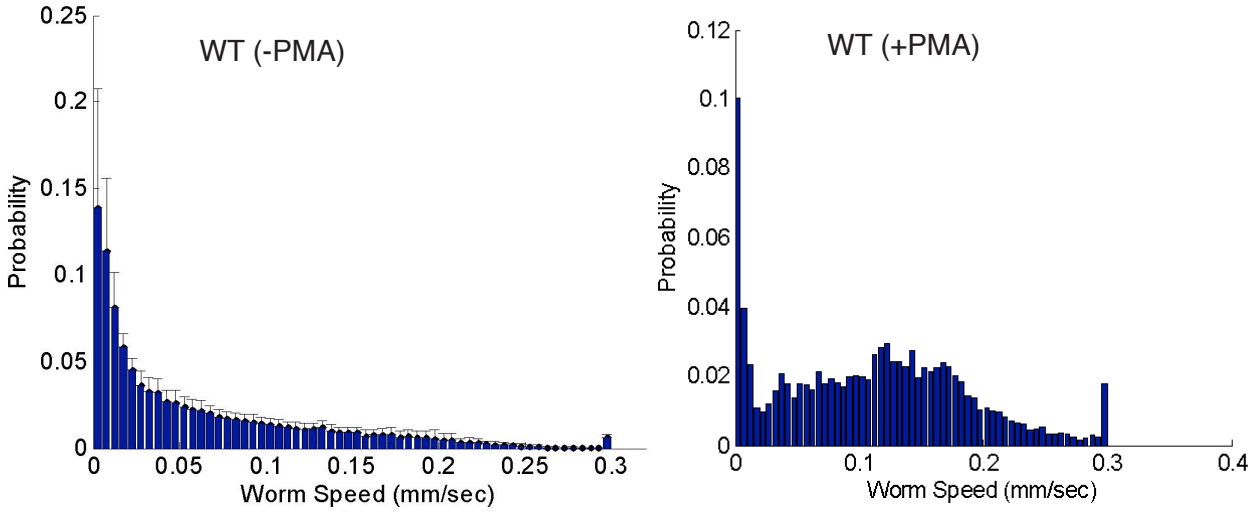

Condition	Wild-type	Phosphomimeitc Syntaxin (QT931)
-PMA	0.076 mm/sec	0.005 mm/sec
+PMA	0.1104 mm/sec	0.009 mm/sec

Figure 6-7 - Exposure to serotonin causes a reduction in locomotion in animals rescued with a mutant form of syntaxin

Wild-type animals exposed to the phorbol ester PMA (a DAG analogue) respond by increasing their rates of locomotion. 15 minutes exposure to PMA shifts the distribution of speeds in wild-type animals to the right (B) compared with that of animals moving on food in the absence of PMA (A), with an average increase in speed from 0.076mm/sec to 0.1104 mm/sec. QT931 animals, rescued with a phosphomimetic form of syntaxin, are also able to increase their average speed on food, from 0.005 mm/sec to 0.009mm/sec, indicating that these animals are able to respond to PMA. (The distribution of speeds in these animals is not shown.) Data obtained from two independent experiments, each taken from videos of 30 animals.

The distribution of speeds in the T252A animals is highly similar to that seen in wild-type animals, confirming that this point mutation rescues the loss of wild-type syntaxin and generates animals capable of wild-type movement under basal conditions. However, should phosphorylation of this site be necessary for slowing, we might expect that these animals would be unable to respond to the presence of serotonin. However, when the animals are exposed to serotonin for 15 minutes, the distribution of speeds shifts to the left in the same way as observed for wild-type animals. This demonstrates that the lack of a phosphorylation site at T252 does not affect the ability of the animals to slow in response to serotonin.

6.4 - Testing Phosphomimentic syntaxin constructs for dominant negative activity

6.4.1 - Wild-type animals carrying phosphomimetic syntaxin have normal locomotion

A question which remains in response to these experiments is whether the phosphomimetic syntaxin represents a low-functioning, possibly misfolded form of syntaxin, which produces viable but highly lethargic offspring as a result of low activity, or if this mutation mimics and endogenous pathway that reduces neurotransmitter release via inhibition of syntaxin.

It is possible that a misfolded protein will have dominant negative effects, such as sequestering factors away from wild-type versions of the protein, or binding to and interfering with the normal function of the wild-type protein.

Therefore we injected wild-type animals with the phosphomimetic syntaxin construct SJN368 at a concentration of 25 ng/µl. We obtained 2 independent lines, and both of these lines had normal locomotion; none displayed the severe lethargy of the syntaxin mutants rescued with this construct. From this we conclude that the construct is does not act in dominant negative fashion.

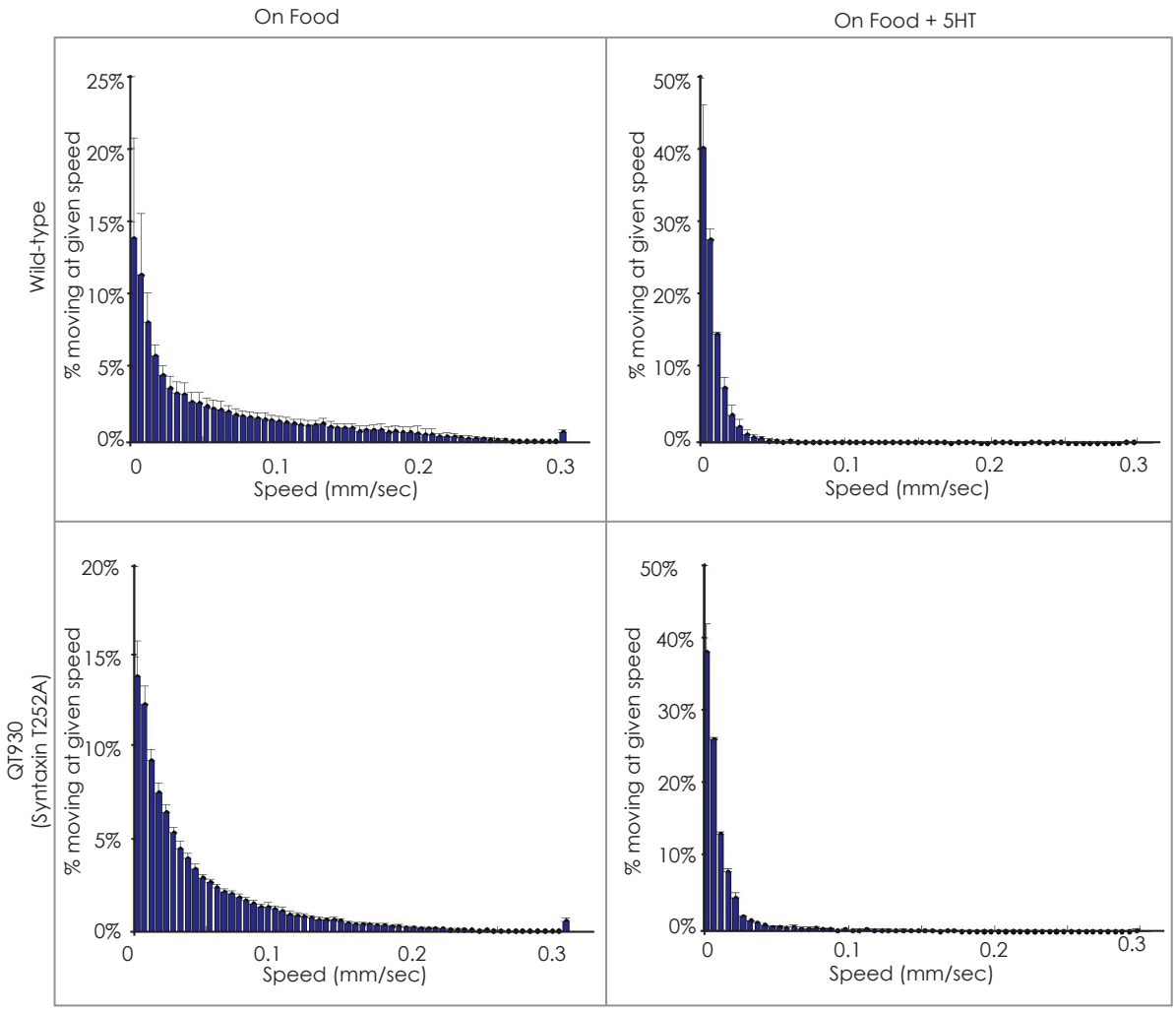

Figure 6-8 - Exposure to serotonin causes a reduction in locomotion in animals rescued with a mutant form of syntaxin

Syntaxin mutant animals rescued with mutant syntaxin which is unable to be phosphorylated by aPKC appear to have wild-type locomotion. We tested the response of these animals to exposure to serotonin. A) Distribution of speeds of wild-type animals on food. Around 15% of animals do not move during the recording, and a fraction of the animals are moving at speeds over 0.1 mm/sec. B) Distribution of speeds in animals carrying the version of syntaxin unable to be phosphorylated by aPKC is very similar to that of wild-type animals. C) 15 minutes exposure to serotonin, over 40% of the animals have stopped moving completely, and virtually no animals are travelling faster than 0.05 mm/sec. D) The response of QT930 animals to 5-HT mimics that of wild-type animals, with nearly 40% of the animals immobile during the video recording, and only a small fraction travelling faster than 0.05 mm/sec. Data obtained from two independent experiments, each taken from videos of 30 animals.

6.8 - Looking for a kinase which may phosphorylate syntaxin in vivo

Our hypothesis for the lethargy seen in the animals carrying a phosphomimetic form of syntaxin is that this mutant syntaxin strongly mimics the effects of an in vivo phosphorylation event at residue T252. If this hypothesis is correct, then we would predict the existence of a kinase associated with this phosphorylation event which,

,when active, should cause slowing of the animal. P We do not expect that the in vivo effects of phosphorylation would be as strongly evident in reduced locomotion as our mutation which mimics permanent phosphorylation; nonetheless we expect animals with an activated kinase would travel slower than wild-type animals, at least under some conditions.

As the research from the Fujita lab was into the effects of an atypical protein kinase C phosphorylation, we decided to investigate the effects of activating a homologous protein in the worm.

6.5 - PKC-3 is an *C. elegans* atypical protein kinase C

The original hypothesis from the Fujita lab in vitro experiment was that an atypical protein kinase C might be recruited by tomosyn to allow phosphorylation of syntaxin (Figure 6-). The model drew on comparisons to the polarity establishing complexes. The kinase in *C. elegans* most homologous to that found in the mammalian complex is PKC-3, which associates with and is correctly localized by the PDZ domain of PAR-3 (Tabuse, Izumi et al. 1998). We set out to make a constitutively active form of PKC-3, a candidate for the kinase which phosphorylates syntaxin at residue T252.

6.5.1 - Constitutively active PKC-3 causes pathfinding defects

We obtained three *pkc-3* cDNAs from Yuji Kohara - YK1447b7, YK284f7, YK526h11 – and grew these according to standard methods. These plasmids were miniprepped, and used as templates for amplifying the full-length cDNA of PKC-3 by PCR. We used primers to introduce unique NcoI and SacI sites for further subcloning, and a NotI site at the 5' end for the introduction of protein tags, such as GFP.

PCR of PKC-3 from YK526h11 produced a band of the predicted size (1800bp) for full-length pkc-3 cDNA, which produced two bands of approximately 1200bp and 700bp when diagnostically digested with NheI, as predicted (for more details, see Methods).

The *pkc-3* cDNA fragment was subcloned into plasmid pSC#205, containing the *acr-2* promoter, which drives expression primarily in the cholinergic neurons of *C. elegans*, together with a few additional neurons in the nerve ring (Nurrish, Segalat et al. 1999). We then generated a constiutitvely active version of PKC-3 by mutating the pseudosubstrate domain, a region of the protein which reduces the kinase activity (Pears, Kour et al. 1990). This activating mutation, where an alanine residue is replaced by a glutamate residue, has been successfully demonstrated in classical, novel and atypical protein kinases (Decock, Gillespie-Brown et al. 1994). We generated PKC-3 constructs containing the

mutation A116E by site-directed mutagenesis, and this construct was named APP3, and will be referred to as PKC-3* to denote the activating mutation.

PKC-3* was injected into wildtype at a concentration of 25ng/µl, along with QT#238, which expresses GFP from the *unc-17* promoter, and a *ttx-3*::GFP co-injection marker. 2 independent lines were obtained, and offspring from these lines appeared uncoordinated.

When examined using our high-power GFP microscope, we could observe classic pathfinding defects in these animals as observed by changes in the *unc-17*-driven GFP pattern. The commisures, the connections between the dorsal and ventral nerve cord, which normally travel across the body of the animal perpendicular to the anterior-posterior axis, were now migrating along the AP axis. These pathfinding defects are likely to be the cause of the uncoordinated locomotion we observed. However, this is a good indication that the PKC-3* construct is active when injected into the worms.

6.5.2 - PKC-3* does not affect neurotransmitter release or the gross behaviour of transformed animals

To try to avoid these pathfinding defects we reinjected our PKC-3* construct into wild-type animals at a concentration of 10 ng/µl. These animals did not appear to have the pathfinding defects seen at the higher concentration.

The locomotion of these transformed animals appears wild-type. There was no gross slowing of the animals, so we decided to test whether there were any changes in neurotransmitter release as a result of the presence of this activated protein.

We tested these animals using the aldicarb assay (Figure 6-9), but saw that they appeared the same as wild-type with respect to aldicarb treatment, indicating that this construct had no effect on the release of acetylcholine.

6.6 - CDC-42 is a small GTPase implicated in the activity of PKC-3 in cell polarity establishment

As the PKC-3* construct was able to cause pathfinding defects, and did not phenocopy the phosphomimetic syntaxin strains for extreme lethargy, we decided to try to activate endogenous PKC-3. We therefore looked to CDC-42, a Rho GTPase associated with the activity of the Par complex, of which PKC-3 is a constituent. CDC-42 and the PAR-3/PAR-6/PKC-3 complex have been shown to function together (Welchman, Mathies et al. 2007), so we reasoned that activating CDC-42 might activate PKC-3, and potentially phenocopy the phosphomimetic syntaxin mutants, if PKC-3 is the endogenous kinase which phosphorylates syntaxin.

6.6.1 - Making constitutively active and dominant negative *cdc-42* constructs

Two mutants of *cdc-42* are available, but neither were suitable for these experiments. *ok825* is a deletion which only affects part of the 3'UTR of *cdc-42*, while *gk388* is deletion which is lethal. We already had available two CDC-42 plasmids: Heat-shock driven *cdc-42* (SJN376) and *p.acr-2* driven *cdc-42* (SJN381). We ordered primers to generate constitutively-active (G12V) and dominant negative (T17N) versions of CDC-42 (see Methods).

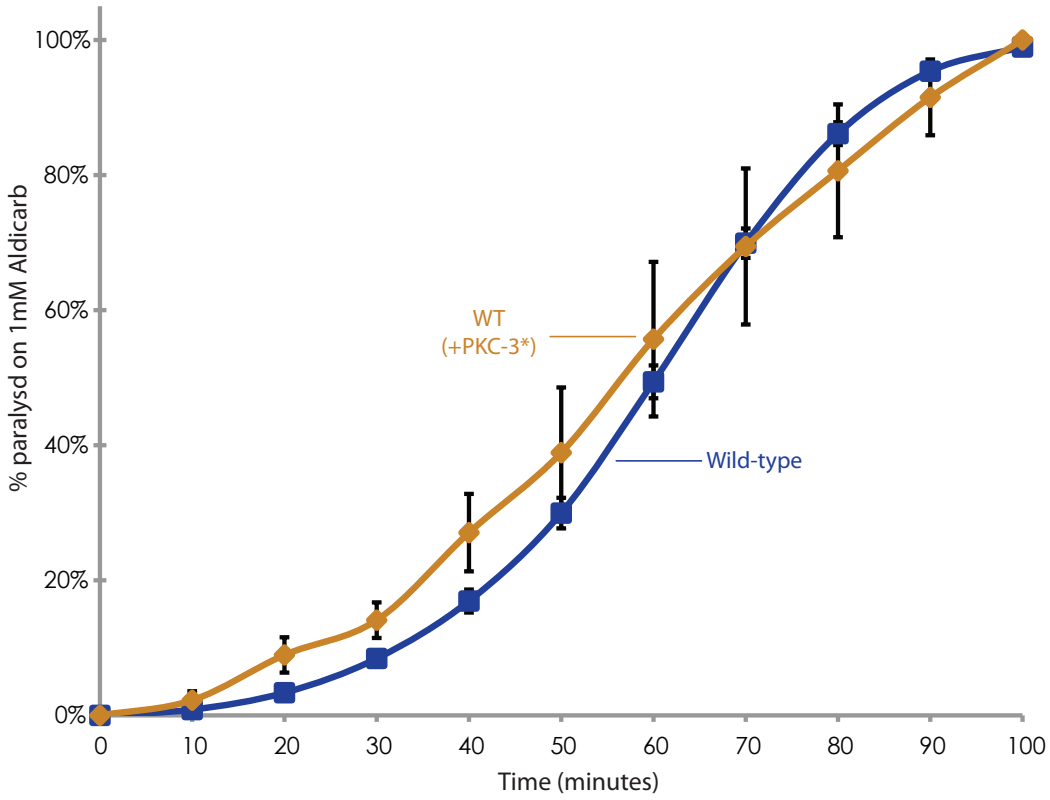

Figure 6-9 - Aldicarb Assay of animals carrying a PKC-3 (gf) construct

Animals overexpressing gain-of-function PKC-3 from the *unc-17* promoter do not display any changes in their response to aldicarb (organge line, n=4).

Using the Quikchange protocol we successfully introduced the constitutively active and dominant negative mutations into the plasmid driven by the *acr-2* promoter (plasmids APP004 and APP005), and generated a heatshock-driven constitutively active CDC-42 (APP006, hsCDC-42*).

6.6.2 - Lines carrying constitutively active, heatshock driven CDC-42 appear wildtype

We injected hsCDC-42* into wild-type animals and obtained 2 independent lines. Prior to heatshock, the animals appeared wild-type. We then subjected these transformed animals to our standard heatshock protocol (see Methods) but no gross behavioural changes were observed in adults.

We therefore performed heat-shock on a mixed population of animals, where we should activate the heat-shock transgene in developing larvae, but we did not see any visible response to activation compared to wild-type control animals. This is surprising given CDC-42 has a well-defined role in development, and suggests that our constitutively-active construct is not active within the transformed animals. However, without tagging the construct with a fluorescent marker such as GFP, we do not know at this stage whether CDC-42 is being expressed.

6.7 - Discussion

We developed a range of mutant syntaxin constructs, based on research conducted by the Fujita lab which indicated that a specific threonine residue in syntaxin was capable of phosphorylation by an atypical protein kinase C in vitro. To mimic this mutation we generated a phosphomimetic version of the worm orthologue of syntaxin, UNC-64, and also a version which was unable to be phosphorylated.

Upon injection into *unc-64* mutant animals, which are homozygous lethal, we found that both of these constructs, and the wild-type form of *unc-64*, were able to rescue the lack of syntaxin function in these mutants.

Interestingly, we noted that the animals rescued with the phosphomimetic form are highly lethargic, and appear almost paralysed. These animals are capable of movement, as seen in videos taken over long (10 hour) time periods, but this movement is at least an order of magnitude slower than that seen in wild-type animals. They are also resistant to aldicarb, an acetylcholinesterase inhibitor (although using a modified protocol to account for their initial low level of movement), which suggests that they have lower levels of neurotransmitter release, and this may be responsible for their impaired locomotion. One issue not addressed as this stage is the level of expression of the three constructs. To compare more precisely the phenotypes across the rescued lines, we could perform quantification of expression of mRNA, using qPCR, or of UNC-64 using a western blot. Alternatively, these experiments could be conducted using the MosSCI single copy

insertion method of transformation, which is predicted to give rise to more wild-type expression levels (Frokjaer-Jensen, Davis et al., 2008).

This led us to speculate that an *in vitro* phosphorylation of syntaxin at this residue, T252, might be involved in a regulated slowing response. We therefore set out to test whether activating the *C. elegans* atypical protein kinase C - PKC-3 - or its upstream activator CDC-42, more commonly associated with the polarity complex involved in development, might be able to phenocopy the lethargy seen in the rescued animals. However, we have so far failed to see an adult phenotype for the activation of PKC-3. We are reasonably confident that the PKC-3* construct, driven by the *acr-2* promoter, is working, because we see pathfinding defects in animals carrying this construct. However, these pathfinding defects make assaying behavioural changes in adults difficult, because we do not know how much of any observed behaviour to ascribe to the developmental defect. When reinjected at lower concentration, we saw no developmental changes with the PKC-3* transgene, but no gross changes in behaviour were observed either. As syntaxin/UNC-64 is a key regulator of neurotransmitter release, we tested whether these animals expressing activated PKC-3 in their cholinergic neurons had any changes in their response to aldicarb, but the transformed animals remained wild-type.

It is possible that the PKC-3* construct is capable of causing adult behavioural changes, but that by being expressed throughout development from the *acr-2* promoter animals are able to compensate for increased PKC-3 activity into adulthood. It would be interesting to see if PKC-3 under the control of a heat-shock promoter, or PKC-3 expressed using tetracycline-response would produce a change in the adult organism, as these methods bypass the potential for compensation during development.

While we were unsuccessful in seeing an adult phenotype for activated, exogenous PKC-3, we attempted to activate endogenous PKC-3 using CDC-42* constructs. However, these constructs did not show any phenotype either in the adult or during developmental stages. We have no evidence to confirm this transgene successfully expressed the CDC-42 protein.

Without further evidence, we cannot be sure whether the mutant UNC-64 protein containing the phosphomimetic mutation is demonstrating the effects of constitutive phosphorylation at residue 252, or whether this version of UNC-64 is simply a misfolded protein, only weakly able to rescue for total loss of syntaxin function in an *unc-64* mutant. Alternatively, this mutation could be interefering with the reported function of the T252 site in the interaction with synaptobrevin, or in the ‘zippering’ of SNARE proteins during fusion (Littleton, Chapman et al., 1998; Lagow, Bao et al., 2007).

To help address this, we examined a second mutated form of syntaxin in which the potential aPKC site is mutated to alanine, preventing phosphorylation. A number of observations about these rescued animals rescued shed additional light on the phosphomimetic mutant phenotype.

The animals rescued with T252A UNC-64 appear wild-type for their locomotion. This indicates that the threonine residue is not essential for the functioning of the protein, i.e. that its loss does not cause constitutive paralysis. The conversion of threonine to alanine is distinctly non-conservative, and yet generates a version of UNC-64 capable of substituting for wild-type. Whether the addition of a glutamic acid residue destabilizes the protein is something that will require further study; for now, we can say that is not the loss of the threonine residue which generates the paralysed phenotype.

Phosphorylation at T252 is not required for syntaxin function. T252A UNC-64 does not cause any gross effects developmental or behavioural effects on rescued animals. If the phosphomimetic mutation is genuinely mimicked regulated phosphorylation then it might be predicted that the inability to phosphorylate at this site might cause animals to move too quickly. However, in the experiments looking at locomotion and aldicarb release, the animals rescued T252A UNC-64 are indistinguishable from wild-type animals. This does not mean that the phosphorylation event is not occurring, but it does suggest that it is rather transient, or that only a small percentage of the UNC-64 is phosphorylated under normal conditions.

Although the alanine mutant is able to move at normal speeds under standard conditions we hypothesized that there might be a lack of slowing under other conditions, consistent with reports of the T254I mutation in Drosophila increasing exocytosis (Lagow, Bao et al., 2007). We investigated whether the animals were able to slow down when exposed to serotonin, a key signal for the dwelling response, and saw that the animals have the same profile of response to the neurotransmitter as wild-type animals. There may be other circumstances in which *C. elegans* will reduce its speed only with wild-type syntaxin, but these remain to be investigated.

Should phosphorylation at site T252 prove to be capable of regulating locomotion, it is likely to only be actively phosphorylated at specific times, as loss of the phosphorylation site has had no discernable effect in our investigations so far. This has led us to look for other situations where *C. elegans* speed changes at distinct times, and a phenotype which has recently been gaining attention is that described as ‘lethargus’ (Raizen, Zimmerman et al. 2008). This phenotype occurs during molting, when the *C. elegans* larval stages shed their outer cuticle. Here the animals enter what is referred to as a ‘sleep-like state’. This

reduction in locomotion is not simply due to lack of the cuticle, but is a state that can be regulated; if the animals are disturbed by touching with a platinum wire they move, and if left undisturbed will compensate for the disturbance by 'resting' longer at the following lethargus stage.

Interestingly, this phenotype is regulated by EGL-4, which is a cyclic GMP-dependent protein kinase. A gain-of-function egl-4 mutant has prolonged periods of rest during molting compared to a wild-type animal (Raizen, Zimmerman et al. 2008). It would be interesting to test whether our animals rescued with a mutant version of syntaxin are either unable to enter lethargus, or have a reduced response to the EGL-4 gain-of-function protein, which would suggest that T252 is a phosphorylation site for EGL-4.

More investigation is needed into the phenotype arising from these mutations. Our model so far suggests that there is no, or a low level of, phosphorylation of syntaxin at the T252 residue under most conditions, but that under certain types of stimuli, phosphorylation occurs, and causes the animals to decrease their rate of locomotion (Figure 6-10).

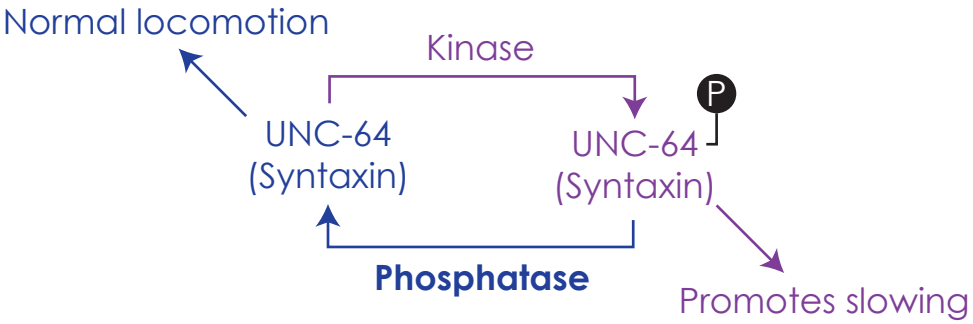

Figure 6-10 - Model of syntaxin regulation

We propose that phosphorylation of syntaxin at site T252 promotes slowing of locomotive behaviour. The absence of an observable effect of loss of this phosphorylation site leads us to suggest that, under standard laboratory conditions, this site is either not phosphorylated, or that any phosphorylation is removed by a regulatory phosphatase which we have yet to identify.

A number of kinases are capable of phosphorylating syntaxin. Casein kinase II (CKII), phosphorylates serine-14 on syntaxin 1A/B (Hirling and Scheller 1996) , and this phosphorylation affects the distribution of syntaxin along axons, positively regulating neurotransmitter release (Folletti, Lin et al, 2000). Lack of CKII activity, and subsequent reductions in syntaxin-1 phosphorylation have recently been implicated as a source of reduced neurotransmitter release in the brains of patients with schizophrenia (Castillo, Ghose et al. 2010). In addition, in non-neuronal systems, protein kinase C phosphorylates syntaxin-4, which increases granule secretion from platelets (Chung,

Polgar et al. 2000). In each of these instances, phosphorylation of syntaxin is a positive regulator of neurotransmitter release. Should the phosphorylation site at T252 prove to be a true endogenous site of regulation of syntaxin activity it may also represent the first example of inhibitory phosphorylation of syntaxin.

7 - TAMOXIFEN REGULATION OF PROTEIN ACTIVITY IN *C. ELEGANS*

7.1 - Introduction

One of the key tools in modern molecular biology is the ability to selectively activate or deactivate proteins in specific cells at specific times. This can be used to introduce exogenous proteins for study, or to allow an organism to pass through development and then activate a protein of interest in the adult organism, such that it does not disrupt normal growth. While *C. elegans* research uses a number of important tools to regulate temporal expression, such as heatshock activation, or spatial regulation, such as cell-specific promoters, it lacks tools for combined temporal-spatial control.

7.1.1 - Methods of cell-specific expression

The ability to use cell-specific promoters that express proteins in a desired subset of cells (Figure 7-1), such as the cholinergic neurons, is a key tool for investigating the site of action of novel proteins, or for overexpressing proteins in specific cell-types (Mello and Fire 1995). For example, two main options are available for cholinergic expression; either the *unc-17* promoter, (Alfonso, Grundahl et al. 1993), used in this thesis for overexpressing activated RHO-1 (Chapter 3) and cell-specific rescue of unc-80 mutants (Chapter 4), or the *acr-2* promoter, used here for driving expression of unc-80 (Chapter 4) or activated PKC-3 (Chapter 6). The endogenous *unc-17* promoter drives expression of the vesicular acetylcholine transporter (Alfonso, Grundahl et al. 1993), which loads acetylcholine into synaptic vesicles, while the *acr-2* promoter is a nicotinic acetylcholine receptor subunit (Squire, Tornoe et al. 1995, Jospin, Qi et al. 2009). Only cells which express transcription factors capable of activating transcription from the specific promoter will express the protein of interest (Figure 7-1).

One disadvantage of these promoters is that they are limited to the endogenous expression pattern and timing of the promoter used. The particular transcription factors and associated DNA binding proteins that regulate endogenous expression from the *unc-17* promoter will drive expression of any exogenous DNA in the same way. We do not as yet have the technology or the knowledge to build our own cell-specific promoters to avoid these issues. We can use promoter fragments to achieve expression in a subset of cells (Teng, Girard et al. 2004; Appleford, Gravato-Nobre et al. 2008), which provide some measure of addtional specificity.

Another approach is to fragment the protein of interest into two halves, each of which is expressed from separate, overlapping promoters. This has been demonstrated with GFP (Zhang, Ma et al. 2004; Feinberg, Vanhoven et al. 2008) and with a caspase (Chelur and Chalfie 2007), but this approach is limited the requirement for a protein which can successfully be reassembled.

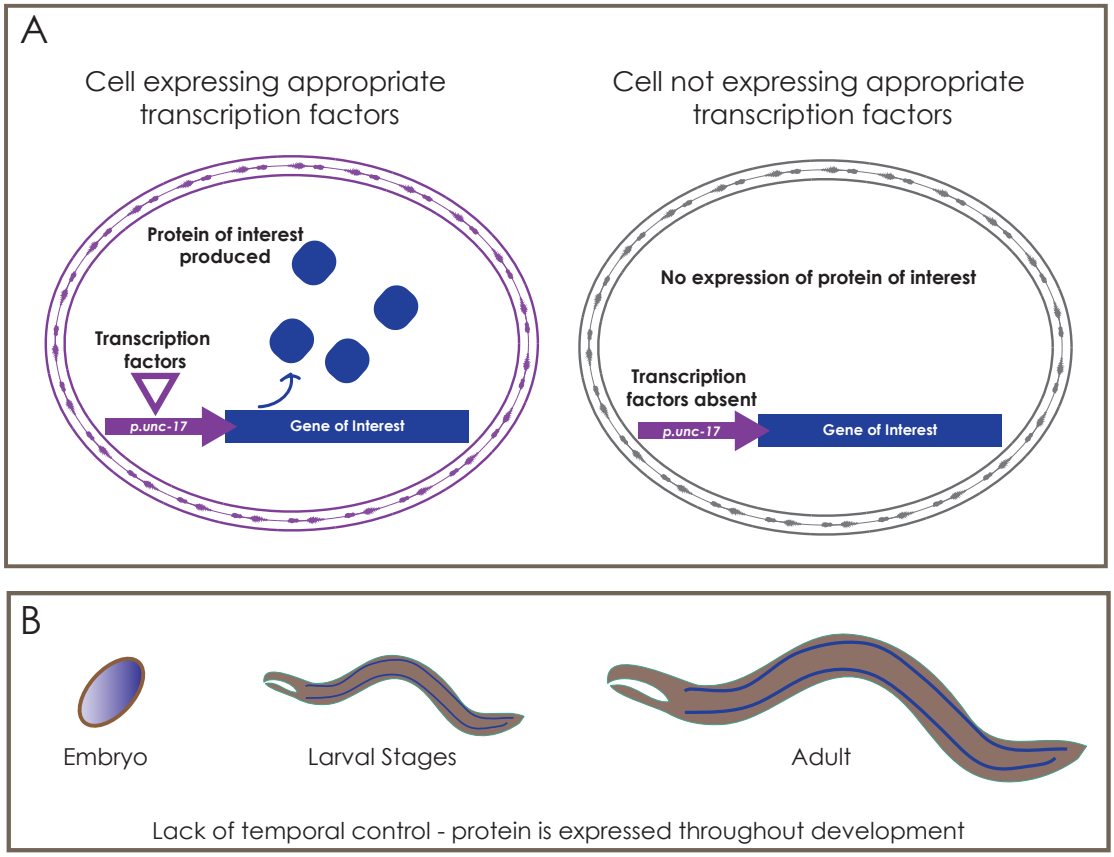

Figure 7-1 Tissue-Specific Expression in *C. elegans*

Tissue-specific promoters, such as the *unc-17* promoter shown here, drive expression only in subset of cells which express the appropriate transcription factors (A). The timing of expression is determined by the endogenous factors acting on the promoter; in the case of the *unc-17* promoter, it is expressed throughout development (B), leading to the possibility of adaptation to whichever exogenous protein is being expressed.

Interestingly, we have seen occasions in which the *unc-17* promoter successfully drives rescuing constructs when the *acr-2* promoter does not appear to (Chapter 4), which is consistent with results seen by other labs with rescue of *pkc-1* mutants (D. Sieburth, personal communication) . This may be due in part to differences in the level of expression, or timing of expression, from these two promoters, which should theoretically have largely overlapping expression patterns.

Another issue with the lack of control given by using cell-specific promoters is that when proteins are expressed throughout the lifetime of the organism there is the possibility for adaptation to occur. When we express RHO-1 from the *unc-17* promoter, which is active

during embroygenesis and into adulthood, there is potential for the animal to compensate for the extra levels of expression of the protein, potentially masking interesting effects.

7.1.1 - Methods of temporal control of expression

It is possible to obtain temporal control of protein expression in *C. elegans*, using the heat-shock promoter (Lis and Wu 1993). The heat-shock factor (HSF-1) is constitutively synthesized, but is inactive until changes in temperature cause it to induce transcription from its specific promoter (Figure 7-2).

This technique has been widely used and to great effect. Our lab has made repeated use of the heat-shock promoter to drive RHO-1 (G14V) expression (McMullan, Hiley et al. 2006). Expression of RHO-1 (G14V) during development has the capacity to cause a variety of developmental defects, such as miswiring of the nervous system, as well as the potential for compensation as mentioned above.

To bypass these effects, we restrain expression of excess RHO-1 until the animal has a fully developed nervous system, and express it by exposing the animals to a series of temperature changes (see Methods for details). Animals overexpressing RHO-1* from the heatshock promoter develop a loopy locomotion highly similar to that seen in animals expressing RHO-1* from the *unc-17* promoter (McMullan, Hiley et al. 2006), along with additional phenotypes which we attribute either to expression in additional cells, or to a lack of compensation during development.

Similarly, when using the RHO-1-specific inhibitor C3 transferase (C3T) (Aktories and Hall 1989), we use heat-shock expression to limit C3T expression to the adult organism. C3T expressed early in development leads to the death of the animals expressing it, meaning we are unable to assay adult phenotype. While heatshock activation of C3T eventually leads to the death of the animals, there is sufficient time (approximately one day) during which assays can be performed to examine adult phenotypes (McMullan, Hiley et al. 2006).

Problems remain with the use of heat-shock to drive expression, however. This method lacks cell specificity; all cells will tend to express the protein under heat-shock control, so it is not possible to examine the effects of expression in a specific tissue type. One possible counter to this is the use of a number of heatshock promoters, which have slightly different patterns of expression (Stringham, Dixon et al. 1992; Ding and Candido 2000),

Another problem with the heat-shock promoter is that it tends to be leaky, i.e. without deliberately inducing expression from the promoter, background changes in temperature can to lead to unwanted expression. For instance, animals carrying the heatshock C3T constructs tend to have reduced levels of neurotransmitter release when grown at room temperature compared with wild-type animals, indicating low background levels of C3T activity (McMullan, Hiley et al. 2006), while the heatshock RHO-1* transgene has been shown to have some activity at 20°C (Diogon, Wissler et al. 2007).

The heatshock activation of protein production, while not offering perfect temporal control, still has the potential to reduce compensation to exogenous protein during development, but at the cost of cell-specificity. A combinatorial approach has been developed which helps overcome some of these problems.

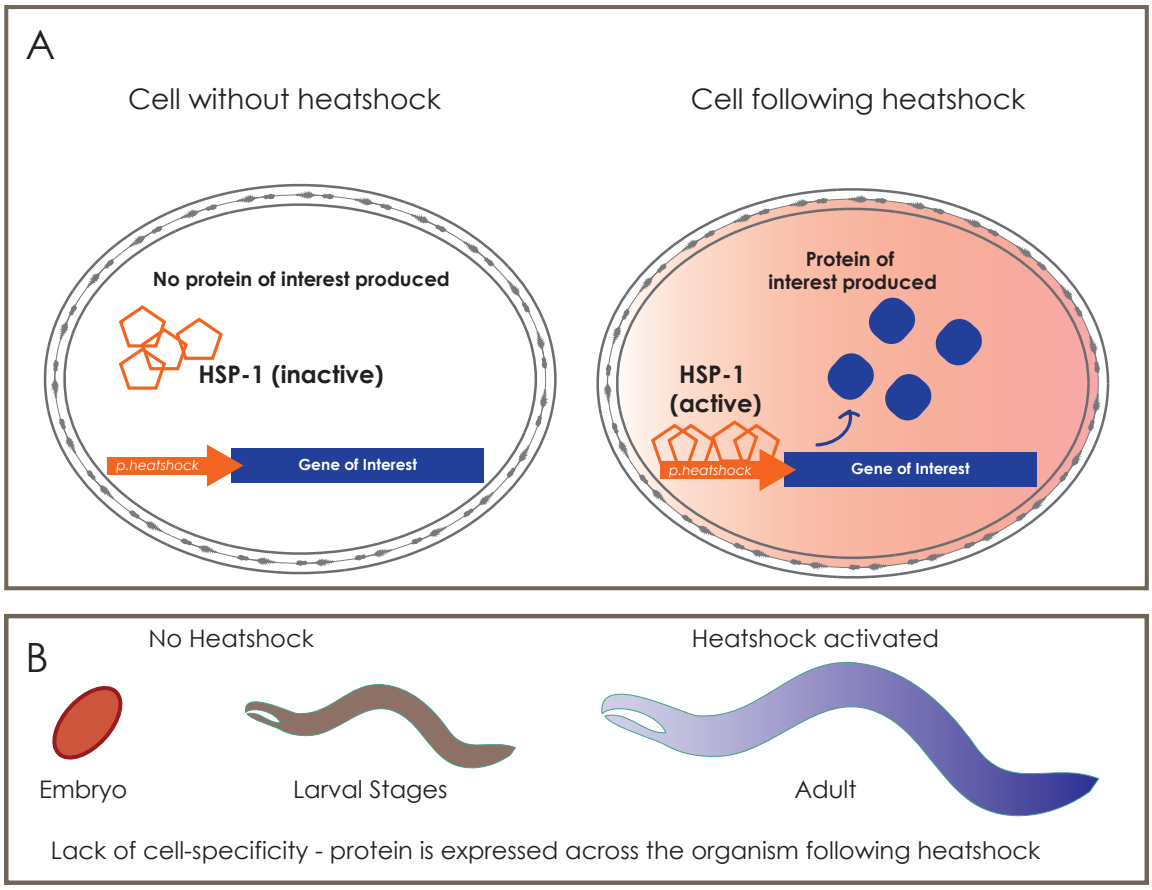

Figure 7-2 Temporal control of protein exprssion in *C. elegans*

The heatshock promoter can be used to temporally control expression of a protein in *C. elegans* by altering the external temperature to activate the endogenous heatshock response. Following this temperature change, HSP-1 binds to the heatshock promoter, driving expression (A). This allows control on the timing of expression, but the heat-shock promoter lacks cell-specificity (B).

7.1 - Combined methods for cell-specific and temporal control of expression - Heat-shock expression in a heat-shock mutant

Animals lacking the heat-shock protein HSF-1 are unable to induce expression from a heat-shock promoter. One method showing promise is to express the heat-shock protein under a cell specific promoter in an *hsf-1* mutant (Bacaj and Shaham 2007).

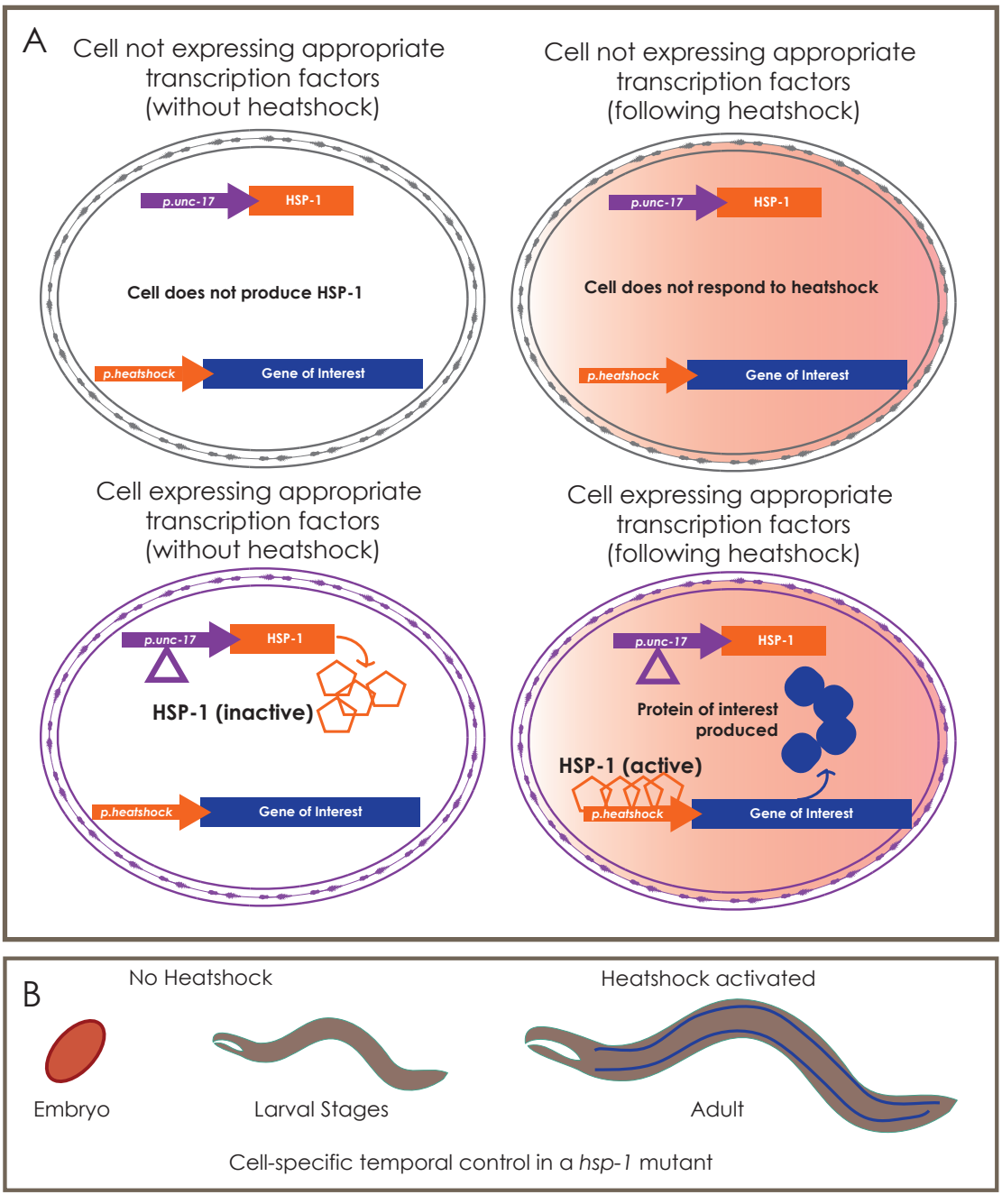

Figure 7-3 Combinatorial promoters produce tissue-specific temporal control of protein expression in *C. elegans*

The heatshock promoter can be combined with a tissue-specific promoter to allow cell-specific, temporal control of expression. The tissue-specific promoter is used to drive the expression of HSP-1 in a hsp-1 mutant, and only those cells expressing HSP-1 are able to respond to heatshock (A). This allows expression in specific cells at a specific developmental stage (B), although this requires the use of a mutant background.

C. elegans has only one heat-shock factor protein, and these mutant animals are deficient in their heat-shock response. A driver plasmid, carrying the HSF-1 construct under control of a cell-specific promoter, is injected into *hsf-1* mutant animals. This driver plasmid is now able to rescue the heat-shock response in a tissue-specific manner, determined by the promoter used (Figure 7-3).

A second construct, termed the responder, is co-transfected with the rescuing HSF-1 plasmid. This construct carries the protein of interest under the control of the heat-shock promoter. On heat-shock activation, the protein of interest is expressed only in those cells which are rescued for heat-shock activity, giving cell-specific, temporal control (Figure 7-3).

While this method offers cell-specificity and temporal regulation, it does have its disadvantages. Temporal control is activated by changes in temperature, but the use of the *hsf-1* mutant background means cells lacking the HSF-1 protein are unable to intiate their endogenous heatshock response, raising the possibility of cellular damage during treatment. *hsf-1* mutants also display a number of mutant phenotypes when grown at 25°C (Bacaj and Shaham 2007), although they appear wild-type at 20°C.

This method also relies on both a cell-specific promoter and a heatshock promoter, and so is potentially subject to the problems inherent in both these methods, such as limited promoter choice and low-level heatshock activation without treatment.

7.1.1 - Recombination as a method of regulation

An alternative use of heatshock to activate protein production involves the use of the FLP recombinase, which removes elements contained between specific FRT sites in DNA. A plasmid containing the gene of interest, containing an inactivating fragment flanked by FRT sites, expressed under a cell-specific promoter, is transfected into animals carrying a plasmid containing the FLP recombinase (which can be expressed under a heatshock promoter). On activation of heatshock, the FLP recombinase removes the inactivating fragment, and transcription of the gene of interest proceeds (Davis, Morton et al. 2008) (Figure 7-4). The cells affected continue to stably produce the protein of interest.

A similar system has been generated using the Cre recombinase, which is capable of removing DNA coded between loxP sites. In this instance two sets of promoters with overlapping cell-types were used to drive the recombinase and the construct of interest, in this case containing flp-21. The flp-21 construct contains a terminator sequence between two loxp sites. The promoters overlap in only a single cell, meaning that activation of this gene occurs in one specific neuron where both the recombinase and the target

plasmid are present (Macosko, Pokala et al. 2009). Switching one of the promoters for a heatshock promoter would make this system temporally regulated as well.

7.1.1 - Alternative methods for temporal regulation of cellular activities

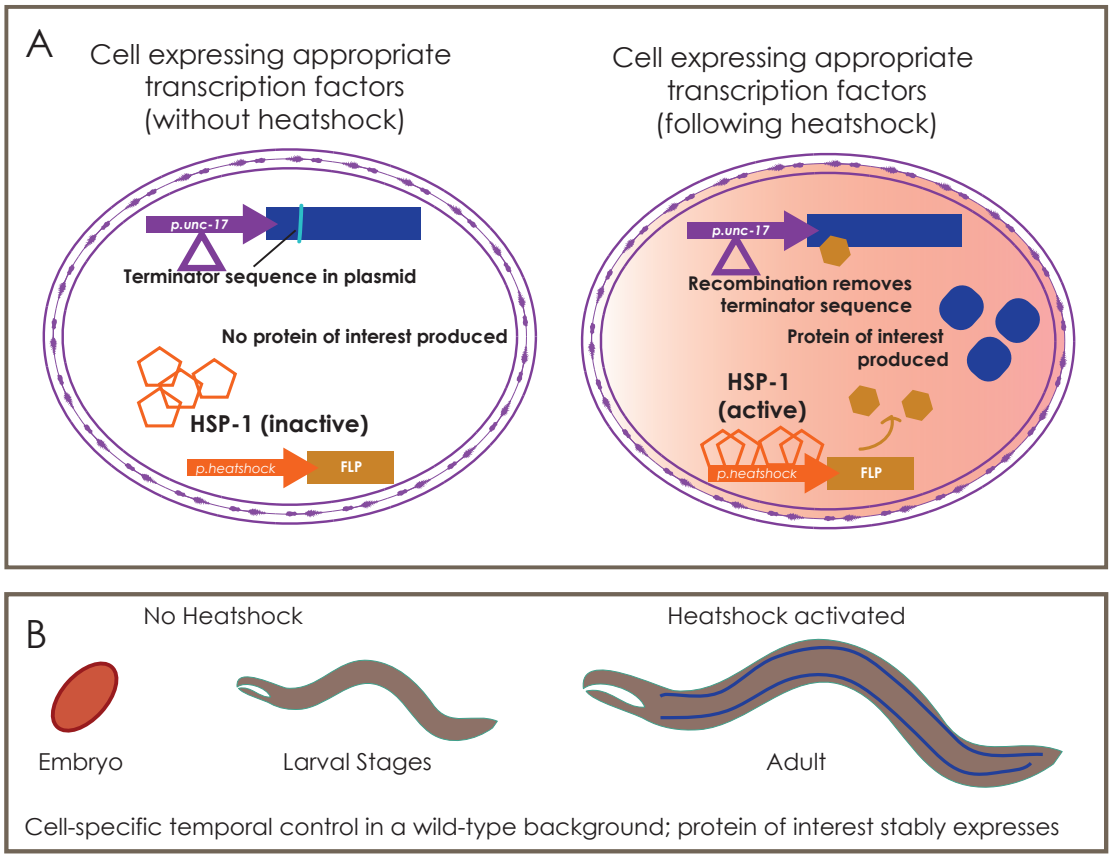

Figure 7-3 Recombinanation can be used to control protein expression in *C. elegans*

A construct containing a terminator sequence is placed under the control of a tissue-specific promoter, but no protein expression occurs until the FLP recombinase is expressed following heatshock (A). This allows for tissue-specific, temporal control, and persistent protein production following heatshock.

Another potential mechanism is the use of the drug tetracycline and the tetracycline-responsive element (Gossen and Bujard 1992; Gossen, Freundlieb et al. 1995). This element is found in bacteria that are able to mount a response to the antibiotic tetracycline, which can configured to drive activation or inhibition of transcription of a target protein. We are currently investigating this system for use in *C. elegans*.

Temporal control of cell activity, meanwhile, can be achieved by using light-activated channels, which allow cell-specific activation based on the production of channelrhodopsin (Nagel, Brauner et al. 2005), or light-activated inhibiton of cells with light-activated

chloride channels . This method is only currently applicable to specific light-activated proteins, however.

A method has also been developed based on the pathway of nonsense-mediated decay (NMD). Genes with long 3' untranscribed regions containing many introns are normally degraded by NMD pathway, but a number of temperature-sensitive mutants exist which prevent this degradation. Transgenes can be engineered under a cell-specific promoter such that their mRNAs are degraded when the animals are maintained at the non-permissive temperature, and successfully translated at the permissive temperature. This offers a mechanism of temporal regulation coupled to cell-specificity, but this requires a mutant background, and has a relatively high background activation of the exogenous genes.

7.1.1 - Current mechanisms of cell-specific, temporal control act at the level of transcription

While these mechanisms are promising, they suffer from a number of additional problems. First, they usually require the presence of two constructs in each strain to be used; these need to be on separate arrays requiring two separate integration events, increasing the workload, although in time these strains would become available to other researchers. The two integrated constructs would each have their own levels of control and regulation, adding additional complexity into the system.

Secondly, while all these methods require the incorporation of a at least 1 trangene, some require additional genomic mutations, while it would be advantageous to conduct these experiments in a background as close to wild-type as possible.

A third point is that these mechanisms control the expression of a protein at the level of transcription. For large proteins, the time it takes to produce and traffic the protein to its site of action can be extensive, and this means that the experiments are not able to examine acute activation of a protein.

7.1 - Tamoxifen regulation

Taking these factors into consideration, we thought that it would be useful to implement a further technique, widely used in mammalian systems, into *C. elegans* biology. This is regulation of protein function by the small molecule tamoxifen, which we believe will provide a complimentary system to those mentioned above.

The modified mammalian estrogen receptor (ER) is fused directly to the protein of interest, such as the Cre recombinase mentioned above (Metzger, Clifford et al. 1995). In this

Cre-fusion case, the presence of tamoxifen regulates recombination and activation of expression of a protein of interest. Again, this relies on a transcriptional level event, and takes time to manifest the activity of the protein of interest. We would rather use an approach where the estrogen receptor is fused directly to the protein of interest, as has been demonstrated with a large number of proteins, including myc (Littlewood, Hancock et al. 1995) and raf (Lloyd, Obermuller et al. 1997).

The presence of the modified estrogen receptor element causes the inactivation of the protein to which it is attached (Figure 7-5). While the exact mechanism of inactivation is still unclear, it is thought that the estrogen receptor is bound by a variety of inactivating polypeptides, with the heat-shock protein Hsp90 being the canonical factor in mammalian systems. *C. elegans* has a number of homologues of Hsp90, including DAF-21 (Birnby, Link et al. 2000). Addition of tamoxifen releases the inhibiting effect of these complexes, and allows the protein of interest to become functional. The only way to discover whether this system works in *C. elegans* is to test it experimentally.

The modified protein construct can be expressed under a cell specific promoter, and transcription and translation progress as dictated by that promoter and any additional elements such as 3'UTR sequences or introns, giving spatial control of expression. The protein is hopefully post-translationally modified and trafficked to its normal location, in an inactive state. Only on addition of tamoxifen does the protein become active; but this activation occurs without the need for further transcription or translation, so the lag between dosing with the drug and activation of the activity of the protein is much shorter than treatment either with heat-shock or with tetracycline. This allows a way to test the response of the cells of interest to an acute increase in protein activity.

There are disadvantages to this method, however. While this approach requires only a single plasmid to be transfected into the target animal, decreasing the complexity of the system, this does mean that each protein must be individually modified to accommodate the estrogen receptor. The protein construct is therefore chimeric, and it is not a certainty that the protein will be active, and this may mean that some proteins are unsuitable targets for this approach.

This technique has been successfully used in a wide variety of mammalian systems, both tissue-culture based and in vivo, and has proven highly successful, for instance in the generation of knock-out mice using tamoxifen-regulated Cre recombinase (Brocard, Warot et al. 1997). We wanted to see whether we could use this system in *C. elegans* to provide a complementary approach to cell-specific, temporal regulation to those discussed previously.

We decided that regulating C3T by adding the estrogen receptor would be both a good test case for the use of tamoxifen regulated activation of a protein, and a very useful tool for our experiments. C3T is a highly toxic protein, and we regularly find that animals transfected with constructs expressing it either die or have pathfinding defects. Given the deleterious nature of the transgene, animals from lines which carry the construct and which have a silenced copy of the transgene have a selective advantage. Therefore, these lines often completely lose the transgene expression (S. Nurrish, personal communication). We reasoned that a line carrying an essentially inactive form of the transgene would be much more stable.

We did consider using expression of GFP fused to the estrogen receptor as our test case. However, following conversations with another lab using the tamoxifen-regulated system, we felt this would be a poor choice because GFP can be resistant to inactivation by the estrogen receptor fusion (Alison Lloyd, personal communication.)

7.1 - Results

7.1.1 - Producing a C3T construct tagged with the mammalian estrogen receptor

We obtained a plasmid containing the modified estrogen receptor as a gift from the Lloyd lab, and were able to combine it with the cDNA for C3T, the RHO-1 specific toxin. We had previously generated a GFP-tagged C3T which is active, demonstrating that N-terminal fusion to the transferase is tolerated.

For ease of reference the modified estrogen receptor-C3T construct will now be referred to as ER:C3T , signifying a tamoxifen-responsive element fused to C3T. The construct is under the control of the *acr-2* promoter, and so will express only in cholinergic neurons, where we have already established a role for RHO-1 (McMullan, Hiley et al. 2006). The fusion protein should be inactive until the addition of tamoxifen, allowing for normal development of the nervous system.

7.1.1 - Transgenic lines containing C3:TMX appear wild-type

The ER:C3T construct was injected into N2 adults at a concentration of 10ng/ul, along with plasmid KP#307 (p.*acr-2*::GFP) as a co-injection marker. It was relatively easy to obtain a transgenic line carrying this construct, which suggested to us that the C3T protein was indeed in an inactive state, as untagged C3T is highly toxic. From a typical set of 20 injections, 6 of the injected animals produced transgenic progeny. Three of the lines gave some transgenic progeny which were malformed, looking dumpy, suggesting

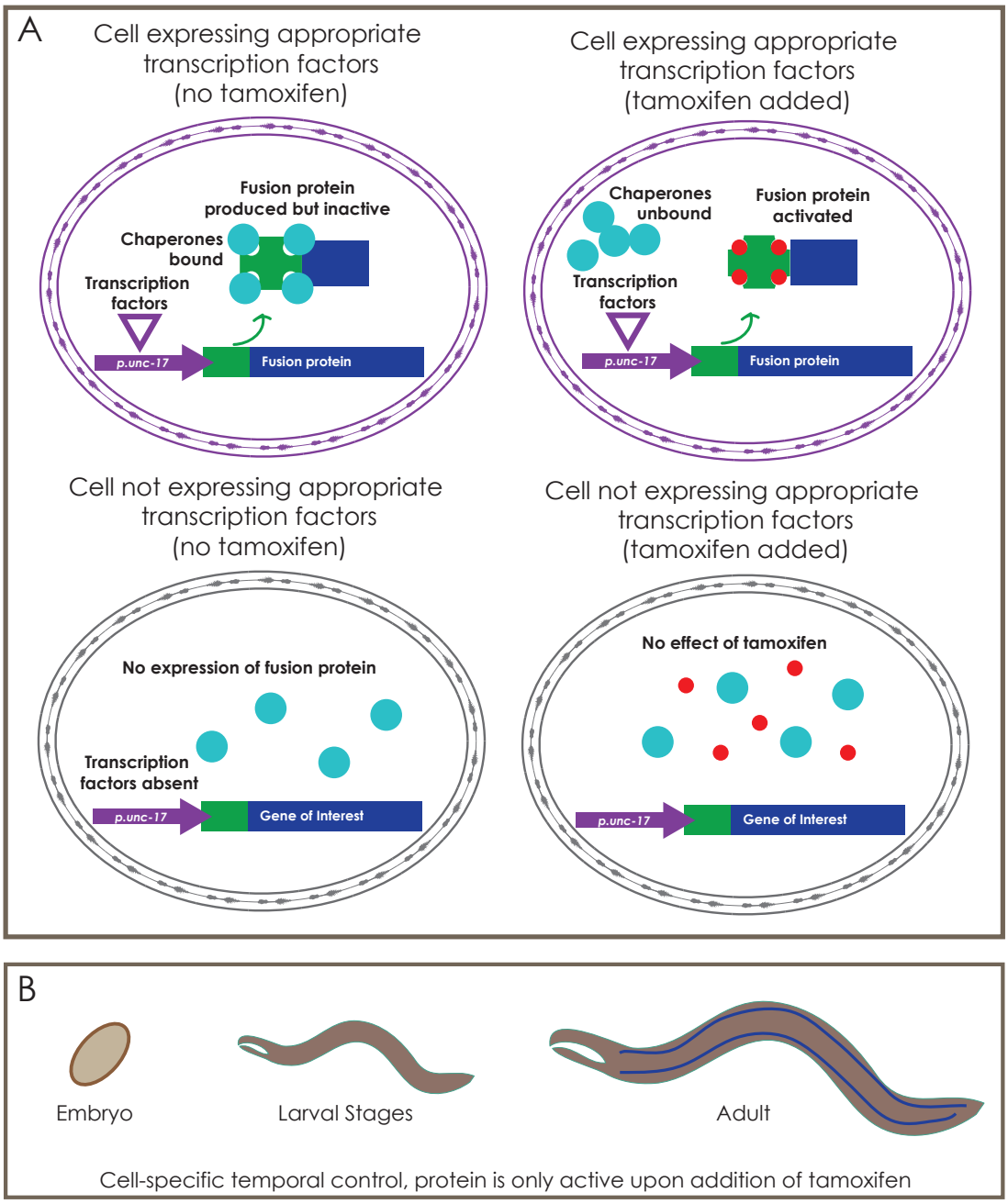

Figure 7-5 Control of protein expression using tamoxifen

The gene of interest is coupled to the modified estrogen receptor (green shape), and expressed from a tissue specific promoter in an inactive state due to the binding of chaperones (light blue circles). Upon addition of tamoxifen (red cirlcles), the estrogen receptor undergoes a conformational cange, the chaperone proteins are released and the protein is activated (B).

that some C3T activity might be present without the addition of tamoxifen. These lines were not frozen.

The remaining three lines of animals carrying this construct, as marked by the presence of the *acr-2*::GFP co-injection marker, appear wild-type, and were named QT947, QT948 and QT949. This marker also allowed us to examine the nervous system wiring for pathfinding defects common with C3T expression, and these animals did not display any defects (data not shown.)

The locomotion of these transformed animals does not appear to be affected by the presence of the RHO-1 inhibitor, in contrast to animals expressing untagged C3, which are lethargic almost to the point of being paralysed (McMullan, Hiley et al. 2006).

7.1.1 - Addition of tamoxifen to wild-type animals has no discernable effect on locomotion or response to aldicarb

One of the potential issues of using tamoxifen to activate proteins tagged with the estrogen receptor is the need to separate the effects of the activated protein from any effects of the drug itself. As part of this testing process, tamoxifen was administered to wild-type animals for us to observe its effects on locomotion and behaviour.

In mammalian tissues, tamoxifen itself is modified to more active compounds, such as 5-OH-Tamoxifen (5-OH-T) which has a far greater affinity for the estrogen receptor. As *C. elegans* may lack the ability to convert the prodrug to its more active form, these experiments make use of 5-OH-Tamoxifen. This has a recommended dilution of 20mg/ml, with 100nM being the recommended final concentration for use in tissue culture experiments.

Based on the use of other pharmacological compounds in *C. elegans* (Rand 1995) and our own protocols for administering compounds such as aldicarb, we diluted the drug in 99% EtOH to 10mg/ml, and prepared NGM plates containing 1µM 5-OH-T, 100 times the tissue culture concentration.

1 day old adult animals were placed onto these plates, and after 5 minutes showed uncoordinated locomotion, where the animals appeared to be dragging their tails rather than moving smoothly. After 1 hour, the animals were highly lethargic, but animals removed at this time point recovered normal locomotion after 2 hours of recovery in the absence of the drug. After 2 hours exposure to tamoxifen, animals were completely paralysed.

Having seen these effects on animals exposed to tamoxifen, we next wanted to try a range of concentrations of the drug, to find a safe exposure limit that would not cause paralysis. We again made NGM plates, this time containing 2nM, 10nM, 20nM, 50nM, 100nM, 200nM, 500nM, and 1µM tamoxifen. We also prepared plates containing an equivalent amount of ethanol as a control.

10 young adult animals were picked to each plate, and examined for paralysis or uncoordinated locomotion at intervals of 10 minutes, 30 minutes, 1 hour and 2 hours. No difference to the control plates was observed at any concentration used over the course of the experiment, in contrast to the results seen previously.

Animals left on these plates overnight exhibited no ill effects to exposure to the drug, so we prepared a further range of dilutions to test exposure to greater concentrations of 5-OH-T. This new set of NGM plates contained 1µM, 2µM, 5µM, 10µM and 20µM concentrations of the drug. After 1 hour of observation, there were no visible changes in locomotion, except at the 20µM concentration range, where animals exposed to 5-OH-T appeared to have slightly shallower body bends. However, after 4 hours, these animals looked wild-type, whereas the animals exposed to 2uM appeared slightly loopy, and 1 of the 10 adult animals on the 5uM plate was paralysed.

7.1.1 - Tamoxifen does not enhance paralysis in combination with the acetylcholinesterase inhibitor, aldicarb

The first experiment, which showed dramatic behavioural changes in response to tamoxifen, appears to be an outlier based on these further experiments. It is possible that the plates used were contaminated with aldicarb from a parallel experiment, so we prepared plates containing both aldicarb and tamoxifen in an attempt to recreate this potential scenario.

Over the course of a two hour experiment, animals were exposed to either 1µM tamoxifen with 100mM aldicarb, 1µM tamoxifen alone, 100mM aldicarb alone or an alcohol-only control, to control for the ethanol in which tamoxifen is suspended. During the course of two hours of observation, there was no visible difference in the paralysis of animals exposed to aldicarb and tamoxifen compared to exposure to aldicarb alone. While the animals paralysed in both situations, this paralysis was not at the fast rate observed in the first experiment, leaving the cause of that paralysis unexplained.

In every case except one we have observed no effect on wild-type adult from exposure to tamoxifen. In that single instance, we saw that animals became paralysed within 1hr after being placed on tamoxifen plates. Having been unable to replicate that result, even

at very high concentrations of tamoxifen, we are unable to say whether this represents a true response to tamoxifen which was uncovered due to an additional, unknown factor, or whether this response was due entirely to some other unknown factor.

7.1.1 - Addition of tamoxifen to ER:C3T animals via NGM plates did not cause paralysis

Having tested the response of wild-type animals to tamoxifen, we attempted to activate the C3T in the ER:C3T lines. We first adminstered tamoxifen via uptake from our NGM plates, as described in the testing of wild-type animals. We used a range of concentrations to attempt to activate the C3T construct: 7µM, 12.5 µM, 21.5µM and 70µM, along with control plates containing an equivalent amounts of ethanol solvent. No effect on locomotion was observed when animals carrying the ER:C3T transgene were placed on these plates for a period of up to 6 hours.

Tamoxifen is light-sensitive, so we wondered whether exposure to light might be inactivating the compound in the plates. We therefore used a further concentration range: 2.5µM, 10µM and 100µM, and a 20µl EtOH plate as control, and kept these plates in a light-proof box to avoid photoinactivation. However, after a period of two days grown in the presence of tamoxifen in the dark, none of the animals from the three independent lines showed any response indicating C3T activation.

It is possible that the drug is inactivated by the salts found in the NGM plate, and therefore we made use of a number of different solvents, including olive oil, to try to prevent this inactivation. We also used a fresh stock of tamoxifen, at 20mg/ml, obtained as a gift from the Lloyd lab, who were successfully using it in their mammalian experiments, in case our own stock had been photoinactivated.

We dissolved the olive oil/tamoxifen mix into the worm mixture, at 0.1µg/ml, 0.2µg/ml, 5µg/ml and 1µg/ml. 10 N2 and 10 ER:C3T L4 animals animals were placed on these plates, and left to grow for 4 days. After this time, none of the animals were paralysed. However, the animals carrying the ER:C3T were not starved, whereas the N2 plates were starved. This suggests that the ER:C3T animals were slower growing, which may be as a very subtle result of carrying the ER:C3T plasmid.

7.1.1 - Direct exposure to tamoxifen did not cause paralysis in ER:C3T animals

A number of drug compounds, such as phorbol esters, aldicarb and levamisole are able to penetrate the cutilcle of the worm by absorption from the NGM plate, but we

wondered whether this mechanism was ineffective for 5-OH-T. Therefore we soaked the ER:C3T expressing worms in a solution of tamoxifen, to expose them directly to a high concentration. Animals expressing ER:C3T were placed in drops of olive oil containing 20mg/ml tamoxifen for up to 2 hours, but did not become paralysed during exposure, or when observed for several days afterwards.

7.1.1 - Injection of Tamoxifen into ER:C3T animals shows some limited effects on behaviour

It is possible that the cuticle is a physical barrier to the entry of the drug. Therefore, we tried to inject the drug into the worms, using tamoxifen dissolved in olive oil. These injections were either into the gonad (to try to induce C3T activation in the developing embryos), intestine or ceolemic space. Of 17 injected animals, 6 were dead one day after injection, and a further 3 were dead three days post-injection. In many of these animals, bubbles of oil were visible. It is not clear whether the retention of oil was responsible for killing these animals, as some of those which survived also contained oil bubbles, or whether the tamoxifen was activating the C3T plasmid with toxic effects. Perhaps more precision targeting of the ceolemic space would give a greater likelihood of activation in the injected animal.

Of the remaining 8 animals, 5 produced offspring which were uncoordinated, and tended to drag their tails when moving. This subtle behavioural change is different to severe paralysis associated with expression of C3, so it is unclear whether it results from some level of C3T activation or from some other effect of the injection procedure. Further injections of tamoxifen failed to produce any uncoordinated offspring. On examining animals from these further rounds of injections with tamoxifen, it was discovered that even some animals not injected appeared to have uncoordinated locomotion, suggesting some background C3T activation.

The net result of these experiments is an inability to see a response to tamoxifen, either in a wild-type background or in animals carrying a construct expressing C3T fused to the estrogen receptor.

7.1 - Conclusions

There are a number of potential reasons why this method was unsuccessful. These could be due to problems with the construct, with the fusion protein or the application of tamoxifen itself. I will address these three briefly in turn.

7.1.1 - The ER:C3T construct may not express efficiently

We do not have evidence that the construct expressing ER:C3T is indeed being expressed in the transfected animals. There are a number of reasons why it might not be expressing well.

First, the modified estrogen receptor contains a sequence with a mammalian codon bias. It is possible that this is an impediment to high expression, and that synthesising an estrogen receptor with a *C. elegans* codon bias might improve the efficiency of this method.

Secondly, including an additional green fluorescent protein (GFP) tag into the construct would provide a serviceable way of checking expression. While the presence of the estrogen receptor might not prevent GFP fluorescence, making it a poor target for observing regulation, the GFP might still act as a good indicator of expression.

Future experiments would be to quantify the level of expression of C3T from the construct; we could make use of a C3T -specific antibody, or an ER antibody. Given more time we would have liked to have used this method to whether C3T is present in our transformed lines.

7.1.1 - The ER:C3T fusion protein may not be activated by tamoxifen in *C. elegans*

If the tagged C3T protein is being expressed, it may be that the C3T is permanently inactivated by the addition of the estrogen receptor, and not able to be activated by the addition of tamoxifen.

We have previously tagged the C3T with GFP without affecting activity, but there may be additional conformational changes induced by the estrogen receptor which completely inactivate the protein.

The mechanism of activation by addition of tamoxifen is somewhat unclear, but is thought to be due to chaperones, such as those involved in the heat-shock response, accumulating around the estrogen receptor and physically masking the effects of whatever protein is attached to the receptor. It may be the case that in *C. elegans* these chaperones bind in a way that is not tractable to tamoxifen addition.

7.1.1 - Tamoxifen delivery to *C. elegans* may be inefficient

The addition of tamoxifen by a number of methods failed to elicit a response in the ER:C3T strain. A simple explanation is that the drug fails to be absorbed by the animals. A wide range of drugs are able to penetrate the *C. elegans* cuticle, but perhaps tamoxifen

is unable to. One way to test this would be to conduct the same experiments using strains which are hypersensitive to drugs due to mutations in their cuticle integrity, such as bus-8 (Partridge, Tearle et al. 2008). It could also be that we are accidentally inactivating the drug through our handling, perhaps by exposure to light or bacteria. It may even be the case that *C. elegans* is able to metabolise tamoxifen to an inactive form, which would make it an unsuitable compound for use in worm biology.

7.1.1 - Final thoughts

We believe a temporally and spatially controlled C3T would allow us to investigate the acute effects of loss of RHO-1 function in more detail than previous techniques allow. While tamoxifen regulation has not proven successful at this stage, its usefulness in mammalian systems indicates that it would be a valuable addition to the tools available *C. elegans* researchers, and one worth pursuing with the modifications suggested above.

Mutant	Allele name	Top Candidates	Identified as not loopy	Confirmed Not Loopy at 15oC	Growth at 20oC	Movement at 20oC	Loopy after heatshock	Sterile after heatshock	Growth after heatshock	Pumping after heatshock	Comments
1.03	nz97	*	Not loopy	Not loopy	Yes	Not loopy	Not loopy	Sterile		Like QT631 w/ hs	pvl 24hrs post hs
1.05	nz92	*	Not loopy	Not loopy	Yes	Not loopy	Not loopy	Not sterile		Faster than QT631 w/ hs	pvl 24hrs post hs NOT sick 24hrs post hs
1.13			Not loopy	Not loopy							
1.22			Not loopy	Not loopy	Yes - but slow growth	Not loopy	Less loopy (than QT631)	Not sterile		Like QT631 w/ hs	pvl
2.06			Not loopy	Not loopy	Yes - but slow growth	Not loopy	Loopy	Not sterile		Like QT631 w/ hs	dpy @ 20oC pvl 24hrs post hs
2.07			Not loopy	Not loopy	Yes	Not loopy	Not loopy	Not sterile		Like QT631 w/ hs	
2.09	nz93	*	Not loopy	Not loopy	Yes	Not loopy	Not loopy	Not sterile		Like N2	pvl 24hrs post hs
2.13			Not loopy	Less loopy (than QT631)	Yes	Loopy	Not loopy	Not sterile		Like QT631 w/ hs	pvl 24hrs post hs
2.14			Not loopy	Not loopy	Yes	Less loopy (than QT631)	Less loopy (than QT631)	Not sterile		Like QT631 w/ hs	
2.15			Not loopy	Not loopy							
2.29	nz96	*	Not loopy	Not loopy	Yes	Not loopy	Not loopy	Not sterile		Faster than QT631 w/ hs	NOT pvl or dar 24hrs post hs NOT sick after hs

Mutant	Allele name	Top Candidates	Identified as not loopy	Confirmed Not Loopy at 15oC	Growth at 20oC	Movement at 20oC	Loopy after heatshock	Sterile after heatshock	Growth after heatshock	Pumping after heatshock	Comments
2.3			Not loopy	Not loopy	Yes	Less loopy (than QT631)	Loopy	Not sterile		Like QT631 w/ hs	pvl and dar 24hrs post hs
2.31			Not loopy	Lethargic, not loopy							
2.34			Not loopy	Less loopy (than QT631)							
3.14			Not loopy	Lethargic, not loopy							
3.26			Not loopy	Not loopy	Yes	Not loopy	Less loopy (than QT631)	Not sterile		Faster than QT631 w/ hs	pvl and slight dar 24hrs post hs
3.36			Not loopy	Not loopy	Yes	Not loopy	Less loopy (than QT631)	Not sterile		Like QT631 w/ hs	pvl and slight dar 24hrs post hs
4.01			Not loopy	Lethargic, not loopy							
4.08			Not loopy	Less loopy (than QT631)	Yes	Loopy	Not loopy	Not sterile		Faster than QT631 w/ hs	
4.09			Not loopy	Lethargic, not loopy							
4.13	nz94	*	Not loopy	Lethargic, not loopy	Yes	Lethargic, not loopy	Not loopy	Sterile		Like QT631 w/ hs	Mapped as UNC-80 mutation and sequenced
4.17			Not loopy								

Mutant	Allele name	Top Candidates	Identified as not loopy	Confirmed Not Loopy at 15oC	Growth at 20oC	Movement at 20oC	Loopy after heatshock	Sterile after heatshock	Growth after heatshock	Pumping after heatshock	Comments
4.2			Not loopy	Lethargic, not loopy							
4.36	nz98	*	Not loopy	Lethargic, not loopy	Yes - but slow growth	Lethargic, not loopy	Lethargic, not loopy	Sterile		Faster than QT631 w/ hs	UNC-80 mutation - not sequenced yet, but does not complement unc-80
4.37			Not loopy	Lethargic, not loopy							
4.42			Not loopy	Less loopy (than QT631)	Yes	Less loopy (than QT631)	Lethargic, not loopy	Not sterile		Like N2	
4.43			Not loopy	Less loopy (than QT631)							
5.03			Not loopy	Not loopy	Yes	Not loopy	Loopy	Sterile		Like QT631 w/ hs	
7.12	nz99	*	Not loopy	Not loopy	Yes	Not loopy	Not loopy	Sterile		Faster than QT631 w/ hs	pvl and dar 24hrs post hs
8.02			Not loopy	Less loopy (than QT631)	Yes	Less loopy (than QT631)	Less loopy (than QT631)	Not sterile		Faster than QT631 w/ hs	pvl 24 hrs post hs
8.07	nz103	*	Not loopy	Less loopy (than QT631)	Yes	Not loopy	Not loopy	Not sterile		Faster than QT631 w/ hs	pvl 24 hrs post hs
9.01			Not loopy	Not loopy	Yes	Less loopy (than QT631)	Not loopy	Sterile		Like QT631 w/ hs	pvl not sick 24hrs post hs
10.01			Not loopy	Not loopy	Yes	Loopy	Not loopy	Not sterile		Faster than QT631 w/ hs	v. few were loopy after hs

Mutant	Allele name	Top Candidates	Identified as not loopy	Confirmed Not Loopy at 15oC	Growth at 20oC	Movement at 20oC	Loopy after heatshock	Sterile after heatshock	Growth after heatshock	Pumping after heatshock	Comments
10.1			Not loopy	Not loopy							
10.17			Not loopy								
11.05			Not loopy	Lethargic, not loopy							
11.06			Not loopy	Lethargic, not loopy							
11.07			Not loopy								
12.09			Not loopy	Less loopy (than QT631)	Yes	Less loopy (than QT631)	Loopy	Sterile		Like QT631 w/ hs	pvl not dar 24hrs post hs
12.1			Not loopy	Not loopy							
13.03			Not loopy	Not loopy							
13.05	nz100	*	Not loopy	Not loopy	Yes	Not loopy	Less loopy (than QT631)	Sterile		Like QT631 w/ hs	
13.09			Not loopy	Not loopy	Yes	Not loopy	Loopy	Sterile		Like QT631 w/ hs	
13.1			Not loopy	Not loopy	Yes - but slow growth	Loopy	Less loopy (than QT631)	Sterile		Faster than QT631 w/ hs	a few were loopy after hs

Mutant	Allele name	Top Candidates	Identified as not loopy	Confirmed Not Loopy at 15oC	Growth at 20oC	Movement at 20oC	Loopy after heatshock	Sterile after heatshock	Growth after heatshock	Pumping after heatshock	Comments
13.11			Not loopy	Not loopy	Yes	Not loopy	Loopy	Sterile		Like QT631 w/ hs	pvl not dar 24hrs post hs
13.12			Not loopy	Not loopy	Yes - but slow growth	Less loopy (than QT631)	Less loopy (than QT631)	Not sterile		Like N2	a few were loopy after hs
13.15	nz101	*	Not loopy	Not loopy	Yes	Not loopy	Not loopy	Not sterile		Like QT631 w/ hs	pvl 24hrs post hs
13.18			Not loopy	Not loopy							
13.19			Not loopy	Lethargic, not loopy							
13.2			Not loopy	Not loopy							
13.25			Not loopy	Not loopy	Yes	Less loopy (than QT631)	Not loopy	Sterile		Like QT631 w/ hs	pvl 24hrs post hs
14.09			Not loopy	Not loopy	Yes	Loopy	Loopy	Sterile		Like QT631 w/ hs	bli
14.1			Not loopy	Less loopy (than QT631)	Yes	Not loopy	Less loopy (than QT631)	Not sterile		Faster than QT631 w/ hs	pvl and slight dar 24hrs post hs
15.01			Not loopy	Not loopy							
15.02	nz95	*	Not loopy	Not loopy	Yes	Not loopy	Not loopy	Not sterile		Faster than QT631 w/ hs	? Wt pumping

Mutant	Allele name	Top Candidates	Identified as not loopy	Confirmed Not Loopy at 15oC	Growth at 20oC	Movement at 20oC	Loopy after heatshock	Sterile after heatshock	Growth after heatshock	Pumping after heatshock	Comments
15.03			Not loopy	Less loopy (than QT631)	Yes	Loopy	Loopy	Not sterile		Like QT631 w/ hs	
15.04			Not loopy								
15.06			Not loopy	Not loopy							
16.03			Not loopy								
16.04			Not loopy	Not loopy	Yes	Loopy	Loopy	Sterile		Like QT631 w/ hs	
16.09			Not loopy	Lethargic, not loopy							
16.11			Not loopy	Not loopy	Yes	Less loopy (than QT631)	Not loopy	Sterile		Like QT631 w/ hs	pvl and dar 24hrs post hs
17.01			Not loopy	Not loopy	Yes	Less loopy (than QT631)	Loopy	Not sterile		Faster than QT631 w/ hs	pvl 24hrs post hs
17.02			Not loopy	Loopy							
18.03			Not loopy	Not loopy	Yes	Not loopy	Not loopy	Not sterile		Faster than QT631 w/ hs	
18.06	nz102	*	Not loopy	Not loopy	Yes	Not loopy	Not loopy	Not sterile		Like QT631 w/ hs	pvl and slight dar 24hrs post hs

Mutant	Allele name	Top Candidates	Identified as not loopy	Confirmed Not Loopy at 15oC	Growth at 20oC	Movement at 20oC	Loopy after heatshock	Sterile after heatshock	Growth after heatshock	Pumping after heatshock	Comments
18.07			Not loopy	Less loopy (than QT631)	Yes	Less loopy (than QT631)	Loopy	Not sterile		Like QT631 w/ hs	
20.03			Not loopy	Not loopy							
20.08			Not loopy	Loopy	Yes	Less loopy (than QT631)	Not loopy	Not sterile		Like N2	some look slightly loopy
20.11			Not loopy	Less loopy (than QT631)	Yes - but slow growth	Loopy	Not loopy	Not sterile		Faster than QT631 w/ hs	some look slightly loopy
21.09			Not loopy								
22.03			Not loopy	Less loopy (than QT631)							
23.04			Not loopy	Lethargic, not loopy							
24.04			Not loopy	Loopy							
24.07			Not loopy								
24.12			Not loopy	Less loopy (than QT631)	Yes	Less loopy (than QT631)	Less loopy (than QT631)	Not sterile		Faster than QT631 w/ hs	some look loopy after hs; Hypersensitive to alidcarb
24.13			Not loopy	Less loopy (than QT631)	Yes	Less loopy (than QT631)	Less loopy (than QT631)	Not sterile		Faster than QT631 w/ hs	pvl 24hrs post hs

Mutant	Allele name	Top Candidates	Identified as not loopy	Confirmed Not Loopy at 15oC	Growth at 20oC	Movement at 20oC	Loopy after heatshock	Sterile after heatshock	Growth after heatshock	Pumping after heatshock	Comments
A.01	nz104	*	Not loopy	Not loopy	Yes	Not loopy	Lethargic, not loopy	Sterile		Faster than QT631 w/ hs	Molting Defect? All worms straight
A.07			Not loopy	Less loopy (than QT631)							Like QT631 in alidcarb assay
A.14		*	Not loopy	Not loopy	Yes	Not loopy	Lethargic, not loopy	Sterile		Like N2	
A.16		*	Not loopy	Not loopy	Yes	Not loopy	Less loopy (than QT631)	Sterile		Faster than QT631 w/ hs	
A.17	nz105	*	Not loopy	Not loopy	Yes	Not loopy	Less loopy (than QT631)	Sterile		Faster than QT631 w/ hs	Pumping is sporadic after hs: . . . - - - - . . . - - - - -
A.20	nz110		Not loopy	Not loopy	Yes	Not loopy	Less loopy (than QT631)	Sterile	Very slow growth	Faster than QT631 w/ hs	Variable growth after hs - between sterile and slow growth; resistant to aldicarb
AA.5			Not loopy	Not loopy	Yes - but slow growth		Loopy	Not sterile	Same as control	Faster than QT631 w/ hs	
AB.01			Not loopy	Not loopy	Yes - but slow growth	Loopy		Sterile			
B.01			Not loopy	Not loopy	Yes	Less loopy (than QT631)	Not loopy	Sterile		Faster than QT631 w/ hs	
B.05			Not loopy	Less loopy (than QT631)	Yes	Less loopy (than QT631)	Less loopy (than QT631)	Not sterile	Slower growth	Faster than QT631 w/ hs	
B.09			Not loopy	Not loopy	Yes	Less loopy (than QT631)	Less loopy (than QT631)	Not sterile	Same as control	Faster than QT631 w/ hs	some look less loopy after hs/growing faster after hs comp. to control?

Mutant	Allele name	Top Candidates	Identified as not loopy	Confirmed Not Loopy at 15oC	Growth at 20oC	Movement at 20oC	Loopy after heatshock	Sterile after heatshock	Growth after heatshock	Pumping after heatshock	Comments
B.13			Not loopy	Less loopy (than QT631)	Yes	Loopy	Less loopy (than QT631)	Sterile		Faster than QT631 w/ hs	
B.20			Not loopy	Not loopy	Yes	Not loopy	Loopy	Sterile		Like QT631 w/ hs	some look dumpy after hs/variable GFP markers/variable growth after hs - between very slow growth and sterile
D.02					Yes	Not loopy		Sterile		Slower than QT631 w/ hs	
D.03	nz111		Not loopy	Not loopy	Yes	Less loopy (than QT631)	Less loopy (than QT631)	Not sterile	Slower growth	Slower than QT631 w/ hs	Resistant to aldicarb
D.07	nz106	*	Not loopy	Not loopy	Yes	Not loopy	Less loopy (than QT631)	Not sterile	Very slow growth	Like QT631 w/ hs	some bag of worms after hs/some lack a GFP marker/looks like completed one generation+eggs only after hs; hypersensitive to aldicarb
D.09			Not loopy		Yes	Not loopy		Sterile			
J.04			Not loopy	Not loopy	Yes - but slow growth	Loopy	Less loopy (than QT631)	Sterile			
J.05			Not loopy	Not loopy	Yes	Less loopy (than QT631)	Not loopy	Not sterile			growing slower than control after hs
J.10			Not loopy	Not loopy	Yes	Less loopy (than QT631)	Less loopy (than QT631)	Not sterile	Same as control	Faster than QT631 w/ hs	more variable@20oC/more eggs, less larvae after hs
K.02			Not loopy	Not loopy			Less loopy (than QT631)	Not sterile	Slower growth	Faster than QT631 w/ hs	some look loopy after hs
L.08			Not loopy	Not loopy	Yes	Not loopy	Less loopy (than QT631)	Not sterile	Slower growth	Slower than QT631 w/ hs	some look loopy after hs, Some worms curled up

Mutant	Allele name	Top Candidates	Identified as not loopy	Confirmed Not Loopy at 15oC	Growth at 20oC	Movement at 20oC	Loopy after heatshock	Sterile after heatshock	Growth after heatshock	Pumping after heatshock	Comments
L.09	nz107	*	Not loopy	Not loopy	Yes	Not loopy	Not loopy	Not sterile	Same as control	Like N2	Molting Defect?/some look loopy after hs, like QT631 in aldicarb assay
L.10	nz108	*	Not loopy	Not loopy	Yes	Less loopy (than QT631)	Not loopy	Not sterile	Very slow growth	Like N2	like QT631 in aldicarb assay
L.13			Not loopy	Not loopy	Yes - but slow growth	Lethargic, loopy	Less loopy (than QT631)	Not sterile	Same as control	Slower than QT631 w/ hs	
L.15	nz109	*	Not loopy	Not loopy	Yes	Not loopy	Not loopy	Not sterile	Same as control	Faster than QT631 w/ hs	growing well after hs; like QT631 in aldicarb assay
O.03			Not loopy	Less loopy (than QT631)	Yes - but slow growth	Less loopy (than QT631)	Less loopy (than QT631)	Sterile		Slower than QT631 w/ hs	more variable@20oC/v. not loopy after hs
Q.02			Not loopy	Not loopy	Yes - but slow growth	Less loopy (than QT631)	Not loopy	Sterile			Hypersensitive to aldicarb
S.01			Not loopy	Not loopy	Yes	Less loopy (than QT631)	Less loopy (than QT631)	Sterile	Very slow growth	Faster than QT631 w/ hs	more variable@20oC/variable GFP markers
S.06			Not loopy	Not loopy	Yes	Lethargic, loopy	Loopy	Sterile			variable growth after hs; hypersensitive to aldicarb
S.08			Not loopy		Yes	Less loopy (than QT631)		Sterile			
S.10			Not loopy	Less loopy (than QT631)	Yes	Less loopy (than QT631)	Less loopy (than QT631)	Not sterile	Same as control	Faster than QT631 w/ hs	look sick after hs
U.01			Not loopy	Not loopy	Yes	Less loopy (than QT631)	Not loopy	Sterile		Faster than QT631 w/ hs	

Mutant	Allele name	Top Candidates	Identified as not loopy	Confirmed Not Loopy at 15oC	Growth at 20oC	Movement at 20oC	Loopy after heatshock	Sterile after heatshock	Growth after heatshock	Pumping after heatshock	Comments
U.05			Not loopy	Not loopy	Yes	Not loopy		Sterile			Variable growth after hs - between sterile and very slow growth; like QT631 in aldicarb assay
U.06					Yes - but slow growth	Not loopy					like QT631 in aldicarb assay
U.07			Not loopy	Not loopy	Yes	Less loopy (than QT631)	Less loopy (than QT631)	Not sterile	Slower growth	Slower than QT631 w/ hs	
W.05			Not loopy	Not loopy	Yes		Less loopy (than QT631)				
X.03			Not loopy	Not loopy		Loopy	Loopy	Not sterile	Same as control	Slower than QT631 w/ hs	

Chromosome	Position	Class	Description	Gene Name	WT Base	Mutated Base	Number WT Reads	Number Varient Reads	Pileup
I	1396032	missense	GCA->ACA[Ala->Thr]	Y92H12BR.7	G	A	0	9	@AaaaaAaaa
I	5990322	missense	GTT->GGT[Val->Gly]	C06A5.3	T	G	1	8	@GGGGGGGG.
I	6514481	missense	TTG->TTC[Leu->Phe]	glh-2	G	C	0	4	@cccc
I	8624283	missense	GGA->AGA[Gly->Arg]	fer-1	C	T	1	12	@.tTTtTTtAttt
II	866038	missense	AGA->ACA[Arg->Thr]	Y46B2A.3	C	G	0	8	@ggGGGGGGg
II	1539427	missense	CTC->TTC[Leu->Phe]	fbxb-44	C	T	0	4	@TTTT
II	2903202	missense	GAG->GGG[Glu->Gly]	Y110A2AM.1	T	C	1	8	@CCCCCCCC,
II	3797203	missense	CAA->CCA[Gln->Pro]	Y8A9A.2	A	C	9	70	@,,,,,,,,[29 C / 40 c / 1 t]
II	5079267	missense	GGC->GCC[Gly->Ala]	dsh-2	C	G	1	11	@GGGGGGGgggg.
II	5079269	missense	TTT->TTG[Phe->Leu]	dsh-2	A	C	1	7	@CCCcccc.
II	7451225	missense	ACG->ATG[Thr->Met]	Y9D1A.2	G	A	0	5	@aAaaa
II	7866906	missense	AGG->TGG[Arg->Trp]	T09A5.12	T	A	0	6	@aaaaAA
II	11212543	missense	CTT->CCT[Leu->Pro]	T06D8.1	T	C	1	7	@.CCCcccc
II	12668766	missense	GAT->GTT[Asp->Val]	rgs-4	A	T	0	4	@ttTT
II	12668767	missense	GAT->GAG[Asp->Glu]	rgs-4	T	G	0	4	@gggG
III	8068400	missense	AGT->AGA[Ser->Arg]	ceh-26	T	A	0	5	@aaaaa
III	8068401	missense	ACT->GCT[Thr->Ala]	ceh-26	A	G	0	5	@ggggg
III	8358762	missense	TCT->TTT[Ser->Phe]	rfp-1	C	T	0	11	@tTTTtTTTTTt
III	9245321	premature_stop	TGG->TAG[Trp->stop]	dat-1	G	A	1	10	@,AaaAAaAAaa
III	10437049	missense	TGT->TAT[Cys->Tyr]	H04D03.1	G	A	1	10	@AAAaAaaaAa,
IV	5849520	missense	CAA->CAT[Gln->His]	C06E7.1	A	T	0	4	@TtTt
IV	6485407	missense	AGA->AGT[Arg->Ser]	Y73B6BL.1	A	T	1	9	@tTTtt.Tttt
IV	7735094	missense	GGT->GAT[Gly->Asp]	clx-1	G	A	1	8	@aaaaAAA,a
IV	9770293	missense	ATT->GTT[Ile->Val]	msp-78	A	G	1	10	@.GGGCgGgggg
IV	10441763	missense	GTA->GGA[Val->Gly]	F13B12.3	T	G	0	4	@GGGG
IV	12931059	missense	CAA->CGA[Gln->Arg]	C32H11.7	A	G	1	9	@GGGGg,GgGg

Chromosome	Position	Class	Description	Gene Name	WT Base	Mutated Base	Number WT Reads	Number Varient Reads	Pileup
V	3326356	missense	AGA->GGA[Arg->Gly]	C17B7.7	A	G	1	7	@Ggggg.gg
V	3326546	missense	AAT->AAA[Asn->Lys]	C17B7.7	T	A	1	10	@aaaaaa,AAAA
V	8706638	missense	CCA->GCA[Pro->Ala]	ZC178.2	G	C	1	9	@CcCccCCC.c
V	12866414	missense	CAG->CCG[Gln->Pro]	T07F10.5	A	C	1	9	@cc.cCcCccc
V	20211027	missense	GAA->GGA[Glu->Gly]	Y113G7B.12	T	C	0	6	@CCCccc
V	20211293	missense	GAT->GAA[Asp->Glu]	Y113G7B.12	A	T	1	7	@TtTt.ttt
X	5700	missense	GAA->AAA[Glu->Lys]	CE7X_3.1	G	A	0	4	@Aaaa
X	1836429	missense	AGT->AAT[Ser->Asn]	T26C11.2	G	A	1	7	@.aAAAAAA
X	11056036	missense	AGA->AGT[Arg->Ser]	C09F12.2	A	T	0	8	@TtTtTttT
X	11767391	missense	TGC->TAC[Cys->Tyr]	ttx-3	C	T	7	52	@.,,,,,,[52 T]
X	11767392	missense	TGC->GGC[Cys->Gly]	ttx-3	A	C	7	80	@.,,,,,,[80 C]
X	15748986	missense	TCG->TTG[Ser->Leu]	ZK678.3	G	A	1	9	@aAa,AaAAaa
X	15748987	missense	TCG->ACG[Ser->Thr]	ZK678.3	A	T	1	10	@tTt,TtTTtTT
I	1649388	frameshift	frameshift (indel, +1 base)	mab-20	X	X	6	5	@,,,,,,gcccc
II	6759911	frameshift	frameshift (indel, -4 bases)	F41G3.2	X	X	4	3	@,,,,ggg
III	12470206	frameshift	frameshift (indel, 2 bases)	Y49E10.29	X	X	3	4	@,.g,ccc

QT788 (*nz97*)

Chromosome	Position	Class	Description	Gene Name	WT Base	Mutated Base	Number WT Reads	Number Varient Reads	Pileup
I	1396032	missense	GCA->ACA[Ala->Thr]	Y92H12BR.7	G	A	0	9	@AaaaaAaaa
I	5990322	missense	GTT->GGT[Val->Gly]	C06A5.3	T	G	1	8	@GGGGGGGG.
I	6514481	missense	TTG->TTC[Leu->Phe]	glh-2	G	C	0	4	@cccc
I	8624283	missense	GGA->AGA[Gly->Arg]	fer-1	C	T	1	12	@.tTTtTTtAttt
II	866038	missense	AGA->ACA[Arg->Thr]	Y46B2A.3	C	G	0	8	@ggGGGGGg
II	1539427	missense	CTC->TTC[Leu->Phe]	fbxb-44	C	T	0	4	@TTTT
II	2903202	missense	GAG->GGG[Glu->Gly]	Y110A2AM.1	T	C	1	8	@CCCCCCCC,
II	3797203	missense	CAA->CCA[Gln->Pro]	Y8A9A.2	A	C	9	70	@.,,,,,,,,[29 C / 40 c / 1 t]
II	5079267	missense	GGC->GCC[Gly->Ala]	dsh-2	C	G	1	11	@GGGGGGGgggg.
II	5079269	missense	TTT->TTG[Phe->Leu]	dsh-2	A	C	1	7	@CCCcccc.
II	7451225	missense	ACG->ATG[Thr->Met]	Y9D1A.2	G	A	0	5	@aAaaa
II	7866906	missense	AGG->TGG[Arg->Trp]	T09A5.12	T	A	0	6	@aaaaAA
II	11212543	missense	CTT->CCT[Leu->Pro]	T06D8.1	T	C	1	7	@.CCCcccc
II	12668766	missense	GAT->GTT[Asp->Val]	rgs-4	A	T	0	4	@ttTT
II	12668767	missense	GAT->GAG[Asp->Glu]	rgs-4	T	G	0	4	@gggG
III	8068400	missense	AGT->AGA[Ser->Arg]	ceh-26	T	A	0	5	@aaaaa
III	8068401	missense	ACT->GCT[Thr->Ala]	ceh-26	A	G	0	5	@ggggg
III	8358762	missense	TCT->TTT[Ser->Phe]	rfp-1	C	T	0	11	@tTTTtTTTTt
III	9245321	premature_stop	TGG->TAG[Trp->stop]	dat-1	G	A	1	10	@.AaaAAaAAaa
III	10437049	missense	TGT->TAT[Cys->Tyr]	H04D03.1	G	A	1	10	@AAAaAaaaAa,
IV	5849520	missense	CAA->CAT[Gln->His]	C06E7.1	A	T	0	4	@TtTt
IV	6485407	missense	AGA->AGT[Arg->Ser]	Y73B6BL.1	A	T	1	9	@tTTtt.Tttt
IV	7735094	missense	GGT->GAT[Gly->Asp]	clx-1	G	A	1	8	@aaaaAAA,a
IV	9770293	missense	ATT->GTT[Ile->Val]	msp-78	A	G	1	10	@.GGGCgGgggg
IV	10441763	missense	GTA->GGA[Val->Gly]	F13B12.3	T	G	0	4	@GGGG
IV	12931059	missense	CAA->CGA[Gln->Arg]	C32H11.7	A	G	1	9	@GGGGg,GgGg

QT788 (*nz97*)

Chromosome	Position	Class	Description	Gene Name	WT Base	Mutated Base	Number WT Reads	Number Varient Reads	Pileup
V	3326356	missense	AGA->GGA[Arg->Gly]	C17B7.7	A	G	1	7	@Ggggg.gg
V	3326546	missense	AAT->AAA[Asn->Lys]	C17B7.7	T	A	1	10	@aaaaaa,AAAA
V	8706638	missense	CCA->GCA[Pro->Ala]	ZC178.2	G	C	1	9	@CcCccCCC.c
V	12866414	missense	CAG->CCG[Gln->Pro]	T07F10.5	A	C	1	9	@cc.cCcCccc
V	20211027	missense	GAA->GGA[Glu->Gly]	Y113G7B.12	T	C	0	6	@CCCccc
V	20211293	missense	GAT->GAA[Asp->Glu]	Y113G7B.12	A	T	1	7	@TtTt.ttt
X	5700	missense	GAA->AAA[Glu->Lys]	CE7X_3.1	G	A	0	4	@Aaaa
X	1836429	missense	AGT->AAT[Ser->Asn]	T26C11.2	G	A	1	7	@.aAAAAAA
X	11056036	missense	AGA->AGT[Arg->Ser]	C09F12.2	A	T	0	8	@TtTtTttT
X	11767391	missense	TGC->TAC[Cys->Tyr]	ttx-3	C	T	7	52	@.,,,,,,[52 T]
X	11767392	missense	TGC->GGC[Cys->Gly]	ttx-3	A	C	7	80	@.,,,,,,[80 C]
X	15748986	missense	TCG->TTG[Ser->Leu]	ZK678.3	G	A	1	9	@aAa,AaAAaa
X	15748987	missense	TCG->ACG[Ser->Thr]	ZK678.3	A	T	1	10	@tTt,TtTTttT
I	1649388	frameshift	frameshift (indel, +1 base)	mab-20	X	X	6	5	@,,,,,,gcccc
II	6759911	frameshift	frameshift (indel, -4 bases)	F41G3.2	X	X	4	3	@,,,,ggg
III	12470206	frameshift	frameshift (indel, 2 bases)	Y49E10.29	X	X	3	4	@,,g,ccc

Chromosome	Position	Class	Description	Gene Name	WT Base	Mutated Base	Number WT Reads	Number Varient Reads	Pileup
I	1883442	missense	GCA->GAA[Ala->Glu]	tag-305	C	A	0	17	@AaaAAaAAAAaaaaAAAA
I	2052578	missense	AAC->TAC[Asn->Tyr]	Y20F4.5	T	A	2	13	@aaAAA,AAAaaa.aa
I	3784062	missense	GGC->GCC[Gly->Ala]	C32E8.4	G	C	0	5	@ccccc
I	4345305	missense	GGC->GCC[Gly->Ala]	anc-1	G	C	0	6	@CCCCCC
I	4345312	missense	AGT->AGA[Ser->Arg]	anc-1	T	A	0	5	@aaaaa
I	6424917	missense	GAC->AAC[Asp->Asn]	ncbp-1	G	A	0	10	@aAaAAaaaaa
I	14886573	missense	CCT->CTT[Pro->Leu]	frm-1	G	A	2	15	@aAA.aaAAA.AAAAAA
II	86186	missense	ATA->ACA[Ile->Thr]	Y46B2A.3	A	G	0	5	@GgGgg
II	1461309	missense	ATC->ACC[Ile->Thr]	Y51H7C.15	A	G	1	12	@Gg.GgGGGGgggG
II	2267957	missense	ATG->ATA[Met->Ile]	K09F6.2	G	A	1	8	@AAaaaaa,a
II	2597713	missense	GAA->GAC[Glu->Asp]	F33H12.6	T	G	1	8	@GggGgGgg,
II	4866998	missense	AAG->ATG[Lys->Met]	col-17	T	A	1	9	@AaA,AAaAaA
II	6022882	missense	TCA->CCA[Ser->Pro]	ZK84.1	T	C	1	7	@cCc,CCCc
II	7871213	missense	CCT->GCT[Pro->Ala]	T01H3.3	G	C	1	10	@cCCCCCCCCC.
II	9338975	missense	GGT->AGT[Gly->Ser]	ttll-12	G	A	0	10	@aAAaAAAAAa
II	11214458	missense	GAC->GAG[Asp->Glu]	T06D8.1	C	G	2	16	@Gg.ggGgggggg.gggg
II	12536804	missense	AGC->AAC[Ser->Asn]	F49C5.3	G	A	0	10	@aaaaAAaAAa
II	12537356	missense	AAA->ACA[Lys->Thr]	F49C5.3	A	C	0	9	@cCCCCCCcc
II	12538384	missense	ATG->GTG[Met->Val]	F49C5.3	A	G	0	14	@GGGGGGgGggGgGG
II	13043073	missense	AAC->AGC[Asn->Ser]	puf-6	T	C	0	13	@ccccCcCCCCccc
II	14145353	missense	CTC->CCC[Leu->Pro]	W03H9.2	A	G	1	9	@gggGGGG.gg
III	57718	missense	AAG->AAT[Lys->Asn]	W05G11.2	G	T	0	6	@TtTTT†
III	741891	missense	AGA->GGA[Arg->Gly]	T17H7.1	A	G	1	9	@g.ggggGGg
III	4784946	missense	GCA->ACA[Ala->Thr]	C38D4.1	C	T	1	15	@tTT.TtTtTtttTTTt
III	11503254	missense	TTA->TTC[Leu->Phe]	Y66D12A.21	T	G	0	4	@GGGG

Chromosome	Position	Class	Description	Gene Name	WT Base	Mutated Base	Number WT Reads	Number Varient Reads	Pileup
IV	2400426	missense	GAT->AAT[Asp->Asn]	Y38F2AR.12	C	T	1	21	@tttTttttttttttTt,TttT
IV	5487180	missense	TTC->CTC[Phe->Leu]	puf-7	T	C	1	7	@CCCCCCc,C
IV	8262551	missense	GCT->GTT[Ala->Val]	vit-6	C	T	0	15	@TTTTTTTTTTTttt
IV	9840852	missense	GTC->GGC[Val->Gly]	kin-24	A	C	1	7	@ccccCC.c
IV	11828164	missense	GCT->GTT[Ala->Val]	M117.6	G	A	2	13	@aAAAAAAaa.aA.aa
IV	12783224	missense	GCA->GTA[Ala->Val]	unc-31	C	T	0	8	@ttTTttt
IV	14512121	missense	GCT->ACT[Ala->Thr]	Y57G11A.5	C	T	0	18	@TTttttttttTTttTT
IV	15965559	missense	CTC->GTC[Leu->Val]	Y105C5B.18	C	G	0	4	@gggG
V	4095088	missense	GTA->ATA[Val->Ile]	nhr-181	G	A	0	11	@aAAAAAAaAaA
V	5755509	readthrough	CAG->AAG[Gln->Lys]	K09H11.11	G	T	0	11	@TTttTttTtt
V	12810473	readthrough	TGA->TTA[stop->Leu]	ZC443.2	C	A	0	6	@aaaaaa
V	12810474	missense	TGA->AGA[stop->Arg]	ZC443.2	A	T	0	6	@tttttt
V	13136453	missense	CTT->ATT[Leu->Ile]	clec-41	G	T	0	17	@TTTTTTtTTTttttTt
V	14108529	missense	GTC->GCC[Val->Ala]	H39E23.3	T	C	0	7	@CCcccCc
V	20211149	missense	GAT->GAA[Asp->Glu]	Y113G7B.12	A	T	0	5	@ttttT
X	1400070	missense	GTT->GCT[Val->Ala]	ZK402.5	A	G	1	8	@CggGGGg.g
X	3407867	missense	CAA->CAT[Gln->His]	vit-5	A	T	1	8	@t.TTtTtT
X	8034682	missense	ACG->GCG[Thr->Ala]	C18A11.6	T	C	2	20	@cCcCCCcCCCCc.cC.cCcCCC
X	8596018		TGC->TCC[Cys->Ser]	F18E9.7	C	G	1	7	@gGGGGG.T

Bibliography

Aktories K, Hall A. 1989. Botulinum ADP-ribosyltransferase C3: a new tool to study low molecular weight GTP-binding proteins. Trends Pharmacol Sci 10: 415-418.

Alberts B, Johnson, A, Lewis, J, Raff, M, Roberts, K, Walter, P. 2008. Molecular Biology of the Cell: Garland Science.

Alfonso A, Grundahl K, Duerr J, Han H, Rand J. 1993. The Caenorhabditis elegans unc-17 gene: a putative vesicular acetylcholine transporter. Science 261: 617.

Anderson P. 1995. Mutagenesis. Pages 31-58 in Epstein HFaS, D. C., ed. Caenorhabditis elegans: Modern Biological Analysis of an organism. New York/London/San Diego: Academic Press.

Appleford PJ, Gravato-Nobre M, Braun T, Woollard A. 2008. Identification of cis-regulatory elements from the C. elegans T-box gene mab-9 reveals a novel role for mab-9 in hypodermal function. Dev Biol 317: 695-704.

Aravamudan B, Broadie K. 2003. Synaptic Drosophila UNC-13 is regulated by antagonistic G-protein pathways via a proteasome-dependent degradation mechanism. J Neurobiol 54: 417-438.

Avery L. 1993. Motor neuron M3 controls pharyngeal muscle relaxation timing in Caenorhabditis elegans. J Exp Biol 175: 283-297.

Avery L, Horvitz HR. 1989. Pharyngeal pumping continues after laser killing of the pharyngeal nervous system of C. elegans. Neuron 3: 473-485.

Avery L, and Thomas, J.H. 1997. Feeding and Defecation. Pages 679–716 in D.L. Riddle TB, B.J. Meyer, and J.R. Priess, ed. C. elegans II, Cold Spring Harbor Laboratory Press.

Baba T, Sakisaka T, Mochida S, Takai Y. 2005. PKA-catalyzed phosphorylation of tomosyn and its implication in Ca2+-dependent exocytosis of neurotransmitter. J Cell Biol 170: 1113-1125.

Bacaj T, Shaham S. 2007. Temporal control of cell-specific transgene expression in Caenorhabditis elegans. Genetics 176: 2651-2655.

Bai J, Hu Z, Dittman JS, Pym EC, Kaplan JM. 2010. Endophilin functions as a membrane-bending molecule and is delivered to endocytic zones by exocytosis. Cell 143: 430-441.

Barker LA, Dowdall MJ, Whittaker VP. 1972. Choline metabolism in the cerebral cortex of guinea pigs. Stable-bound acetylcholine. Biochem J 130: 1063-1075.

Barrière AF, M.-A. 2006. Isolation of C. elegans and related nematodes in Community TCeR, ed. Wormbook.

Beg AA, Jorgensen EM. 2003. EXP-1 is an excitatory GABA-gated cation channel. Nat Neurosci 6: 1145-1152.

Ben-Ari Y. 2002. Excitatory actions of gaba during development: the nature of the nurture. Nat Rev Neurosci 3: 728-739.

Berri S, Boyle JH, Tassieri M, Hope IA, Cohen N. 2009. Forward locomotion of the nematode C. elegans is achieved through modulation of a single gait. HFSP J 3: 186-193.

Betz A, Ashery U, Rickmann M, Augustin I, Neher E, Sudhof TC, Rettig J, Brose N. 1998. Munc13-1 is a presynaptic phorbol ester receptor that enhances neurotransmitter release. Neuron 21: 123-136.

Bigelow H, Doitsidou M, Sarin S, Hobert O. 2009. MAQGene: software to facilitate C. elegans mutant genome sequence analysis. Nat Methods 6: 549.

Birnby DA, Link EM, Vowels JJ, Tian H, Colacurcio PL, Thomas JH. 2000. A transmembrane guanylyl cyclase (DAF-11) and Hsp90 (DAF-21) regulate a common set of chemosensory behaviors in caenorhabditis elegans. Genetics 155: 85-104.

Block MR, Glick BS, Wilcox CA, Wieland FT, Rothman JE. 1988. Purification of an N-ethylmaleimide-sensitive protein catalyzing vesicular transport. Proc Natl Acad Sci U S A 85: 7852-7856.

Bounoutas A, Chalfie M. 2007. Touch sensitivity in Caenorhabditis elegans. Pflugers Arch 454: 691-702.

Bounoutas A, Zheng Q, Nonet ML, Chalfie M. 2009. mec-15 encodes an F-box protein required for touch receptor neuron mechanosensation, synapse formation and development. Genetics 183: 607-617, 601SI-604SI.

Boyle JH. 2010. C. elegans locomotion: an integrated approachUniversity of Leeds, Leeds.

Branicky R, Hekimi S. 2006. What keeps C. elegans regular: the genetics of defecation. Trends Genet 22: 571-579.

Brenner S. 1974. The genetics of Caenorhabditis elegans. Genetics 77: 71-94.

Brenner S. 1988. Forward. Pages ix-xiii. in Wood WB, ed. The Nematode Caenorhabditis elegans.

N.Y.: Cold Spring Harbor.

Broadie K, Prokop A, Bellen HJ, O'Kane CJ, Schulze KL, Sweeney ST. 1995. Syntaxin and synaptobrevin function downstream of vesicle docking in Drosophila. Neuron 15: 663-673.

Brocard J, Warot X, Wendling O, Messaddeq N, Vonesch JL, Chambon P, Metzger D. 1997. Spatio-temporally controlled site-specific somatic mutagenesis in the mouse. Proc Natl Acad Sci U S A 94: 14559-14563.

Brockie PJaM, A. V. 2006. Ionotropic glutamate receptors: genetics, behavior and electrophysiology in Jorgensen EMaK, J.M, ed. Wormbook.

Brose N, Rosenmund C, Rettig J. 2000. Regulation of transmitter release by Unc-13 and its homologues. Curr Opin Neurobiol 10: 303-311.

Brundage L, Avery L, Katz A, Kim UJ, Mendel JE, Sternberg PW, Simon MI. 1996. Mutations in a C. elegans Gqalpha gene disrupt movement, egg laying, and viability. Neuron 16: 999-1009.

Calixto A, Chelur D, Topalidou I, Chen X, Chalfie M. 2010. Enhanced neuronal RNAi in C. elegans using SID-1. Nat Methods 7: 554-559.

Carvelli L, McDonald PW, Blakely RD, Defelice LJ. 2004. Dopamine transporters depolarize neurons by a channel mechanism. Proc Natl Acad Sci U S A 101: 16046-16051.

Castillo MA, Ghose S, Tamminga CA, Ulery-Reynolds PG. 2010. Deficits in syntaxin 1 phosphorylation in schizophrenia prefrontal cortex. Biol Psychiatry 67: 208-216.

Ceccarelli B, Hurlbut WP, Mauro A. 1973. Turnover of transmitter and synaptic vesicles at the frog neuromuscular junction. J Cell Biol 57: 499-524.

Chalfie M, Sulston J. 1981. Developmental genetics of the mechanosensory neurons of Caenorhabditis elegans. Dev Biol 82: 358-370.

Chalfie M, Tu Y, Euskirchen G, Ward WW, Prasher DC. 1994. Green fluorescent protein as a marker for gene expression. Science 263: 802-805.

Chalfie M, Sulston JE, White JG, Southgate E, Thomson JN, Brenner S. 1985. The neural circuit for touch sensitivity in Caenorhabditis elegans. J Neurosci 5: 956-964.

Charlie NK, Schade MA, Thomure AM, Miller KG. 2006. Presynaptic UNC-31 (CAPS) is required to activate the G alpha(s) pathway of the Caenorhabditis elegans synaptic signaling network. Genetics 172: 943-961.

Chase DL, Patikoglou GA, Koelle MR. 2001. Two RGS proteins that inhibit Galpha(o) and Galpha(q) signaling in C. elegans neurons require a Gbeta(5)-like subunit for function. Curr Biol 11: 222-231.

Chase DL, Pepper JS, Koelle MR. 2004. Mechanism of extrasynaptic dopamine signaling in Caenorhabditis elegans. Nat Neurosci 7: 1096-1103.

Chase DL 2007. Biogenic amine neurotransmitters in C. elegans in Jorgensen EM, J.M, ed. Wormbook.

Chelur DS, Chalfie M. 2007. Targeted cell killing by reconstituted caspases. Proc Natl Acad Sci U S A 104: 2283-2288.

Chen BL, Hall DH, Chklovskii DB. 2006. Wiring optimization can relate neuronal structure and function. Proc Natl Acad Sci U S A 103: 4723-4728.

Cho W, Stahelin RV. 2006. Membrane binding and subcellular targeting of C2 domains. Biochim Biophys Acta 1761: 838-849.

Chronis N, Zimmer M, Bargmann CI. 2007. Microfluidics for in vivo imaging of neuronal and behavioral activity in Caenorhabditis elegans. Nat Methods 4: 727-731.

Chung K, Lu H. 2009. Automated high-throughput cell microsurgery on-chip. Lab Chip 9: 2764-2766.

Chung K, Crane MM, Lu H. 2008. Automated on-chip rapid microscopy, phenotyping and sorting of C. elegans. Nat Methods 5: 637-643.

Chung SH, Polgar J, Reed GL. 2000. Protein kinase C phosphorylation of syntaxin 4 in thrombin-activated human platelets. J Biol Chem 275: 25286-25291.

Clark SG, Shurland DL, Meyerowitz EM, Bargmann CI, van der Bliek AM. 1997. A dynamin GTPase mutation causes a rapid and reversible temperature-inducible locomotion defect in C. elegans. Proc Natl Acad Sci U S A 94: 10438-10443.

Colavita A, Culotti JG. 1998. Suppressors of ectopic UNC-5 growth cone steering identify eight genes involved in axon guidance in Caenorhabditis elegans. Dev Biol 194: 72-85.

Collingridge GL. 2003. The induction of N-methyl-D-aspartate receptor-dependent long-term potentiation. Philos Trans R Soc Lond B Biol Sci 358: 635-641.

Consortium TCeG. 1998. Genome sequence of the nematode C. elegans: a platform for investigating biology. Science 282: 2012-2018.

Conti E, Izaurralde E. 2005. Nonsense-mediated mRNA decay: molecular insights and mechanistic variations across species. Curr Opin Cell Biol 17: 316-325.

Crane MM, Chung K, Lu H. 2009. Computer-enhanced high-throughput genetic screens of C. elegans in a microfluidic system. Lab Chip 9: 38-40.

Cronin CJ, Feng Z, Schafer WR. 2006. Automated imaging of C. elegans behavior. Methods Mol Biol 351: 241-251.

Culotti JG, Russell RL. 1978. Osmotic avoidance defective mutants of the nematode Caenorhabditis elegans. Genetics 90: 243-256.

Dal Santo P, Logan MA, Chisholm AD, Jorgensen EM. 1999. The inositol trisphosphate receptor regulates a 50-second behavioral rhythm in C. elegans. Cell 98: 757-767.

Dash PK, Orsi SA, Moody M, Moore AN. 2004. A role for hippocampal Rho-ROCK pathway in long-term spatial memory. Biochem Biophys Res Commun 322: 893-898.

Davis GW. 2006. Homeostatic control of neural activity: from phenomenology to molecular design. Annu Rev Neurosci 29: 307-323.

Davis MW, Morton JJ, Carroll D, Jorgensen EM. 2008. Gene activation using FLP recombinase in C. elegans. PLoS Genet 4: e1000028.

Davis MW, Hammarlund M, Harrach T, Hullett P, Olsen S, Jorgensen EM. 2005. Rapid single nucleotide polymorphism mapping in C. elegans. BMC Genomics 6: 118.

de Bono M, Bargmann CI. 1998. Natural variation in a neuropeptide Y receptor homolog modifies social behavior and food response in C. elegans. Cell 94: 679-689.

De Camilli P, Takei K. 1996. Molecular mechanisms in synaptic vesicle endocytosis and recycling. Neuron 16: 481-486.

Decock JB, Gillespie-Brown J, Parker PJ, Sugden PH, Fuller SJ. 1994. Classical, novel and atypical isoforms of PKC stimulate ANF- and TRE/AP-1-regulated-promoter activity in ventricular cardiomyocytes. FEBS Lett 356: 275-278.

Denver DR, et al. 2009. A genome-wide view of Caenorhabditis elegans base-substitution mutation processes. Proc Natl Acad Sci U S A 106: 16310-16314.

Di Giovanni J, et al. 2010. V-ATPase membrane sector associates with synaptobrevin to modulate neurotransmitter release. Neuron 67: 268-279.

Diana G, Valentini G, Travaglione S, Falzano L, Pieri M, Zona C, Meschini S, Fabbri A, Fiorentini C. 2007. Enhancement of learning and memory after activation of cerebral Rho GTPases. Proc Natl Acad Sci U S A 104: 636-641.

Ding L, Candido EP. 2000. HSP43, a small heat-shock protein localized to specific cells of the vulva and spermatheca in the nematode Caenorhabditis elegans. Biochem J 349: 409-412.

Diogon M, Wissler F, Quintin S, Nagamatsu Y, Sookhareea S, Landmann F, Hutter H, Vitale N, Labouesse M. 2007. The RhoGAP RGA-2 and LET-502/ROCK achieve a balance of actomyosin-dependent forces in C. elegans epidermis to control morphogenesis. Development 134: 2469-2479.

Doitsidou M, Poole RJ, Sarin S, Bigelow H, Hobert O. 2010. C. elegans mutant identification with a one-step whole-genome-sequencing and SNP mapping strategy. PLoS One 5: e15435.

Dougherty EC, Calhoun HG. 1948. Possible significance of free-living nematodes in genetic research. Nature 161: 29.

Duerr JS, Han HP, Fields SD, Rand JB. 2008. Identification of major classes of cholinergic neurons in the nematode Caenorhabditis elegans. J Comp Neurol 506: 398-408.

Dybbs M, Ngai J, Kaplan JM. 2005. Using microarrays to facilitate positional cloning: identification of tomosyn as an inhibitor of neurosecretion. PLoS Genet 1: 6-16.

Edgley M, D'Souza A, Moulder G, McKay S, Shen B, Gilchrist E, Moerman D, Barstead R. 2002. Improved detection of small deletions in complex pools of DNA. Nucleic Acids Res 30: e52.

Etienne-Manneville S, Hall A. 2002. Rho GTPases in cell biology. Nature 420: 629-635.

Feinberg EH, Vanhoven MK, Bendesky A, Wang G, Fetter RD, Shen K, Bargmann CI. 2008. GFP Reconstitution Across Synaptic Partners (GRASP) defines cell contacts and synapses in living nervous systems. Neuron 57: 353-363.

Feng Z, Cronin CJ, Wittig JH, Jr., Sternberg PW, Schafer WR. 2004. An imaging system for standardized quantitative analysis of C. elegans behavior. BMC Bioinformatics 5: 115.

Fesce R, Grohovaz F, Valtorta F, Meldolesi J. 1994. Neurotransmitter release: fusion or 'kiss-and-run'? Trends Cell Biol 4: 1-4.

Fire A, Xu S, Montgomery MK, Kostas SA, Driver SE, Mello CC. 1998. Potent and specific genetic interference by double-stranded RNA in Caenorhabditis elegans. Nature 391: 806-811.

Flames N, Hobert O. 2009. Gene regulatory logic of dopamine neuron differentiation. Nature 458: 885-889.

Flibotte S, et al. 2010. Whole-genome profiling of mutagenesis in Caenorhabditis elegans. Genetics 185: 431-441.

Foletti DL, Lin R, Finley MA, Scheller RH. 2000. Phosphorylated syntaxin 1 is localized to discrete domains along a subset of axons. J Neurosci 20: 4535-4544.

Fraser AG, Kamath RS, Zipperlen P, Martinez-Campos M, Sohrmann M, Ahringer J. 2000. Functional genomic analysis of C. elegans chromosome I by systematic RNA interference. Nature 408: 325-330.

Frokjaer-Jensen C, Davis MW, Hopkins CE, Newman BJ, Thummel JM, Olesen SP, Grunnet M, Jorgensen EM. 2008. Single-copy insertion of transgenes in Caenorhabditis elegans. Nat Genet 40: 1375-1383.

Fujita Y, et al. 1998. Tomosyn: a syntaxin-1-binding protein that forms a novel complex in the neurotransmitter release process. Neuron 20: 905-915.

Futai M, Oka T, Sun-Wada G, Moriyama Y, Kanazawa H, Wada Y. 2000. Luminal acidification of diverse organelles by V-ATPase in animal cells. J Exp Biol 203: 107-116.

Gilon P, Rorsman P. 2009. NALCN: a regulated leak channel. EMBO Rep 10: 963-964.

Goda Y, Sudhof TC. 1997. Calcium regulation of neurotransmitter release: reliably unreliable? Curr Opin Cell Biol 9: 513-518.

Gossen M, Bujard H. 1992. Tight control of gene expression in mammalian cells by tetracycline-responsive promoters. Proc Natl Acad Sci U S A 89: 5547-5551.

Gossen M, Freundlieb S, Bender G, Muller G, Hillen W, Bujard H. 1995. Transcriptional activation by tetracyclines in mammalian cells. Science 268: 1766-1769.

Gotta M, Abraham MC, Ahringer J. 2001. CDC-42 controls early cell polarity and spindle orientation in C. elegans. Curr Biol 11: 482-488.

Govek EE, Newey SE, Van Aelst L. 2005. The role of the Rho GTPases in neuronal development. Genes Dev 19: 1-49.

Gracheva EO, Burdina AO, Touroutine D, Berthelot-Grosjean M, Parekh H, Richmond JE. 2007a. Tomosyn negatively regulates CAPS-dependent peptide release at Caenorhabditis elegans synapses. J Neurosci 27: 10176-10184.

Gracheva EO, Burdina AO, Touroutine D, Berthelot-Grosjean M, Parekh H, Richmond JE. 2007b. Tomosyn negatively regulates both synaptic transmitter and neuropeptide release at the C. elegans neuromuscular junction. J Physiol 585: 705-709.

Gracheva EO, Burdina AO, Holgado AM, Berthelot-Grosjean M, Ackley BD, Hadwiger G, Nonet ML, Weimer RM, Richmond JE. 2006a. Tomosyn inhibits synaptic vesicle priming in Caenorhabditis elegans. PLoS Biol 4.

Gray JM, Karow DS, Lu H, Chang AJ, Chang JS, Ellis RE, Marletta MA, Bargmann CI. 2004. Oxygen sensation and social feeding mediated by a C. elegans guanylate cyclase homologue. Nature 430: 317-322.

Groffen AJ, Jacobsen L, Schut D, Verhage M. 2005. Two distinct genes drive expression of seven tomosyn isoforms in the mammalian brain, sharing a conserved structure with a unique variable domain. J Neurochem 92: 554-568.

Gupta BP, Sternberg PW. 2003. The draft genome sequence of the nematode Caenorhabditis briggsae, a companion to C. elegans. Genome Biol 4: 238.

Hajdu-Cronin YM, Chen WJ, Patikoglou G, Koelle MR, Sternberg PW. 1999. Antagonism between G(o)alpha and G(q)alpha in Caenorhabditis elegans: the RGS protein EAT-16 is necessary for G(o)alpha signaling and regulates G(q)alpha activity. Genes Dev 13: 1780-1793.

Hammarlund M, Watanabe S, Schuske K, Jorgensen EM. 2008. CAPS and syntaxin dock dense core vesicles to the plasma membrane in neurons. J Cell Biol 180: 483-491.

Harris TW, et al. 2010. WormBase: a comprehensive resource for nematode research. Nucleic Acids Res 38: D463-467.

Hart AC. 2005. Behaviour in Ambros V, ed. Wormbook.

Hatsuzawa K, Lang T, Fasshauer D, Bruns D, Jahn R. 2003. The R-SNARE motif of tomosyn forms SNARE core complexes with syntaxin 1 and SNAP-25 and down-regulates exocytosis. J Biol Chem 278: 31159-31166.

Hawasli AH, Saifee O, Liu C, Nonet ML, Crowder CM. 2004. Resistance to volatile anesthetics by mutations enhancing excitatory neurotransmitter release in Caenorhabditis elegans. Genetics 168: 831-843.

Hedgecock EM, Russell RL. 1975. Normal and mutant thermotaxis in the nematode Caenorhabditis elegans. Proc Natl Acad Sci U S A 72: 4061-4065.

Heuser JE, Reese TS. 1973. Evidence for recycling of synaptic vesicle membrane during transmitter release at the frog neuromuscular junction. J Cell Biol 57: 315-344.

Hiley E, McMullan R, Nurrish SJ. 2006. The Galpha12-RGS RhoGEF-RhoA signalling pathway regulates neurotransmitter release in C. elegans. EMBO J 25: 5884-5895.

Hills T, Brockie PJ, Maricq AV. 2004. Dopamine and glutamate control area-restricted search behavior in Caenorhabditis elegans. J Neurosci 24: 1217-1225.

Hirling H, Scheller RH. 1996. Phosphorylation of synaptic vesicle proteins: modulation of the alpha SNAP interaction with the core complex. Proc Natl Acad Sci U S A 93: 11945-11949.

Hodgkin J. 1983. Male Phenotypes and Mating Efficiency in CAENORHABDITIS ELEGANS. Genetics 103: 43-64.

Hodgkin J, Horvitz HR, Brenner S. 1979. Nondisjunction Mutants of the Nematode CAENORHABDITIS ELEGANS. Genetics 91: 67-94.

Hodgkin J, Papp A, Pulak R, Ambros V, Anderson P. 1989. A new kind of informational suppression in the nematode Caenorhabditis elegans. Genetics 123: 301-313.

Horvitz HR, Sulston JE. 1980. Isolation and genetic characterization of cell-lineage mutants of the nematode Caenorhabditis elegans. Genetics 96: 435-454.

Horvitz HR, Brenner S, Hodgkin J, Herman RK. 1979. A uniform genetic nomenclature for the nematode Caenorhabditis elegans. Mol Gen Genet 175: 129-133.

Horvitz HR, Chalfie M, Trent C, Sulston JE, Evans PD. 1982. Serotonin and octopamine in the nematode Caenorhabditis elegans. Science 216: 1012-1014.

Hoshi K, Shingai R. 2006. Computer-driven automatic identification of locomotion states in Caenorhabditis elegans. J Neurosci Methods 157: 355-363.

Houssa B, de Widt J, Kranenburg O, Moolenaar WH, van Blitterswijk WJ. 1999. Diacylglycerol kinase theta binds to and is negatively regulated by active RhoA. J Biol Chem 274: 6820-6822.

Humeau Y, Popoff MR, Kojima H, Doussau F, Poulain B. 2002. Rac GTPase plays an essential role in exocytosis by controlling the fusion competence of release sites. J Neurosci 22: 7968-7981.

Humphrey JA, Hamming KS, Thacker CM, Scott RL, Sedensky MM, Snutch TP, Morgan PG, Nash HA. 2007a. A putative cation channel and its novel regulator: cross-species conservation of effects on general anesthesia. Curr Biol 17: 624-629.

Husson SJ, Clynen E, Baggerman G, Janssen T, Schoofs L. 2006. Defective processing of neuropeptide precursors in Caenorhabditis elegans lacking proprotein convertase 2 (KPC-2/EGL-3): mutant analysis by mass spectrometry. J Neurochem 98: 1999-2012.

Husson SJ, Janssen T, Baggerman G, Bogert B, Kahn-Kirby AH, Ashrafi K, Schoofs L. 2007. Impaired processing of FLP and NLP peptides in carboxypeptidase E (EGL-21)-deficient Caenorhabditis elegans as analyzed by mass spectrometry. J Neurochem 102: 246-260.

Huttner WB, Schmidt A. 2000. Lipids, lipid modification and lipid-protein interaction in membrane budding and fission--insights from the roles of endophilin A1 and synaptophysin in synaptic vesicle endocytosis. Curr Opin Neurobiol 10: 543-551.

Ishida H, Zhang X, Erickson K, Ray P. 2004. Botulinum toxin type A targets RhoB to inhibit lysophosphatidic acid-stimulated actin reorganization and acetylcholine release in nerve growth factor-treated PC12 cells. J Pharmacol Exp Ther 310: 881-889.

Jacob TC, Kaplan JM. 2003. The EGL-21 carboxypeptidase E facilitates acetylcholine release at Caenorhabditis elegans neuromuscular junctions. J Neurosci 23: 2122-2130.

Jaffe AB, Hall A. 2005. Rho GTPases: biochemistry and biology. Annu Rev Cell Dev Biol 21: 247-269.

Jansen G, Hazendonk E, Thijssen KL, Plasterk RH. 1997. Reverse genetics by chemical mutagenesis in Caenorhabditis elegans. Nat Genet 17: 119-121.

Jayanthi LD, Apparsundaram S, Malone MD, Ward E, Miller DM, Eppler M, Blakely RD. 1998. The Caenorhabditis elegans gene T23G5.5 encodes an antidepressant- and cocaine-sensitive dopamine transporter. Mol Pharmacol 54: 601-609.

Jorgensen EM. 2005. GABA in Kaplan JM, ed. Wormbook.

Jorgensen EM, Mango SE. 2002. The art and design of genetic screens: caenorhabditis elegans. Nat Rev Genet 3: 356-369.

Jorgensen EM, Hartwieg E, Schuske K, Nonet ML, Jin Y, Horvitz HR. 1995. Defective recycling of synaptic vesicles in synaptotagmin mutants of Caenorhabditis elegans. Nature 378: 196-199.

Jospin M, Watanabe S, Joshi D, Young S, Hamming K, Thacker C, Snutch TP, Jorgensen EM, Schuske K. 2007. UNC-80 and the NCA ion channels contribute to endocytosis defects in synaptojanin mutants. Curr Biol 17: 1595-1600.

Jospin M, Qi YB, Stawicki TM, Boulin T, Schuske KR, Horvitz HR, Bessereau JL, Jorgensen EM, Jin Y. 2009. A neuronal acetylcholine receptor regulates the balance of muscle excitation and inhibition in Caenorhabditis elegans. PLoS Biol 7: e1000265.

Kamath RS, et al. 2003. Systematic functional analysis of the Caenorhabditis elegans genome using RNAi. Nature 421: 231-237.

Kass J, Jacob TC, Kim P, Kaplan JM. 2001. The EGL-3 proprotein convertase regulates mechanosensory responses of Caenorhabditis elegans. J Neurosci 21: 9265-9272.

Kimble J. 1981. Alterations in cell lineage following laser ablation of cells in the somatic gonad of Caenorhabditis elegans. Dev Biol 87: 286-300.

Koelle MR, Horvitz HR. 1996. EGL-10 regulates G protein signaling in the C. elegans nervous system and shares a conserved domain with many mammalian proteins. Cell 84: 115-125.

Koh TW, Bellen HJ. 2003. Synaptotagmin I, a Ca2+ sensor for neurotransmitter release. Trends Neurosci 26: 413-422.

Lackner MR, Nurrish SJ, Kaplan JM. 1999a. Facilitation of synaptic transmission by EGL-30 Gqalpha and EGL-8 PLCbeta: DAG binding to UNC-13 is required to stimulate acetylcholine release. Neuron 24: 335-346.

Lackner MR, Kornfeld K, Miller LM, Horvitz HR, Kim SK. 1994. A MAP kinase homolog, mpk-1, is involved in ras-mediated induction of vulval cell fates in Caenorhabditis elegans. Genes Dev 8: 160-173.

Lagow RD, Bao H, Cohen EN, Daniels RW, Zuzek A, Williams WH, Macleod GT, Sutton RB, Zhang B. 2007. Modification of a hydrophobic layer by a point mutation in syntaxin 1A regulates the rate of synaptic vesicle fusion. PLoS Biol 5: e72.

Lear BC, Lin JM, Keath JR, McGill JJ, Raman IM, Allada R. 2005. The ion channel narrow abdomen is critical for neural output of the Drosophila circadian pacemaker. Neuron 48: 965-976.

Lee JH, Daud AN, Cribbs LL, Lacerda AE, Pereverzev A, Klockner U, Schneider T, Perez-Reyes E. 1999. Cloning and expression of a novel member of the low voltage-activated T-type calcium channel family. J Neurosci 19: 1912-1921.

Lehman K, Rossi G, Adamo JE, Brennwald P. 1999. Yeast homologues of tomosyn and lethal giant larvae function in exocytosis and are associated with the plasma membrane SNARE, Sec9. J Cell Biol 146: 125-140.

Lewis JA, Hodgkin JA. 1977. Specific neuroanatomical changes in chemosensory mutants of the nematode Caenorhabditis elegans. J Comp Neurol 172: 489-510.

Lewis JAaF, J.T. 1995. Methods in Cell Biology, vol. 45.

Li CaK, K. 2008. Neuropeptides in Jorgensen EMaK, J.M, ed. Wormbook.

Li H, Ruan J, Durbin R. 2008. Mapping short DNA sequencing reads and calling variants using mapping quality scores. Genome Res 18: 1851-1858.

Li W, Feng Z, Sternberg PW, Xu XZ. 2006. A C. elegans stretch receptor neuron revealed by a mechanosensitive TRP channel homologue. Nature 440: 684-687.

Liegeois S, Benedetto A, Garnier JM, Schwab Y, Labouesse M. 2006. The V0-ATPase mediates apical secretion of exosomes containing Hedgehog-related proteins in Caenorhabditis elegans. J Cell Biol 173: 949-961.

Lis J, Wu C. 1993. Protein traffic on the heat shock promoter: parking, stalling, and trucking along. Cell 74: 1-4.

Littleton JT, Chapman ER, Kreber R, Garment MB, Carlson SD, Ganetzky B. 1998. Temperature-sensitive paralytic mutations demonstrate that synaptic exocytosis requires SNARE complex assembly and disassembly. Neuron 21: 401-413.

Littlewood TD, Hancock DC, Danielian PS, Parker MG, Evan GI. 1995. A modified oestrogen receptor ligand-binding domain as an improved switch for the regulation of heterologous proteins. Nucleic Acids Res 23: 1686-1690.

Liu LX, et al. 1999. High-throughput isolation of Caenorhabditis elegans deletion mutants. Genome Res 9: 859-867.

Lloyd AC, Obermuller F, Staddon S, Barth CF, McMahon M, Land H. 1997. Cooperating oncogenes converge to regulate cyclin/cdk complexes. Genes Dev 11: 663-677.

Lochrie MA, Mendel JE, Sternberg PW, Simon MI. 1991. Homologous and unique G protein alpha subunits in the nematode Caenorhabditis elegans. Cell Regul 2: 135-154.

Lockery SR, Goodman MB. 2009. The quest for action potentials in C. elegans neurons hits a plateau. Nat Neurosci 12: 377-378.

Lonart G, Sudhof TC. 2000. Assembly of SNARE core complexes prior to neurotransmitter release sets the readily releasable pool of synaptic vesicles. J Biol Chem 275: 27703-27707.

Lou X, Korogod N, Brose N, Schneggenburger R. 2008. Phorbol esters modulate spontaneous and Ca2+-evoked transmitter release via acting on both Munc13 and protein kinase C. J Neurosci 28: 8257-8267.

Lu B, Su Y, Das S, Liu J, Xia J, Ren D. 2007. The neuronal channel NALCN contributes resting sodium permeability and is required for normal respiratory rhythm. Cell 129: 371-383.

Lu B, Su Y, Das S, Wang H, Wang Y, Liu J, Ren D. 2009. Peptide neurotransmitters activate a cation channel complex of NALCN and UNC-80. Nature 457: 741-744.

Lu B, Zhang Q, Wang H, Wang Y, Nakayama M, Ren D. 2010. Extracellular calcium controls background current and neuronal excitability via an UNC79-UNC80-NALCN cation channel complex. Neuron 68: 488-499.

Lu TZ, Feng ZP. 2011. A sodium leak current regulates pacemaker activity of adult central pattern generator neurons in lymnaea stagnalis. PLoS One 6: e18745.

Lundquist E. 2006. Small GTPases in Greenwald I, ed. Wormbook.

Macosko EZ, Pokala N, Feinberg EH, Chalasani SH, Butcher RA, Clardy J, Bargmann CI. 2009. A hub-and-spoke circuit drives pheromone attraction and social behaviour in C. elegans. Nature 458: 1171-1175.

Madison JM, Nurrish S, Kaplan JM. 2005. UNC-13 interaction with syntaxin is required for synaptic transmission. Curr Biol 15: 2236-2242.

Mahoney TR, Liu Q, Itoh T, Luo S, Hadwiger G, Vincent R, Wang ZW, Fukuda M, Nonet ML. 2006. Regulation of synaptic transmission by RAB-3 and RAB-27 in Caenorhabditis elegans. Mol Biol Cell 17: 2617-2625.

Malenka RC, Madison DV, Nicoll RA. 1986a. Potentiation of synaptic transmission in the hippocampus by phorbol esters. Nature 321: 175-177.

Malenka RC, Madison DV, Andrade R, Nicoll RA. 1986b. Phorbol esters mimic some cholinergic actions in hippocampal pyramidal neurons. J Neurosci 6: 475-480.

McDonald PW, Hardie SL, Jessen TN, Carvelli L, Matthies DS, Blakely RD. 2007. Vigorous motor activity in Caenorhabditis elegans requires efficient clearance of dopamine mediated by synaptic localization of the dopamine transporter DAT-1. J Neurosci 27: 14216-14227.

McEwen JM, Madison JM, Dybbs M, Kaplan JM. 2006. Antagonistic regulation of synaptic vesicle priming by Tomosyn and UNC-13. Neuron 51: 303-315.

McIntire SL, Jorgensen E, Horvitz HR. 1993. Genes required for GABA function in Caenorhabditis elegans. Nature 364: 334-337.

McKay SJ, et al. 2003. Gene expression profiling of cells, tissues, and developmental stages of the nematode C. elegans. Cold Spring Harb Symp Quant Biol 68: 159-169.

McMullan R, Nurrish SJ. 2007. Rho deep in thought. Genes Dev 21: 2677-2682.

McMullan R, Nurrish SJ. 2011. The RHO-1 RhoGTPase Modulates Fertility and Multiple Behaviors in Adult C. elegans. PLoS One 6: e17265.

McMullan R, Hiley E, Morrison P, Nurrish SJ. 2006. Rho is a presynaptic activator of neurotransmitter release at pre-existing synapses in C. elegans. Genes Dev 20: 65-76.

Mello C, Fire A. 1995. DNA transformation. Methods Cell Biol 48: 451-482.

Mendel JE, Korswagen HC, Liu KS, Hajdu-Cronin YM, Simon MI, Plasterk RH, Sternberg PW. 1995. Participation of the protein Go in multiple aspects of behavior in C. elegans. Science 267: 1652-1655.

Metzger D, Clifford J, Chiba H, Chambon P. 1995. Conditional site-specific recombination in mammalian cells using a ligand-dependent chimeric Cre recombinase. Proc Natl Acad Sci U S A 92: 6991-6995.

Miller KG, Emerson MD, Rand JB. 1999. Goalpha and diacylglycerol kinase negatively regulate the Gqalpha pathway in C. elegans. Neuron 24: 323-333.

Miller KG, Alfonso A, Nguyen M, Crowell JA, Johnson CD, Rand JB. 1996. A genetic selection for Caenorhabditis elegans synaptic transmission mutants. Proc Natl Acad Sci U S A 93: 12593-12598.

Morgan PG, Sedensky M, Meneely PM. 1990a. Multiple sites of action of volatile anesthetics in Caenorhabditis elegans. Proc Natl Acad Sci U S A 87: 2965-2969.

Morgan PG, Sedensky MM, Meneely PM, Cascorbi HF. 1988. The effect of two genes on anesthetic

response in the nematode Caenorhabditis elegans. Anesthesiology 69: 246-251.

Nagel G, Brauner M, Liewald JF, Adeishvili N, Bamberg E, Gottschalk A. 2005. Light activation of channelrhodopsin-2 in excitable cells of Caenorhabditis elegans triggers rapid behavioral responses. Curr Biol 15: 2279-2284.

Nassel DR. 2009. Neuropeptide signaling near and far: how localized and timed is the action of neuropeptides in brain circuits? Invert Neurosci 9: 57-75.

Nguyen M, Alfonso A, Johnson CD, Rand JB. 1995. Caenorhabditis elegans mutants resistant to inhibitors of acetylcholinesterase. Genetics 140: 527-535.

Nigon V, Dougherty EC. 1950. A dwarf mutation in a nematode; a morphological mutant of Rhabditis briggsae, a free-living soil nematode. J Hered 41: 103-109.

Nishizuka Y. 1988. The molecular heterogeneity of protein kinase C and its implications for cellular regulation. Nature 334: 661-665.

Nonet ML, Grundahl K, Meyer BJ, Rand JB. 1993. Synaptic function is impaired but not eliminated in C. elegans mutants lacking synaptotagmin. Cell 73: 1291-1305.

Nonet ML, Saifee O, Zhao H, Rand JB, Wei L. 1998. Synaptic transmission deficits in Caenorhabditis elegans synaptobrevin mutants. J Neurosci 18: 70-80.

Nonet ML, Staunton JE, Kilgard MP, Fergestad T, Hartwieg E, Horvitz HR, Jorgensen EM, Meyer BJ. 1997. Caenorhabditis elegans rab-3 mutant synapses exhibit impaired function and are partially depleted of vesicles. J Neurosci 17: 8061-8073.

Norman KR, Fazzio RT, Mellem JE, Espelt MV, Strange K, Beckerle MC, Maricq AV. 2005. The Rho/Rac-family guanine nucleotide exchange factor VAV-1 regulates rhythmic behaviors in C. elegans. Cell 123: 119-132.

Nurrish S, Ségalat L, Kaplan JM. 1999a. Serotonin inhibition of synaptic transmission: Galpha(0) decreases the abundance of UNC-13 at release sites. Neuron 24: 231-242.

Ono Y, Fujii T, Igarashi K, Kuno T, Tanaka C, Kikkawa U, Nishizuka Y. 1989. Phorbol ester binding to protein kinase C requires a cysteine-rich zinc-finger-like sequence. Proc Natl Acad Sci U S A 86: 4868-4871.

Palfreyman M, Jorgensen, E. M. 2008. Roles of SNARE proteins in synaptic vesicle fusion. In Molecular Mechanisms of Neurotransmitter Release. Pages 35-59, Humana Press.

Partridge FA, Tearle AW, Gravato-Nobre MJ, Schafer WR, Hodgkin J. 2008. The C. elegans glycosyltransferase BUS-8 has two distinct and essential roles in epidermal morphogenesis. Dev Biol 317: 549-559.

Pears CJ, Kour G, House C, Kemp BE, Parker PJ. 1990. Mutagenesis of the pseudosubstrate site of protein kinase C leads to activation. Eur J Biochem 194: 89-94.

Perez-Mansilla B, Nurrish S. 2009. A network of G-protein signaling pathways control neuronal activity in C. elegans. Adv Genet 65: 145-192.

Pierce-Shimomura JT, Morse TM, Lockery SR. 1999. The fundamental role of pirouettes in Caenorhabditis elegans chemotaxis. J Neurosci 19: 9557-9569.

Pierce-Shimomura JT, Chen BL, Mun JJ, Ho R, Sarkis R, McIntire SL. 2008a. Genetic analysis of crawling and swimming locomotory patterns in C. elegans. Proc Natl Acad Sci U S A 105: 20982-20987.

Raizen DM, Zimmerman JE, Maycock MH, Ta UD, You YJ, Sundaram MV, Pack AI. 2008. Lethargus is a Caenorhabditis elegans sleep-like state. Nature 451: 569-572.

Ramot D, Johnson BE, Berry TL, Jr., Carnell L, Goodman MB. 2008. The Parallel Worm Tracker: a platform for measuring average speed and drug-induced paralysis in nematodes. PLoS One 3: e2208.

Rand JB. 2007. Acetylcholine in Jorgensen EMaK, J.M, ed. Wormbook.

Rand JBaJ, C. D. 1995. Genetic Pharmacology: Interactions between Drugs and Gene Products in Caenorhabditis elegans. Pages 187-204 in Epstein HF, ed. Caenorhabditis elegans Modern Biological Analysis of an Organsim.

Raymond V, Mongan NP, Sattelle DB. 2000. Anthelmintic actions on homomer-forming nicotinic acetylcholine receptor subunits: chicken alpha7 and ACR-16 from the nematode Caenorhabditis elegans. Neuroscience 101: 785-791.

Reynolds NK, Schade MA, Miller KG. 2005. Convergent, RIC-8-dependent Galpha signaling pathways in the Caenorhabditis elegans synaptic signaling network. Genetics 169: 651-670.

Richmond JE, Davis WS, Jorgensen EM. 1999. UNC-13 is required for synaptic vesicle fusion in C. elegans. Nat Neurosci 2: 959-964.

Ridley AJ, Hall A. 1992. The small GTP-binding protein rho regulates the assembly of focal adhesions and actin stress fibers in response to growth factors. Cell 70: 389-399.

Rockman MV, Kruglyak L. 2009. Recombinational landscape and population genomics of Caenorhabditis elegans. PLoS Genet 5: e1000419.

Saifee O, Wei L, Nonet ML. 1998a. The Caenorhabditis elegans unc-64 locus encodes a syntaxin that interacts genetically with synaptobrevin. Mol Biol Cell 9: 1235-1252.

Sakisaka T, Baba T, Tanaka S, Izumi G, Yasumi M, Takai Y. 2004. Regulation of SNAREs by tomosyn and ROCK: implication in extension and retraction of neurites. J Cell Biol 166: 17-25.

Sarin S, Prabhu S, O'Meara MM, Pe'er I, Hobert O. 2008. Caenorhabditis elegans mutant allele identification by whole-genome sequencing. Nat Methods 5: 865-867.

Sarin S, Bertrand V, Bigelow H, Boyanov A, Doitsidou M, Poole RJ, Narula S, Hobert O. 2010. Analysis of multiple ethyl methanesulfonate-mutagenized Caenorhabditis elegans strains by whole-genome sequencing. Genetics 185: 417-430.

Sawin ER, Ranganathan R, Horvitz HR. 2000. C. elegans locomotory rate is modulated by the environment through a dopaminergic pathway and by experience through a serotonergic pathway. Neuron 26: 619-631.

Schade MA, Reynolds NK, Dollins CM, Miller KG. 2005. Mutations that rescue the paralysis of Caenorhabditis elegans ric-8 (synembryn) mutants activate the G alpha(s) pathway and define a third major branch of the synaptic signaling network. Genetics 169: 631-649.

Schoch S, Deak F, Konigstorfer A, Mozhayeva M, Sara Y, Sudhof TC, Kavalali ET. 2001. SNARE function analyzed in synaptobrevin/VAMP knockout mice. Science 294: 1117-1122.

Schuske KR, Richmond JE, Matthies DS, Davis WS, Runz S, Rube DA, van der Bliek AM, Jorgensen EM. 2003. Endophilin is required for synaptic vesicle endocytosis by localizing synaptojanin. Neuron 40: 749-762.

Sedensky MM, Meneely PM. 1987. Genetic analysis of halothane sensitivity in Caenorhabditis elegans. Science 236: 952-954.

Segalat L, Elkes DA, Kaplan JM. 1995. Modulation of serotonin-controlled behaviors by Go in Caenorhabditis elegans. Science 267: 1648-1651.

Shen Y, Sarin S, Liu Y, Hobert O, Pe'er I. 2008. Comparing platforms for C. elegans mutant identification using high-throughput whole-genome sequencing. PLoS One 3: e4012.

Sieburth D, Madison JM, Kaplan JM. 2007. PKC-1 regulates secretion of neuropeptides. Nat Neurosci 10: 49-57.

Sieburth D, et al. 2005. Systematic analysis of genes required for synapse structure and function. Nature 436: 510-517.

Snutch TP, Monteil A. 2007. The sodium "leak" has finally been plugged. Neuron 54: 505-507.

Sollner T, Whiteheart SW, Brunner M, Erdjument-Bromage H, Geromanos S, Tempst P, Rothman JE. 1993. SNAP receptors implicated in vesicle targeting and fusion. Nature 362: 318-324.

Souza RP, Rosa DVF, Romano-Silva MA, Zhen M, Meltzer HY, Lieberman JA, Remington G, Kennedy JL, Wong AHC. 2010. Lack of association of NALCN genetic variants with schizophrenia. Psychiatry research.

Speca DJ, et al. 2010. Conserved role of unc-79 in ethanol responses in lightweight mutant mice. PLoS Genet 6.

Speese S, Petrie M, Schuske K, Ailion M, Ann K, Iwasaki K, Jorgensen EM, Martin TF. 2007. UNC-31 (CAPS) is required for dense-core vesicle but not synaptic vesicle exocytosis in Caenorhabditis elegans. J Neurosci 27: 6150-6162.

Speese SD, Trotta N, Rodesch CK, Aravamudan B, Broadie K. 2003. The ubiquitin proteasome system acutely regulates presynaptic protein turnover and synaptic efficacy. Curr Biol 13: 899-910.

Spencer AG, Orita S, Malone CJ, Han M. 2001. A RHO GTPase-mediated pathway is required during P cell migration in Caenorhabditis elegans. Proc Natl Acad Sci U S A 98: 13132-13137.

Squire MD, Tornoe C, Baylis HA, Fleming JT, Barnard EA, Sattelle DB. 1995. Molecular cloning and functional co-expression of a Caenorhabditis elegans nicotinic acetylcholine receptor subunit (acr-2). Receptors Channels 3: 107-115.

Steven R, Zhang L, Culotti J, Pawson T. 2005. The UNC-73/Trio RhoGEF-2 domain is required in separate isoforms for the regulation of pharynx pumping and normal neurotransmission in C. elegans. Genes Dev 19: 2016-2029.

Steven R, Kubiseski TJ, Zheng H, Kulkarni S, Mancillas J, Ruiz Morales A, Hogue CW, Pawson T, Culotti J. 1998. UNC-73 activates the Rac GTPase and is required for cell and growth cone migrations in C. elegans. Cell 92: 785-795.

Stringham EG, Dixon DK, Jones D, Candido EP. 1992. Temporal and spatial expression patterns of the small heat shock (hsp16) genes in transgenic Caenorhabditis elegans. Mol Biol Cell 3: 221-233.

Sulston J, Dew M, Brenner S. 1975. Dopaminergic neurons in the nematode Caenorhabditis elegans. J Comp Neurol 163: 215-226.

Sulston JE, Brenner S. 1974. The DNA of Caenorhabditis elegans. Genetics 77: 95-9104.

Sulston JE, Horvitz HR. 1977. Post-embryonic cell lineages of the nematode, Caenorhabditis elegans. Dev Biol 56: 110-156.

Sulston JE, White JG. 1980. Regulation and cell autonomy during postembryonic development of Caenorhabditis elegans. Dev Biol 78: 577-597.

Sulston JE, Schierenberg E, White JG, Thomson JN. 1983. The embryonic cell lineage of the nematode Caenorhabditis elegans. Dev Biol 100: 64-119.

Suzuki H, Kerr R, Bianchi L, Frokjaer-Jensen C, Slone D, Xue J, Gerstbrein B, Driscoll M, Schafer WR. 2003. In vivo imaging of C. elegans mechanosensory neurons demonstrates a specific role for the MEC-4 channel in the process of gentle touch sensation. Neuron 39: 1005-1017.

Swayne LA, et al. 2009. The NALCN ion channel is activated by M3 muscarinic receptors in a pancreatic beta-cell line. EMBO Rep 10: 873-880.

Sweitzer SM, Hinshaw JE. 1998. Dynamin undergoes a GTP-dependent conformational change causing vesiculation. Cell 93: 1021-1029.

Tabara H, Grishok A, Mello CC. 1998. RNAi in C. elegans: soaking in the genome sequence. Science 282: 430-431.

Tabuse Y, Izumi Y, Piano F, Kemphues KJ, Miwa J, Ohno S. 1998. Atypical protein kinase C cooperates with PAR-3 to establish embryonic polarity in Caenorhabditis elegans. Development 125: 3607-3614.

Tall GG, Krumins AM, Gilman AG. 2003. Mammalian Ric-8A (synembryn) is a heterotrimeric Galpha protein guanine nucleotide exchange factor. J Biol Chem 278: 8356-8362.

Tavernarakis N, Shreffler W, Wang S, Driscoll M. 1997. unc-8, a DEG/ENaC family member, encodes a subunit of a candidate mechanically gated channel that modulates C. elegans locomotion. Neuron 18: 107-119.

Teng Y, Girard L, Ferreira HB, Sternberg PW, Emmons SW. 2004. Dissection of cis-regulatory elements in the C. elegans Hox gene egl-5 promoter. Dev Biol 276: 476-492.

Thomas JH. 1990. Genetic analysis of defecation in Caenorhabditis elegans. Genetics 124: 855-872.

Timmons L, Court DL, Fire A. 2001. Ingestion of bacterially expressed dsRNAs can produce specific and potent genetic interference in Caenorhabditis elegans. Gene 263: 103-112.

Tokuoka SM, Saiardi A, Nurrish SJ. 2008. The mood stabilizer valproate inhibits both inositol- and diacylglycerol-signaling pathways in Caenorhabditis elegans. Mol Biol Cell 19: 2241-2250.

Trimble WS, Cowan DM, Scheller RH. 1988. VAMP-1: a synaptic vesicle-associated integral membrane protein. Proc Natl Acad Sci U S A 85: 4538-4542.

Udo H, Jin I, Kim JH, Li HL, Youn T, Hawkins RD, Kandel ER, Bailey CH. 2005. Serotonin-induced regulation of the actin network for learning-related synaptic growth requires Cdc42, N-WASP, and PAK in Aplysia sensory neurons. Neuron 45: 887-901.

van Blitterswijk WJ, Houssa B. 2000. Properties and functions of diacylglycerol kinases. Cell Signal 12: 595-605.

van der Linden AM, Simmer F, Cuppen E, Plasterk RH. 2001. The G-protein beta-subunit GPB-2 in Caenorhabditis elegans regulates the G(o)alpha-G(q)alpha signaling network through interactions with the regulator of G-protein signaling proteins EGL-10 and EAT-16. Genetics 158: 221-235.

van Swinderen B, Saifee O, Shebester L, Roberson R, Nonet ML, Crowder CM. 1999. A neomorphic syntaxin mutation blocks volatile-anesthetic action in Caenorhabditis elegans. Proc Natl Acad Sci U S A 96: 2479-2484.

van Swinderen B, Metz LB, Shebester LD, Mendel JE, Sternberg PW, Crowder CM. 2001. Goalpha regulates volatile anesthetic action in Caenorhabditis elegans. Genetics 158: 643-655.

Wang H, Ren D. 2009. UNC80 functions as a scaffold for Src kinases in NALCN channel function. Channels (Austin) 3: 161-163.

Ward S. 1973. Chemotaxis by the nematode Caenorhabditis elegans: identification of attractants and analysis of the response by use of mutants. Proc Natl Acad Sci U S A 70: 817-821.

Washbourne P, et al. 2002. Genetic ablation of the t-SNARE SNAP-25 distinguishes mechanisms

of neuroexocytosis. Nat Neurosci 5: 19-26.

Watson N, Linder ME, Druey KM, Kehrl JH, Blumer KJ. 1996. RGS family members: GTPase-activating proteins for heterotrimeric G-protein alpha-subunits. Nature 383: 172-175.

Weber T, Zemelman BV, McNew JA, Westermann B, Gmachl M, Parlati F, Sollner TH, Rothman JE. 1998. SNAREpins: minimal machinery for membrane fusion. Cell 92: 759-772.

Weimer RM, Richmond JE, Davis WS, Hadwiger G, Nonet ML, Jorgensen EM. 2003. Defects in synaptic vesicle docking in unc-18 mutants. Nat Neurosci 6: 1023-1030.

Welchman DP, Mathies LD, Ahringer J. 2007. Similar requirements for CDC-42 and the PAR-3/PAR-6/PKC-3 complex in diverse cell types. Dev Biol 305: 347-357.

White JG, Southgate, E., Thomson, J.N., Brenner, S. 1986. The Structure of the Nervous System of the Nematode Caenorhabditis Elegans. Philosophical Transactions of the Royal Society, London B 314: 1-340.

Wicks SR, Yeh RT, Gish WR, Waterston RH, Plasterk RH. 2001. Rapid gene mapping in Caenorhabditis elegans using a high density polymorphism map. Nat Genet 28: 160-164.

Williams SL, Lutz S, Charlie NK, Vettel C, Ailion M, Coco C, Tesmer JJ, Jorgensen EM, Wieland T, Miller KG. 2007. Trio's Rho-specific GEF domain is the missing Galpha q effector in C. elegans. Genes Dev 21: 2731-2746.

Winston WM, Sutherlin M, Wright AJ, Feinberg EH, Hunter CP. 2007. Caenorhabditis elegans SID-2 is required for environmental RNA interference. Proc Natl Acad Sci U S A 104: 10565-10570.

Wissmann A, Ingles J, Mains PE. 1999. The Caenorhabditis elegans mel-11 myosin phosphatase regulatory subunit affects tissue contraction in the somatic gonad and the embryonic epidermis and genetically interacts with the Rac signaling pathway. Dev Biol 209: 111-127.

Wissmann A, Ingles J, McGhee JD, Mains PE. 1997. Caenorhabditis elegans LET-502 is related to Rho-binding kinases and human myotonic dystrophy kinase and interacts genetically with a homolog of the regulatory subunit of smooth muscle myosin phosphatase to affect cell shape. Genes Dev 11: 409-422.

Yamanaka T, Horikoshi Y, Sugiyama Y, Ishiyama C, Suzuki A, Hirose T, Iwamatsu A, Shinohara A, Ohno S. 2003. Mammalian Lgl forms a protein complex with PAR-6 and aPKC independently of PAR-3 to regulate epithelial cell polarity. Curr Biol 13: 734-743.

Yau DM, Yokoyama N, Goshima Y, Siddiqui ZK, Siddiqui SS, Kozasa T. 2003. Identification and molecular characterization of the G alpha12-Rho guanine nucleotide exchange factor pathway in Caenorhabditis elegans. Proc Natl Acad Sci U S A 100: 14748-14753.

Yeh E, et al. 2008. A putative cation channel, NCA-1, and a novel protein, UNC-80, transmit neuronal activity in C. elegans. PLoS Biol 6: e55.

Yokoyama S, Shirataki H, Sakisaka T, Takai Y. 1999. Three splicing variants of tomosyn and identification of their syntaxin-binding region. Biochem Biophys Res Commun 256: 218-222.

Yook KJ, Proulx SR, Jorgensen EM. 2001. Rules of nonallelic noncomplementation at the synapse in Caenorhabditis elegans. Genetics 158: 209-220.

Yu FH, Yarov-Yarovoy V, Gutman GA, Catterall WA. 2005. Overview of molecular relationships in the voltage-gated ion channel superfamily. Pharmacol Rev 57: 387-395.

Zallen JA, Peckol EL, Tobin DM, Bargmann CI. 2000. Neuronal cell shape and neurite initiation are regulated by the Ndr kinase SAX-1, a member of the Orb6/COT-1/warts serine/threonine kinase family. Mol Biol Cell 11: 3177-3190.

Zhang L, Chung BY, Lear BC, Kilman VL, Liu Y, Mahesh G, Meissner RA, Hardin PE, Allada R. 2010. DN1(p) circadian neurons coordinate acute light and PDF inputs to produce robust daily behavior in Drosophila. Curr Biol 20: 591-599.

Zhang S, Ma C, Chalfie M. 2004. Combinatorial marking of cells and organelles with reconstituted fluorescent proteins. Cell 119: 137-144.

Zhou KM, Dong YM, Ge Q, Zhu D, Zhou W, Lin XG, Liang T, Wu ZX, Xu T. 2007. PKA activation bypasses the requirement for UNC-31 in the docking of dense core vesicles from C. elegans neurons. Neuron 56: 657-669.